PROCEEDINGS OF THE FIRST ERDA SEMIANNUAL SOLAR PHOTOVOLTAIC CONVERSION PROGRAM CONFERENCE

University of California
Los Angeles, CA
July 22-25, 1975

Organized by the Jet Propulsion Laboratory
for the Energy Research and Development Administration
with participation by the
National Science Foundation (NSF)

(NASA-CR-143107) PROCEEDINGS OF THE FIRST ERDA SEMIANNUAL SOLAR PHOTOVOLTAIC CONVERSION PROGRAM CONFERENCE (Jet Propulsion Lab.) 744 p HC $18.75 CSCL 10A
N76-12472
THRU
N76-12508
Unclas
G3/44 03845

JPL Document 5040-13

JET PROPULSION LABORATORY
CALIFORNIA INSTITUTE OF TECHNOLOGY
PASADENA, CALIFORNIA

PREFACE

This report of the Proceeding of the Subject Meeting has been assembled to provide the participants and other interested parties with a compilation of abstracts of the talks given. Copies of visual aids used have been printed in the best available form.

CONTENTS

INTRODUCTION

Session I: Photovoltaic Systems -①

Session II: Low-Cost Silicon Solar Arrays

CONTENTS (Contd)

Session III: Test and Demonstration

Session IV: Concentrator Systems

Session V: Polycrystalline Silicon Cells

Session VI: Compound Semiconductor Solar Cells

CONTENTS (Contd)

Session VII: Other Approaches 1

Session VIII: Other Approaches 2

CONTENTS (Contd)

Attendee List

Semi-Annual National Solar Photovoltaic Conversion Program Review Meeting

University of California
Los Angeles, CA, July 22-25, 1975

Dr. Richard W. Ahrons
Innotech Corporation
181 Main Street
Norwalk, CT 06851

Mr. Larry Anderson
Chemistry Department
Ohio State University
Columbus, OH 43212

Dr. Richard L. Anderson
Department of Electrical Engineering
Syracuse University
Syracuse, NY 13210

Dr. Wayne Anderson
College of Engineering
Rutgers University
New Brunswick, NJ 08903

Dr. William W. Anderson
Electrical Engineering Department
Ohio State University
Columbus, OH 43212

Mr. William Bachman
Jet Propulsion Laboratory
4800 Oak Grove Drive
Pasadena, CA 91103

Dr. Charles Backus
College of Engineering Science
Arizona State University
Tempe, AZ 85281

Mr. Ron Barchet
General Electric Company
Corporation Research & Development
P. O. Box 43
Schenectady, NY 12301

Mr. Fred Bartels
Spectrolab
12500 Gladstone Avenue
Sylmar, CA 91342

Dr. Ronald L. Bell
Varian Central Research Lab
611 Hansen Way
Palo Alto, CA 94303

Dr. Raymond Berg
Sandia Laboratories
Albuquerque, NM 87115

Dr. Elliot Berman
Boston University
Boston, MA 02215

Mr. D. T. Bernatowicz
NASA-Lewis Research Center
21000 Brookpark Road
Cleveland, OH 44135

Dr. Karl Böer
Institute of Energy Conversion
University of Delaware
Newark, DE 19711

Mr. Piet Bos
Electric Power Research Institute
3412 Hillview Avenue
Palo Alto, CA 94304

Dr. H. Brandhorst
NASA-Lewis Research Center
21000 Brookpark Road
Cleveland, OH 44135

Mr. Gerald W. Braun
Southern California Edison Co.
2244 Walnut Grove Avenue
Rosemead, CA 91770

Dr. T. P. Brody
Westinghouse Electric Corporation
Research and Development
Pittsburgh, PA 15235

Dr. Richard Bube
Department of Materials Science
Stanford University
Stanford, CA 94305

Attendee List

Mr. Irving G. Calish
Innotech Corporation
181 Main Street
Norwalk, CT 06851

Dr. William T. Callaghan
Jet Propulsion Laboratory
4800 Oak Grove Drive
Pasadena, CA 91103

Mr. W. F. Carroll
Jet Propulsion Laboratory
4800 Oak Grove Drive
Pasadena, CA 91103

Mr. Paul Caruso
Solar Power Corporation
Braintree, MA 02184

Mr. John Castle
Spectrolab
12500 Gladstone Avenue
Sylmar, CA 91342

Mr. Arnold S. Cherdak
Mitre Corporation
McLean, VA 22101

Professor T. L. Chu
Electronic Sciences Center
Southern Methodist University
Dallas, TX 75275

Mr. Ted Ciszek
IBM, Department 267
East Fishkill, Route 52
Hopewell Junction, NY 12533

Mr. J. W. Cleland
Holifield National Laboratory
P. O. Box X
Oak Ridge, TN 37830

Dr. George Craford
Director of R&D
Monsanto
3400 Hillview Avenue
Palo Alto, CA 94304

Dr. Denis J. Curtin
COMSAT Laboratories
P. O. Box 115
Clarksburg, MD 20734

Dr. Edgar DeMeo
Department of Engineering
Brown University
Providence, RI 02912

Mr. James N. Deyo
NASA-Lewis Research Center
21000 Brookpark Road
Cleveland, OH 44135

Mr. Donald Dinger, AMXFB-ZN
Commander
USAMERDC
Fort Belvoir, VA 22060

Mr. Edward Divita
Jet Propulsion Laboratory
4800 Oak Grove Drive
Pasadena, CA 91103

Dr. Wolfgang Doeffler
Honeywell
2600 Ridgeway Parkway
Minneapolis, Minn. 55413

Mr. Robert Easter
Division of Solar Energy
Energy Research & Development Adm.
1800 G Street, N.W.
Washington, D. C. 20545

Dr. Joseph Feinstein
Varian Central Research Lab
611 Hansen Way
Palo Alto, CA 94303

Dr. Leon Florschuetz
Arizona State University
Tempe, AZ 85281

Mr. Richard L. Foley
RCA Labs
Princeton, NJ 08540

Attendee List

Mr. Robert G. Forney
Jet Propulsion Laboratory
4800 Oak Grove Drive
Pasadena, CA 91103

Mr. Gordon Gaines
Battelle Columbus Lab.
505 King Avenue
Columbus, OH 43201

Dr. John Galt
Sandia Laboratory
Albuquerque, NM 87115

Mr. Edward Gillis, AMKFB-E
Commander
USAMERDC
Fort Belvoir, VA 22060

Mr. John V. Goldsmith
Jet Propulsion Laboratory
4800 Oak Grove Drive
Pasadena, CA 91103

Mr. Paul Goldsmith
TRW Systems
One Space Park
Redondo Beach, CA 92078

Dr. R. L. Gordon
Battelle Northwest Laboratories
P. O. Box 999
Richmond, WA 99352

Mr. Al Green
Code 601
Naval Weapons Center
China Lake, CA 93555

Dr. G. Haacke
American Cyanamid Company
Chemical Research Division
Stamford, CT 06904

Dr. Gregory Haas
Mitre Corporation
McLean, VA 22101

Mr. Richard T. Haenle
Jet Propulsion Laboratory
4800 Oak Grove Drive
Pasadena, CA 91103

Mr. Robert L. Harkey
Jet Propulsion Laboratory
4800 Oak Grove Drive
Pasadena, CA 91103

Mr. Walter A. Hasbach
Jet Propulsion Laboratory
4800 Oak Grove Drive
Pasadena, CA 91103

Mr. Walter Hausz
General Electric
Aerospace Group TEMPO
816 State Street
Santa Barbara, CA 93102

Mr. Frederic A. Heim
Sensor Technology, Inc.
21012 Lassen Street
Chatsworth, CA 91311

Dr. Ed Hsieh
University of California
Lawrence Livermore Laboratory
P. O. Box 808
Livermore, CA 94550

Mr. Lee P. Hunt
Dow Corning Corporation
Hemlock, MI 48626

Mr. H. K. Kan
Aerospace Corporation
P. O. Box 92957
Los Angeles, CA 90009

Dr. Lawrence Kazmerski
Electrical Engineering Dept.
University of Maine
Orona, ME 04473

Attendee List

Dr. Gordon Kent
Department of Electrical Engineering
Syracuse University
Syracuse, NY 13210

Mr. Aaron Kirpich
General Electric Corporation
Adv. Energy Programs
King of Prussia Park
P. O. Box 8661
Philadelphia, PA 19108

Dr. W. Kohn
University of California, San Diego
P. O. Box 109
La Jolla, CA 92037

Mr. Al Kran
IBM
East Fishkill, Route 52
Hopewell Junction, NY 12533

Dr. Henry Kressel
RCA Labs
David Sarnoff Research Center
Princeton, NJ 08540

Professor B. Lalevic
College of Engineering
Rutgers University
New Brunswick, NJ 08903

Mr. Alan LaRue
Aerospace and Defense Group
Honeywell, Inc.
15250 Ventura Blvd.
Sherman Oaks, CA 91403

Dr. Stuart Lee
Fluor Corporation
2500 S. Atlantic Boulevard
Los Angeles, CA 90040

Dr. Stanley L. Leonard
The Aerospace Corporation
P. O. Box 91957
Los Angeles, CA 90009

Dr. Fred Lindholm
University of Florida
Electrical Engineering
Gainesville, FL 32601

Dr. J. Lindmayer
Solarex Corporation
1335 Piccard Drive
Rockville, MD 20850

Mr. Norman Lutkefeder
Federal Energy Administration
12th & Pennsylvania Ave., N.W.
Washington, D. C. 20461

Mr. Harold L. Macomber
Jet Propulsion Laboratory
4800 Oak Grove Drive
Pasadena, CA 91103

Dr. Leonard M. Magid
Energy Research & Development Adm.
1800 G Street, N.W.
Washington, D. C. 20545

Mr. James McCormick
Dow Corning
Hemlock, MI 48626

Mr. J. McCristall
Optical Coating Laboratory
15251 East Don Julian Road
City of Industry, CA 91746

Dr. John D. Meakin
Institute of Energy Conversion
University of Delaware
Newark, DE 19711

Mr. A. I. Mlavsky
Mobil Tyco Solar Energy Corp.
16 Hickory Drive
Waltham, MA 02154

Dr. Joseph Morabito
Bell Labs
55 Union Boulevard
Allentown, PA 18103

Attendee List

Dr. Tapan Mukherjee
National Science Foundation
Div. of Adv. Eng. Research & Tech.
1800 G Street, N.W.
Washington, D. C. 20545

Dr. Marc Nicolet
Department of Electrical Engineering
California Institute of Technology
Pasadena, CA 91109

Dr. Arthur J. Nozik
Allied Chemical Materials Research
P. O. Box 1021R
Morristown, NJ 07960

Mr. Henry Oman
The Boeing Company
P. O. Box 3999
Seattle, WA 98124

Dr. D. J. Page
Westinghouse Electric Corp., R&D
310 Beulah Road
Pittsburgh, PA 15235

Dr. P. F. Pittman
Westinghouse Electric Corp., R&D
310 Beulah Road
Pittsburgh, PA 15235

Dr. Morton Prince
Division of Solar Energy
Energy Research & Development Admin.
1800 G Street, N.W.
Washington, D. C. 20545

Dr. Ari Rabl
Argonne National Laboratory
9700 South Cass Avenue
Argonne, IL 60439

Professor Paul M. Raccah
The Belfer Graduate School
Yeshiva University
Amsterdam Avenue & 186th Street
New York, NY 10033

Mr. E. L. Ralph
Spectrolab
12500 Gladstone Avenue
Sylmar, CA 91342

Dr. J. J. Rasmussen
Battelle Northwest Laboratories
P. O. Box 999
Richmond, WA 99352

Dr. K. V. Ravi
Mobil Tyco Solar Energy Corp.
16 Hickory Drive
Waltham, MA 02154

Mr. David Richardson
Arthur D. Little, Inc.
Acorn Park
Cambridge, MA 02140

Mr. Robert Riel
Westinghouse Electric, R&D
310 Beulan Road
Pittsburgh, PA 15235

Dr. Albert Rose
Department of Electrical Engg.
California Institute of Technology
Pasadena, CA 91109

Dr. Lou Rosenblum
NASA-Lewis Research Center
21000 Brookpark Road
Cleveland, OH 44135

Mr. Irwin Rubin
Sensor Technology Inc.
21012 Lassen Street
Chatsworth, CA 91311

Mr. Ralph Ruth - D/540, HA32
Rockwell International
Autonetics Division
3370 Miraloma Avenue
Anaheim, CA 92803

Attendee List

Dr. C. T. Sah
Electrical Engineering Dept.
University of Illinois
Urbana, IL 61801

Dr. George Samara
Sandia Laboratory
Albuquerque, NM 87115

Mr. Dan Schneiderman
Jet Propulsion Laboratory
4800 Oak Grove Drive
Pasadena, CA 91103

Dr. Donald Schueler
Div. of Solar Energy
Energy Research & Development Adm.
1800 G Street, N.W.
Washington, D. C. 20545

Dr. S. Schultz
Physics Department
University of California, San Diego
P. O. Box 109
La Jolla CA 92037

Mr. E. A. Sequeira
Jet Propulsion Laboratory
4800 Oak Grove Drive
Pasadena, CA 91103

Dr. John Shewchun
Department of Engineering
Brown University
Providence, RI 02912

Mr. F. A. Shirland
Westinghouse Electric Corp., R&D
310 Beulah Road
Pittsburgh, PA 15235

Dr. Wigbert Siekhaus
University of California
Lawrence Berkeley Laboratory
Berkeley, CA 94720

Dr. Richard J. Stirn
Jet Propulsion Laboratory
4800 Oak Grove Drive
Pasadena, CA 91103

Mr. H. Kurt Strass
Energy Systems Division
Office of Energy Programs
National Aeronautics & Space Adm.
Washington, D. C. 20546

Dr. R. P. Stromberg
Sandia Laboratory
Albuquerque, NM 87115

Dr. Steven J. Valenty
General Electric Company
Schenectady, NY 12301

Dr. Gene Wakefield
Semiconductor Group
Texas Instruments, Inc.
P. O. Box 5012
Dallas, TX 75222

Dr. Douglas Warschauer
Div. of Solar Energy
Energy Research & Development Adm.
1800 G Street, N.W.
Washington, D. C. 20545

Dr. Mason Watson
The Aerospace Corporation
P. O. Box 92957
Los Angeles, CA 90009

Dr. Ronald Wichner
University of California
Lawrence Livermore Laboratory
P. O. Box 808
Livermore, CA 94550

Mr. Paul Wiener
Jet Propulsion Laboratory
4800 Oak Grove Drive
Pasadena, CA 91103

Attendee List

Dr. Brown Williams
RCA Labs
David Sarnoff Research Center
Princeton, NJ 08540

Professor Martin Wolf
University of Pennsylvania
260 Towne Building
Philadelphia, PA 19174

Mr. Charles Wrigley
Solarex Corporation
1335 Piccard Drive
Rockville, MD 20850

Mr. William Yerkes
16562 Knollwood Drive
Granada Hills, CA 91344

Dr. Sol Zwerdling
Argonne National Laboratory
9700 South Cass Avenue
Argonne, IL 60439

INTRODUCTION

The National Photovoltaic Conversion Program

Leonard M. Magid
Division of Solar Energy
Energy Research and Development Administration
Washington, D. C. 20545

I wish to welcome all of you to this, the first of the Semi-Annual National Solar Photovoltaic Conversion Program Review Meetings held under the sponsorship of the new Energy Research and Development Administration (ERDA).

As most of you must know by now, with the creation of ERDA on January 19, 1975, the lead Agency role in Solar Energy, as well as the major parts of each of the solar technologies including photovoltaics, was transferred from the National Science Foundation (NSF) to ERDA. NSF is expected, however, to continue to play a significant role in the National Photovoltaic Conversion Program, primarily in areas of basic research and applied technology in what I trust will be a closely coordinated effort with ERDA within the overall interests of the National Program. Dr. Tap Mukherjee, the NSF Photovoltaic Conversion Program Manager, will shortly be outlining the NSF role in this effort.

ERDA STRUCTURE

With respect to the ERDA program, Figure 1 shows the functional organization under the leadership of Dr. Robert Seamans, Jr., the ERDA Administrator. The Division of Solar Energy is part of the Office of the Assistant Administrator for Solar, Geothermal and Advanced Energy Systems, headed by Dr. John M. Teem, as shown in Figure 2.

The organization of the Division of Solar Energy is given in Figure 3. The Photovoltaic Branch is located within the Office of the Assistant Director for Solar Electric Applications headed by Dr. Dick Blieden. Dr. Mort Prince, one of the original developers of the silicon solar cell has recently been named the Chief of the Photovoltaics Branch.

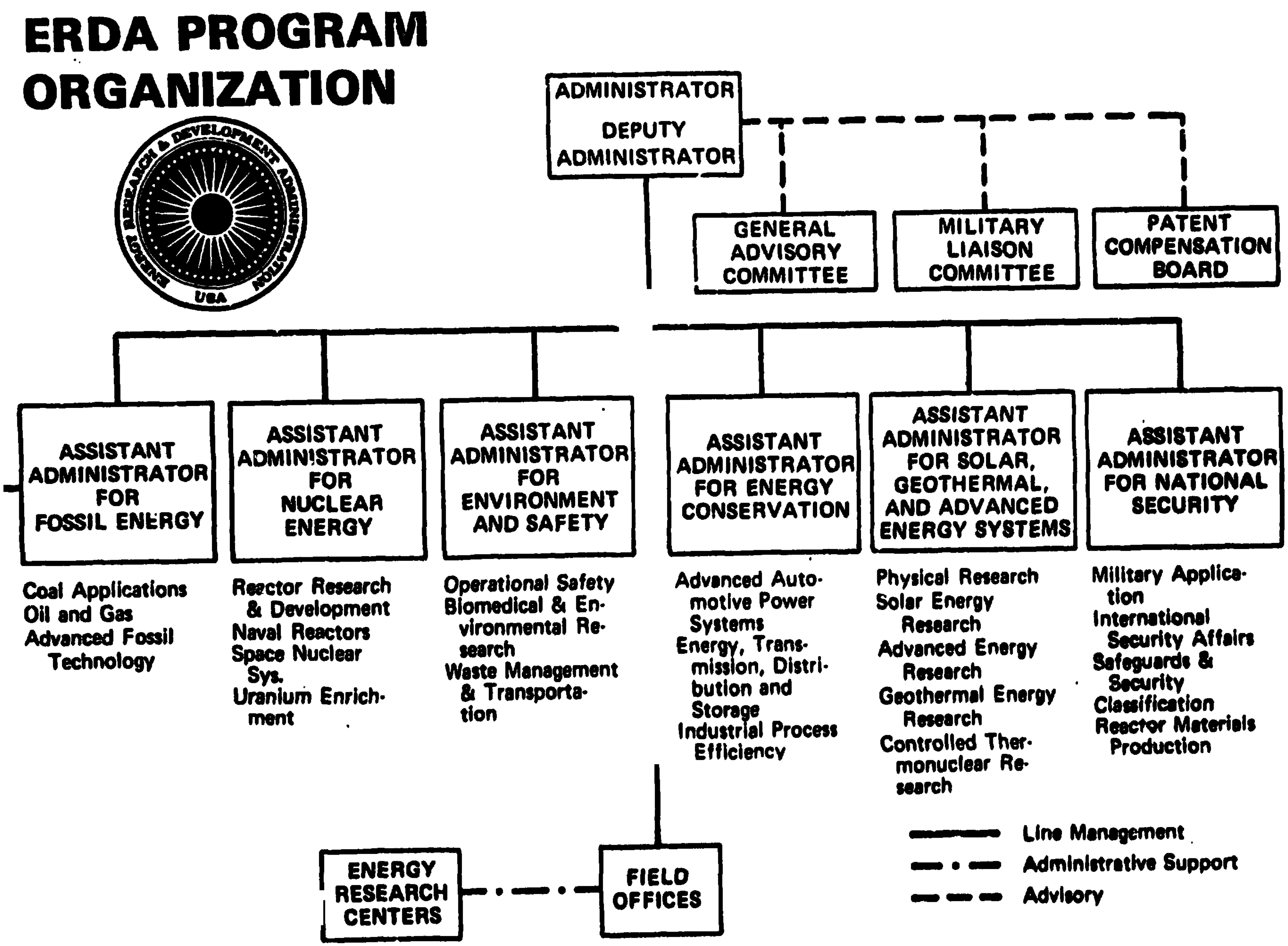
ERDA PROGRAM ORGANIZATION
ENERGY RESEARCH & DEVELOPMENT ADMINISTRATION USA
ADMINISTRATOR
DEPUTY ADMINISTRATOR
GENERAL ADVISORY COMMITTEE
MILITARY LIAISON COMMITTEE
PATENT COMPENSATION BOARD
ASSISTANT ADMINISTRATOR FOR FOSSIL ENERGY
Coal Applications
Oil and Gas
Advanced Fossil Technology
ASSISTANT ADMINISTRATOR FOR NUCLEAR ENERGY
Reactor Research & Development
Naval Reactors
Space Nuclear Sys.
Uranium Enrichment
ASSISTANT ADMINISTRATOR FOR ENVIRONMENT AND SAFETY
Operational Safety
Biomedical & Environmental Research
Waste Management & Transportation
ASSISTANT ADMINISTRATOR FOR ENERGY CONSERVATION
Advanced Automotive Power Systems
Energy, Transmission, Distribution and Storage
Industrial Process Efficiency
ASSISTANT ADMINISTRATOR FOR SOLAR, GEOTHERMAL, AND ADVANCED ENERGY SYSTEMS
Physical Research
Solar Energy Research
Advanced Energy Research
Geothermal Energy Research
Controlled Thermonuclear Research
ASSISTANT ADMINISTRATOR FOR NATIONAL SECURITY
Military Application
International Security Affairs
Safeguards & Security
Classification
Reactor Materials Production
ENERGY RESEARCH CENTERS
FIELD OFFICES
Line Management
Administrative Support
Advisory

FIG. 1

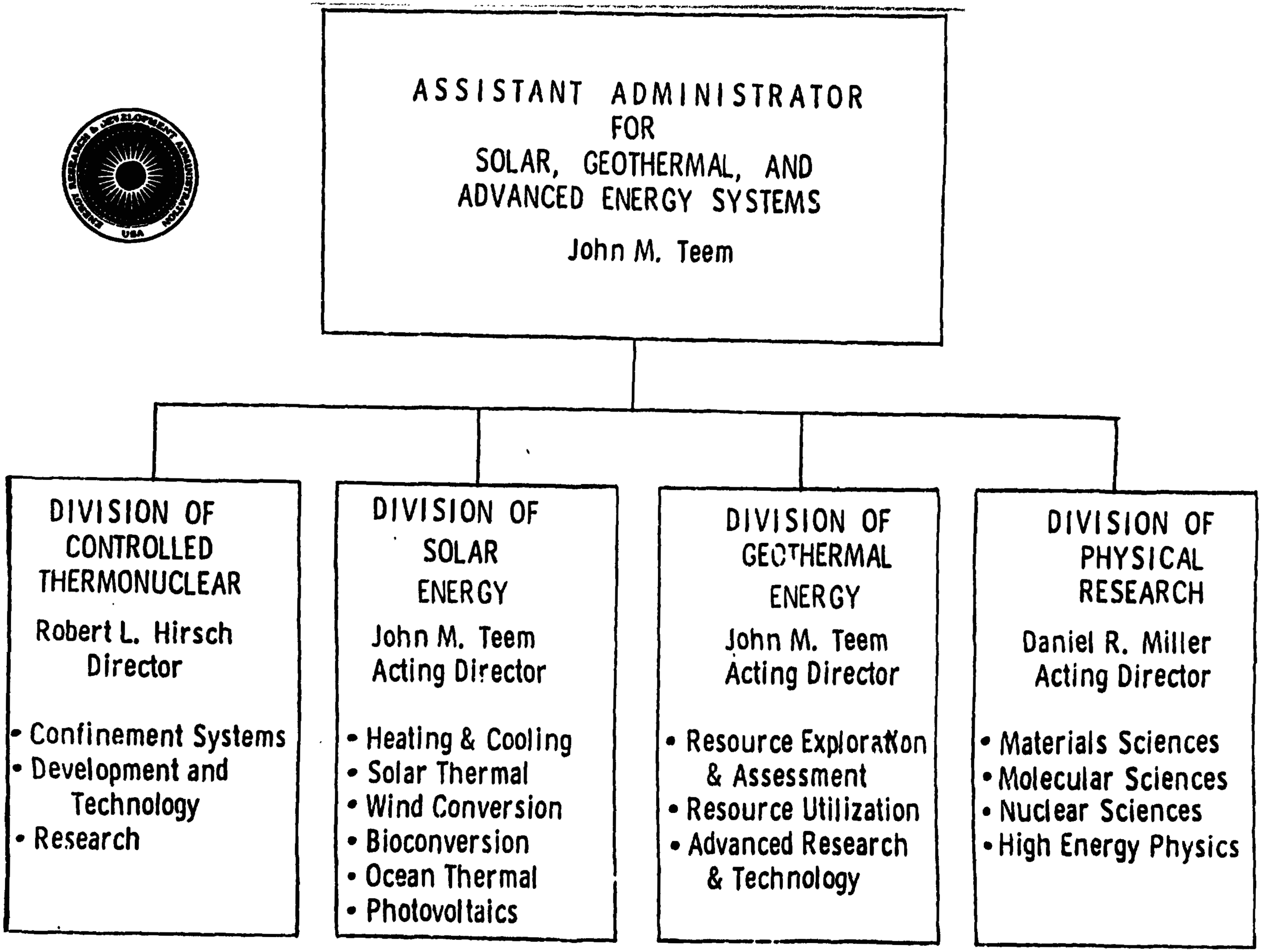

ASSISTANT ADMINISTRATOR
FOR
SOLAR, GEOTHERMAL, AND
ADVANCED ENERGY SYSTEMS
John M. Teem

DIVISION OF
CONTROLLED
THERMONUCLEAR
Robert L. Hirsch
Director

- Confinement Systems
- Development and Technology
- Research

DIVISION OF
SOLAR
ENERGY
John M. Teem
Acting Director

- Heating & Cooling
- Solar Thermal
- Wind Conversion
- Bioconversion
- Ocean Thermal
- Photovoltaics

DIVISION OF
GEOTHERMAL
ENERGY
John M. Teem
Acting Director

- Resource Exploration & Assessment
- Resource Utilization
- Advanced Research & Technology

DIVISION OF
PHYSICAL
RESEARCH
Daniel R. Miller
Acting Director

- Materials Sciences
- Molecular Sciences
- Nuclear Sciences
- High Energy Physics

FIG. 2

DIVISION OF SOLAR ENERGY

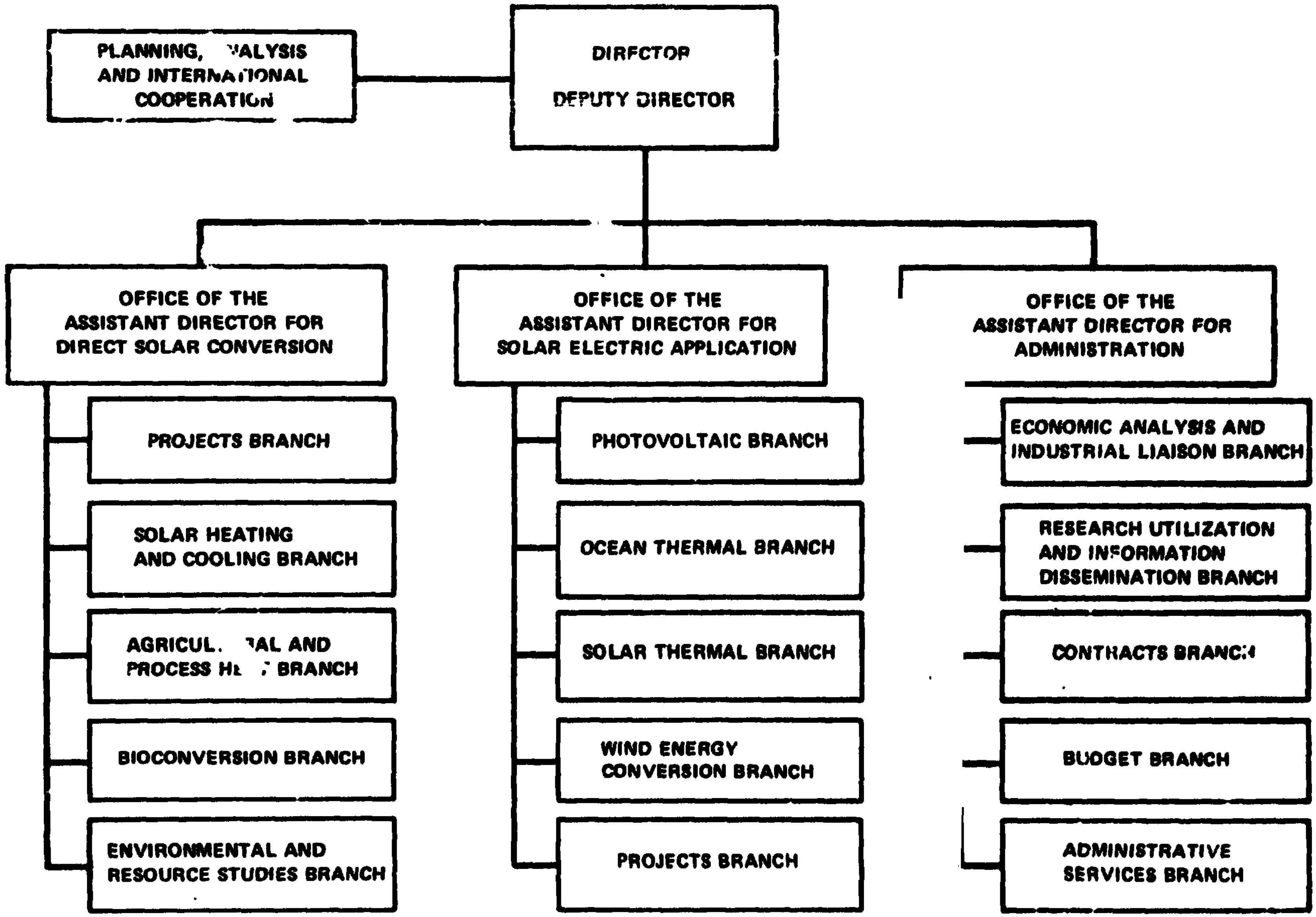

FIG. 3

OBJECTIVES OF THE PROGRAM

The general objective of the ERDA Photovoltaic Conversion Program is to develop low-cost reliable Solar Photovoltaic Conversion Systems (SPCS) and to stimulate the creation of a viable industrial and commercial capability to produce and distribute these systems for widespread use in residential and commercial applications. A program has been developed to achieve the following specific objectives:

- Conduct research, development and demonstrations to show a factor of ten reduction in solar array prices and to establish the viability of this technology in the latter half of this decade.
- Conduct a focused research and development effort on advanced technologies for photovoltaic devices that show a potential reduction in solar array prices of one hundred or greater.
- Conduct systems and applications studies to identify suitable demonstrations of cost-effective photovoltaic energy conversion systems.
- Conduct experimental system tests and demonstrations of photovoltaic power systems for a variety of residential, commercial and industrial applications.
- Conduct demonstrations to establisn the viability of advanced technologies in the first half of the next decade.

PROGRAM STRUCTURE

The structure of the ERDA Photovoltaic Conversion Program designed to implement these objectives is shown in Figures 4 and 5.

The principal programmatic emphasis will be placed initially on the research, development, and demonstration of low-cost reliable silicon arrays. This will be guided and supported by systems and applications studies that will develop the conceptual design and analysis of a variety of system applications with emphasis on the efficiencies, reliabilities and lifetimes required for viable photovoltaic electric power systems. Initial assessments of the markets for photovoltaic applications will also be developed.

UNITED STATES
ENERGY RESEARCH AND DEVELOPMENT ADMINISTRATION

NATIONAL PHOTOVOLTAIC CONVERSION PROGRAM

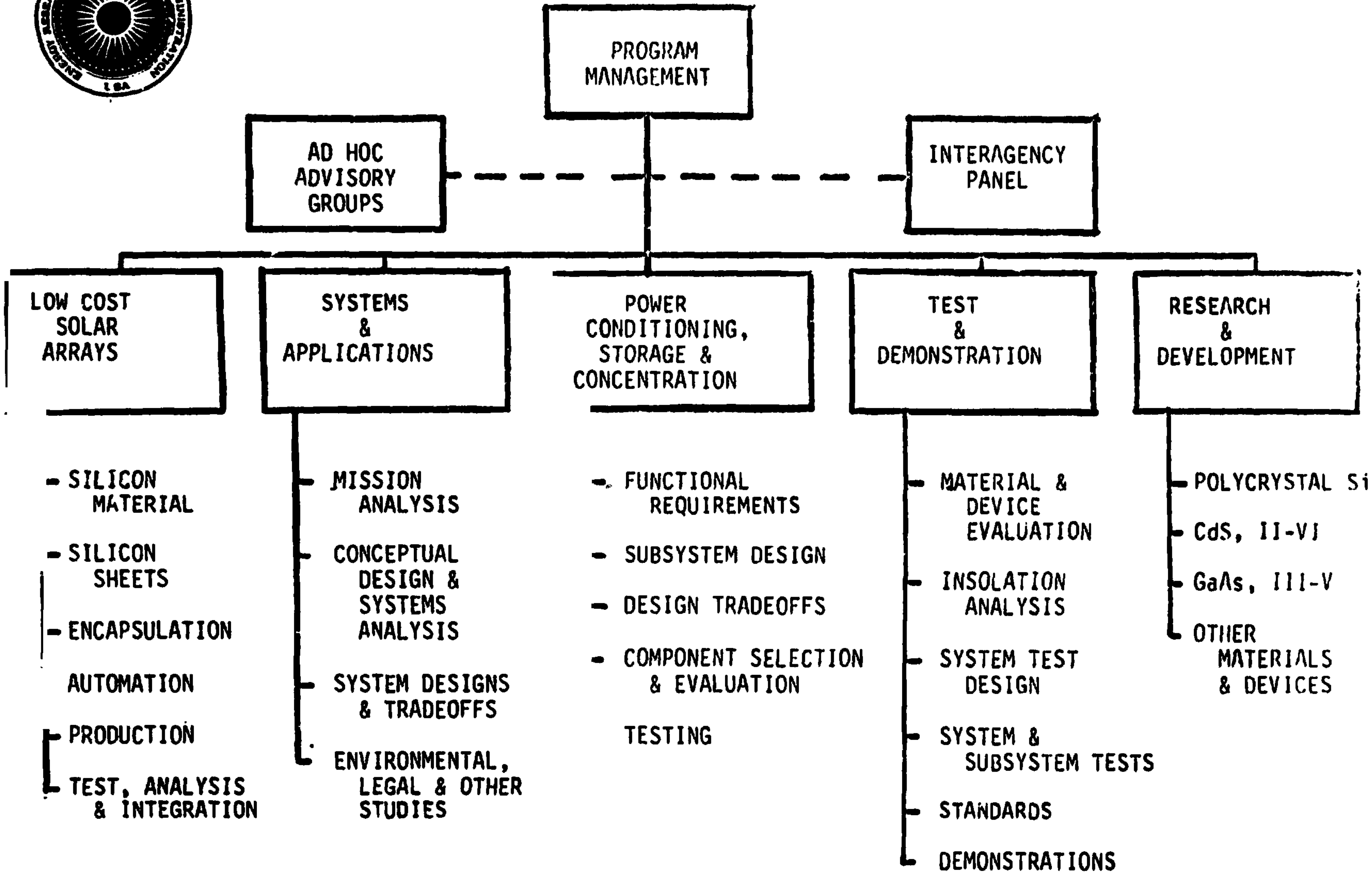

FIG. 4

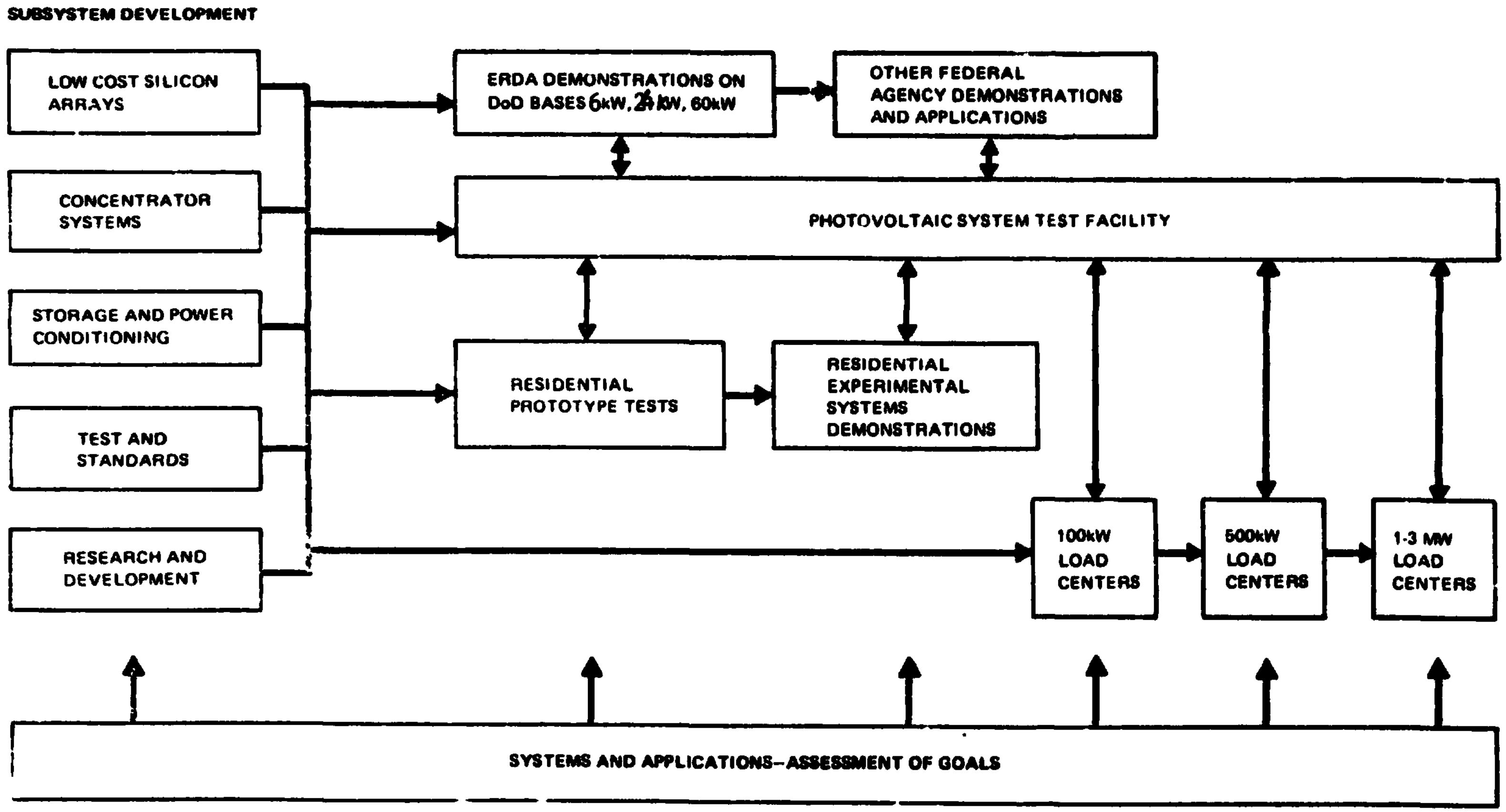

Fig. 5. Photovoltaic energy conversion-structure

The research and development element of the program is aimed at improving overall SPCS performance and utility through a variety of studies on: new methods of single crystal and thin-film growth; development of alternate low-cost solar-cell materials and techniques; methods for improving basic cell efficiencies; improved cell encapsulation for longer lifetimes; and improved high-volume, automated material and cell fabrication techniques.

The power conditioning and storage element of the program will identify specific requirements for solar cells when used in electric power systems, particularly with respect to the need for storage to compensate for the day-night solar cycle and effects that transient conditions such as cloud cover and bad weather imposed on storage systems. In addition, this area must also analyze the constraints imposed upon the system design by utility-grid interfacing problems including the conversion of low voltage DC output to AC.

Studies on the use of optical concentrators to reduce the costs of photovoltaic power systems by reducing the number or size of solar cells required to provide a specific electrical power output is another element of the program.

The testing and evaluation of solar cell materials and devices, the collection and dissemination of insolation data at sites throughout the country and the establishment of standards for solar cell performance, reliability and lifetimes are included in the test and standards element of the program.

Finally, the structure and content of the SPCS program will be guided by continuing mission analysis studies aimed at evaluating alternative applications for photovoltaic systems and their major subsystems, identifying the most promising ones and establishing the pertinent cost and performance goals. System design and analysis studies will be conducted concurrently and will lead to conceptual designs for photovoltaic systems in several size ranges and to the identification and resolution of critical subsystem interface problems. A series of studies to determine possible economic, environmental, social, or legal impacts (and associated constraints) resulting from large-scale deployment of photovoltaic power systems will also be undertaken.

PROGRAM PLAN

A program plan that addresses the technical and institutional problems of SPCS is presented in the ten-year planning milestones shown in Figure 6. This plan consists of the milestone schedules for seven major programs elements: Systems and Applications, Low-Cost Silicon Arrays, Concentrator Systems, Test and Standards, Research and Development, Storage and Power Conditioning, and Assessment of Goals.

Primary emphasis is expected to be placed through the mid 1980's on tasks to improve technical design efficiency, reliability, lifetimes and energy payback times of photovoltaic solar arrays through silicon technology development. Particular stress will be placed on: production of low cost silicon materials; array encapsulation materials and techniques; improved cell and environmentally-satisfactory array design; and high-volume, cost-effective automated array assembly techniques. By FY 83 it is expected that a pilot plant will be established with the capability for producing in excess of 5 million square meters per year of silicon sheet to be sold at less than $18 per square meter. By FY 84, it may be possible to establish an industrial facility with the capability for producing approximately 2000 metric tons per year of silicon material at a market price of less than $10 per kilogram. By FY 85 a total plant capacity should be established capable of producing in excess of 500 MWe peak per year of encapsulated solar array modules at a market price of less than $500 per peak KWe.

In FY 76 a series of Federally-sponsored tests and demonstrations of a wide variety of applications of solar photovoltaic conversion systems will be initiated. More specifically:

- Several DOD applications of solar photovoltaic conversion systems will begin in 1976 to establish the technical feasibility of their use at remote DOD bases.
- Initial ERDA residential system tests will begin in 1978.
- Large-scale ERDA demonstration systems totaling up to 10 MWe (peak) will begin in the early 1980's.

Test and evaluation of energy storage and power processing systems will be conducted throughout this time period. A standards laboratory will be established to perform exposure and life tests on arrays and materials, and establish failure mechanism and accelerated endurance tests. Studies will be conducted to resolve questions of ownership and liability of experimental system demonstration equipment, and modifications of labor practices, building codes and architectural design guides needed to accommodate photovoltaic systems. Technology transfer will be accomplished through conferences, workshops, press releases, manuals, and technical and trade publications. Local industry and small business participation will be encouraged in this demonstration phase.

PLANNING MILESTONES FOR SOLAR PHOTOVOLTAIC CONVERSION PROGRAM

FY	75	76	77	78	79	80	81	82	83	84	85
1. SYSTEMS & APPLICAT. ENG. & ANALYSIS			Prel. Design Spec.		Detail Design Spec.						
DEMONSTRATIONS		45kW	170kW	285kW	600kW	1MW	2MW	4MW	7MW	10MW	
2. LOW-COST SILICON ARRAYS TECH. DEVELOPMENT					$5000/kW Estab.	$500/kW Feas. Demo.		$2000/kW Estab.		$1000/kW Estab.	$500/kW Estab.
LARGE-SCALE PROD.		170kW Delv.	150kW Delv.	270kW Delv.	500kW Delv.	1MW Delv.	2MW Delv.	3MW Delv.	4MW Delv.		
3. CONCENTRATOR SYSTEMS				$5000/kW Estab.		$2000/kW Estab.		$1000/kW Estab.			$250/kW Estab.
4. TEST & STANDARDS		Test Fac. Oper.			Solar Cell Perf. Spec.						
5. RESEARCH & DEVELOP.						10% Eff. Thin-Film Demo.				$100 to	$300/kW Thin Film Feas. Demo.
6. STORAGE & POWER COND.			Eval. Tasks Init.	Prelim. Subsyst. Tests	Cand. Subsys. Selected		Dev. & Proto-Test Comp.		Hardware Devlpd.		
7. ASSMT. OF GOALS						Plant Ownership Deter.					

Fig. 6.

During the FY 76 to FY 79 period, research and development will be conducted to determine storage and power conditioning interface requirements. The performance, reliability, and cost of current storage and power conditioning subsystems will be evaluated and new designs will be specifically engineered for photovoltaic applications. Subsystem and interface engineering and tests necessary to adapt storage and power conditioning subsystems to solar photovoltaic applications will be completed by the early 80's, as will studies needed to determine environmental, legal and safety impacts of storage and power conditioning subsystems and methods of removing or alleviating these impacts.

Figure 7 indicates the planned growth in the rate of production of solar photovoltaic conversion systems in terms of the expected peak power of SPC systems produced annually. This includes expected ERDA purchases through 1983; the expected rate of the free market without Federal government purchases; the total expected Federal government purchases, including SPC systems purchased by other agencies of the Federal government for cost-effective applications, and the total annual expected production rate in the United States to meet both Federal purchases and the non-government market demands for solar photovoltaic conversion systems.

Study and experimental tasks will be undertaken between FY 76 and FY 84 to examine technology limitations and design and cost tradeoffs of concentrator systems in the areas of cell and array efficiency, concentrator ratios, methods of concentration, cooling techniques and tracking techniques. Studies and experimental tasks will be completed by FY 80 to examine processes for manufacturing concentrator systems and to establish requirements for incorporating these techniques into array assembly processes. This effort will be paralleled by feasibility, cost-effectiveness and marketability studies to determine whether to manufacture concentrator systems. To accelerate the cost reduction of concentrator systems and provide hardware for demonstrations of solar photovoltaic power systems using concentrators, several large Federal procurements of low-cost concentrator systems will be considered during the course of this effort.

By 1980, advanced cell concepts will have been examined emphasizing studies of design limitations and cost tradeoffs for thin film technology. Studies will also be conducted to examine tradeoffs with respect to design, conversion efficiency, reliability, lifetimes, utilization of natural resources, energy payback times and the overall economics of advanced techniques and systems for the purpose of selecting viable new candidate devices

PHOTOVOLTAICS PRODUCTION GOALS

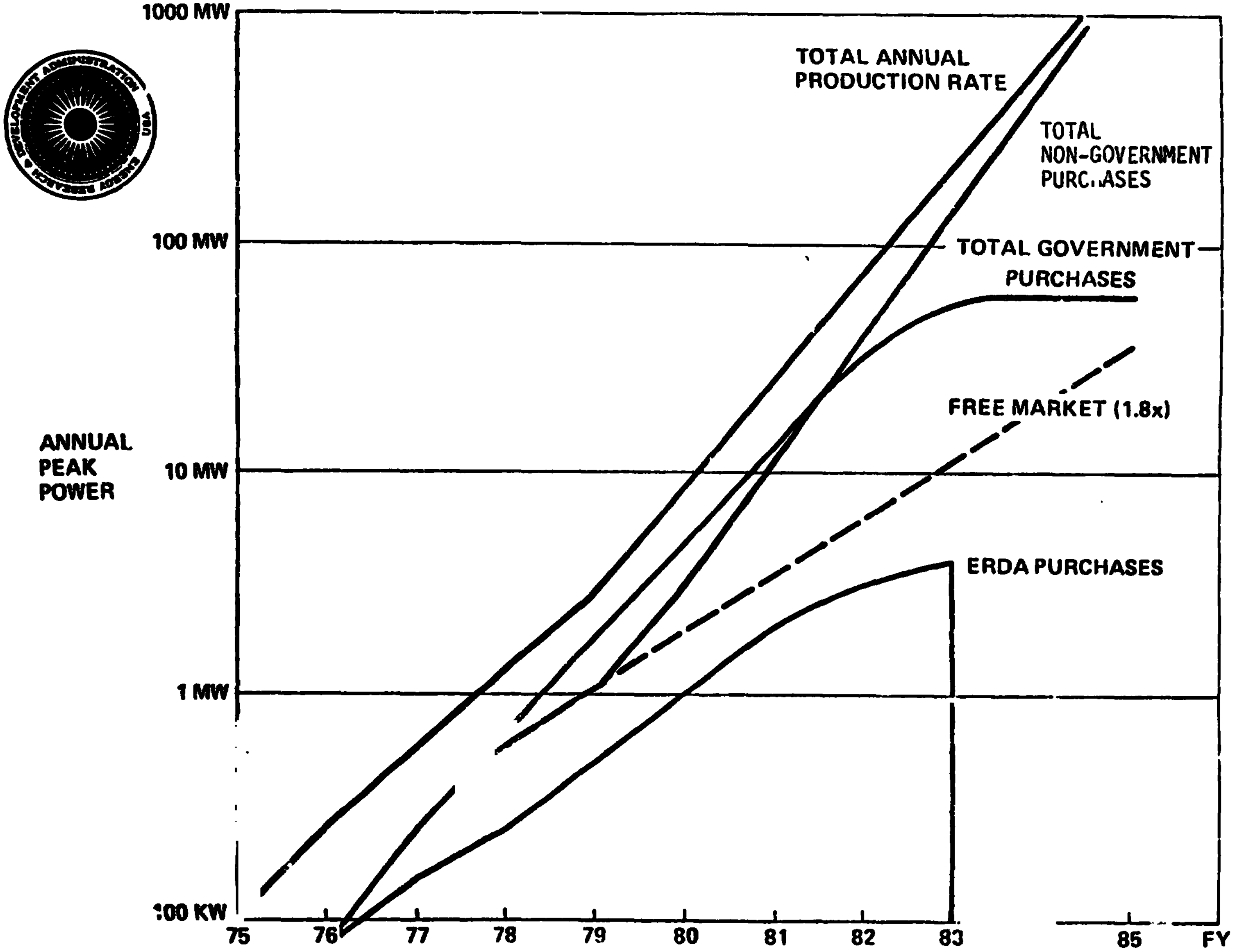

FIG. 7

MAJOR MILESTONES AND DECISION POINTS

Major planning milestones of the SPCS program are:

- FY 1976, identify the most promising applications of SPCS for military use, and initiate DOD tests of these systems to establish their technical feasibility.
- FY 1976, specify interim measurement techniques for tests and standards and have photovoltaic test facility operational.
- FY 1977, complete preliminary photovoltaic system design specification and define solar cell performance specifications.
- FY 1978, initiate residential experimental systems demonstrations and operate $5000/peak KWe concentrator systems.
- FY 1979, specify post-1985 systems and subsystems, demonstrate operational solar arrays at $5000/peak KWe.
- FY 1980, demonstrate operational concentrators at $2000/peak KWe, the feasibility of manufacturing and marketing solar arrays at a price of $500/peak KWe, and 10% efficiency for thin-film solar cells.
- By 1985, promote the establishment of total installed industrial production plant capacity of 500 MWe/yr of silicon solar arrays at a market price of less than $500/peak KWe and demonstrate the feasibility of thin-film solar arrays priced at $100 to $300 per peak KWe.

UTILIZATION PLAN

The Federal role in the plan for utilization of SPC systems will be to undertake, coordinate and direct RD&D to improve performance-to-cost ratios, reduce techno-economic risks and uncertainties, verify the estimated operational characteristics of solar electric systems, and establish their economic viability. Early large-scale demonstrations will be undertaken to enhance public and user acceptance and accelerate industrial implementation of solar photovoltaic systems. A series of studies will be conducted to determine possible environmental, legal, societal, or institutional impacts, as well as means for removing these types of constraints on public and user acceptability. Studies will be conducted to address questions of ownership of commercial manufacturing facilities and operational power plants. Related programs of other Federal agencies include: 1) studies of the basic characteristics of materials and novel devices for photovoltaic energy conversion (NSF); 2) establishment of high efficiency silicon solar arrays for space applications and studies of satellite solar power systems (NASA); and 3) studies of market conditions and the use of Federal and local incentives (such as tax reductions) to induce solar cell development and use (FEA).

Various types of information and data on SPC systems will be compiled and entered into the Solar Energy Information Data Bank, including:

- Reports, Journal articles, dissertations, monographs, project descriptions, and other written materials pertaining to research, development and applications of solar photovoltaic conversion systems;
- Technical information on the design, construction, and maintenance of solar photovoltaic conversion systems;
- General information on solar photovoltaic conversion system applications disseminated to the public;
- Physical and chemical properties and possible environmental impacts of materials required for solar photovoltaic conversion systems activities and equipment; and
- Engineering performance data on equipment and devices utilizing solar photovoltaic energy conversion.

The data will also be supplied by ERDA as appropriate, to Federal, State and local government organizations, and their contractors; universities, colleges and not-for-profit organizations, and the private sector, including the public, industry, commercial organizations, etc.

Finally, I wish to both congratulate and thank Bob F [illegible] s staff at JPL, our meeting organizer, for putting together such an [illegible] meeting.

NSF/RANN - SOLAR PHOTOVOLTAIC CONVERSION PROGRAM

OBJECTIVES

- CONDUCT FOCUSSED RESEARCH OF ADVANCED TECHNOLOGIES FOR SOLAR CELLS THAT SHOW A POTENTIAL REDUCTION IN ARRAY COST TO 30-10¢/WATT
- CONDUCT RESEARCH ON LONG-RANGE APPLICATIONS OF DIRECT SOLAR ELECTRIC CONVERSION AND STORAGE
- SUPPORT NATIONAL SOLAR ENERGY PROGRAM BY PROVIDING TECHNOLOGY BASE NECESSARY FOR DEMONSTRATION PROJECTS

JULY 22, 1975

NSF/RANN - SOLAR PHOTOVOLTAIC CONVERSION PROGRAM

STRATEGY

* RESEARCH ON PROJECTS APPROACHING DECISION POINT FOR TRANSFER TO ERDA
* EMPHASIS ON RESEARCH IN ADVANCED AND INNOVATIVE TECHNOLOGY
* RESEARCH ON NEW MATERIALS, METHODS AND NOVEL DEVICES OTHER THAN THOSE BASED ON SILICON SINGLE CRYSTAL SOLAR CELL ARRAYS

JULY 22, 1975

NSF/RANN - SOLAR PHOTOVOLTAIC CONVERSION PROGRAM

MANAGEMENT

* COORDINATION WITH ERDA PROJECTS
* REVIEW PRIORITIES ON THE BASIS OF NATIONAL PROGRAM MILESTONES
* WORK WILL BE PERFORMED PRIMARILY BY UNIVERSITIES AND NOT-FOR-PROFIT ORGANIZATIONS
* INDUSTRIAL FIRMS WILL BE USED WHEN SPECIAL CAPABILITIES ARE REQUIRED
* PROCUREMENT VIA UNSOLICITED PROPOSALS

JULY 22, 1975

UTILIZATION

- ERDA, PRINCIPAL USER
- NATIONAL PHOTOVOLTAIC PROGRAM REVIEW MEETING (GRANTEES AND CONTRACTORS)
- SEMINARS, WORKSHOPS
- PUBLICATION OF REPORTS

NSF/RANN - SOLAR PHOTOVOLTAIC CONVERSION PROGRAM

PROGRAM STRUCTURE

- CdS/Cu_2S THIN FILM SOLAR CELLS
- Cu_xS AND Cu_2S/M SYSTEM
- LARGE AREA POLYCRYSTALLINE Si THIN FILM SOLAR CELLS
- GALLIUM ARSENIDE AND III-V SEMICONDUCTORS
- CADMIUM TELLURIDE AND II-VI SEMICONDUCTORS

JULY22, 1975

NSF/RANN - SOLAR PHOTOVOLTAIC CONVERSION PROGRAM

PROGRAM STRUCTURE

- Cu_2O/Cu SOLAR CELLS
- $CuInS_2$ AND TERNARY THIN FILM CELLS
- CERAMIC AND SEMICONDUCTOR OXIDE CELLS
- ORGANIC POLYMER FILMS AND REDOX CELLS

JULY 22, 1975

NATIONAL SCIENCE FOUNDATION

SOLAR PHOTOVOLTAIC CONVERSION PROGRAM

Program Manager - Tapan Mukherjee

The National Science Foundation Photovoltaic Conversion Program focusses on advanced and innovative technologies necessary to meet the long-range goals of the National Solar Energy Program. The principal objective of NSF/RANN program is to provide the technology base for low-cost thin film solar cells that will meet ERDA milestone of achieving 10-30¢/watt array cost. The planning philosophy is to investigate high risk and potentially high pay-off concepts. Research will be carried out to the demonstration stage and then the projects will be transferred to ERDA to be included in the national plan of demonstration and implementation. The dynamics of this planning philosophy provides continuous opportunity for incorporation of novel ideas and new thrusts as resources become available after ERDA transfer. The Program Unit Concept was developed from the common characteristics of the projects retained by the National Science Foundation after the transfer of major components to ERDA. In general, these projects seek specific alternatives to silicon single crystal solar cell arrays and are oriented to the study of materials and prototype devices.

SESSION I

PHOTOVOLTAIC SYSTEMS

FEA PLANS FOR FEDERAL INCENTIVES AND MARKET EVALUATION

(Norman Lutkefeder)

FEDERAL LAWS COVERING SOLAR ENERGY

- FEDERAL ENERGY ADMINISTRATION ACT (PL 93-275) MAY 7, 1974
- HOUSING AND COMMUNITY DEVELOPMENT ACT (PL 93-383) AUGUST 22, 1974
- SOLAR HEATING AND COOLING DEMONSTRATION ACT (PL 93-409) SEPTEMBER 3, 1974
- ENERGY REORGANIZATION ACT (PL 93-438) OCTOBER 11, 1974
- SOLAR ENERGY R,D&D ACT (PL 93-473) OCTOBER 26, 1974
- FEDERAL NONNUCLEAR ENERGY R&D ACT (PL 93-577) DECEMBER 31, 1974

FEDERAL ENERGY ADMINISTRATION

- SOLAR ENERGY -

ROLE

- CONDUCT BROAD-BASED ANALYSES REGARDING DIRECTION AND SCOPE OF SOLAR RELATED ENDEAVORS FROM AN OVERALL ENERGY DEVELOPMENT/CONSERVATION VIEWPOINT
- DEVELOP, IMPLEMENT AND COORDINATE PROGRAMS AND POLICIES TO FACILITATE THE WIDESPREAD APPLICATION AND ACCELERATED UTILIZATION OF PROVEN SOLAR TECHNOLOGIES

FEDERAL ENERGY ADMINISTRATION
- SOLAR ENERGY -

COMMERCIALIZATION EFFORT IS

- CONCURRENT, NOT JUST SEQUENTIAL TO RESEARCH, DEVELOPMENT & DEMONSTRATION
- PREDICATED ON TWO MAJOR ASSUMPTIONS
    1. A REASONABLY SUCCESSFUL R, D&D PROGRAM
    2. WITHOUT AGGRESSIVE FEDERAL PROGRAM TO COMMERCIALIZE SOLAR ENERGY TECHNOLOGIES, THE SIGNIFICANT PIB PROJECTIONS FOR ENERGY SAVINGS WILL NOT BE REALIZED

FEDERAL ENERGY ADMINISTRATION

- SOLAR ENERGY -

PROGRAM AREAS

- IDENTIFY AND, WHERE APPROPRIATE, REMOVE ECONOMIC, INSTITUTIONAL, AND LEGAL BARRIERS TO WIDESPREAD COMMERCIAL APPLICATION
- STIMULATE MARKET DEMAND
- DEVELOP INDUSTRY CAPABILITY
- PERFORM TRADE-OFF STUDIES TO ASSURE SOLAR ENERGY DEVELOPMENT PROGRAMS ARE PROPERLY INTERWOVEN WITH:
  - OTHER ENERGY DEVELOPMENT ENDEAVORS
  - ENERGY CONSERVATION PROGRAMS

ORIGINAL PAGE IS
OF POOR QUALITY

FEDERAL ENERGY ADMINISTRATION

- SOLAR ENERGY -

PROJECTS CURRENTLY BEING ADDRESSED

- ASSESS FOREIGN MARKETS FOR U.S. SOLAR PRODUCTS--WITH DOC/BIC
- DEVELOP EARLY MARKET FOR SOLAR ELECTRIC SYSTEMS (PHOTOVOLTAIC AND WIND CONVERSION) VIA DOD'S ENERGY SELF-SUFFICIENCY PROGRAM FOR REMOTE MILITARY FORCES--WITH DOD & ERDA
- DEVELOP COMPREHENSIVE PROGRAM DEFINITION REQUIRED UNDER P.L. 93-473--WITH ERDA & OTHERS
- DETERMINE IMPACT OF VARIOUS INCENTIVES AND, IF APPROPRIATE, DEVELOP MODEL LEGISLATION AND/OR CONTRIBUTE TO CURRENT CONGRESSIONAL INITIATIVES--WITH OTHERS
- ACCELERATE DEVELOPMENT OF "DEFINITIVE" PERFORMANCE CRITERIA AND INDUSTRY STANDARDS TO ASSURE THAT PUBLIC IS PROVIDED WITH QUALITY PRODUCTS--WITH ERDA, HUD, NBS, DOD & OTHERS
- ACCELERATE USE OF SOLAR HEATING AND COOLING SYSTEMS IN GOVERNMENT BUILDINGS--WITH ERDA, DOD, GSA & OTHERS

SOLAR ENERGY

U.S. SENATE PROPOSED BILLS - 1975

NUMBER	SPONSOR	COMMITTEE	DATE ENTERED	PURPOSE
S 28	MOSS	FINANCE	JAN. 15	TAX INCENTIVE
S 168	DOMENICI	FINANCE	JAN. 16	TAX INCENTIVE
S 311	McCLURE	FINANCE	JAN. 21	PROMOTE R&D
S 489	ABOUREZK	JUDICIARY	JAN. 29	ANTI-TRUST
S 875	HART	BANKING, HOUSING & URBAN AFFAIRS	FEB. 27	LOW-INTEREST LOANS
S 1112	GRAVEL	FINANCE	MAR. 7	ENERGY TRUST FUND (R,D&D)
S 622 (AMEND)	FANNIN	INTERIOR & INSULAR AFFAIRS	APR. 7	LOW INTEREST LOANS & LOAN GUARANTEES
S 973	BENSTEN	FINANCE	MAR. 6	PROMOTE R&D
S 1379	FANNIN	FINANCE	APR. 8	TAX INCENTIVES

SOLAR ENERGY
U.S. HOUSE OF REPRESENTATIVES
PROPOSED BILLS - 1975

NUMBER	SPONSOR	COMMITTEE	DATE ENTERED	PURPOSE
HR 36	TEAGUE	SCIENCE & TECH.	JAN. 14	ENERGY CONSERVATION R&D CORPORATION
HR 1505	VANIK	WAYS & MEANS	JAN. 15	TAX INCENTIVE
HR 1697	McCLORY	WAYS & MEANS	JAN. 20	TAX INCENTIVE
HR 2873	CONTE	JUDICIARY	FEB. 5	ANTI-TRUST
HR 3849	GUDE	BANKING, CURRENCY & HOUSING	FEB. 27	LOW-INTEREST LOANS RESIDENTIAL BLDGS.
HR 4407	HARRINGTON	JUDICIARY	MAR. 6	ANTI-TRUST
HR 5959	WYLIE	WAYS & MEANS	APR. 15	TAX INCENTIVE
HR 6584	GUDE	WAYS & MEANS	MAY 1	TAX CREDIT/AMORTIZATION NON-RESIDENTIAL BLDGS.
HR 6860	ULLMAN	WAYS & MEANS	MAY 9	TAX INCENTIVE

MISSION ANALYSIS OF PHOTOVOLTAIC SOLAR ENERGY SYSTEMS

Stanley L. Leonard, The Aerospace Corporation

The overall objectives of The Aerospace Corporation's photovoltaic mission analysis program have been a) to develop procedures for the technical and economic evaluation of terrestrial applications (missions) for the photovoltaic conversion of solar energy and b) to use these procedures to identify the missions most likely to find a significant place in the U. S. energy marketplace in the 1980-2000 period. The greatest emphasis in the study is being placed on two main classes of missions: on-site applications, in which the photovoltaic system serves the electric power demand of a load-point that is co-located with the system, and central station power plant applications. Fuel production applications and a variety of special-purpose missions are also being studied, albeit at a considerably lower level of effort.

Much of the effort during the early part of the reporting period was devoted to the development of the computer software needed in the methodology for evaluating on-site missions. The procedure employs computer simulation to determine performance characteristics. These results are then used, along with a model for the operation of a complete utility system, to determine the amount of back-up energy that the utility grid must provide and the amount of additional generation capacity that is needed in order to maintain reliable service. The economic evaluation of the mission then requires the comparison of the total cost of the energy provided to the on-site load-points in two different situations, one in which photovoltaic systems satisfy most of the demand and one in which the entire load is served directly by the utility grid. This procedure treats the economics of the mission essentially from the utility point of view. The costs associated with the distribution of back-up power are thereby included implicitly.

The evaluation methodology for on-site missions have been used in analyzing a representative base-line mission/system concept in some detail and in assessing the sensitivity of the result to variations in mission or system characteristics. The baseline concept is a residential photovoltaic system located in Phoenix. The analysis presumes the existence of a substantial number of such systems within the service area of an electric utility system; the demand served by photovoltaic systems amounts to about 0.6% of the total system demand. It was found that the use of such residential on-site systems can be expected to become economically competitive in 1990 if photovoltaic array costs can be reduced to about $100 per peak kW.

The sensitivity analyses have included studies of the effect on performance of variations in array size, in storage capacity, in geographical location (seven different sites), and in types of demand (residential, commercial, or industrial). Both flat-plate and Winston collectors have been investigated and a comparison has been made between performance of collectors with fixed orientation and collectors whose tilt is adjusted monthly. In addition, a brief study was made of the sensitivity of the economic evaluation to variations in photovoltaic conversion efficiency, in the costs of essential subsystems, and in the cost of fuel for competing power sources.

A second major effort, begun late in the reporting period, has been devoted to implementing procedures for evaluating central station power plant applications. This task consists largely in adapting procedures that were developed in an earlier Aerospace Corporation analysis of missions for solar-thermal energy conversion. At the close of the reporting period, this adaptation process is essentially complete and preliminary runs are being made. An improved model for dispatching the output of a solar energy plant is also being developed; it will be incorporated into the methodology when complete.

A start has also been made on the development of evaluation procedures for fuel production (e.g., electrolytic hydrogen) missions. Central to this evaluation will be the cost of competitive fuel (or of hydrogen produced in other ways), and a study of the projected (1980-2000) costs of such fuels is under way.

During the remainder of the grant period (two months), representative central station power plant missions will be evaluated. The improved dispatch routine will be incorporated into the methodology, as will procedures for evaluating the combined effect of the use of three solar plants, each located at a different site. The study of projected fuel costs will be completed and used in an assessment of the competitive position of electrolytic hydrogen produced with power from photovoltaic arrays.

A proposal for a follow-on study has been submitted to ERDA. It calls for an extension in both breadth and depth of the mission analysis effort and for the provision of direct program support to the ERDA photovoltaic conversion program office. The proposed funding for the Mission Analysis portion of the study is approximately $400K, while that for the Program Support segment is $62K, for a total of $462K.

The Aerospace Corporation

Mission Analysis of Photovoltaic Solar Energy Systems

CONTRACTING AGENCY:
NATIONAL SCIENCE FOUNDATION
RESEARCH APPLIED TO NATIONAL NEEDS

GRANT NUMBER:	GI-44099
PERIOD OF GRANT:	15 MONTHS [1 June 1974-31 August 1975]
AMOUNT OF GRANT:	$233,900
PRINCIPAL INVESTIGATOR:	DR. A. B. GREENBERG

STUDY OBJECTIVES AND SCOPE

DEVELOP PROCEDURES FOR EVALUATING CANDIDATE PHOTOVOLTAIC SYSTEMS AS APPLIED IN ALTERNATIVE MISSIONS

ASSESS ALTERNATIVE MISSIONS FOR PHOTOVOLTAIC SYSTEMS AND IDENTIFY THOSE OF GREATEST POTENTIAL

- FOUR SPECIFIC MISSION CLASSES
  - ON-SITE (supplemental) POWER
  - CENTRAL STATION POWER
  - FUEL/FEEDSTOCK PRODUCTION
  - SPECIAL PURPOSE APPLICATIONS
- GEOGRAPHICAL AREA - SOUTHWESTERN U.S.
- TIME PERIOD - 1980-2000

ESTABLISH TECHNICAL AND ECONOMIC GOALS FOR SYSTEM, SUBSYSTEM, AND COMPONENT DESIGN AND PERFORMANCE

DETERMINE THE MARKET CAPTURE POTENTIAL AND IMPACT ON RESOURCES OF THE PREFERRED PHOTOVOLTAIC CONVERSION MISSION(S)

Planned Activity: 1 January-30 June, 1975

- CONTINUE EVOLUTIONARY DEVELOPMENT OF SYSTEM SIMULATION SUBROUTINES
- FINISH EVALUATION OF ON-SITE MISSIONS
  - USE SYSTEM-SIMULATION MODEL TO EVALUATE PERFORMANCE
  - INVESTIGATE COST/PERFORMANCE TRADEOFFS IN SUBSYSTEM DESIGN
  - CARRY OUT PRELIMINARY COST/PERFORMANCE OPTIMIZATION
  - DETERMINE COST OF DELIVERED ENERGY, COMPARE WITH CONVENTIONAL SYSTEMS
- DEVELOP AND BEGIN APPLICATION OF METHODOLOGY FOR EVALUATING FUEL-PRODUCTION MISSIONS
- BEGIN APPLICATION OF PREVIOUSLY DEVELOPED METHODOLOGY TO EVALUATION OF CENTRAL-STATION POWER PLANTS
- REVIEW EXISTING STUDIES OF SPECIAL-PURPOSE APPLICATIONS
- ASSESS IMPACT ON PHOTOVOLTAIC-SYSTEM DEVELOPMENT OF EXTERNAL ISSUES
  - ENVIRONMENTAL FACTORS
  - DEMANDS ON NATURAL RESOURCES
  - INSTITUTIONAL CONSTRAINTS

Mission Methodology — On - Site

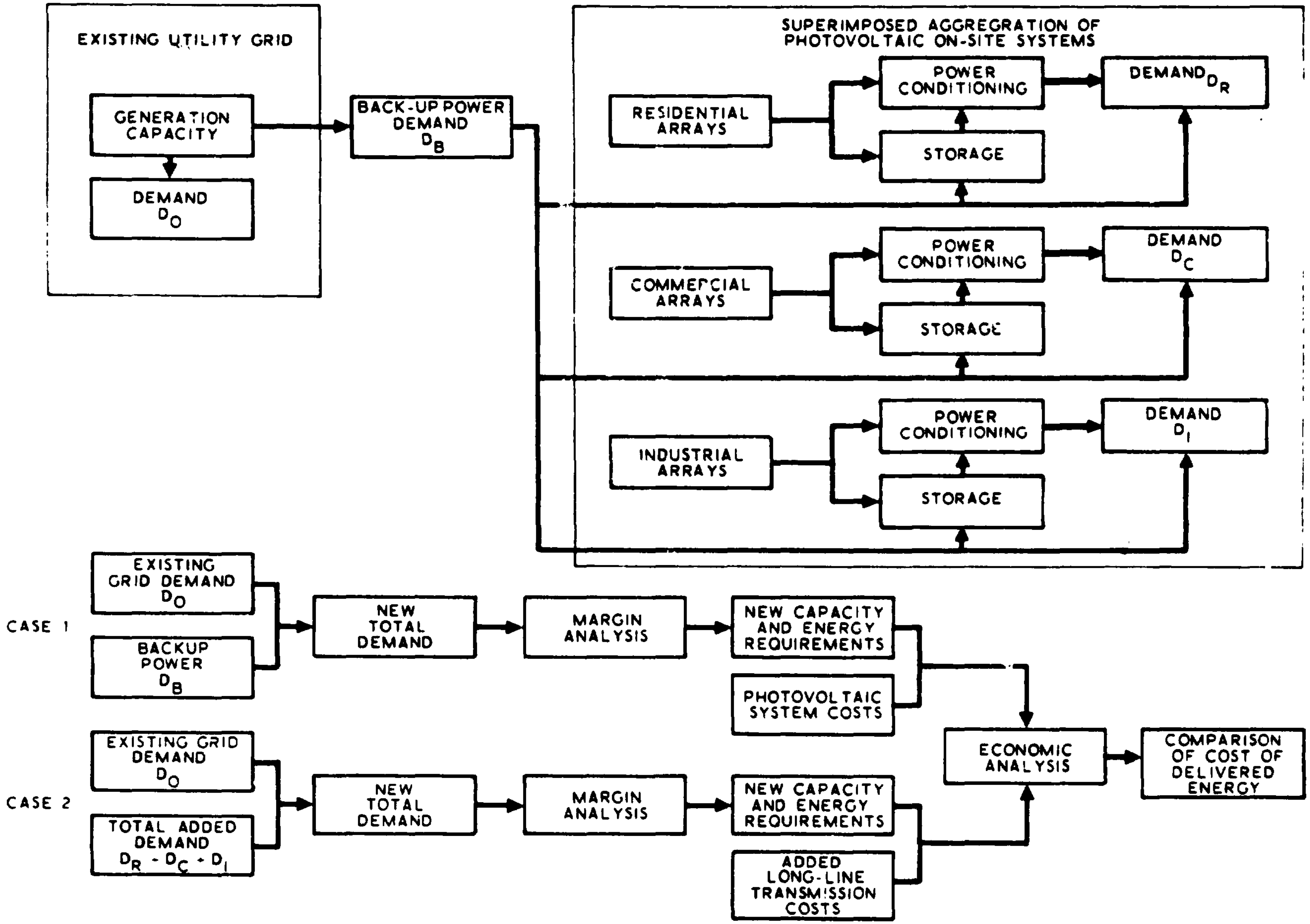

Residential Photovoltaic System in Phoenix

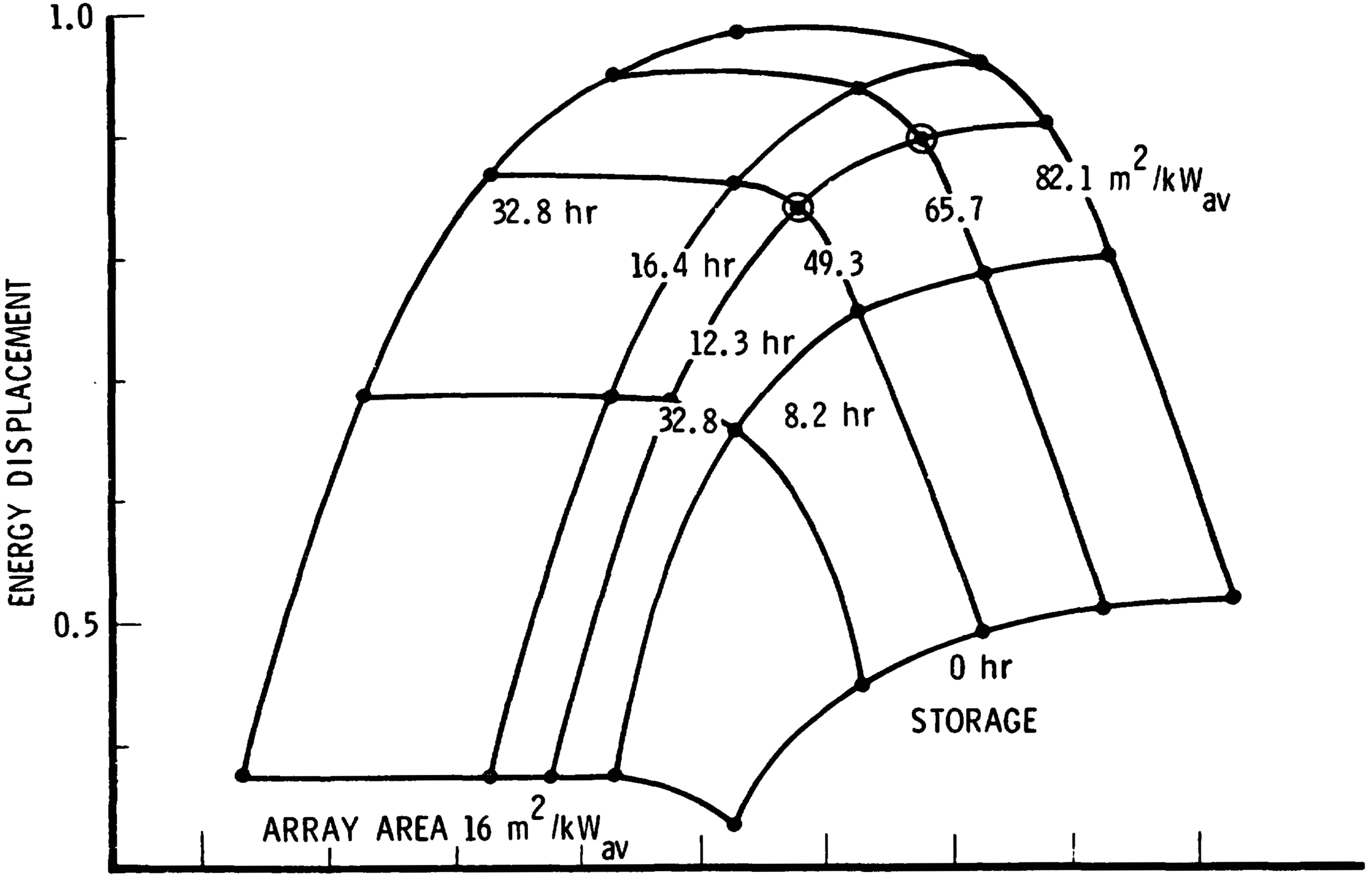

Required Additional Conventional Generation Capacity

CASE	MULTIPLYING FACTOR	ARRAY AREA (m^2/kW_{av})	STORAGE CAPACITY (hr)	FORECASTING	REQUIRED NEW CAPACITY (MW)
PHOENIX INSOLATION SYNTHETIC RESIDENTIAL DEMAND TILT ADJUSTED MONTHLY	1	49.3	12.3	NO	4.0
		49.3	12.3	YES	0.019
		65.7	12.3	NO	1.8
		65.7	12.3	YES	0
		0	0	-	190.0
	10	49.3	12.3	NO	150.0
		49.3	12.3	YES	4.7
		65.7	12.3	NO	58.0
		65.7	12.3	YES	0
		0	0	-	2169.0

Cost of Meeting New Residential Demand

1990 PRESENT VALUE IN MILLIONS OF 1990 DOLLARS

	AVERAGE NEW DEMAND 121.8 MW	 1218 MW
CONVENTIONAL ALTERNATIVE		
• CAPITAL COST (coal plant at $[illegible]/KW)	116.7	1331.8
• OPERATING COSTS		
FUEL (coal at 4.54 mills/KW_h)	84.9	849.0
O&M (coal plant, $15.97/$KW_{av}$)	36.8	368.0
• TRANSMISSION (100 miles at $450/MW-mile)	8.6	97.6
TOTAL	247.0	2646.4
PHOTOVOLTAIC		
(array area = $6(10^6)m^2$, storage = $1.5(10^6)KW_h$)		
• CAPITAL COST		
STORAGE (at $20/$KW_h$)	30.0	300.0
POWER CONDITIONING ($35/KW)	10.3	103.0
ELECTRICAL WIRING ($7/KW)	4.5	45.0
ARRAY/SUPPORT STRUCTURES ($X/$m^2$)	6X	6X
• PHOTOVOLTAIC O&M (2 mills/KW_h)	35.0	350.0
• BACKUP ENERGY		
FUEL (coal at 4.54 mills/KW_h)	14.0	140.0
O&M (coal plant, $15.97/KW.	6.0	60.0
• BACKUP CAPACITY (coal p[illegible] .4/KW)	2.5	92.0
TOTAL	102.3 + 6X	10[illegible]0.0 + 6X

Allowed Array Costs

CASES	AVERAGE DEMAND 121.8 MW				AVERAGE DEMAND 1218 MW			
	ARRAY PLUS SUPPORT		ARRAY ALONE (support at $15/m2)		ARRAY PLUS SUPPORT		ARRAY ALONE (support at $15/m2)	
	$/ m^2	$/ kW_{pk}	$/ m^2	$/ kW_{pk}	$/ m^2	$/ kW_{pk}	$/ m^2	$/ kW_{pk}
NO FORECASTING								
BASELINE CASE	24.12	227.55	9.12	86.04	25.94	244.72	10.94	103.21
$\eta(70^\circ) = 16\%$	38.59	227.00	23.59	138.76	41.50	244.12	26.50	155.88
STORAGE $50/kWh	16.62	156.79	1.62	15.28	18.44	173.96	3.44	32.45
POWER CONDITIONING $100/kW	20.92	197.36	5.92	55.85	22.74	214.53	7.74	73.02
PERFECT FORECASTING								
BASELINE CASE	23.38	220.57	8.38	79.06	26.27	247.83	11.27	106.32
$\eta(70^\circ) = 16\%$	37.41	220.06	22.41	131.82	42.04	247.29	27.04	159.06
STORAGE $50/kWh	15.88	149.81	0.88	8.30	18.77	177.08	3.77	35.57
POWER CONDITIONING $100/kW	20.18	190.38	5.18	48.87	23.07	217.64	8.07	76.13

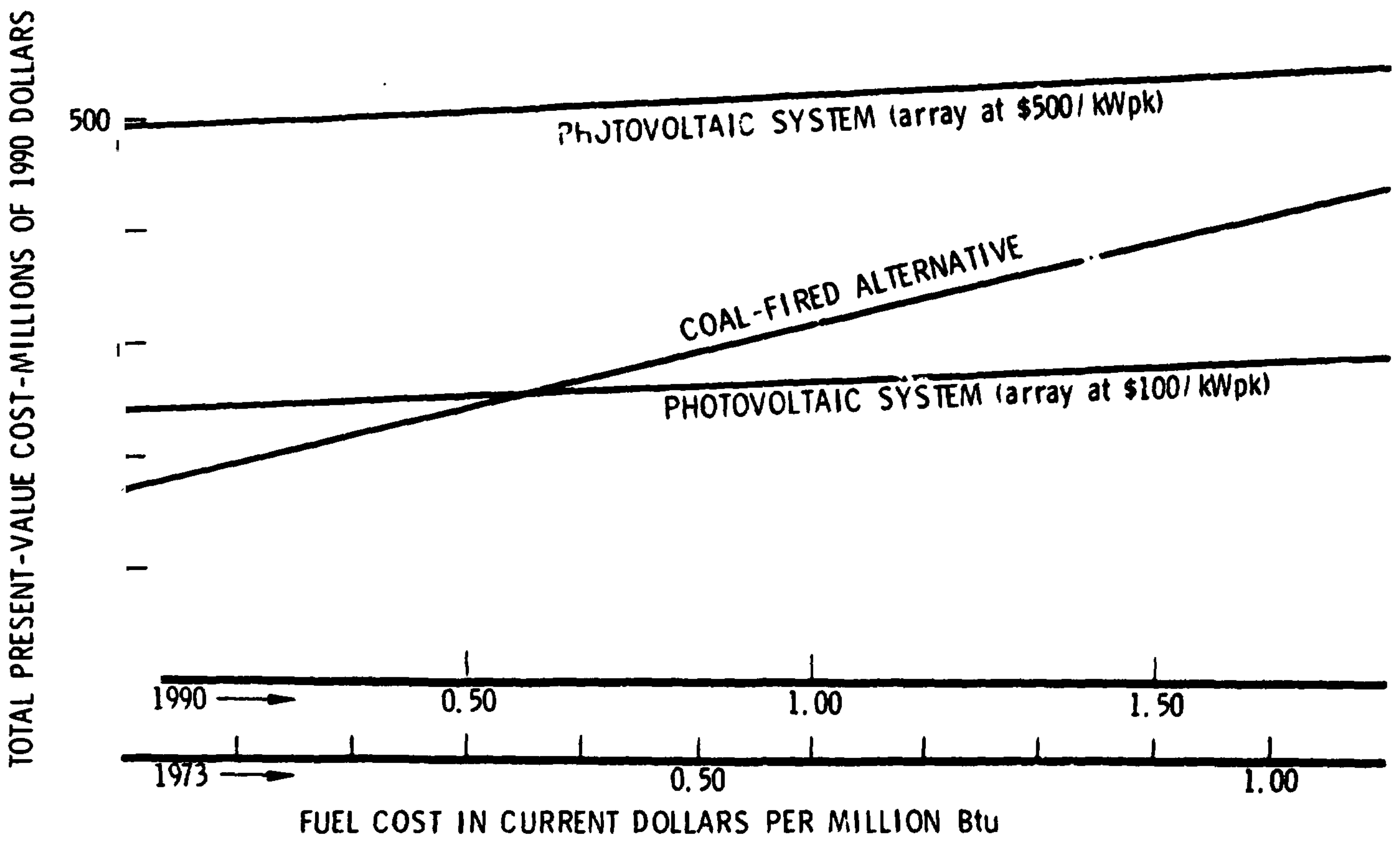
TOTAL PRESENT-VALUE COST-MILLIONS OF 1990 DOLLARS
500
PHOTOVOLTAIC SYSTEM (array at $500/ KWpk)
COAL-FIRED ALTERNATIVE
PHOTOVOLTAIC SYSTEM (array at $100/ KWpk)
1990
0.50
1.00
1.50
1973
0.50
1.00
FUEL COST IN CURRENT DOLLARS PER MILLION Btu

Phoenix Residential System

WINSTON COLLECTOR X = 4

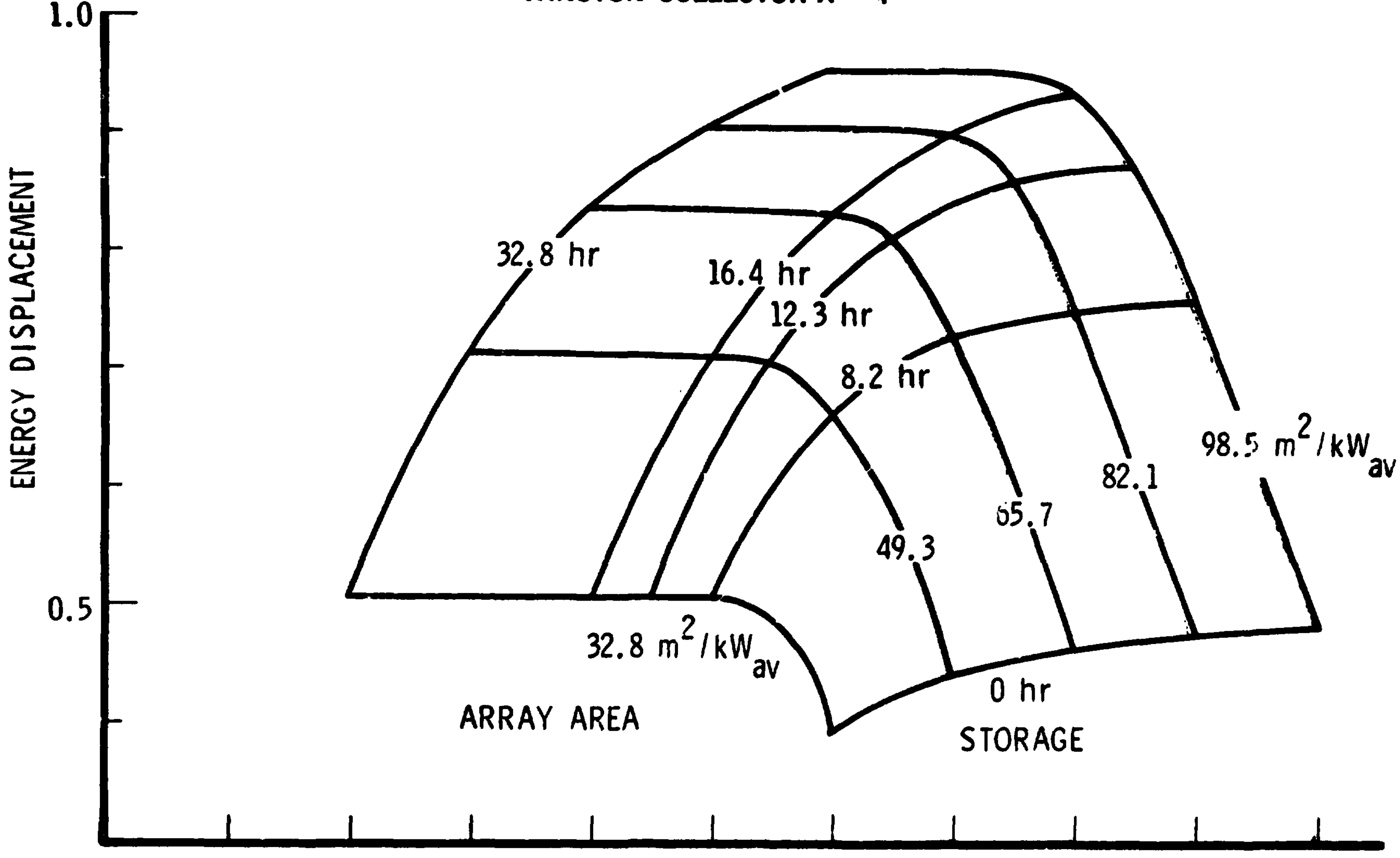

Performance - Flat Plate Collector

FIXED TILT vs ADJUSTABLE TILT

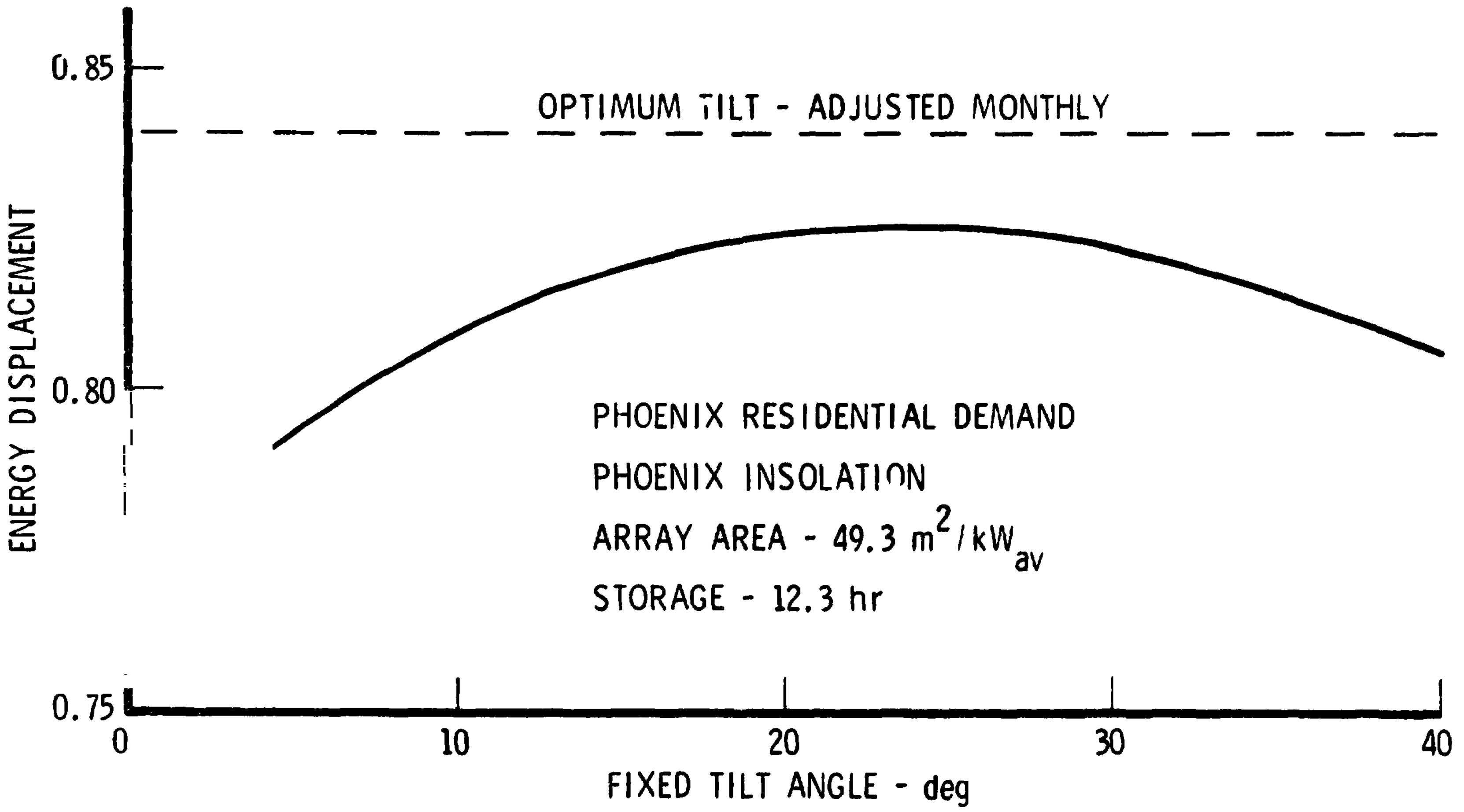

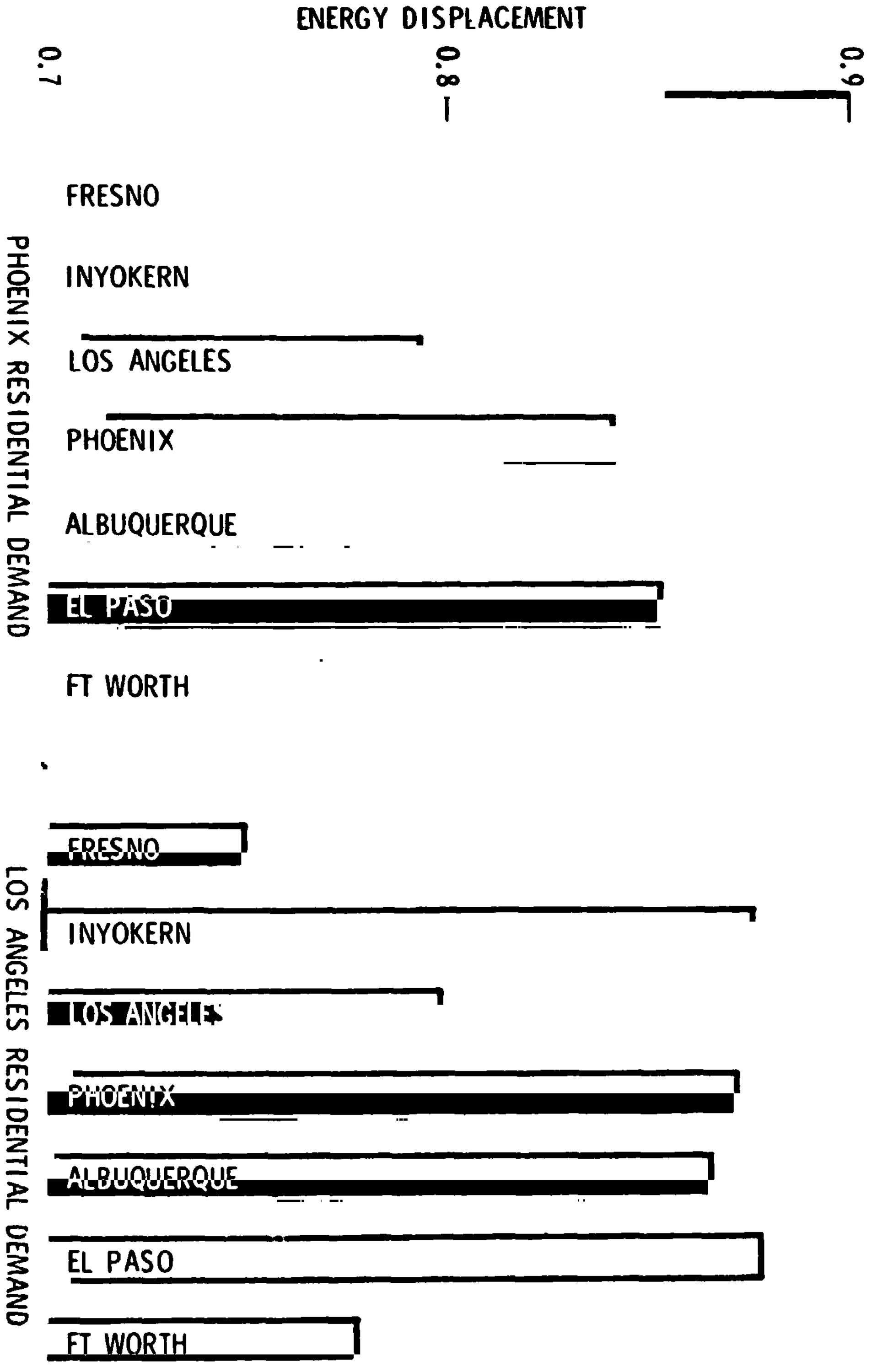
ENERGY DISPLACEMENT
0.7
0.8
0.9
PHOENIX RESIDENTIAL DEMAND
FRESNO
INYOKERN
LOS ANGELES
PHOENIX
ALBUQUERQUE
EL PASO
FT WORTH
LOS ANGELES RESIDENTIAL DEMAND
FRESNO
INYOKERN
LOS ANGELES
PHOENIX
ALBUQUERQUE
EL PASO
FT WORTH

Energy Displacement-On-Site Systems in Phoenix

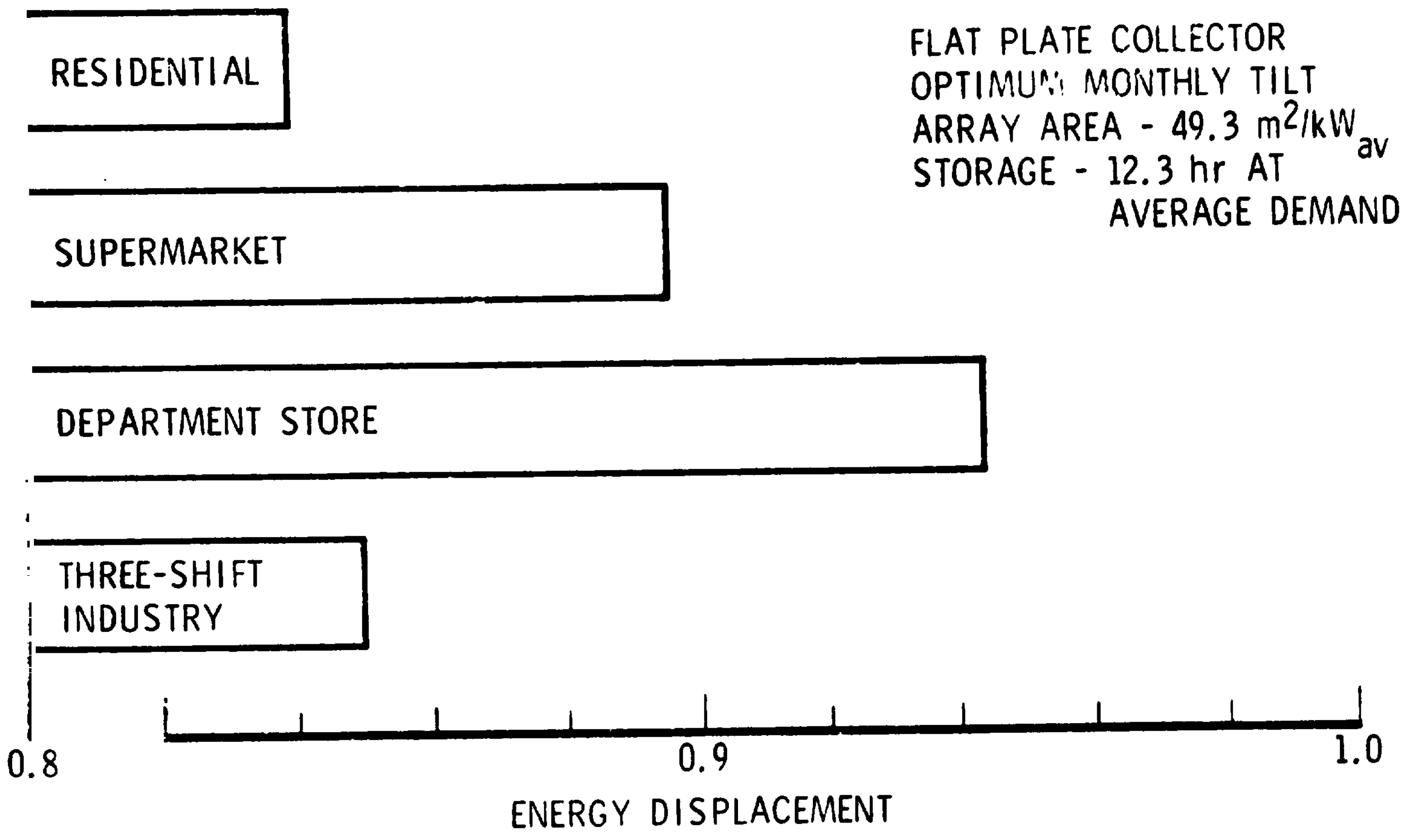

FLAT PLATE COLLECTOR
OPTIMUM MONTHLY TILT
ARRAY AREA - 49.3 m^2/kW_{av}
STORAGE - 12.3 hr AT
AVERAGE DEMAND

Summary of Key Results

1 JAN TO 1 JUL 1975

ON-SITE MISSIONS

- RESIDENTIAL/COMMERCIAL/INDUSTRIAL DEMAND REPRESENTATIONS PREPARED
- SIMULATION MODEL SOFTWARE COMPLETED
- TECHNICAL/ECONOMIC EVALUATION PROCEDURE OPERATIONAL
- ANALYSIS OF REPRESENTATIVE MISSIONS/SYSTEMS
- PERFORMANCE SENSITIVITY STUDIES
  - GEOGRAPHICAL LOCATIONS
  - DEMAND TYPE
  - ARRAY TYPE
  - ARRAY AREA
  - STORAGE CAPACITY
- INITIAL ECONOMIC SENSITIVITY STUDIES
  - FORECASTING vs NO FORECASTING
  - MARKET PENETRATION
  - SUBSYSTEM COSTS

CENTRAL STATION MISSIONS

- SIMULATION MODEL SOFTWARE ADAPTED FROM SOLAR THERMAL CASE
- POWER PLANT ECONOMIC MODEL ADAPTED
- IMPROVED DISPATCH MODEL UNDER DEVELOPMENT
- INITIAL TECHNICAL/ECONOMIC EVALUATION RUNS UNDER WAY

FUEL PRODUCTION MISSIONS

- EVALUATION PROCEDURE ADOPTED
- INVESTIGATION OF PROJECTED COSTS OF COMPETITIVE FUELS UNDER WAY

Planned Activities

1 JUL TO 31 AUG 1975

CENTRAL STATION MISSIONS

- TECHNICAL/ECONOMIC EVALUATION OF REPRESENTATIVE EXAMPLES
  - BASELOAD
  - INTERMEDIATE
  - PEAKING
- IMPLEMENT IMPROVED DISPATCH ROUTINE
- DEVELOP/IMPLEMENT MODEL FOR THREE SOLAR PLANTS AT DIFFERENT SITES

FUEL PRODUCTION MISSIONS

- DETERMINE PROJECTED COST OF HYDROGEN FROM PHOTOVOLTAIC ELECTROLYSIS
- COMPARE WITH PROJECTED COSTS OF COMPETITIVE FUELS

SPECIAL PURPOSE APPLICATIONS

- REVIEW EXISTING STUDIES

Planned Renewal Request

MISSION ANALYSIS AND PROGRAM SUPPORT FOR THE SOLAR PHOTOVOLTAIC CONVERSION PROGRAM

SUGGESTED PERIOD: 1 OCTOBER 1976 - 30 SEPTEMBER 1977

ESTIMATED COST: MISSION ANALYSIS - $400K; PROGRAM SUPPORT - $62K

MAJOR OBJECTIVES:

- MISSION ANALYSIS
  - USE DEVELOPED METHODOLOGY FOR SYSTEMATIC EVALUATION OF ON-SITE ELECTRIC AND CENTRAL STATION APPLICATIONS
  - EXTEND COVERAGE TO THE 48 CONTIGUOUS STATES
  - DEVELOP AND UTILIZE PROCEDURES FOR EVALUATION OF PHOTOVOLTAIC TOTAL ENERGY SYSTEMS
  - DETERMINE TECHNICAL AND ECONOMIC REQUIREMENTS FOR SYSTEMS/SUBSYSTEMS
  - ASSESS SOCIETAL IMPACT OF WIDE-SPREAD USAGE
- PROGRAM SUPPORT
  - ASSIST IN MONITORING ERDA SYSTEMS ANALYSIS CONTRACTS
  - PROVIDE PLANNING ASSISTANCE

STATUS OF THE PHOTOVOLTAIC CONCEPTUAL DESIGN AND SYSTEMS ANALYSIS RFP

Leonard M. Magid
Division of Solar Energy
Energy Research and Development Administration
Washington, D. C. 20545

The National Photovoltaic Conversion Program has recently awarded three contracts totaling slightly more than $1.4M for the first Conceptual Design and Systems Analysis (Phase Zero) studies of solar photovoltaic conversion systems.

The systems to be analyzed, as shown in Figure 1, include:

1. An on-site residential system in the 1 to 10 peak kW demand range.
2. A central station power plant in the 50 to 1,000 MW demand range.
3. An intermediate range application in the 100 kW to 10 MW level.

The awards, each for a 12 month effort starting in June 1975, are to:

General Electric Corp.	-	$472K
Spectrolab, Inc.	-	$413K
Westinghouse Electric Corporation	-	$528K

In addition to the technical evaluations, each study will also provide an assessment of the financial, environmental, legal, institutional and related issues associated with the actual implementation of photovoltaic conversion systems. To accomplish these objectives, the project have formed teams that include engineers, architects, economists, lawyers and representatives from utilities and university research centers, as indicated in Figure 2.

CONCEPTUAL DESIGN AND SYSTEMS ANALYSIS
OF PHOTOVOLTAIC POWER SYSTEMS

SYSTEMS TO BE ANALYZED

1. **ON-SITE RESIDENTIAL**

   1 - 10 kWe PEAK DEMAND

   30 - 100 kWh DAILY DEMAND

2. **CENTRAL STATION POWER PLANT**

   50 - 1000 MWe DEMAND

3. **INTERMEDIATE RANGE SYSTEM**

   100 KWe - 10 MWe DEMAND

FIG. 1

ENERGY RESEARCH & DEVELOPMENT ADMINISTRATION USA

CONCEPTUAL DESIGN AND SYSTEMS ANALYSIS OF PHOTOVOLTAIC POWER SYSTEMS

I. GENERAL ELECTRIC CORP. - $472K

WITH: SHELDAHL CORP.
PENNSYLVANIA POWER AND LIGHT CO.

II. SPECTROLAB, INC. - $413K

WITH: BECHTEL CORP.
FACILITIES SYSTEMS ENGIN. CORP.
MIDWEST RESEARCH INSTITUTE
ARIZONA STATE UNIVERSITY

III. WESTINGHOUSE ELECTRIC CORP. - $528K

WITH: BURT, HILL AND ASSOCIATES
CHARLES RIVER ASSOCIATES
FORD, BACON AND DAVIS
PHILADELPHIA ELECTRIC CO.
TRW
UNIVERSITY OF PENNSYLVANIA

FIG. 2

SESSION II

LOW-COST SILICON SOLAR ARRAYS

N76 12474

LOW-COST SILICON SOLAR ARRAY PROJECT

John V. Goldsmith
Jet Propulsion Laboratory
California Institute of Technology

ABSTRACT

The responsibility to conduct ERDA's Low-cost Silicon Solar Array Project, which is a part of the overall Solar Photovoltaics Program, has been delegated to the California Institute of Technology's Jet Propulsion Laboratory (JPL). An Industry Briefing formally announcing this Project was conducted February 5, 1975. The objectives of the Project include a 1985 goal to reduce silicon solar array prices to less than $500/KW. These low-cost arrays further shall have lifetimes greater than 20 years, conversion efficiencies greater than 10% and a national rate of units manufactured greater than 500MW per year. A Project team, led by Robert Forney, has been organized at JPL. This team is divided presently into five major Task areas: Silicon Material, Large Area Silicon Sheet, Module Encapsulation, Automated Array, and Large Scale Production. The Tasks are all part of one integrated effort dedicated to reaching the Project's 1985 objectives. Specifically, the Silicon Material Task is to concentrate on reducing the basic solar cell quality silicon material price to less than $30/Kg with a goal of less than $10/Kg. The Large Area Silicon Sheet Task is to convert the low-cost material into large areas of silicon with the required properties and dimensional thicknesses that will permit their conversion into high efficiency solar cells. The added price goal of this process is less than $1.60/sq. ft. The Encapsulation Task is to produce low-cost, long-life, greater than 20-year lifetime encapsulation materials and techniques. The Automated Array Task is to convert the sheets of silicon into solar arrays utilizing facilities, designs and processes that will result in the less than $500/KW objective. The Large Scale Production Process Task has as its primary objective the supply of silicon solar array modules to ERDA's Photovoltaic Program Demonstration and System Test and Analysis Projects. Approximately 10 megawatts of these modules are presently planned to be procured from Industry with gradually increasing annual buys over the next eight years. It is anticipated these buys will stimulate the market and assist Industry in developing better modules at lower cost. This Large Scale Production Task will benefit from the technology advancement achieved in the previously described four Tasks and could serve as a practical test of improved designs and production techniques. It is a goal that hardware procured through the Large Scale Production Task will be bought for less than $5 per watt by 1979 and $2 per watt by 1983.

This Low-cost Silicon Solar Array Project is to be a National effort involving the best talents in Industry and Universities. Requests for Proposals in the first four Task areas were solicited during April, and proposals are now under evaluation. A Request for Proposals for the first 40 kilowatts of solar array modules required in the Large Scale Production Task will be released in the near future.

LOW COST SILICON SOLAR ARRAY PROJECT
ORGANIZATION

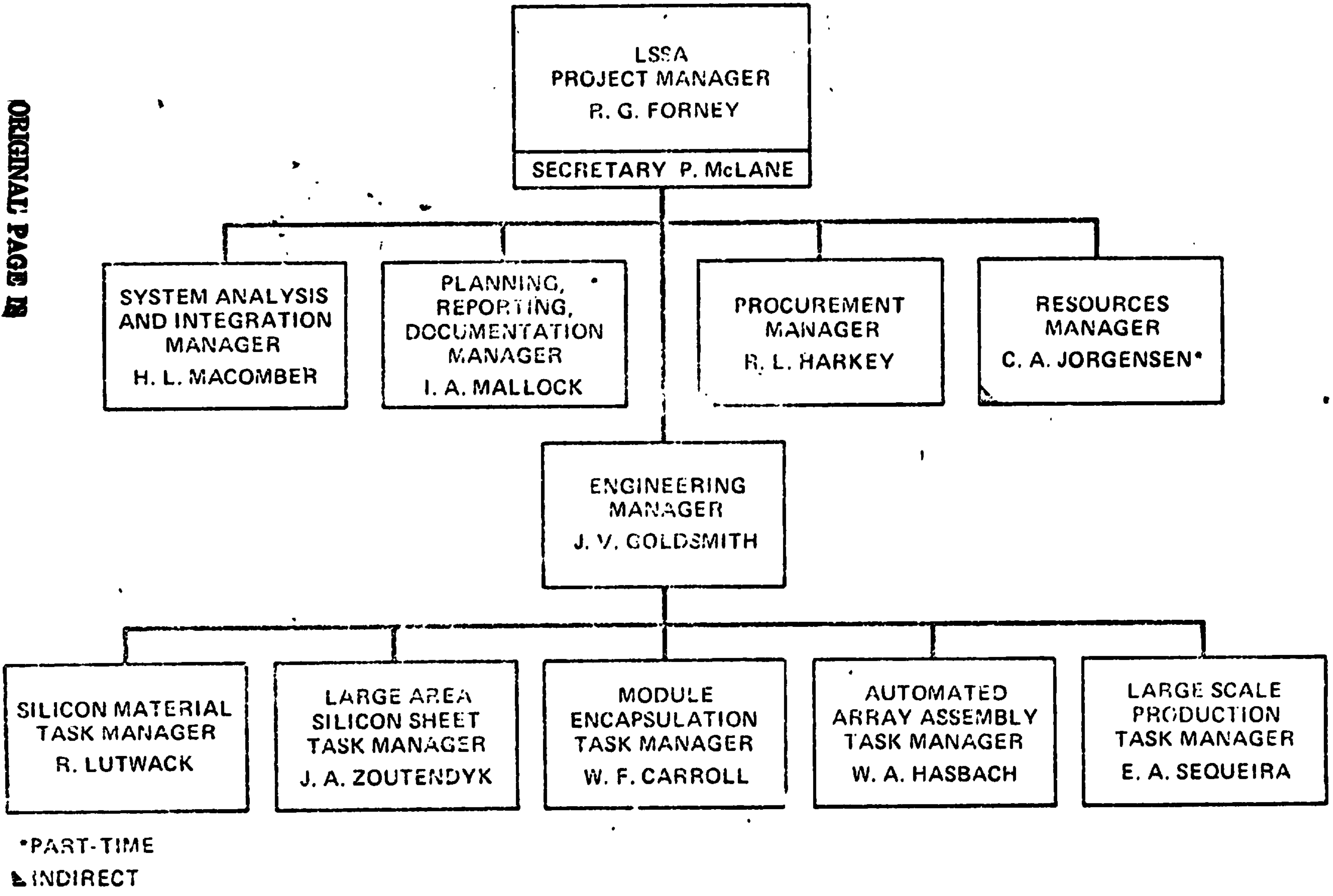

ORIGINAL PAGE IS
OF POOR QUALITY

LOW-COST SILICON SOLAR ARRAY PROJECT

RELATIVE ROLES OF GOVERNMENT AND INDUSTRY

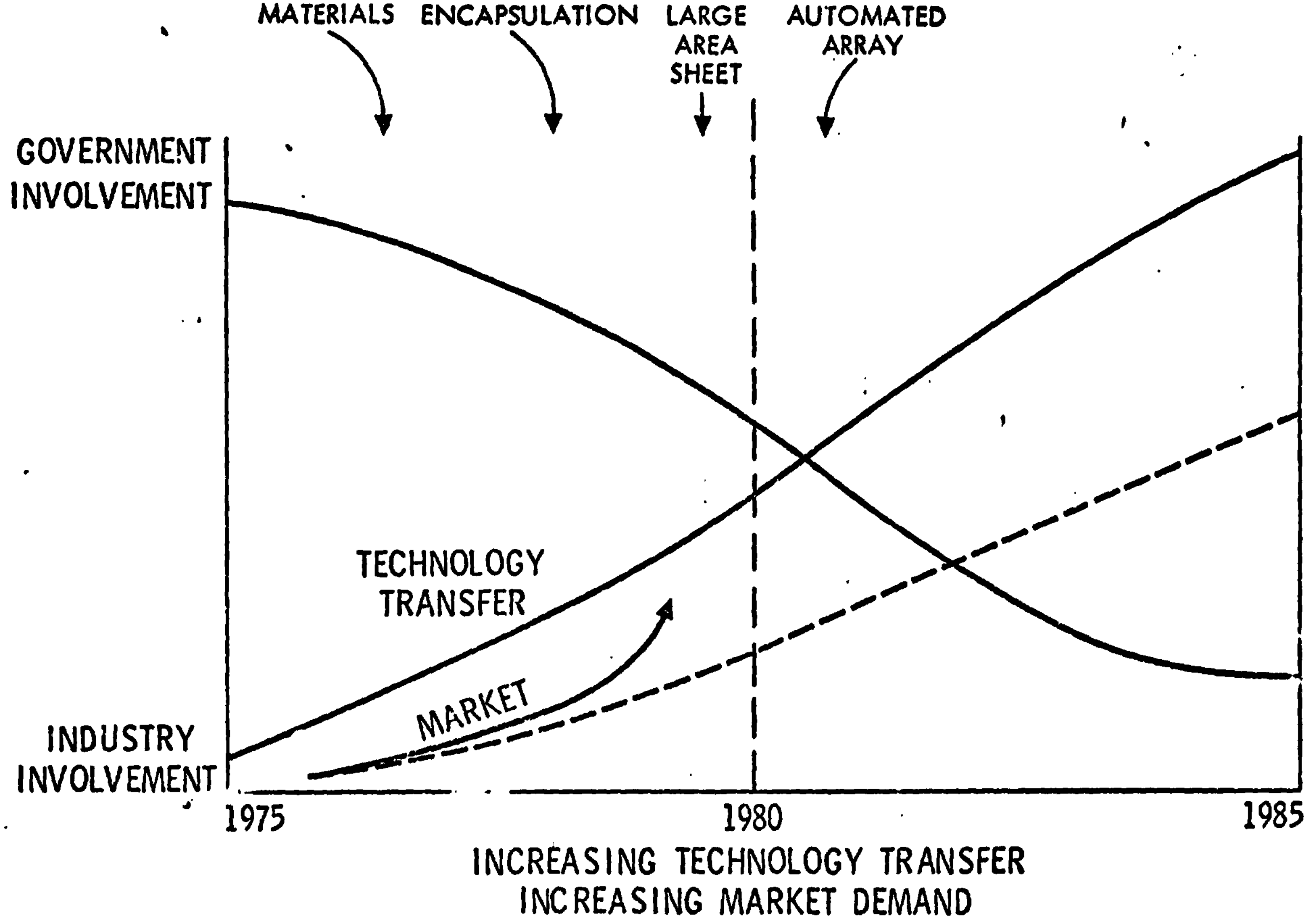

LOW-COST SILICON SOLAR ARRAY PROJECT

1985 PROJECT TECHNICAL REQUIREMENTS

1985 PROJECT TECHNICAL REQUIREMENTS

● EFFICIENCY	> 10% Array
● LIFETIME	> 20 years
● COST	< $500 /KW
● PRODUCTION RATE	> 500 MW/yr

KEY NEEDS:

- LOW COST SOLAR CELL QUALITY SILICON MATERIAL
- LOW COST, HIGH EFFICIENCY SILICON SHEET DEVICES
- LONG LIFE, PRACTICAL SOLAR ARRAY ENCAPSULANTS
- INTEGRATED, VALUE ENGINEERED, AUTOMATED ARRAY FABIRCATION

LOW-COST SILICON·SOLAR·ARRAY PROJECT

SUMMARY IMPROVEMENTS REQUIRED

	1975	1985
SILICON MATERIAL	$ 60 / kg	< $30 / kg
SILICON WAFER	$ 28 / sq ft	< 1.60 / sq ft
ARRAY FABRICATION	$140 / sq ft	< 1.60 / sq ft
	(~ 30,000 / kW)	(< 500 / kW).

LOW COST SILICON SOLAR ARRAY PROJECT
TASK INTERACTIONS

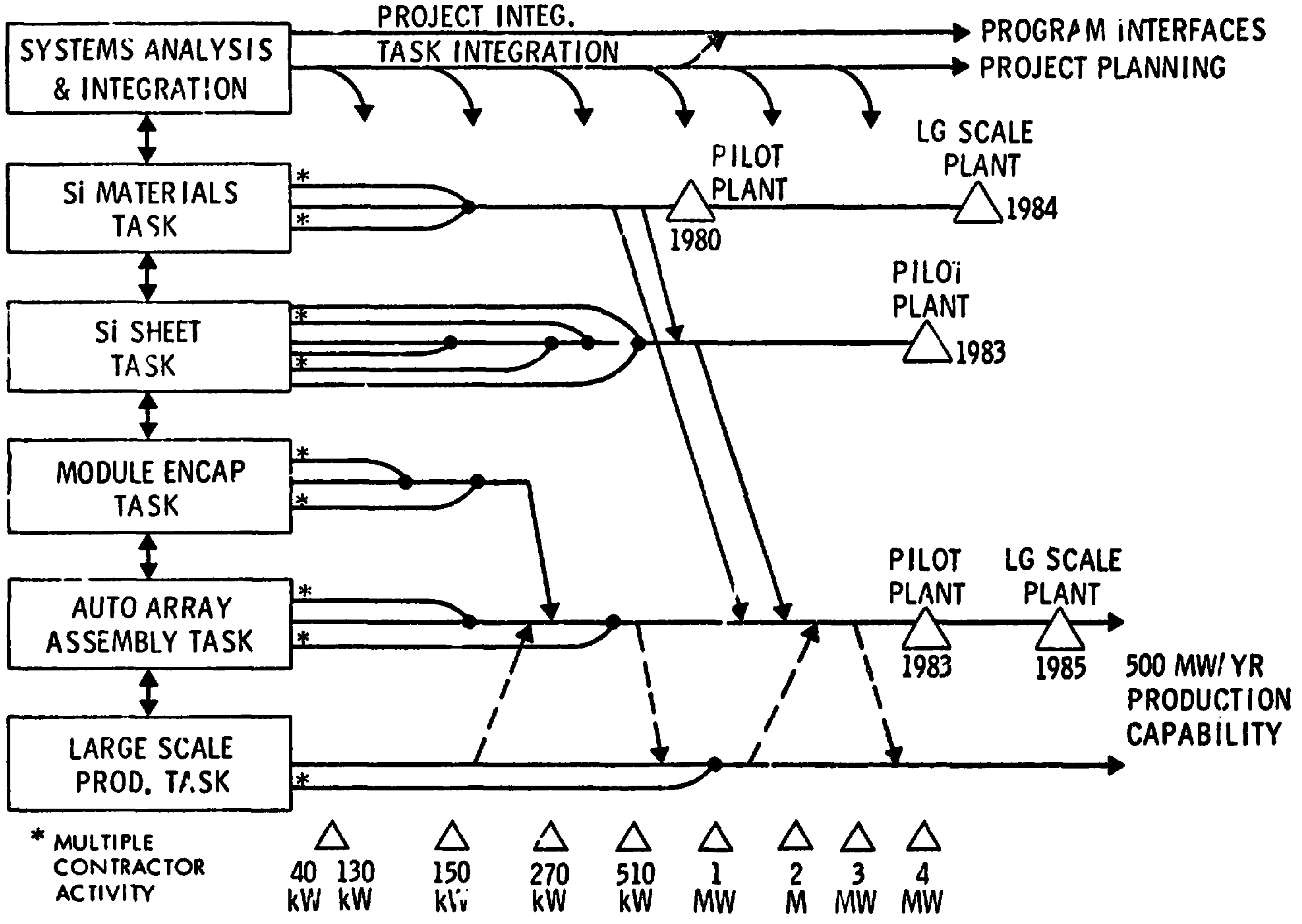

PHOTOVOLTAIC CONVERSION OF SOLAR ENERGY

Contract #W7405-eng-26

OAK RIDGE NATIONAL LABORATORY

March 75 - July 76

$180,000

J. W. Cleland, R. D. Westbrook

H. L. Davis and R. F. Wood

1) Objective

The first and most immediate objective of the photovoltaic conversion work at ORNL is the development of a thorough understanding of and techniques for controlling certain factors which are known to degrade the electrical characteristics of p-n junctions in silicon semiconductor devices. The most important of these factors is the nonuniform distribution of phosphorus which is introduced by conventional doping techniques. As a possible means of circumventing this problem a thorough study of nuclear doping is currently being emphasized. The second objective of the program is the identification and control of point, line and surface imperfections which act as recombination centers to degrade the minority carrier lifetime in both single and polycrystalline silicon, and in other III-V and II-VI semiconductors. A third objective of the program is the identification and study of new solar cell materials and growth methods.

2) Past Activity

This project, though recently initiated, is closely related to other research at ORNL, e.g., the work on ultra-pure germanium, nuclear doping, crystal growth, optical and electrical properties of solids, pure materials research, chemical vapor deposition, electron microscopy, semiconductor device modeling and testing, and organic semiconductors.

3) Current Effort

The first phase of this work is being devoted to the applicability of "nuclear doped" silicon to the silicon solar cell. All methods presently used in the preparation of silicon for semiconductor devices introduce a nonuniform distribution of any chemical dopant. It has been demonstrated that the distribution of phosphorus, the standard n-type dopant, takes the form of striations which intersect and degrade the characteristics of a p-n junction. These striations can be greatly reduced by nuclear doping, in which the ^{30}Si of normally available silicon transmutes to ^{31}P after thermal neutron capture with a half-life of 2.6 hours. Also, no other impurities are introduced by the nuclear doping process in contrast to the possibility of inadvertant contamination of the melt with copper, gold, etc. during normal doping procedures. The performance of high power silicon diodes, thyristors and avalanche detectors is significantly improved for nuclear-doped Si over that for conventionally doped material, and a similar improvement may be attainable in the efficiency of silicon solar cells.

We have irradiated wafers and ingot sections of both single crystal and polycrystalline silicon in various reactor locales with a thermal to epithermal neutron ratio from unity to 2,000, and have introduced 10^{13} to 10^{16} phosphorus cm^{-3}. The times and temperatures required to remove (n,γ) and fast neutron lattice damage are being studied, and electrical property measurements are in use to determine the carrier concentration, mobility, and minority carrier lifetime as a function of the total flux, thermal/epithermal ratio, and annealing requirements. Electron microscope and microscopic spreading resistance measurements are in progress, and test specimens are also being evaluated at other laboratories as regards their performance as avalanche detectors, high voltage power rectifiers and thyristors, ~~and~~ solar cells.

4) Future Plans

After the first stage of the research program is well advanced, and definitive results on the role played by the nonuniform distribution of dopants have been obtained, the emphasis will shift toward studies of electron-hole recombination processes. This part of the program will rely heavily on a close interplay between experimental and theoretical research. Advanced optical techniques and spin-resonance (where applicable) will be used to determine the lattice sites, concentration, energy levels and lifetimes associated with those impurities and point imperfections which introduce deep traps and act as recombination centers. The role played by dislocations, grain boundaries, and surfaces in promoting recombination and thus reducing the minority carrier lifetime will be thoroughly studied by optical, Auger electron, LEED and electron microscopy techniques. The theoretical work will be directed toward a determination of the energy levels, wave functions and lifetimes of electrons and holes at deep traps and in the vicinity of line and surface imperfections. These are particularly important studies because the ultimate success of photovoltaic conversion as an alternative source of energy is likely to depend on the possibility of using polycrystalline, amorphous or highly impure silicon or other materials.

Single crystal ingots of silicon will be grown by float zone refining and Czochralski pulling and a systematic study will be made of the requirements for control of point defects, defect clusters, dislocations, twins, stacking faults and unwanted chemical impurities. Crystals with varying concentrations of those impurities most frequently found in silicon will be grown for use in lifetime studies. Samples of silicon from newer growth processes such as edge-defined, film-fed growth and internal zone growth will be procured and prepared for testing. Studies of growth methods for III-V, II-VI, polycrystalline, amorphous and organic semiconductors will be surveyed. The possible use of Shottky barriers instead of p-n junctions will be explored because such an approach may lead to simplified fabrication procedures and hence reduced costs.

5) Survey of Key Results to Date

The most serious problem that was anticipated with the nuclear doping technique was the removal of radiation damage that is introduced as a consequence of (n,γ) recoils following thermal neutron absorption, and as a consequence of all other damage mechanisms activated by the reactor irradiation. We have now produced phosphorus concentrations in silicon from 10^{13} to 10^{16} cm^{-3} by neutron doping, and in all cases have been able to recover the carrier mobility and a substantial percentage of the carrier lifetime by suitable annealing schedules. We find that generally the mobility returns to normal at lower temperatures than the lifetime, but as the annealing study is incomplete at this time we do not know the upper limit, if any, of lifetime recovery.

DEVELOPMENT OF A 20% EFFICIENT SOLAR CELL

Grant No. GI-43090

15 Months

Initiated 1 June 1974

$119,400

Principal Investigator:
Dr. Joseph Lindmayer
SOLAREX CORPORATION
1335 Piccard Drive
Rockville, Maryland

Presented At
National Solar Photovoltaic Program Review Meeting
Los Angeles, California
July 22-25, 1975

ABSTRACT

The efficiency of silicon solar cells has been increased significantly in the last few years, particularly after the introduction of the violet cell. With the onset of the terrestrial photovoltaic program, it became apparent that techniques should be found for high efficiency inexpensive solar cells. This Grant was given just for such a purpose. The actual work has proceeded along the lines which are basic to inexpensive technologies, such as the use of CZ crystals, chemical surface preparation, short junction formation in quantity, back junction formation by simple alloying, no clean room operation, etc.

Progress in efficiency during the grant period was continuous and the 20% efficiency has been just about reached by this time as is indicated in the attached figures. The reason for the gradual improvement is that nature resists the idea of large jumps; improvement in one parameter usually results in degradation of another and this continuous cross talk is the reason for graduality.

Much of the efficiency of silicon solar cells was limited by the generation of three types of defect states: bulk states, surface induced states, and surface states. The magnitude and distribution of these defects affect the three basic parameters, photocurrent, photovoltage and fill factor.

A. Current

The quantum yield of the cells have been improved continuously. The short wavelength response is controlled by defect states near the front junction while the red response is controlled by bulk states and by defects generated near the back surface. The total collection efficiency is approximately 78% at the moment for flat surfaces but can be increased by some 5-6% with textured surfaces. There is clearly room for continued improvement in the current collection efficiency.

B. Photovoltage

The complex matter of photovoltage has been attached heavily both theoretically and experimentally. A general mathematical treatment indicates that the practical limit of a room temperature photovoltage of about 600 mV is controlled by surface thermal generation current. We believe that the problem has been theoretically identified with this work and, therefore, gives an important guideline for the experimental approaches. We believe that with sufficient experimental effort, the photovoltage could be raised much above 600 mV.

C. Fill Factor

Great improvements have been accomplished in the control of the fill factor and it can now be held very close to the ideal value; namely in the range of 78-80%. These excellent results indicate the potential return that can be obtained by minimization of defect states.

The combined theoretical and experimental effort which went in many directions during the grant could not encompass detailed studies of all the related phenomena but has been instrumental in establishing a range of parameters that can provide consistently high conversion efficiencies.

DEVELOPMENT OF A 20% EFFICIENT SOLAR CELL

GRANT NO. GI-43090
15 MONTHS, INITIATED 1 JUNE 1974

$119,400

PRINCIPAL INVESTIGATOR:
JOSEPH LINDMAYER
SOLAREX CORPORATION

OBJECTIVES

INCREASE TERRESTRIAL EFFICIENCY OF SILICON SOLAR CELLS TO 20%

UTILIZE POTENTIALLY INEXPENSIVE TECHNOLOGIES

APPROACH

IMPROVE OPTICAL COUPLING W. AR COATING AND TEXTURING

IMPROVE SHORT AND LONG WAVELENGTH RESPONSE

IMPROVE FILL FACTOR TOWARD THEORETICAL VALUES

STUDY PHOTOVOLTAGE LIMITATIONS

LAST 6 MONTHS ACTIVITY

CONTINUED STUDIES FOR BETTER FRONT JUNCTION FORMATION

MAPPING ELEMENTS AND COMPOUNDS FOR REAR HIGH-LOW JUNCTION FORMATION

CHARACTERIZATION OF LOW TEMPERATURE DIFFUSION

DEFECT GENERATION STUDIES

IMPROVE AND SIMPLIFY TANTALUM OXIDE COATING

STUDY TEXTURING

COMPARE P-ON-N AND N-ON-P

IMPROVE MEASUREMENT TECHNIQUES

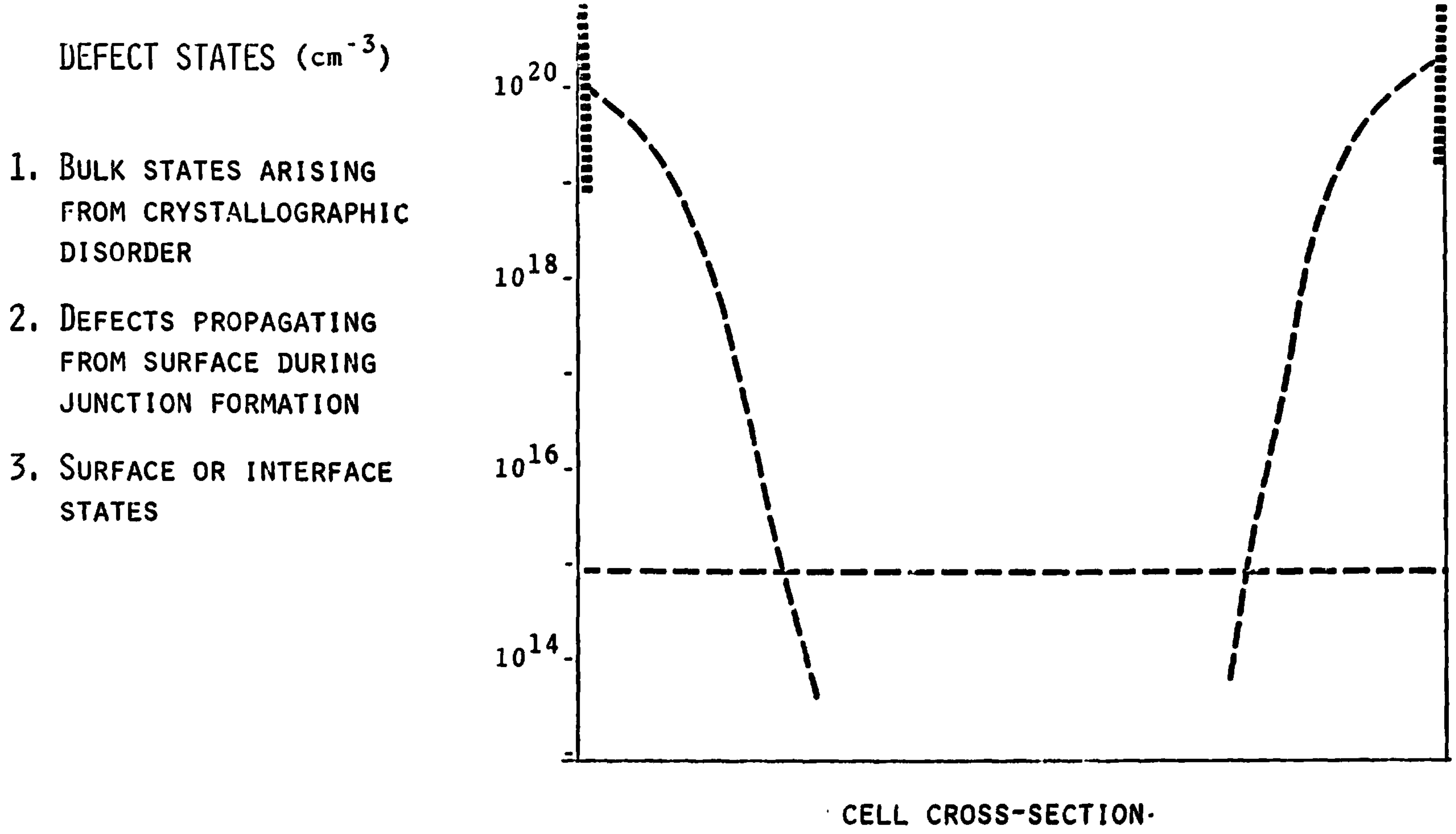

THREE BASIC TYPES OF DEFECTS IN SILICON CELLS

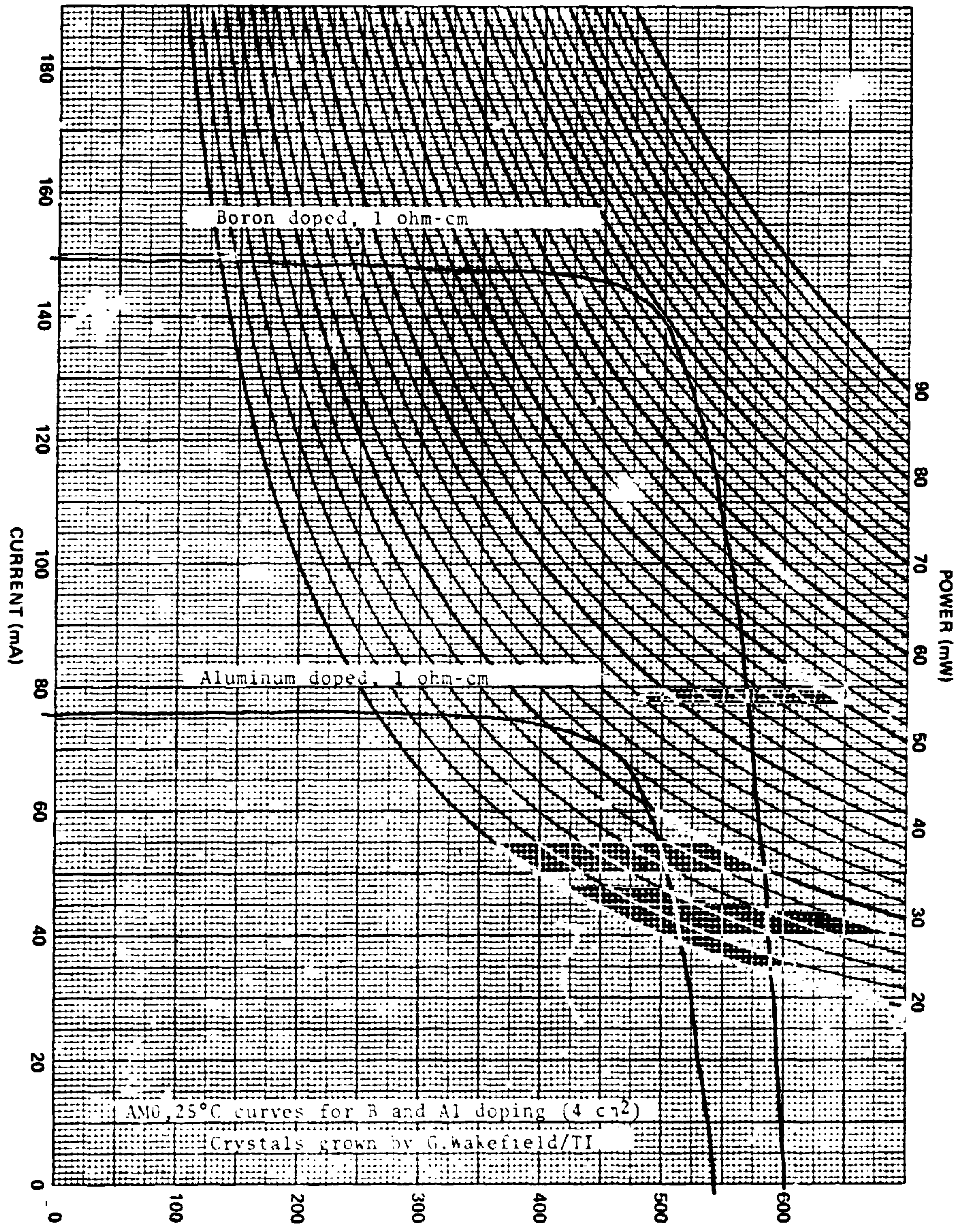
Boron doped, 1 ohm-cm
Aluminum doped, 1 ohm-cm
AM0,25°C curves for B and Al doping (4 cm²)
Crystals grown by G.Wakefield/TI
CURRENT (mA)
0
20
40
60
80
100
120
140
160
180
VOLTAGE (mV)
0
100
200
300
400
500
600
POWER (mW)
20
30
40
50
60
70
80
90

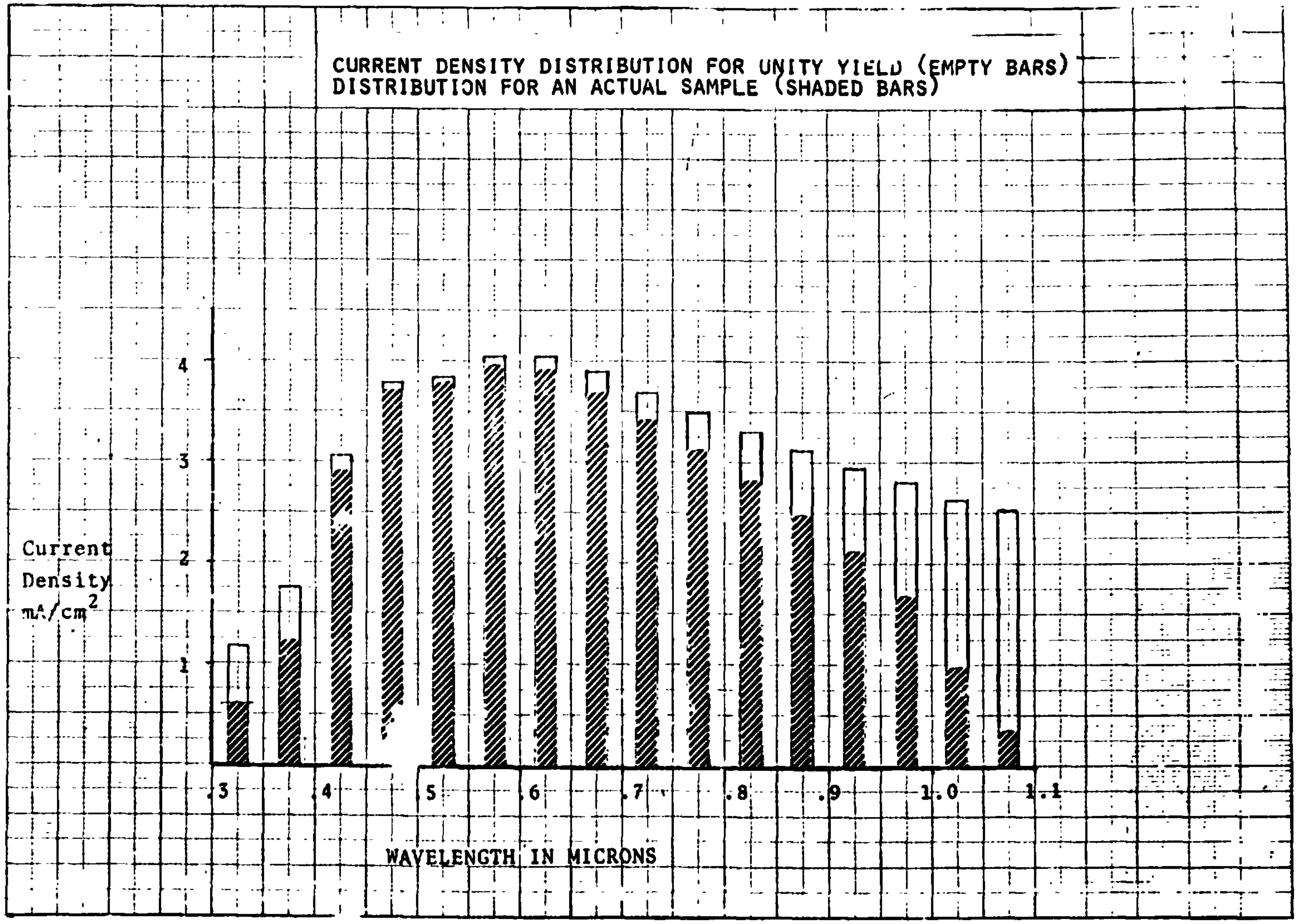

CURRENT DENSITY DISTRIBUTION FOR UNITY YIELD (EMPTY BARS)
DISTRIBUTION FOR AN ACTUAL SAMPLE (SHADED BARS)

SHEET RESISTANCE OF DIFFUSED PHOSPHORUS LAYER AS A FUNCTION OF TEMPERATURE (10 MIN.)

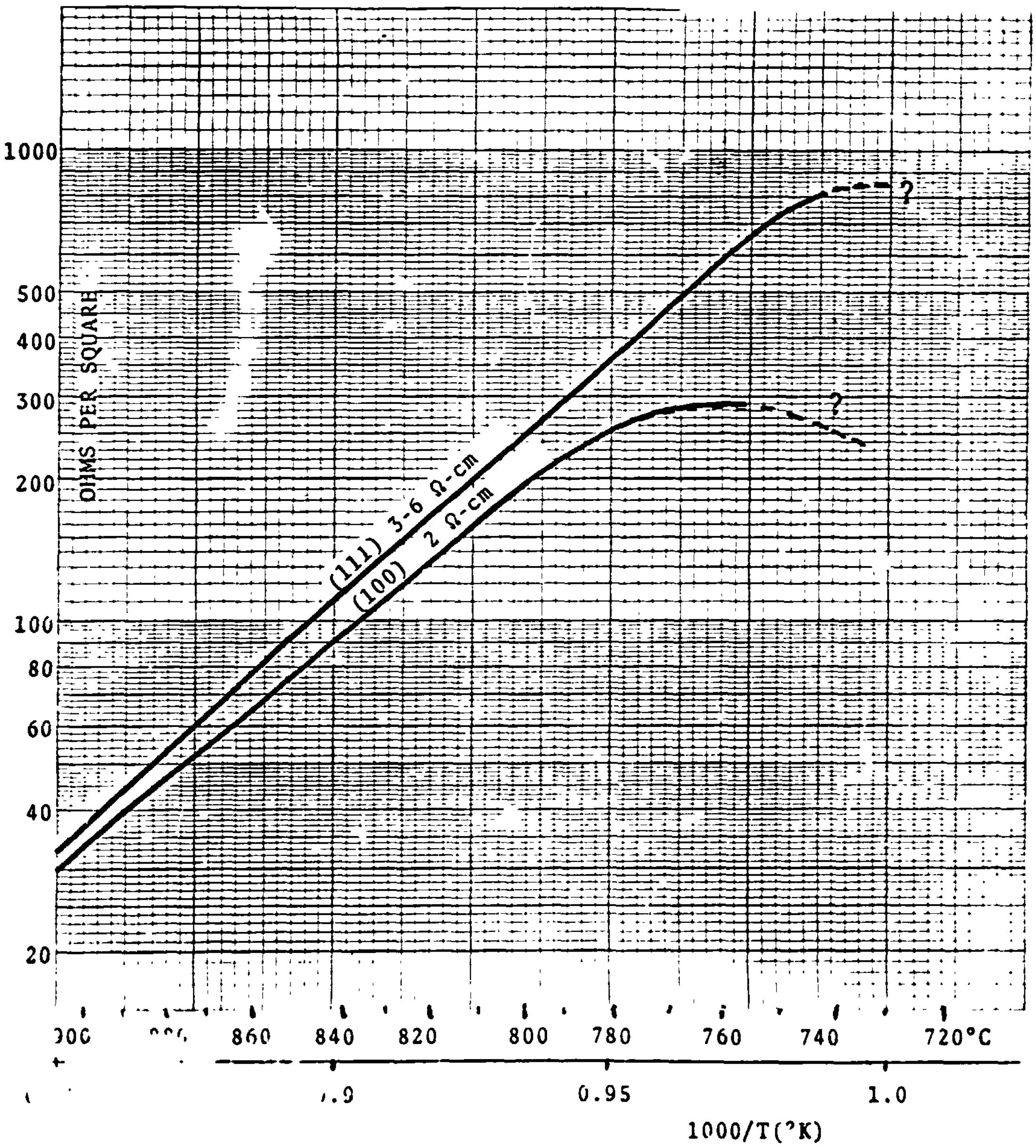

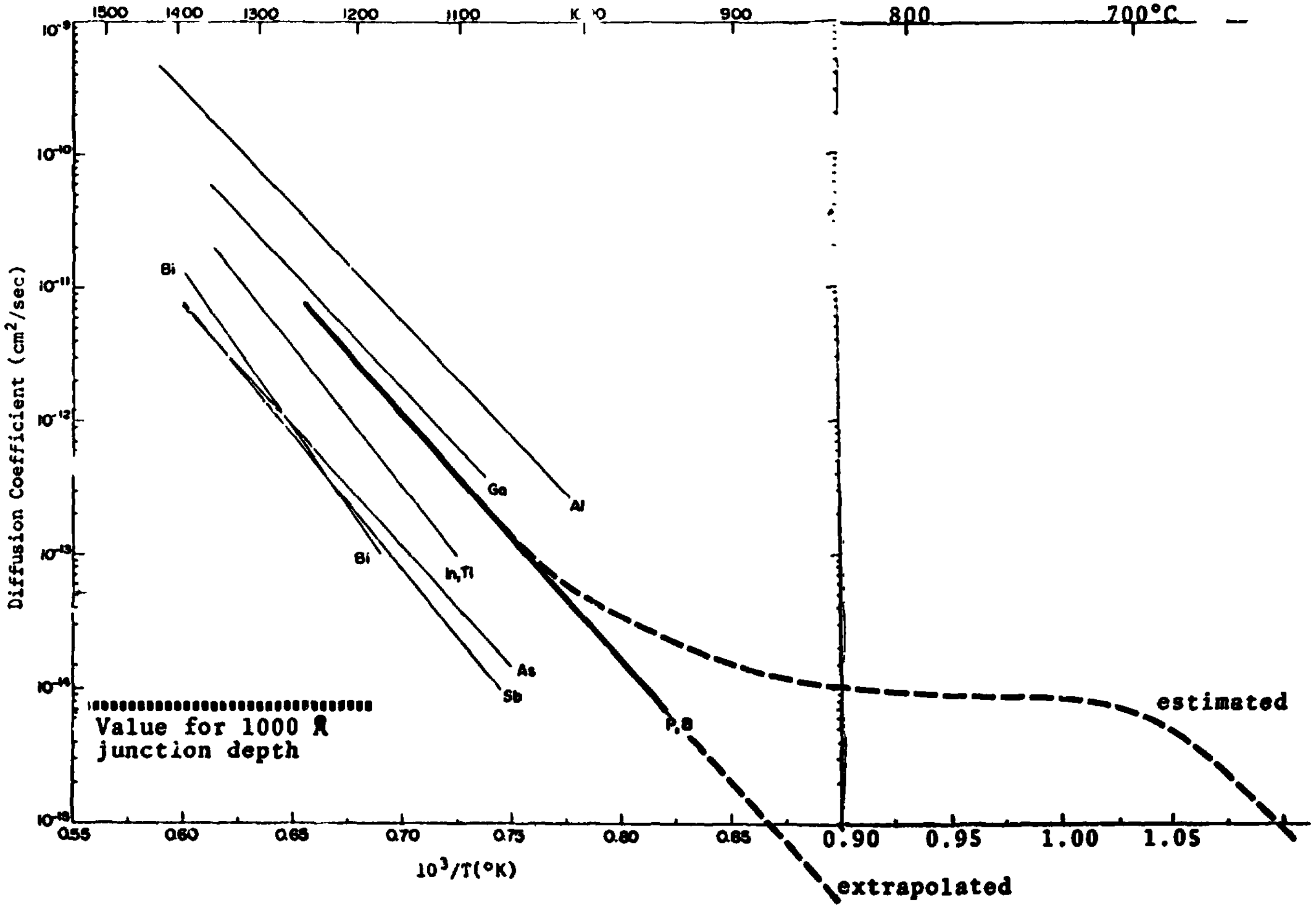

ESTIMATED PHOSPHORUS DIFFUSION CONSTANT AS COMPARED TO PUBLISHED VALUES

TABLE FOR DIFFERENT BACK LAYERS

Compound	Character	Remarks
B glass	p-type	spin-on
Ga glass	n-type	spin-on
CeO_2	n-type	electron beam
Cr	p-type	filament
Si (p-type)	n-type	electron beam
Ti	p-type	filament
Ta_2O_5	p-type	electron beam
Ni	n-type	electron beam
SiO	n-type	electron beam
Si (metallurgical)	p-type	electron beam
Ge	n-type	electron beam
MoO_3	n-type	electron beam
Mn	n-type	electron beam
Mo	?	electron beam
V	?	electron beam
Sn	n-type	electron beam
Al_2O_3	p-type	electron beam
AlP	n-type	electron beam
B_2O_3	?	electron beam

INFRARED RESPONSE

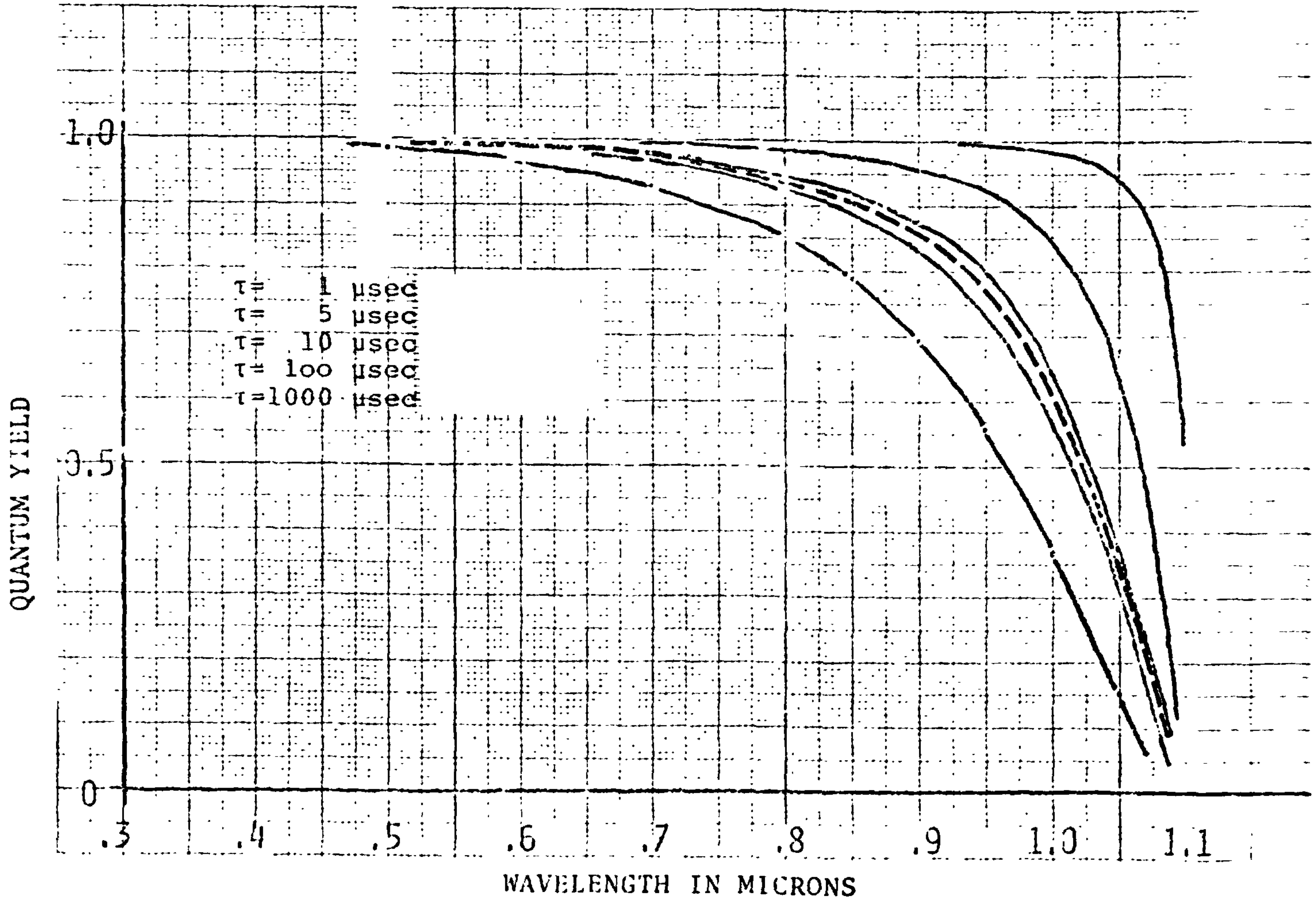

Quantum curves (precalculated) help to determine lifetime in the neighborhood of the back contact (dashed line)

TEXTURING FOR LIGHT TRAPPING

Alkaline Etches

Acid Etches

Preferential Etching With and Without Masking

1) Bare cell reflection may be reduced from 35% to 12%
2) Coated with organic matter, below 10% reflection
3) Texturing offers only 6-7% gain if AR coating is used
4) Difficult to hold fill factor with textured surface
5) Some slow degradation may occur with (100) plane

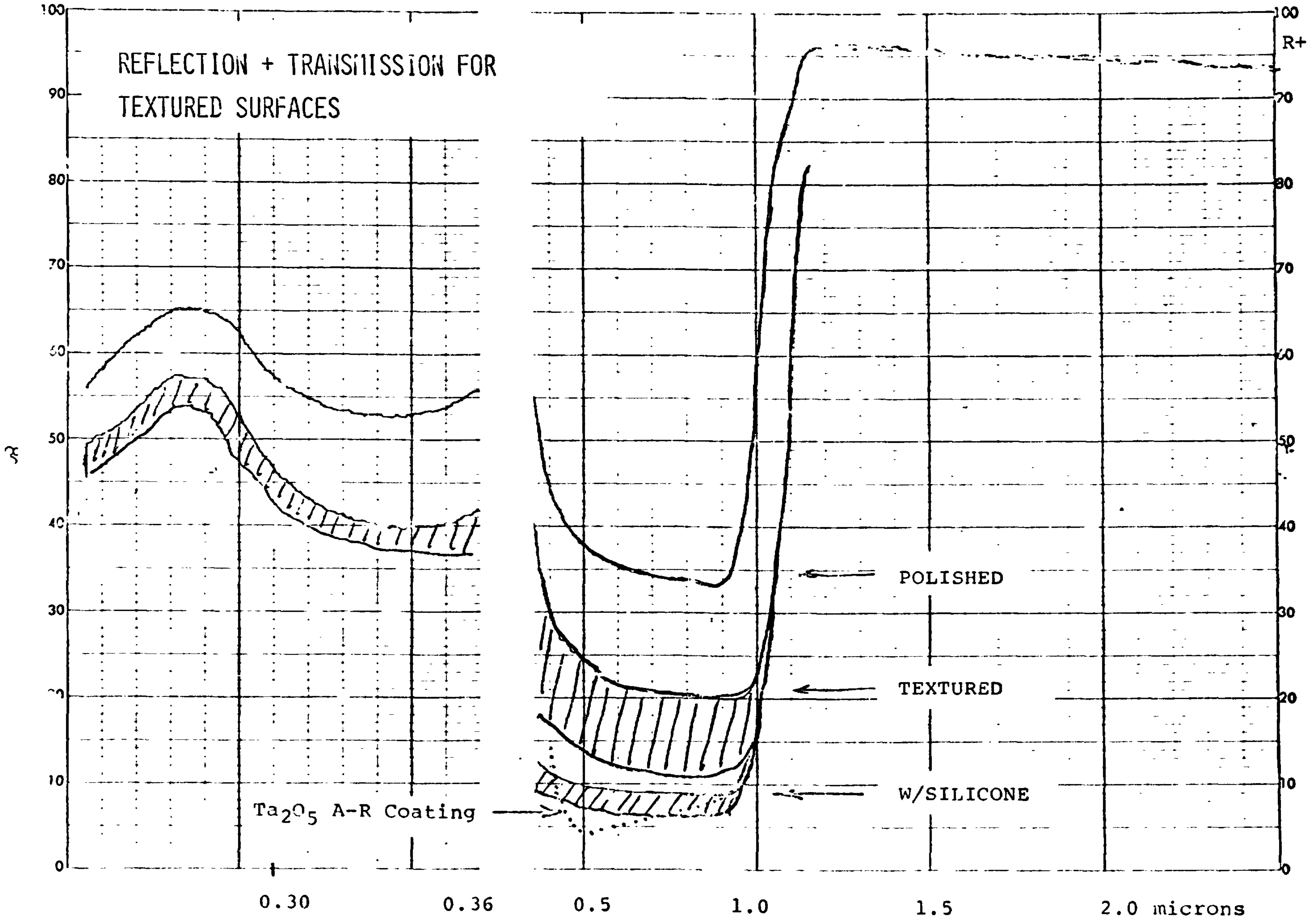

REFLECTION + TRANSMISSION FOR TEXTURED SURFACES

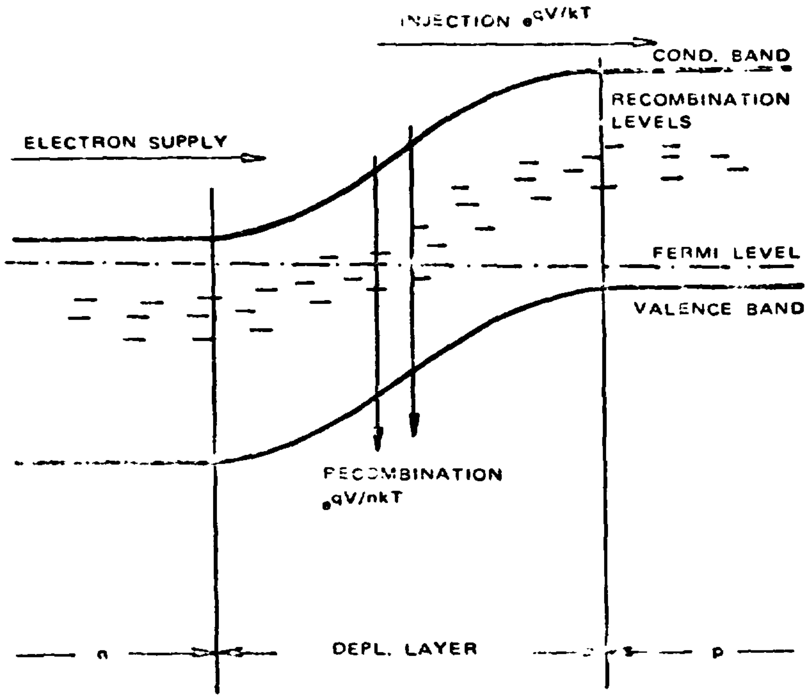

Figure 3. Energy barrier at an n-p junction. Space charge recombination current through recombination centers in the middle of the barrier is the first current component that flows as a forward bias is applied in a p-n junction. True injection will start at higher voltages.

J. Lindmayer, COMSAT TECHNICAL REVIEW VOLUME 2 NUMBER 1, SPRING 1972

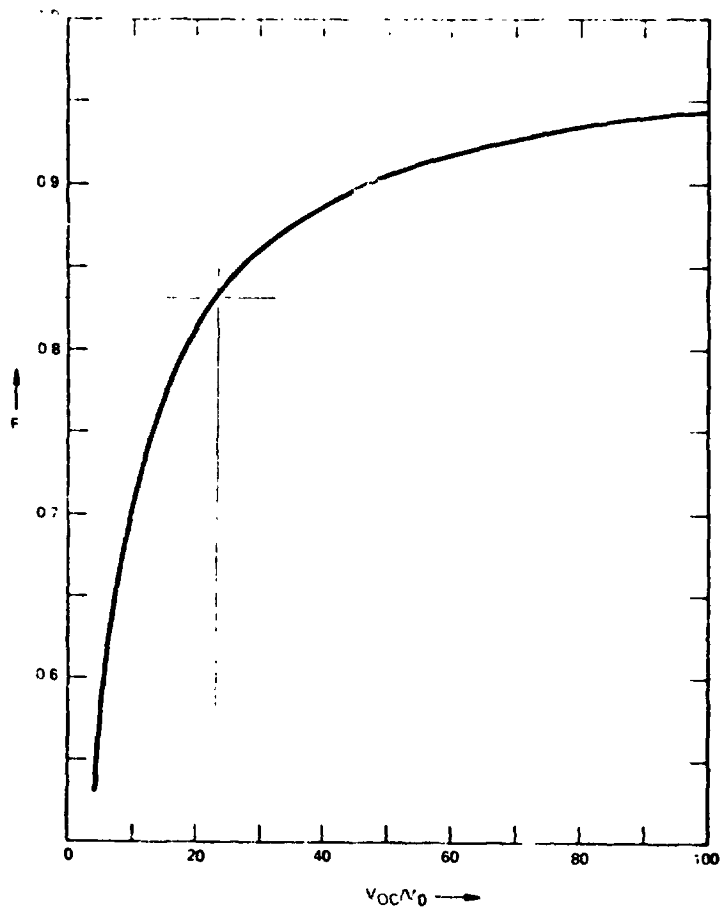

The fill factor could be as high as 83% at $V_{OC}=600$ mV and $V_0=26$ mV
Actual values reached 80% with 4 cm^2; harder to maintain for large areas.

$J_0 = \frac{q n_i^2}{N} \frac{D}{W}$		REVERSE CURRENT DENSITY WITH HIGH REAR CONTACT RECOMBINATION
$J_0 = \left. \frac{q\ n_i^2}{N + \frac{J_{sc}}{qW}} \frac{D}{L} \tanh W/L \right\rvert_{s=0}$	LEADING TO VOLTAGE INCREMENT OF BOTH KIND	BULK REVERSE CURRENT DENSITY WITH LOW REAR CONTACT RECOMBINATION (s=0), CONTRIBUTING TO INCREASED PHOTOVOLTAGE
$J_F = \frac{q n_i^2 D}{\int_0^{x_J} N\, dx}$	LEADING TO VOLTAGE LIMITATION	REVERSE CURRENT FROM TOP LAYER LIMITS PHOTOVOLTAGE WHEN THE BULK CURRENT IS MINIMIZED

DETAILED CALCULATION MAY BE FOUND IN LAST QUARTERLY REPORT

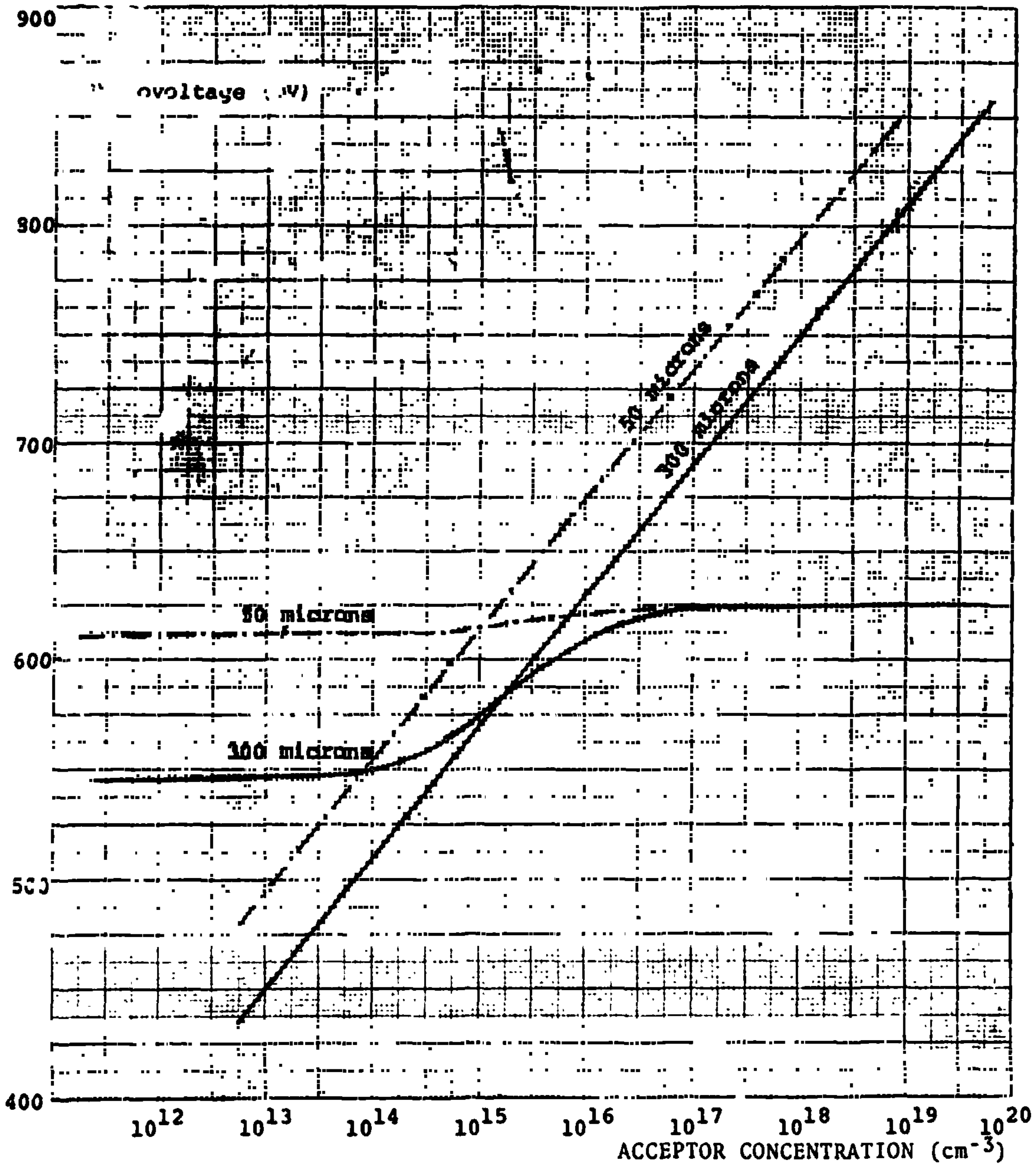

CALCULATED PHOTOVOLTAGE FOR TWO CELL THICKNESSES. THE PARALLEL LINES ARE FROM THE BULK CONTRIBUTION ALONE (CONVENTIONAL), AT LOW DOPING LEVELS IMPROVEMENTS ARE SEEN FROM REDUCED REAR RECOMBINATION, AT HIGH DOPING REVERSE CURRENT OF TOP LAYER LIMITS PHOTOVOLTAGE.

C.2

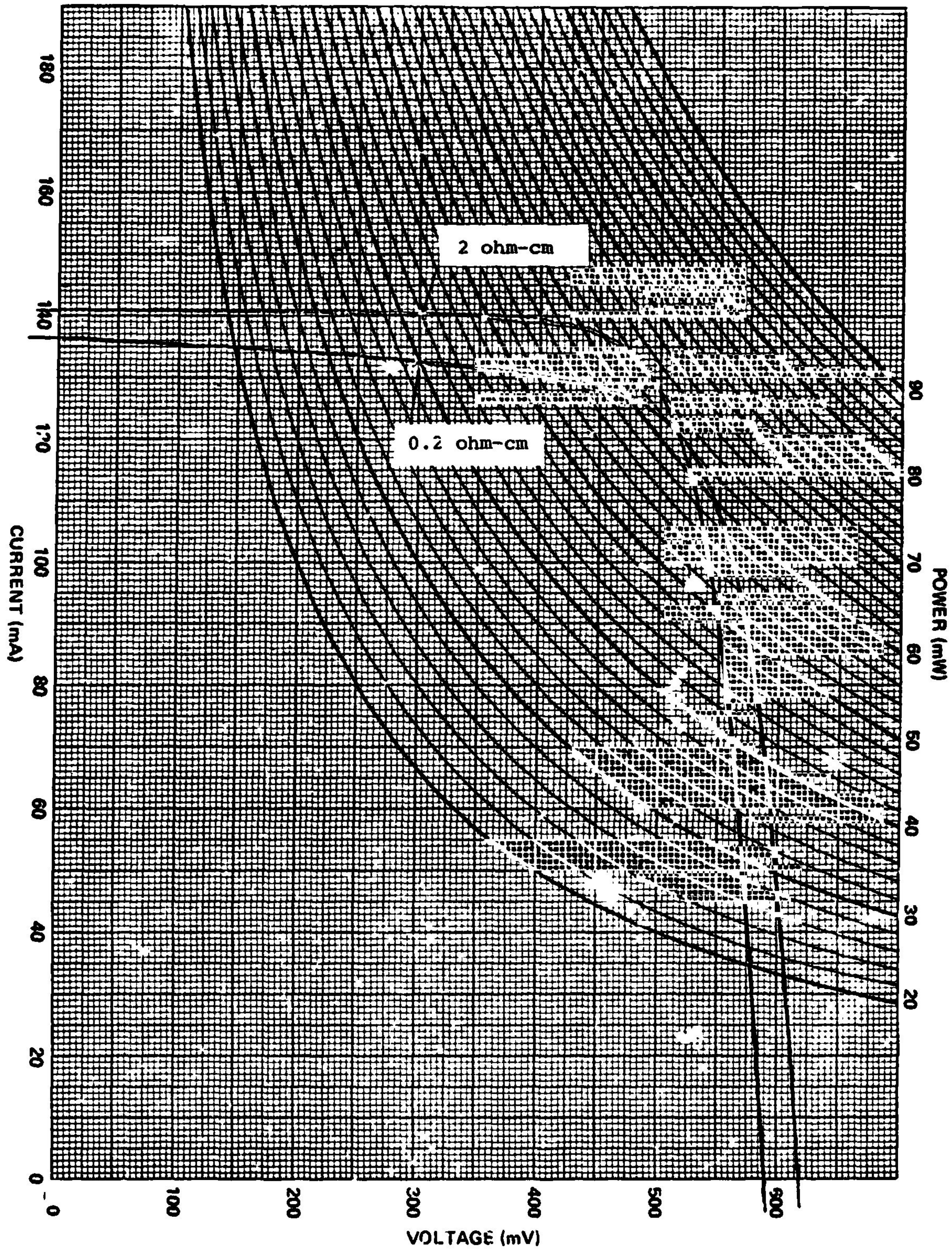
2 ohm-cm
0.2 ohm-cm
CURRENT (mA)
0
20
40
60
80
100
120
140
160
180
VOLTAGE (mV)
0
100
200
300
400
500
600
POWER (mW)
20
30
40
50
60
70
80
90

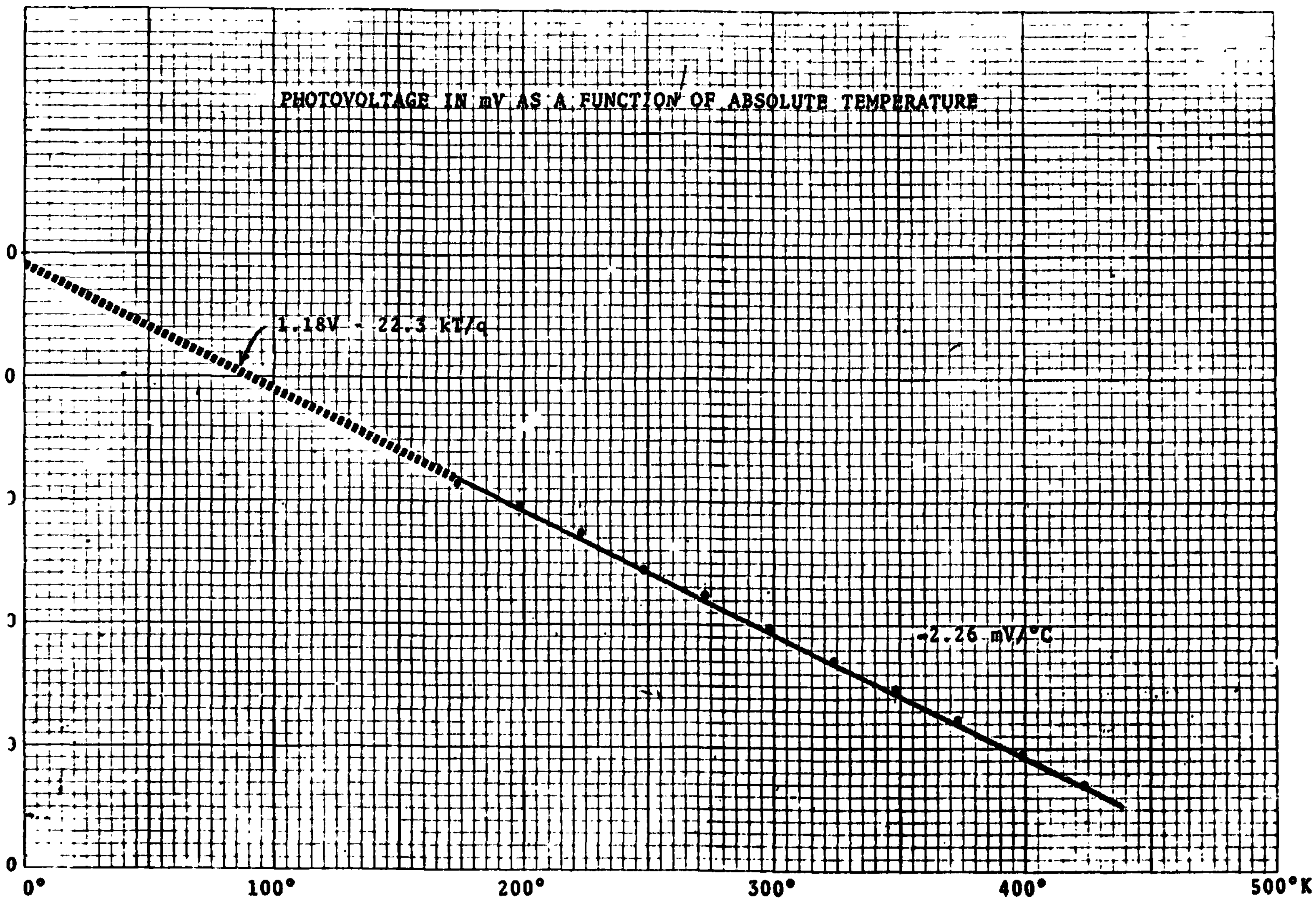

PHOTOVOLTAGE IN mV AS A FUNCTION OF ABSOLUTE TEMPERATURE

PROGRESS IN TERRESTRIAL EFFICIENCY

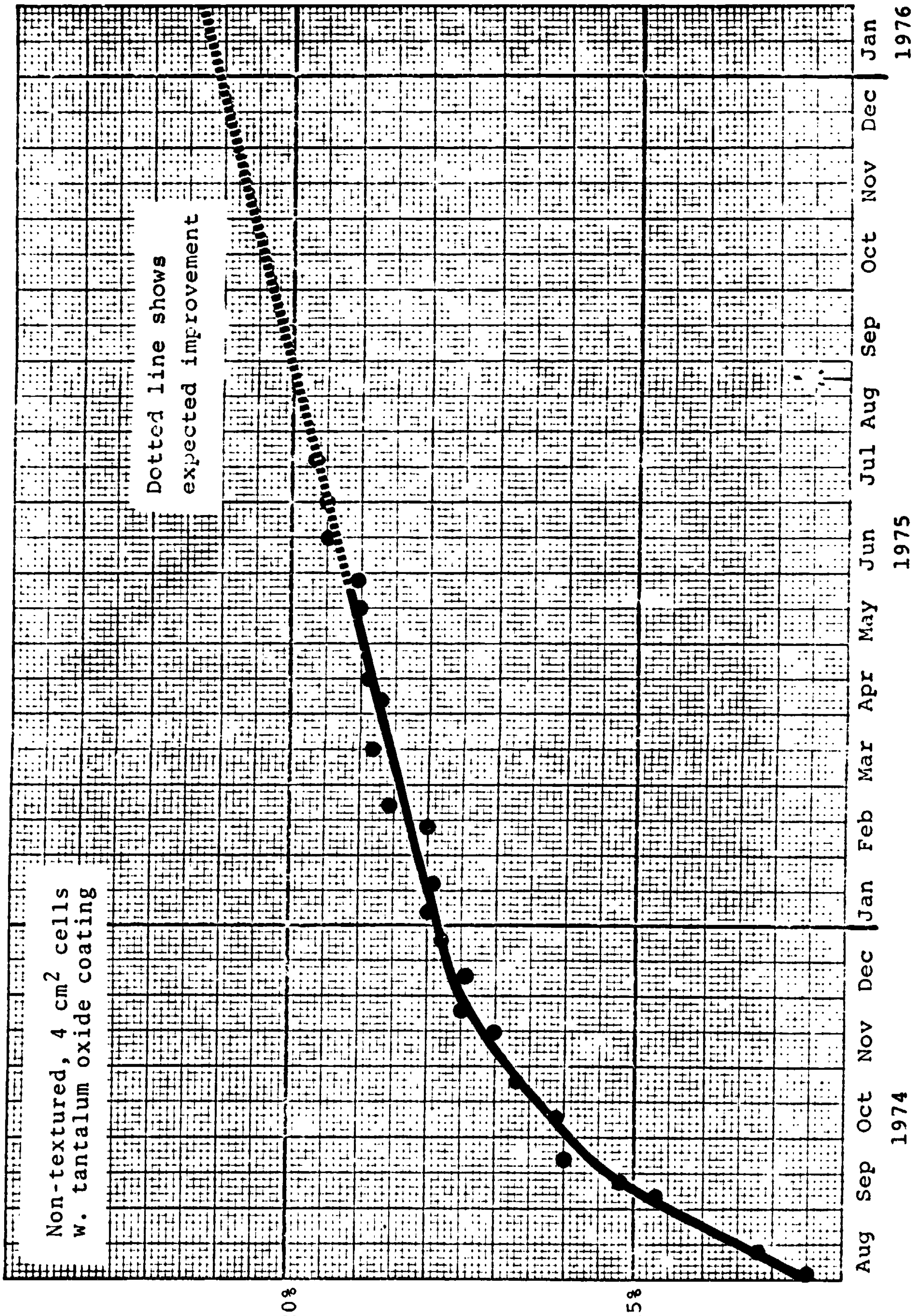

PRECEDING PAGE BLANK NOT FILMED

SUMMARY OF KEY RESULTS

IMPROVED TANTALUM OXIDE COATINGS
TEXTURING MAY LEAD TO LONG TERM DEGRADATION
HIGH FILL FACTORS AROUND 80%
BETTER UNDERSTANDING OF PHOTOVOLTAGE PROBLEMS
HIGHER PHOTOVOLTAGE, ABOVE 600 mV
BETTER RESPONSE
EFFICIENCY NEAR OR AT 20%
EFFICIENCY IMPROVES WITH CONCENTRATION

PLANNED ACTIVITY FOR NEXT 6 MONTHS

GRANT ENDS IN AUG. 1975; RENEWAL REQUESTED

IF RENEWED, THE EFFICIENCY RANGE ABOVE 20% WOULD BE EXAMINED, INCLUDING BASIC RESEARCH ON EFFECTS OBSERVED BUT NOT WELL UNDERSTOOD

SOLAR SILICON DEFINITION GRANT

AER 75 - 03972

PRINCIPAL INVESTIGATOR - DR. G. F. WAKEFIELD

TEXAS INSTRUMENTS INCORPORATED
DALLAS, TEXAS 75222

This project is being conducted to define a preliminary chemical purity specification for solar grade silicon. The specification should permit the utilization of less pure (than semiconductor grade) silicon to manufacture solar cells having efficiencies of at least 10% AMO. Lower purity solar silicon should be obtainable for significantly reduced cost than semiconductor silicon, since lower cost processing approaches could be utilized. The criticality of this goal is easily appreciated from the fact that silicon presently contributes 20% to cost of solar panels. Reduction of the panel cost to one tenth present cost is obviously material limited. Economies of scale and learning do not forecast the required cost reduction since semiconductor silicon is already an established, relatively large scale industry. This program was thus conducted on a compressed time scale to allow earliest consideration of the reduced purity requirements.

The approach on this project was to prepare crystals from high purity silicon doped to known level with many common impurities. This impure silicon was fabricated into small area diodes and solar cells to evaluate the effect of the impurities on device performance. Measurements were made of the I-V characteristics (with emphasis on the slope of the recombination and injection influenced curves), the photoresponse behavior and lifetime measurement by photoconductive decay technique. Following selection of the maximum levels of impurities tolerable within the performance criteria, samples of impure silicon were fabricated into solar cells by several solar cell manufacturers. The performance of these cells was compared to performance of cells fabricated simultaneously from semiconductor silicon by the same manufacturer to eliminate processing variables. The results of the diode evaluation showed that up to several ppm of most common impurities were tolerable in the raw material silicon used for crystal growth. The impure silicon provided for solar cell manufacturers tests was grown from silicon containing 10 ppm of each of the impurities being studied, for a total impurity level of 120 ppm in the melt.

The solar cells made from the impure silicon were consistently lower in performance by .5 to 1% absolute from all sources. The V_{OC} and I_{SC} were reduced .5750 to .565 V and 31 to 20 ma/cm^2 for 2" diameter cells semiconductor grade silicon and the impure silicon respectively. Cells from the impure silicon thus performed 90% as well as cells made from silicon having 10^4 - 10^5 higher purity level. The consistency of data from several sources of fabrication and the normal distribution shape of the yield curve tend to support the validity of the data.

A preliminary specification was drafted, reviewed with government and producers, and included in the grant final report.

SOLAR SILICON DEFINITION

SOLAR SILICON DEFINITION GRANT

NSF GRANT NO: AER75-03972

PERIOD: 15 OCTOBER 1974
TO
31 OCTOBER 1975

PRINCIPAL INVESTIGATOR:
DR. GENE WAKEFIELD

PERFORMED AT:
TEXAS INSTRUMENTS

GRANT AMOUNT: $172,400

JULY 1975 AER75-03972

SOLAR SILICON DEFINITION

TEXAS INSTRUMENTS/SOUTHERN METHODIST UNIVERSITY

GOAL:

- ESTABLISH A SPECIFICATION FOR SOLAR GRADE SILICON RAW MATERIAL WHICH CAN BE USED TO OPTIMIZE PERFORMANCE VS. MATERIAL COST FOR SOLAR CELLS TO PROVIDE A REALISTIC TARGET FOR LOW COST SILICON MANUFACTURING METHODS.

APPROACH:

- DEFINE AN IMPURITY PROPERTY VS. PERFORMANCE MATRIX WHICH WILL ALLOW DETERMINATION OF IMPURITY TOLERANCE LEVEL. EVALUATE MATERIAL AS P-N DIODE TO SELECT MATERIAL FOR FABRICATION OF SOLAR CELLS BY SOLAR CELL MANUFACTURERS. EVALUATE SOLAR CELLS.

- SYNTHESIZE SOLAR GRADE SPECIFICATION AND PUBLISH AFTER REVIEW WITH INDUSTRY AND NSF.

JULY 1975 AER75-03972

SOLAR SILICON DEFINITION

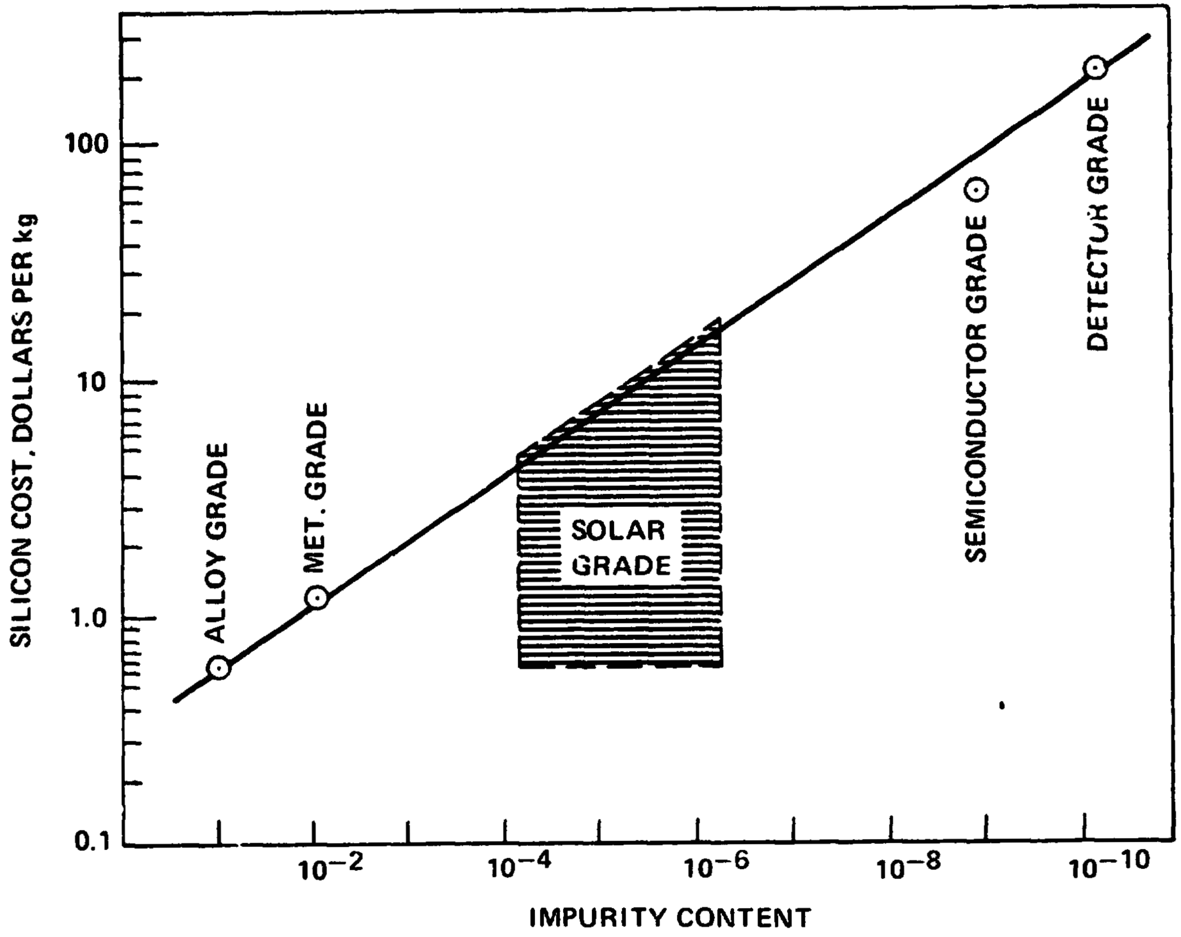

JULY 1975 AER75-03972

SOLAR SILICON DEFINITION
EXPERIMENTAL APPROACH

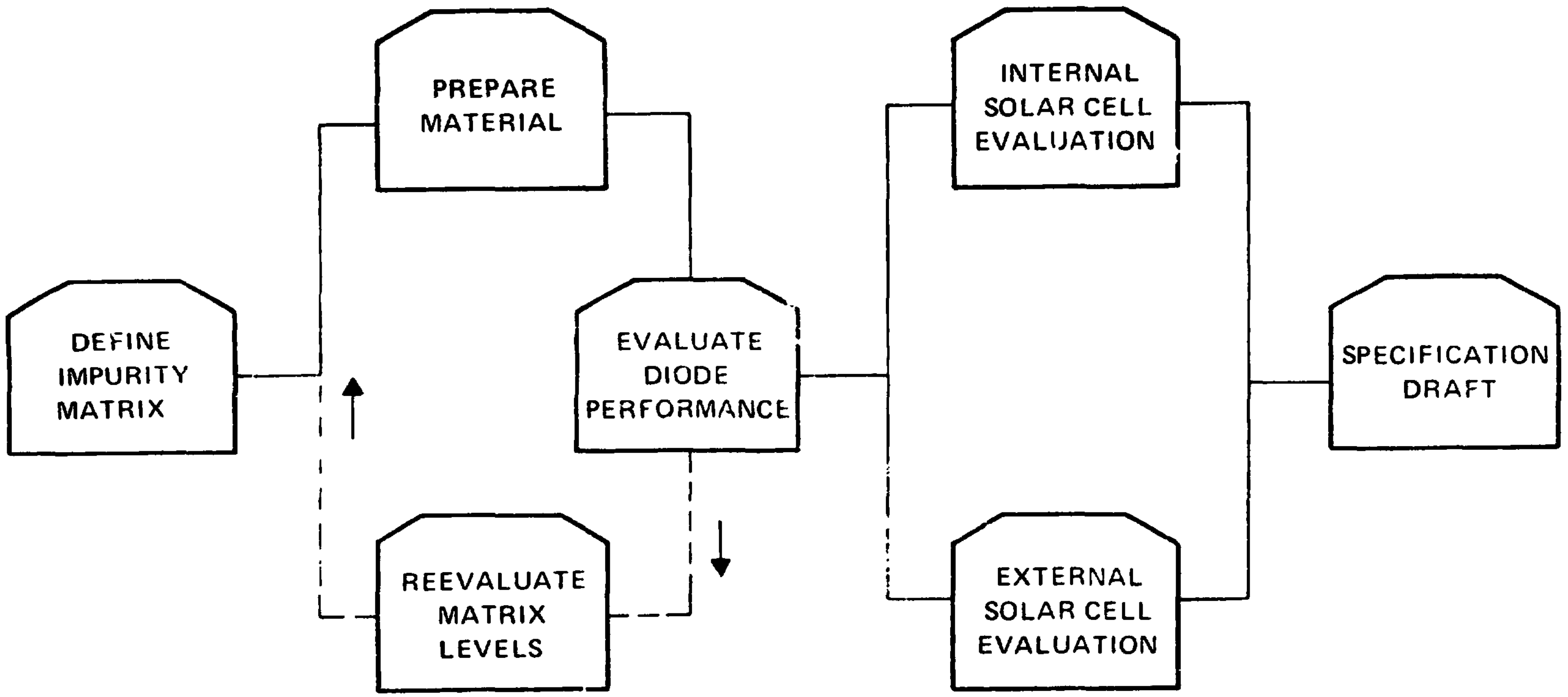

JULY 1975 AER75-03972

SOLAR SILICON DEFINITION GRANT

PLANNED ACTIVITY	RESULT
● COMPLETE DIODE FABRICATION AND EVALUATION	● COMPLETED
● FABRICATE AND EVALUATE SOLAR CELLS	● SOLAR SILICON WITH 100 ppm IMPURITIES YIELDED 90% OF PERFORMANCE OF SEMICONDUCTOR SILICON
● PREPARE SPECIFICATION FOR IMPURITY CONTENT OF SILICON	● PRELIMINARY SPECIFICATION FOR SOLAR SILICON WRITTEN
● REVIEW AND PUBLISH SPECIFICATION	● SPECIFICATION REVIEWED AND PUBLISHED.

JULY 1975 AER75-03972

SOLAR SILICON DEFINITION

IMPURITY MATRIX FOR SOLAR SILICON DEFINITION

IMPURITY	GROUP	CONCENTRATION LEVELS LOG N, ATOMS/CC			SOLID SOLUBILITY
SODIUM	IA	15	17		9×10^{18}
MAGNESIUM	IIA	14	15	16	5×10^{18}
ALUMINUM	IIIA	14	15	16	2×10^{19}
COPPER	IB	13	14	15	1×10^{18}
GOLD	IB	14	15	16	1×10^{17}
ZINC	IIB	14	15	16	6×10^{16}
TITANIUM	IVB	13	14	15	1×10^{15}
VANADIUM	VB	13	14	15	5×10^{15}
CHROMIUM	VIB	13	14	15	5×10^{15}
MANGANESE	VIIB	13	14	15	4×10^{16}
IRON	VIII	14	15	16	3×10^{16}
NICKEL	VIII	14	15	16	1×10^{17}

JULY 1975 AER75-03972

SOLAR SILICON DEFINITION

INFLUENCE OF IMPURITIES ON SILICON SOLAR CELLS

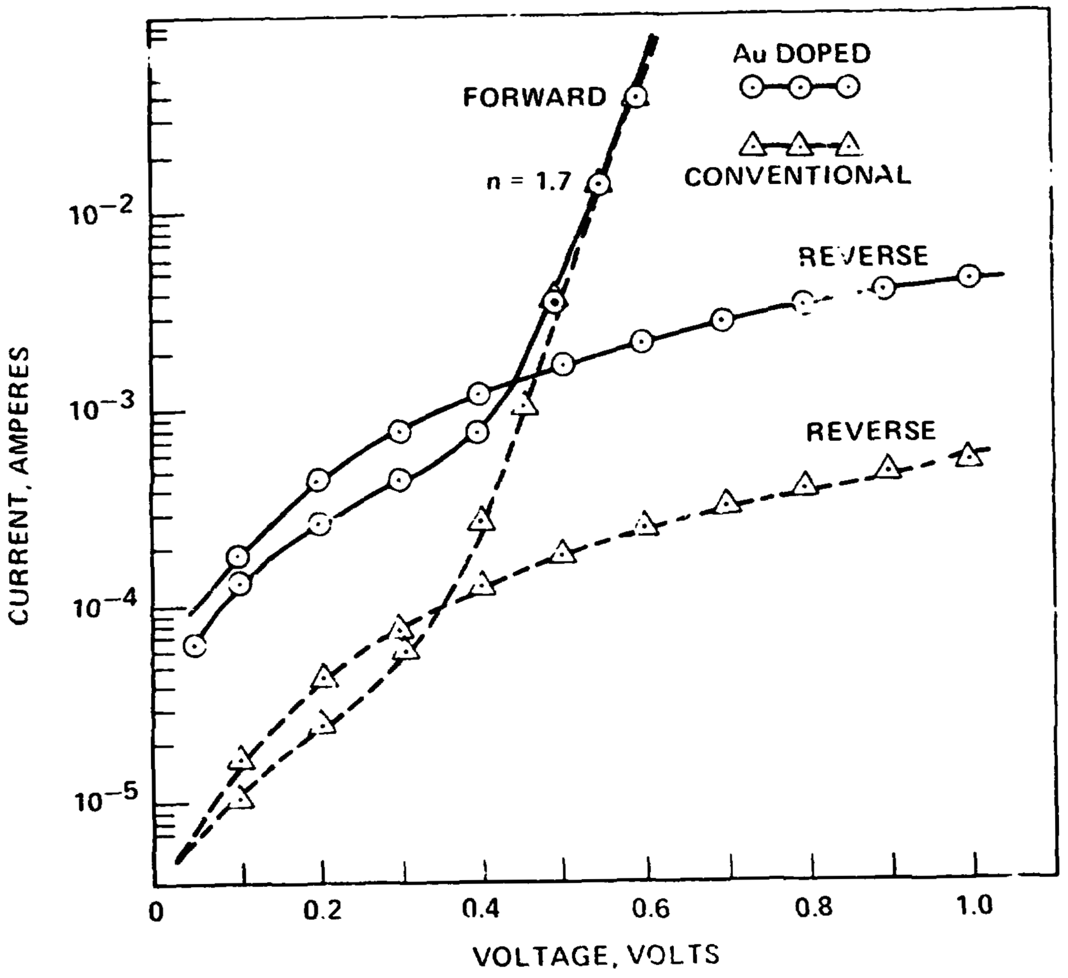

GOLD IMPURITY:
BEFORE PROCESSING
1 X 10^{16} a/cc;
AFTER PROCESSING .
7 X 10^{14} a/cc.

JULY 1975 AER75-03972

SOLAR SILICON DEFINITION

INFLUENCE OF IMPURITIES ON SILICON SOLAR CELLS

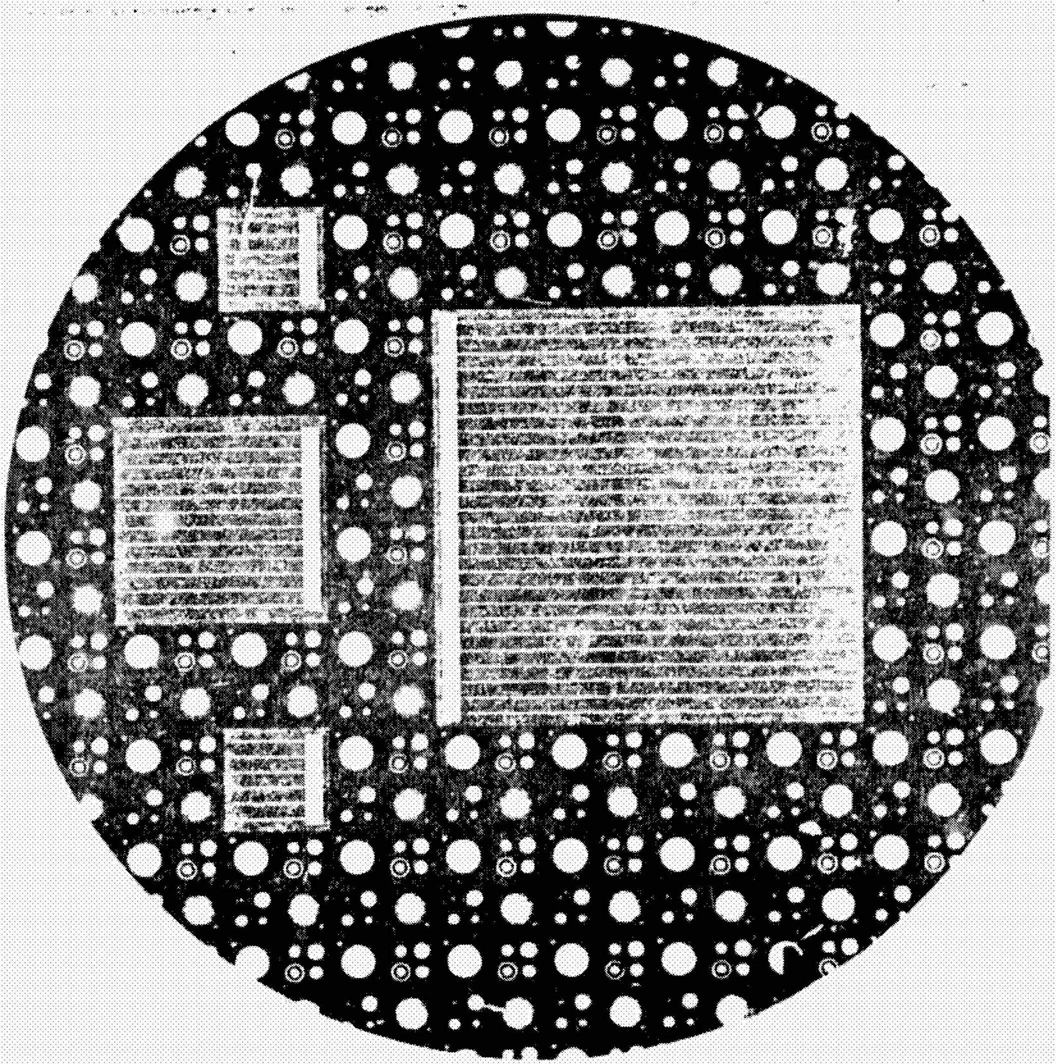

JUNCTION AREAS FROM
2×10^{-4} TO 4 cm^2

TEST PATTERN FOR DIODES
AND SOLAR CELLS

JULY 1975 AER75 03972

INFLUENCE OF IMPURITIES ON SILICON SOLAR CELLS

SUMMARY OF PHOTORESPONSE FROM DOPED SILICON SOLAR CELLS

IMPURITY	CONCENTRATION, a/cc X 10^{15}	PERFORMANCE*
COPPER	.3–2	.95
CHROMIUM	.1	.96
TITANIUM	.01–1	.88
MANGANESE	.01–.1	.94
VANADIUM	.01–.1	1
MAGNESIUM	.1–1	1
NICKEL	.01+.1	.97
IRON	.01–.7	.98
ALUMINUM	20	.7
GOLD	.7	.9

*RATIO OF SEMICONDUCTOR SILICON CELLS.

JULY 1975 AER75-03972

SOLAR SILICON DEFINITION

SILICON SOLAR CELL EVALUATION

CRYSTAL NUMBER	MELT COMPOSITION* ppm	RESISTIVITY OHM-CM, TYPE	FABRICATOR	RATIO TO "PURE" SILICON PERFORMANCE**
N	0.35 P	1, n	ALL	1 (AM1)
18	10 EA Ni, Cu, Cr, Mg, Mn, Ti, V 50 Fe; 0.35 P	0.8, n	TI	.88
			MOBIL TYCO	.95
			SOLAREX	.94 (.85)***
			SOLAR POWER CO.	.92
P	0.35 B	1, p	ALL	1 (AM0)
19	100 Al	0.9, p	TI	.6
			CENTRALAB	.66
			SOLAREX	.47
			MOBIL TYCO	.4

*BALANCE SEMICONDUCTOR GRADE SILICON

**BY SAME FABRICATOR

***RATIO TO WACKER SILICON, RESTIVITY ~ 8 OHM-CM

JULY 1975 AER75-03972

SOLAR SILICON DEFINITION

DISTRIBUTION OF SOLAR CELL CONVERSION EFFICIENCY

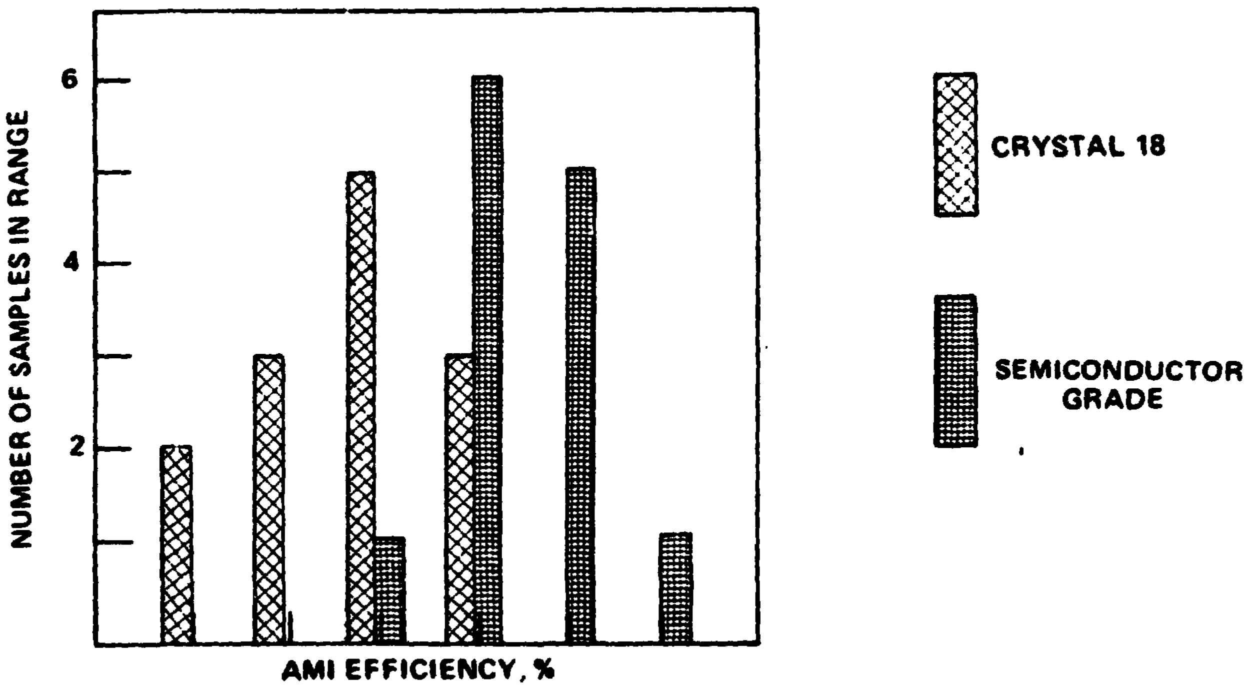

FABRICATED BY SOLAR POWER CORPORATION

JULY 1975 AER75-03972

SOLAR SILICON DEFINITION

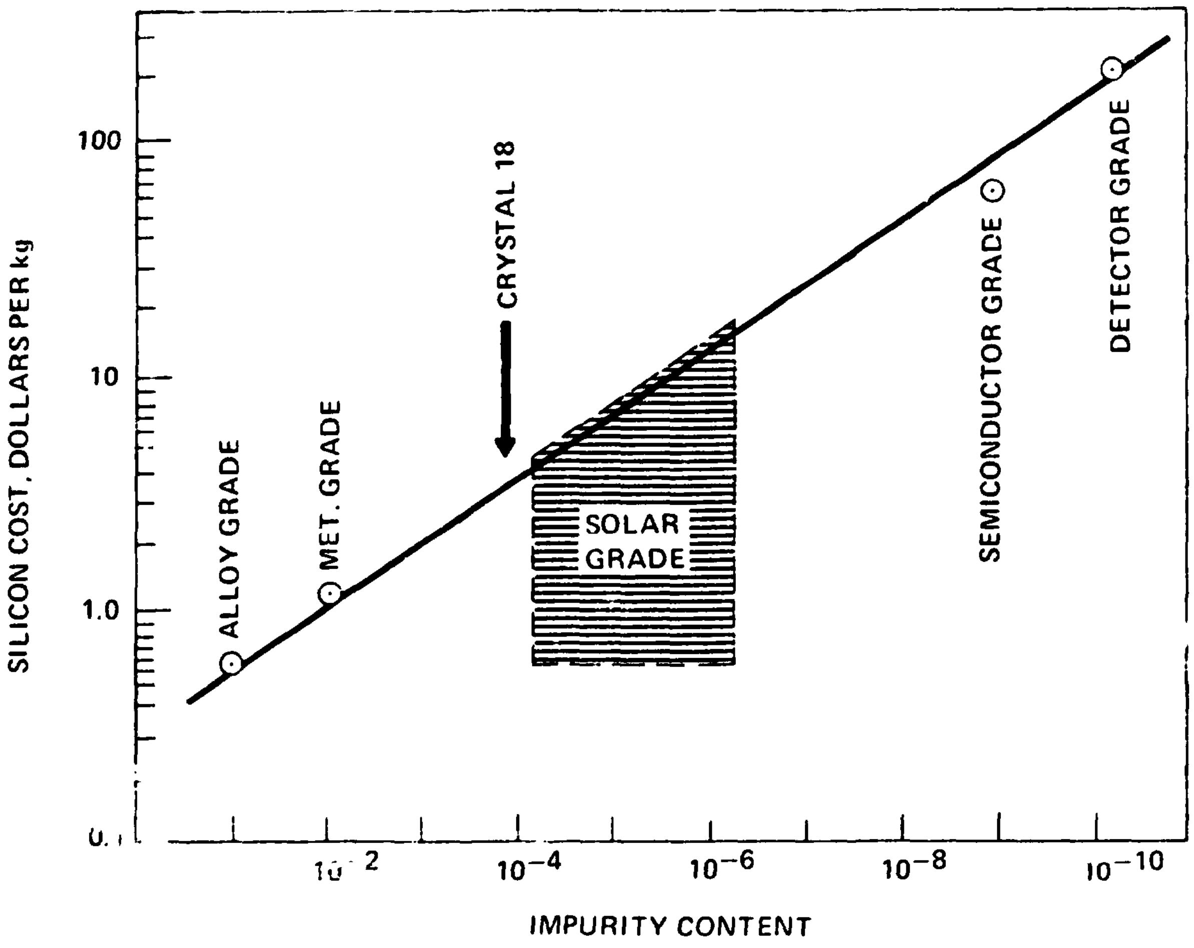

SOLAR SILICON DEFINITION

PRELIMINARY SPECIFICATION FOR SOLAR SILICON

RAW MATERIAL:

MAXIMUM IMPURITIES (ppm)

IRON	25	VANADIUM	5
NICKEL	5	COPPER	5
CHROMIUM	5	OXYGEN	5
MAGNESIUM	5	CARBON	5
MANGANESE	5	ALUMINUM	1
TITANIUM	5	BORON	.01

PHOSPHORUS .01

CRYSTAL SHEET:

SOLAR SILICON SHEET (FROM ANY METHOD) SHOULD BE DISLOCATION FREE MATERIAL EQUIVALENT TO CZOCHRALSKI CRYSTAL PULLED FROM ABOVE RAW MATERIAL.

JULY 1975 AER75-03972

SOLAR SILICON DEFINITION

SUMMARY OF KEY RESULTS

- DIODE AND SOLAR CELL PREFORMANCE OF DEVICES FABRICATED FROM SOLAR SILICON SHOWED EFFICIENCY (AM0) $>$ 10%.
- INFLUENCE OF IMPURITIES ON CZOCHRALSKI CRYSTAL GROWTH MINIMAL.
- PRELIMINARY SPECIFICATION FOR SOLAR SILICON WAS PREPARED ALLOWING PPM AMOUNTS OF COMMON METALS.
- LOW COST SILICON MANUFACTURING METHODS FOR SOLAR SILICON ARE LIKELY.

JULY 1975 AER75-03972

EFG RIBBON GROWTH

K. V. Ravi
Mobil Tyco Solar Energy Corporation
Waltham, Massachusetts 02154

The review will cover two projects entitled "Continuous Silicon Solar Cells" (Harvard-Tyco) and "Scale-Up of Program on Continuous Silicon Solar Cells."

Past activities in the theoretical aspects of EFG ribbon growth have dealt with capillary effects, die effects, thermal effects and crystal shape effects. This program was concluded in March and the final report is near completion. Effort since the last review meeting has been devoted to the examination of the shape of the meniscus at the ribbon edges. It has been determined that the height of the meniscus at the ribbon edges was underestimated in the earlier theory. Present theoretical findings along with analogue experiments indicate that the side meniscus lifts the edge meniscus effectively increasing the meniscus height at the edges. This finding has important consequences in the stable growth of high quality ribbons. Other factors considered include the effects of crystal orientation on ribbon shape or morphology.

The experimental aspects of growth have dealt with continuous ribbon growth and factors contributing to ribbon quality. Continuous ribbons of up to 80 ft (1 in. wide, 8 to 10 mils thick) in length have been grown. With the use of top or die heaters in resistance heated crystal growth systems, the control of vertical temperature gradients as well as the height of the meniscus above the die is possible. By employing a high meniscus mode of operation of the system a few crystals of very high quality with respect to defect densities (dislocations, twins and SiC particles) have been grown. The crystals also maintain a constant orientation over long lengths.

The quality aspects of ribbon crystals have been under continuous investigation with new insights into the characteristics of linear boundaries and SiC particles being developed.

A summary of the states of EFG ribbons was presented in the IEEE 11th Annual Photovoltaic Specialists Conference.

TITLE PAGE

I

TITLE:	CONTINUOUS SILICON SOLAR CELLS		
ORGANIZATIONS:	HARVARD UNIVERSITY/TYCO LABORATORIES, INC.		
PERIOD:	MARCH 1973 - MARCH 1975		
AMOUNT:	$300,700 TOTAL	HARVARD	$111,000
		TYCO	189,700
PRINCIPAL INVESTIGATORS:	PROFESSOR BRUCE CHALMERS - HARVARD DR. A. I. MLAVSKY - TYCO		

II

TITLE:	SCALE-UP OF PROGRAM ON CONTINUOUS SILICON SOLAR CELLS
ORGANIZATION:	MOBIL TYCO SOLAR ENERGY CORPORATION
PERIOD:	MAY 1974 - JULY 1975
AMOUNT:	$321,000
PRINCIPAL INVESTIGATOR:	DR. A. I. MLAVSKY

THEORETICAL CONSIDERATIONS

1. CAPILLARY EFFECTS
2. DIE EFFECTS
3. THERMAL EFFECTS
4. CRYSTAL SHAPE EFFECTS

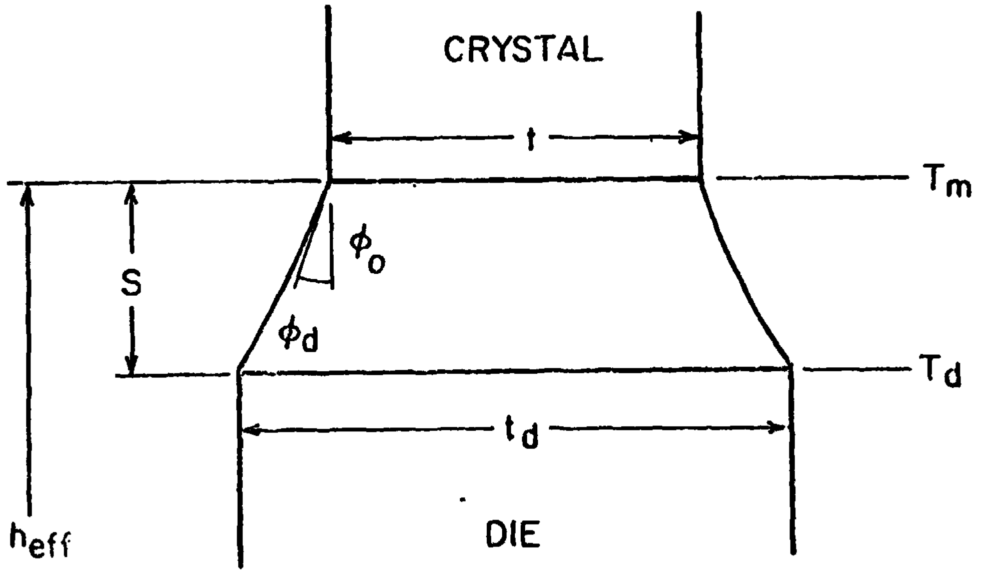

REQUIREMENT FOR CONSTANT CROSS-SECTION GROWTH OF SILICON:

$\phi_o = 11° \pm 1°$ FOR {111} ORIENTATION

$\phi_o < 11°$ FOR OTHER ORIENTATIONS

THE ANISOTROPY OF ϕ_o AFFECTS THE RIBBON MORPHOLOGY.

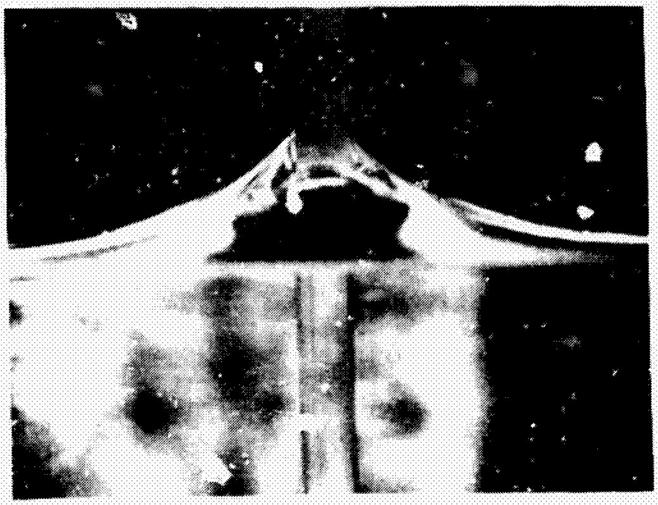

(a)

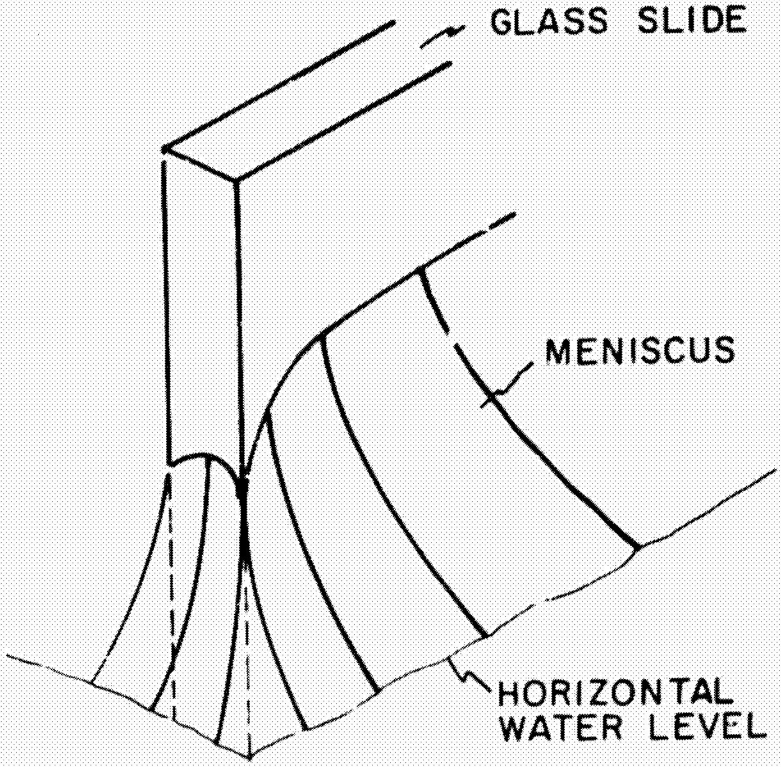

(b)

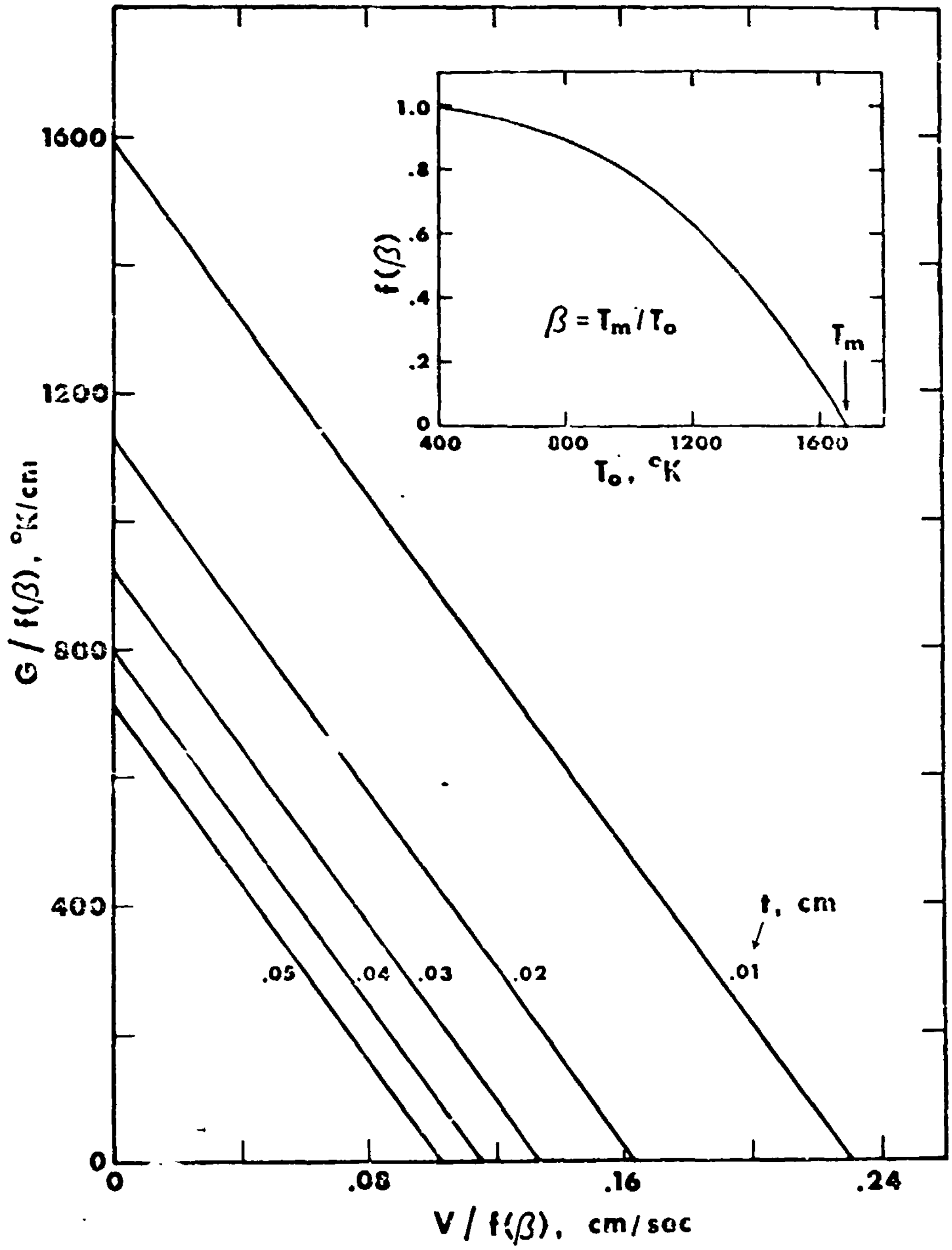
1600
1200
800
400
0
G / f(β), °K/cm
0
.08
.16
.24
V / f(β), cm/sec
t, cm
.05
.04
.03
.02
.01
1.0
.8
.6
.4
.2
0
f(β)
β = Tm / To
Tm
400
800
1200
1600
To, °K

EQUIPMENT AND PROCESS DEVELOPMENT

1. RF HEATED SYSTEM - PROBLEMS RELATING TO CONTINUOUS GROWTH.
2. RESISTANCE HEATED SYSTEMS - PROBLEMS RELATING TO CONTINUOUS GROWTH AND CRYSTALLINITY CONSIDERATIONS.

PROBLEMS ADDRESSED IN CONTINUOUS RIBBON GROWTH

1. SCALE UP OF CRUCIBLE AND ASSOCIATED COMPONENTS.
2. DIE DESIGN FOR MENISCUS CONTROL AND MENISCUS DIMENSIONS.
3. RIBBON GUIDANCE AND COLLECTION OR SPOOLING APPARATUS.

CONTINUOUS RIBBON GROWTH - CURRENT STATUS

MAXIMUM LENGTH	WIDTH	THICKNESS (AVERAGE)	GROWTH RATE (AVERAGE)	COMMENTS
80 FT	1 IN.	~8-10 MILS	~1 IN./MIN	RUN TERMINATED DUE TO DEPLETION OF MELT.
60 FT	1 IN.	~3-10 MILS	~1 IN./MIN	RUN TERMINATED.
40 FT	1 IN.	~8-10 MILS	~1 IN./MIN	RUN TERMINATED

PROBLEMS ADDRESSED IN RIBBON QUALITY

1. CONTROL OF VERTICAL TEMPERATURE GRADIENTS.
2. MENISCUS CONTROL CONSIDERATIONS.
3. HIGH MENISCUS MODE (HMM) OF OPERATION.

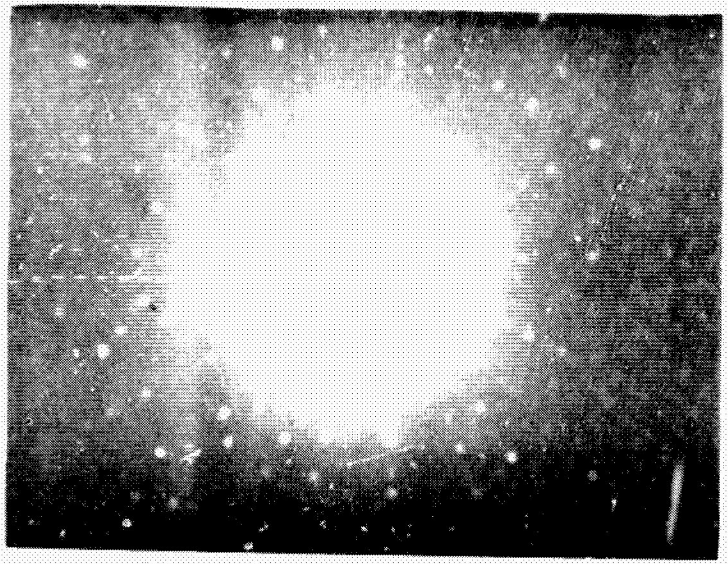

SEED - GROWTH PLANE (111)
GROWTH DIRECTION $[\bar{2}11]$

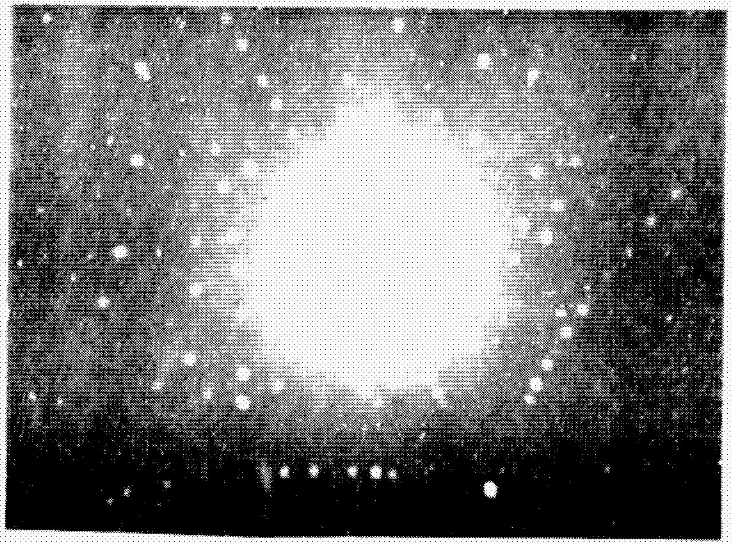

5 CM FROM SEED - 35° FROM (111)

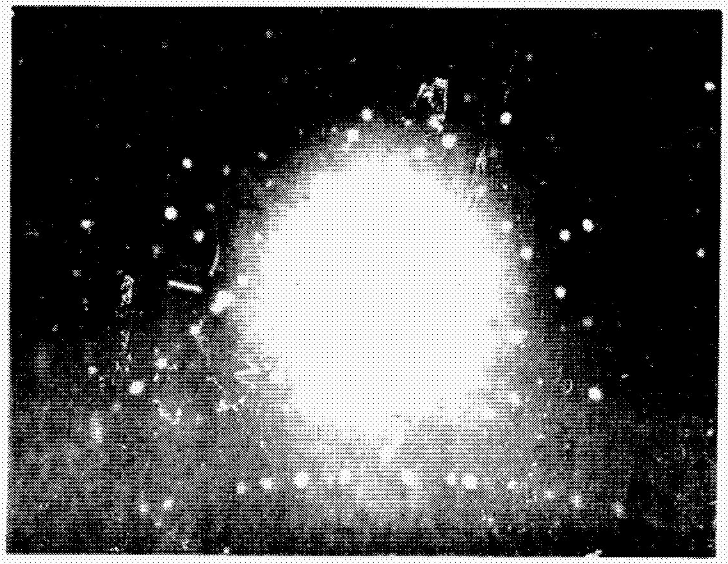

14.5 CM FROM SEED - 16° FROM (111)

45 CM FROM SEED - 16° FROM (111)

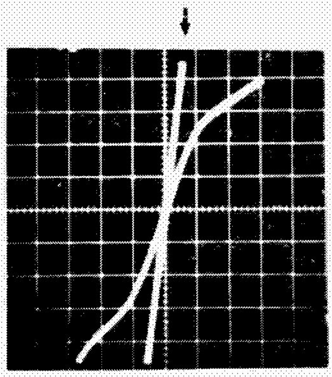

1-3

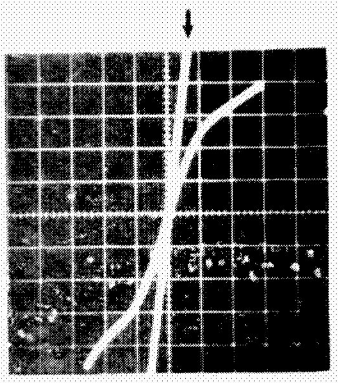

1-2

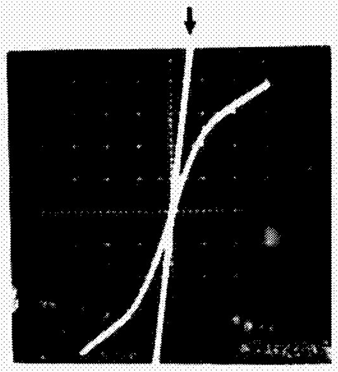

2-4

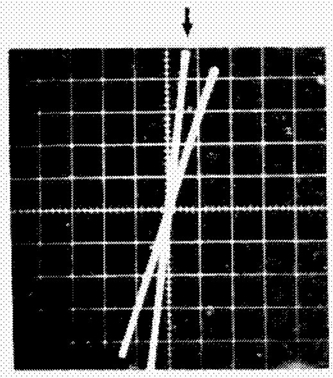

1-4

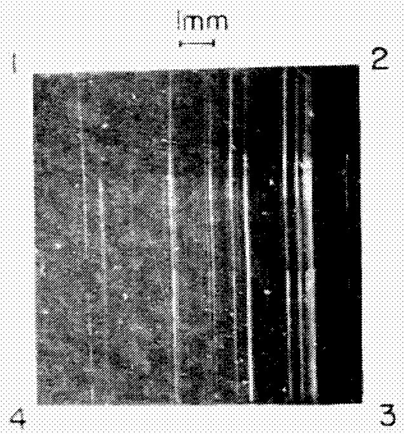

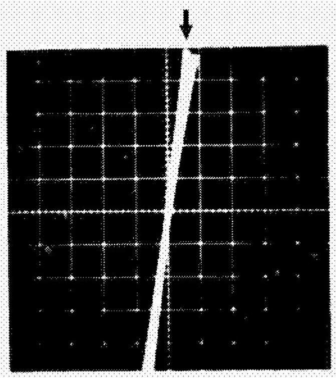

2-3

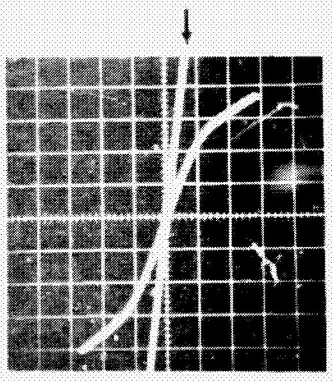

3-4

1.5 Ω-cm FZ →

SAMPLE: 14-55-3-7

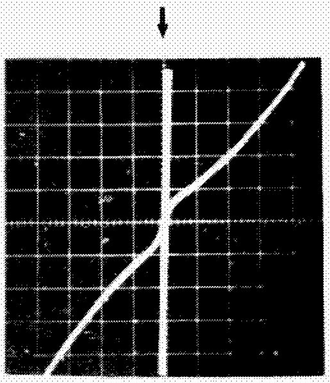

2-4

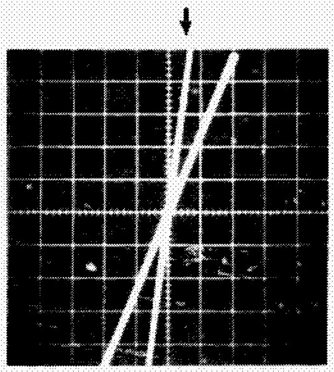

1-2

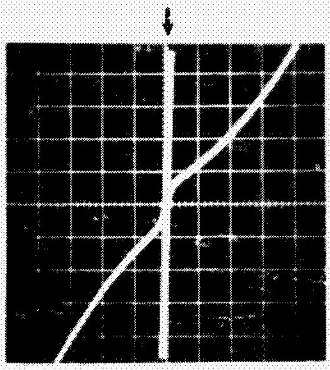

1-3

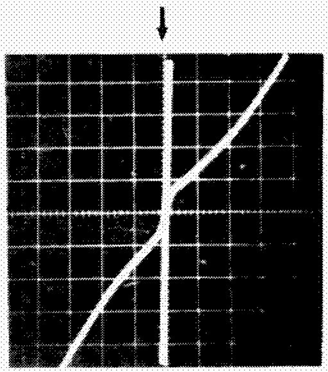

2-3

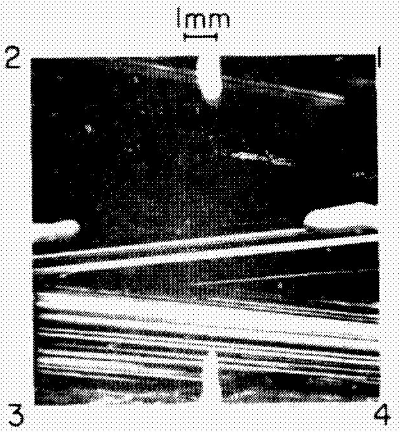

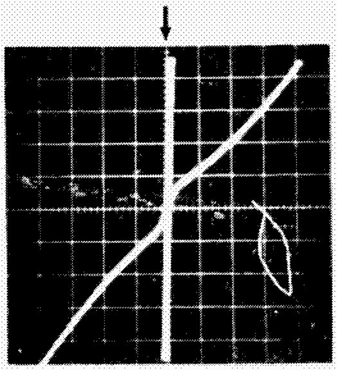

1-4

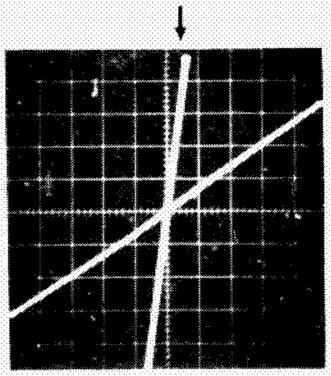

3-4

1.5 Ω -cm FZ →

SAMPLE: 14-38-3-4

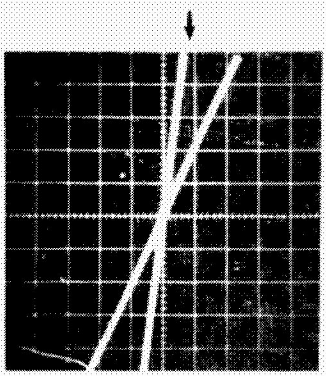

1-3

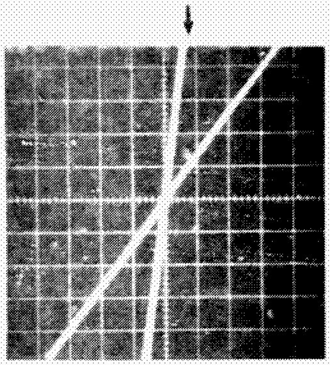

1-2

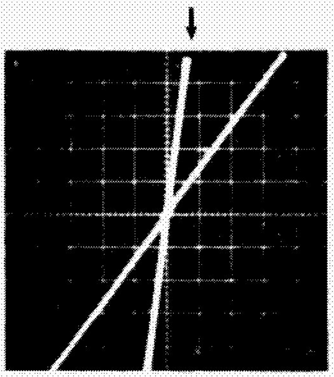

2-4

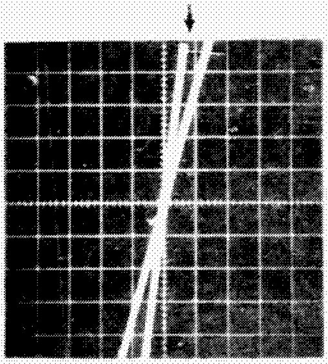

1-4

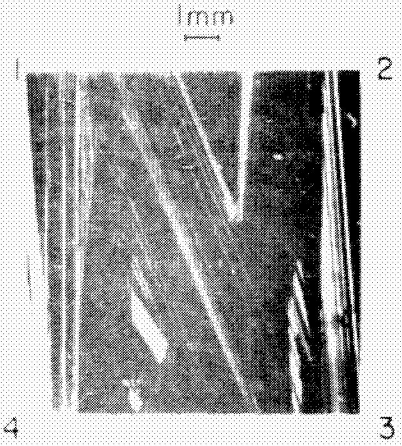

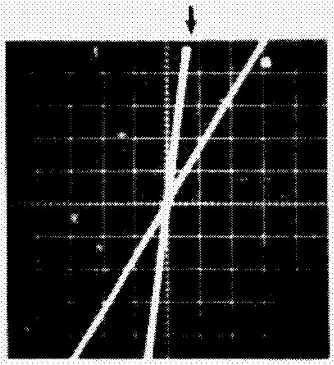

2-3

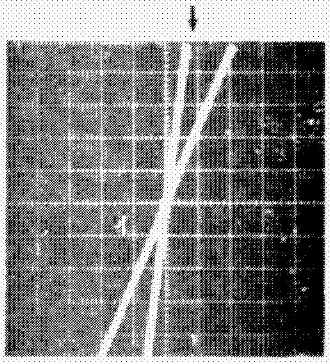

3-4

1.5 Ω -cm FZ →

SAMPLE 14-39-4-5

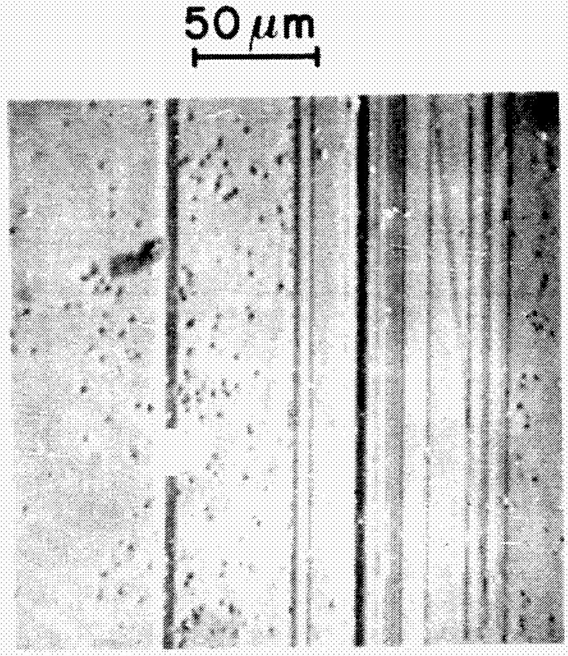
50 μm

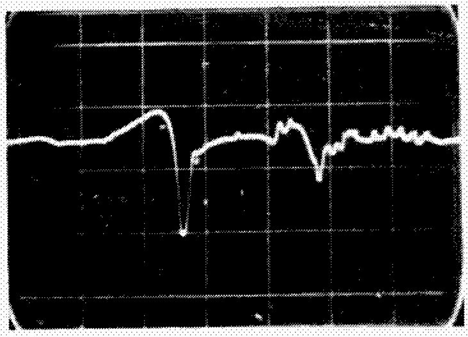

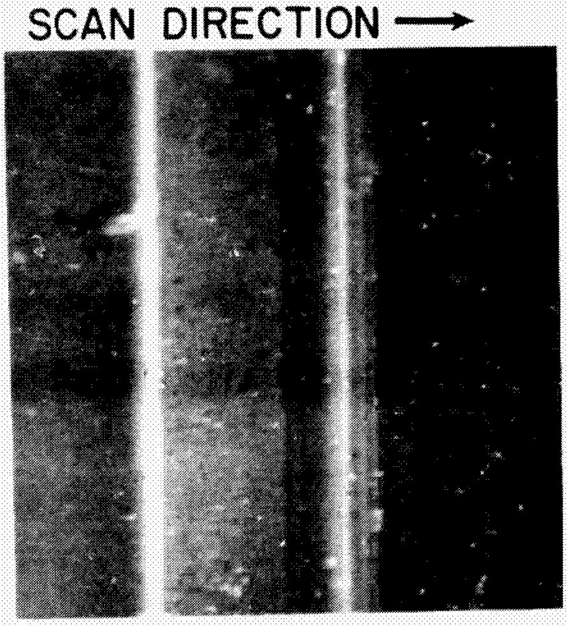
SCAN DIRECTION →

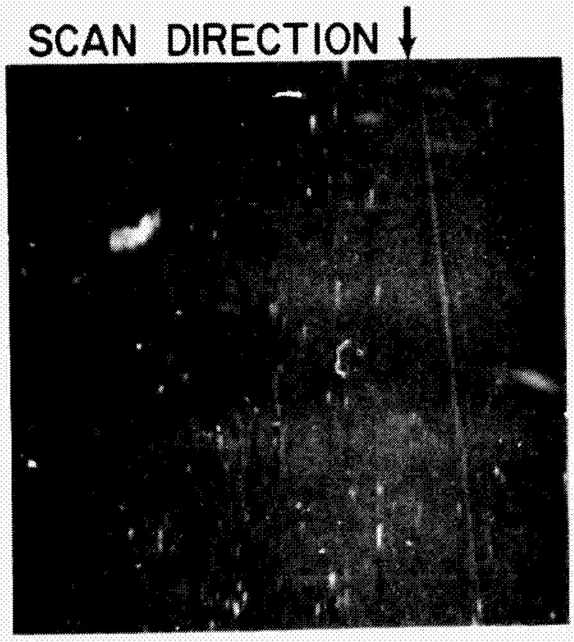
SCAN DIRECTION ↓

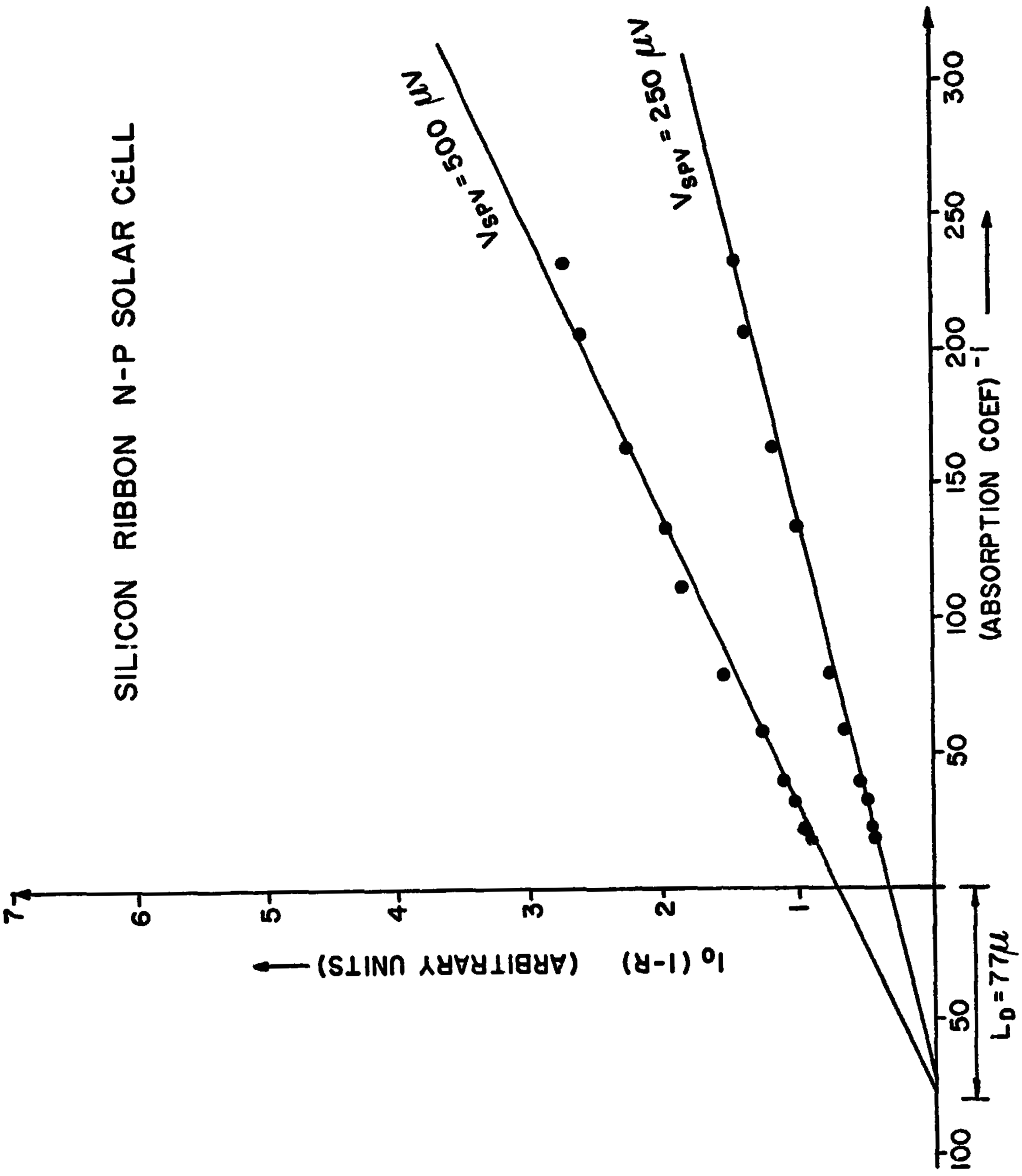
SILICON RIBBON N-P SOLAR CELL
$V_{SPV} = 500\ \mu V$
$V_{SPV} = 250\ \mu V$
$I_0\ (1-R)$ (ARBITRARY UNITS)
1
2
3
4
5
6
7
(ABSORPTION COEF)$^{-1}$
50
100
150
200
250
300
100
50
$L_D = 77\mu$

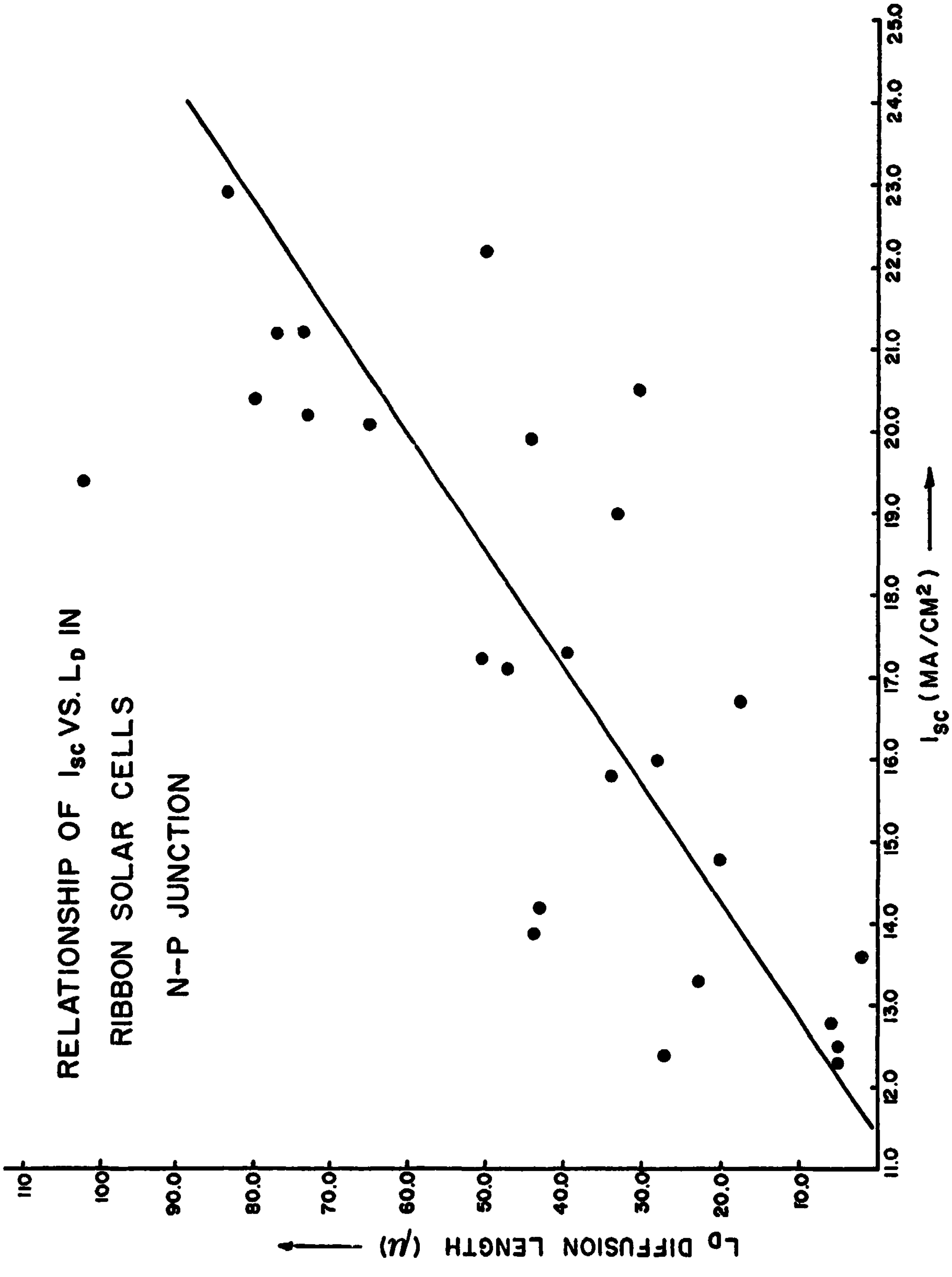

RELATIONSHIP OF I_{sc} VS. L_D IN RIBBON SOLAR CELLS

N-P JUNCTION

SUMMARY OF KEY RESULTS

1. THEORETICAL UNDERSTANDING OF MENISCUS SHAPE AND STABILITY AT RIBBON EDGES.

2. THEORETICAL RELATIONSHIPS BETWEEN CRYSTAL ORIENTATION AND RIBBON DIMENSIONS HAVE BEEN DETERMINED.

3. FACTORS RELATING TO THERMAL EFFECTS AND CRYSTAL SHAPE CONTROL HAVE BEEN ANALYZED.

4. CONTINUOUS RIBBON GROWTH HAS BEEN ACHIEVED WITH THE MAXIMUM LENGTH TO DATE BEING 80 FT (1 IN. WIDE, 8-10 MILS THICK).

5. THE STRUCTURAL CHARACTERISTICS OF RIBBONS AND STRUCTURE - PROPERTY RELATIONSHIPS HAVE BEEN STUDIED.

6. A FEW HIGH QUALITY RIBBONS WHICH PROPAGATE AND MAINTAIN SEED ORIENTATIONS HAVE BEEN GROWN. THIS GROWTH HAS BEEN ACHIEVED WITH THE HIGH MENISCUS MODE OF OPERATION OF THE SYSTEM.

STATUS SUMMARY

A. BASIS ESTABLISHED FOR EXPERIMENTAL DEVELOPMENT OF FAST, WIDE RIBBON.

B. CONDITIONS ESTABLISHED FOR CONTINUOUS UNATTENDED GROWTH.

C. EFFECT OF GROWTH PARAMETERS ON QUALITY UNDERSTOOD TO PERMIT SYSTEMATIC QUALITY IMPROVEMENT

- A + B + C -

LOW COST HIGH QUALITY SHEET PRODUCTION

EFG SILICON RIBBON SOLAR CELLS

K. V. Ravi, H. B. Serreze, H. E. Bates, A. D. Morrison
D. N. Jewett and J. C. T. Ho

Mobil Tyco Solar Energy Corporation
Waltham, Massachusetts 02154

Presented at the

11th

PHOTOVOLTAIC SPECIALISTS CONFERENCE

PHOENIX, ARIZONA
MAY 6-8, 1975

Sponsored by IEEE
In Cooperation with the
National Science Foundation
The Energy Research & Development Admin.
and Arizona State University

EFG SILICON RIBBON SOLAR CELLS

K. V. Ravi, H. B. Serreze, H. . . Bates, A. D. Morrison
D. N. Jewett and J. C. T. Ho

Mobil Tyco Solar Energy Corporation
Waltham, Massachusetts 02154

SUMMARY

The growth and characteristics of edge-defined, film-fed grown (EFG) silicon ribbons are discussed. Factors involved in the growth of continuous lengths of 1 in. wide ribbons are examined. The structural and electrical characteristics of the ribbons have been studied and the results are presented. Solar cells have been fabricated using the ribbon crystals and typical AM0 efficiencies of 6 to 10% have been realized.

INTRODUCTION

Among the principal factors that affect economically and technically the attainment of large scale silicon photovoltaic systems is crystal growth. The cost factors associated with the conventional Czochralski growth technique are such that alternative procedures for obtaining single crystal silicon in ribbon form by direct solidification from the melt are desirable. One such technique is the edge-defined, film-fed growth (EFG) process whose features have been discussed elsewhere (1, 2). Initial results of ribbon growth experiments relating to silicon were reported in previous meetings of this conference (3, 4) and elsewhere (4a). It is the intent here to present an update of this technology. A discussion of the growth aspects of silicon ribbon is followed by a description of the structural characteristics of the state-of-the-art ribbon. Structure property relationships have been studied with specific emphasis on the effects of linear defect boundaries on photo-generated signals in the material. Data on ribbon solar cells is presented in the concluding section of this paper.

RIBBON GROWTH

The most prominent characteristic of the EFG technique is the ability to grow ribbons of a given dimension with good shape control. In order to attain this dimensional control, a die is inserted between the bulk of the melt and the growing interface. This produces several advantages, but also certain engineering constraints which must be considered in the growth of silicon ribbons by EFG.

Briefly, the advantages of the EFG process are: the isolation of the growth interface from the bulk of the melt; the production of an interface which stays at a constant location relative to the isotherms in the system - instead of fluctuating up and down with the melt - the development of a fluid flow system which ensures that the composition of the ribbon will be that of the melt feeding the ribbon; and, of course, direct shaping of the crystal. The basic requirement is the existence of a die material which is wet by, but which does not significantly react with molten silicon.

The die material currently being used is graphite. Graphite presents a number of problems which have to be overcome in its use as a die for EFG. The most apparent problem is the formation of silicon carbide in the form of a layer and in particulate form within and on top of the die during ribbon growth. The particles, about 0.05 to 0.1 mm in the largest dimension, create a rough surface on the die. They often protrude from the bottom of the meniscus, appearing cold and black in contrast to the meniscus of molten silicon. These cold precipitates cause projections of the growth interface towards the cold region. These projections cause a rough solid-liquid interface thereby leading to instability and, possibly, structural defects.

Although graphite reacts with molten silicon, the reaction rates have been observed to be slow enough for the successful development of ribbon growth technology. Up to 65 feet of ribbon has been grown from a single die. Examination of the dies following the sustained growth of long lengths of ribbon has not revealed the presence of significantly more SiC on top of the die as compared to carbide formation on dies through which small lengths of ribbon ($<$ 10 ft) have been grown. Typical examples of dies from which short and long ribbons have been grown are shown in Fig. 1. Further, die erosion or distortion effects were not observed in any of the dies used for long growth runs.

The die, which provides the advantages of shaping, isolation from the melt, etc. also imposes certain requirements in terms of design of the die and of the thermal environment surrounding the die. In addition, certain operating or process constraints exist which have to be considered in order to achieve successful growth. For example, the amount of melt which is in proximity to the growing ribbon is quite small in comparison to Czochralski growth. Therefore, loss of very small amounts of heat can provide enough of a temperature decrease to cause solidification of the ribbon at the die top.

Silicon has approximately twice the thermal conductivity of graphite. As a result, more heat flux per cross sectional area travels up the column of liquid silicon than up the graphite die. In addition, the outside and top edges of the die tend to be cold with respect to the molten silicon, since in typical rf heated systems, the outer sloping face of the die is free to radiate heat away, and the only source of heat to that portion of the die is the die holder or lower structures. In this case the interface will tend to curve downward towards the die edges; if the temperature of the liquid near the die top approaches the melting point, there will be a tendency for the interface to advance towards the die edges.

There are other areas where a detailed consideration of the thermal environment at the top of the die is crucial. For instance in spreading a small seed into a full width ribbon there are several different thermal stages which are observed. Before seeding takes place, the temperature along the top of the die is nearly uniform and is just above the melting point. Upon seeding there is additional heat loss up the seed by means of conduction which tends to decrease the temperature at the top of the die and causes the silicon to freeze. Heat is added at this time in order to remelt the silicon, or [illegible]cally the melt temperature is raised before seeding to allow for this heat l[illegible] the seed has been melted and the meniscus has been established, growth may begin. However, at this point the silicon at either side of the seed is much hotter than the silicon directly under the seed. Therefore, the ribbon will tend to taper instead of spreading. In order to overcome this tapering, growth speed is increased rapidly until the heat of solidification at the narrow seed is generated rapidly enough to compensate for extra heat lost up the seed. At this point the silicon under the growing seed may be hotter than the silicon on either side of the seed, and the ribbon will then spread in response to the temperature gradient.

One difficulty with this approach is that the growth rate must be raised very rapidly to a high level and this may entail dropping the heat input to the top of the die to such an extent that the rest of the silicon freezes and the growth is aborted. Full width seeding with a growth system which is essentially isothermal along the die top has been developed to avoid this situation. The edges of the die and ribbon radiate enough extra heat away to allow the ribbon to stay at full width.

In developing this technology, three meniscus shapes (Fig. 2) have been used as simple guides to the thermal environment during ribbon growth. The first shape, (Fig. 2A) concave with respect to the ribbon (meniscus closer to the die at the center), is attained when the ends of the ribbon are hot with respect to the center of the die. Growing with this meniscus shape causes the ribbon to taper. Attempts to spread the ribbon by decreasing the temperature lead to freezing of the ribbon to the center of the die.

The opposite thermal condition (Fig. 2B), the ends of the ribbon cold with respect to the center, leads to a meniscus convex with respect to the ribbon (meniscus closer to the die at the ends). In this case the ribbon will spread rapidly, but it is difficult to prevent the edges of the ribbon from freezing to the die.

Finally, a meniscus curved up on one end and down on the other results from one end being hotter than the other. A ribbon grown in this environment tends to taper on one side and spread on the opposite (Fig. 2C). This phenomenon is also caused by having the die, susceptor, heat shields, or other components slightly out of balance. Tightening of component specifications and special care in assembly of the growth set up are the major ways to avoid this problem. The vertical gradient variations are also crucially important. These gradients determine allowable growth speeds, sensitivity of meniscus height to changing growth speeds, etc.

Silicon ribbons have been grown from three different types of furnaces and with three types of pulling mechanisms. The initial experimental work was done with high frequency induction systems. These are characterized by simple growth set up design, good visibility and rapid power adjustment capability. The disadvantages include higher power consumption, rf interference in control devices, and the presence of a single power zone. The motor generator induction furnace has the advantages of the rf system but uses less power and produces less electronic interference. It still is characterized by one hot zone. Fig. 3 shows a typical example of an rf heated growth station.

The resistance furnaces which have been more recently developed have independent top heating zones which permit the attainment of continuously variable thermal gradients within the die. In addition, the combination of reliability, low power consumption (a factor of 3 less than rf heating), low electronic interference, and design flexibility make this approach more desirable. Its drawbacks are associated with the more complicated, larger system enclosures and the added requirements imposed on heating element design. Fig. 4 shows an example of a resistance heated system.

Two types of vertical pulling mechanism have been used. The hydraulic piston system first used provides a very smooth stroke, but it is quite bulky, not easily controllable and difficult to monitor. The second type uses a motor driven ball screw assembly which, with suitable mechanical damping, provides easily controlled and monitored pulling. Finally, two different continuous belt puller designs have been used to grow continuous ribbon. The advantages of electric control and monitoring are still present, and of course there is an unlimited pull stroke. The major problems are providing adequate mechanical guid[illegible] the ribbon, avoiding ribbon "wander" within the belts of the pullers, and in the [illegible]ing of seed holders which can move through the belts with a minimum of disturbance in the transition from seed holder to ribbon. All of these systems have been used to successfully grow 1 inch wide ribbons. As mentioned above, ribbons of lengths up to 65 feet have been grown employing continuous belt pullers. The ribbons have been sufficiently strain free to permit reeling on to ~ 3 ft diameter reels. Fig. 5 shows the reeling mechanism on a growth station.

RIBBON CHARACTERISTICS

The two most significant ribbon characteristics in addition to dimensional control are the chemical purity and crystallographic structure.

Chemical Purity

Because of the intimate contact between the liquid and the die during the growth process it is necessary not only that the die material itself not introduce significant numbers of electrically active impurities, but also that impurities in (and on) the die be minimized. Carbon is electrically inactive in silicon; however, the total impurity content of typical high purity commercial graphites can be of the order of 100 to 600 ppm. Transition metals are generally present as major fractions of the total, as are aluminum and silicon. Fabrication and handling of graphite dies can also, of course, introduce a broad spectrum of impurities. Since nothing is known about the kinetics of impurity transfer from the bulk of the die to the melt, it is safest to assume that all impurity atoms present in the die will be immediately introduced into the melt, and thus to strive to lower the impurity levels in the graphite as far as possible. As an example, it is found that the typical graphite die material being used (DFP-2 grade having been subjected to a high temperature purification treatment by the manufacturer) contains approximately 5 ppm of iron. This translates into approximately 6×10^{16} atoms of iron in a 2.5 cm wide by 3.05 cm long, ~0.5 cm thick graphite die.

A typical melt used with this size die contains about 10 cm^3 of silicon. Complete transfer of the Fe to the melt would then produce a level of 4×10^{15} atoms/cm^3 of Fe in the silicon. If in fact only 10% of the total finds its way into the melt, the resulting 4×10^{14} atoms/cm^3 of Fe is still a fairly high concentration for a deep level impurity. Given these considerations, the course of effort followed to achieve suitable low impurity levels in graphite dies is discussed below.

Vacuum Firing

The first approach to cleaning graphite dies was vacuum outgassing. This process evolved from a fairly mild 1500°C, 10^{-2} torr treatment which probably only removed the more volatile contaminants introduced during fabrication, giving typical ribbon resistivities of 0.5 Ω-cm, to a 1900°C, 10^{-5} torr, one hour treatment, which, when applied to dies made from DFP-2 (i.e., pre-purified) graphite allowed fairly consistent growth of ribbon of 1 to 2 Ω-cm, p-type resistivity. Solar cells produced from these ribbons typically performed at about 1/2 to 2/3 the level of control cells made from commercial Czochralski silicon. Spectral response data, showing reduced red-response for the EFG-ribbon cells relative to the Czochralski cells, were taken to indicate the presence of lifetime killing impurities which presumably were not being removed by the vacuum-firing treatment.

Hydrogen Chloride Firing

The use of high temperature treatments in chlorine or fluorine-containing atmospheres for the production of nuclear-grade and spectrographic graphites is fairly well-known (5). The treatment works by diffusion of impurity atoms from within the bulk of the graphite grains to their surfaces, there to react with the halogen atoms forming volatile halides which are carried away in the gas phase.

Consequently, a procedure for the post fabrication purification of the dies has been established involving the heating of the dies at temperatures of ~1300°C in an atmosphere of argon and anhydrous HCl with a 5% HCl content by volume. The purification times are typically 5 hours. As a result of this process significant improvements in purity have been observed as evidenced by electrical measurements and solar cell data from ribbons grown from purified dies.

Crystallographic Structure

Typical ribbon crystals currently being grown by the EFG process are characterized by a large density of crystallographic defects. A detailed analysis of defect types and densities in many ribbons has been made and the following is a brief discussion of these characteristics. By far the most predominant defect types observed are twins and dislocations with occasional low angle grain boundaries. In addition, silicon carbide (SiC) particles are observed as inclusions distributed randomly across the length and the width of the ribbon. Typical characteristics of current ribbons can be described as follows.

Twins

Twin boundaries of varying densities and orientations are observed. Both growth twins and deformation twins are formed, typical examples of which are in Fig. 6. Deformation twins are sometimes characterized by the presence of dislocations in their vicinity and appear as fine narrow bands, whereas growth twins are typically wide and generally free of dislocations. At least three modes of twin nucleation appear to be operative in the crystals. (a) Twins have been observed to nucleate at SiC particles embedded in the ribbon; a typical example is shown in Fig. 7. (b) twin nucleation at the seed-crystal interface is a common occurrence with both deformation twins and growth twins forming at the interface; examples of this are shown in Fig. 8. (c) growth instabilities represented by local changes in ribbon dimensions have also been observed to generate twins as shown in Fig. 9.

Dislocations

Most of the dislocations observed appear to be deformation induced. This is evident from the observation that the dislocations are aligned along close packed planes to form slip bands. A typical case is shown in Fig.10. Dislocation-twin interactions are frequently observed with local dislocation pile-ups (Fig. 11). Dislocation generation around SiC particles is also observed.

SiC Particles

The inclusion of SiC particles in ribbon crystals can occur as a result of three possible mechanisms; (a) precipitation of dissolved carbon in the solid in the form of SiC subsequent to solidification. (b) precipitation of SiC at the solid-liquid interface as a result of carbon rejection from the solidifying crystal into the meniscus, and (c) the pick-up of SiC particles by the interface from the top of the die with subsequent incorporation into the solid.

Although a definitive determination of the relative importance of these processes has not yet been obtained, initial studies indicate that by far the most frequently occurring process is the pick-up of SiC particles by the solid-liquid interface from the die and the attendant inclusion of the particles in the ribbon. Typical particle densities are in 1-2 particles/cm^2 range.

The influence of seed orientation on the morphology of linear boundaries (twins and arrayed dislocations) is observed to be quite marked. For example, ribbons with a (110) $<1\bar{1}2>$ orientation are found to have predominantly linear boundaries parallel to the ribbon edges.

A number of avenues are available for obtaining ribbon quality improvements. One approach is discussed here which involves the control of the vertical temperature gradient within the die to minimize the dissolution and reprecipitation of carbon in the form of SiC. A reduction in the vertical temperature gradient is achieved by the use of an independent top or die heater in a resistance heated crystal growth apparatus (Fig. 4). By suitably controlling the temperature at the die top the temperature difference between the silicon in the crucible and the silicon at the top of the die (the meniscus) can be kept at the minimum. By this means short lengths of ribbon have been grown with significantly reduced defect densities as compared with ribbons grown under conditions of large vertical temperature gradients within the die.

Table I shows the average defect densities observed in the ribbon. It is apparent that densities of both linear boundaries (twins and slip bands) and dislocations are lower in crystals grown from resistance heated systems employing die heaters to appropriately control temperature gradients.

Table II lists the average electrical properties of ribbon crystals with data on typical Czochralski crystals of similar resistivity for comparison. A characteristic that is immediately apparent is the relatively large range in properties observed in the ribbon crystals. This fact in addition to the largely linear morphology

Table I. Average Defect Densities of EFG Silicon Ribbons (20 in. after growth initiation)

	RF Furnace	Resistance Furnace
Parallel Boundaries/cm	7.5×10^2	3.9×10^2
Dislocations/cm^2	1.2×10^6	3×10^5

(Data represents average values from 20 specimens grown in an rf heated apparatus and 10 specimens from a resistance furnace).

Table II. Average Electrical Properties of EFG Silicon Ribbon: Boron Doped - 1.1 Ω-cm.

	Average	Range	Typical Czochralski Values
Resistivity:	1.8 Ω-cm	0.4 - 5.2	1.8
Mobility:	215 cm^2/V·sec	60 - 320	350
Photoconductivity Decay Time:	8 μsec	0.2 - 37	15
Absorption Coefficient at 1.8 μm:	16 cm^{-1}	0.1 - 65	0.05 - 0.5

(Based on 33 samples from 14 ribbons grown from one rf system).

of defects observed in the ribbon, indicates that a full understanding of local defect-property relationships is required to obtain a complete characterization of the crystals.

STRUCTURE PROPERTY RELATIONSHIPS

The conversion efficiencies of silicon solar cells are dependent, among other things, upon the presence or absence of non-radiative recombination centers and upon defect-impurity factors that reduce the minority carrier lifetime in the bulk of the crystal. The presence of large densities of crystallographic defects and transition metals in ribbon crystals undoubtedly adversely affects solar cell properties. In order to determine the specific effects of defects on electrical characteristics, a relatively detailed examination of structure-property relationships is needed. A variety of procedures has been adopted to evaluate the specific electrical effects of particular defects. Among the most dominant defects, as previously discussed, are linear boundaries represented by twin and slip bands. These linear boundaries have been observed to exhibit highly anisotropic properties. The local electrical characteristics of the ribbons were determined by measuring the local photovoltage and photocurrent generated by a laser beam incident on a ribbon solar cell. By scanning the laser beam across the width of the ribbon and recording the photogenerated signal, it was possible to evaluate both the distribution of properties across the width, as well as the effects of local linear defect boundaries. Fig. 12 shows three typical traces of the short circuit current response produced in a ribbon solar cell by a scanned laser beam at three different regions of a long ribbon. Two effects are notable in these plots. The current response at the edges of the ribbon is markedly reduced in comparison with the response at regions removed in comparison with the response at regions removed from the edges, and localized small scale variations in the signal are evident across the entire ribbon width. The localized reduction in photocurrent has been directly related to the presence of linear boundaries. The optical micrograph in Fig. 12 indicates a set of parallel boundaries which cause the particular reduction in short circuit current shown by the arrows on the plots. A one-to-one correlation between the presence of linear boundaries and a local reduction in photogenerated signals has been observed.

When the defect morphology is more complicated, as in the case of intersecting boundaries, the effects on electrical characteristics are further exacerbated. This is demonstrated in Fig. 13 where the short circuit current generated at a region containing multiple intersecting boundaries is much lower than that generated in regions either free of boundaries or containing non-intersecting parallel boundaries.

This distinction in the properties of intersecting and non-intersecting boundaries has also been observed in the breakdown characteristics of mesa diodes fabricated in ribbon crystals (6) as well as in solar cell properties (7).

An indication of the range of light generated current response in a ribbon as a result of the presence of linear boundaries can be obtained by comparing the theoretically expected spectral response of a solar cell for different minority carrier diffusion lengths in the base material with the experimentally determined short circuit response at the wavelength of the laser beam (He-Ne laser with a wavelength of 633 nm). Fig. 14 shows a plot of the theoretically determined spectral response for different values of diffusion length. (See Appendix for a discussion of the theoretical basis used to obtain the plots in Fig. 14). The range of values for the collection efficiency (Q) at 633 nm obtained from the laser measurements is superimposed over the theoretical plots. Q values were calculated from Eq. 1 in the Appendix by taking the peak of short circuit photocurrent response due to the laser beam excitation (λ = 633 nm. No (incident photon flux density) = 4.8×10^{17} photons/cm^2 sec) as the maximum and the valley response as the minimum in the range. It is observed that the peak response corresponding to defect-free regions indicates that the diffusion length for minority carriers is $\sim 30\ \mu$ whereas the diffusion length at the linear boundaries is $\sim 5\ \mu$. A reduction in the minority carrier diffusion length of a factor of six results at the defect boundaries. This range, of course, is for a specific ribbon and could vary as a function of the particular processes, such as die purification techniques employed during ribbon growth.

The change in the diffusion length at the boundaries indicates either a reduction in the mobility or lifetime. This can be the result of the direct effect of the defect boundaries as a consequence of the strain associated with the boundaries or as a result of the presence of dangling bonds associated with dislocations. However, a detailed analysis of the I-V characteristics of ribbons containing linear boundaries suggests that an association of impurities with the boundaries is a more likely reason for the unusual electrical behavior (8). A more precise indication of the localized conduction behavior of linear boundaries was obtained by a scanning electron microscope operated in the electron beam induced current (EBIC) mode (9). This technique permits the investigation of the electrical effects of localized defect-impurity complexes in semiconductors (10, 11). The current generated in a diffused n^+p junction (a solar cell) by a scanning electron beam is amplified and displayed on a CRT. By operating the instrument in a single line scan mode the local interaction between the beam generated carriers and the linear defects can be observed. Fig. 15 shows a secondary electron image of a set of linear boundaries. The waveform shows the EBIC signal obtained when the beam is scanned across the linear boundaries by employing a single line scan. The instrument was operated at 30 kV with a beam current of 200 μA and spot size of ~1500 Å. When the beam crosses a linear boundary a local reduction in the EBIC signal is observed. The waveform represents the net flow of charge carriers at the space charge region of the p n junction in the region containing the linear boundaries. The abrupt change in the EBIC signal indicates that the boundaries function as local regions of low minority carrier lifetime in the ribbons. Further discussion of this phenomenon will be presented elsewhere (8).

RIBBON SOLAR CELLS

Solar cells have been fabricated from randomly sampled ribbon blanks, thus ensuring that all qualities of ribbon have been included. Typical junction depths sought were ~0.5 μm with phosphorous diffusion being performed in an oxidizing ambient. Cells up to 1 in. × 4 in. in size have been fabricated (Fig. 16) using Al - Ag contacts formed by evaporation through a mask. The data presented in this paper is from 1 cm × 2 cm solar cells.

As expected, the particular characteristics of ribbon crystals introduce certain unique problems in solar cell fabrication and performance. The effects of parallel and intersecting boundaries on solar cell properties have been reported elsewhere (7). The effects of non-random properties across the ribbon width discussed in the previous section are also reflected in solar cell performance. By selecting 1 cm × 2 cm specimens from both the central regions and the edges of 1 in. wide ribbons the influence of the edges on cell performance could be determined. Table III shows a comparative analysis of the properties of cells from the two regions. Significant degradation of cell characteristics from the edges of the ribbon supports the data presented in the previous section.

Spectral response measurements on ribbon solar cells indicated certain unique characteristics in terms of the short wavelength response of the cells. Ribbon cells were typically observed to function better toward the blue end of the spectrum as compared to Czochralski cells made under identical conditions. Figure 17 shows this result. The effects of die purification (vacuum heat treatment and halogen treatment as discussed in the Ribbon Characteristics section) are also

Table III. Solar Cell Data for Specimens Selected from Ribbon Edges and Ribbon Center

		Mean Values				
Type of Cell	No. of Cells	V_{oc} (mV)	I_{sc}/A (mA/cm^2)	P_{max}/A (mW/cm^2)	Fill Factor	Reverse Leakage (μA)
Center	7	529	18.7	7.0	0.71	620
Edge	7	516	17.8	5.8	0.62	2.1 mA

indicated. The reduced response of the ribbon cells in the red end of the spectrum is as expected. (The HCl die purification treatment shows the expected improvement in red response). The blue response however, is observed to be better for ribbon solar cells as compared to Czochralski cells. Typically, blue response can be improved by shallower junction depths (12). Consequently the junction depths for a large number of ribbon and control Czochralski specimens were measured and a difference of ~50% was observed in the depths with the ribbon specimens having shallower junctions when diffused under identical conditions. The mechanism involved in this phenomenon is being investigated and will be reported shortly (13).

Figure 18 shows typical I-V characteristics of current state-of-the-art ribbon solar cells. Typical efficiencies of 6 to 10% under approximate AM0 conditions have been realized, which compare very favorably with conventional Czochralski solar cells.

CONCLUSIONS

One inch wide ribbons ~8 to 10 mils thick have been grown continuously to various lengths up to 65 ft. The carbon dies used show no observable distortion or erosion indicating that continuous ribbon growth can be achieved with carbon dies.

Purification procedures adopted have demonstrated that impurities in the carbon dies can be reduced to improve the purity of the ribbons.

An initial study of defect distributions and structure property relatioships has shown that defect impurity association appears to cause the major problem in ribbon crystals. Improvements in electrical characteristics can be achieved by suitable reductions in both impurity content and defect densities. The use of resistance heated ribbon growth systems with controllable thermal environments has reduced defect densities markedly.

Solar cell efficiencies attainable with appropriate device process technology in ribbon crystals are around 6 to 10% under AM0 illumination conditions. These efficiencies have been attained with a current state-of-the-art material which includes relatively high densities of twins and dislocations in addition to transition metal impurities. Improvements in ribbon characteristics can be achieved by more refined thermal design of growth systems, improved purity, and a reduction in and control of defect densities and distribution.

ACKNOWLEDGEMENTS

The authors would like to gratefully acknowledge the invaluable technical assistance of D. Bliss, B. Little. H. Rao, A. Sood, V. White and D. Yates. The excellent art work is by C. Taylor. Valuable discussions with Dr. A. I. Mlavsky and Professor B. Chalmers have greatly contributed to this work.

Portions of this work were supported by NASA Contract NAS7-100 and NSF Grants GI-43873 and GI-37067.

APPENDIX

The collection efficiency Q (λ) of a photovoltaic cell can be expressed as:

$$Q(\lambda) = \frac{J_{s.c.}(\lambda)}{q\,N_{abs}(\lambda)} \qquad (1)$$

where

$J_{s.c.}(\lambda)$ = Short circuit density of the cell, (amp/cm^2)

$N_{abs}(\lambda)$ = Photon flux density being absorbed in the cell, (photon/cm^2 sec).

= $No\,(1-R)\,(1-e^{-\alpha(\lambda)\ell})$

and

No = Incident photon flux density, (photon/cm^2 sec).

R = Reflectivity of the cell surface.

$\alpha(\lambda)$ = Absorption coefficient as a function of photon wavelength λ, (cm^{-1}).

ℓ = Thickness of the cell, (cm).

By programming the expression for Q (α) formulated by Dale and Smith (14) in such a form that the input parameters depend on (for an N^+/P junction): the minority carrier diffusion length Ln in the p-type base material, junction depth Xj, surface layer carrier mobility μ_p, and lifetime τ_p, surface impurity concentration to base impurity concentration ratio Ns/NB, cell thickness ℓ, and surface recombination velocity Vs, the value of Q (α) the total collection efficiency can be calculated (15). The conversion of Q (α) to Q (λ) is accomplished by using the absorption data of Dash and Newman (16).

REFERENCES

1. B. Chalmers, H. E. LaBelle, Jr., A. I. Mlavsky, J. Crystal Growth, 13/14, 84 (1972).
2. J. C. Swartz, T. Surek, and B. Chalmers, J. Mat. Sci., 4, 255 (1975).
3. H. E. Bates, F. H. Cocks, A. I. Mlavsky, IEEE Photovoltaic Specialists Conference Record, 9th, (1972) p. 386.
4. H. E. Bates, D. N. Jewett, and V. E. White, IEEE Photovoltaic Specialists Conference Record, 10th (1973) p. 197.

4a. T. F. Ciszek, Mat. Res. Bull., 7, 731 (1972).

5. Industrial Graphite Engineering Handbook, Union Carbide Corporation, p. 605 (1970).
6. J. C. T. Ho and K. V. Ravi, to be published.
7. H. B. Serreze, J. C. Swartz, G. Entine and K. V. Ravi, Mat. Res. Bull. 9, 1421 (1974).
8. A. K. Sood, C. V. Hari Rao, H. E. Bates and K. V. Ravi, Recent News Paper No. 424 Spring Meeting of the Electrochemical Society, Toronto (1975).
9. J. J. Lander, H. Schreiber and T. M. Buck, Appl. Phys. Letters, 3, 206 (1963).
10. K. V. Ravi, C. J. Varker and C. E. Volk; J. Electrochem. Soc. 120, 533 (1973).
11. K. V. Ravi and C. J. Varker; Appl. Phys. Letters, 25, 69 (1974).
12. J. Lindmayer and J. F. Allison, COMSAT Tech. Rev. 3, 1 (1973).
13. H. B. Serreze and K. V. Ravi, to be published.
14. B. Dale and F. P. Smith, J. Appl. Phys., 32, 1377 (1961).
15. J. C. T. Ho, A. Kirkpatrick and F. T. C. Bartel, NASA Contract No. NAS2-5516, Ames Research Center (1970).
16. W. C. Dash and R. Newman, Phys. Rev. 99, 1151 (1955).

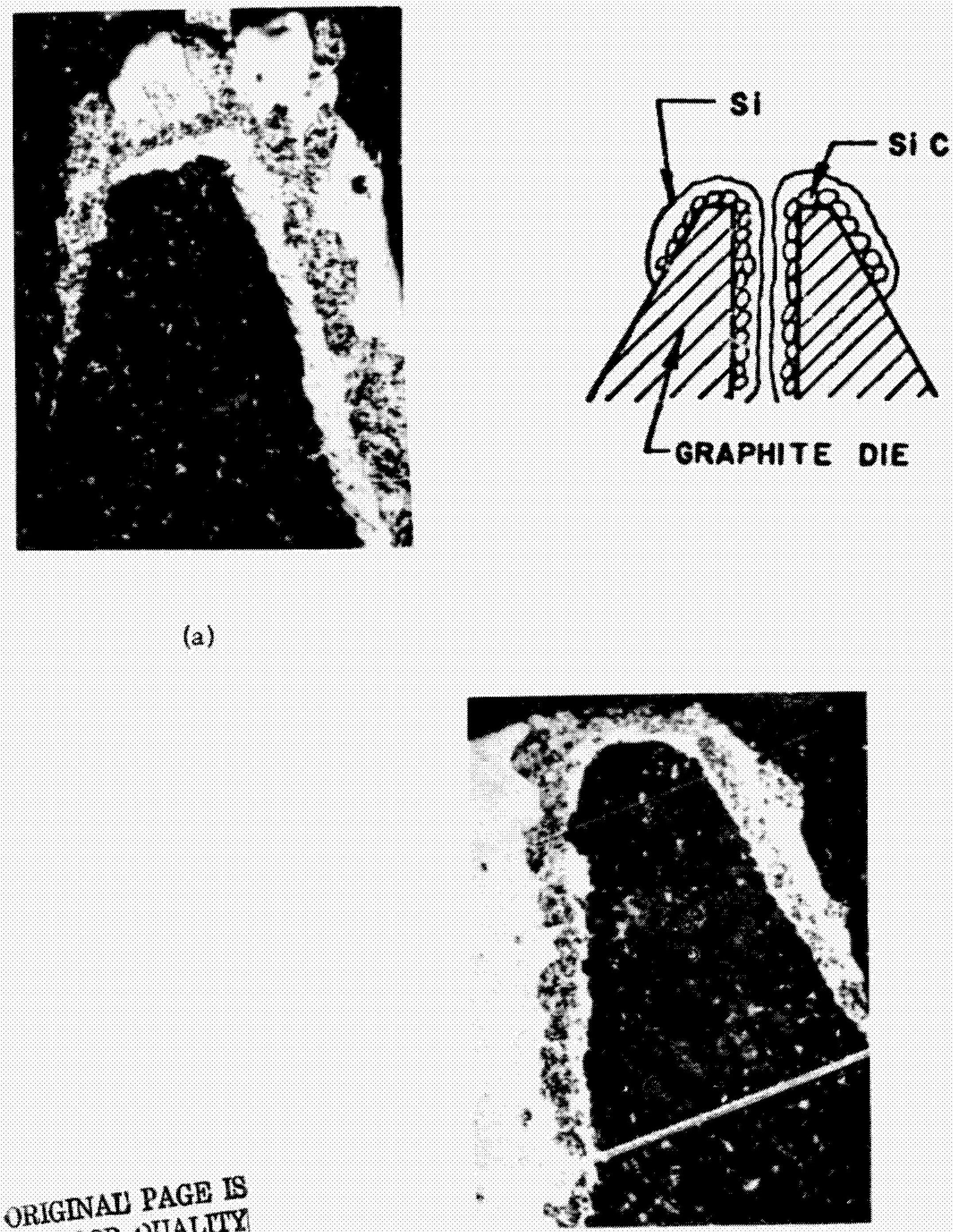

(a)

(b)

Fig. 1. Typical examples of dies from which short (< 10 ft) and long (> 40 ft) ribbons have been grown (a and b respectively).

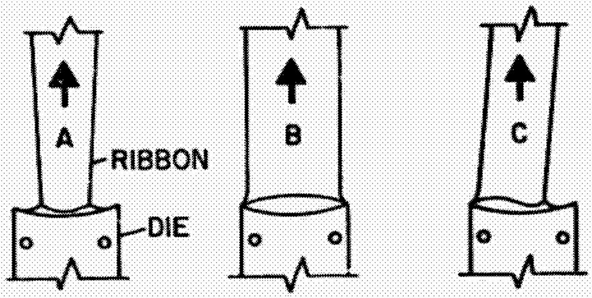

Fig. 2. Schematic sketches of meniscus shapes. See text for discussion.

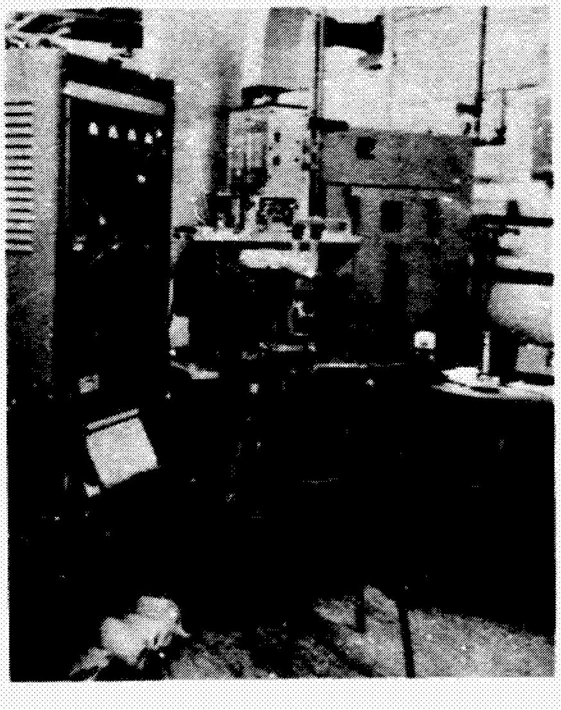

Fig. 3. Typical example of an rf heated ribbon growth apparatus.

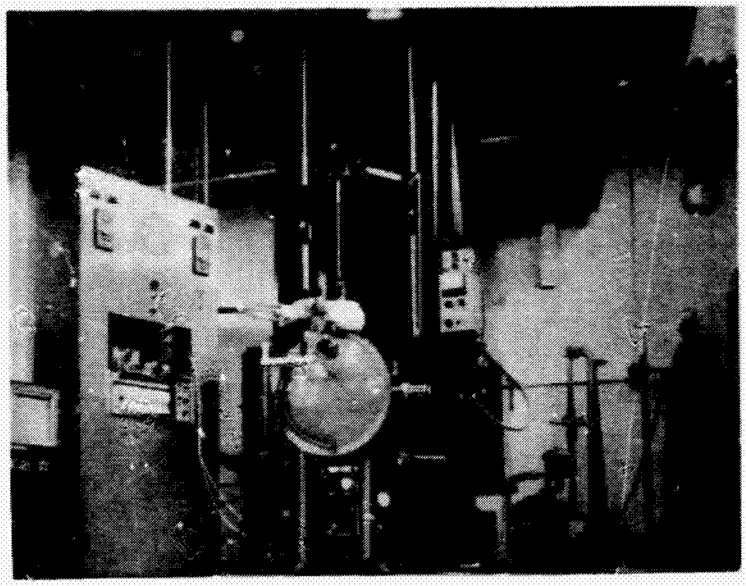

Fig. 4. Resistance heated ribbon growth apparatus.

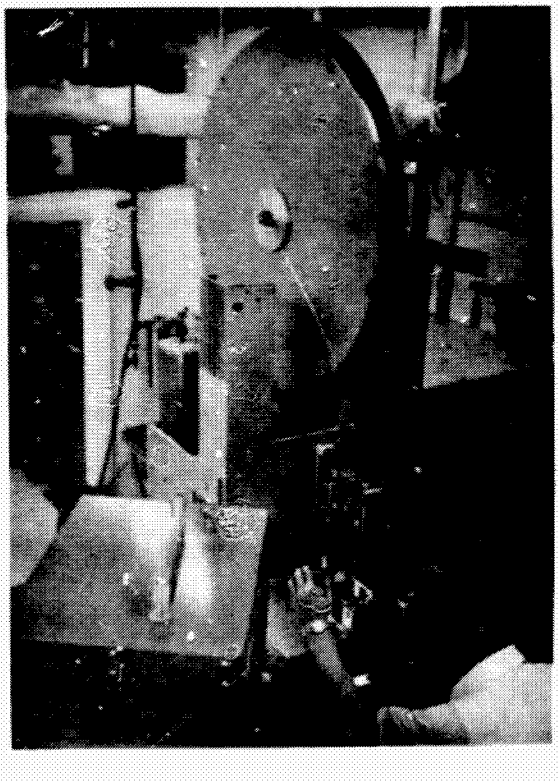

Fig. 5. Approximately 3 ft diameter reeling mechanism mounted on a continuous belt puller. The ribbon crystal can be observed emerging from the belt puller and on the reel.

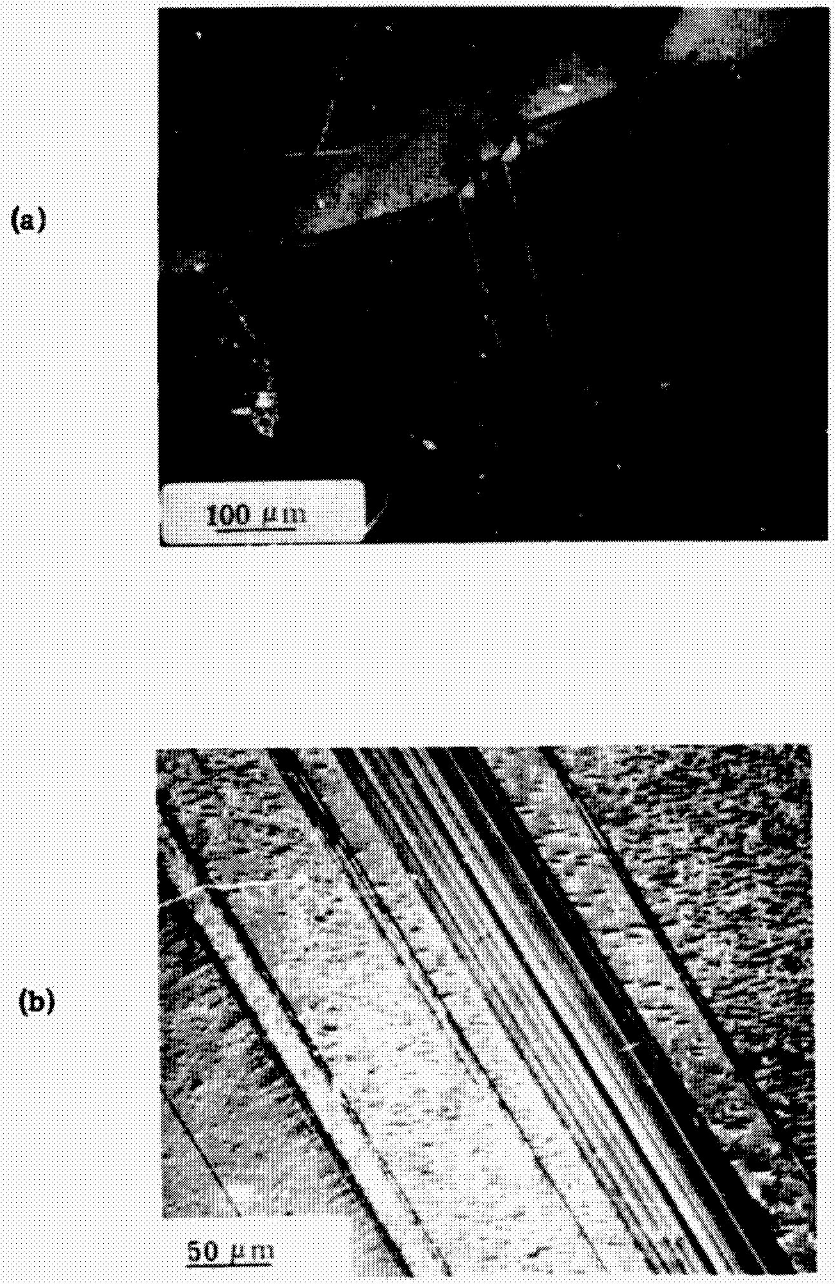

Fig. 6. Typical examples of growth twins (a) and deformation twins (b). Growth twins are typically wide and generally not associated with dislocation. Deformation twins often occur as closely spaced linear boundaries frequently in association with dislocations.

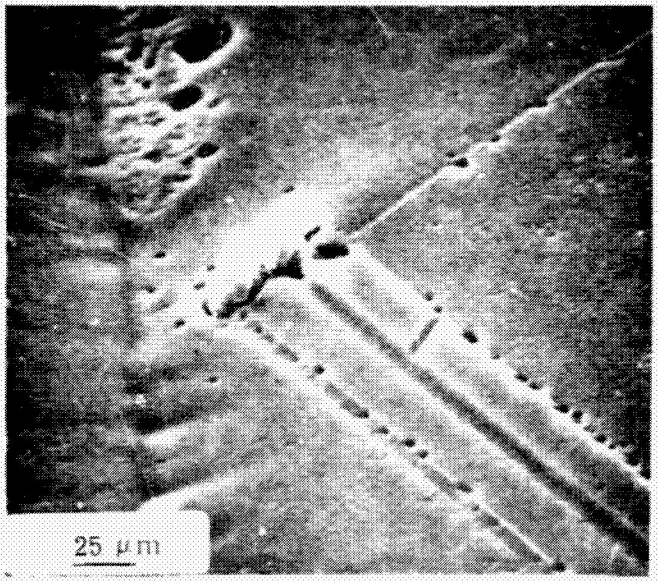

Fig. 7. Twin nucleation from SiC particles embedded in the ribbon.

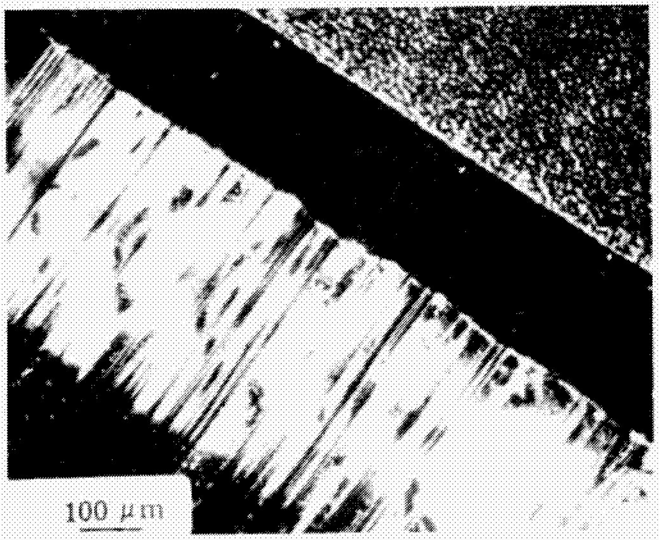

Fig. 8. Twin nucleation at the seed crystal interface.

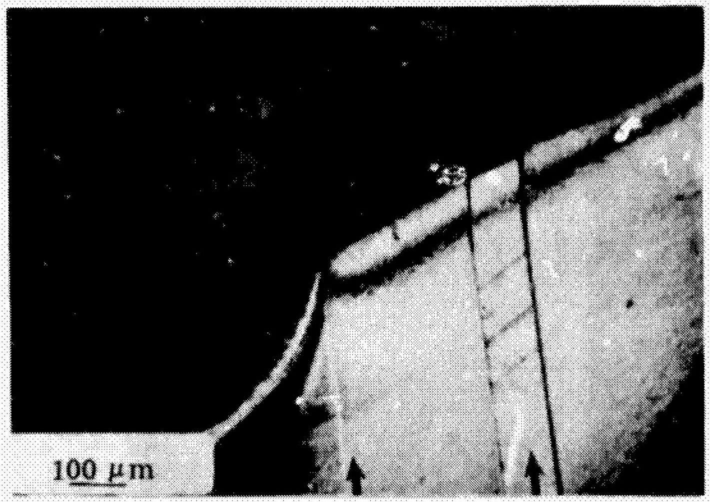

Fig. 9. Twin nucleation due to growth instabilities as represented by changes in ribbon dimensions. Arrows indicate regions of the ribbon which have changed dimension locally and nucleated defects

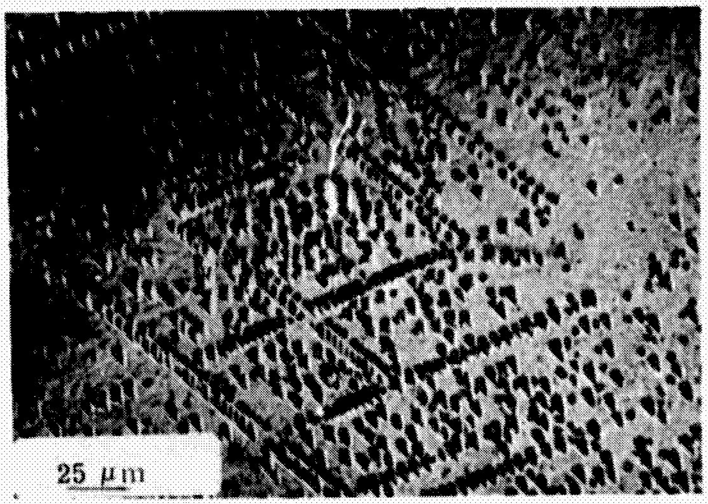

Fig. 10. Deformation induced dislocations aligned along close packed planes. Dislocation pile-ups are also observable in the micrograph.

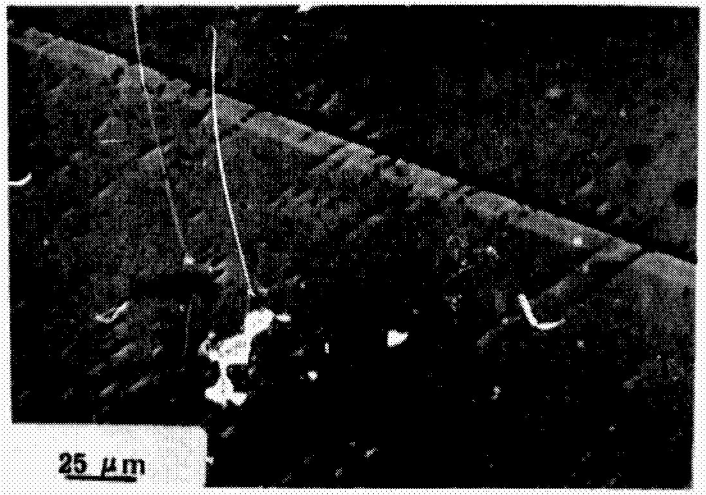

Fig. 11. Dislocation pile-ups against twin boundaries.

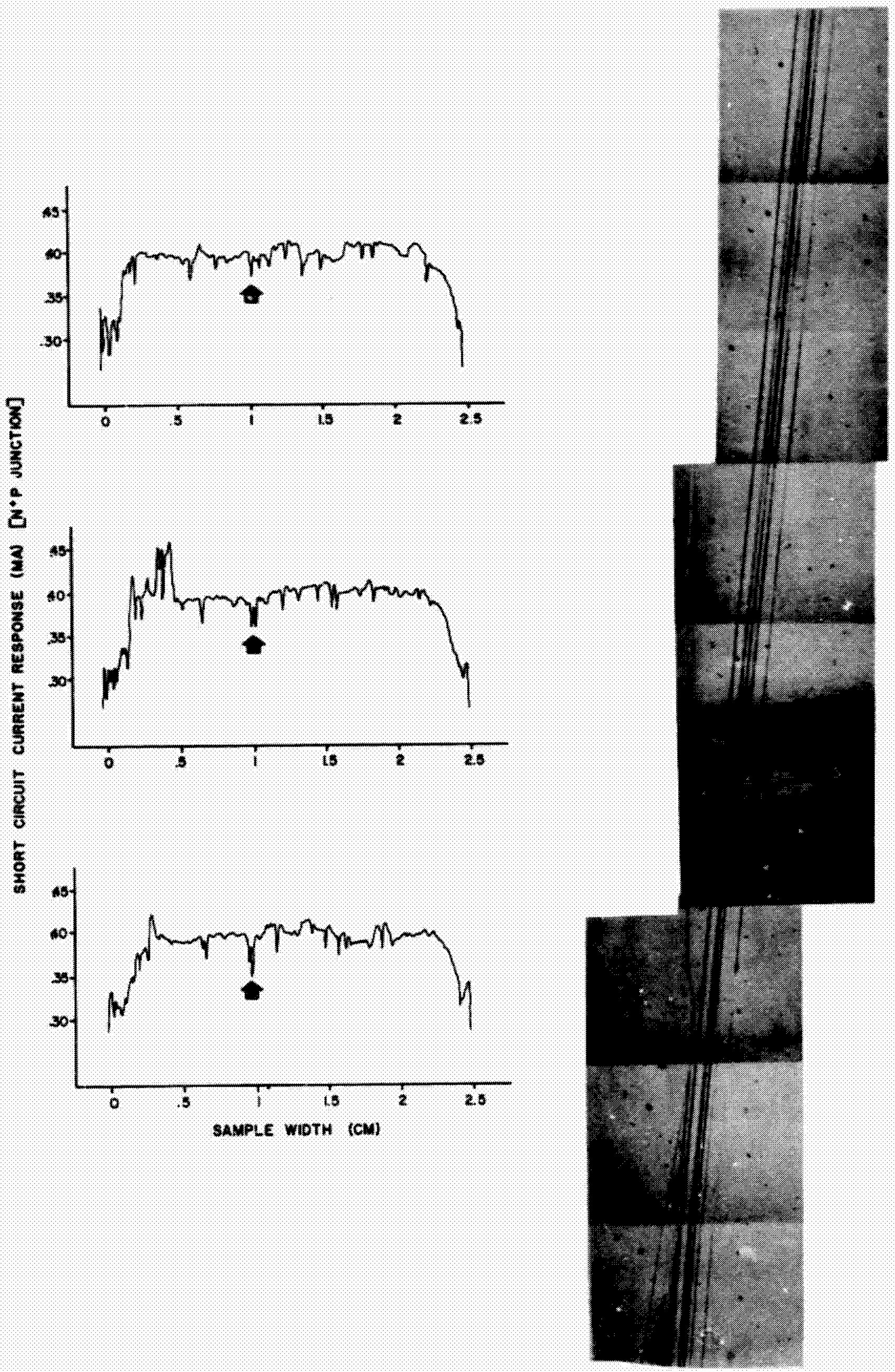

Fig. 12. Short circuit current response plotted as a function of distance across the ribbon width. The three plots were obtained from three regions along the ribbon length. Micrograph shows twin boundaries which caused the particular current indicated by the arrows on the plots.

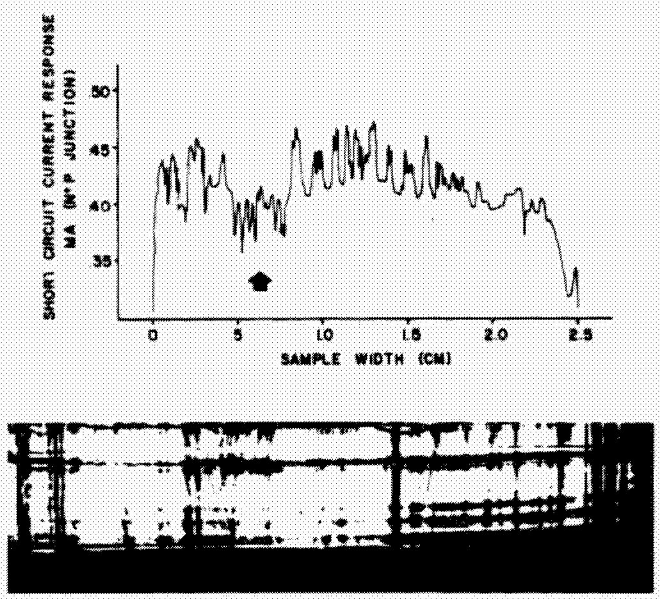

Fig. 13. The effect of intersecting boundaries on laser beam induced short circuit current. Arrow indicates the region on the plot corresponding to the region in the ribbon containing intersecting boundaries.

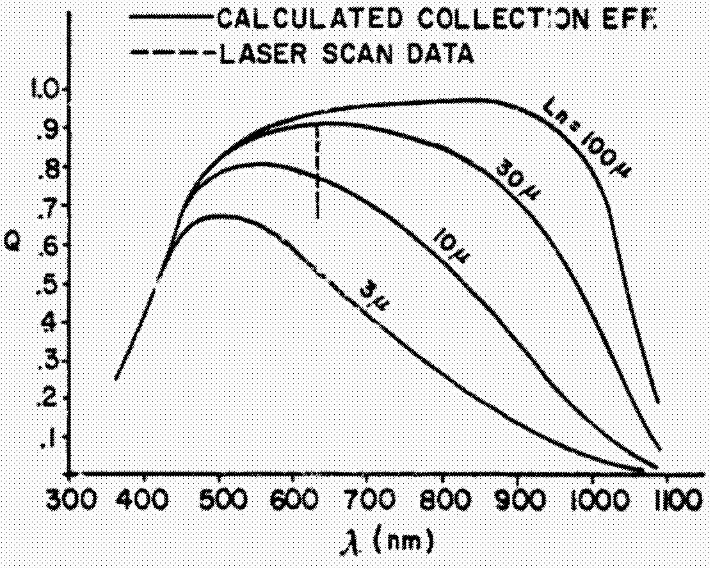

Fig. 14. Theoretically determined spectral response for different values of diffusion lengths in the base region. The laser scan data is superimposed over the theoretical plots. Data used to obtain the plots were: $X_j = 0.25$ μm; $N_S/N_O = 10^5$; $\mu p = 10$ cm^2/V·sec; $\tau_p = 10^{-10}$ sec; $\ell = 10$ mils; $V_s = 10^5$ cm/sec.

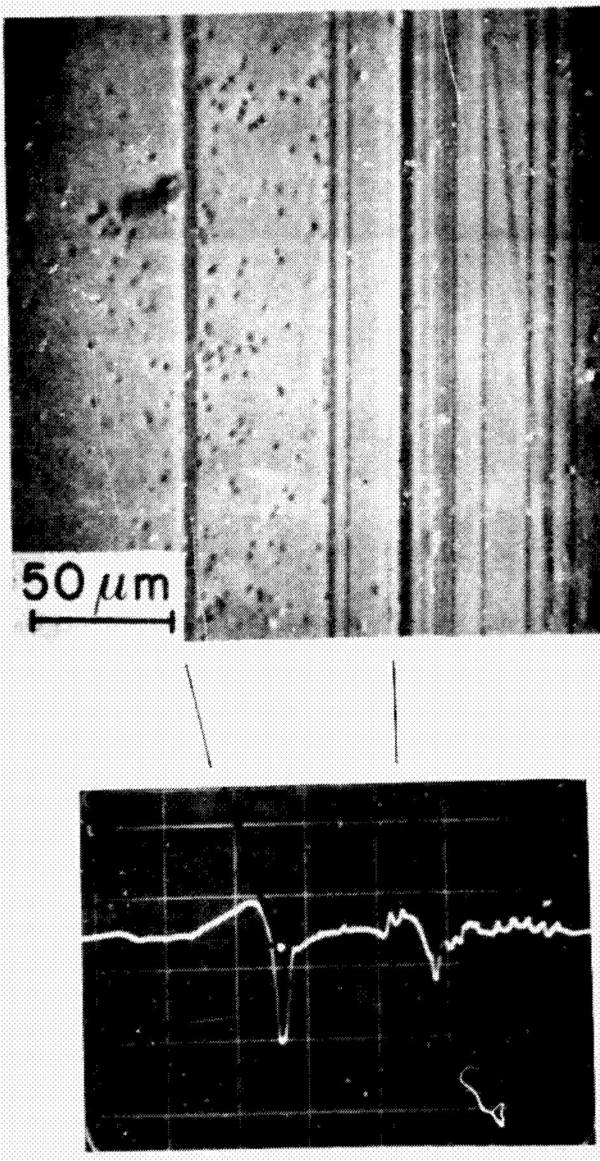

Fig. 15. Secondary electron image of linear boundaries in a ribbon crystal. Waveform shows the EBIC signal when the electron beam is scanned across the boundaries. A direct correlation between the boundaries and a local reduction in the EBIC is observed.

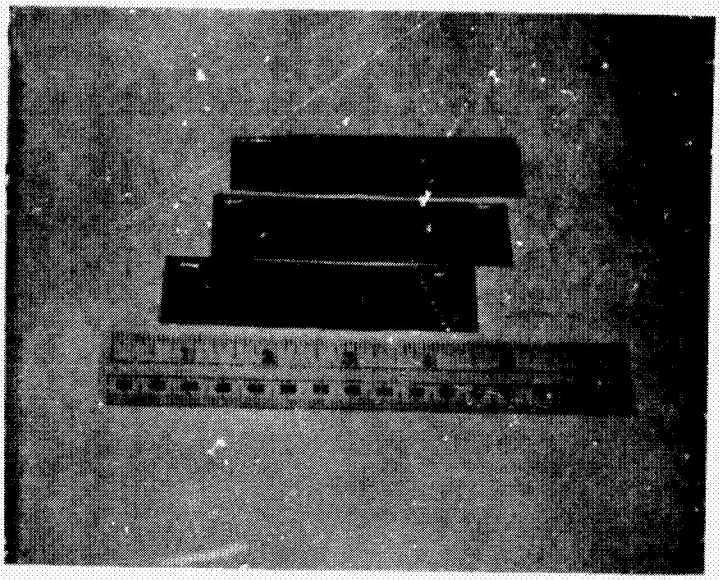

Fig. 16. Typical examples of 1 in. × 4 in. ribbon solar cells.

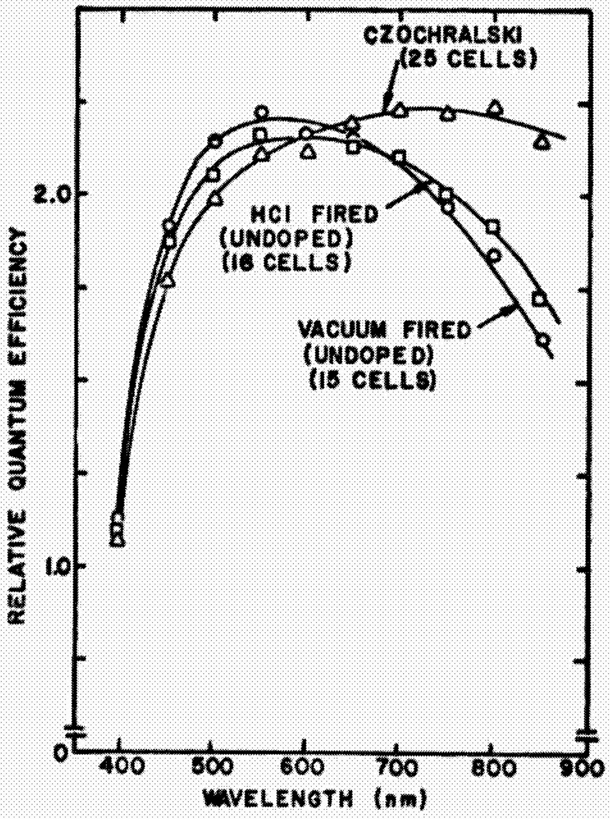

Fig. 17. Comparison of spectral response measurements made on Czochralski and ribbon solar cells. See text for discussion.

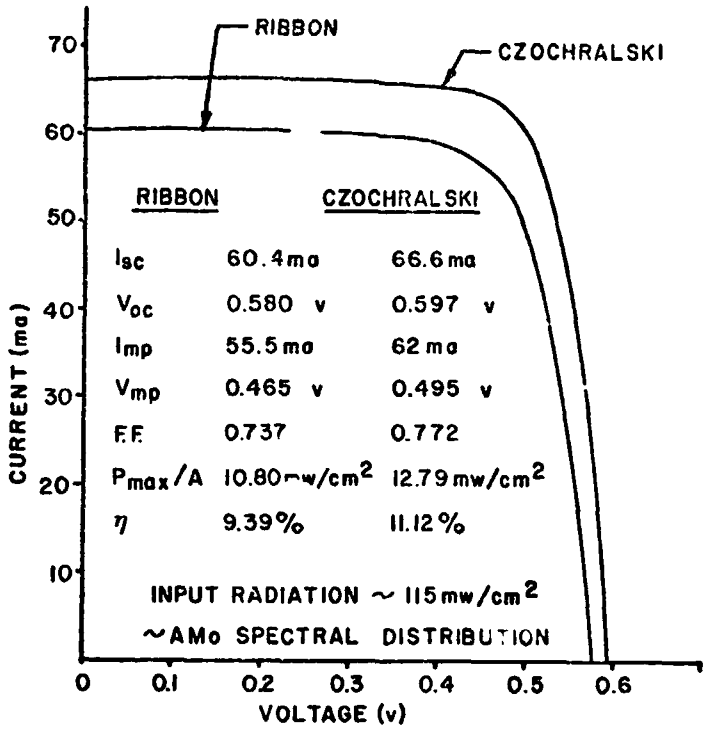

	RIBBON	CZOCHRALSKI
I_{sc}	60.4ma	66.6ma
V_{oc}	0.580 v	0.597 v
I_{mp}	55.5ma	62 ma
V_{mp}	0.465 v	0.495 v
F.F.	0.737	0.772
P_{max}/A	10.80 mw/cm^2	12.79 mw/cm^2
η	9.39%	11.12%

INPUT RADIATION ~ 115mw/cm^2
~AMo SPECTRAL DISTRIBUTION

Fig. 18. Typical I-V characteristics of current state-of-the-art ribbon solar cells. This data was obtained from ribbons displaying typical defect structures listed in Table I. An I-V curve from a control Czochralski cell is also shown. The cells have been AR coated.

SILICON RIBBON GROWTH USING A CAPILLARY ACTION SHAPING TECHNIQUE

G. H. Schwuttke/T. F. Ciszek/A. Kran
International Business Machines Corp.
East Fishkill Laboratories
Hopewell Junction, New York 12533

JPL SUBCONTRACT 954144
National Solar Photovoltaic Program Review Meeting
July 22-25, 1975

ABSTRACT

A review of work performed since the inception date (May 8, 1975) is presented, along with an outline of the project concept and work plan (Figs. 1-3).

The crystal growth method involves Meniscus shaping at the vertex of a wettable die. As ribbon growth depletes the melt meniscus, capillary action supplies replacement material (Fig. 4). Because of the die/melt proximity, a durable, nonreactive die is desirable. A number of materials (Fig. 5) have been collected for die evaluation and are being machined. Crystal growth to date has been done with graphite and silicon carbide dies. Graphite dies lead to particle inclusions in the ribbon surface. We have positively identified the particles as beta silicon carbide (Fig. 6). Silicon carbide particles and carbon cause defect nucleation in otherwise defect-free ribbons (Fig. 7). We have grown a number of 12 mm wide x 0.5 mm thick x 1 m long ribbons to thoroughly characterize the state-of-the-art multi-crystalline ribbons, and are in the process of scale-up to 25 mm widths while studying process changes for improved ribbon structure.

Two projects which were begun before the inception date were completed during the past two months. An expression for maximum potential ribbon growth rates was derived an the results are shown graphically in Figs. 8-9. Current rates for 0.05 cm thick ribbons (about 2 cm/min.) are approximately 30% of the maximum value. The second completed project involved the growth of silicon tubes 6 mm in wall thickness, and over 1 m in length by the capillary action shaping technique (Fig. 10-12). Tube structure was similar to that of ribbons. Planar defects and some large angle grain boundaries were present, with the largest grains extending over one quarter of the tube circumference.

In conjunction with and support of the technology development effort, an economic evaluation and computer-aided simulation of materials, processes and resources is being performed for the purpose of clarifying the complex interactions between economic and physical variables. Objectives are listed in Fig. 13.

To date, a methodology for analyzing a given processing step has been defined and ribbon pulling was chosen as the initial modeling effort. The assigned parameters of the mathematical model are shown in Figure 14, and Figure 15 lists the parameters which are subsequently calculated. The data flow model is shown in Figure 16. An example of the computer generated input/output formats is presented in Figures 17 and 18. Figures 19 through 23 address the remaining review items.

SILICON RIBBON GROWTH USING A CAPILLARY ACTION SHAPING TECHNIQUE

G. H. SCHWUTTKE, PROGRAM MANAGER

914-897-3140

JPL CONTRACT NUMBER: 954144

(SUBCONTRACT UNDER NASA CONTRACT NAS7-100)
(TASK ORDER NO. RD-152)
EFFECTIVE DATE OF CONTRACT: 5/8/75
CONTRACT EXPIRATION DATE: 12/31/76
CONTRACT AMOUNT: $214,133.

**ORIGINAL PAGE IS
OF POOR QUALITY**

OBJECTIVES

1. TECHNOLOGICAL ASSESSMENT OF RIBBON GROWTH OF SILICON USING A CAPILLARY ACTION SHAPING TECHNIQUE.
2. ECONOMIC EVALUATION OF RIBBON SILICON GROWN BY A CAPILLARY ACTION SHAPING TECHNIQUE AS LOW COST SILICON.

SYNOPSIS OF PROGRAM OF STUDY, PRINCIPAL INVESTIGATORS

1. CRYSTAL GROWTH OF SILICON RIBBONS (T. F. CISZEK)
2. CHARACTERIZATION OF SILICON RIBBONS (G. H. SCHWUTTKE)
3. ECONOMIC EVALUATIONS AND COMPUTER AIDED SIMULATION OF RIBBON GROWTH (A. KRAN)

STATEMENT OF WORK

1. EVALUATION OF DIE MATERIALS AND DESIGNS
2. DETERMINATION AND OPTIMIZATION OF BASIC GROWTH PROCESSES
3. STUDY PROCESS EFFECTS ON RIBBON PROPERTIES
4. STUDY REQUIREMENTS FOR MULTIPLE AND CONTINUOUS GROWTH
5. EVALUATION OF CHARACTERIZATION PROCESSES
6. ECONOMIC ANALYSIS OF RIBBON AND CZOCHRALSKI TECHNIQUES

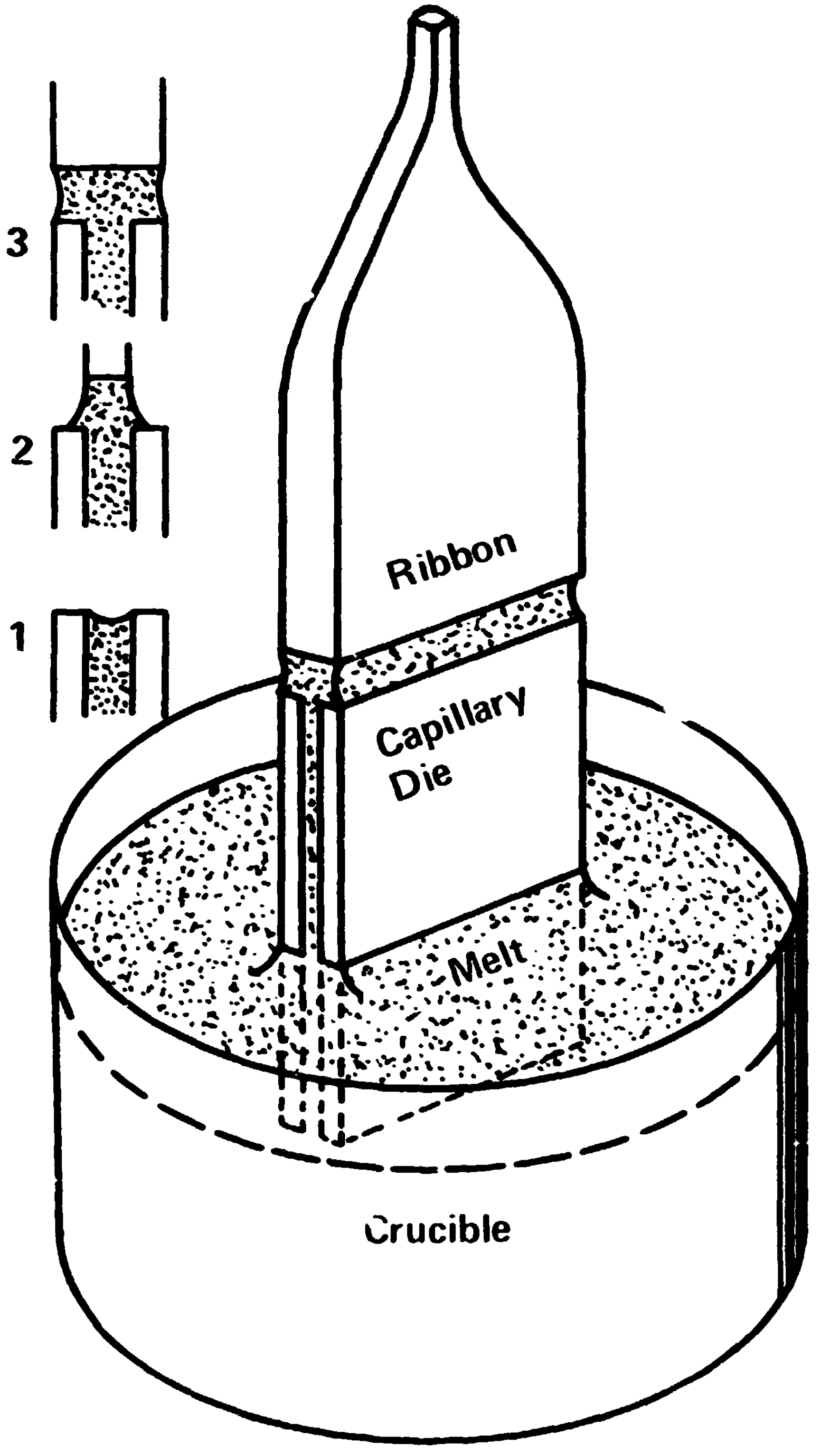
3
2
1
Ribbon
Capillary
Die
Melt
Crucible

DIE MATERIALS UNDER INVESTIGATION

ZIRCONIUM BORIDE (HOT PRESSED

TITANIUM BORIDE (HOT PRESSED)

BORON CARBIDE (HOT PRESSED)

ALUMINUM BORIDE

SILICON NITRIDE

SILICON CARBIDE (RECRYSTALLIZED)

VITRIOUS CARBON

IDENTIFICATION OF YELLOWISH-GREEN INCLUSION

CRYSTAL		ASTM CARD #1-1119 Beta SiC	
d	I_o	d	I/I_1
2.51	S	2.51	100
2.[illegible]	M	2.17	20
1.54	M	1.54	63
1.315	M	1.31	50
1.27	W	1.26	5
		1.09	6
1.00	W	1.00	18
0.975	W	0.97	6
0.89	W	0.89	13
0.84	W	0.84	10

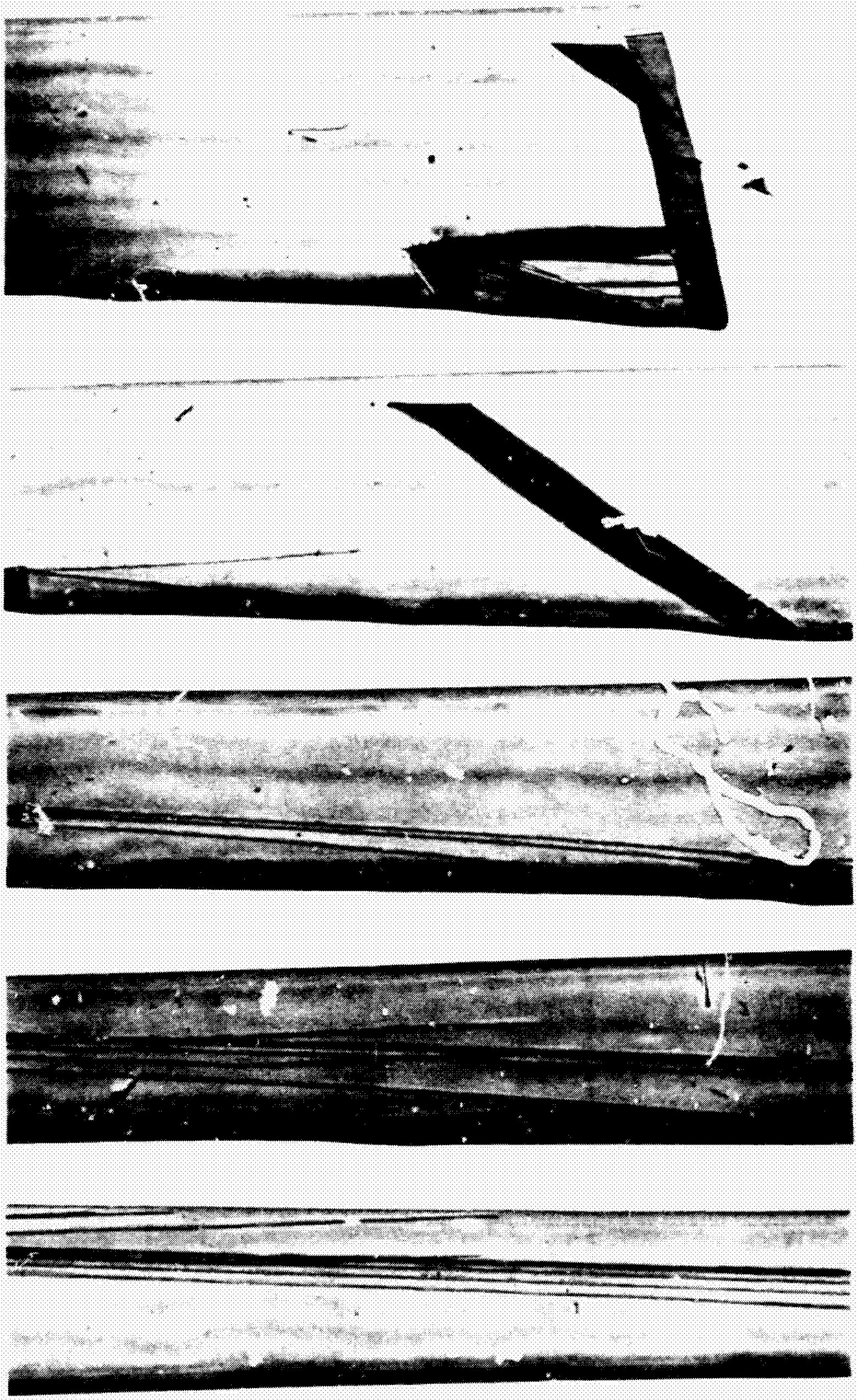

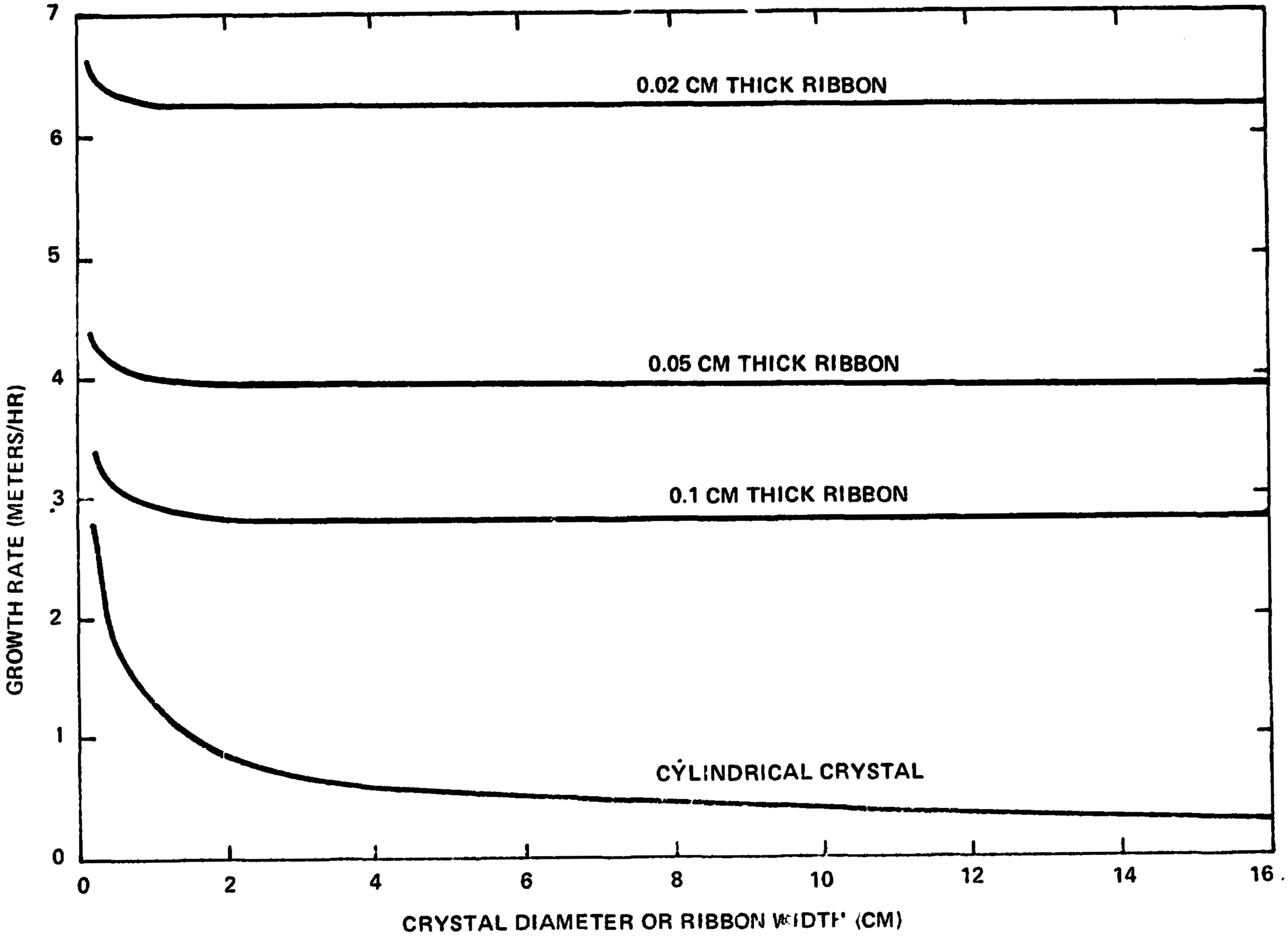
7
6
5
4
3
2
1
0
GROWTH RATE (METERS/HR)
0
2
4
6
8
10
12
14
16
CRYSTAL DIAMETER OR RIBBON WIDTH (CM)
0.02 CM THICK RIBBON
0.05 CM THICK RIBBON
0.1 CM THICK RIBBON
CYLINDRICAL CRYSTAL

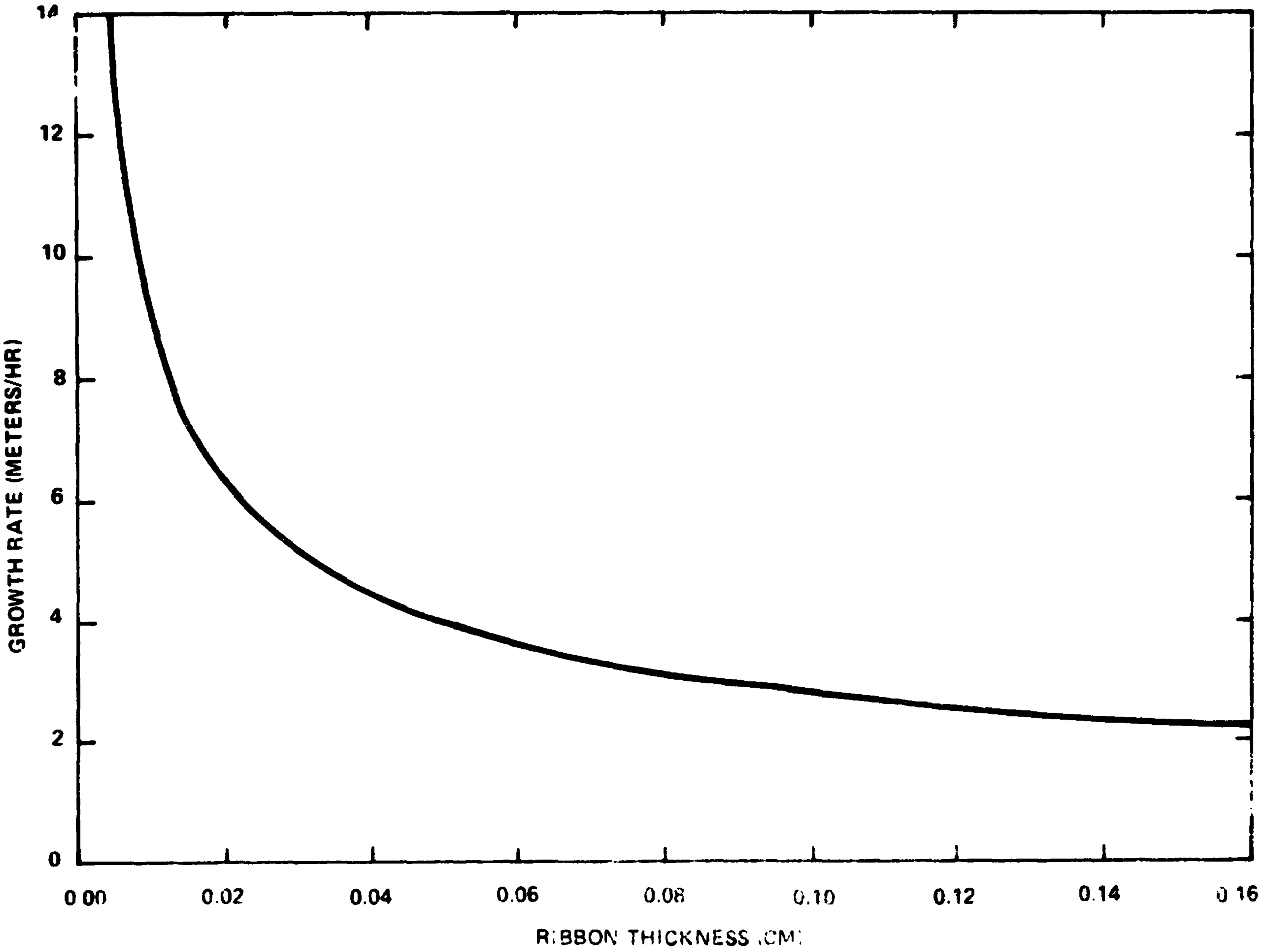
14
12
10
8
6
4
2
0
GROWTH RATE (METERS/HR)
0.00
0.02
0.04
0.06
0.08
0.10
0.12
0.14
0.16
RIBBON THICKNESS (CM)

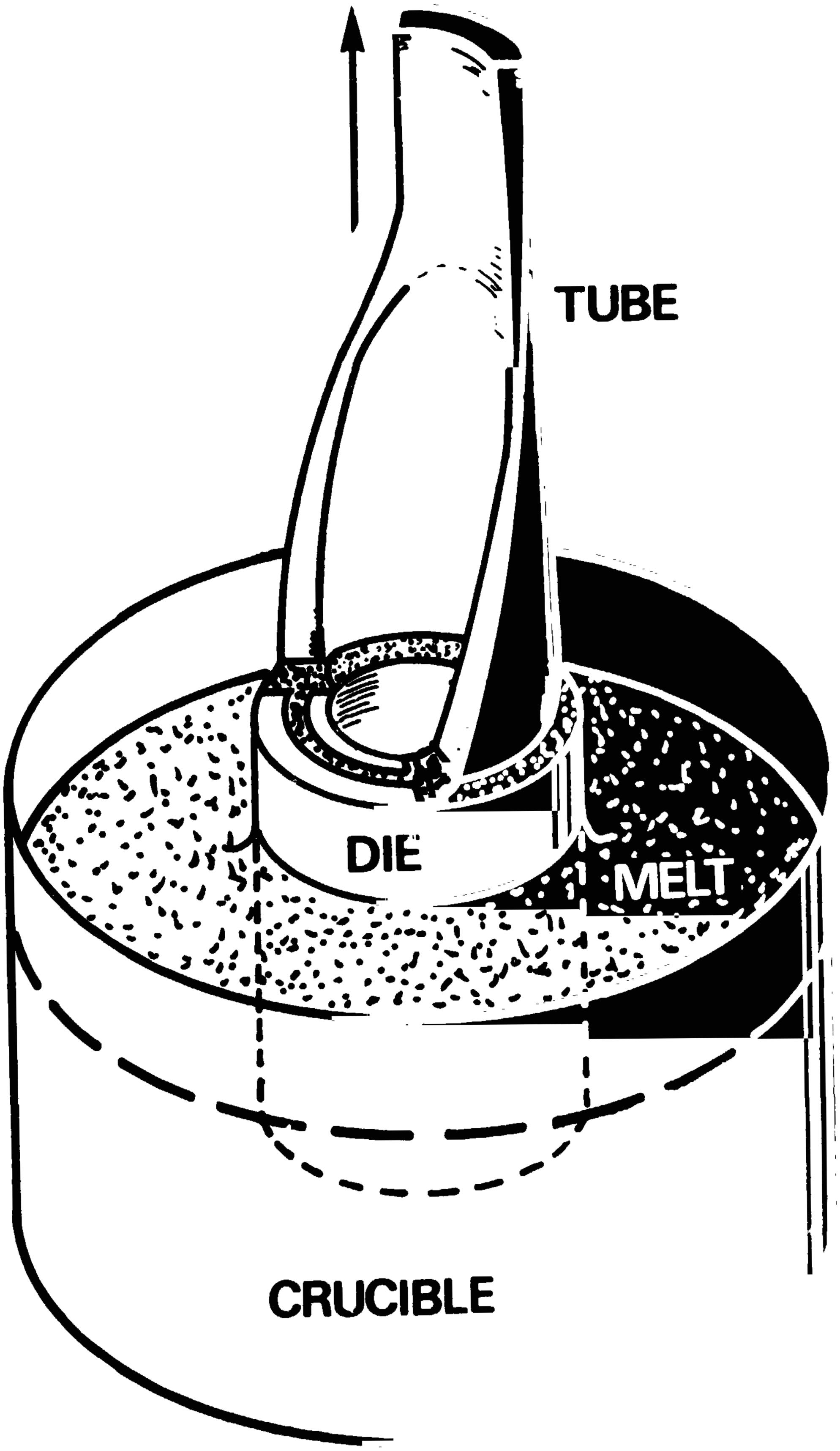
TUBE
DIE
MELT
CRUCIBLE

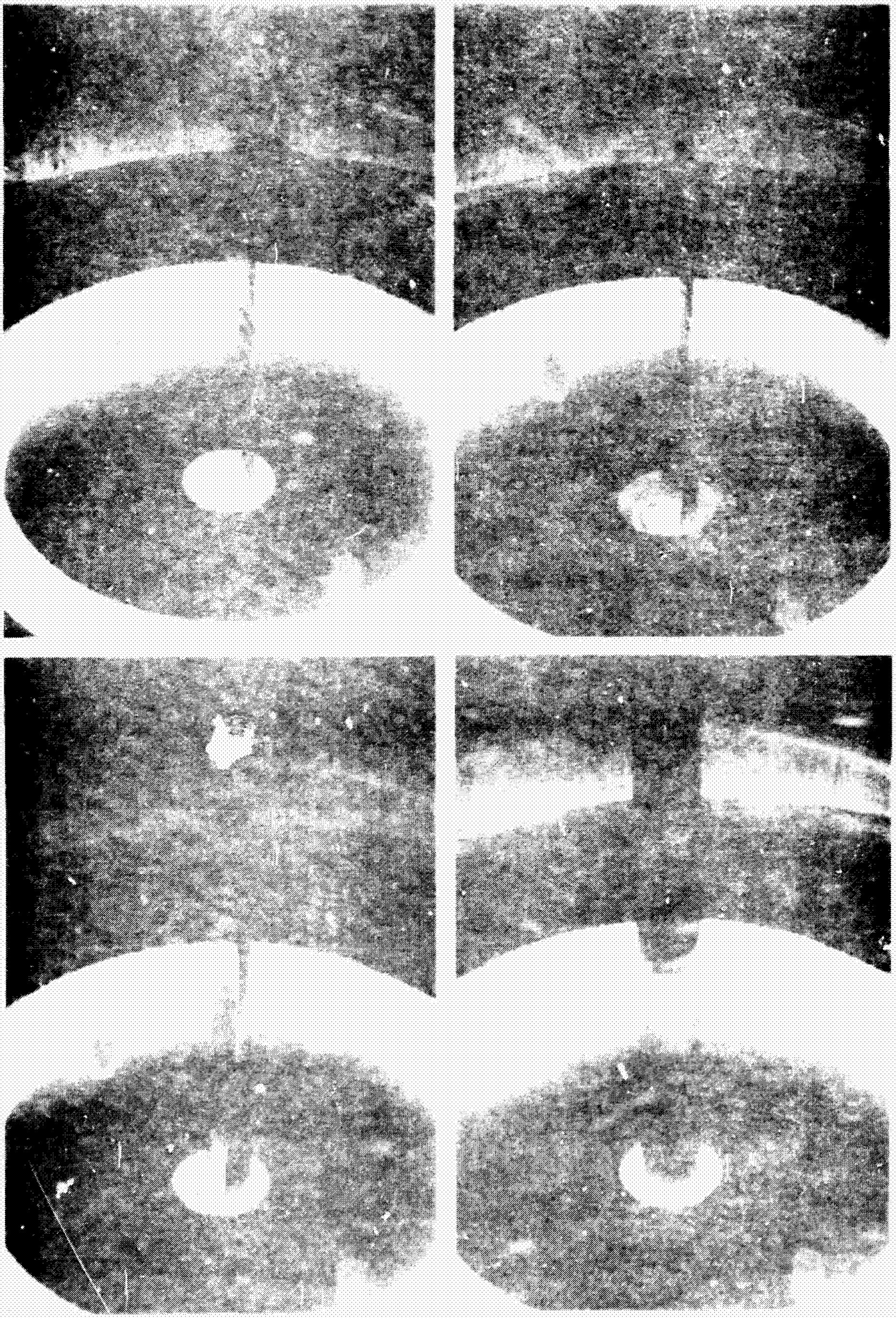

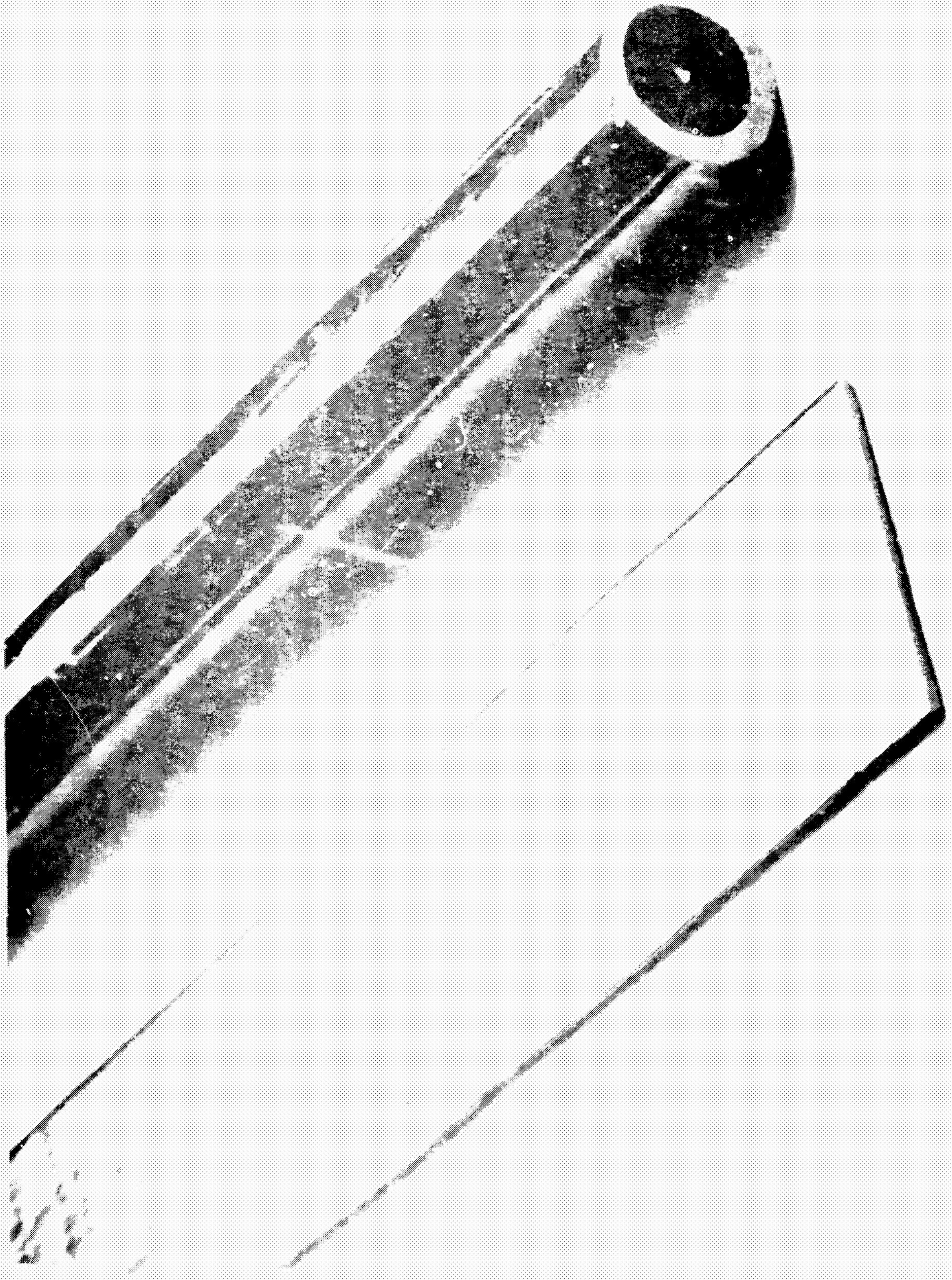

OBJECTIVE OF COMPUTER AIDED MODELING

- TO UNDERSTAND THE RESPECTIVE IMPORTANCE OF PARAMETERS AND THEIR ASSIGNED VALUES
- TO AID IN SENSITIVITY STUDIES
- TO ASSESS THE IMPACT OF TECHNOLOGY IMPROVEMENTS ON THE ECONOMIC OUTLOOK FOR PHOTOVOLTAICS
- TO GAIN INSIGHT ON ASSUMPTIONS AND TECHNOLOGY PROJECTIONS

MATHEMATICAL MODEL

1. ASSIGNED PARAMETERS

CC = CRUCIBLE COST, \$
CH = ENERGY TO OPERATE EQUIPMENT, KW
CP = POWER COST, \$/KWH
DS = SILICON DENSITY, 2.33 G/CM^3
EC = CONVERSION EFFICIENCY, %
ED = ENERGY DENSITY, PEAK AT AM1, %
EP = EQUIPMENT PRICE, \$
HW = WORK WEEK, HOURS
FC = FACTOR, %
IN = INTERST, %
LP = POLY SILICON COST, \$/KG
LR = REMELTED MATERIAL, %
LY = POLY YIELD TO RIBBON, %
MA = MACHINE AVAILABILITY, %
NU = NUMBER OF YEARS
PE = ANNUAL SALARY OF ENGINEER, \$
PS = ANNUAL SALARY OF SUPERVISOR, \$
PT = ANNUAL SALARY OF TECHNICIAN, \$
RG = RIBBON GROWTH RATE, M/HR
RS = RIBBONS GROWN SIMULTANEOUSLY
RT = RIBBON THICKNESS, MM
RW = RIBBON WIDTH, CM
RY = RIBBON GROWTH YIELD, %

2. CALCULATED PARAMETERS

AG = AREA GROWTH RATE, M^2/HR
CR = CAPITAL RECOVERY FACTOR
DC = DIRECT COST, $\$/M^2$
EC = CAPITAL EQUIPMENT COST, $\$/M^2$
GA = GENERAL & ADMINISTRATIVE COST, $\$/M^2$
LC = POLY SILICON COST, $\$/M^2$
NC = ENERGY COST AT MATERIAL LEVEL, $/KW
NH = WORKING HOURS PER YEAR
PC = PERSONAL COST, $\$/M^2$
PR = PROFIT, $\$/M^2$
OH = OVERHEAD, $\$/M^2$
SS = SERVICES & SUPPLIES, $\$/M^2$
TO = COST OF TOTAL OPERATIONS, $\$/M^2$
YF = YIELD FACTOR

DATA FLOW MODEL

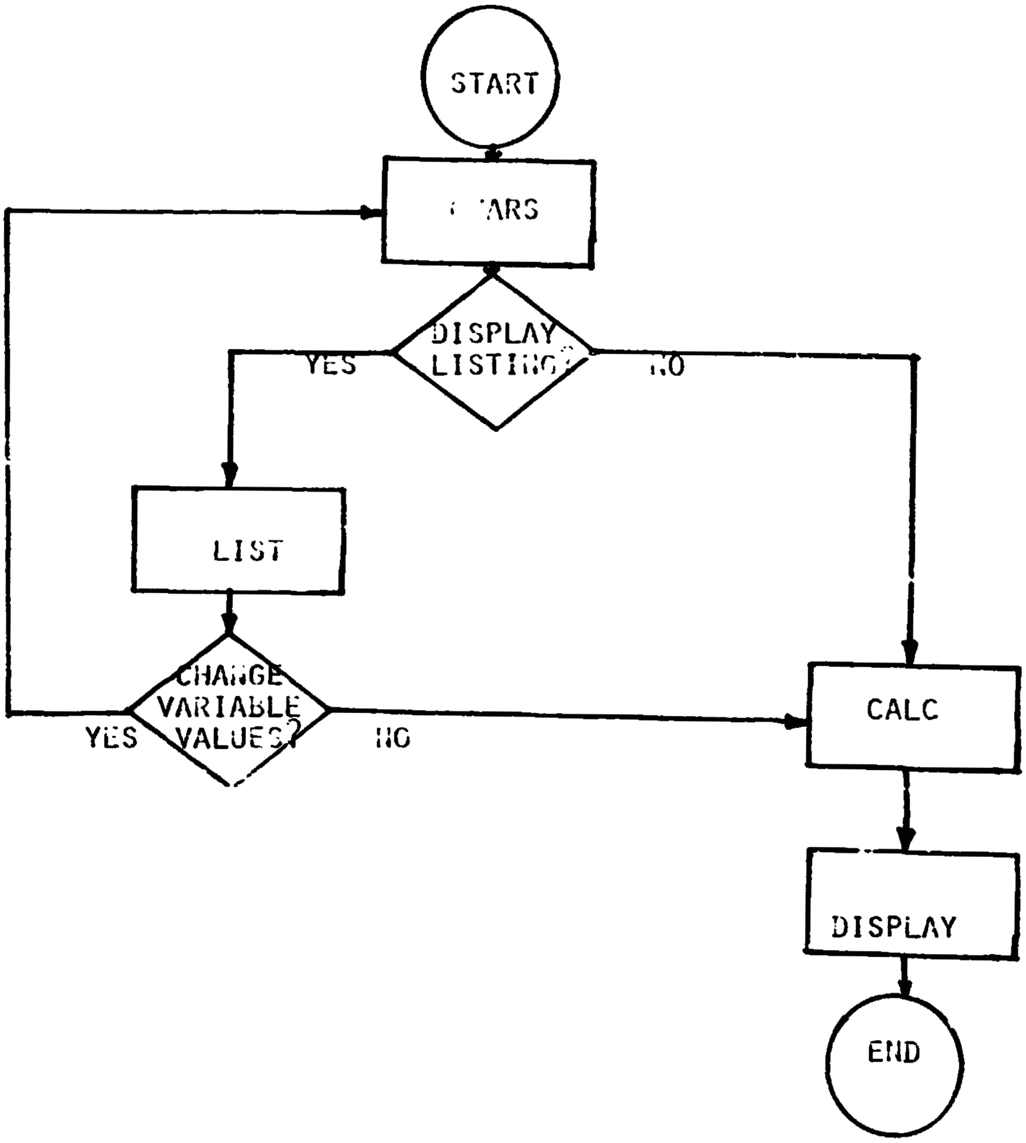

```
        LIST OF RIBBON PARAMETERS AND THEIR ASSIGNED VALUES
        ---------------------------------------------------

   RIBBON DATA
1  RIBBONS GROWN SIMULTANEOUSLY - 1 1 1
2  RIBBON WIDTH, CM - 3 3 3
3  RIBBON GROWTH RATE,M/HR - 2.3 2.3 2.3
4  RIBBON THICKNESS, MM - 0.2 0.2 0.2
5  YIELD OF GOOD RIBBON, PERCENT - 60 70 80

   DIRECT COST
6  RIBBON FURNACE, DOLLARS - 25000 25000 25000
7      EQUIPMENT LIFE, YEARS - 7
8      INTEREST RATE, PERCENT - 8
9      EQUIPMENT AVAILABILITY, PERCENT - 70

10 PERSONNEL PER SHIFT
11     NO. OF SUPERVISORS - 0.05 AT A YEARLY RATE OF - 25000
12     NO. OF ENGINEERS - 0.1  AT A YEARLY RATE OF - 20000
13     NO. OF TECHNICIANS - 0.5  AT A YEARLY RATE OF - 10000

14 POLY SILICON COST, DOLS/KG - 65 65 65
15 POLY YIELD TO RIBBON,PERCENT - 80 80 80

16 SERVICES AND SUPPLIES
17     ONE CRUCIBLE PER DAY AT A COST OF - 30 DOLLARS
18     POWER COST AT - 0.05 DOLLARS PER KWH
19     ENERGY TO OPERATE EQUIPMENT - 20 KW

   OVERHEAD - 50 PCT OF PERSONNEL+ 10 PCT OF RAW MATL COST
   G AND A - 10  PERCENT OF DIRECT COST+OVERHEAD

   PROFIT BEFORE TAX, PERCENT - 10 OF DC+O/H+GaA

   MISCELLANEOUS
20 WORKWEEK, HOURS - 120
21 CONVERSION EFFICIENCY, PERCENT -   7.5
22 ENERGY DENSITY AT AM1,KW/M SQ PEAK - 1
```

ECONOMICS OF SILICON RIBBON - ONE RIBBON PULLER

PRINTED FROM A. KRAN'S SF WSS: 06.55 HOURS, 07/14/75

RIBBONS GROWN SIMULTANEOUSLY	1.00	1.00	1.00
RIBBON WIDTH, CM	5.00	5.00	3.00
AVG AREA GROWTH RATE, SQ M/HOUR	0.05	0.05	0.04
COMBINED YIELD FACTOR	0.48	0.56	0.64
DIRECT COST IN DOLS/SQ METER			
EQUIPMENT CAPITAL RECOVERY	27.02	25.67	20.71
PERSONNEL	142.34	122.01	106.75
POLY SILICON COST	63.10	54.00	47.53
SERVICES/SUPPLIES	67.29	57.00	50.47
SUBTOTAL:	300.55	257.44	225.26
OVERHEAD COST IN DOLS/SQ METER	74.29	64.03	56.41
G&A EXPENSES IN DOLS/SQ METER	37.45	32.15	28.17
PROFIT IN DOLLARS/SQ METER	41.29	35.36	30.93
TOTAL COST IN DOLS/SQ METER	455.20	388.98	340.02
DOLLARS PER KG	6042.07	5186.42	4544.22

ORIGINAL PAGE IS
OF POOR QUALITY

3. PLANNED ACTIVITY TO DATE (3 MONTHS)

DESIGN A COMPUTER-AIDED MODEL TO ESTABLISH A RELATIONSHIP BETWEEN THE COMPLEX INTERACTIONS OF ECONOMIC AND PHYSICAL VARIABLES.

PLANNED ACTIVITY FOR NEXT 6 MONTHS

- USE MODEL TO PERFORM ENGINEERING/ECONOMIC ANALYSIS
- DEFINE SIMILAR MODEL FOR CHRALSKI GROWTH
- PERFORM COMPARISON STUDIES

MAJOR PROBLEMS

NONE

SUMMARY OF KEY RESULTS

RIBBON GROWTH MODEL HAS BEEN DEFINED AND DEBUGGED. LITTLE [illegible] DATE.

PLANNED RENEWAL REQUESTS

TOO EARLY TO FORMULATE PLANS.

N76 12476

RESEARCH AND DEVELOPMENT OF LOW COST PROCESSES FOR INTEGRATED SOLAR ARRAYS

M. Wolf/L. Crossman

ABSTRACT

The current phase of the project is directed toward assembling adequate knowledge to permit the technical and economic feasibility assessment of competing process approaches which are expected to optimally fit into an extremely low cost, large volume process sequence leading to high efficiency solar arrays (Fig. 1). In this endeavor, one of the approaches investigated in the silicon reduction and purification area, namely the upgraded arc-furnace process, has both a much larger background of available information and appears technically and economically exceedingly attractive, so that it has now reached the stage of transition from preliminary feasibility studies to advanced experimentation, with significantly larger requirements for equipment and funding.

The emphasis has continued on the 2 areas of Si reduction and purification and of sheet generation. However, the work has recently been concentrated on gaining information about one reduction process combined with purification (higher purity arc furnace with gas blowing and gradient freezing; Dow-Corning) one transport process with purification and polycrystal sheet growth potential (SiF_2), on plastic deformation for sheet generation, and on float zone sheet recrystallization.

The previously unexplored Si transport properties of the SiF_2 reaction at atmospheric pressure have been further investigated. It has been firmly established that the SiF_2 gas can be moved without

decomposition at constant temperature both above 1000° C (see clear zone in deposition tube shown in Fig. 4) and below 100° C, with Si depostion occuring at the intermediate temperatures. Since the rate limiting step has been found to be the SiF_2 formation reaction, which is currently carried out at 1150° C, extrapolation through thermodynamic considerations indicates the possibility of obtaining increased transport rates (up to 0.75 g Si per of gas (STP) moved through the system) by raising the reaction temperature above the Si melting point. Considerable effort was spent in purifying the SiF_4 gas which was found to contain O_2 and other impurity gases, as purchased. This purification eliminated the formation of fluorosilicate byproducts which have been depositing in the piping system, but did not otherwise significantly affect the transport reaction.

Considerable progress was made in the exploration of the high temperature mechanical properties of polycrystalline Si, with the objective of assessing the feasibility of plastic deformation, such as rolling. Data are being accumulated to generate "forming limit diagrams" with temperature and strain rate as parameters. Such diagrams have been recently introduced as design tools in metal forming (Fig. 6). The experiments carried out by axial compression of Si cylinders at temperatures from 1250 to 1350° C have shown that the method of forming limit diagrams is also applicable to silicon. Deformations by up to 70% at strain rates up to 1%/s have indicated that plastic deformation of Si may be a suitable forming method (Fig. 7). Earlier problems with the anisotropic crystal structures in the "polyrods" resulting from the $SiHCl_3$ purification process (Fig. 8) have been overcome by raising temperature and strain. Also, crystallization has been observed to take place, including grain growth by an order of magnitude (Figures 9 and 10).

The float zone recrystallization equipment to be used for the exploration of the conversion of polycrystalline sheet to single crystal sheet by, heating with a planar electron beam is now completed, with experimentation scheduled to begin (Fig. 12).

The investigation of solution growth processes has been tentatively terminated with the finding that the known solvents for properties which do not appear to be conducive to fast growth rates of sheets of high semiconductor quality (Fig. 14).

In preparation for the ultimate economic analysis of competing processes, a thorough economic evaluation, with evolution forecast, of the Czochralski process as a baseline has been carried out, with the result that the primary limiting item is the crucible cost due to the current one time use. Re-use potential may lead to an ultimate single crystal cost near \$13. -/m^2 without cutting or device processing costs, in lieu of approximately \$25. -/m^2 with one time use of the crucible. This assumes the availability of \$4. -/kg polycrystal Si (Fig. 15).

RESEARCH AND DEVELOPMENT OF LOW COST PROCESSES
FOR
INTEGRATED SOLAR ARRAYS

Grant: ERDA EC(1-1)--2721
Previously: NSF/RANN/SE/GI-29729

Work performed at
University of Pennsylvania/Dow Corning Corp.

Period of Grant

April 15, 1975 - Jan. 14, 1976
(Prior Apr. 15, 1974 to April 14, 1975)

Grant Value: $299,733

(preceding: $317,005)

Principal Investigators

M. Wolf/L. Crossman

OBJECTIVE

DEMONSTRATE FEASIBILITY OF NEW TECHNOLOGY
SUITABLE FOR INTEGRATED PROCESS (QUARTZ SAND TO ARRAY)
YIELDING HIGH EFFICIENCY Si ARRAYS AT $15.00 TO 40.00/$M^2$.

CURRENT PHASE:

ASSEMBLE ADEQUATE INFORMATION TO PERMIT
TECHNO/ECONOMIC ASSESSMENT OF PROCESS ALTERNATES
BEFORE START OF PROCESS DEVELOPMENT.

CARRY OUT EXPERIMENTAL RESEARCH
ON HIGH POTENTIAL APPROACHES, NOT ALREADY UNDER
DEVELOPMENT ELSEWHERE, TO OBTAIN NECESSARY INFORMATION.

FIGURE 1

PLANNED ACTIVITY-PAST 6 MONTH PERIOD

PLAN	ACTION
1.1 SiF_2 TRANSPORT PROCESS:	
A) DETERMINE OPTIMUM DEPOSITION TEMPERATURE	'RATE(T) DETERMINATION PROGRESSING, NOT RATE LIMITING STEP.
B) DETERMINE TRANSPORT DISTANCE AND TEMPERATURE BEFORE DECOMPOSITION	'EXPERIM'N CONTINUING WITH EQUIPMENT MODIFICATION.
C) ELUCIDATE REACTION KINETICS	'GAS PURIFICATION INSTITUTED. EXPERIMENTATION CONTINUING.
D) DETERMINE IMPURITY SEPARATION	'IN PROGRESS.
1.2 STUDY ARC FURNACE TECHNOLOGY, METAL REDUCTION AND ELECTROLYSIS OF SI, SILICATES AS RAW MATERIALS.	'TECHNOLOGY ASSESSED, WORK ON ELECTROLYSIS, METAL REDUCTION. SILICATES TENTATIVELY TERMINATED.
1.3 PREPARE EQUIPMENT FOR MET-GRADE SI UPGRADING	'EXPERIMENTATION INITIATED.
2.1 COMPLETE MOLTEN ZONE REGROWTH APPARATUS AND START EXPERIMENTATION.	'APPARATUS COMPLETED.
2.2 STUDY SOLUTION GROWTH OF SI LAYERS.	'PROPERTIES OF BINARY SOLUTIONS TABULATED, WORK TENTATIVELY TERMINATED.
2.3 STUDY PLASTIC DEFORMATION (ROLLING OF SI AND GRAIN GROWTH METHOD).	'HIGH TEMPERATURE PROPERTIES OF SI BEING DETERMINED.
2.4 COMPLETE PROCESS EVALUATION METHOD.	'CZOCHRALSKI PROCESS ANALYZED AS BASE LINE.

FIGURE 2

SiF_4/SiF_2 TRANSPORT PROCESS

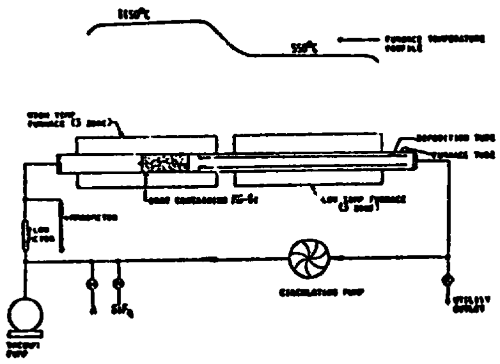

OB .TIVE

'DEVELOP LOW COST PROCESS FOR CONVERTING MG-Si TO SOLAR GRADE POLYCRYSTAL SHEET

GOALS

'DETERMINE IF TRANSPORT RATES COMMENSURATE WITH PRODUCTION GOALS ACHIEVABLE

'DETERMINE IF ADEQUATE PURIFICATION ACHIEVABLE

'ESTABLISH OPTIMUM MEANS FOR COUPLING TO SUBSEQUENT PROCESSES (EPITAXIAL GROWTH, ETC.)

PROGRESS

'EFFECTIVE TRANSPORT POSSIBLE AT ATMOSPHERIC PRESSURE:

1. Si TRANSPORT RATE ≥ 0.05 G/ℓ GAS MOVED
2. NO SiF_2 DECOMPOSITION FOR 3 S ABOVE 1100°C
3. NO SiF_2 DECOMPOSITION OVER 50 CM AT 250°C, FOLLOWED BY DEPOSITION AT 550°C.
4. RATE LIMITING STEP:
   Si DISSOLUTION
5. WIDE TEMP. RANGE FOR DEPOSITION:
   500 - 1000°C
6. DECOMPOSITION INDEPENDENT OF FILM THICKNESS
7. RECRYSTALLIZATION OF AMORPHOUS DEPOSIT OBSERVED
8. DEPOSITION RATE APPROX. EQUAL ON Si WAFERS, SiO_2 WAFERS, HOT TUBE WALLS
9. INFLUENCE OF IMPURITY GASES NOT OBVIOUS.
10. PRELIMINARY IMPURITY ANALYSES INCONCLUSIVE

FIGURE 3

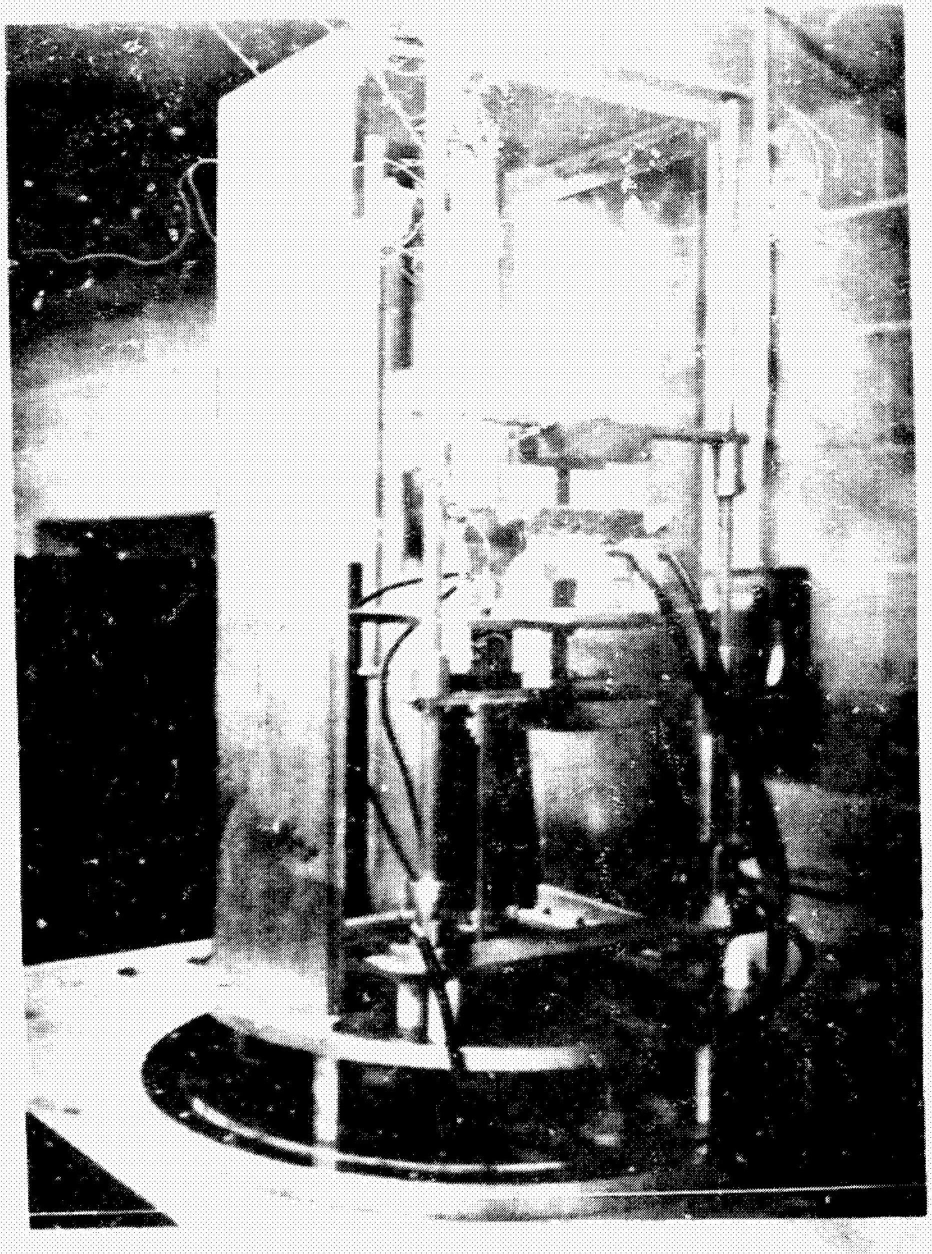

ELECTRON BEAM ZONE MELTING
APPARATUS (PIERCE GUN)

ORIGINAL PAGE IS
OF POOR QUALITY

PLASTIC DEFORMATION OF SILICON

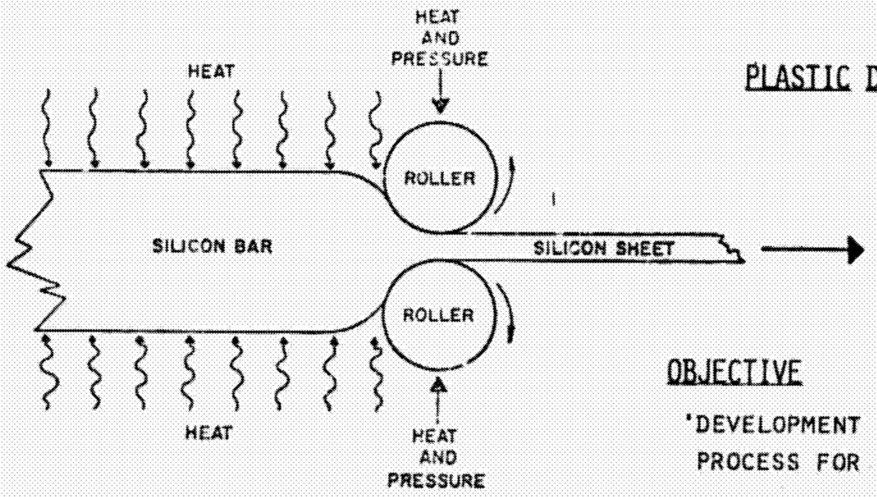

OBJECTIVE

- DEVELOPMENT OF HIGH SPEED SOLID STATE PROCESS FOR SILICON SHEET FORMATION

GOALS

- INVESTIGATE SI PLASTICITY AT TEMPERATURES BELOW MELTING POINT.
- DETERMINE PROCESS RATE.
- ESTABLISH MATERIALS AND PROCESS PARAMETERS TO DEMONSTRATE WORKING FEASIBILITY.
- DETERMINE PRODUCT CHARACTERISTICS (ELECTRICAL, ETC.)
- OPTIMIZE PRODUCT MORPHOLOGY.

PROGRESS

- FORMING LIMIT DIAGRAM FOR SILICON BEING DETERMINED.
- POLYCRYSTALLINE SILICON UNIAXIALLY COMPRESSED AT DEFORMATION RATES $\leq$ 1% PER SECOND.
- CRYSTALLOGRAPHIC TEXTURE OF POLYCRYSTALLINE SILICON (SIHCL$_3$ PROCESS) DETERMINED - (X-RAY DIFFRACTOMETER).
- GRAIN GROWTH OBSERVED AFTER ANNEALING AND STRAINING, GRAINS UP TO 1MM DIAMETER.

FIGURE 5

KUHN 1973

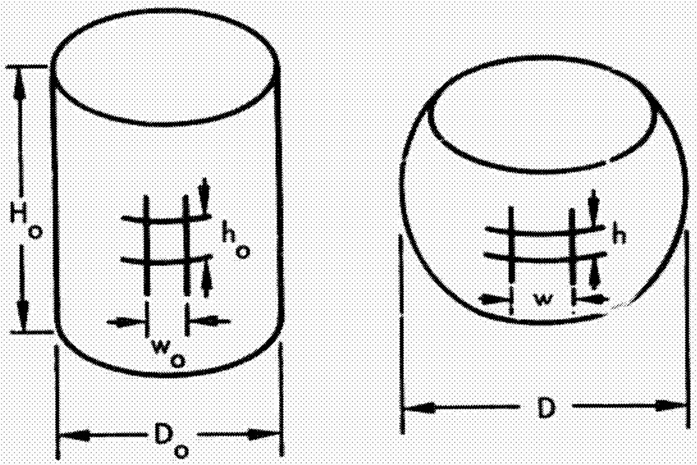

AXIAL STRAIN $\epsilon_z = \ln(h/h_o)$

HOOP STRAIN $\epsilon_\theta = \ln(w/w_o)$ or $\ln(D/D_o)$

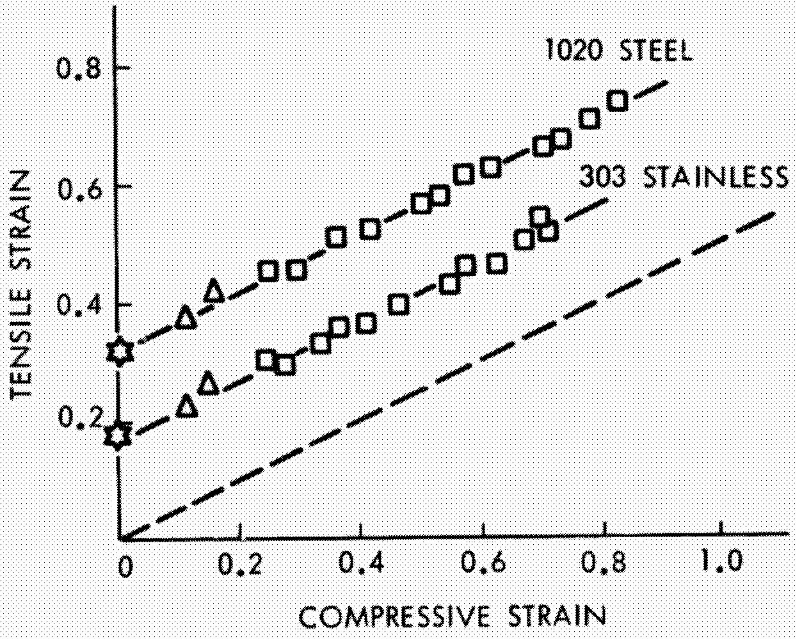

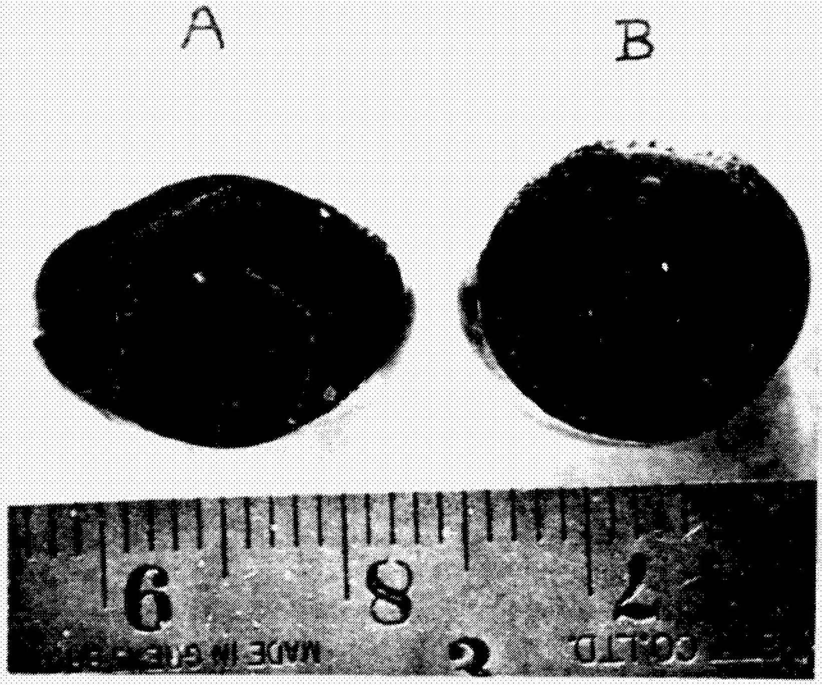

ANISOTROPIC DEFORMATION

A. 40% DEFORMATION AT 1280°C

B. 40% DEFORMATION AT 1350°C

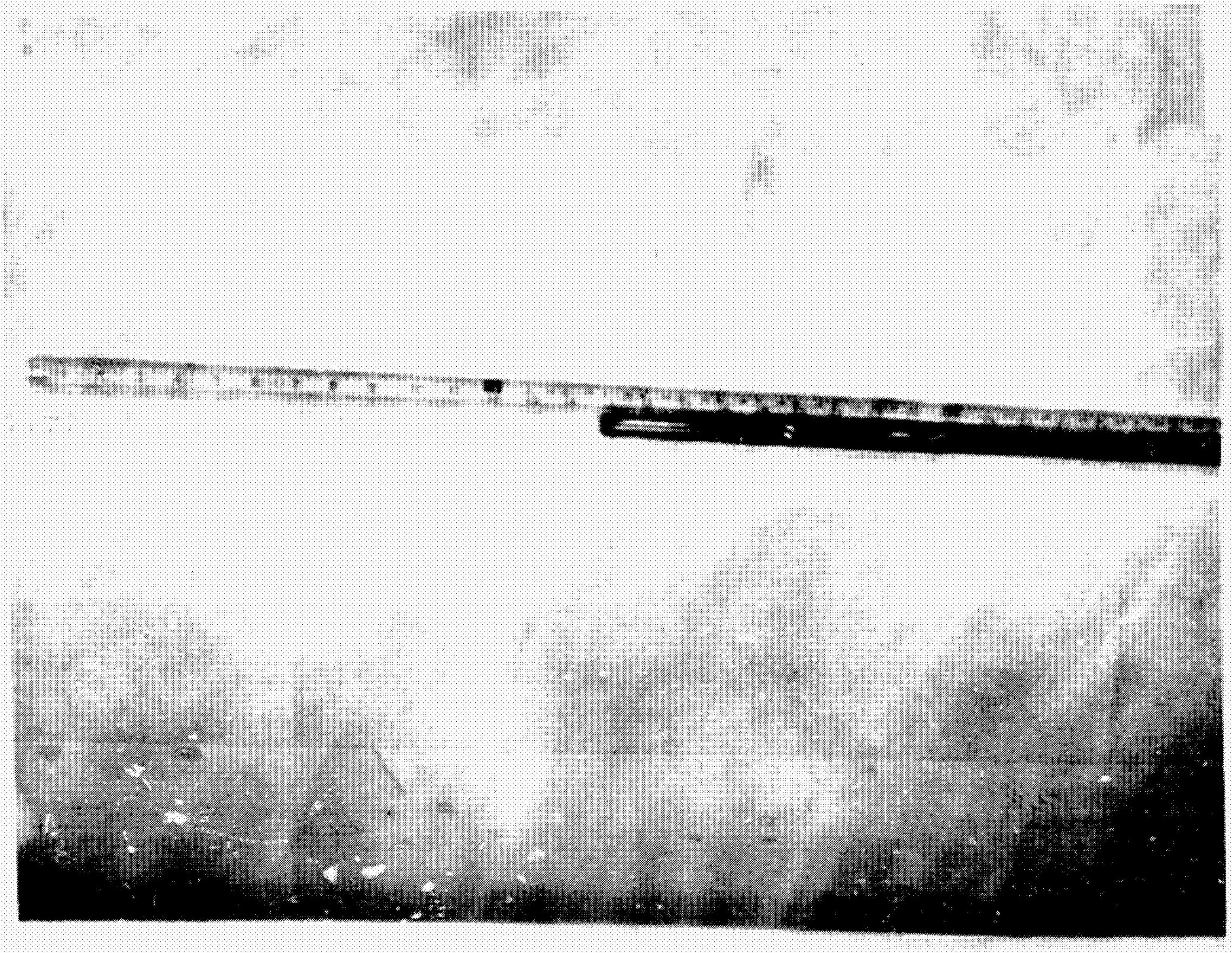

HIGH TEMPERATURE (>1000°C)
SiF_2 TRANSPORT

ORIGINAL PAGE IS
OF POOR QUALITY

ORIGINAL PAGE IS
OF POOR QUALITY

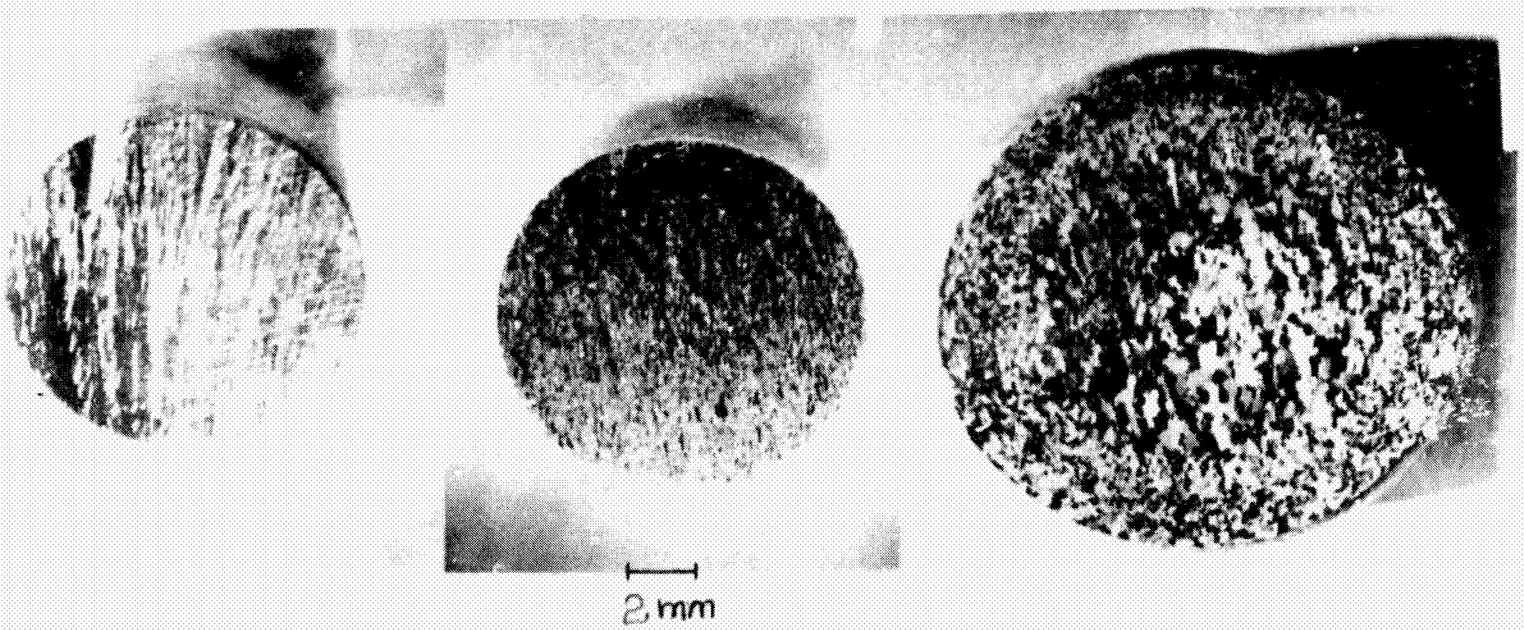

RECRYSTALLIZATION

AS RECEIVED

(b) ANNEALING
OF (a)
T = 1350°C
Δt = 4 HRS.

(c) ANNEALING AFTER
PLASTIC
DEFORMATION
T = 1350°C
Δt = 4 HRS.

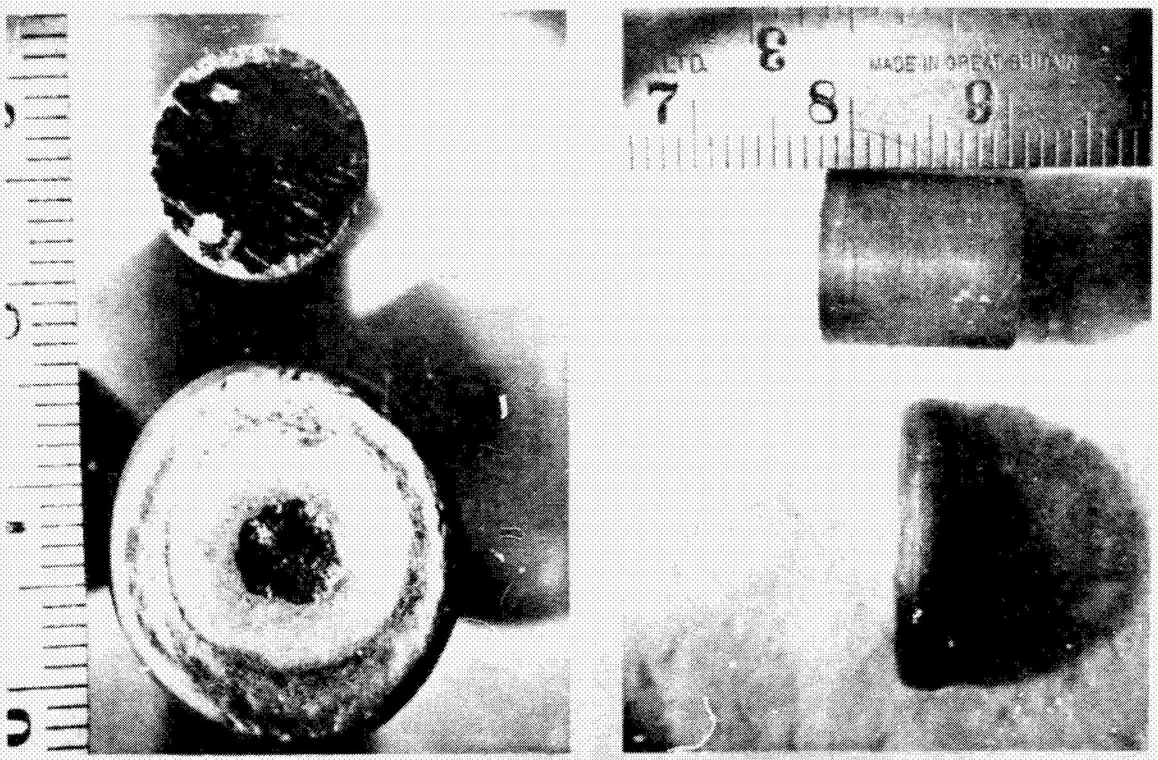

(a) TOP VIEW (b) SIDE VIEW

PLASTIC DEFORMATION

$\dot{\varepsilon} = 10^{-3}$ SEC^{-1}

$T = 1350\,^{\circ}C$

$\sigma = 10$ Kg·mm^{-2} (15×10^{3} P.S.I)

$\Delta L \cdot L^{-1} = 70\ \%$

FLOATING MOLTEN ZONE RECRYSTALLIZATION

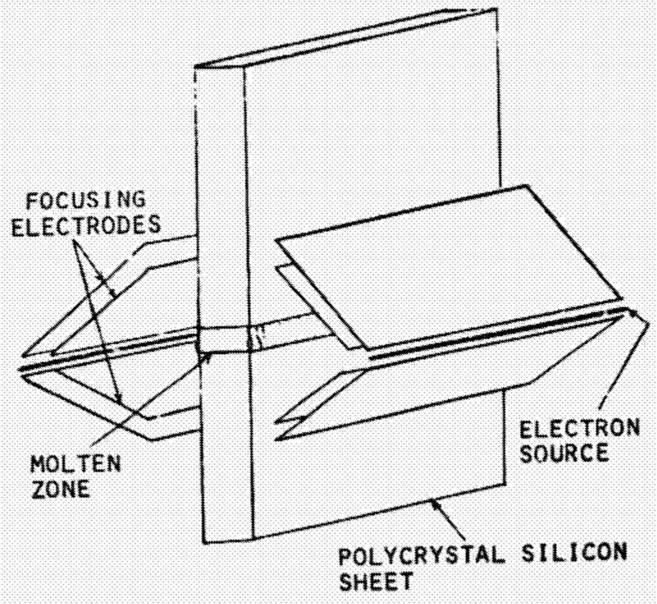

OBJECTIVE

- PRODUCE SINGLE CRYSTAL SHEET FROM FINE GRAIN POLYCRYSTALLINE SI SHEET.

GOALS

- PRODUCE STABLE FLOATING MOLTEN ZONES IN SHEET DOWN TO 100 µM THICKNESS.
- DEMONSTRATE ADEQUATE RECRYSTALLIZATION RATE WITH ACCEPTABLE MORPHOLOGY.
- DEMONSTRATE COMPATIBILITY OF PROCESS WITH CONTINUOUS FLOW CONCEPT.

PROGRESS

- MAXIMUM THEORETICAL RECRYSTALLIZATION RATE AND CORRESPONDING E-GUN OPERATIONAL PARAMETERS DETERMINED.
- CONSTRUCTION OF MOLTEN ZONE REGROWTH APPARATUS COMPLETED.

FIGURE 11

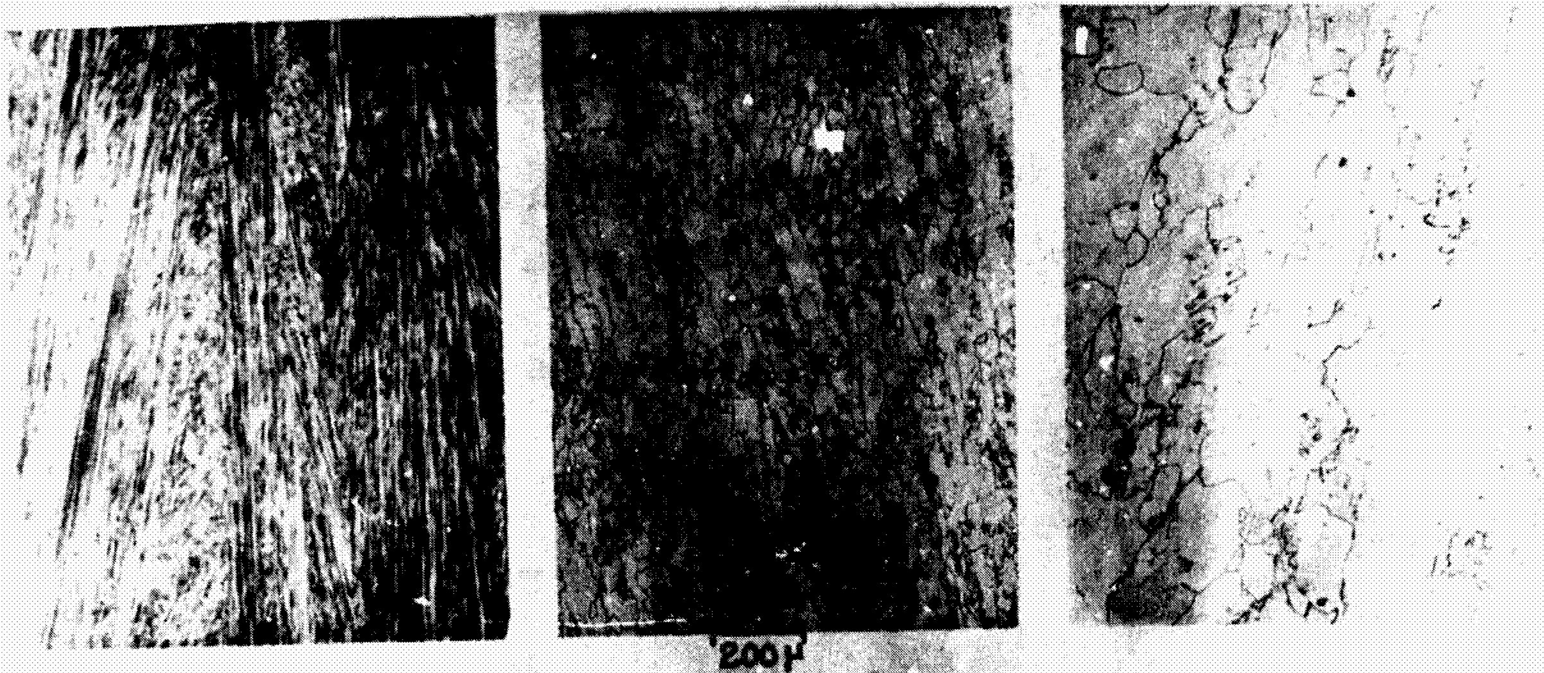

GRAIN SIZE

a) AS RECEIVED

(b) ANNEALING
OF (a)
T = 1350°C
Δt = 4 HRS.

(C) ANNEALING
AFTER PLAS.
DEFORMATION
T = 1350°C
Δt = 4 HRS.

BINARY SOLUTION GROWTH OF SILICON

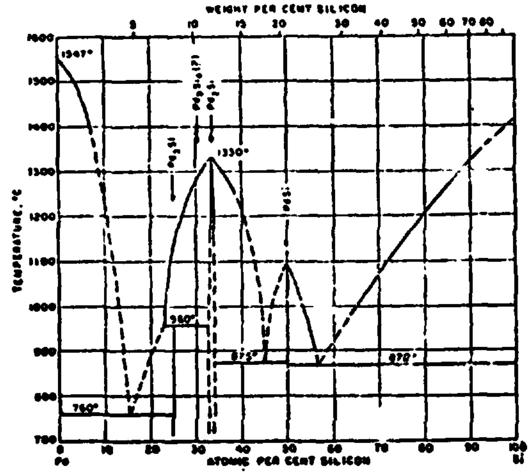

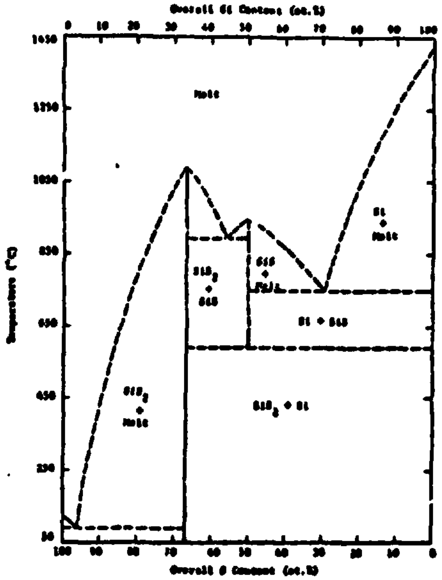

OBJECTIVE

'LOW TEMPERATURE GROWTH OF SILICON SHEET

GOALS

'SURVEY POTENTIAL BINARY SYSTEMS, DETERMINE SUITABILITY

'DETERMINE IF ACCEPTABLE GROWTH RATES ACHIEVABLE

'DETERMINE IF ACCEPTABLE MATERIAL PROPERTIES ACHIEVABLE

'ESTABLISH OPTIMUM BINARY SYSTEM

PROGRESS

'PROPERTIES OF POTENTIAL SOLUTIONS TABULATED AND GROUPED.

'EXPERIMENTAL WORK POSTPONED.

FIGURE 13

CANDIDATE MATERIALS FOR SILICON SOLUTION GROWTH

I M.P. ≤ 600°C LIQ. SOL'Y. ≤ 5% AT M.P.	II M.P. ≥ 950°C LIQ SOL'Y. HIGH	III M.P. ≤ 950°C; LIQ. SOL'Y. HIGH ELECTR. ACTIVE OR LIFETIME KILLER
Li In Pb Sn Zn	As Cr Ni Th B Fe O Ti Ba Hf P U Be Hg Pt V C Mg Pu W Ca Mn Re Y Ce Mo Sr Zr Co Nb Ta	Ag Al Au Cu Ga Li Sb

600° ≤ M.P. ≤ 950°C LIQ. SOL'Y. HIGH, NEUTRAL	Si ALLOYS NOT CHARACTERIZED
S (?) Pd	Cd N Pr Se Cs Na Rb Sm Ir Nd Rh Te K Np Ru Tl La Os Sc Yb

FIGURE 14

ATTRIBUTE	CURRENT DATA	PROJECTED DATA		
CRYSTAL DIAMETER, INCHES	3	4	6	8
WAFER THICKNESS, MM	0.4	0.24	0.20	0.20
KERF, MM	0.28	0.16	0.12	0.12
QUARTZ CRUCIBLE COST, $/KG	19.19	12.00	12.00	12.00
REPLACEMENT PARTS, $/KG	11.96	5.60	3.60	3.45
CAPITAL COSTS, $/KG	9.81	4.68	3.00	2.87
ALL OTHER DIRECT COSTS, $/KG	6.68	3.78	1.96	1.43
SILICON AT $4/KG	5.50	5.50	5.50	5.50
COST OF CYL. SILICON, AFTER 20% G&A	62.79	36.77	30.17	29.20
WAFER COST, $/M²	113.65	42.44	25.64	24.82

FIGURE 15. CZOCHRALSKI GROWTH COST SUMMARY

PROBLEMS

1. LOW SUPPLIER INVENTORIES AND LONG DELIVERY TIMES CAUSE DELAYS.
2. SiF_4 AND SI PURITY
3. SHORT GRANT PERIODS PREVENT PH.D. THESIS USE.

STAFF

	SiF_2 TRANSPORT		PLASTIC DEFORMATION		RECRYSTALLIZATION	
FACULTY	MACDIARMID WOLF	0.2 0.15	GRAHAM POPE	0.1 0.15	WOLF ZEMEL	0.15 0.1
RE. SPEC.	NOEL	0.5	-	-	NOEL	0.4
POST. DOC.	-	-	KULKURNI	1.0	STARTING SEPT.	-
TECHN.	GORMAN	0.7	-	-	GORMAN	0.3
STUDENT	2	1.0	1	0.3	1	0.6

SUMMARY OF KEY RESULTS

1.1.1 PRELIMINARY EVALUATION COMPLETED:

- COMMERCIAL MG-SI PROCESS SELECTED FOR UPGRADING
- SiF_2 POTENTIALLY USEFUL WITH MG-SI UPGRADING FOR TRANSPORT/PURIFICATION
- AL REDUCTION OF SiO_2 AND SiO REACTIONS POTENTIALLY FEASIBLE ROUTES

1.2.1 SiF_2 TRANSPORTABLE AT ATMOSPHERIC PRESSURE W/O DECOMPOSITION ABOVE 1100°C AND BELOW 100°C.

1.2.2 SILICON TRANSPORT RATE DETERMINED BY SiF_2 FORMATION REACTION.

1.2.4 MG-SI UPGRADED

- USING GAS BLOWING
- USING UNIDIRECTIONAL SOLIDIFICATION
- 10.7% (AMO) EFFICIENT CELL PRODUCED

2.1.1 EQUIPMENT FOR MOLTEN ZONE RECRYSTALLIZATION COMPLETED.

2.2.1 MATERIALS FOR BINARY MELT SOLUTION GROWTH TABULATED AND GROUPED.

2.2.2 SILICON PLASTICALLY DEFORMED $\geq$ 1250°C UP TO 70% AT DEFORMATION RATES $\leq$ 1%.

2.3.1 STRAIN-ANNEALING OBSERVED, GRAIN GROWTH BY FACTOR ~ 10 TO 1MM DIA.

PLANNED ACTIVITY-NEXT 6 MONTHS

1. SiF_2 TRANSPORT PROCESS:

   A) COMPLETE PRELIMINARY INVESTIGATION OF TRANSPORT PARAMETERS.

      INITIATE STUDY OF REACTION KINETICS.

   B) EVALUATE IMPURITY SEPARATION CAPABILITIES.

2. EXPERIMENTAL STUDY OF FLOATING MOLTEN ZONE PROCESS IN THIN SI SHEETS.

3. CONTINUE CHARACTERIZATION OF HIGH TEMPERATURE MECHANICAL PROPERTIES OF SILICON.

   COMPLETE AT LEAST ONE FORMING LIMIT DIAGRAM.

4. EXTEND PROCESS EVALUATION METHOD AND ECONOMIC ANALYSIS.

LOW-COST PROCESSES FOR SOLAR-GRADE SILICON

under

RESEARCH AND DEVELOPMENT OF LOW-COST PROCESSES
FOR INTEGRATED SOLAR ARRAYS

GRANT NSF/RANN/SE/GI-29729

for

15 April 1974 - 14 July 1975

at

$144,892

by

LEE P. HUNT
DOW CORNING CORPORATION

LEON D. CROSSMAN, ASSOC. PRINCIPLE INVESTIGATOR

under subcontract to

UNIVERSITY OF PENNSYLVANIA
MARTIN WOLF, PRINCIPLE INVESTIGATOR

Presented at

NATIONAL SOLAR PHOTOVOLTAIC PROGRAM REVIEW MEETING
LOS ANGELES, CALIFORNIA

July 22-25, 1975

ABSTRACT

Dow Corning's objective is to determine the best process for the high-volume production of solar-grade silicon (SoG-Si) at less than $10/kg within the ERDA milestone of having a pilot plant available by mid-1980.

The overall process screening approach (Visual Aid 2) which began with over 200 possible reactions leading to silicon has reduced this number to ten (V.A.3.) which still fall within the constratints mentioned above. Two of these reactions involve the direct reduction of silica to silicon via aluminum or carbon[*]. Seven other reactions involve the use of various reductants to convert silica to silicon via intermediate silicon monoxide. The tenth reaction uses recyclable SiF_4 to transport <u>in situ</u> produced silicon via intermediate SiF_2; this is currently under study by the University of Pennsylvania.

The reactions described above, in addition to processes involving silicates and/or electrolytic techniques, have been divided into two broad categories (V.A.4.): (1) metallurgicalgrade silicon (MG-Si) process upgrading, and (2) other processes. This was done since the commercial process for producing MG-Si already meets the high-volume, low-cost guidelines for SoG-Si[**] and, therefore, has a good probability of meeting the mid-1980 pilot plant milestone. The "other processes: are still in the conceptualization or research stage.

Upgrading the MG-Si process is being pursued in four associated areas in order to improve the purity of the normally 98% material (V.A.5.). The first two work areas involve purification of raw materials entering the process in addition to upgrading the arc furnace itself. These areas will be pursued, assuming contract extension. Success appears very favorable based upon suggestions from raw materials suppliers, arc furnace manufacturers, and MG-Si producers (B.A.9.).

The second two areas of process upgrading comprise improving the purity of the silicon after it leaves the arc furnace by reactive gas blowing and unidirectional freezing. Since both methods have been shown to reduce aluminum and heavy metal impurities by one to two orders-of-magnitude (V.A.7.), it is planned to study these methods in conjunction in a specially designed gradient furnace. Neither of the two methods, however, significantly reduce the levels of boron or phosphorus thereby stressing the need for initiating efforts in the raw material and arc furnace areas. The delivery time for an experimental arc furnace results in this item being on the critical path for meeting the mid-1980 pilot plant milestone (V.A. 14).

---

[*] This is today's commercial, submerged-electrode, arc furnace process for metallurgical-grade silicon.

[**] One furnace can generate greater than 10,000 tons per year of MG-Si selling at $1/kg.

The best cell produced to date was fabricated from MG-Si that had been blown with an O_2-Cl_2 mixture, unidirectionally solidified, and 6-float-zone passed (to determine a base boron level of 0.04 ohm-cm). The cell showed a 10.7% AMO efficiency with I_{sc} = 33 ma/cm^2 and V_{oc} = 0.62 v (V.A.8.).

In the "other processes" category, the use of silicates as a silicon source and of electrolysis as a process were studied. Silicates were deemed unfavorable since their inherent chemical composition involves the presence of another metallic element (V.A.11.). The best electrolytic process uses a 1000°C fused salt of silica in cryolite. Preliminary analysis of this process was viewed pessimistically for the reasons cited in V.A.10.

A summary of key results appears in Visual Aid 12.

Summarized future plans appear in Visual Aid 15.

DOW CORNING OBJECTIVE

TO DETERMINE THE BEST PROCESS FOR PRODUCING SILICON FOR SOLAR ARRAYS

- AT <$10/KG
- AT HIGH VOLUME RATES
- WITHIN ERDA MILESTONES

V.A.2.

PROCESS SCREENING PROCEDURE

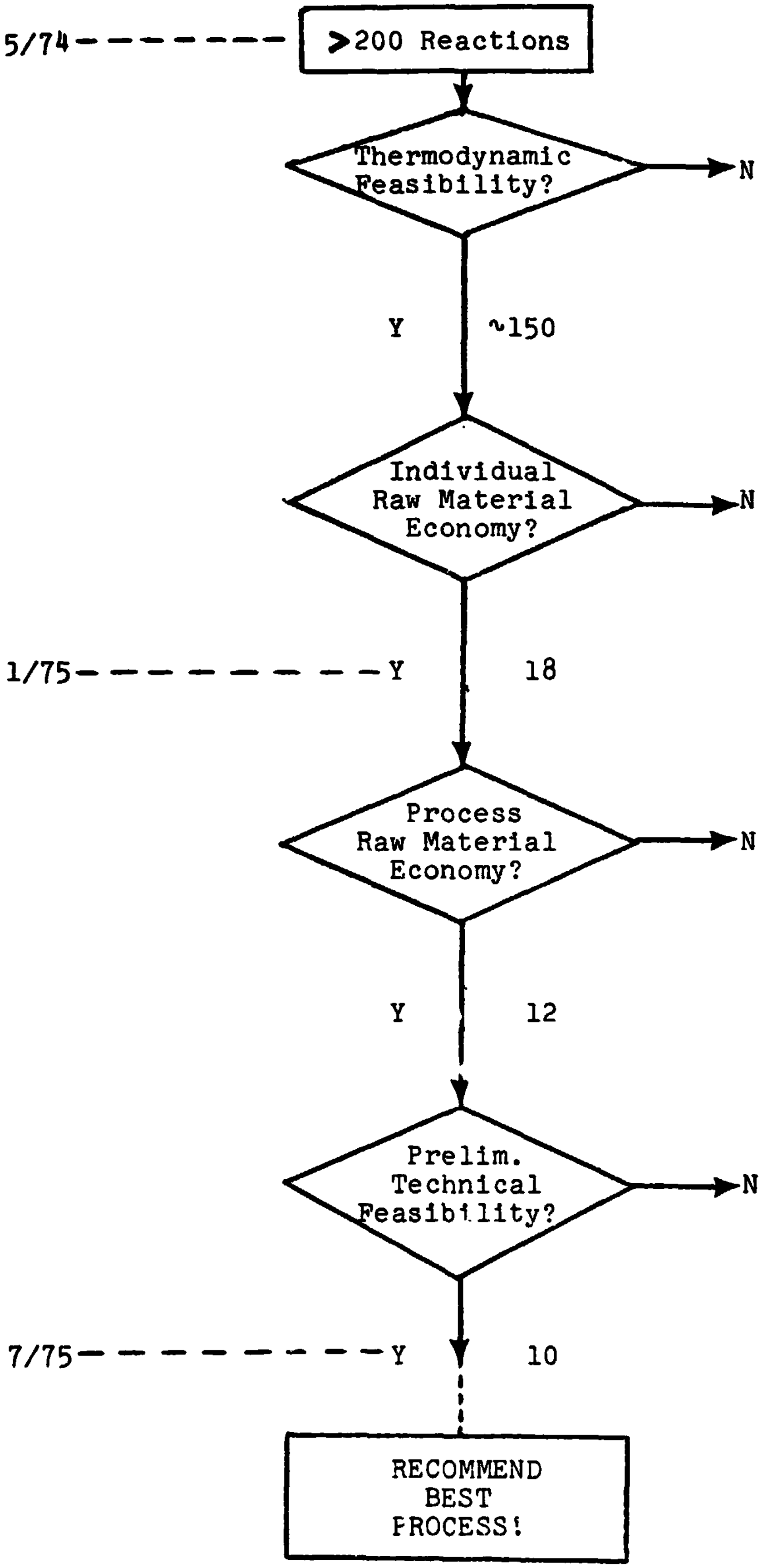

REMAINING PROCESSES

No. Reactions	1975 Raw Mat'l. Cost For Reaction ($/kg Si)	Reaction Type
2	0.12 for C 0.97 for Al	$SiO_2 \xrightarrow{C^* \text{ or } Al} Si$
1	0.12 (SiF_4 recycled)	$SiO_2 \xrightarrow{2C} Si \xrightarrow{SiF_4} 2SiF_2 \xrightarrow[-SiF_4]{} Si$
7	0.12 min. to 2.06 max.	$SiO_2 \xrightarrow{Al,\ C,\ \text{or } Mg} SiO \xrightarrow{Al,\ C,\ H_2 \text{ or } Mg} Si$

* Commercial Arc Furnace Process

PROCESS CATAGORIZATION

- UPGRADING THE METALLURGICAL-GRADE SI PROCESS
  - A PROVEN COMMERCIAL PROCESS
  - CAPABLE OF MEETING MILESTONES SOONER THAN R&D STAGE PROCESSES
  - ALL SI COMPOUNDS FROM REDUCTION OF QUARTZITE
  - CURRENT MG-S [illegible] TS $1/KG
  - PRESENT RATES >10,000 T/Y PER FURNACE

- OTHER PROCESSES
  - SiO GENERATED IN ARC FURNACE
  - SiF_2 TO TRANSPORT SI
  - ELECTROLYTIC
  - SILICATES

V.A.5.

UPGRADING MG-SI PROCESS

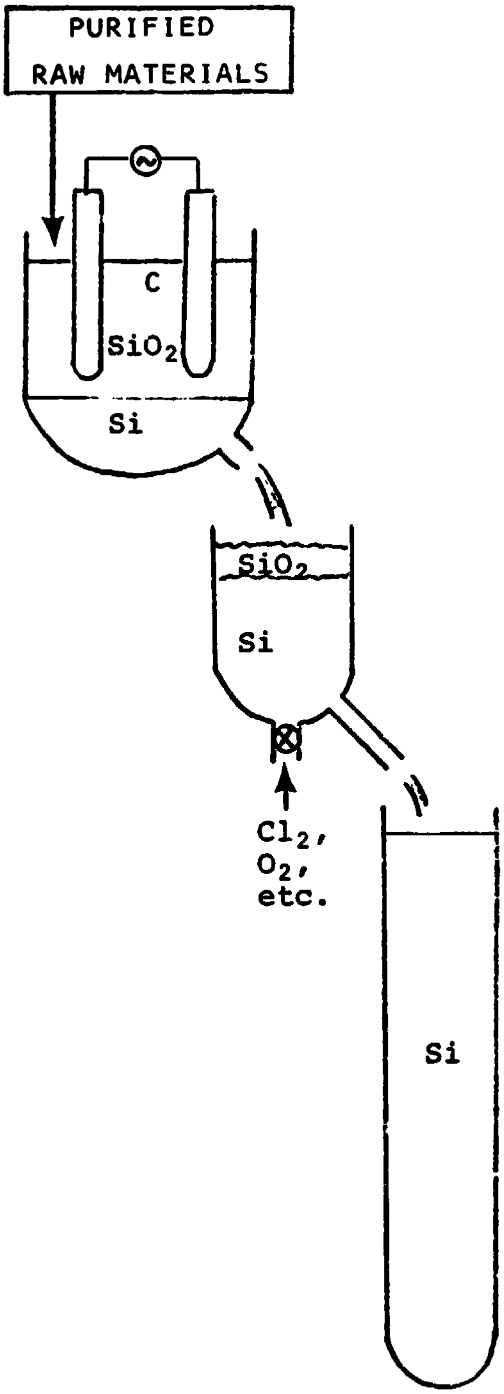

	AREAS OF WORK	IMPURITY STATUS
I.	RAW MATERIALS	B REMOVED? P + OTHERS TO BE TESTED.
II.	ARC FURNACE	B,P, + OTHERS TO BE TESTED.
III.	REACTIVE GAS BLOWING AND/OR SLAGGING	AL & HEAVY METALS REMOVED.
IV.	UNIDIRECTIONAL SOLIDIFICATION	AL & HEAVY METALS REMOVED.

UPGRADING MG-SI BY UNIDIRECTIONAL SOLIDIFICATION (WORK AREA IV)

	Impurity Levels (ppma)		
Impurity	MG-Si	CZO Seed	CZO 50% Point
B	39	39	44
P	37	23	21
Al	780	<10	60
Cu	40	< 4	< 4
Fe	910	< 5	140
Heavy Metals*	20-150	< 6	< 5-20

* Ti, V, Cr, Mn, Ni

UPGRADING MG-SI BY REACTIVE GAS BLOWING
(WORK AREA III)

BEST DATA TO DATE VIA EMISSION SPECTROSCOPY

	IMPURITIES IN MG-SI (PPMA)		
IMPURITY	NOT BLOWN	CL_2 BLOWN	O_2 BLOWN
B	39*	38*	36*
P	23	21	23
AL	1600	83	470
CU	35	4	4
FE	1600	40	40
HEAVY METALS†	50-100	< 5	5-40

* ~0.04 OHM-CM BY FZ EVALUATION

† TI, V, CR, MN, NI

V.A.8.

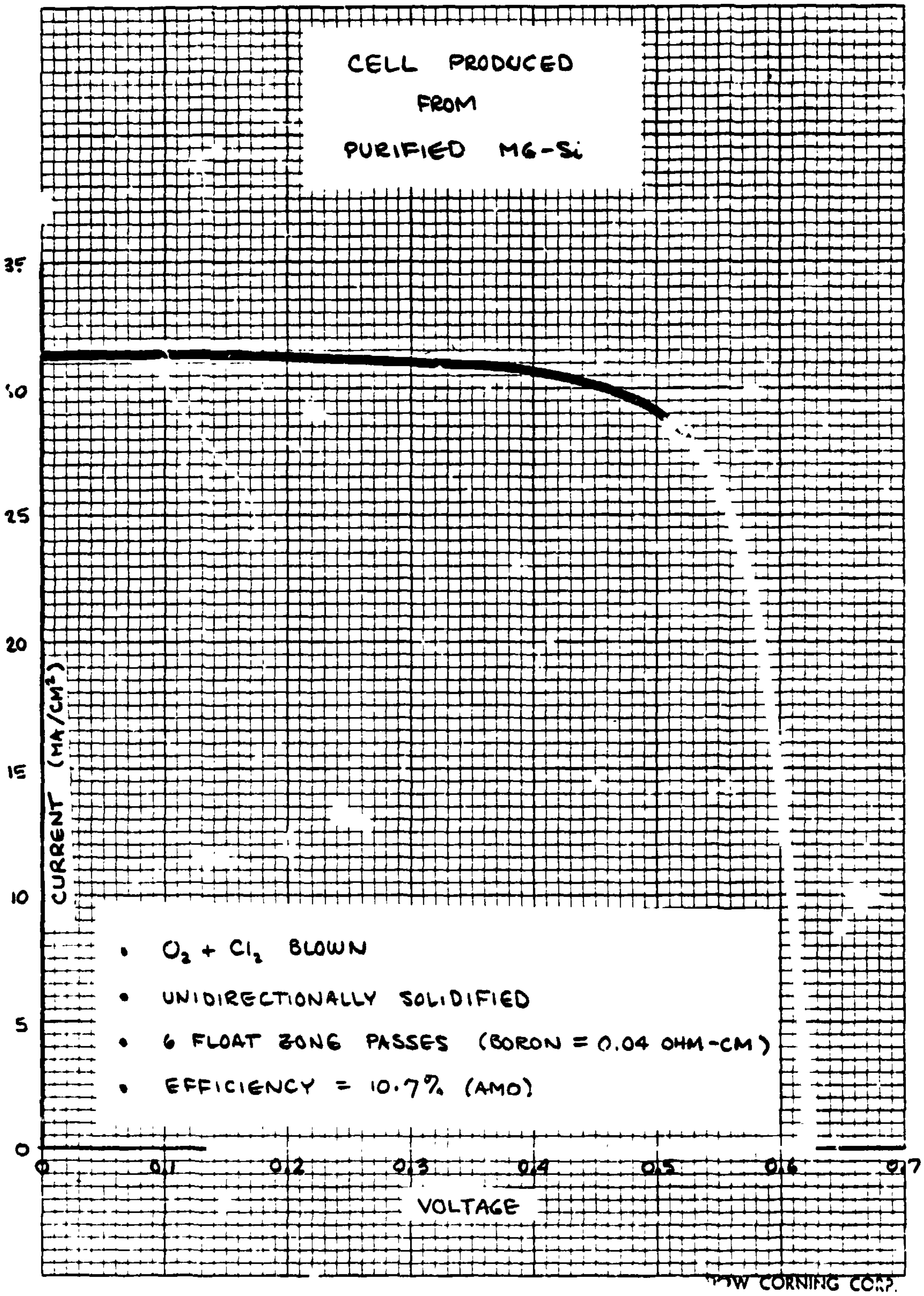
CELL PRODUCED
FROM
PURIFIED MG-Si
35
30
25
20
15
10
5
0
CURRENT (MA/CM²)
0
0.1
0.2
0.3
0.4
0.5
0.6
0.7
VOLTAGE
• O₂ + Cl₂ BLOWN
• UNIDIRECTIONALLY SOLIDIFIED
• 6 FLOAT ZONE PASSES (BORON = 0.04 OHM-CM)
• EFFICIENCY = 10.7% (AMO)
DOW CORNING CORP.

V.A.9.

UPGRADING POLY-SI PROCESS
(WORK AREAS I & II)

I. RAW MATERIALS

- Impurities Flow Through Furnace
    - Quartzite Can Be Upgraded (B < 1 ppma)
    - Carbon Sources Can Be Upgraded
    - Effect Of B From Raw Mat'l → Poly-Si Documented

II. ARC FURNACE

- Upgrade Liner, Tap Hole Plug, Ladle, Etc.
- Needed To
    - Test Raw Materials
    - Generate SiO
- Have Visited Manufacturers of Arc Furnace and Poly-Si

OTHER PROCESSES

- ELECTROLYTIC (BEST)

	SiO_2 IN Na_3SiF_6 ELECTROLYSIS	ARC FURNACE
TECHNOLOGY EXTENT	EXPERIMENTAL	COMMERCIAL
PRODUCTION RATE (KG SI/HR)	0.1	1000-2000
SI PURITY (WT. %)	99	98
PROCESS ENERGY (KWH/KG SI)	34	13

PESSIMISTIC DUE TO

- 4 ORDERS-OF-MAGNITUDE LOWER RATE
- SAME PURITY LEVEL
- HIGHER PROCESS ENERGY

OTHER PROCESSES

- SILICATES (E.G., $Al_2Si_2O_7 \equiv Al_2O_3 \bullet 2SiO_2$)
  - RULED OUT DUE TO INHERENT IMPURITY CONTENT

SUMMARY OF KEY RESULTS

TEN PROCESSES REMAIN IN RUNNING

- MG-SI UPGRADING FURTHEST ADVANCED COMMERCIALLY
- SiF_2 BY UNIVERSITY OF PENNSYLVANIA
- AL REDUCTION OF SiO_2 REMAINS
- REST INVOLVE SIO

MG-SI UPGRADED

- USING GAS BLOWING
- USING UNIDIRECTIONAL SOLIDIFICATION
- 10.7% EFFICIENT CELL PRODUCED

CRITICALITY OF EXPERIMENTAL ARC FURNACE IDENTIFIED

ELECTROLYSIS PROCESSES VIEWED PESSIMISTICALLY

SILICATES RULED OUT

MAJOR PROBLEMS

TECHNICAL

- REMOVAL OF B AND P

COST

- CAPITAL FOR EXPERIMENTAL ARC FURNACE
- MANPOWER TO IMPLEMENT ALL PROGRAM PHASES

SCHEDULE

- MEETING ERDA MILESTONES

V.A.14.

ACTION REQUIRED TO MEET PILOT PLANT MILESTONE FOR WORK AREAS I AND II

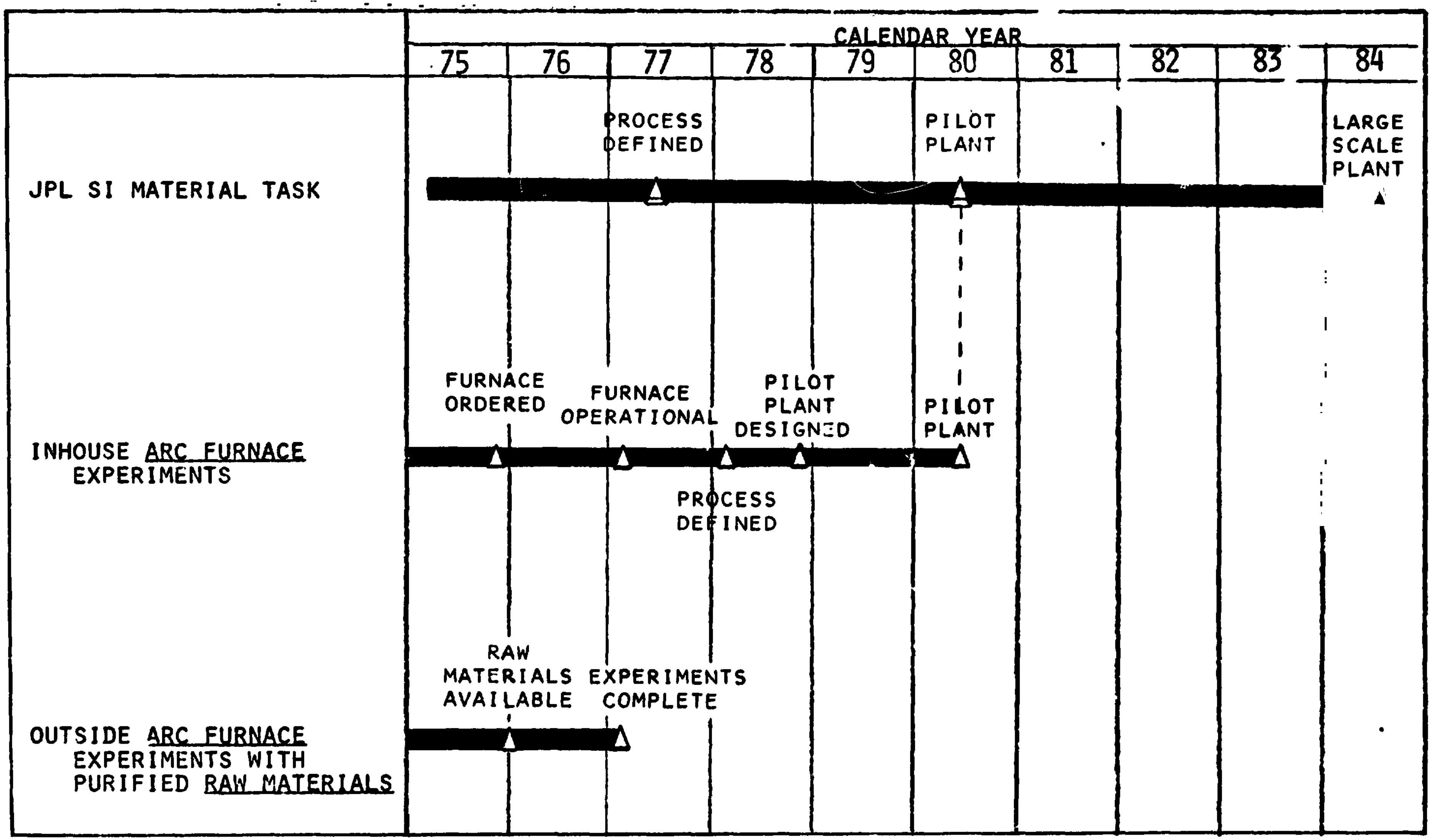

SIX MONTH GOALS UNDER REQUESTED CONTINUATION OF FUNDING

PERIOD: 15 JULY 1975 -- 14 JANUARY 1976

COST: $56,600 ORIGINAL ESTIMATE
$129,529 CURRENT REQUEST

MAJOR GOALS (ASSUMES INTERFACING WITH JPL PROGRAM):

- MG-SI UPGRADING
  - 10/75 SLAGGING FEASIBILITY DETERMINED
  - 10/75 PURCHASE OF EXPERIMENTAL ARC FURNACE INITIATED
  - 11/75 FEASIBILITY DETERMINED OF COMBINED BLOWING/FREEZING IN GRADIENT FURNACE
  - 12/75 RAW MATERIALS AVAILABLE FOR UPGRADING
  - 12/75 PLANS COMPLETE FOR EXTERNAL ARC FURNACE EXPERIMENTS
- SILICON MONOXIDE
  - 10/75 PROCESS POTENTIAL EVALUATED
  - 12/75 EXPERIMENTS INITIATED
- ALUMINUM REDUCTION OF QUARTZITE
  - 7/75 ENERGY ANALYSIS PERFORMED
  - 9/75 PROCESS POTENTIAL EVALUATED
  - 12/75 EXPERIMENTS INITIATED
- ENERGY ANALYSIS
  - 9/75 COMPLETE FROM QUARTZITE TO CELL

SESSION III

TEST AND DEMONSTRATION

PHOTOVOLTAIC TEST AND DEMONSTRATION PROJECT FOR THE NATIONAL PHOTOVOLTAIC CONVERSION PROGRAM

BY JAMES N. DEYO
NASA-LEWIS RESEARCH CENTER
CLEVELAND, OHIO

PRESENTED AT THE ERDA-NATIONAL SOLAR PHOTOVOLTAIC
PROGRAM REVIEW MEETING JULY 22-25, 1975
LOS ANGELES, CALIFORNIA

N76 12478

PHOTOVOLTAIC TEST AND DEMONSTRATION PROJECT FOR THE NATIONAL PHOTOVOLTAIC CONVERSION PROGRAM

by James N. Deyo

NASA-Lewis Research Center
Cleveland, Ohio

Abstract

As part of the overall effort to develop ways of utilizing solar energy as a national energy source, the Energy Research and Development Administration (ERDA) has established the National Photovoltaic Conversion Program. The overall objective of this program is to develop low-cost reliable photovoltaic systems suitable for a variety of terrestrial applications, and to stimulate the creation of a viable industrial capability to provide them. The program, now being implemented, is composed of several interrelated yet separate projects. Each project addresses a major segment of the effort required to achieve the program objective.

One of these projects, recently assigned to and now being developed by the Lewis Research Center of NASA, is concerned with conducting photovoltaic system tests and demonstrations covering a wide range of applications having national significance. Experience gained through this project will be used to evaluate emerging systems technology, provide systems-related guidance to the other projects of the program, and develop information for future photovoltaic program planning.

The project is divided into three basic activities. Objectives of the first activity, "Tests and Model System Demonstrations", are to determine the operating characteristics for a variety of photovoltaic conversion systems and subsystems and to confirm by tests and demonstrations that these systems can satisfy potentially attractive national applications. Solar cell modules for this activity will be provided by the Low Cost Silicon Solar Array Project being conducted by JPL for ERDA. In a similar manner, guidance in the selection of application categories for demonstration will be provided through mission and impact studies conducted by the Systems and Application Project of the national program. The second basic activity of the project is concerned with "Device Performance and Diagnostics". Objectives here are concerned with devising and developing the methodology, techniques, and equipment to make standardized measurements of solar cell and module performance and performance-related characteristics. This activity will therefore provide to the photovoltaic community a centralized source for standardized performance measurements and information of a reference and diagnostic nature. The third basic activity of the project will address the endurance of solar cell modules and arrays and the mechanisms affecting the materials of construction which induce performance degradation and failure. This activity will be carried out through accelerated and real time environmental testing, under conditions of intended use, of solar cell module materials of construction as well as complete modules. Laboratory investigations of methods of evaluating encapsulant material stability and degradation will be undertaken. Material and module samples for testing will be solicited from the photovoltaic community as well as being provided by the other projects of the national program.

Currently efforts in each of the three activity areas are being implemented through initial funding provided by ERDA. In addition, planning is going forward to more fully develop the basic project plans outlined to date and to identify new tasks which must be initiated through FY 76 and later ERDA funding to maintain the project schedule. Charts in the attached visual aid material indicate the basic project plans and tentative test and demonstration categories. As noted earlier in the systems test and demonstrtion activity, final selection of application categories will be guided by information from the Systems and Application Project of the national program.

NATIONAL PHOTOVOLTAIC CONVERSION PROGRAM

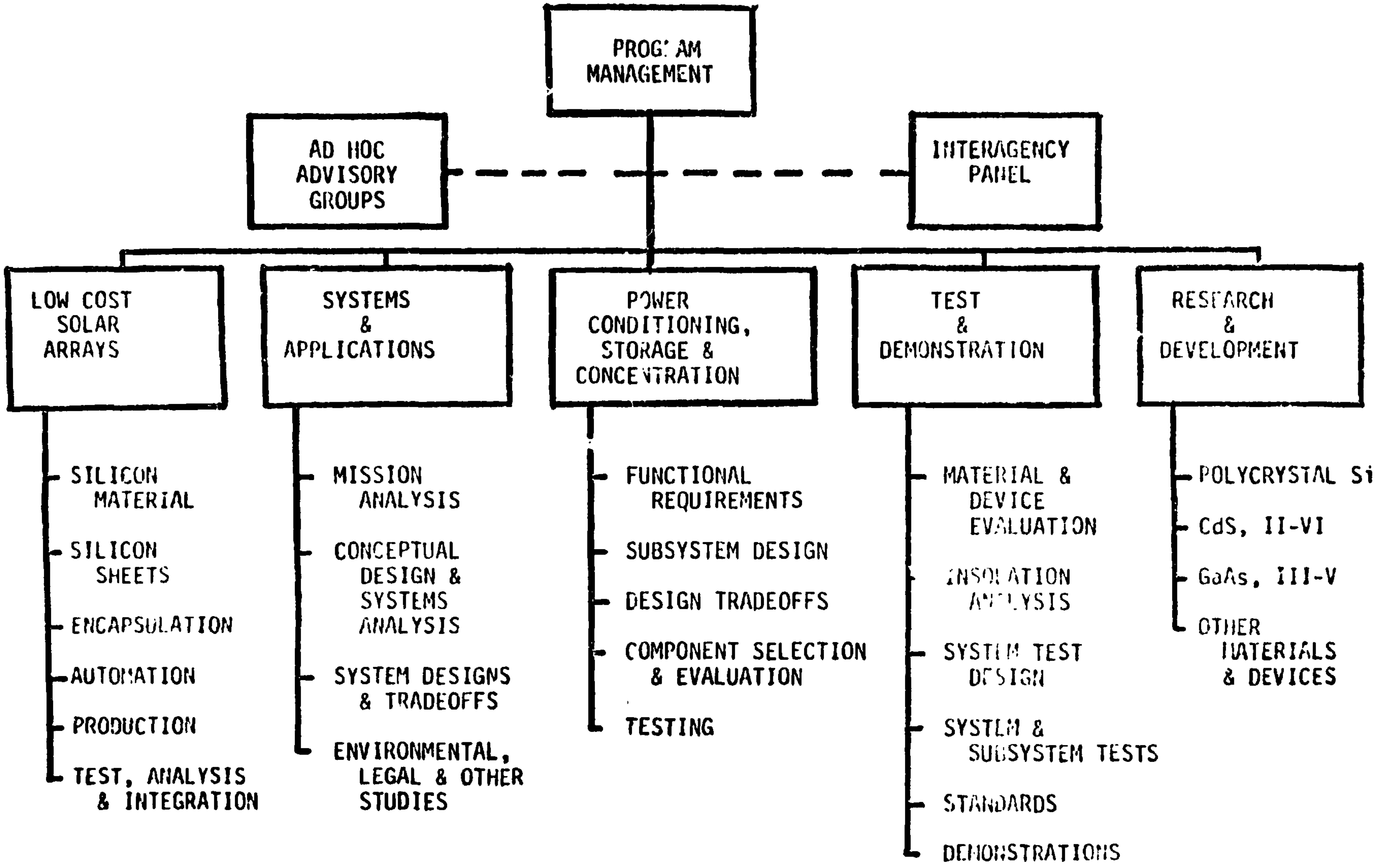

TEST AND DEMONSTRATION PROJECT

MAJOR ACTIVITIES:

- TESTS AND MODEL SYSTEM DEMONSTRATIONS
- DEVICE PERFORMANCE AND DIAGNOSTICS
- ENDURANCE TESTING

TESTS AND MODEL SYSTEM DEMONSTRATIONS

OBJECTIVES:

- DETERMINE OPERATING CHARACTERISTICS FOR A VARIETY OF P/V CONVERSION SYSTEMS & SUBSYSTEMS
- CONFIRM BY TESTS & DEMONSTRATIONS THAT P/V SYSTEMS CAN SATISFY POTENTIALLY ATTRACTIVE APPLICATIONS HAVING NATIONAL IMPACT

TESTS AND MODEL SYSTEM DEMONSTRATIONS

TECHNICAL APPROACH:

- INITIAL TESTS EMPHASIZE LOW POWER LEVELS & SYSTEM SIMPLICITY
- INCREASE P[illegible] LEVELS & SYSTEM FUNCTIONS BASED ON TEST RESULTS & ON-GOING STUDIES
- SOLAR CELL MODULES SUPPLIED BY "LCSSCA" ON REFERENCE CATEGORIES

TEST & MODEL SYSTEM DEMONSTRATION CATEGORIES*

ERDA:

0.1 - 1.0 kW REMOTE APPLICATIONS
5 - 15 kW RESIDENTIAL
100 - 500 kW LOAD CENTERS
1 - 3 MW LOAD CENTERS

ERDA / DOD:

1 - 3 kW LOAD CENTER
3 - 12 kW LOAD CENTER
12 - 60 kW LOAD CENTER

LeRC TEST CAPABILITY:

UP TO 100 kW P/V SYSTEM TEST FACILITY
5-15 kW PROTOTYPE RESIDENCE
COMPONENT & SUBSYSTEM SUPPORT TESTING

*REFERENCE CATEGORIES FOR PLANNING PURPOSES

CANDIDATES FOR REMOTE APPLICATIONS

FY '76 & '77

- U.S. COAST GUARD
  - 2ND DISTRICT (WESTERN RIVERS) (50)
  - 1ST DISTRICT (ATLANTIC-N.E.) (48)
  - REEF LIGHTS (7)
  - MAJOR LIGHT STATION (1)

- NOAA - RAMOS (40)

- U.S. GEOLOGICAL SURVEY
  - RIVER GAUGE STATION (100)
  - LANDSAT PLATFORM (20)

- OTHER POTENTIAL CANDIDATES
  - FAA (REMOTE NAVAIDS - BEACONS)
  - DOT (HIGHWAY AIDS-BARRIERS)
  - USDA - FOREST SERVICE (FIRE MON., COMM.)

PHOTOVOLTAIC SYSTEM TEST FACILITY

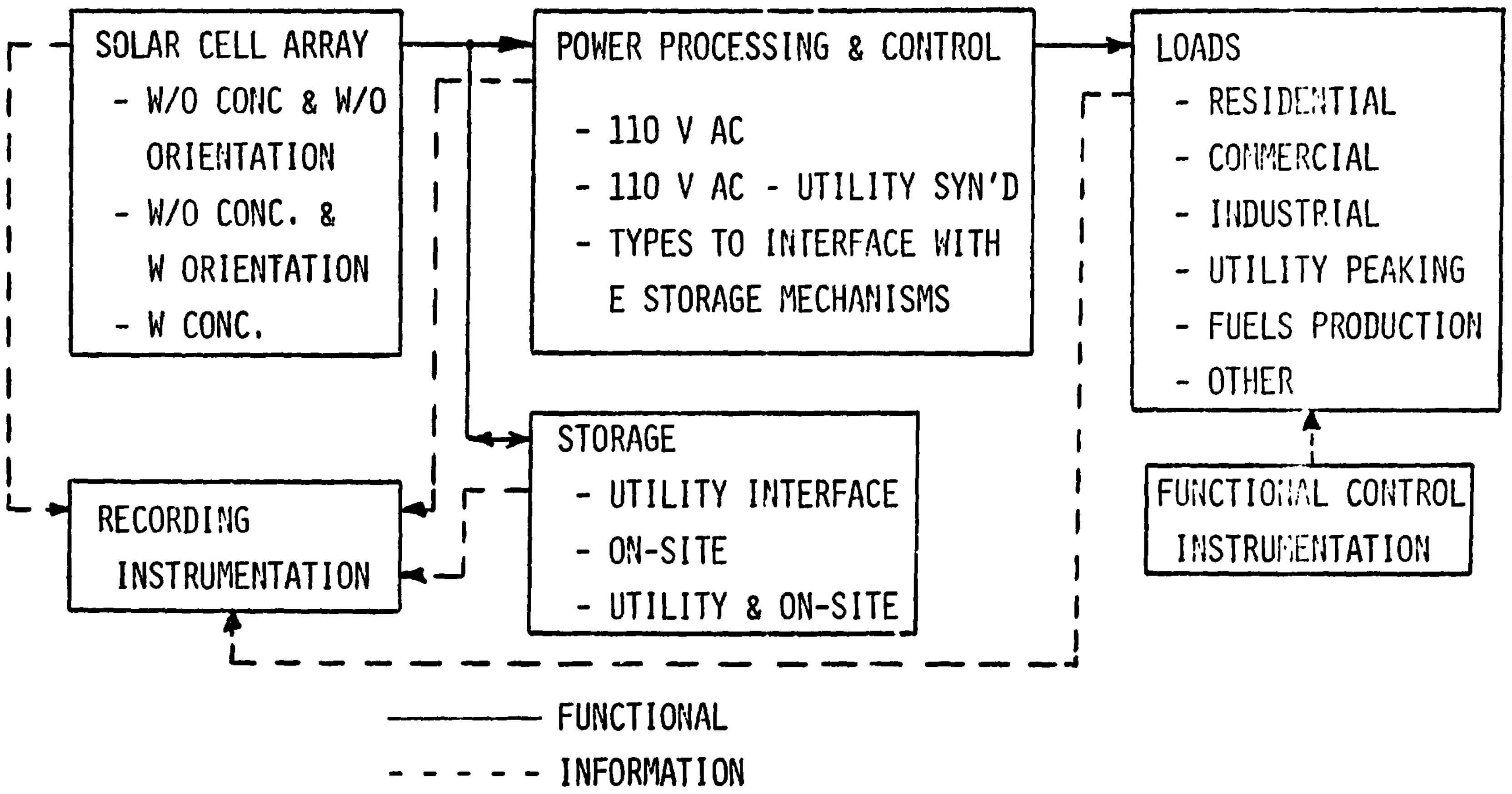

ERDA - TEST AND DEMONSTRATION PROJECT

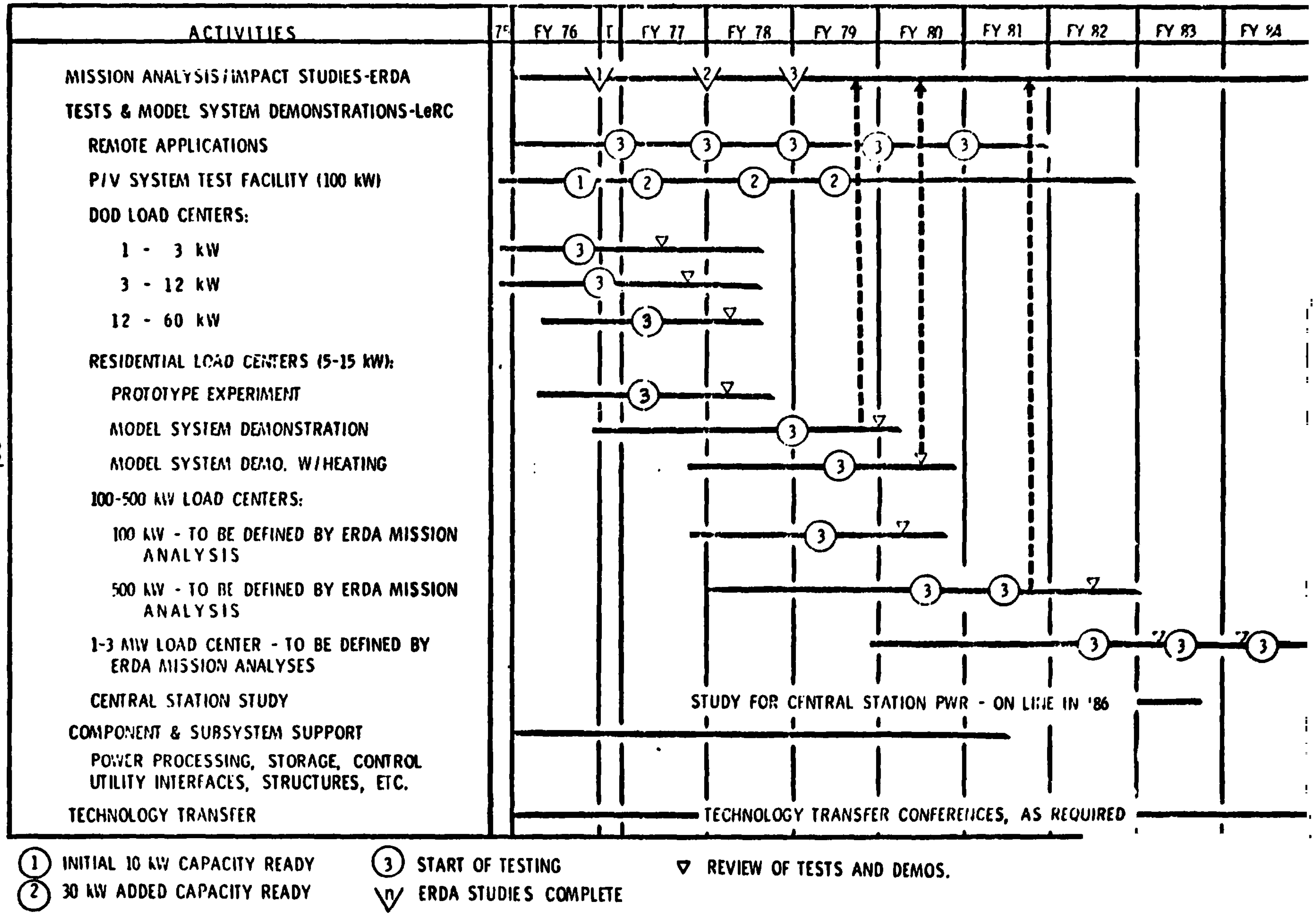

DEVICE PERFORMANCE AND DIAGNOSTICS

OBJECTIVES:

PROVIDE FOR:

- ACCURATE AND REPRODUCIBLE MEASUREMENTS OF SOLAR CELL AND MODULE PERFORMANCE
- DIAGNOSTIC MEASUREMENTS ON SOLAR CELLS
- ESTABLISH MATERIALS DIAGNOSTICS INFORMATION CENTER(S)

DEVICE PERFORMANCE AND DIAGNOSTICS

TECHNICAL APPROACH:

- DEVISE A STANDARD ACCURATE LABORATORY MEASUREMENT BASED ON A REPRESENTATIVE SOLAR TERRESTRIAL SPECTRUM
- ESTABLISH CELL AND MODULE STANDARD MEASUREMENT LABORATORIES AT LERC

DEVICE PERFORMANCE AND DIAGNOSTICS

MAJOR ACTIVITIES:

- WORKSHOPS AND COMMITTEES TO PROVIDE PHOTOVOLTAIC COMMUNITY INPUT FOR MEASUREMENT METHODS
- MEASUREMENT PROCEDURES MANUAL
- STANDARD METHODOLOGY FOR CELL AND MODULE REFERENCE PERFORMANCE MEASUREMENTS
- STANDARD CELL MEASUREMENT FACILITY
- CALIBRATION OF REFERENCE CELLS
- MODULE MEASUREMENT FACILITY
- DEVICE ELECTRICAL DIAGNOSTICS FACILITY

ERDA - TEST AND DEMONSTRATION PROJECT

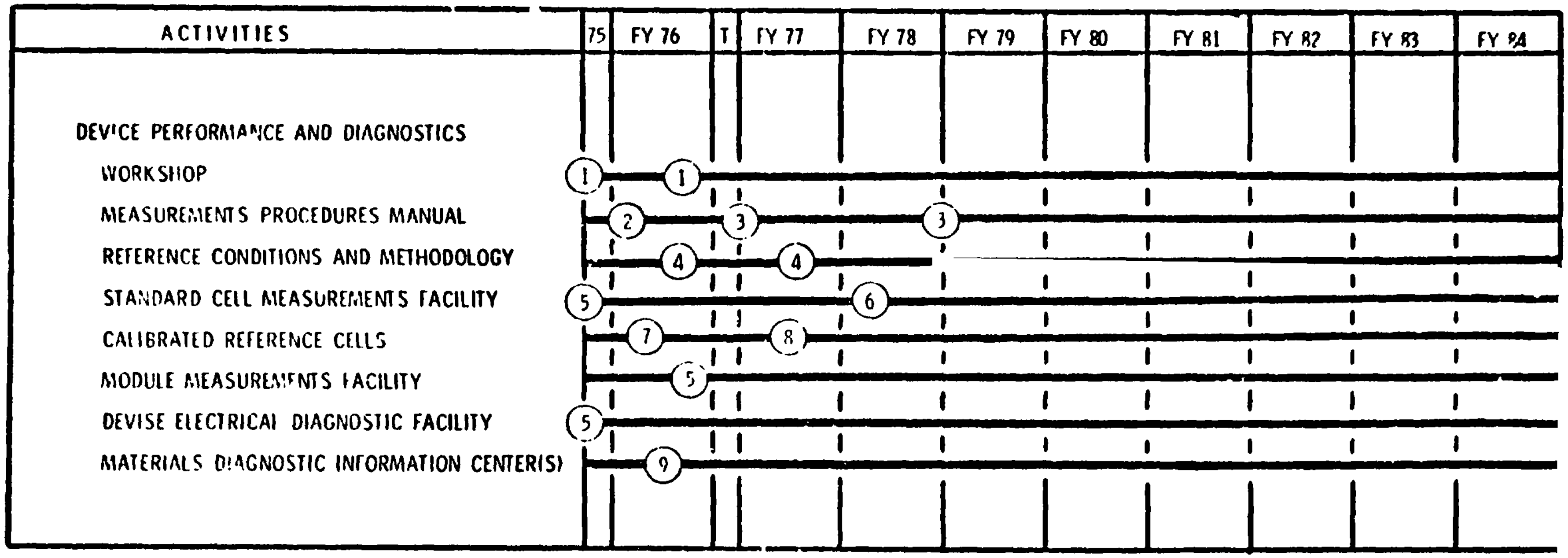

① CONVENE WORKSHOP
② DISTRIBUTE INTERIM MANUAL
③ DISTRIBUTE UPDATED MANUAL
④ EVALUATE REFERENCE COND. & METHODS
⑤ FACILITY OPERATIONAL
⑥ FACILITY IMPROVEMENTS OPERATIONAL
⑦ DISTRIBUTE INTERIM REF. CELLS
⑧ DISTRIBUTE UPDATED REF. CELLS
⑨ CENTER OPERATIONAL

ENDURANCE TESTING

OBJECTIVES:

- DETERMINE ENDURANCE OF SOLAR CELL MODULES, ARRAYS, AND COMPONENT MATERIALS OF CONSTRUCTION UNDER ENVIRONMENTAL CONDITIONS OF INTENDED USE
- DEVELOP METHODS OF EVALUATING FAILURE MECHANISMS AND PREDICTING MODULE ENCAPSULANT LIFE

ENDURANCE TESTING

TECHNICAL APPROACH:

- ESTABLISH CAPABILITY FOR ACCELERATED AND REAL TIME ENVIRONMENTAL TESTING
- TEST MODULES AND MATERIALS FROM "LCSSCA" PROJECT
- SOLICIT MODULES AND MATERIALS OF CONSTRUCTION FROM P/V COMMUNITY FOR EVALUATION
- CONDUCT INVESTIGATIONS OF ENCAPSULANT FAILURE MECHANISMS TO ESTABLISH PREFERRED METHODS OF PREDICTING LIFETIMES

ERDA - TEST AND DEMONSTRATION PROJECT

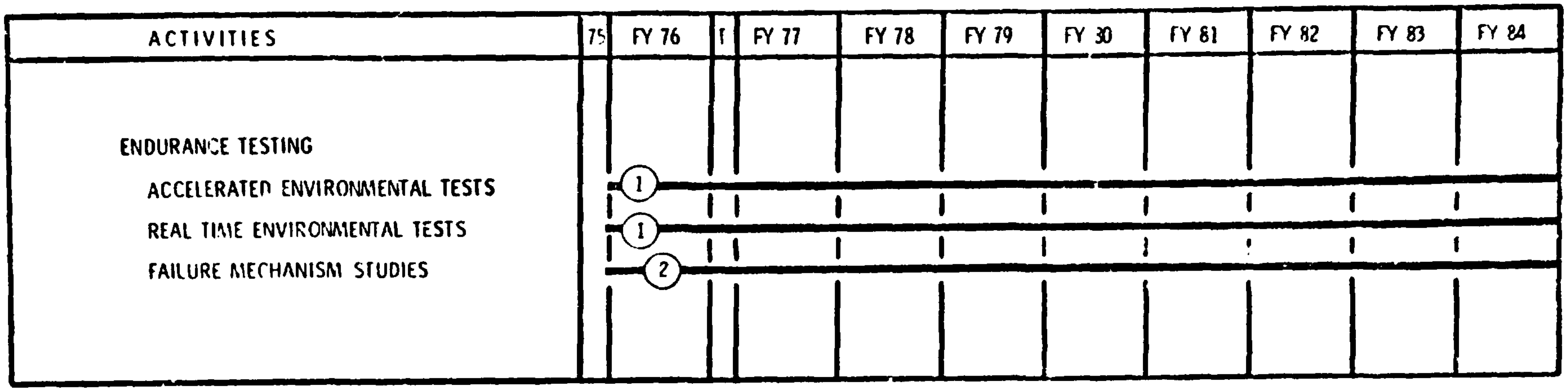

① FACILITIES AVAILABLE FOR MAT'L. EVAL.

② STUDIES INITIATED

STATUS OF ERDA-DOD APPLICATIONS PLANS

Title of Project: DOD PHOTOVOLTAICS DEMONSTRATION STUDY

Period of Contract: 7 July - 2 August 1975

Value of Contract: $30,000

Author: Donald B. Dinger
Associate Technical Director (R&D)
US Army Mobility Equipment Research and
Development Center

Principal Investigators: Richard T. Sale
Edward A. Gillis

Presented on 23 July 1975 at

NATIONAL SOLAR PHOTOVOLTAIC PROGRAM

REVIEW MEETING

Los Angeles, California

The Army Mobility Equipment Research and Development Center (USAMERDC) is presently conducting a one month DOD Demonstration Study sponsored by ERDA. The objective of this study effort is to produce a demonstration program which will define the role of Solar Terrestrial Photovoltaic (P/V) systems as power sources for DOD applications. To accomplish this goal, numerous potential demonstrations of DOD applications are being identified and analyzed. After the best demonstration projects are selected, the P/V power source requirements and an implementation plan for each demonstration project will be developed.

USAMERDC has been assigned DOD program management responsibility for investigation of terrestrial applications of solar P/V devices. This assignment includes the study which is the subject of this paper as well as conducting the demonstrations evolving from the study. In addition, USAMERDC has been tasked to establish a Tri-Service coordinating mechanism relative to application of P/V devices and has been funded for a study to identify early market potential for P/V devices within DOD.

In spite of limited experience in Solar P/V devices, USAMERDC is well qualified to perform the P/V activity outlined above. One of USAMERDC's primary missions is R&D in Electric Power Generation and Distribution. Of particular significance are major R&D activities in power conditioning and energy storage. Expertise and experience in these technologies will be most beneficial in establishing requirements for P/V power sources.

DOD is dedicated to conservation of energy and reduction of dependence on hydrocarbon fuel. The military is also interested in determining applications where P/V offers a tactical advantage. There may also be applications which prove cost effective, such as remote locations which have a high logistics burden due to resupply of fuel. Characteristics of P/V systems which make them attractive to the military for electric power sources include high reliability, low maintenance, unattended operation, long life, silent operation and reduced logistics.

ERDA is committed to purchase 90 KW of P/V power systems which will be supplied to DOD for demonstrations to provide DOD with a basis for future military utilization of P/V devices. Two 3 KW systems will be available on 1 January 1976 for installation in the selected demonstration projects. Two 12 KW systems will be provided on 1 April, and the final 60 KW system will be supplied in August 1976.

USAMERDC's study approach is t initially identify multiple DOD applications, analyze their power system requirements relative to use of P/V units, and recommend the most promising applications to DOD and ERDA for selection of the demonstration projects. A preliminary systems analysis will be performed and an implementation plan will be developed for each of the selected projects. The final task will be the preparation of a report summarizing results of the study.

The first two weeks of the study were primarily devoted to identifying potential applications of P/V power sources and developing evaluation criteria. Numerous agencies have been contacted and there has been good response at all levels; potential applications have been provided by all the Services. Candidate demonstration systems and locations are being analyzed using the derived evaluation criteria. Technical data regarding available batteries and power conditioning devices are being accumulated. The most promising demonstration candidates in each of the three power sizes (3 KW, 12 KW, and 60 KW) will be submitted by 25 July. Following selection of the demonstration projects the systems engineering, systems analysis, and implementation plan for each project will be initiated.

The evaluation criteria place emphasis on military market potential and military advantages. The military market potential is an indicator of both potential energy savings and production base potential. The application should benefit from use of a P/V power source; there should be an improved mission capability. In addition to the above primary considerations,the suitability of P/V to integration with the load utilizing available storage and power conditioning equipment is important. Candidates are also being evaluated to determine if there are similar applications in the civilian sector and their potential for an impressive demonstration which can readily "sell" the advantages of utilizing P/V in military applications.

USAMERDC's projected role in the DOD demonstration program includes:

a. Assisting in development, fabrication and assembly of the Photovoltaic power source.

b. Installation of the power system at the demonstration site and integration of it with the load.

c. Operation and maintenance of each demonstration project.

d. Monitoring system performance for at least 12 months to determine capability of P/V source to provide sufficient power to required quality, as dictated by the using equipment.

e. Evaluation of the P/V power system's design using recorded data; determine if there is adequate or surplus storage and/or array, etc.

DOD PHOTOVOLTAICS DEMONSTRATION STUDY

PERFORMED BY: U.S. ARMY MOBILITY EQUIPMENT RESEARCH & DEVELOPMENT CENTER
FORT BELVOIR, VIRGINIA

STUDY DURATION: 7 JULY 1975 - 2 AUGUST 1975

AMOUNT: $30,000

PRINCIPAL INVESTIGATORS: RICHARD T. SALE
EDWARD A. GILLIS

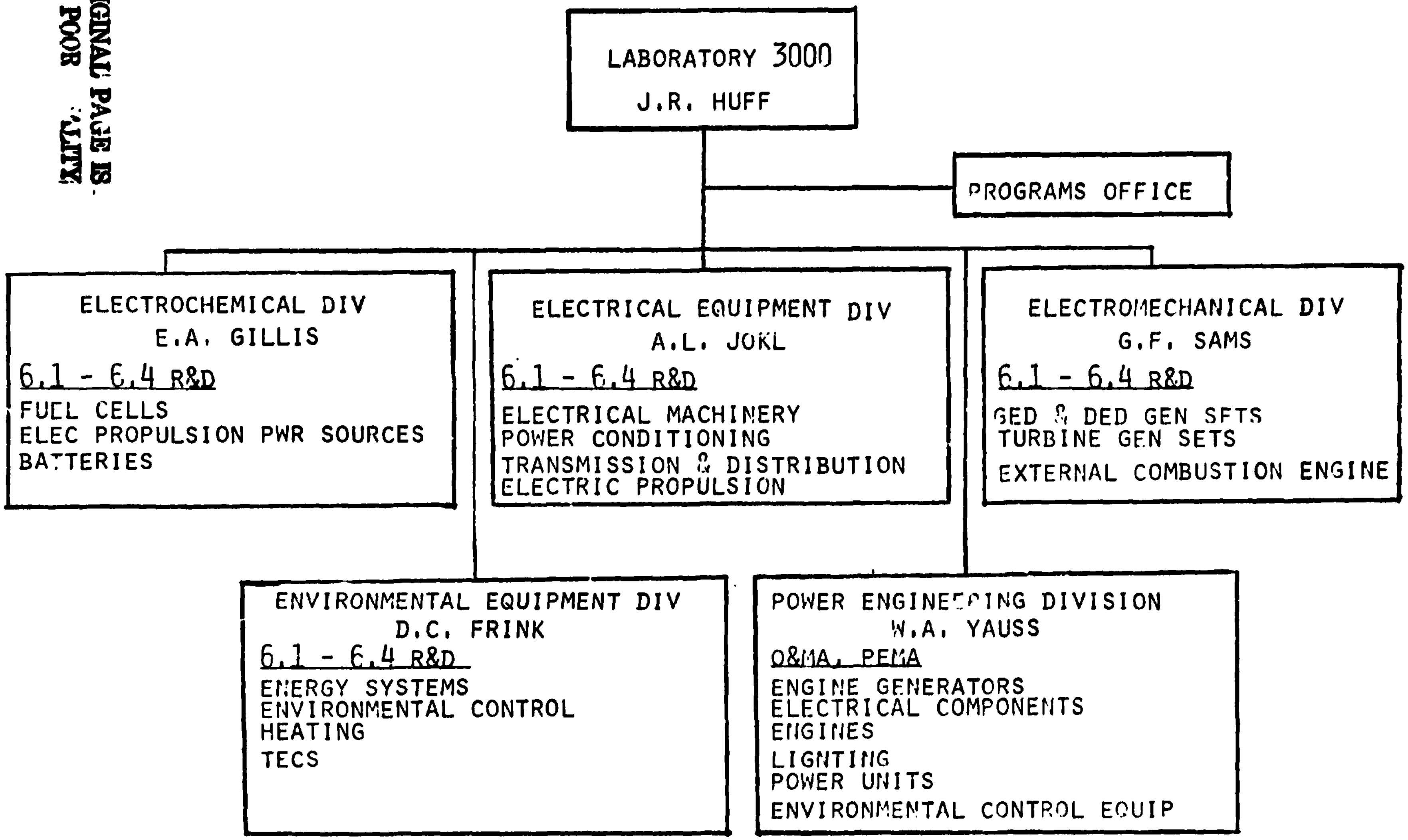

LABORATORY 3000
J.R. HUFF
PROGRAMS OFFICE
ELECTROCHEMICAL DIV
E.A. GILLIS
6.1 - 6.4 R&D
FUEL CELLS
ELEC PROPULSION PWR SOURCES
BATTERIES
ELECTRICAL EQUIPMENT DIV
A.L. JOKL
6.1 - 6.4 R&D
ELECTRICAL MACHINERY
POWER CONDITIONING
TRANSMISSION & DISTRIBUTION
ELECTRIC PROPULSION
ELECTROMECHANICAL DIV
G.F. SAMS
6.1 - 6.4 R&D
GED & DED GEN SETS
TURBINE GEN SETS
EXTERNAL COMBUSTION ENGINE
ENVIRONMENTAL EQUIPMENT DIV
D.C. FRINK
6.1 - 6.4 R&D
ENERGY SYSTEMS
ENVIRONMENTAL CONTROL
HEATING
TECS
POWER ENGINEERING DIVISION
W.A. YAUSS
O&MA, PEMA
ENGINE GENERATORS
ELECTRICAL COMPONENTS
ENGINES
LIGHTING
POWER UNITS
ENVIRONMENTAL CONTROL EQUIP

ACTIVE TECHNICAL AREAS

- ENERGY STORAGE
  - MAGNETIC
  - PNEUMATIC
  - BATTERY
  - FLYWHEEL
  - HYDROGEN
- STORAGE CONVERTERS
  - FUEL CELL
  - ROTATING ELECTRICAL MACHINE
  - HEAT ENGINE
- POWER CONDITIONING

MILITARY INTEREST IN PHOTOVOLTAICS

- CONSERVE ENERGY - REDUCE DEPENDENCE ON POL
- APPLICATIONS WHICH RESULT IN TACTICAL ADVANTAGES - INCREASE ABILITY TO PERFORM MISSION
- APPLICATIONS WHICH ARE COST EFFECTIVE - SUCH AS REMOTE SITES WHERE LOGISTICS BURDEN CAN BE SUBSTANTIALLY REDUCED
- P/V CHARACTERISTICS WHICH OFFER ADVANTAGES FOR SELECTED MILITARY APPLICATIONS
    - HIGH RELIABILITY, LOW MAINTENANCE
    - UNATTENDED OPERATION
    - LONG LIFE
    - SILENT
    - REDUCED LOGISTICS
- INCREASE PRODUCTION BASE TO ENHANCE PRIVATE SECTOR USAGE AND INCREASE AVAILABILITY OF PETROLEUM FOR CRITICAL MILITARY APPLICATIONS

SOLAR ELECTRIC POWER

DOD PROGRAM MANAGEMENT RESPONSIBILITY

- MARKET SURVEY
- DEMONSTRATION
- TRI-SERVICE COORDINATION

DOD DEMONSTRATION PROGRAM - 90KW

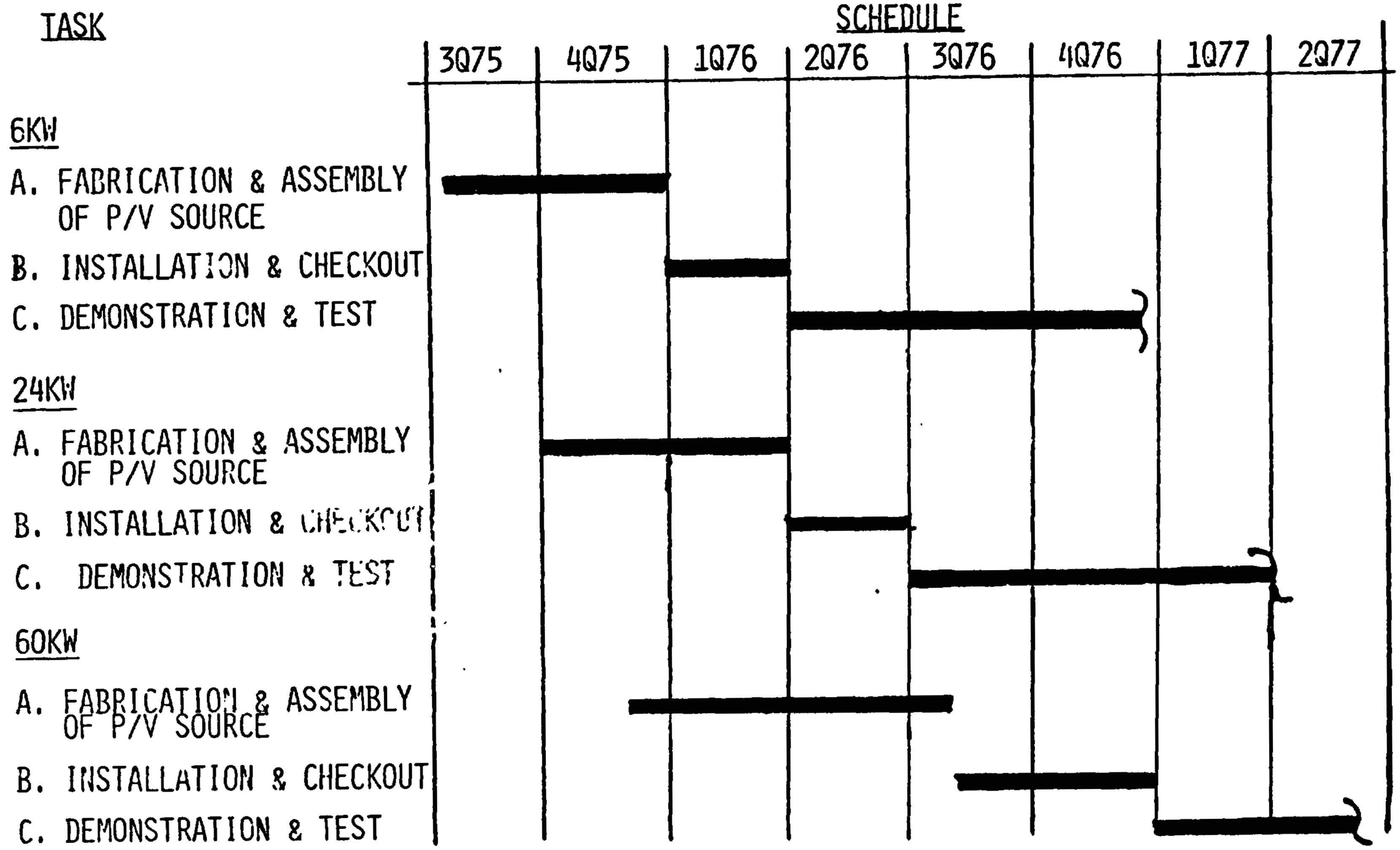

OBJECTIVES

- DEFINE DEMONSTRATION PROJECTS OF SOLAR TERRESTRIAL PHOTOVOLTAICS AS A POWER SOURCE FOR DOD APPLICATIONS
- SELECT DEMONSTRATION PROJECTS WHICH OFFER HIGH POTENTIAL MILITARY PAYOFF
- PROVIDE HARDWARE AND SYSTEM REQUIREMENTS NECESSARY TO DEVELOP AND ASSEMBLE THE COMPLETE P/V POWER SOURCE FOR EACH DEMONSTRATION PROJECT

STUDY APPROACH

- IDENTIFY DOD SYSTEMS REQUIREMENTS
- ANALYZE POWER SYSTEM REQUIREMENTS RE APPLICATION OF P/V POWER SOURCES
- SUBMIT RECOMMENDED APPLICATIONS TO DOD AND ERDA FOR SELECTION OF DEMONSTRATION PROJECTS
- DEVELOP IMPLEMENTATION PLAN FOR EACH SELECTED DEMONSTRATION PROJECT
- PREPARE REPORT

STUDY SCHEDULE

TASK

A. IDENTIFY DOD REQUIREMENT FOR VARIOUS APPLICATIONS

B. ANALYZE REQUIREMENTS

C. SELECT POTENTIAL SITE FOR MOST PROMISING APPLICATIONS

D. RECOMMEND DEMONSTRATION PROJECTS TO DOD AND ERDA

E. SELECTION OF PROJECTS

F. PRELIMINARY SYSTEMS ENGR. AND SYSTEMS ANALYSIS

G. DEVELOP IMPLEMENTATION PLAN FOR SELECTED PROJECTS

H. SUBMIT REPORT SUMMARIZING RESULTS

STATUS

- NUMEROUS APPLICATIONS IDENTIFIED BY DOD AGENCIES
- EVALUATION CRITERIA DEVELOPED
- CANDIDATE SYSTEMS ANALYZED
- RATIONALE SUPPORTING RELATIVE RATINGS OF APPLICATIONS BEING DOCUMENTED
- POWER CONDITIONING AND STORAGE DATA BEING ACCUMULATED
- RECOMMENDED LOCATION OF DEMONSTRATION PROJECTS BEING FINALIZED
- MOST PROMISING CANDIDATES FOR DEMONSTRATION PROJECTS WILL BE SUBMITTED BY 25 JULY

AGENCIES CONTACTED

DOD

OFFICE OF THE ASSISTANT SECRETARY OF DEFENSE FOR INSTATLLATIONS AND LOGISTICS

COORDINATORS FOR ENERGY - ARMY, NAVY, AIR FORCE

PROJECT MANAGER - MOBILE ELECTRIC POWER

DEFENSE COMMUNICATIONS AGENCY

ARMY

CORPS OF ENGINEERS

HARRY DIAMOND LABORATORIES

ELECTRONICS COMMAND

NIGHT VISION LABORATORY

ARMY SECURITY AGENCY

SHARPE DEPOT
MASSTER

AVIATION COMMAND

MISSILE COMMAND

ARMAMENTS COMMAND

PICATINNY ARSENAL

FRANKFORD ARSENAL

AGENCIES CONTACTED (CONTINUED)

NAVY

- NAVAL RESEARCH LABORATORY (ACTING AS FOCAL POINT FOR OTHER ORGANIZATIONS)
- NAVAL WEAPONS CENTER
- NAVAL ELECTRONICS LABORATORY
- NAVAL CIVIL ENGINEERING LABORATORY

AIR FORCE

- WRIGHT PATTERSON AFB, PROPULSION LAB
- CIVIL ENGINEERING OFFICE (PENTAGON)
- AIR FORCE ACADEMY
- TYNDALL AFB
- BOLLING AFB

MARINE CORPS

- CONCEPTS AND ANALYSIS BRANCH
- MOBILE ELECTRIC POWER GROUP
- COMMAND, CONTROL AND COMMUNICATIONS (QUANTICO)

NASA - LEWIS

JPL

EVALUATION CRITERIA

- PRIMARY IMPORTANCE
    - MILITARY MARKET POTENTIAL
    - MILITARY ADVANTAGES
- SECONDARY IMPORTANCE
    - SUITABILITY AS A POWER SOURCE RELATIVE TO LOAD AND DEPLOYMENT
- OTHER CONSIDERATIONS
    - SIMILAR CIVILIAN APPLICATIONS
    - IMPRESSIVE DEMONSTRATION

EXAMPLES OF APPLICATIONS SUBMITTED

6 KW

- CATHODIC PROTECTION
- NIGHT VISION DEVICES
- RADIOS

24 KW

- INSTRUMENT LANDING SYSTEM
- WATER WELL PUMP
- WATER PURIFICATION

60 KW

- REMOTE RADAR SITE
- HELOSHED, MOBILE COMMUNICATIONS UNIT
- WAREHOUSE (FORKLIFT BATTERIES)

USAMERDC PROJECTED EFFORT IN DEMONSTRATIONS

- ASSIST IN DEVELOPMENT, FABRICATION AND ASSEMBLY OF P/V POWER SOURCE
- INSTALLATION AND INTEGRATION
- OPERATE AND MAINTAIN EACH DEMONSTRATION SYSTEM
- MONITOR SYSTEM PERFORMANCE, ADEQUACY OF SOURCE TO MEET LOAD REQUIREMENTS
- EVALUATE POWER SYSTEM DESIGN

TERRESTRIAL PHOTOVOLTAIC MEASUREMENTS WORKSHOP PROJECT
FOR THE
NATIONAL PHOTOVOLTAIC CONVERSION PROGRAM

BY HENRY W. BRANDHORST, JR.

NASA-LEWIS RESEARCH CENTER

CLEVELAND, OHIO

PRESENTED AT THE ERDA-NATIONAL SOLAR PHOTOVOLTAIC
PROGRAM REVIEW MEETING JULY 22-25, 1975
LOS ANGELES, CALIFORNIA

N76 12480

REVIEW OF TERRESTRIAL PHOTOVOLTAIC MEASUREMENTS WORKSHOP

by Henry W. Brandhorst, Jr.

NASA-Lewis Research Center
Cleveland, Ohio

Abstract

A Terrestrial Photovoltaic Measurements Workshop was held at the NASA-Lewis Research Center, March 19-21, 1975. The purpose of this meeting (figure 1) was to make recommendations on measurement methods and the terrestrial solar intensity and spectrum to be used by investigators in the Solar Photovoltaic Energy Conversion Program.

The workshop was divided into three major areas, each with a chairman, as shown in figure 2. Approximately 95 people from 45 different organizations (Federal Government, universities, and companies) attended. About 25 papers covering these three areas were presented. The proceedings of this meeting will be available shortly.

Broad agreement was obtained on an interim method for making terrestrial solar cell measurements. The major recommendations of the workshop are shown in figure 3. These recommendations have been translated into an interim test procedure to be used by all photovoltaic investigators. The session chairmen and workshop coordinator together developed this document which is now available to all investigators.

The key aspects of this procedure are summarized in figures 4 and 5. Figure 4 shows the only acceptable measurement techniques: three to be used with natural sunlight measurements, and one with artificial light sources. Pyranometers or pyrheliometers are to be used in a well-defined manner and are not to be used with artificial light sources.

The use of standard solar cells to set simulator irradiance levels or to monitor solar irradiance in outdoor measurements is a proven, reliable method developed in the space program. It is necessary that the standard cells be made from the same material and have essentially the same spectral response as the test cells. Such cells must either be supplied by, or traceable to, the NASA-Lewis Research Center, which is serving the ERDA as the national testing laboratory. These cells should become available no later than October 1975. Figure 5 shows the recommended standard test conditions and definitions to be used in reporting cell performance data. Figure 6 shows the Air Mass Two spectral distribution to be used for all theoretical calculations. Integrated intensity for this curve is 75 mW/cm^2.

With this basis, it is hoped that uniform measurements and calculations can be made by all investigators. However, these recommended procedures are interim procedures. It is planned that another workshop be held in April 1976 so that new results can be presented and modifications made to these interim test conditions as required.

In summary (figure 7), a Terrestrial Photovoltaic Measurements Workshop was held in March 1975. The recommendations of this workshop have been translated into an interim terrestrial solar cell test procedure to be used by all investigators. A second workshop is planned in April 1976 to modify this interim test procedure as required.

TERRESTRIAL PHOTOVOLTAIC MEASUREMENTS WORKSHOP

MARCH 19-21, 1975

NASA-LEWIS RESEARCH CENTER

PURPOSE: TO MAKE RECOMMENDATIONS ON MEASUREMENT METHODS AND TERRESTRIAL SOLAR INTENSITY AND SPECTRUM TO BE USED BY INVESTIGATORS IN THE SOLAR PHOTOVOLTAIC CONVERSION PROGRAM

TERRESTRIAL PHOTOVOLTAIC MEASUREMENTS WORKSHOP

TECHNICAL ORGANIZATION

SESSION I - SOLAR INTENSITY AND SPECTRUM CONDITIONS FOR TERRESTRIAL PHOTOVOLTAICS

JOHN HICKEY/EPPLEY LABORATORIES, CHAIRMAN

SESSION II - TERRESTRIAL SUNLIGHT SIMULATION

HENRY CURTIS/NASA-LEWIS RESEARCH CENTER, CHAIRMAN

SESSION III - METHODOLOGY FOR MEASUREMENT AND CALIBRATION OF SOLAR CELLS

EUGENE RALPH/SPECTROLAB, CHAIRMAN

RECOMMENDATIONS OF THE TERRESTRIAL PHOTOVOLTAIC MEASUREMENTS WORKSHOP

- MEASUREMENTS OF SOLAR CELL PERFORMANCE IN TERRESTRIAL SUNLIGHT ARE THE MOST ACCEPTABLE.
- AN ARTIFICIAL LIGHT SOURCE SUCH AS A FILTERED Xe ARC LAMP IS TO BE USED FOR LABORATORY MEASUREMENTS.
- CALIBRATED SOLAR CELLS ARE TO BE USED TO ADJUST THE ARTIFICIAL LIGHT SOURCE INTENSITY.
- AN ABSOLUTE SPECTRAL RESPONSE MEASUREMENT TECHNIQUE IS NEEDED.
- A SINGLE AIR MASS TWO SOLAR SPECTRAL DISTRIBUTION CURVE SHOULD BE USED IN ALL THEORETICAL CALCULATIONS.
- A CENTRALIZED NATIONAL LABORATORY SHOULD BE ESTABLISHED TO PERFORM REFERENCE PHOTOVOLTAIC MEASUREMENTS, TO ISSUE CALIBRATED SOLAR CELLS, AND TO SUPPORT NECESSARY R&D.

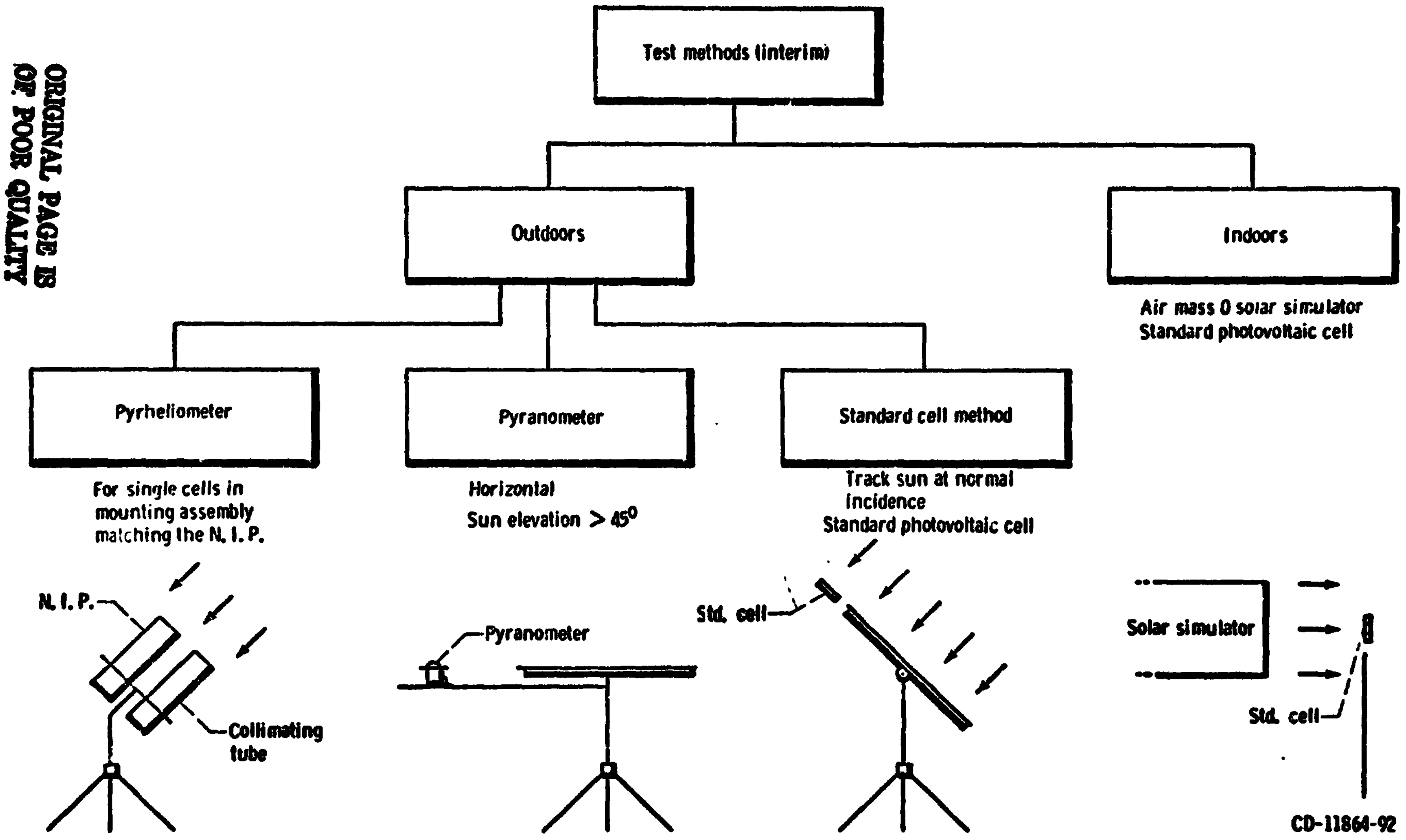
Test methods (interim)
Outdoors
Indoors
Air mass 0 solar simulator
Standard photovoltaic cell
Pyrheliometer
Pyranometer
Standard cell method
For single cells in
mounting assembly
matching the N. I. P.
Horizontal
Sun elevation > 45°
Track sun at normal
incidence
Standard photovoltaic cell
N. I. P.
Collimating
tube
Pyranometer
Std. cell
Solar simulator
Std. cell
CD-11864-92

Figure 1.

STANDARD TEST CONDITIONS AND DEFINITIONS

TEMPERATURE - 28 ± 2° C

INTENSITY - 100 mW/cm^2 FOR SUNLIGHT SIMULATOR
AS SET WITH STANDARD CELL

TEST CELL AREA - TOTAL CELL AREA

SHORT CIRCUIT CURRENT - $V_{LOAD} < 20$ mV

OPEN CIRCUIT VOLTAGE - $R_{LOAD} > 10^4\ \Omega$

FILL FACTOR - $\frac{P_{max}}{V_{oc} \times I_{sc}}$

EFFICIENCY (%, - $\frac{P_{max}}{A_{Total} \times \text{IRRADIANCE}} \times 100$

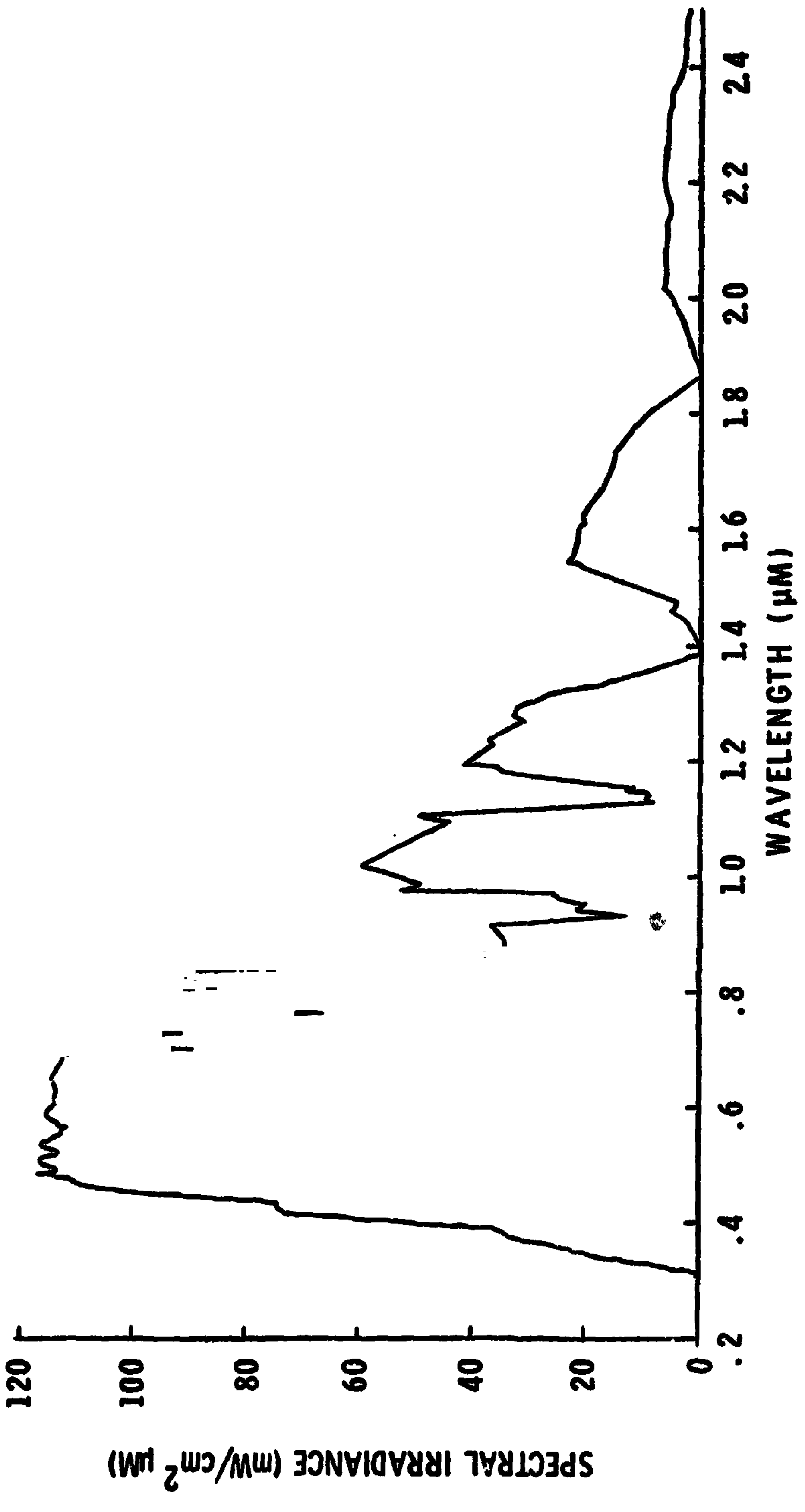
SPECTRAL IRRADIANCE (mW/cm^2 µM)
120
100
80
60
40
20
0
.2
.4
.6
.8
1.0
1.2
1.4
1.6
1.8
2.0
2.2
2.4
WAVELENGTH (µM)

SUMMARY

- FIRST TERRESTRIAL PHOTOVOLTAIC MEASUREMENTS WORKSHOP HELD IN MARCH 1975
- INTERIM TERRESTRIAL SOLAR CELL TESTING PROCEDURES HAVE BEEN DOCUMENTED FOR USE BY ALL INVESTIGATORS
- A SECOND WORKSHOP IS PLANNED FOR APRIL 1976 TO MODIFY INTERIM TEST PROCEDURES AS REQUIRED

SESSION IV

CONCENTRATOR SYSTEMS

INVESTIGATION OF TERRESTRIAL PHOTOVOLTAIC POWER SYSTEMS WITH SUNLIGHT CONCENTRATION

BY

ARIZONA STATE UNIVERSITY

AND

SPECTROLAB, INC.

ERDA CONTRACT	E(11-1)-2590
CONTRACT PERIOD	JANUARY 1, 1975 TO DECEMBER 31, 1975
CONTRACT AMOUNT	$249,274
SPECTROLAB SUBCONTRACT	$118,175

PRINCIPAL INVESTIGATOR:
CHARLES E. BACKUS
COLLEGE OF ENGINEERING
SCIENCES
ARIZONA STATE UNIVERSITY
TEMPE, AZ 85231

N76 12481

INVESTIGATION OF TERRESTRIAL PHOTOVOLTAIC POWER SYSTEMS WITH SUNLIGHT CONCENTRATION

Arizona State University
and
Spectrolab, Inc.

This joint program was started January 15, 1974. The first year was mostly analytical effort looking at the component and system characteristics expected for concentration configurations. Those studies resulted in the conclusions given in Table I and indicated very encouraging prospects if the assumptions made could be verified. The program being pursued in the second year is to experimentally verify the first year's conclusion. (See Table II).

The analytical model of the silicon solar cells for high illumination is being used to design cells for different concentration factors. Figure 1 shows that a cell design using one centimeter length grid fingers (w=1 cm) can be made that would have an efficiency at 100 suns that is 90% of the efficiency of a typical cell at one sun. This may require about 30 fingers per centimeter and thus the deposition of the grid should be achievable with conventional techniques. These results were obtained by keeping the internal voltage drop constant by varying the internal resistance. The decrease in efficiency comes from the greater coverage of the surface with grids as the concentration increases. Figure 2 shows the importance of base material resistivity on cell design for high concentration.

One of the important parameters indicated on the first year's program was the dependence of the system cost for passively cooled arrays on the thermal conductance between cell and ambient air. Therefore a wind tunnel was constructed (See Figure 3) to measure these values in a controlled environment.

Table III gives the description of the heat rejection geometries being investigated in this tunnel. Figures 4 and 5 give typical results for the configurations tested to date.

Calculations on additional concentration configurations are continuing and also the dependence of their characteristics on various design parameters. As a typical example Figure 6 shows how mirror surface inaccuracies affect the energy distribution incident at the cells. System cost studies are continuing as shown in Figures 7 and 8.

Four concentrator system desi[illegible] been made and will be built during the next six months. The[illegible] are:

1) A non-tracting system (c[illegible]tration ratio 7.5) See Figure 9
2) A circular Fresnel system (concentration ratio 16) See Figure 10
3) A fixed mirror system (concentration ratio 40) See Figure 11
4) A 5 foot diameter, parabolic reflector system with concentration ratios up to about 100 or more.

TABLE I

CONCLUSIONS FROM FIRST YEAR'S PROGRAM (ANALYTICAL)

- CONCENTRATION SYSTEMS CAN BE CHEAPER THAN FLAT ARRAYS EVEN AT PROJECTED COSTS FOR CELLS (50 ¢/PEAK WATT)

- CONVENTIONALLY PROCESSED SILICON CELLS CAN OPERATE AT LIGHT INTENSITIES UP TO 200 SUNS AT EFFICIENCIES COMPARABLE TO CURRENT PRODUCTION SPACE CELLS

- PASSIVE COOLING TECHNIQUES CAN BE ADEQUATE FOR RELATIVELY HIGH CONCENTRATION RATIOS (~50)

TABLE II

PROPOSED SECOND YEAR PROGRAM

DURATION: JANUARY 1, 1975 - DECEMBER 31, 1975

REQUESTED FUNDING: $249,274

TEAM: ARIZONA STATE UNIVERSITY (PRIME)
SPECTROLAB DIVISION, TEXTRON, INC. ($118,175 SUBCONTRACT)

OBJECTIVE: TO VERIFY THE ENCOURAGING ANALYTICAL STUDIES BY EXPERIMENTS

PROPOSED TASKS:

I. EXPERIMENTAL DEVELOPMENT OF CONCENTRATION CELLS
(GRID CONTACTS, INCREASE VOLTAGE, FABRICATE ASSEMBLIES)

II. THERMAL ANALYSIS AND TESTING
(WIND DEPENDENCE FOR PASSIVE, ACTIVE COOLING FOR HIGH CR > 100)

III. CONCENTRATED SOLAR CELL SYSTEM TESTING
(5 SYSTEMS - FLAT ARRAY AND CR OF ABOUT 3, 10, 40 AND 100)

IV. SYSTEM PERFORMANCE AND COST ANALYSIS
(COMPLETE COST ANALYSIS AND ESTABLISH CONFIDENCE LEVEL)

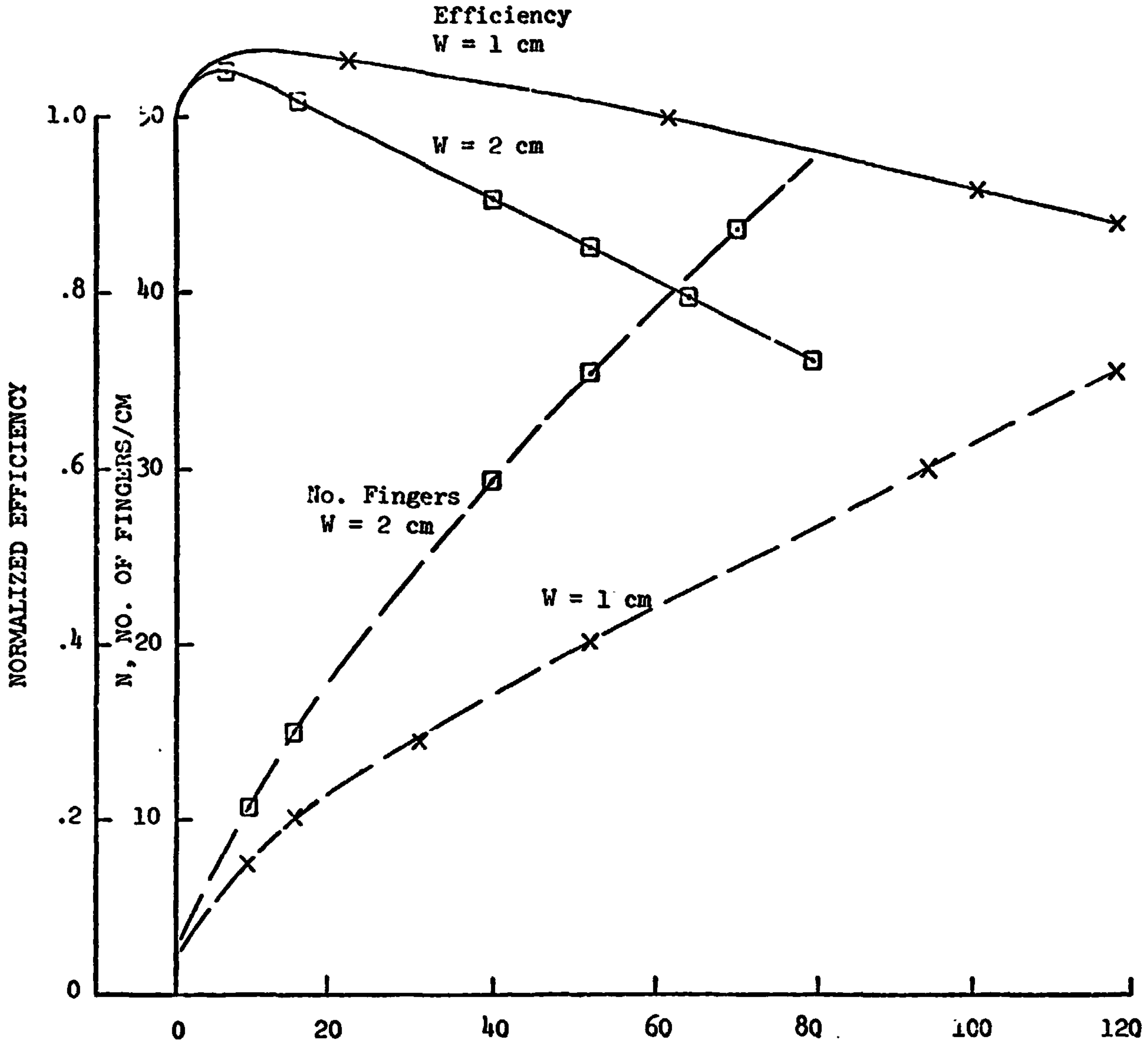

CONCENTRATION

FIGURE 1

NORMALIZED EFFICIENCY & NO. OF FINGERS/CM

vs.

CONCENTRATION LEVEL

Finger Width = .009 cm
Diffused Layer Sheet Resistance = 50 Ω/square
Base Material Resistivity = 0.1 ohm-cm
Cell Thickness = .025 cm
Sheet Resistance of Metalization = .004 Ω/square

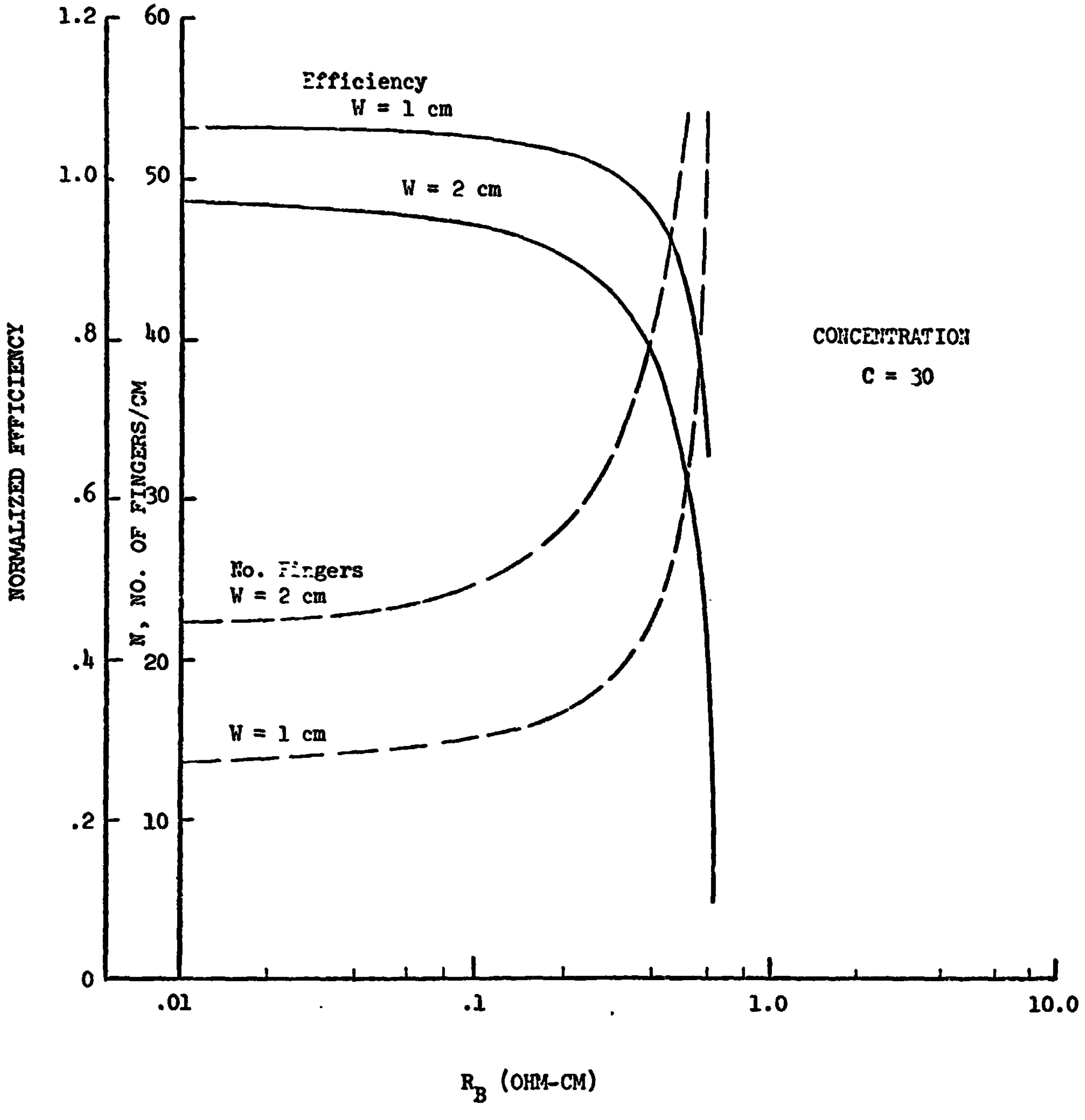

FIGURE 2

NORMALIZED EFFICIENCY & NO. OF FINGERS/CM

vs.

MATERIAL BASE RESISTIVITY

Finger Width = .009 cm
Diffused Layer Sheet Resistance = 50 Ω/square
Cell Thickness = .025 cm
Sheet Resistance of Metalization = .004 Ω/square

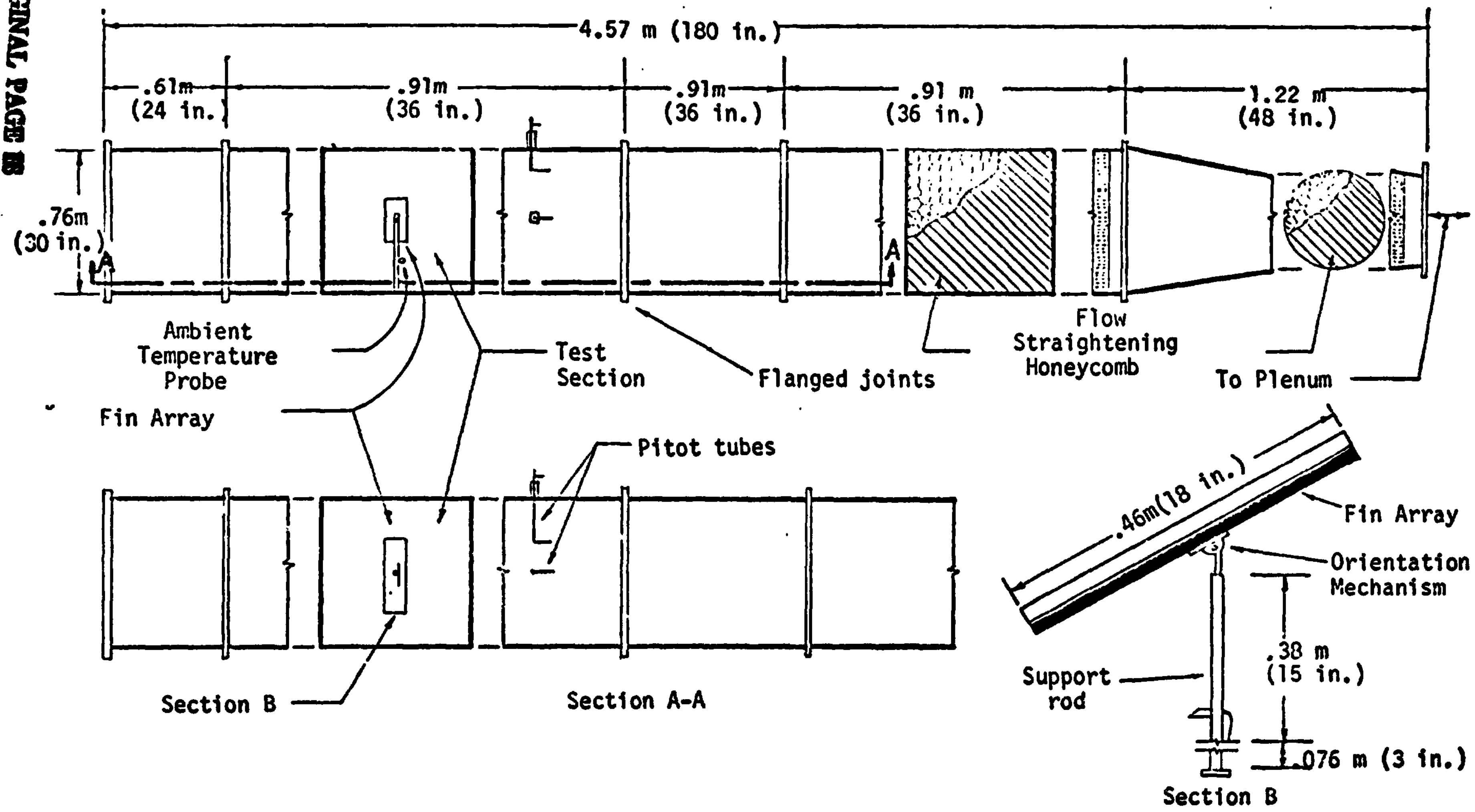

FIGURE 3

LOW SPEED WIND TUNNEL AND TEST MOUNT FOR MEASUREMENT OF COOLING RATES FROM FINNED HEAT SINKS AS A FUNCTION OF AIR FLOW SPEED AND DIRECTION

FIGURE 4

MEASURED THERMAL CONDUCTANCES FOR FRONT SURFACE OF BASELINE FLAT PLATE AS A FUNCTION OF AIR FLOW SPEED AND DIRECTION

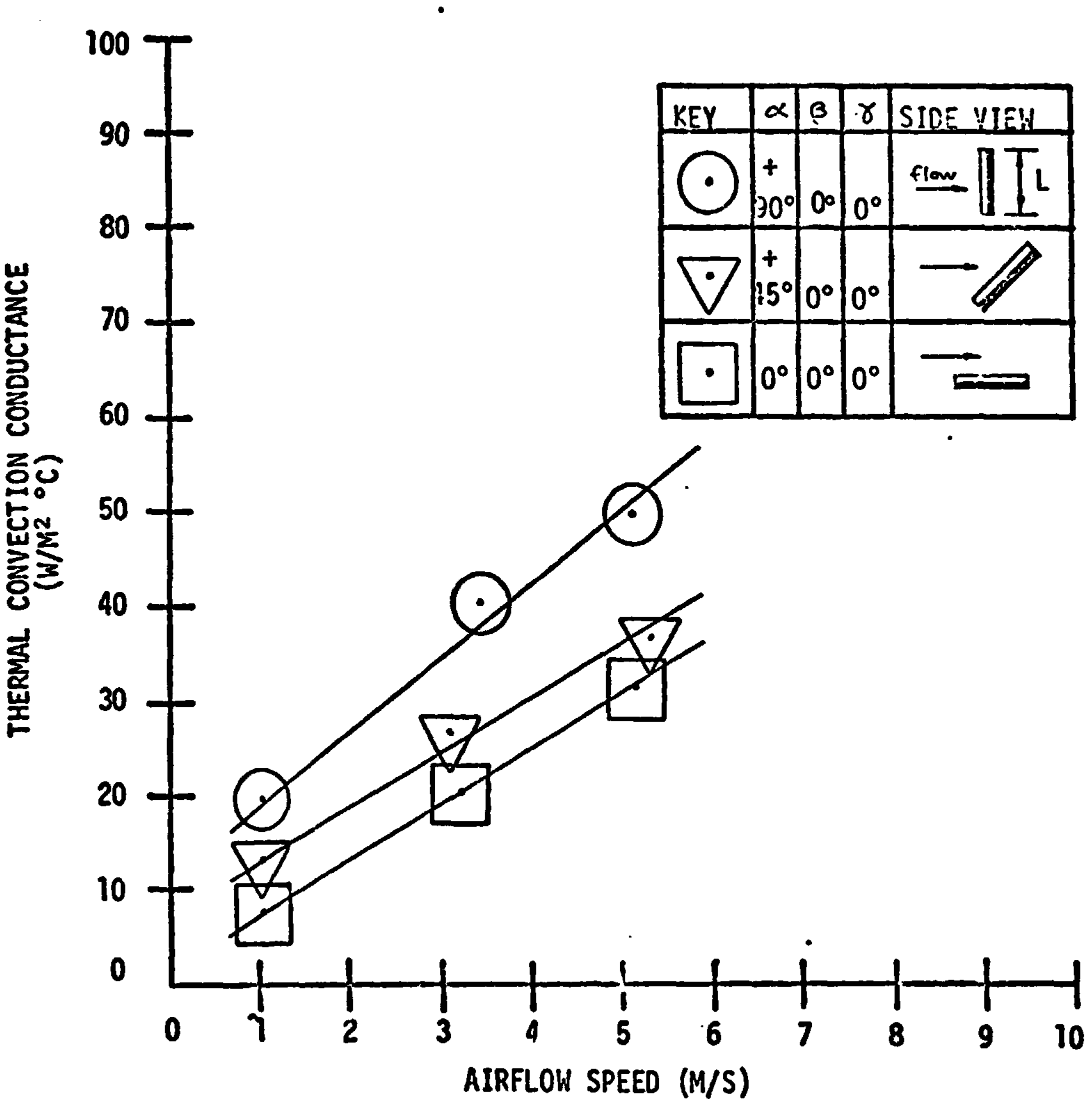

FIGURE 5

MEASURED THERMAL CONVECTION CONDUCTANCES PER UNIT BASE AREA FOR STUBBY TRAPEZOIDAL LONGITUDINAL FINNED SURFACE AS A FUNCTION OF AIR FLOW SPEED AND DIRECTION (SEE TABLE III FOR DIMENSIONS)

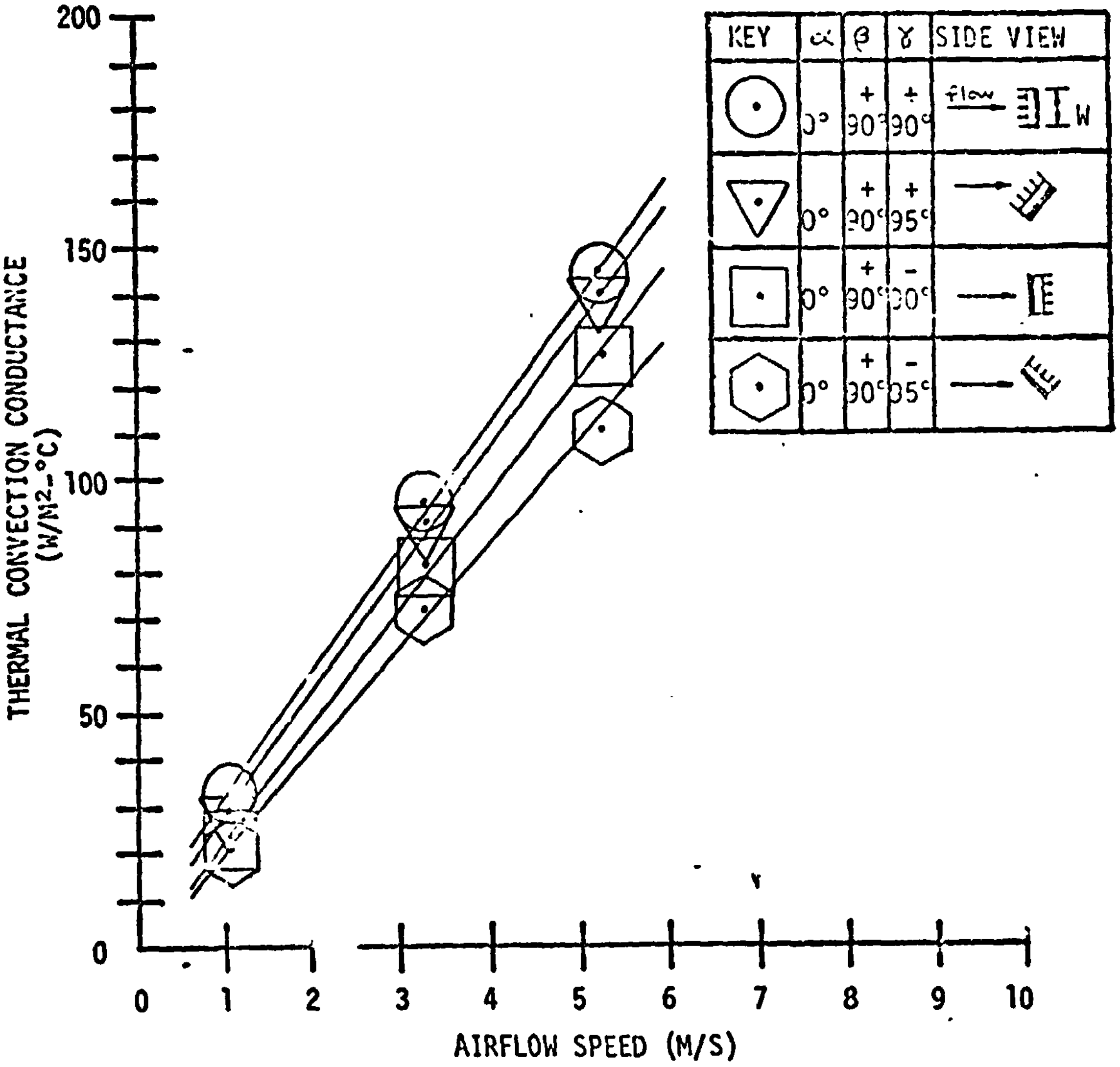

ARRAY DESCRIPTION		ARRAY DIMENSIONS								
		N_f	A_t/A_b	L	W	B_1	B_2	H_f	S_1	Z
FLAT PLATE		0	1	.459m (18.0")	.076m (3.00")	-	-	-	-	.0030m (.12")
FINNED PLATE WITH STUBBY TRAPEZOIDAL FINS	LONGITUDINAL	21	4.59	.459m (18.0")	.093m (3.66")	.00038m (.015")	.00076m (.030")	.0081m (.32")	.0046m (.18")	.0020m (.08")
	TRANSVERSE	101	4.47	.462m (18.2")	.089m (3.50")					
FINNED PLATE WITH LONG TRAPEZOIDAL FINS	LONGITUDINAL	12	7.86	.462m (18.2")	.103m (4.06")	.00051m (.02")	.0025m (.10")	.305m (1.20")	.0091m (.36")	.0046m (.18")
	TRANSVERSE	49	7.25	.459m (18.0")	.102m (4.00")					

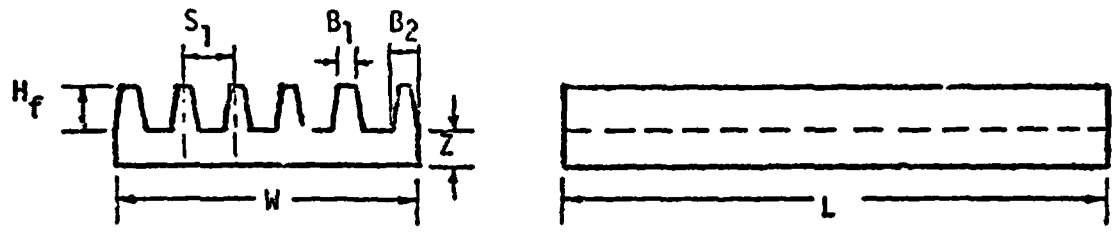

TABLE III

SUMMARY OF DIMENSIONS OF ALUMINUM FINNED PLATE TEST MODELS

c.4

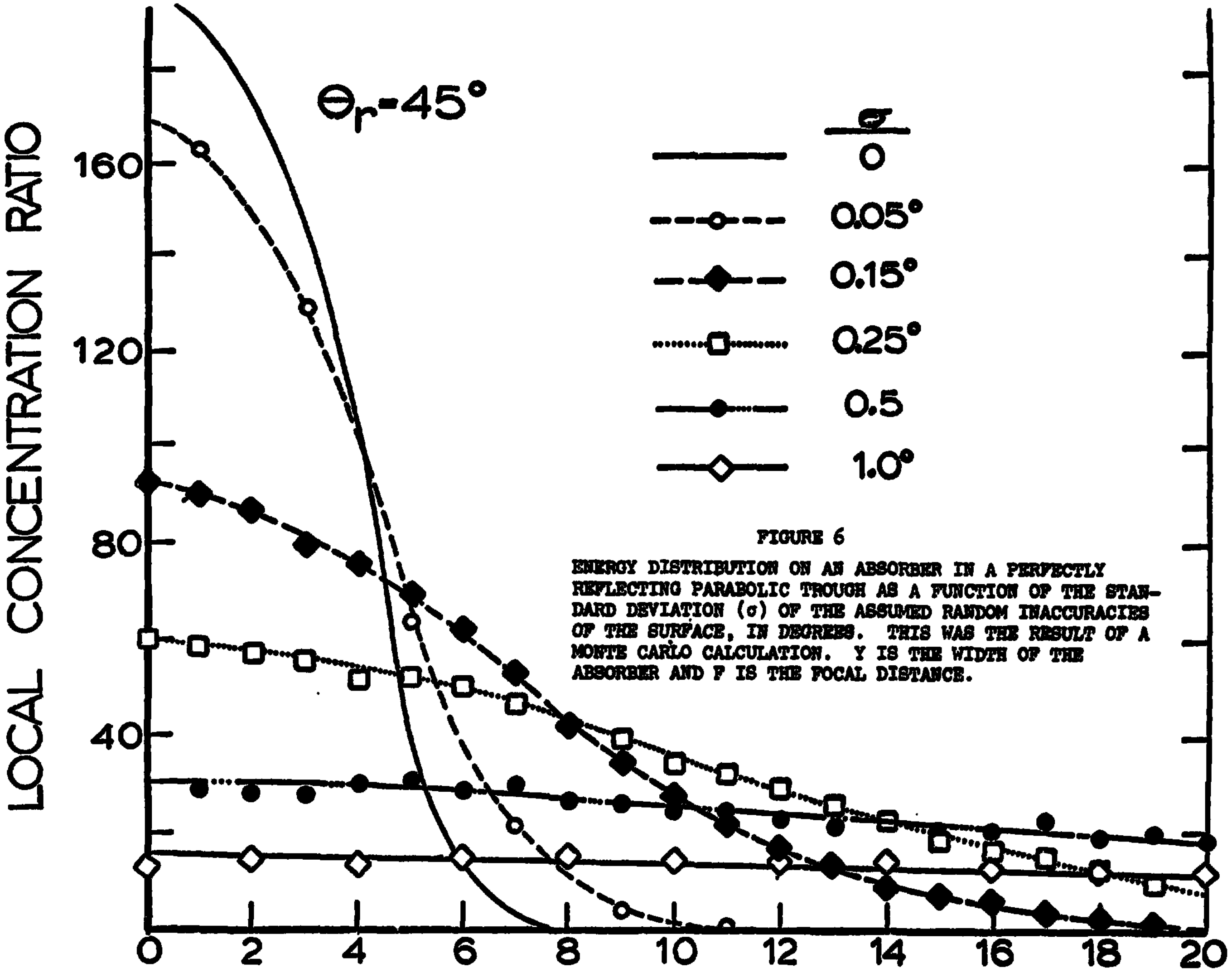

FIGURE 6

ENERGY DISTRIBUTION ON AN ABSORBER IN A PERFECTLY REFLECTING PARABOLIC TROUGH AS A FUNCTION OF THE STANDARD DEVIATION (σ) OF THE ASSUMED RANDOM INACCURACIES OF THE SURFACE, IN DEGREES. THIS WAS THE RESULT OF A MONTE CARLO CALCULATION. Y IS THE WIDTH OF THE ABSORBER AND F IS THE FOCAL DISTANCE.

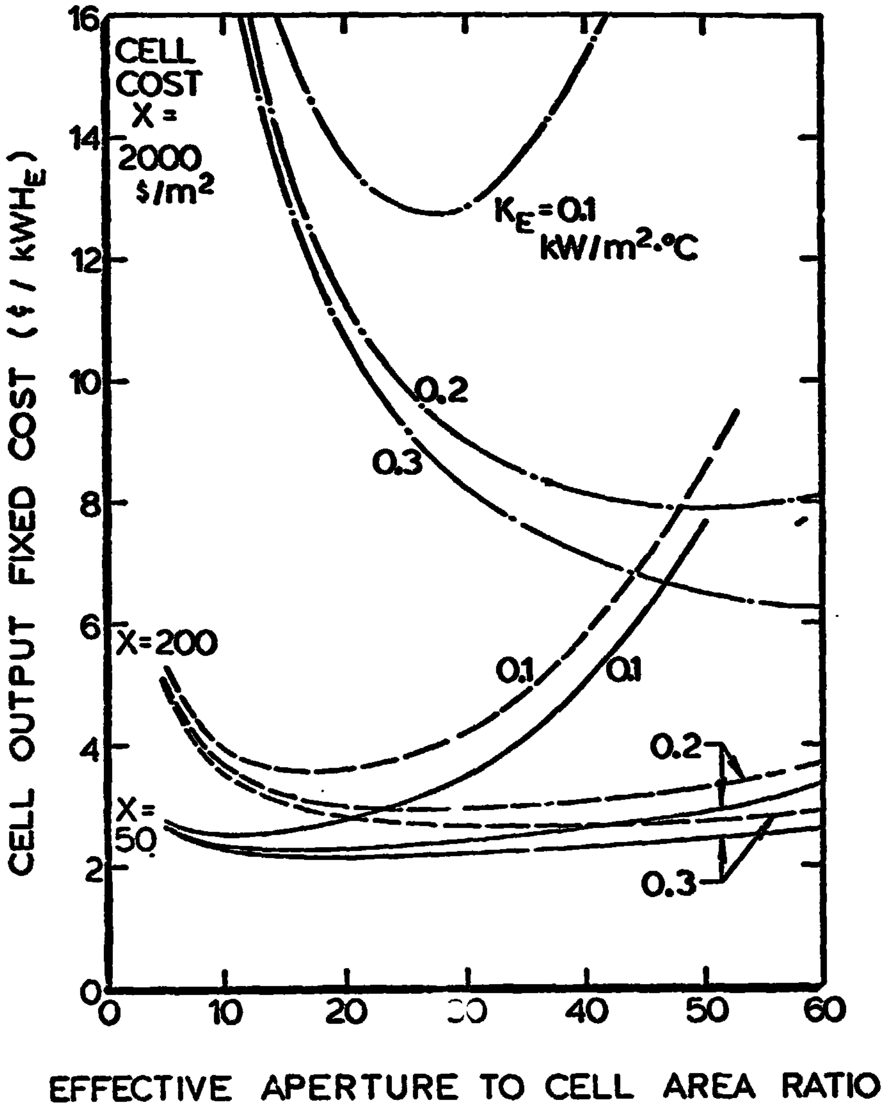

FIGURE 7

ELECTRICAL OUTPUT COST AVERAGED OVER A YEAR IN ALBUQUERQUE FOR A FIXED MIRROR CONCENTRATOR WITH AN ASSUMED COST OF 20$/m^2 FOR THE REFLECTOR AND A PACKING FACTOR OF 0.35. SILICON SOLAR CELLS, PASSIVELY COOLED WERE ASSUMED WITH THE THERMAL CONDUCTANCES OF K_E=0.1, 0.2 and 0.3 AS A PARAMETER. THE INCLUDED ANGLE FOR THE MIRROR WAS 120° WITH A 15° TILT AND A 15° INCLINATION USED.

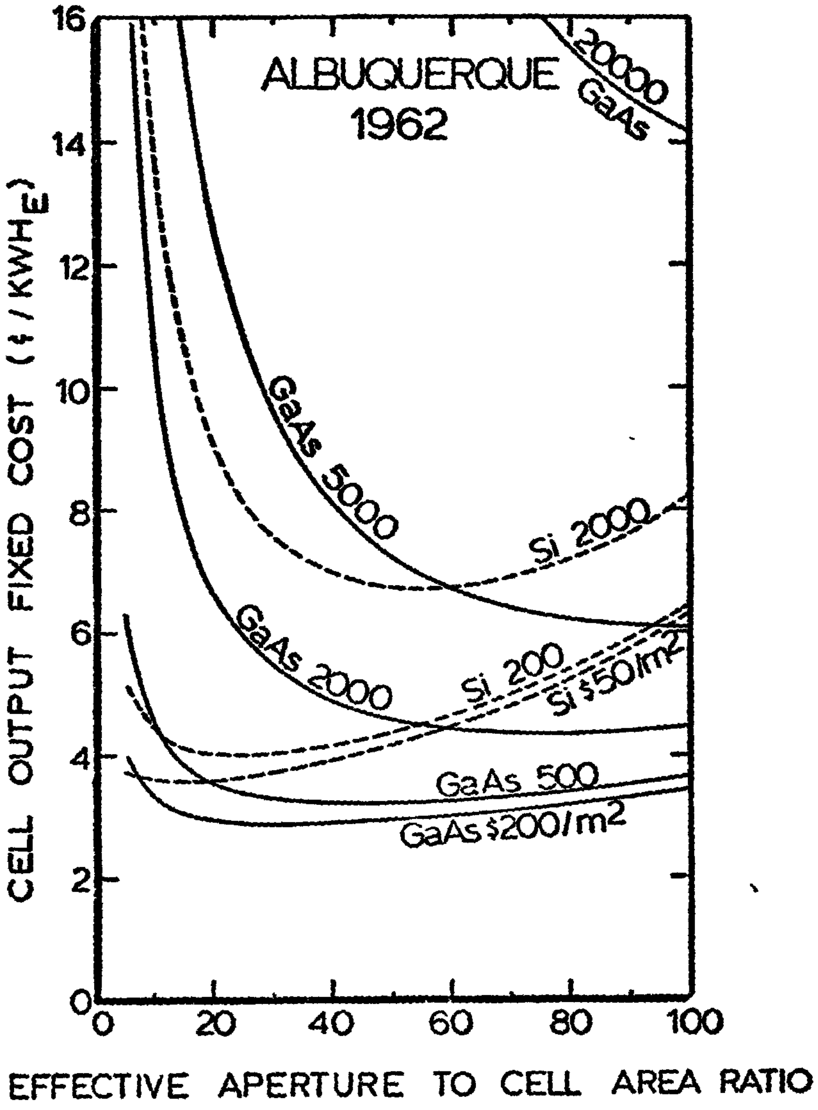

FIGURE 8

A COMPARISON OF S_i AND GaAs SYSTEMS FOR VARIOUS ASSUMED COSTS FOR THE CELLS IN $/m^2, PASSIVELY COOLED, K_e=0.4 KW/M^2-°C, REFLECTIVITY OF 0.85 AND CELL ABSORPTIVITY OF 0.8, Si CELLS WERE 15% EFFICIENT AT 25°C GOING LINEAR TO 0 AT 270°C. GaAs WAS 20% AT 25°C GOING TO 0 AT 400°C

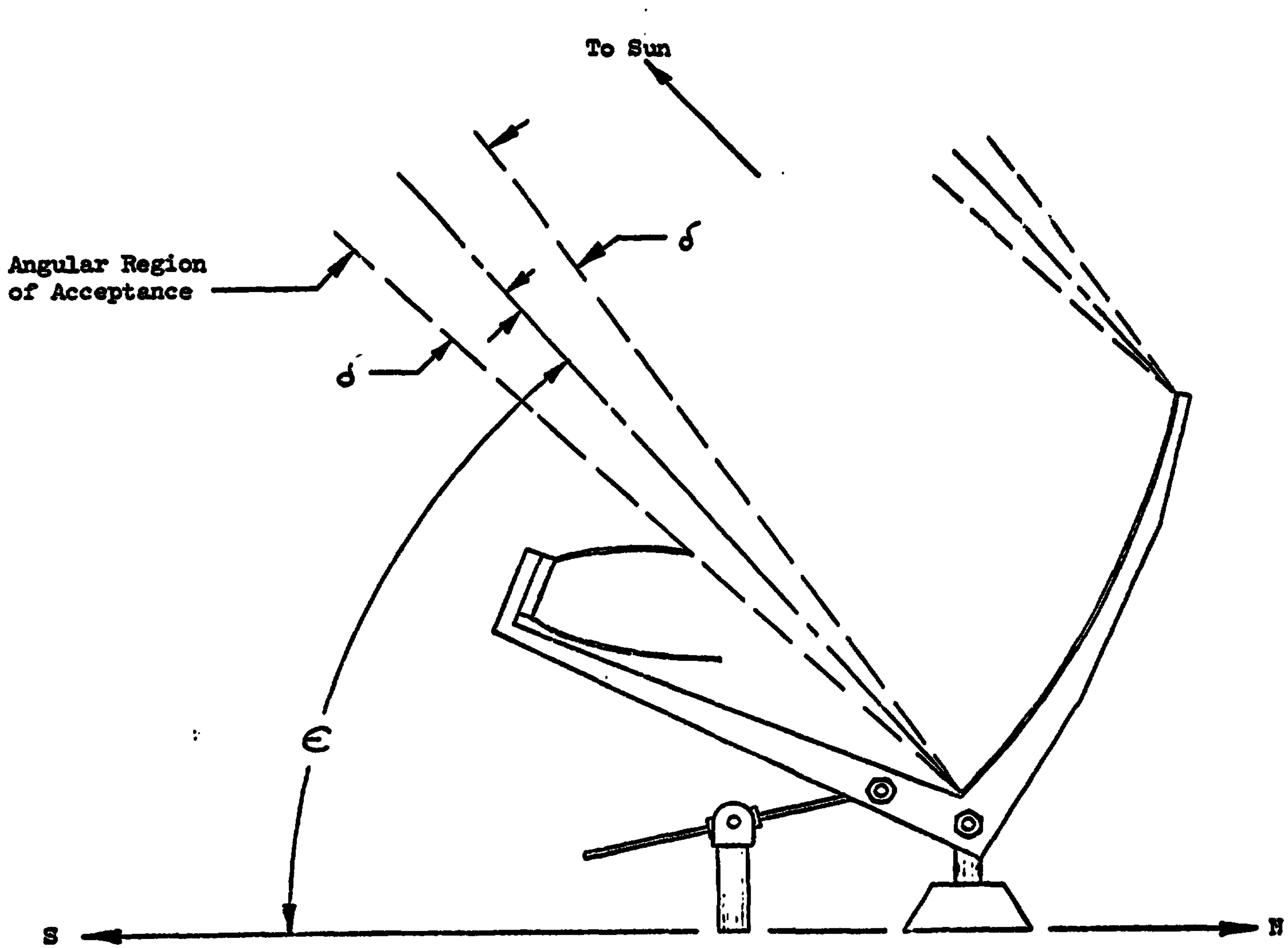

FIGURE 9
MOUNTING ORIENTATION OF PTCEC

THIS NON-TRACKING CONCENTRATOR SYSTEM USES A PARABOLIC TROUGH AND A COMPOUND ELIPTICAL CONCENTRATOR ORIENTED IN THE EW DIRECTION. GEOMETRICAL CONCENTRATION FACTOR IS 7.5

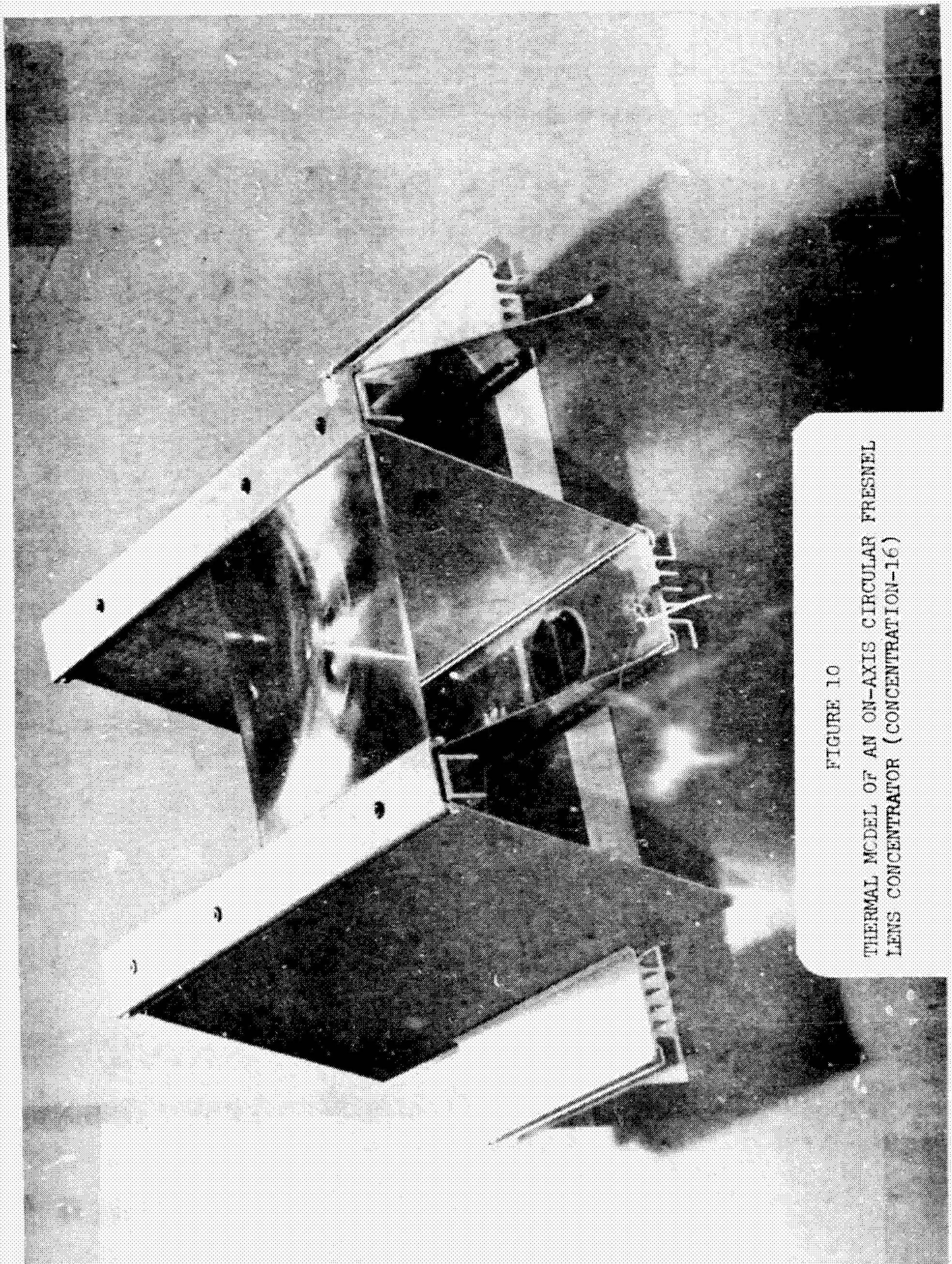

FIGURE 10

THERMAL MODEL OF AN ON-AXIS CIRCULAR FRESNEL LENS CONCENTRATOR (CONCENTRATION-16)

ORIGINAL PAGE IS
OF POOR QUALITY

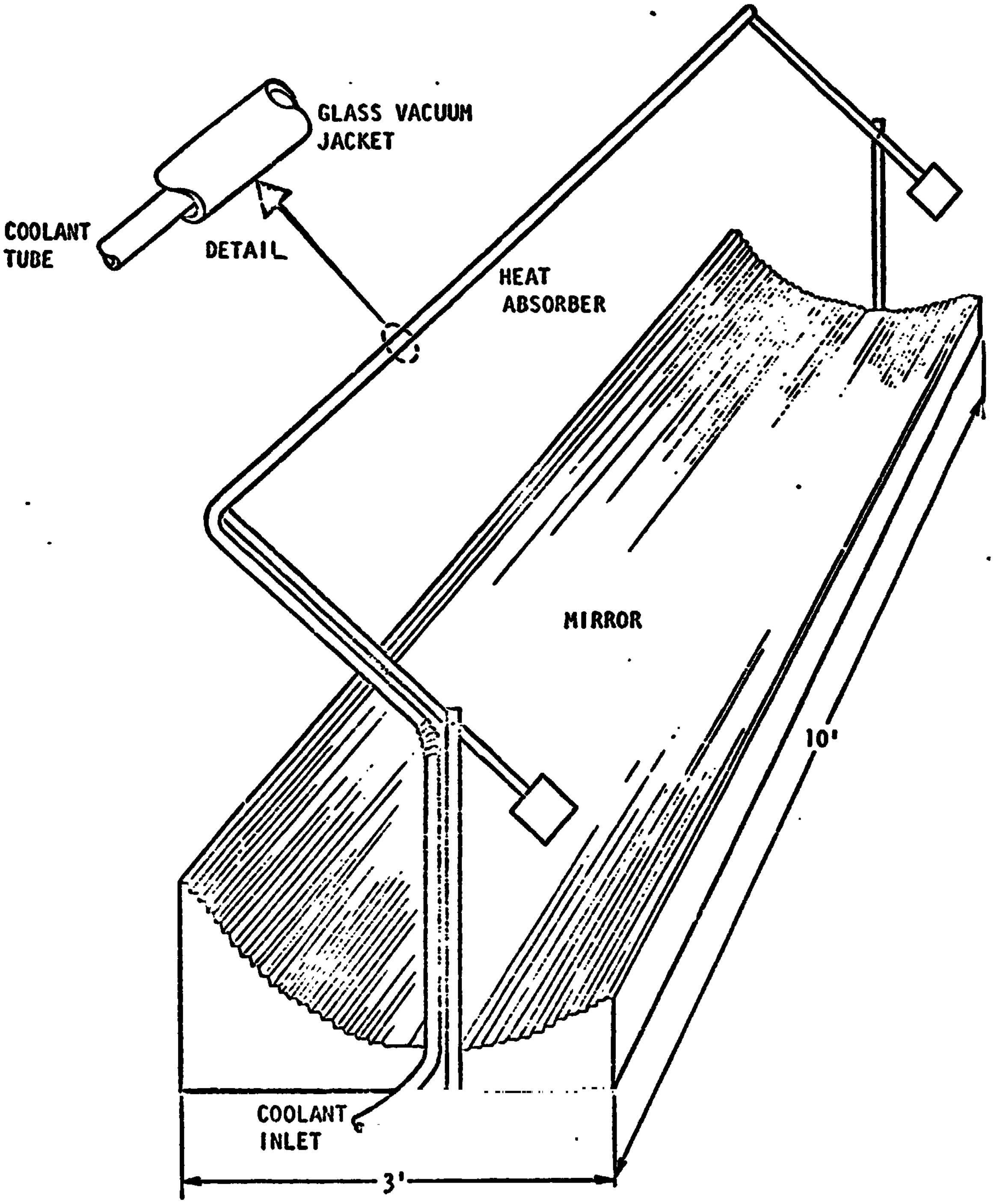

FIGURE 11
Model of fixed-mirror concentrator

N76 12482

PHOTOVOLTAIC APPLICATIONS OF COMPOUND PARABOLIC CONCENTRATOR (CPC)

GRANT: 31-109-ENG-38

ORGANIZATION PERFORMING WORK: ARGONNE NATIONAL LABORATORY

PERIOD OF GRANT: 26 MARCH -- 30 JUNE

AMOUNT OF AWARD: $30,000

PRINCIPAL INVESTIGATOR: ROLAND WINSTON

COMPOUND PARABOLIC CONCENTRATOR

CPC

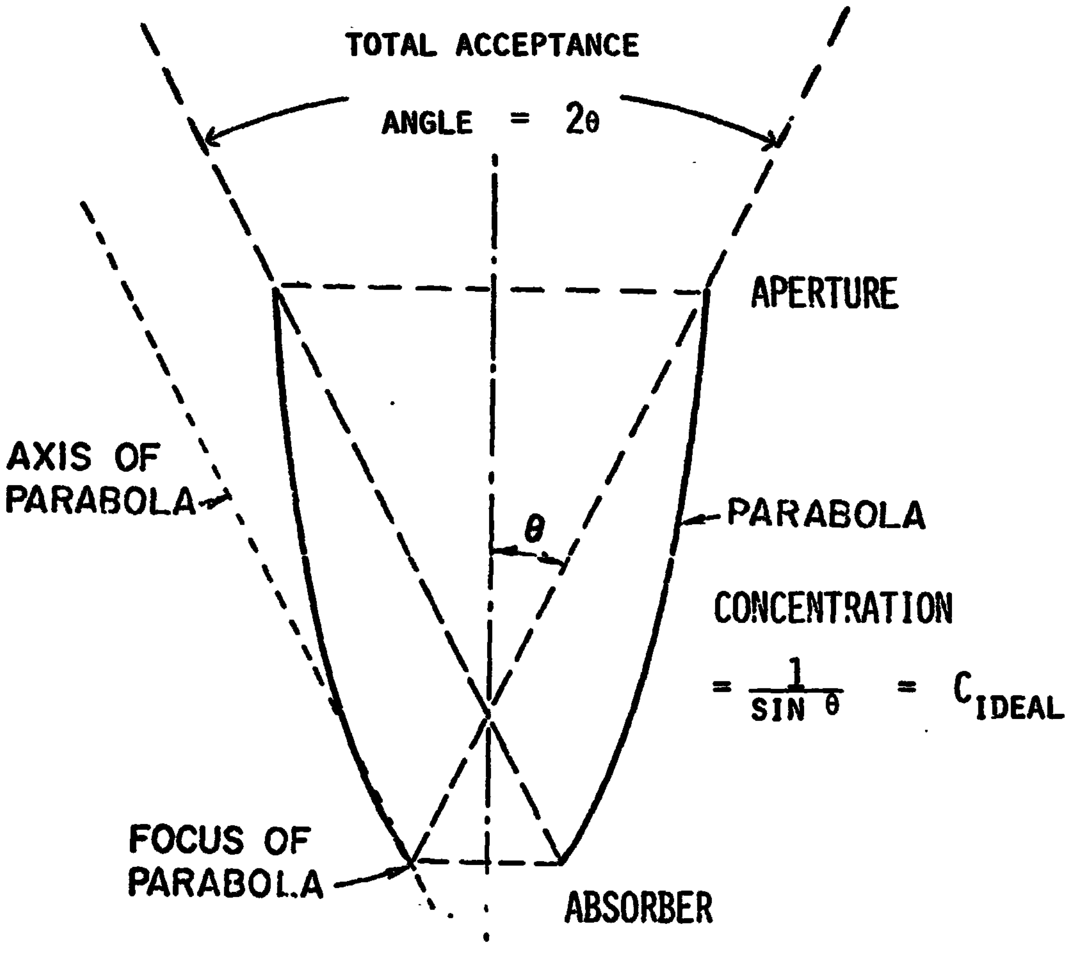

REPORTS

A. RABL, "Optical and Thermal Properties of Compound Parabolic Concentrators", Argonne Report SOL 75-01

A. RABL, "Comparison of Solar Concentrators", Argonne Report SOL 75-02.

A. RABL, et al., "Report on Concentrating Flat Plate Compound Parabolic Collectors".

R. GIUGLER, et al., "X 10 Compound Parabolic Concentrators", also Progress Reports NSF/RANN/SE-AER-74-01C65/PR/74/4 and 75-01065/PR/75/1.

OVERALL OBJECTIVE OF PROJECT

DETERMINE SUITABILITY OF CPC FOR PHOTOVOLTAIC APPLICATIONS, IN PARTICULAR

- INVESTIGATE TECHNICAL PROBLEMS (COOLING, GRID SPACING, ETC.)
- OPTIMIZE CONCENTRATOR DESIGN,
- CALCULATE SYSTEM COST.

TASKS PERFORMED BY MOBIL TYCO

1. DETERMINATION OF THE PERFORMANCE CHARACTERISTICS OF STATE-OF-THE-ART (I.E., CZOCHRALSKI N ON P) SILICON SOLAR CELLS AS A FUNCTION OF CONCENTRATION RATIO (UP TO 10 TIMES) AND TEMPERATURE (20 - 100°C).

2. MAXIMIZATION OF SOLAR CELL PERFORMANCE UNDER CONCENTRATION AND AT ELEVATED TEMPERATURES, INCLUDING ELECTRODE GRID DESIGN, JUNCTION DEPTH, AND ANTIREFLECTION COATING.

3. ANALYSIS OF CPC/SOLAR CELL PERFORMANCE AS A FUNCTION OF CONCENTRATION RATIO AND DEGREE OF TRUNCATION (AND HENCE OF ACCEPTANCE ANGLE), INCLUDING DETERMINATION OF THE ENERGY DISTRIBUTION ON THE CELL TO PROVIDE DESIGN GUIDANCE FOR THE LOCATION OF THE GRID STRUCTURE.

4. ANALYSIS OF THE COST EFFECTIVENESS OF THE CPC/SILICON SOLAR CELL SYSTEM.

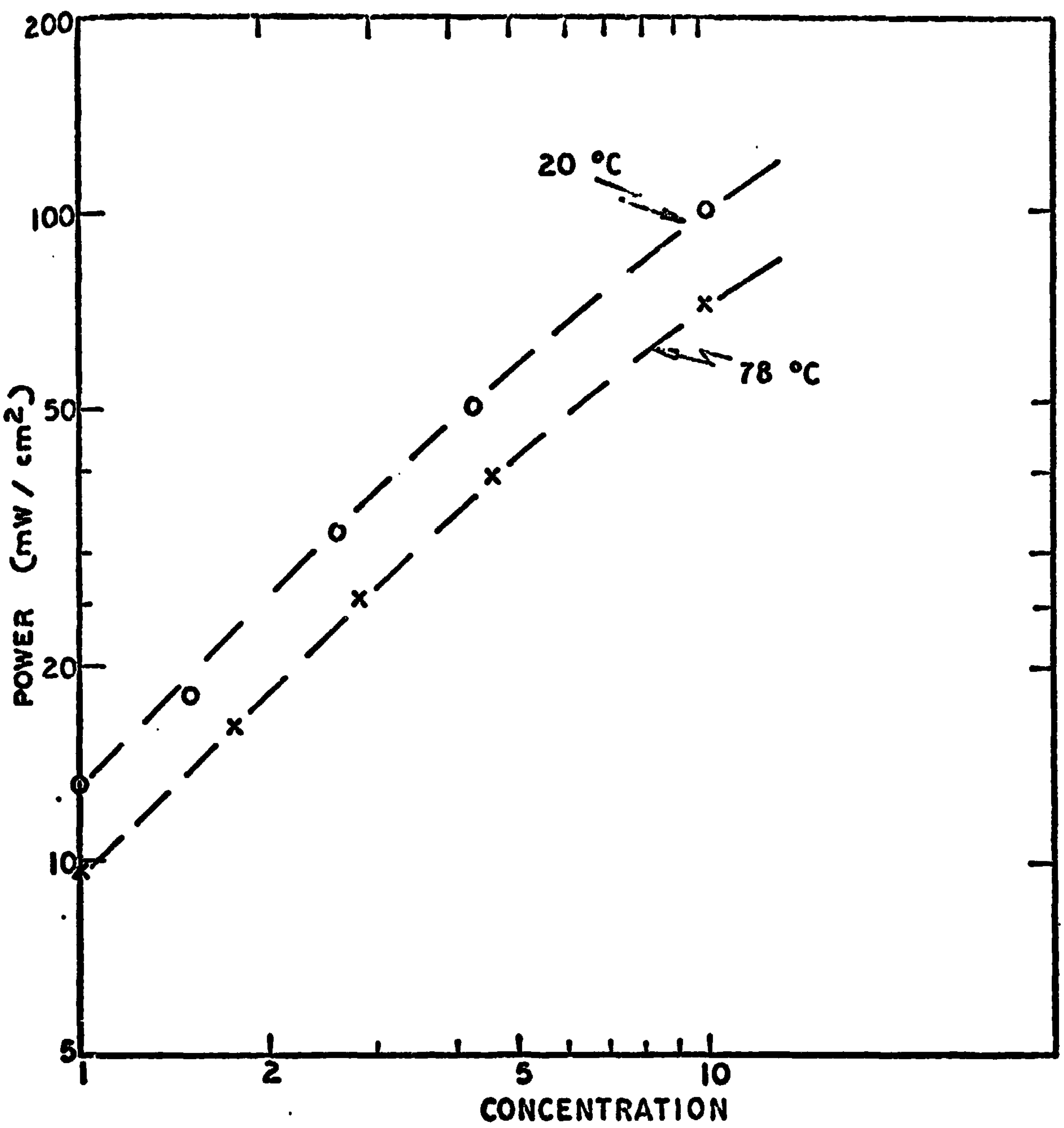

Power output versus concentration for 20° and 78°C. The average decrease in efficiency was 0.4%/°C. The AR coating was 1200 Å and the junction depth was 0.25 μm.

(MEASURED WITH 20 MIRROR HELIOSTAT)

EFFICIENCY OF 8 X CPC AND SI PHOTOCELL COMBINATION WAS MEASURED.

(ALUMINUM WITH REFLECTIVITY 85%, ACTUAL CONCENTRATION = 6, FOR MECHANICAL REASONS)

MEASURED OUTPUT: 5 X

TEMPERATURE DEPENDENCE OF EFFICIENCY

- 0.5% PER °C (THEOR.)

- 0.4% PER °C (EXP.)

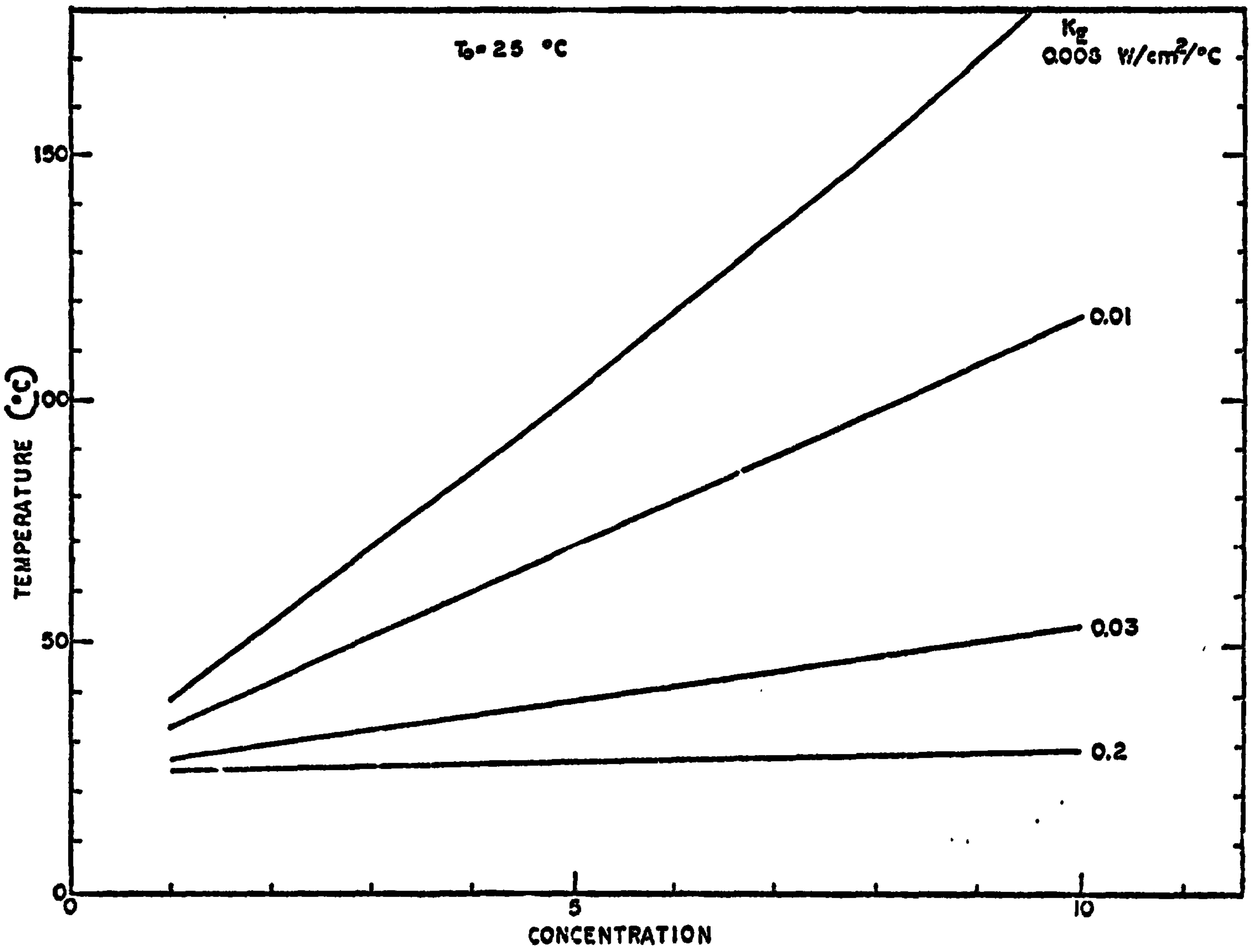

Temperature of a silicon solar cell as a function of concentration for different types of cooling. $K_e = 0.005 \text{ W/cm}^2/°\text{C}$ corresponds to a flat strip, 0.03 a finned heat sink in a slight breeze, 0.2 cooling by a circulating liquid, and 0.01 to some intermediate cooling. The ambient temperature was 25 C.

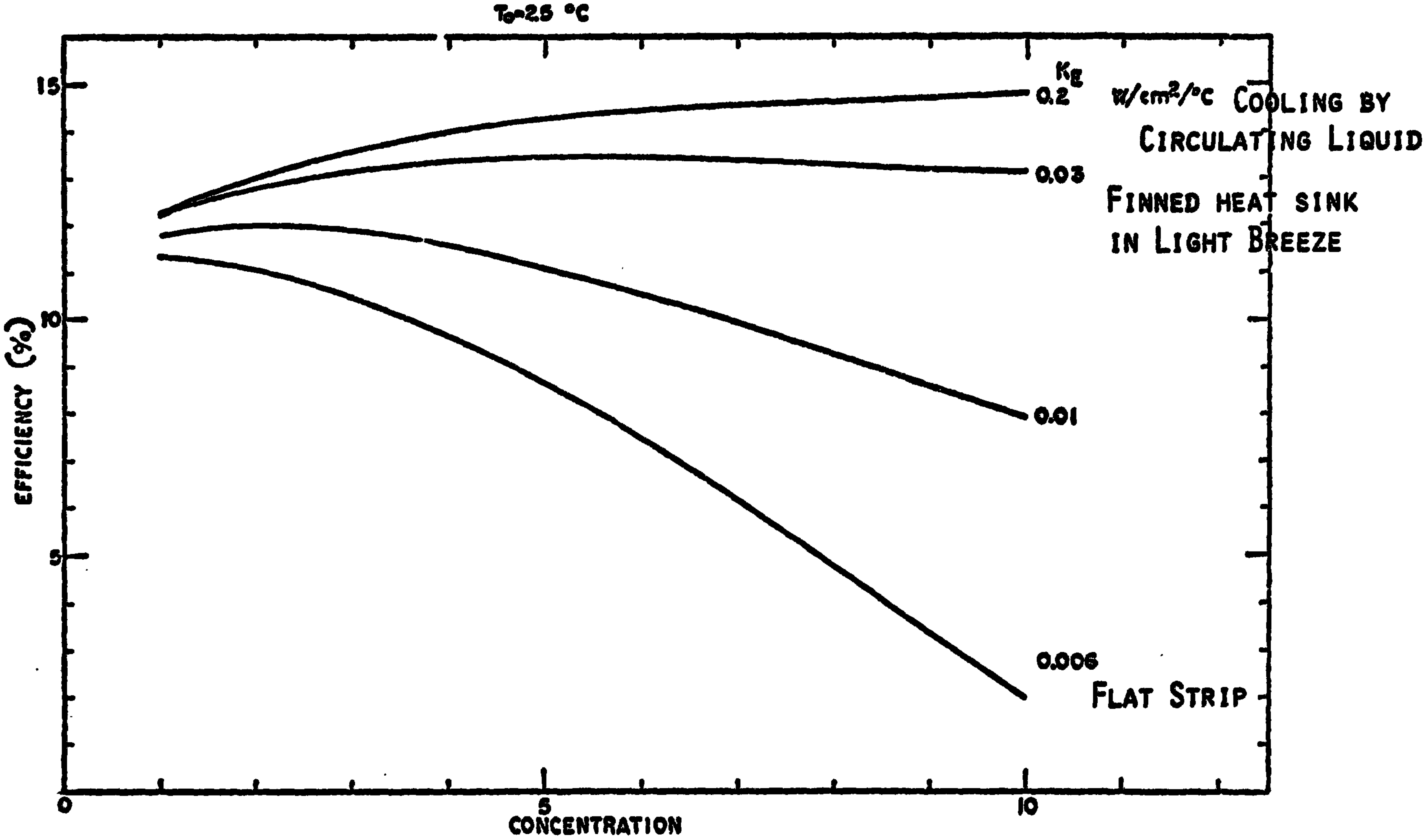

Solar cell conversion efficiency as a function of concentration. For the types of cooling schemes corresponding to various values at K_e, see the preceding figure or text.

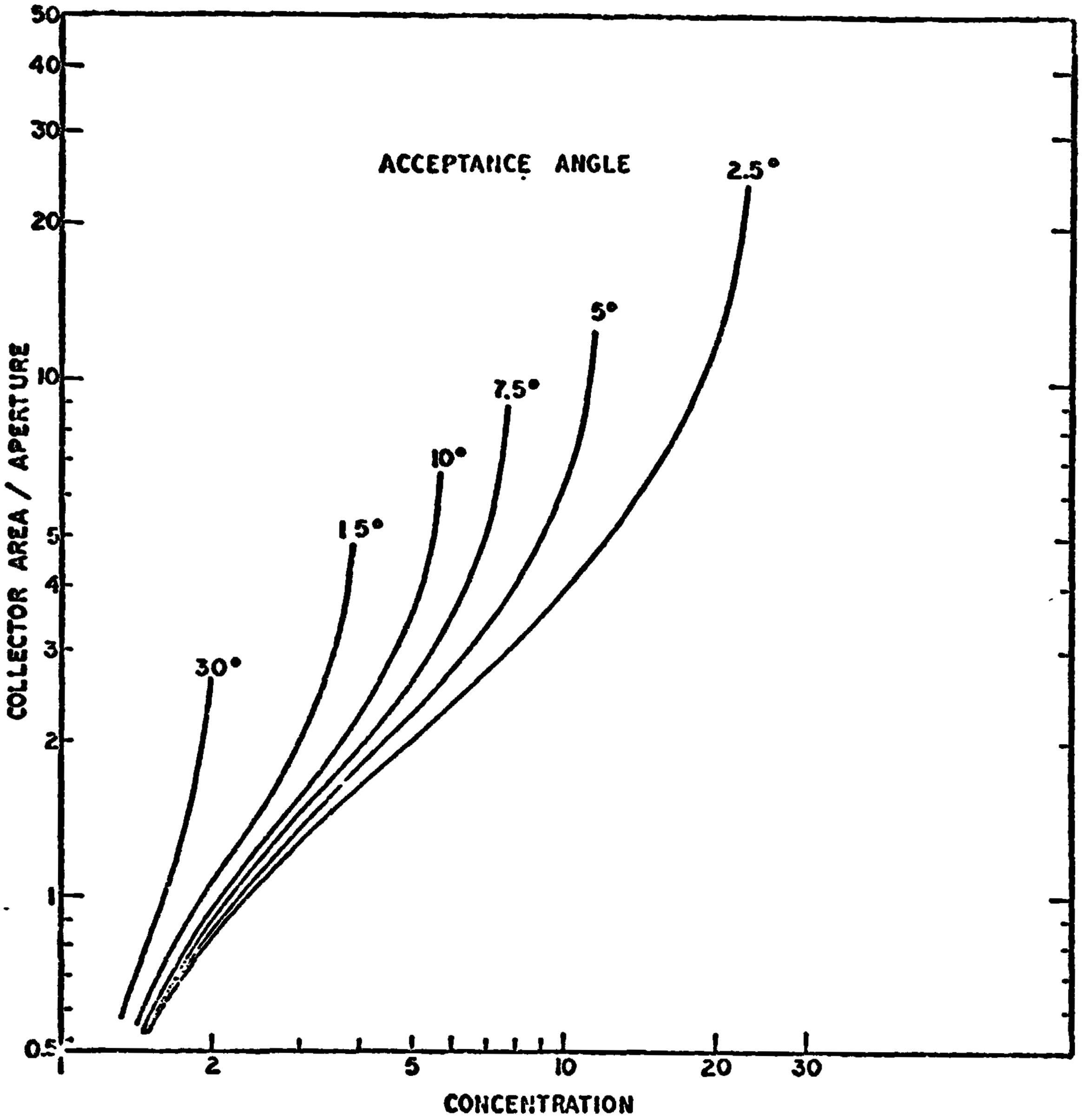

Fig. 39. The collector area per unit lengths divided by the aperture per unit length as a function of concentration for a CPC. Acceptance angles between 2.5 and 30° were used.

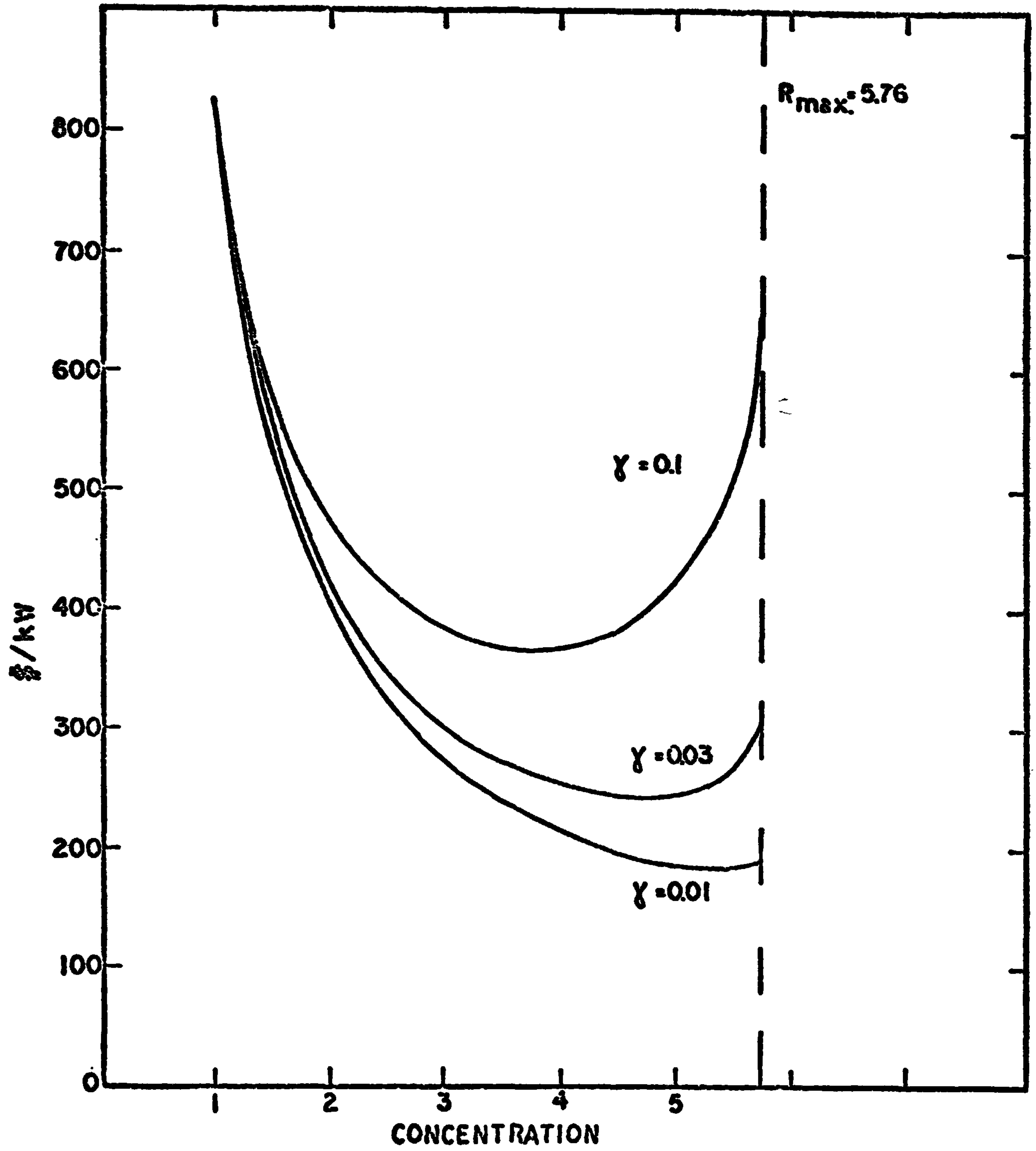

The cost in $/kW of a CPC system versus concentration. γ is the ratio of reflector costs per unit area to Si solar cell costs. An acceptance angle of 10° and $K_e = 0.003\ \mathrm{W/cm^2/°C}$ were used.

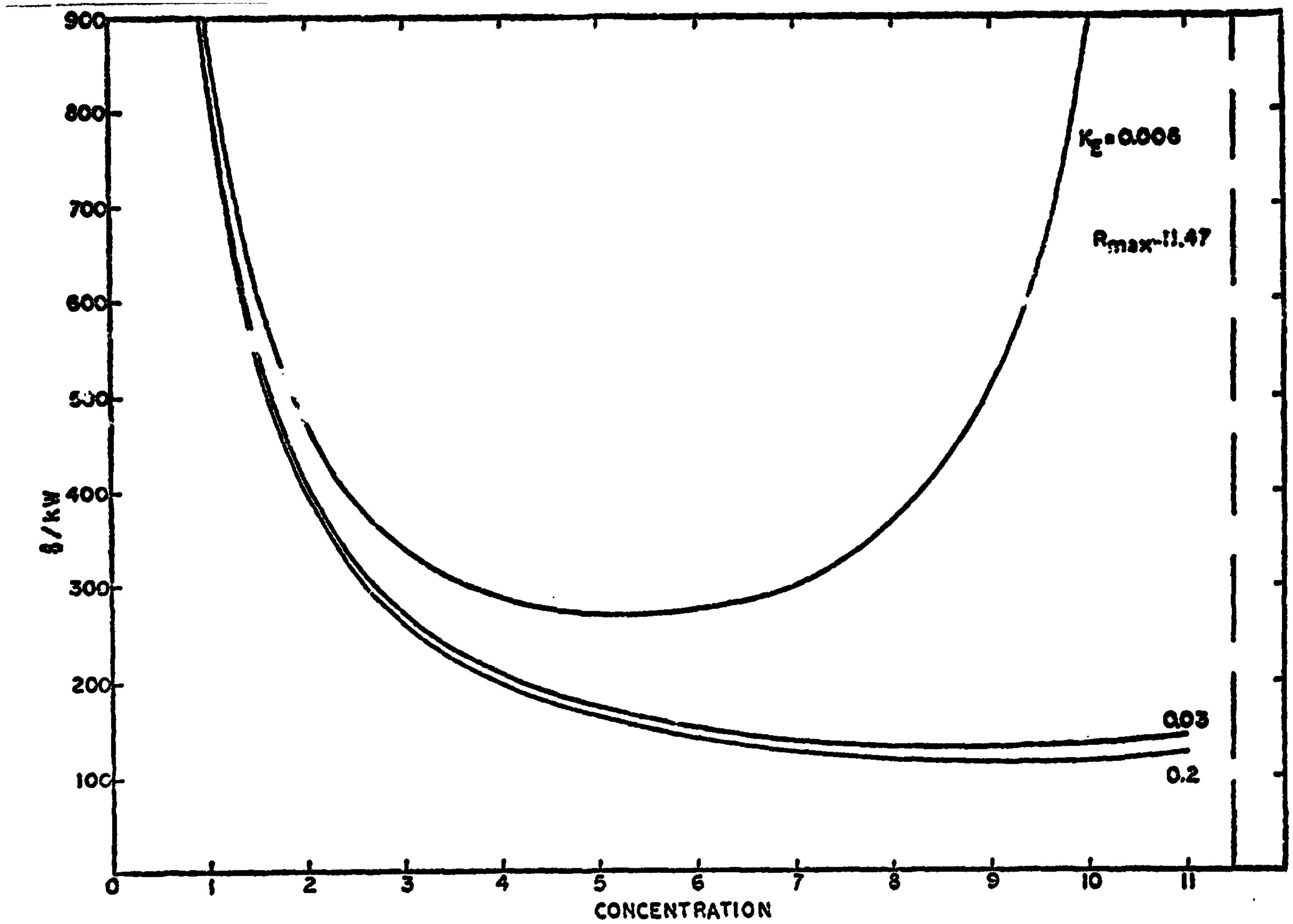

The cost in $/kW of a CPC system versus concentration for different types of cooling. See the text for types of cooling corresponding to different values of K_e. The acceptance angle is 5 °

KEY RESULTS OF MOBIL TYCO

1. SILICON SOLAR CELLS CAN READILY BE DESIGNED TO INCREASE IN EFFICIENCY WITH CONCENTRATION UP TO 10 SUNS. SIMPLE IMPROVEMENTS IN GRID STRUCTURE PERMIT THE ATTAINMENT OF THE REQUISITE VALUE OF SERIES RESISTANCE.

2. THE SPECIFIC CELL PARAMETERS REQUIRED TO ACHIEVE ENHANCED EFFICIENCY WITH INCREASING CONCENTRATION HAVE BEEN DEFINED, AND THESE ARE READILY ATTAINABLE WITH MINIMUM MODIFICATION OF STANDARD SOLAR CELL FABRICATION TECHNIQUES.

3. RAY TRACING COMPUTER PROGRAM HAS BEEN DEVELOPED TO DETERMINE ENERGY DISTRIBUTION AT EXIT OF CPC.

4. THE COST OF A CPC/SOLAR CELL SYSTEM WAS DETERMINED AS A FUNCTION OF CONCENTRATION RATIO. TOTAL COST OF A CPC/SOLAR CELL SYSTEM WILL BE BETWEEN 4 AND 5 TIMES LOWER THAN FOR FLAT PLATE SILICON CELL ARRAYS.

THE STATEMENT OF WORK FOR SPECTROLAB

EVALUATE FOR PHOTOVOLTAIC APPLICATIONS THE USE OF THE CPC DESIGN AS A FIELD COLLECTOR -- IN CONJUNCTION WITH A PRIMARY FOCUSING CONCENTRATOR. THE PRIMARY FOCUSING CONCENTRATOR MAY BE A PARABOLIC REFLECTOR, AN ARRAY OF FRESNEL MIRRORS, A FRESNEL LENS OR SOME OTHER TYPE.

SINGLE CPC vs. TWO COMPONENT SYSTEMS

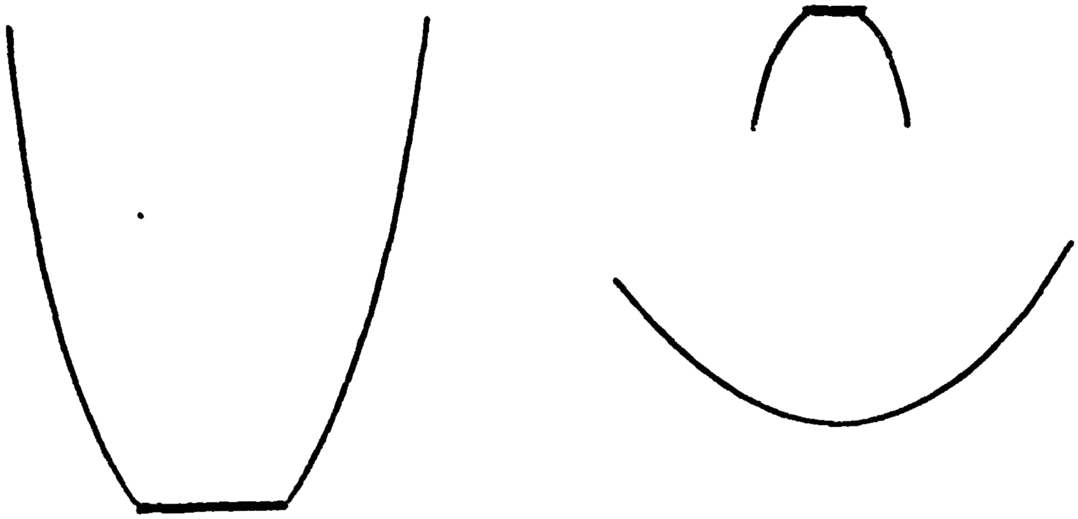

TWO COMPONENT SYSTEM ACHIEVES ABOUT 90% OF C_{IDEAL}.

VERY FAVORABLE REFLECTOR/APERTURE RATIO,

PREFERABLE FOR $C \gtrsim 10$

(WITH OFF AXIS DESIGN MAY BE PREFERABLE FOR $C \gtrsim 6$)

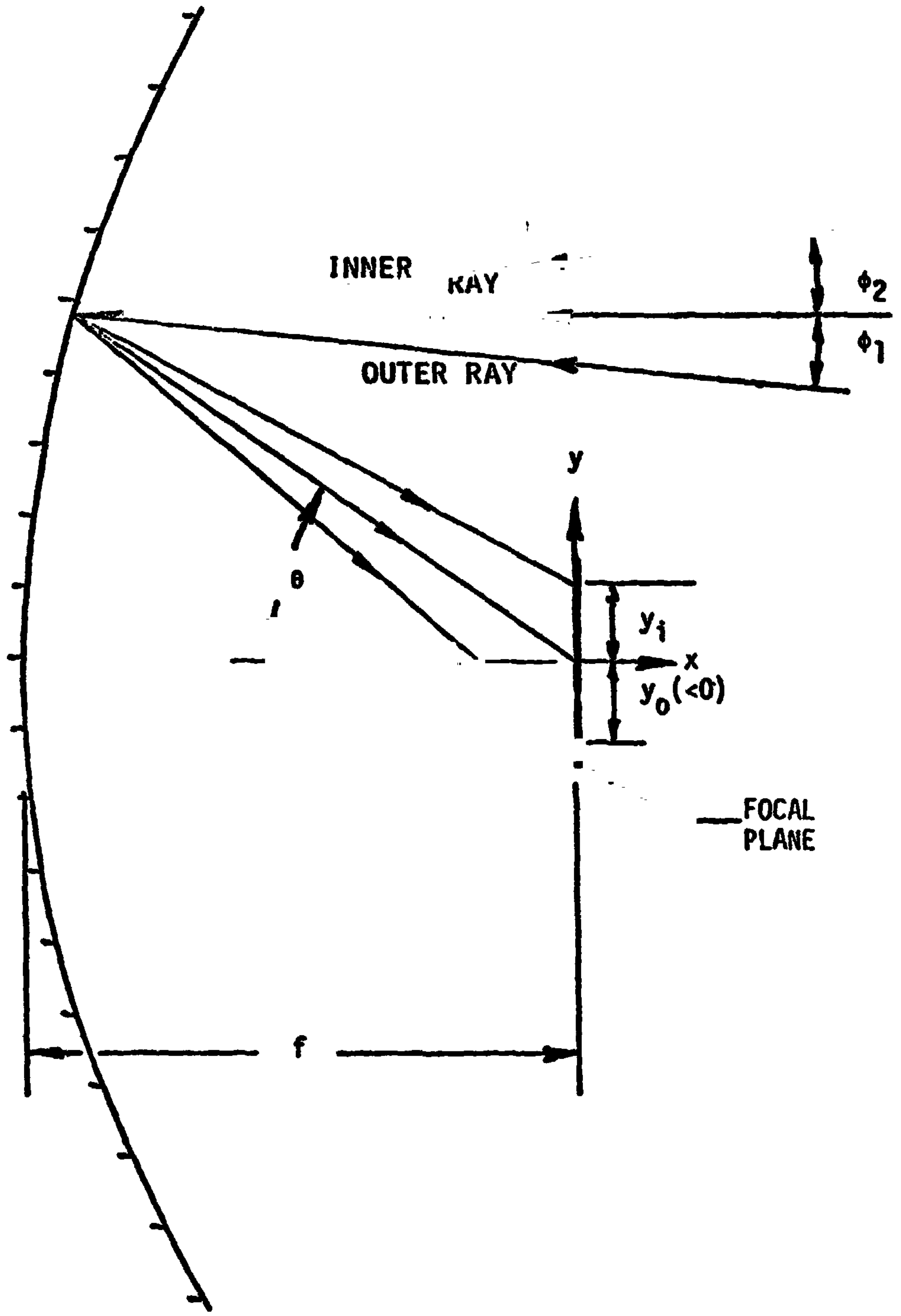

PARABOLIC TROUGH WITH RIM ANGLE $\theta = 65°$, ACCEPTANCE HALF ANGLE $\delta = 2.5°$.

HIGHLY NONUNIFORM FLUX DISTRIBUTION AT ABSORBER

$$P_{MAX}/P_{AVERAGE} = 15$$

(SIMILAR CONCLUSIONS FOR OTHER SINGLE STAGE CONCENTRATORS.)

PARABOLIC TROUGH WITH CPC SECOND STAGE

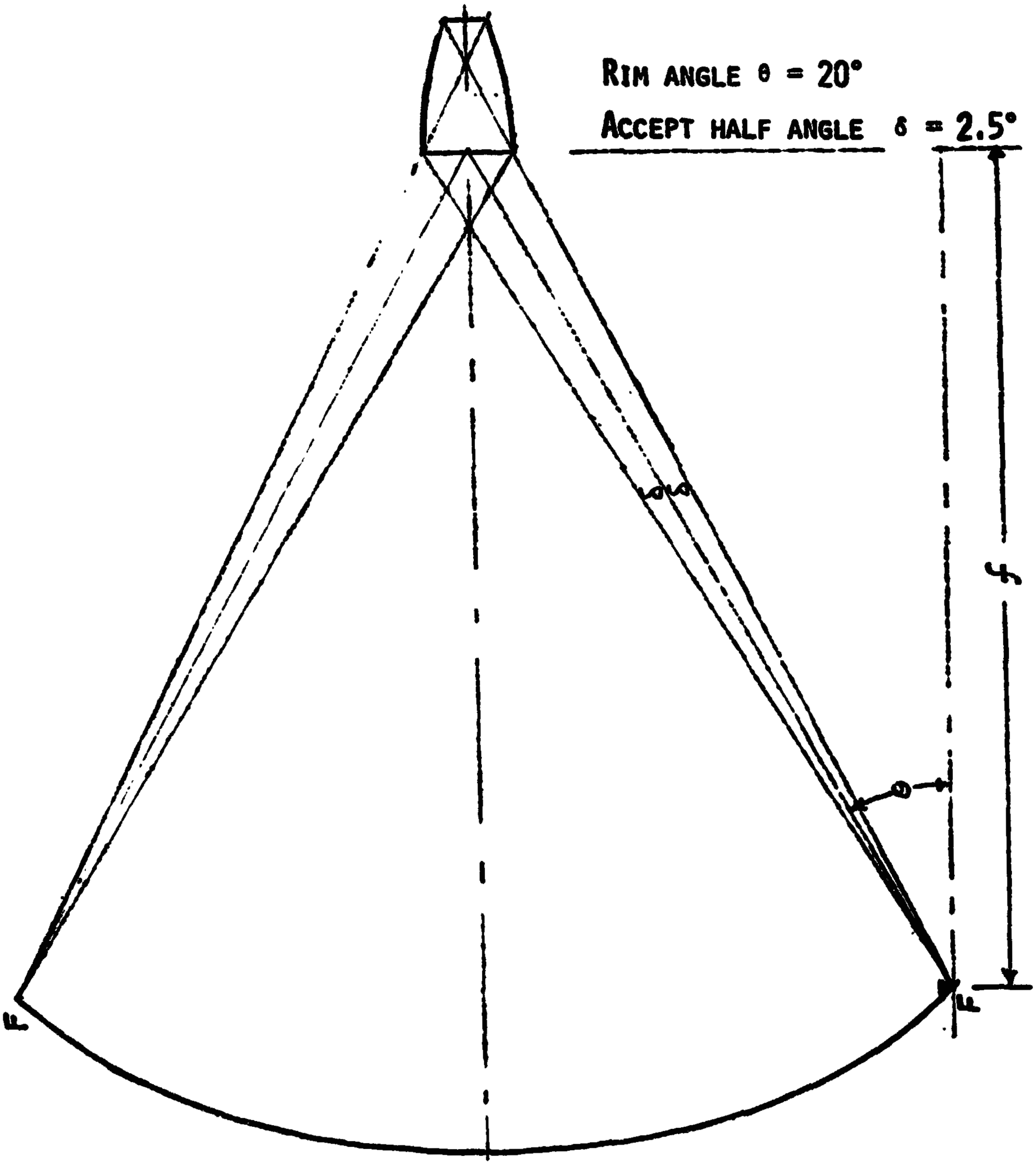

RIM ANGLE $\theta = 20°$

ACCEPT HALF ANGLE $\delta = 2.5°$

FLUX DISTRIBUTION AT ABSORBER NEARLY UNIFORM

$P_{MAX}/P_{AVERAGE} = 1.2$

CPC APPLICATION PROJECT

RESULTS OF PHOTOVOLTAIC APPLICATION STUDY

- CPC AS FIELD COLLECTOR IN HYBRID SYSTEM
  (SPECTROLAB / ASU)

CONCLUSION OF STUDY

TWO-ELEMENT DESIGN IS SUBSTANTIALLY BETTER THAN ANY SINGLE ELEMENT DESIGN STUDIED, FOR USE WITH PHOTOVOLTAIC CELLS BECAUSE :

a. ADDITIONAL CONCENTRATION OF ~2. 5 POSSIBLE

b. FLUX DISTRIBUTION IS SMOOTHED OUT
(PEAK / AVERAGE INTENSITY = x15 FOR PARABOLIC TROUGH, = 1. 2 FOR HYBRID SYSTEM)

c CPC CAN BE DESIGNED TO REJECT HEAT. HENCE DOES NOT ADD TO OVERALL COST OF SINGLE ELEMENT SYSTEM

RECOMMENDATION :

FURTHER STUDY LEADING TO DESIGN OF CONCENTRATOR SYSTEMS OPTIMIZED FOR SPECIFIC APPLICATIONS AND FABRICATION AND TEST OF PROTOTYPES

ORIGINAL PAGE IS
OF POOR QUALITY

CPC APPLICATION PROJECT
PHOTOVOLTAIC SCHEDULE
FY 1976

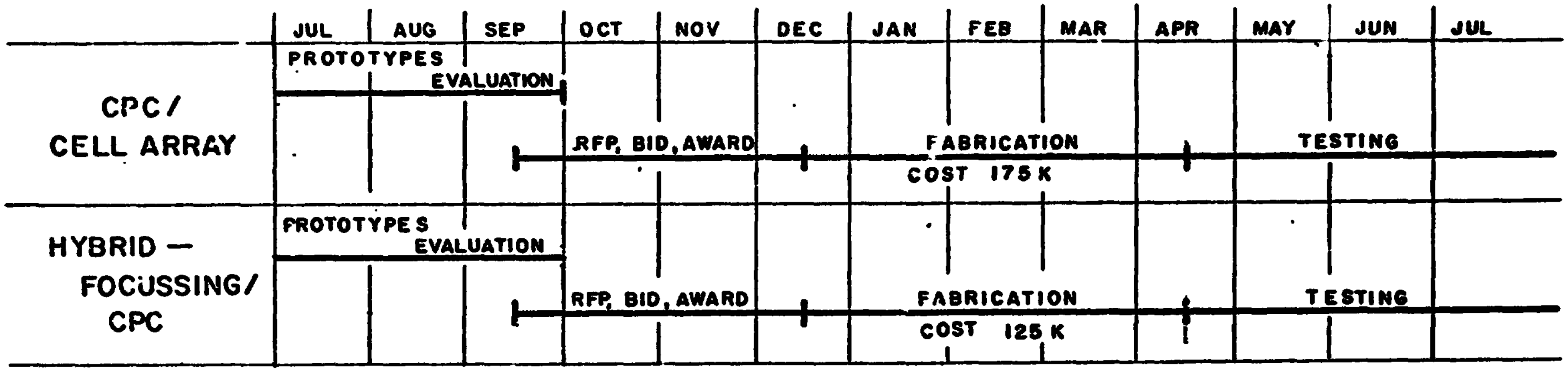

TOTAL COST — 300K

N76 12483

INTEGRATED PHOTOVOLTAIC-THERMAL SOLAR ENERGY CONVERSION SYSTEMS

George A. Samara

Sandia Laboratories, Albuquerque, New Mexico 87115

(Internally Funded)

Principal Investigators: D. G. Schueler
R. P. Stromberg

Person in Charge: G. A. Samara

presented at

National Solar Photovoltaic Program Review Meeting

July 22-25 (1975) Los Angeles, California

ABSTRACT

One potential solution to the economic viability of solar energy is the application of total energy concepts to solar energy conversion systems. The total energy concept envisions providing a major fraction of the energy requirements of residential and light commercial buildings from solar energy. Specifically, electricity, air conditioning, space heating and hot water would be provided.

The overall objective of this Sandia program is (i) to demonstrate the feasibility of a combined photovoltaic-thermal solar total energy system, and (ii) to develop the hardware which can provide the proper ratio of electrical and thermal energy for residential and commercial applications at a cost competitive with alternate energy sources.

The approach adopted is based on solar concentration (initially 40-50 suns). Sunlight is concentrated on photovoltaic cells (currently single crystal silicon) which absorb the light and convert some of the solar energy into electricity. The remainder of the absorbed energy, which is converted into heat in the cell, is extracted as useful thermal energy by a circulating fluid. Since we find that the dollar values of the electrical and thermal energies produced by the combined system are nearly equivalent for the applications envisioned here, the cost-effectiveness of the combined collector system is essentially doubled compared to photovoltaic concentration systems which do not make use of the excess heat.

The program consists of four closely coordinated tasks: (1) Systems Analysis, (2) Silicon Cell Development for High Illumination, High Temperature Operation, (3) Development of the Combined Photovoltaic-Thermal Collector, and (4) Systems Demonstrations. Work on the first three tasks is well under way. The basic plan for the program is to build on existing broad technology bases and to concentrate on developing an overall technical and economic view of the combined total energy systems. In the early phases of this program we have emphasized modeling and computer simulation of both solar cell and overall system configuration and performance, in parallel efforts which seek to define critical or important design parameters.

The successful utilization of solar energy depends on achieving the proper balance between (i) the solar input power, (ii) the power load to the system, (iii) the energy storage requirements, and (iv) the available conventional power sources. In addition, since both solar input power and load power requirements are time varying functions, dynamic systems modeling techniques [illegible] needed to determine the optimal system configuration and energy st[illegible]y necessary to support load demands for all available time histo[illegible]wer and load

data for any given application. Towards this end Sandia has developed a large solar energy systems computer analysis code (SOLSYS). We are employing this code to assess the technical and economic feasibility of the combined system relative to various utilization scenarios. Initial studies have dealt with configuring individual residences using Albuquerque solar and load data.

The Silicon Cell Development task has emphasized the redesign of the cell to yield high efficiency at the operating conditions of the combined system (40-50 suns and temperatures to $\sim$ 100°C). A Sandia-developed numerical semiconductor device analysis code which yields one-dimensional numerical solutions of the carrier transport equations throughout the thickness of the cell is being used and has proved to be an indispensable aid towards achieving the desired goal. Analyses have been carried out on a number of cell designs at solar intensities ranging from 1 to 140 suns and temperatures from 27 to 200°C. A design has been selected and is being experimentally tested which yields 12% conversion efficiency at 50 suns and 100°C. The modifications needed, in comparison with the conventional cell, include lowering the substrate resistivity by an order of magnitude to $\sim 0.3\ \Omega$-cm, reducing the junction depth from 0.5 to 0.2 μm, decreasing the diffused surface layer concentration to $N_D \simeq 1\times10^{20}\,\mathrm{cm}^{-3}$, and optimizing the top surface metallization. Experimental results on Sandia-built modified cells have thus far given excellent confirmation of the code results.

A combined photovoltaic-thermal collector has been built and is now being tested. Initial tests have concentrated on evaluating the thermal efficiency of the collector before and after the silicon cells are mounted. With likely improvements in bonding between cells and receiver and in the absorptivity of the cells, thermal efficiencies > 50% can be expected for the combined receiver operating at 100°C.

Since we are still in the early stages of this program it is expected that the analytical and experimental work under the various tasks will continue for the near future. The systems analysis will be expanded to include other cities and other loads; the modified cell work will emphasize optimizing the top-surface metallization; and the combined collector work will concentrate on optimizing both electrical and thermal efficiencies and gaining operational experience under field conditions. Plans for a complete integrated system development model will be formulated.

The attached figures elaborate on and further illustrate certain aspects and accomplishments of the program.

OVERALL OBJECTIVES:

- To Demonstrate the Feasibility of Combined Photovoltaic-Thermal Solar Energy Systems
- To Develop the Hardware Which can Provide the Proper Ratio of Electrical and Thermal Energy for Pertinent Applications at a Cost Competitive with Alternate Energy Sources

PROGRAM TASKS:

1. Systems Analysis
    a. Computer Simulation
    b. System Configurations
2. Silicon Cell Development for Solar Concentration
    a. Code Simulation and Analysis
    b. Cell Fabrication
    c. Performance Testing
3. Combined Collector Development
    a. Modeling
    b. Fabrication and Testing
4. Systems Demonstrations
    a. Development Models
    b. Full-Scale Demonstrations

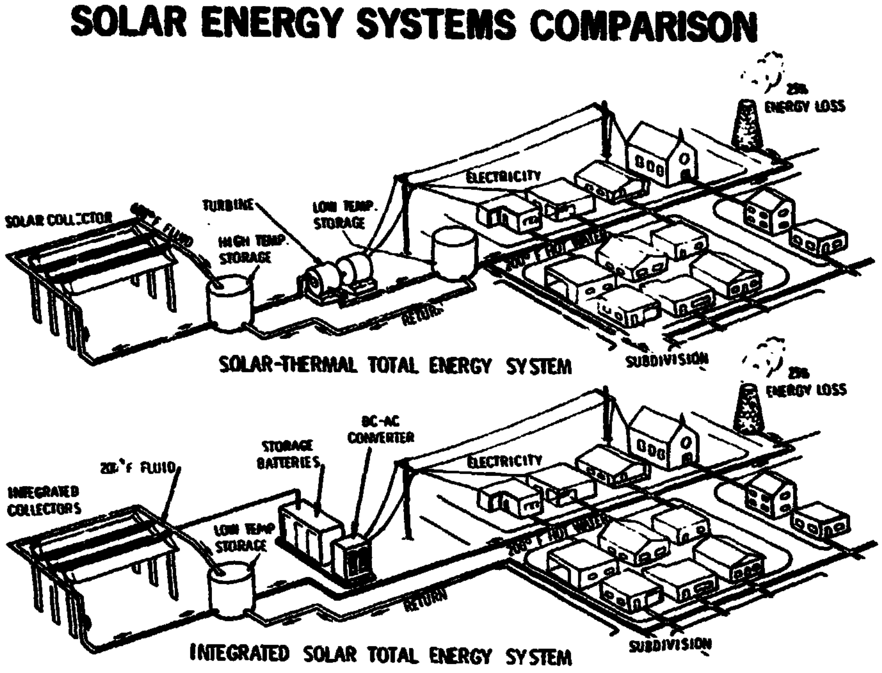

FIGURE 1 (top) A solar energy system using solar-thermal conversion and thermal cascading.

(bottom) A solar energy system using combined photovoltaic and thermal conversion.

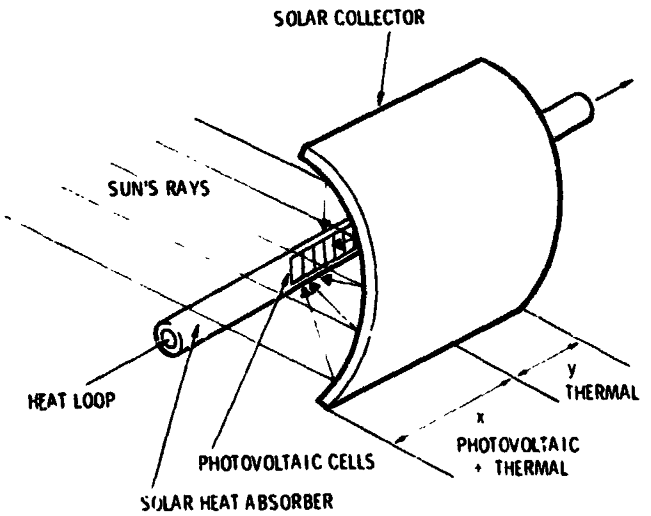

FIGURE 2. An integrated photovoltaic-thermal solar concentrating collector.

ORIGINAL PAGE IS OF POOR QUALITY

TABLE I

Calculated Performances of Conventional and Optimized Solar Cells at T = 100° C

	Conventional			Optimized		
	1 sun	40 suns	100 suns	1 sun	40 suns	100 suns
V_{oc} [V]	0.379	0.481	0.499	0.447	0.568	0.597
J_{sc} [mA/cm^2] (per sun)	41.9 (41.9)	1757. (43.9)	4476. (44.8)	43.6 (43.6)	1749. (43.7)	4395. (43.9)
FF	0.720	0.629	0.486	0.743	0.769	0.754
η^* [%]	7.0	8.2	6.7	8.9	11.8	12.2

$^*\gamma = 0.96$

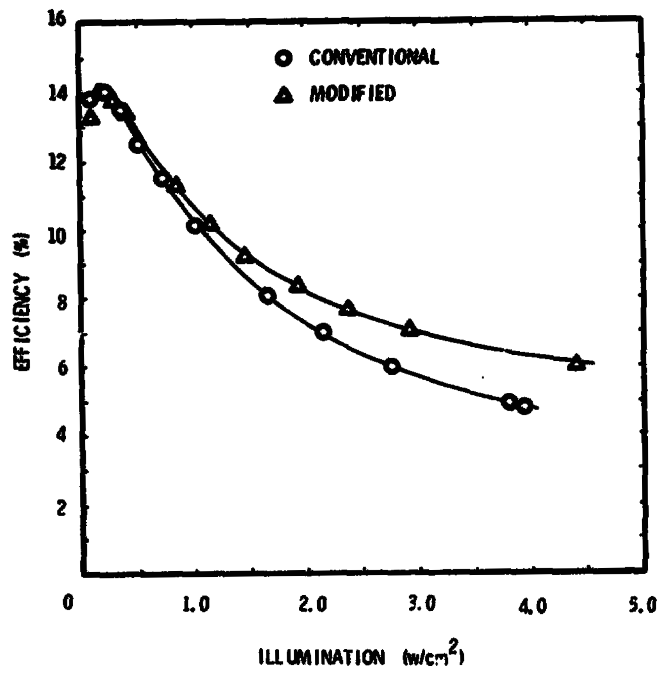

Fig. 3

Efficiency versus illumination intensity for a conventional silicon cell and our modified silicon cell at 26°C. Front surface electrode pattern is not optimized.

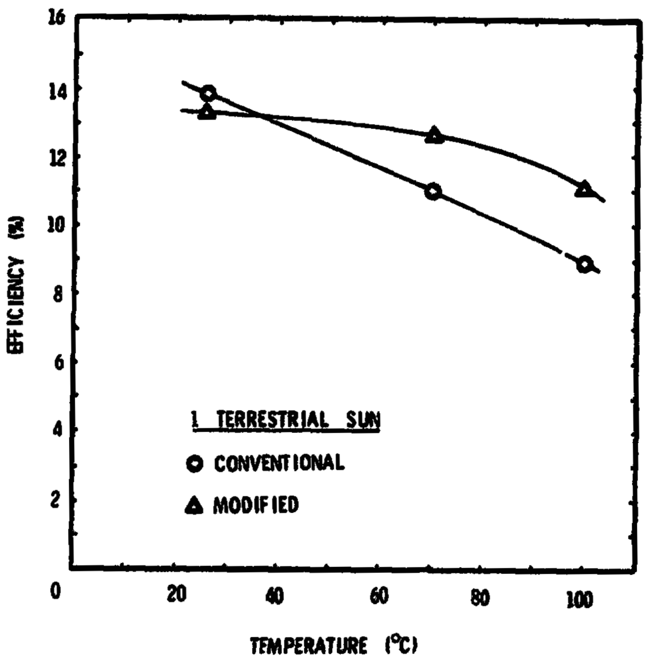

Fig. 4

Efficiency versus temperature for a conventional silicon cell and our modified silicon cell at 1 terrestrial sun (0.1 W/cm^2). Front surface electrode pattern is not optimized.

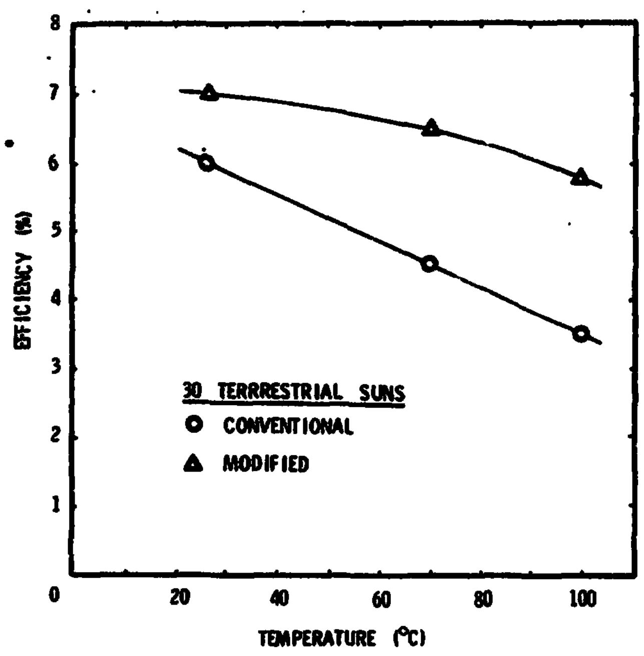

Fig. 5 Efficiency versus temperature for a conventional silicon cell and our modified silicon cell at 1 terrestrial sun (0.1 W/cm^2). Front surfece electrode pattern is not optimized.

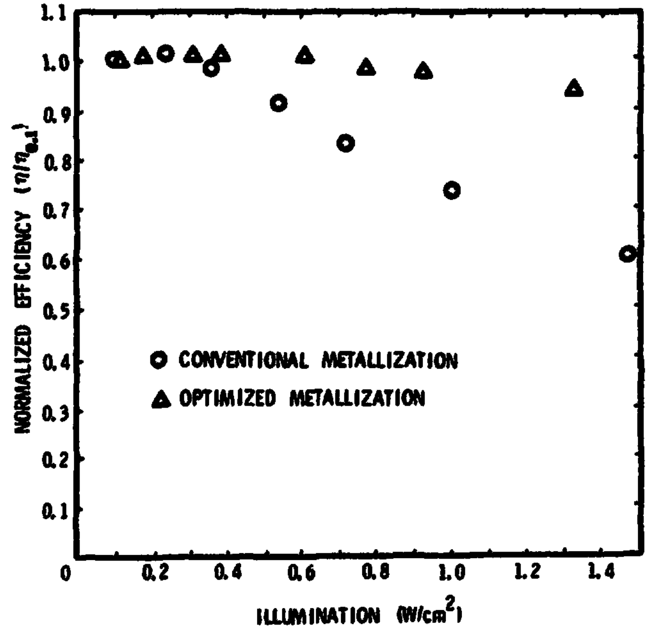

Fig. 6 Normalized efficiency versus illumination for conventional silicon cells with conventional and optimized front surface electrode patterns.

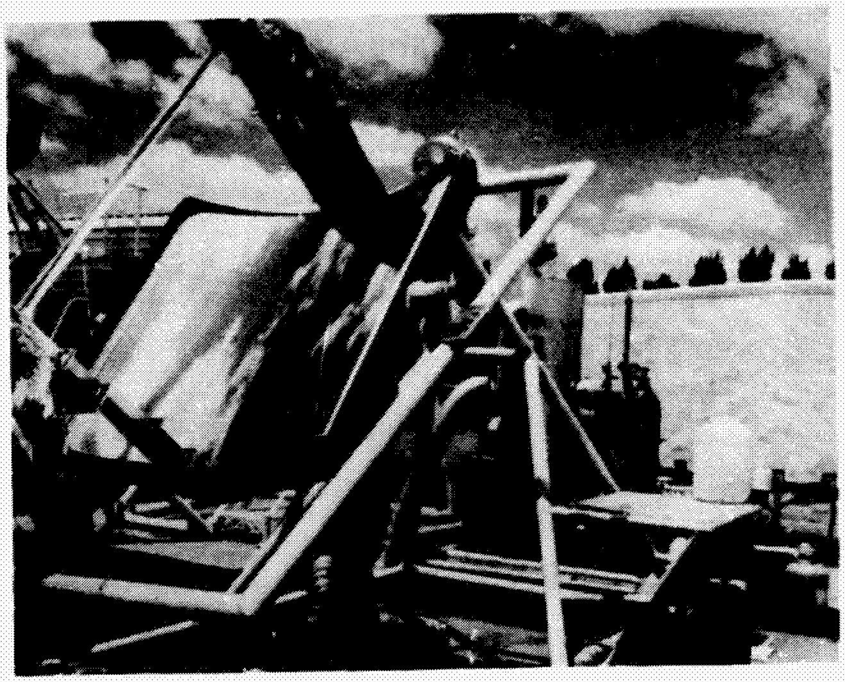

Fig. 7 Reflector and integrated receiver pipe under test.

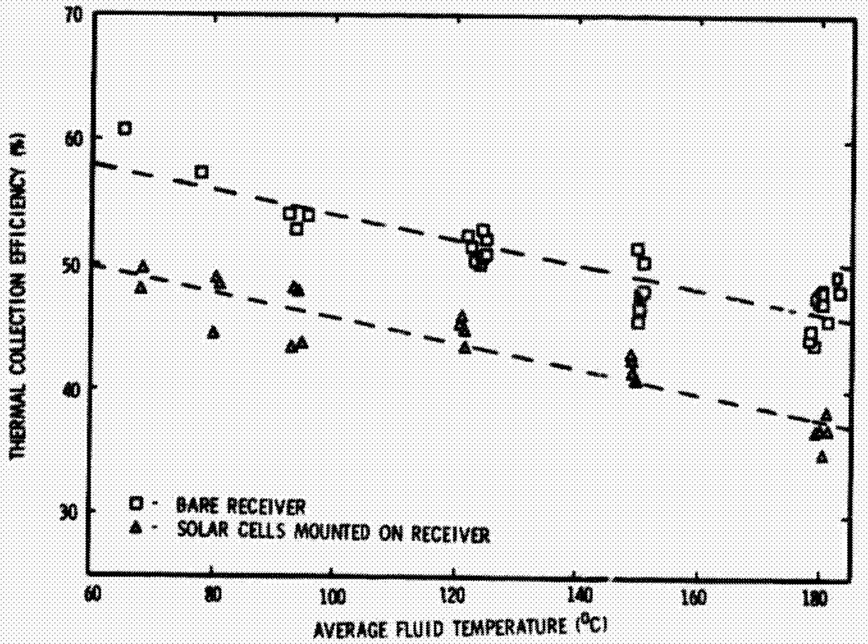

THERMAL EFFICIENCY MEASUREMENTS AS FUNCTION OF COOLANT FLUID TEMPERATURE.

Fig. 8

SUMMARY

- Sandia's Solar Energy Systems Computer Analysis Code (SOLSYS) is Being Utilized to Assess the Technical and Economic Feasibility of Combined Photovoltaic Systems Relative to Various Utilization Scenarios.
- Combined Systems Using Concentrators and High Efficiency (≥ 10%) Silicon Cells can Provide Residences (or Communities) with a Reasonable Balance of Electrical and Thermal Energy.
- The Device Analysis Code has been Used to Redesign the Silicon Cell for High Temperature, High Illumination Operation.
- A Design Yielding 12% Efficiency at 50 Suns and 100°C has been Selected.
- Modified Cells have been Fabricated and Tested. Results have Confirmed Code Predictions.
- A Combined Collector has been Built and is being Tested. Thermal Efficiencies > 50% at 50 Suns and 100°C can be expected.

SESSION V

POLYCRYSTALLINE SILICON CELLS

N76 12484

DEVELOPMENT OF LOW COST THIN FILM POLYCRYSTALLINE SILICON SOLAR CELLS FOR TERRESTRIAL APPLICATIONS

NSF Grant AER 73-07843

(GI-38981)

Period of Grant

June 1, 1973 - November 30, 1976

Value of Grant: $449,000

Ting L. Chu, Southern Methodist University

Principal Investigator

Presented at the National Photovoltaic Program Review Meeting

July 22-25, 1975

Los Angeles, California

I. Objective

The objective of this grant is to develop low-cost thin film polycrystalline silicon solar cells for terrestrial utilization. The technical approaches consist of (1) the deposition, characterization, and optimization of silicon p-n junction structures on graphite and metallurgical silicon substrates, (2) the purification of metallurgical silicon, (3) the fabrication and characterization of solar cells from purified metallurgical silicon, and (4) the fabrication and characterization of large area cells, 30 cm^2 or larger in area.

II. Past Activity

During 1974, major efforts were directed to (1) the deposition and characterization of silicon on graphite and metallurgical silicon substrates by the thermal reduction of trichlorosilane, and (2) the fabrication and evaluation of silicon solar cells on these substrates. The microstructure of silicon deposited on graphite substrates by the trichlorosilane process was optimized, and the average size of crystallites was 20-30 μm. Using appropriate dopants during the deposition process, many solar cells of the configuration n^+-silicon/p-silicon/graphite were fabricated, and their AMO efficiencies were limited to about 1.5%. The grain size of vapor deposited silicon on graphite substrates was improved by rapid melting and solidification, and silicon p-n junction solar cells with AMO efficiencies (no anti-reflection coating) up to 2% were produced.

Metallurgical silicon plates were prepared by unidirectional solidification of the melt in a boron nitride container and were used as substrates for the deposition of silicon by the trichlorosilane process. Silicon deposited on metallurgical silicon plates by the trichlorosilane process was found to be epitaxial with respect to the substrate. Many solar cells of the configuration n^+-silicon/p-silicon/metallurgical silicon were prepared, and their AMO efficiencies (no anti-reflection coating) were up to 2.6%.

III. Current Effort

The recent work has been directed to (1) the improvement in the structural properties of silicon on graphite substrates, (2) the optimization of solar cell characteristics on graphite and metallurgical silicon substrates, and (3) the purification of metallurgical silicon. A zone-melting technique has been developed for the recrystallization of silicon on graphite substrates, and the microstructure of silicon was improved considerably. Silicon p-n junction solar cells on graphite substrates with AMO efficiencies up to 2.5% have been produced. The conversion efficiency of n^+-silicon/p-silicon/metallurgical silicon solar cells appears to be limited by the grain boundaries in the p-layer. This grain boundary effect has been reduced by increasing the dopant concentration in the p-layer, and the AMO efficiency of n^+-silicon/p^+-silicon/metallurgical silicon solar cells was up to 3.5%.

The purification of metallurgical silicon by chemical treatment of the melt and the floating-zone technique has been carried out. The treatment of molten metallurgical silicon with chlorine, chlorine-oxygen mixture, etc., was found to be effective in reducing the concentration of most metallic impurities, except iron. The floating zone technique was found to be effective in reducing the concentration of most impurities, except boron, in metallurgical silicon. Solar cells with AMO efficiencies higher than 4% have been produced from two zone-pass material.

IV. Future Plans

Future work will be directed toward the improvement of conversion efficiencies of solar cells on graphite and metallurgical silicon substrates, including (1) the refinement of the zone-melting technique for the recrystallization of silicon on graphite substrates, (2) the purification and characterization of metallurgical silicon, and (3) the optimization of the thickness and resistivity of the silicon layer.

V. Key Results to Date

The AMO efficiencies (no anti-reflection coating) obtained to date are 2.5% for solar cells deposited on graphite substrates, 3.5% for solar cells deposited on metallurgical silicon substrates, and 4.5% for solar cells fabricate from purified metallurgical silicon.

DEVELOPMENT OF LOW COST THIN FILM POLYCRYSTALLINE SILICON SOLAR CELLS FOR TERRESTRIAL APPLICATIONS

NSF Grant AER 73-07843
(GI-38981)

Work performed at

Southern Methodist University and Texas Instruments, Incorporated

Period of Grant

June 1, 1973 - November 30, 1976

Amount of Award: $449,000

Principal Investigator

Ting L. Chu, Southern Methodist University

POLYCRYSTALLINE SILICON SOLAR CELLS

INTRODUCTION

- Overall Objective: To develop low-cost thin film polycrystalline silicon solar cells for terrestrial utilization.
- Approaches:
  - Deposition and characterization of silicon on graphite and metallurgical silicon substrates by the trichlorosilane ($SiHCl_3$) process.
  - Fabrication, characterization, and optimization of solar cells on graphite and metallurgical silicon substrates.
  - Purification of metallurgical silicon.
  - Fabrication and characterization of solar cells from purified metallurgical silicon.
- Key results reported at the last review (December, 1974):
  - The microstructure of silicon deposited on graphite by the trichlorosilane process was optimized. The average size of crystallites was 20-30 µm.
  - Silicon p-n junction solar cells with AMO efficiencies up to 1.5% have been produced on graphite substrates.
  - The grain size of vapor deposited silicon on graphite was improved by rapid melting and solidification. Solar cells with AMO efficiencies up to 2% have been produced.
  - Silicon p-n junction solar cells on metallurgical silicon with AMO efficiencies up to 2.6% have been produced by the trichlorosilane process.

TLC: 2

POLYCRYSTALLINE SILICON SOLAR CELLS

PLANNED ACTIVITY FOR LAST SIX MONTHS

PLAN	ACTION
• Deposition and characterization of silicon on pyrolytic carbon-coated graphite substrates by the thermal reduction of trichlorosilane.	• Silicon layers deposited on carbon-coated graphite substrates under a wide range of conditions, and their microstructure and crystallography evaluated.
• Improvement in structural properties of silicon on graphite substrates.	• Zone-melting technique developed for the recrystallization of silicon.
• Deposition and characterization of silicon solar cells on graphite substrates.	[illegible]-n junction solar cells with AMO efficiencies up to 2.5% have been produced.
• Deposition and optimization of silicon solar cells on metallurgical silicon substrates.	• P-n junction solar cells with AMO efficiencies up to 3.5% have been produced.
• Purification of metallurgical silicon and fabrication of solar cells from purified silicon.	• Metallurgical silicon purified by chemical treatment and floating-zone techniques. Solar cells with AMO efficiencies higher than 4% have been produced.

TLC; 3

POLYCRYSTALLINE SILICON SOLAR CELLS - PROGRESS TO DATE

DEPOSITION OF SILICON ON CARBON-COATED GRAPHITE

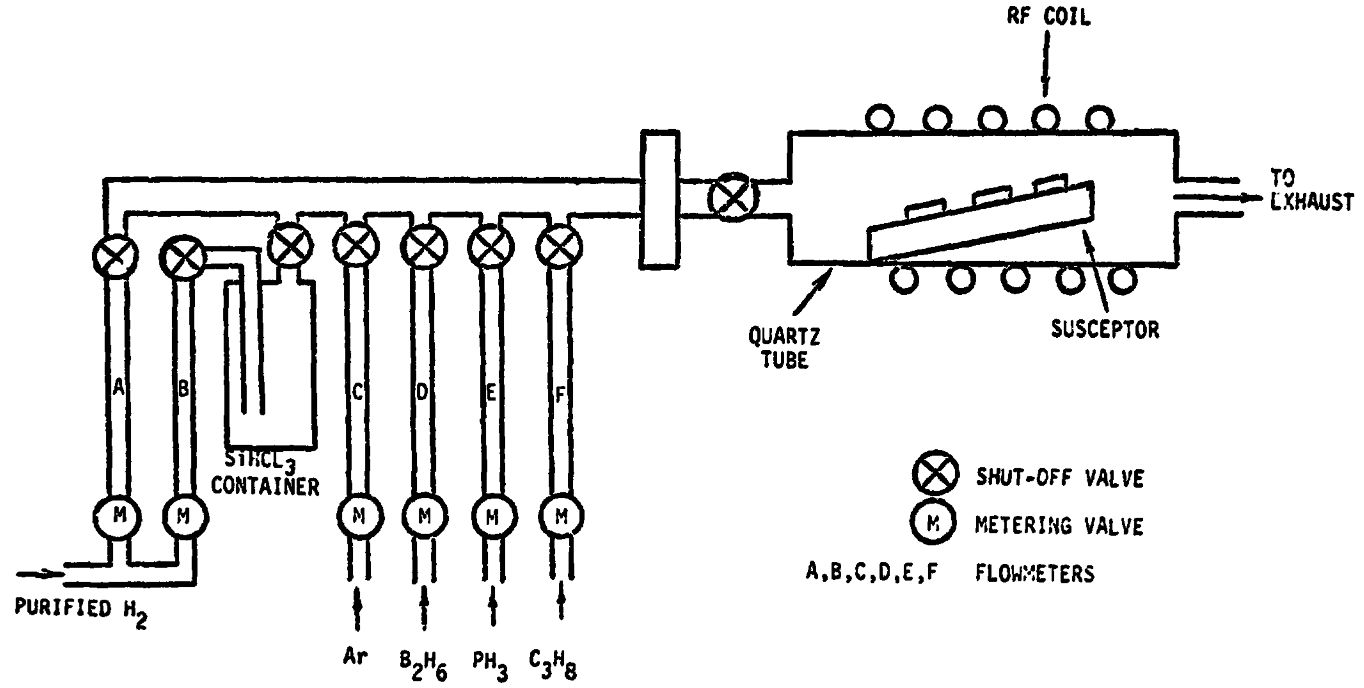

Schematic of the Apparatus for the Deposition of Carbon and Silicon

- Reactions: Thermal decomposition of propane for the deposition of carbon.
  Thermal reduction of trichlorosilane for the deposition of silicon.
- Substrate Temperature: 1100° - 1250° C
- Deposition Rate: 0.3 - 0.8 μm/min for carbon
  0.3 - 2 μm/min for silicon

TLC; 4

POLYCRYSTALLINE SILICON SOLAR CELLS - PROGRESS TO DATE

PROPERTIES OF SILICON ON CARBON/GRAPHITE SUBSTRATES

- MICROSTRUCTURE

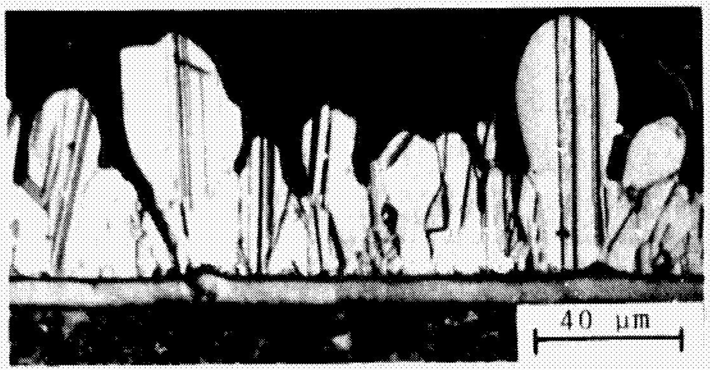

1250° C, 0.3 μm/min

1250° C, 1.5 μm/min

- CRYSTALLOGRAPHIC PROPERTIES

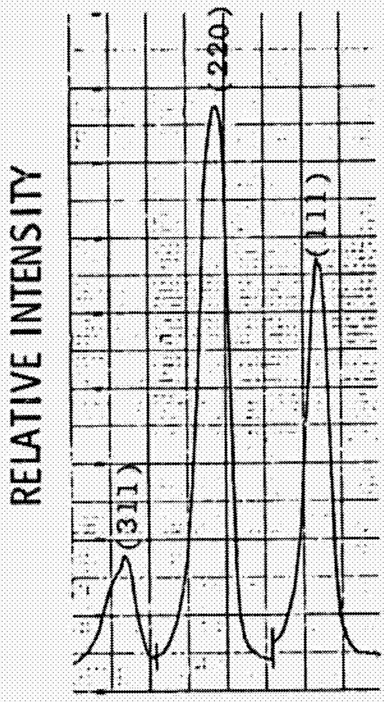

1000°C, 1 μm/min

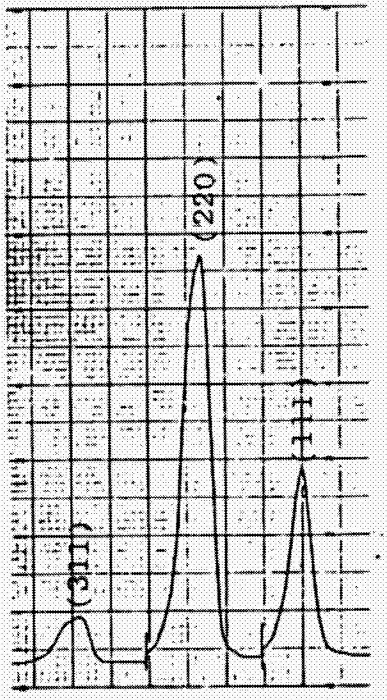

1000°C, 0.2 μm/min

- CONCLUSION: Silicon on carbon/graphite is similar to silicon on graphite in microstructure, crystallographic properties, and solar cell characteristics.

TLC; 5

POLYCRYSTALLINE SILICON SOLAR CELLS - PROGRESS TO DATE

SILICON SOLAR CELLS ON GRAPHITE SUBSTRATES

- BY CONVENTIONAL CVD

0.2 - 0.4 μm, 0.002 - 0.003 ohm-cm N-SILICON
10 - 20 μm, 0.5 - 2 ohm-cm P-SILICON
10 - 40 μm, 0.002 - 0.005 ohm-cm P-SILICON
GRAPHITE SUBSTRATE (OR CARBON-COATED GRAPHITE)

- BY CVD AND RECRYSTALLIZATION

0.2 - 0.4 μm, 0.002 - 0.003 ohm-cm N-SILICON
10 - 20 μm, 0.5 - 2 ohm-cm P-SILICON
VAPOR-DEPOSITED P^+ -SILICON RECRYSTALLIZED
GRAPHITE SUBSTRATE (OR CARBON-COATED GRAPHITE)

- AVERAGE GRAIN SIZE: 15 - 20 μm
- AMO EFFICIENCY: 1.5%

TLC; 6

POLYCRYSTALLINE SILICON SOLAR CELLS - PROGRESS TO DATE

RECRYSTALLIZATION OF SILICON ON GRAPHITE SUBSTRATES

- APPROACHES
  - Rapid Melting and Solidification
  - Zone-Melting

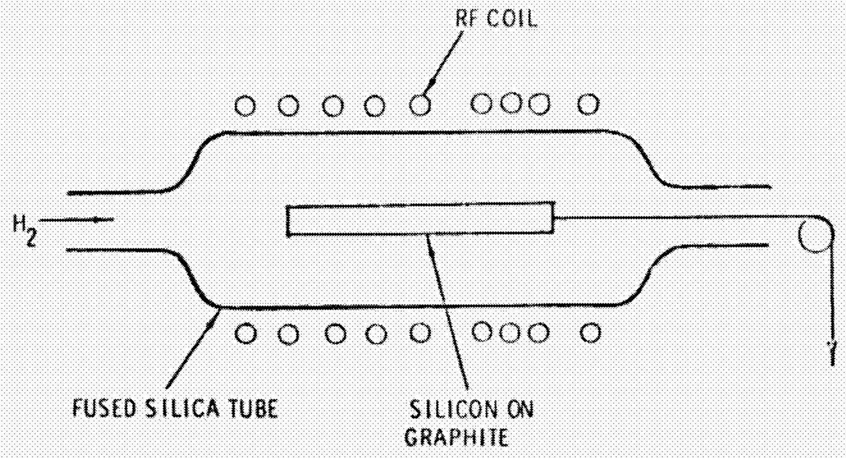

Scnematic of the Zone-Melting Apparatus

TLC; 7

- SILICON BY ZONE-MELTING

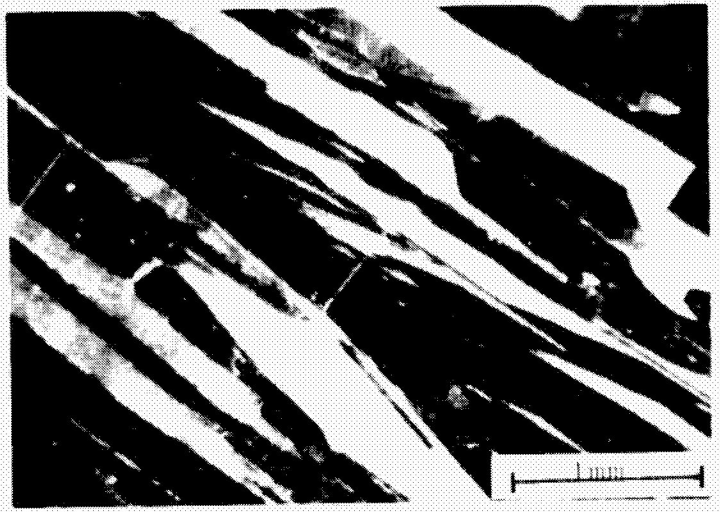

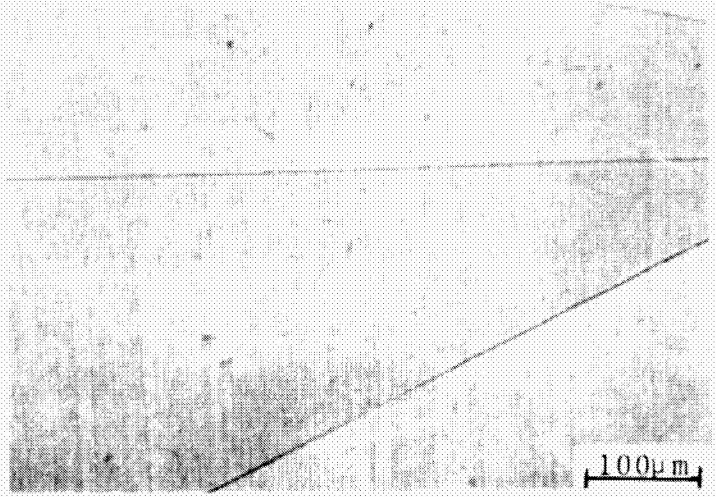

POLYCRYSTALLINE SILICON SOLAR CELLS - PROGRESS TO DATE

SILICON SOLAR CELLS, 2.5 CM X 2.5 CM, ON GRAPHITE SUBSTRATE

- Dark Characteristics

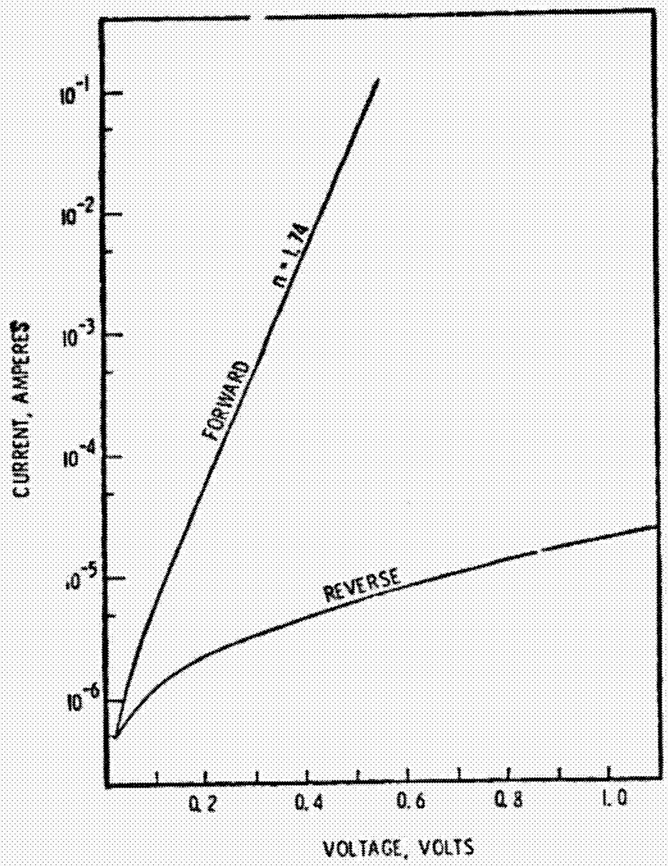

TLC, 8

- Characteristics under Illumination at 135 mW/cm^2.

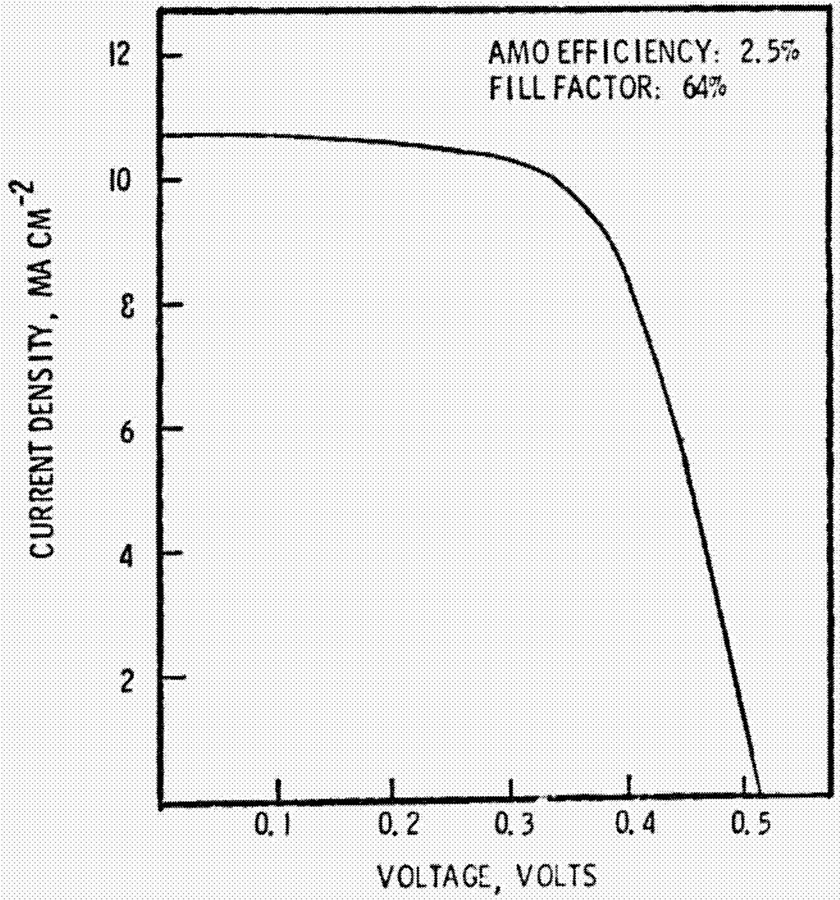

POLYCRYSTALLINE SILICON SOLAR CELLS - PROGRESS TO DATE

SILICON SOLAR CELLS ON UNIDIRECTIONALLY SOLIDIFIED METALLURGICAL SILISON

DARK CURRENT-VOLTAGE CHARACTERISTICS

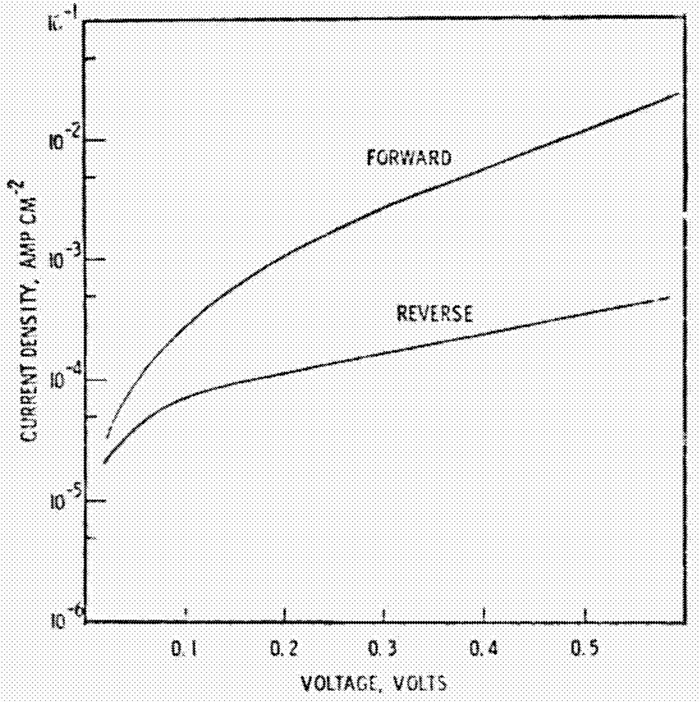

0.4 μm 0.005 OHM-CM N-SILICON
20 μm 1 OHM-CM P-SILICON
P$^+$ SUBSTRATE

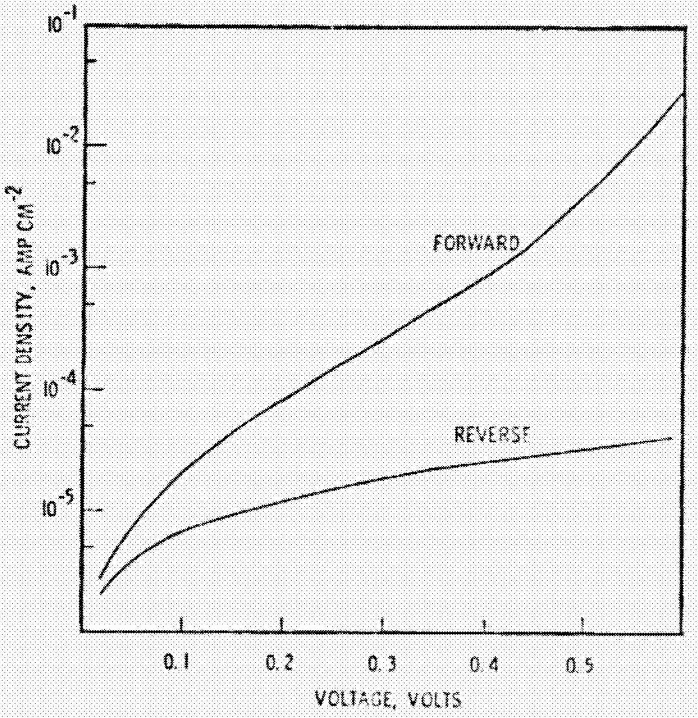

0.4 μm 0.005 OHM-CM N-SILICON
5 μm 0.06 OHM-CM P-SILICON
P$^+$ SUBSTRATE

TLC; 9

POLYCRYSTALLINE SILICON SOLAR CELLS - PROGRESS TO DATE

SILICON SOLAR CELLS ON UNIDIRECTIONALLY SOLIDIFIED METALLURGICAL SILICON

- Characteristics under illuminations at 135 MW/cm^2

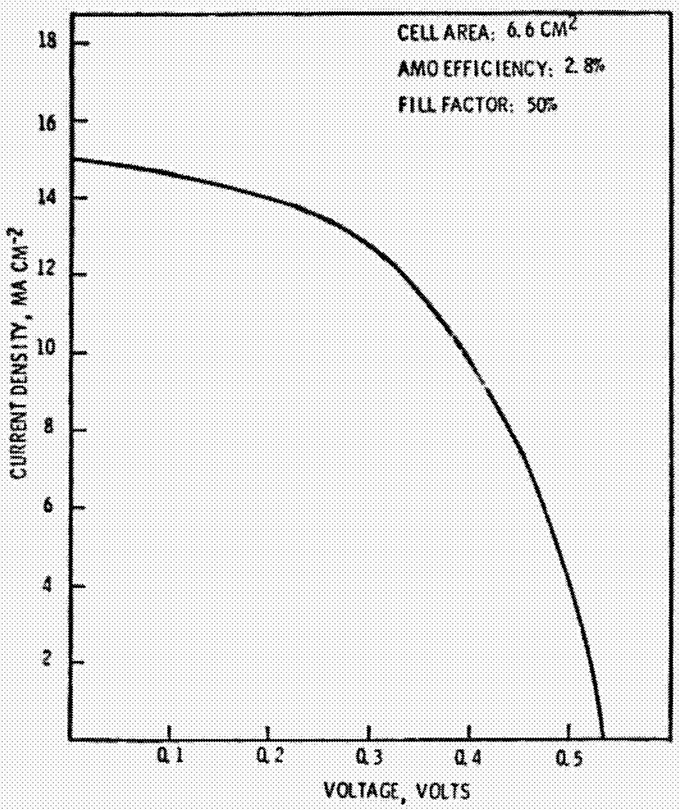

N$^+$-SILICON/P-SILICON/SUBSTRATE

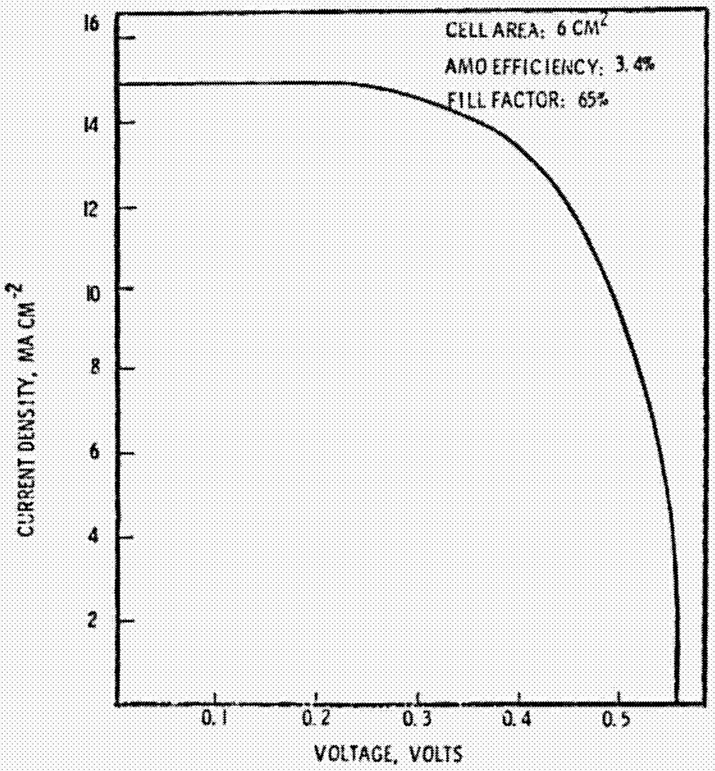

N$^+$-SILICON/P$^+$-SILICON/SUBSTRATE

- CONCLUSION: Grain boundary effects in polycrystalline silicon can be reduced by doping.

TLC; 10

POLYCRYSTALLINE SILICON SOLAR CELLS - PROGRESS TO DATE

SILICON SOLAR CELLS ON CZOCHRALSKI METALLURGICAL SILICON

- SUBSTRATE

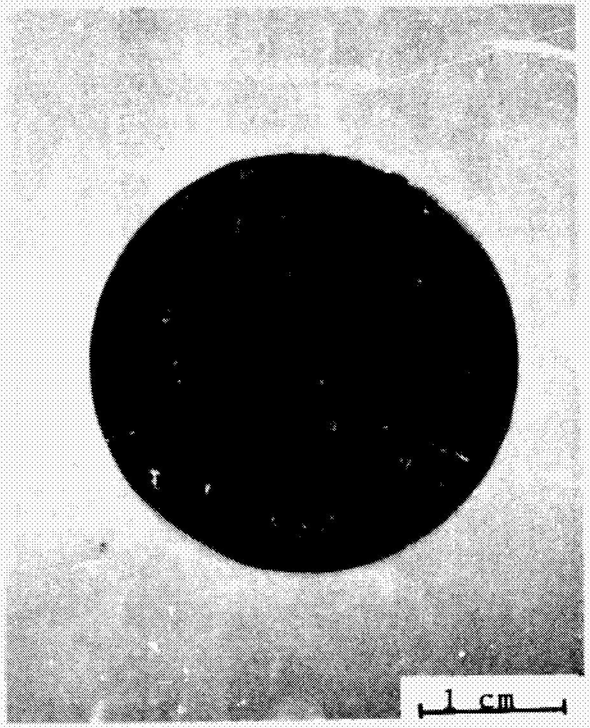

- DARK CURRENT VOLTAGE CHARACTERISTICS

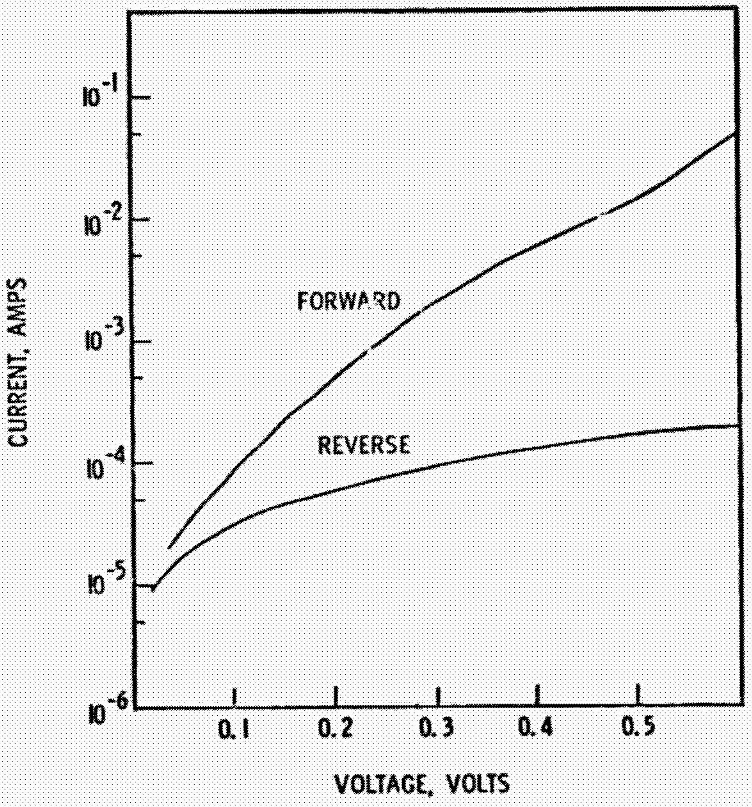

N^+-SILICON/P-SILICON/CZOCHRALSKI
METALLURGICAL SILICON

TLC; II

POLYCRYSTALLINE SILICON SOLAR CELLS - PROGRESS TO DATE

SILICON SOLAR CELLS ON CZOCHRALSKI PULLED METALLURGICAL SILICON

- Characteristics under illuminations at 135 MW/cm^2

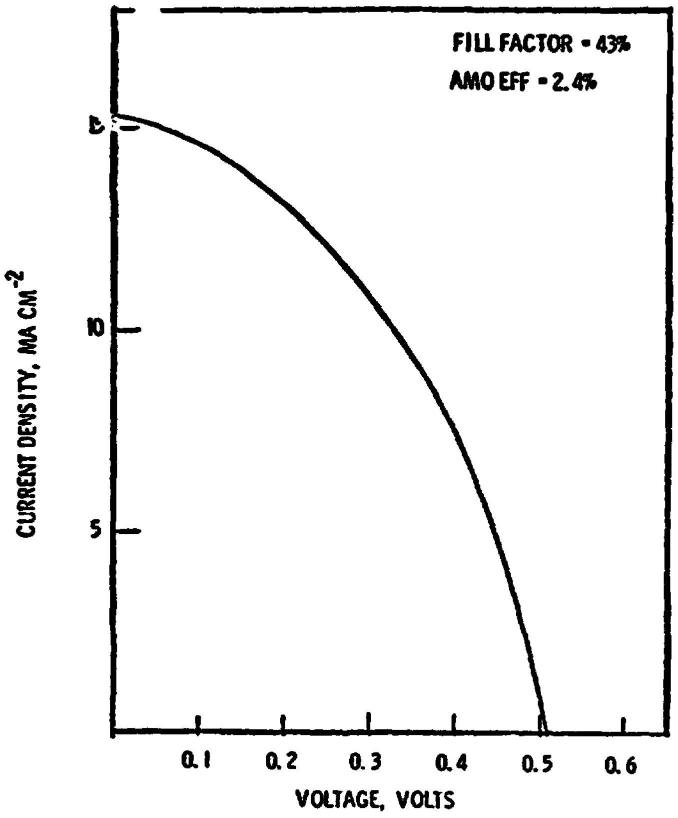

DIFFUSED CELL

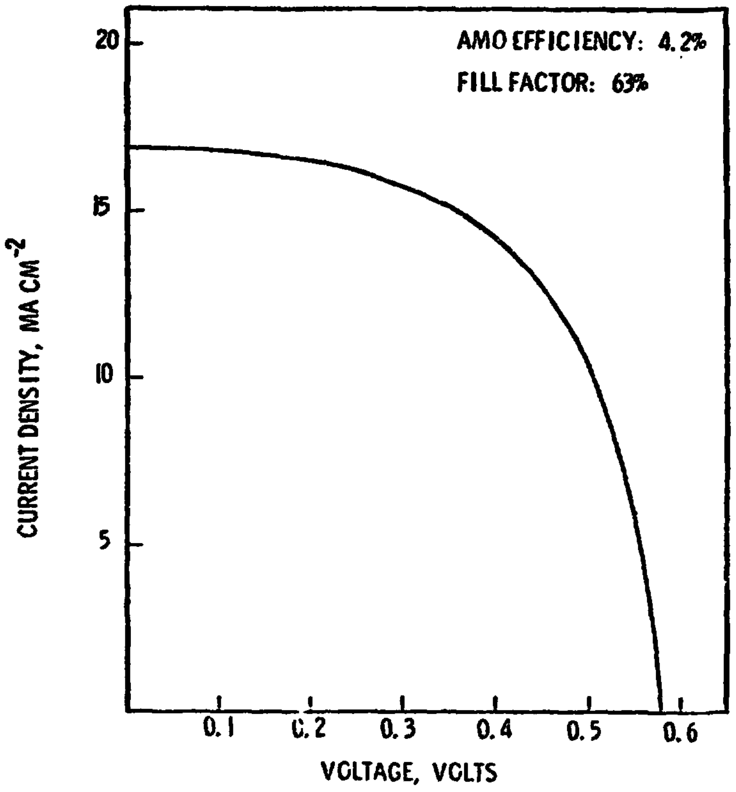

N$^+$-SILICON/P-SILICON/SUBSTRATE

TLC; 12

POLYCRYSTALLINE SILICON SOLAR CELLS - PROGRESS TO DATE

PURIFICATION OF METALLURGICAL SILICON

- TECHNIQUES: Floating-zone and chemical treatment of melt
- RESULTS:

IMPURITY CONCENTRATION, PPM BY WEIGHT

	Metal. Silicon	2 Zone Passes	Cl_2 Treat.	Cl_2+O_2 Treat.	GeO_2-SiO_2 Treat.
Al	>>5,000	1-10	10-100	1-10	10-100
Fe	>>1,000	1-10	>>1000	>>1000	300-3000
B	10-100	10-100	1-10	1-10	1-10
V	100-1000	N. D.	10-100	30-300	10-100
Cu	10-100	<0.1	1-10	10-100	1-10
Ti	30-300	N. D.	10-100	30-300	10-100
Mn	30-300	N. D.	30-300	30-300	30-300
Mg	10-100	0.1-1	0.1-1	3-30	0.1-1
Cr	30-300	N. D.	1-10	10-100	1-10
Ni	10-100	N. D.	10-100	10-100	10-100

TLC; 13

POLYCRYSTALLINE SILICON SOLAR CELLS - PROGRESS TO DATE

SILICON SOLAR CELLS FROM TWO ZONE-PASS METALLURGICAL SILICON BY DIFFUSION

- Dark Characteristics

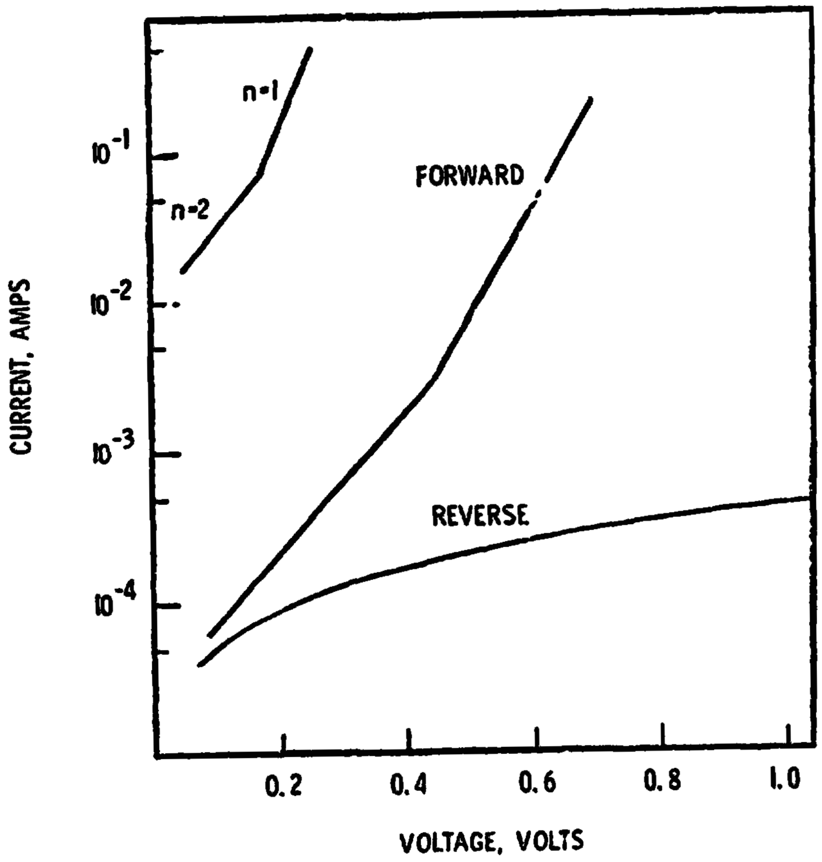

- Characteristics under Illumination at 135 mW/cm^2.

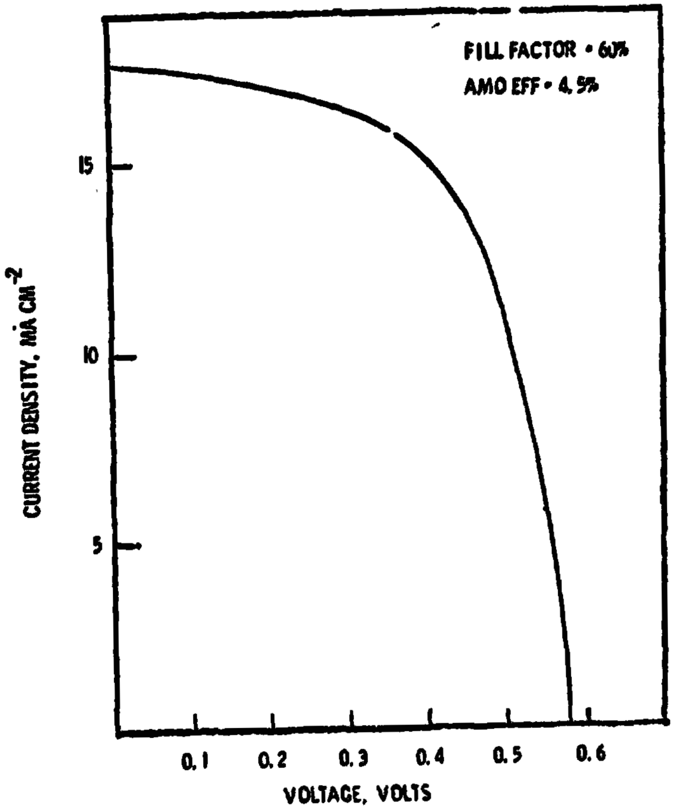

TLC; 14

POLYCRYSTALLINE SILICON SOLAR CELLS

SUMMARY OF KEY RESULTS

- Silicon deposited on carbon/graphite substrates is similar to silicon deposited on graphite substrates in structural and crystallographic properties and solar cell characteristics.
- A simple zone-melting technique has been developed to improve structural properties of silicon on graphite substrates. Solar cells with AMO efficiencies of up to 2.5% have been produced.
- Grain boundary effects in silicon on metallurgical silicon substrates can be reduced by doping. Silicon solar cells with AMO efficiencies up to 3.5% have been produced.
- Chemical treatment of the melt is effective in reducing the concentration of most metallic impurities, except iron, in metallurgical silicon.
- Zone-refining is effective in reducing the concentration of most impurities, except boron, in metallurgical silicon. Solar cells with AMO efficiencies higher than 4% have been produced.

TLC, 15

POLYCRYSTALLINE SILICON SOLAR CELLS

MAJOR PROBLEMS

- Silicon Solar Cells on Graphite
    - Non-reproducible structural properties of silicon
    - High series resistance of solar cells
- Silicon Solar Cells on Metallurgical Silicon
    - Casting of silicon substrates with large crystallites
    - Relatively high cost of casting
- Purification of Metallurgical Silicon
    - Removal of iron by chemical treatment
    - Relatively high cost of zone-refining

TLC; 16

POLYCRYSTALLINE SILICON SOLAR CELLS

PLANNED ACTIVITY FOR NEXT SIX MONTHS

- Further improvement in the recrystallization of silicon on graphite.
- Preparation of substrates from purified metallurgical silicon.
- Optimization of solar cell characteristics on graphite and metallurgical silicon substrates.
- Critical evaluation of the purification of metallurgical silicon by zone-refining.
- Characterization of metallurgical silicon purified by chemical treatment.

TLC; 17

GLASS-SI HETEROJUNCTION SOLAR CELLS

NSF GRANT AER74-17631

DEPARTMENT OF ELECTRICAL AND COMPUTER ENGINEERING
SYRACUSE UNIVERSITY
SYRACUSE, NEW YORK

INNOTECH CORPORATION
NORWALK, CONNECTICUT

PERIOD OF GRANT: 1 AUGUST 1974 - 31 JULY 1975

FUNDING FOR 1 AUGUST 1974 - 31 JULY 1975: $313,900

AUTHOR: R.W. AHRONS
INNOTECH CORPORATION

PRINCIPAL INVESTIGATOR:

R.L. ANDERSON
SYRACUSE UNIVERSITY

N76 12485

GLASS-Si HETEROJUNCTION SOLAR CELLS

The objective of this program is the development of a low temperature, low-cost process to combine a wide band gap top surface material with silicon to form a heterojunction solar cell. The top material, in addition to forming a junction, provides an optically transparent window, low resistance contact, and an optical match for low reflectivity. The requirements for an overall low-cost array require, in addition to a low-cost process, a low cost substrate material such as polycrystalline silicon.

Progress during this six month period is best indicated by the achievement of an increase in efficiency on polycrystal silicon from an initial 2% to over 7% (as measured both at INNOTECH and NASA-Lewis facilities). The cells were produced in the 2 cm by 2 cm and 1 cm by 1cm size, with top-side grid metallization. The polycrystalline silicon has crystal grains varying from 5μm to 5mm. The junction is an n+/n heterojunction between an SnO_2-based glass and the polycrystalline silicon. Voltages of up to 475mV were measured under open circuit conditions.

For single crystal substrates, efficiencies very close to 10% were measured. These cells had the same structure as the polycrystalline cells described above. Open-circuit voltages as high as 529mV were measured.

Short-circuit current density for single crystal approaches 30mA/cm^2 for the polycrystalline units; the short-circuit is about 90% of the short-current measured for the single crystal units. We believe this demonstrates the potential of solar cells using polycrystalline materials to achieve 90% of the efficiency of a non-textured single-crystal solar cell.

The cells are n+-type SnO_2 based glass on an n-type silicon forming an n+/n junction. Theoretical investigation of the current generation model and barrier layer model is underway. The built-in voltage and the resulting open-circuit voltage is process dependent.

Work on p+/n heterojunction using In_2O_3-based glass resulted in cells of 3% efficiency on polycrystalline material and 4% efficiency on single crystal material. Values of 337 mV were achieved for open-circuit voltage. This low voltage is the main limit for high efficiencies.

Work on other glass/silicon systems did not show appreciable promise. Cells with fine grain polycrystalline material had lower photocurrent than the polycrystalline material reported on above.

As the number of grain boundaries increases, further losses in current must be tolerated. The experiments were limited and information as to V_{OC} reduction due to reduction of effective lifetime with fine grain sizes could not be determined.

Initial work on spray coating of glass on silicon substrates showed very promising results. We believe this method can lead to a vacuum-free process.

The contract work for the next year will be focused towards achieving 10% efficiency on polycrystalline materials and 14% efficiency on single crystal cells. Further understanding of the n^+/n glass-Si heterojunction will be a prime effort. We are excited about this technology as representing a potentially lower cost, viable alternate to diffusion.

GLASS-SI HETEROJUNCTION SOLAR CELLS
NSF GRANT AER74-17631

DEPARTMENT OF ELECTRICAL AND COMPUTER ENGINEERING
SYRACUSE UNIVERSITY
SYRACUSE, NEW YORK

INNOTECH CORPORATION
NORWALK, CONNECTICUT

PERIOD OF GRANT: 1 AUG. 1974 - 31 JULY 1975

FUNDING FOR 1 AUG. 1974 - 31 JULY 1975: $313,900

PRINCIPAL INVESTIGATOR:

R.L. ANDERSON
SYRACUSE UNIVERSITY

OVERALL OBJECTIVES OF PROJECT

THE PURPOSE OF THIS PROJECT IS TO INVESTIGATE THE FEASIBILITY OF FABRICATING LOW-COST SOLAR CELLS SUITABLE FOR TERRESTRIAL APPLICATION. THESE CELLS CONSIST OF GLASS-SILICON HETEROJUNCTIONS. SPECIFIC GOALS INCLUDE THE PREPARATION AND CHARACTERIZATION OF GLASS-MONOCRYSTALLINE Si AND GLASS-POLYCRYSTALLINE Si HETEROJUNCTIONS, AND MODELING THESE DEVICES.

PLANNED ACTIVITY LAST 6 MONTHS

- DEVELOP PRELIMINARY THEORY OF HETEROJUNCTION SOLAR CELLS
- INCREASE OPEN CIRCUIT VOLTAGE ON EXISTING AND NEW GLASS/SILICON MATERIAL SYSTEMS
- PRODUCE LARGE SIZE CELLS ON VARIOUS SUBSTRATES
- DEVELOP PROCESSING TECHNIQUES
- INCREASE FILL FACTOR

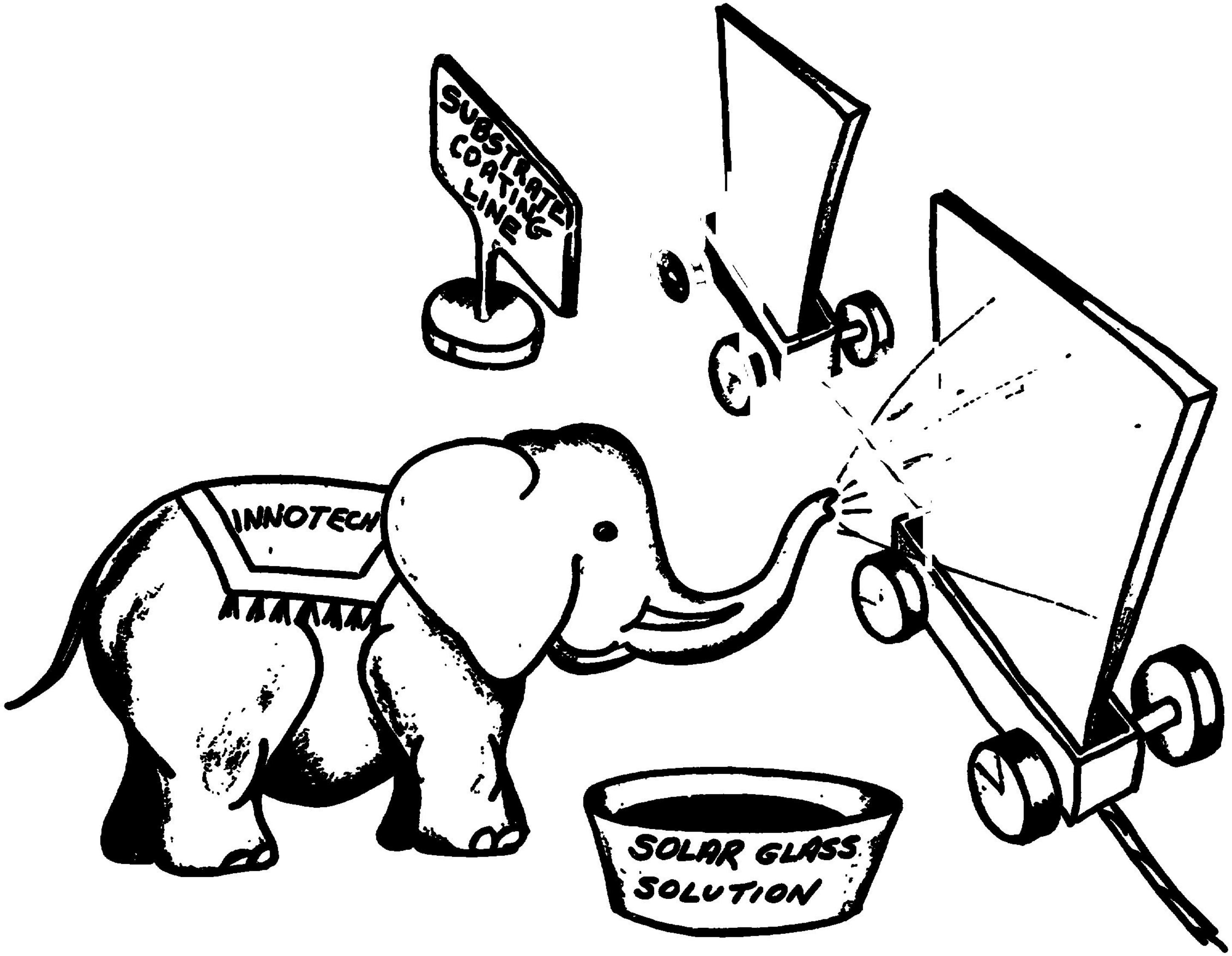

LOW COST SOLAR CELL PROCESSING LINE

PROJECT CONCEPTS

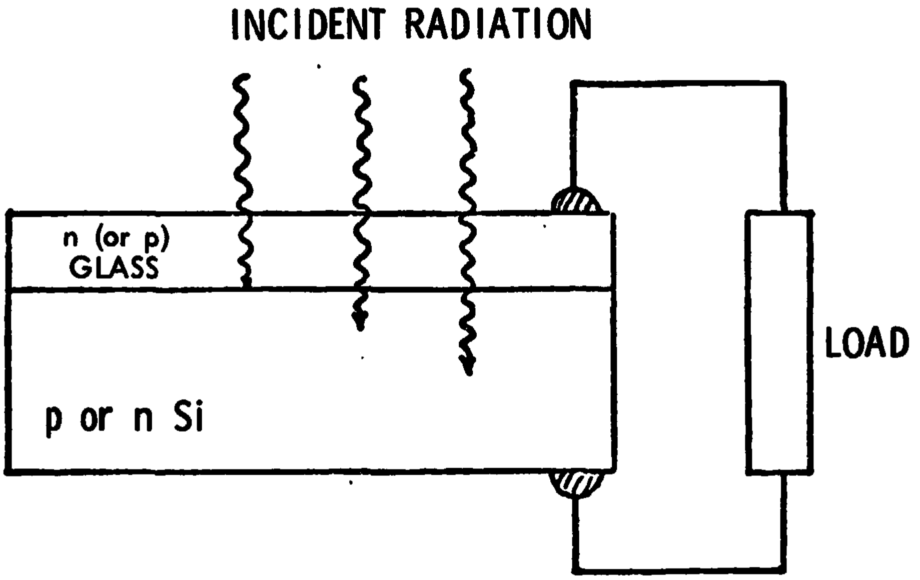

SCHEMATIC DIAGRAM OF GLASS-Si HETEROJUNCTION CELL

ADVANTAGES OF CELL

1. OPTICALLY TRANSPARENT WINDOW
2. LOW SERIES RESISTANCE
3. LOW REFLECTIVITY
4. LOW COST

BEST CELL RESULTS

Evap. $n^+ - SnO_2$ / n-Si CELL

@AM1 100 mW/cm²

AREA	Voc	Isc	FF	Eff.	Location
	mV	mA	%	%	
4cm²	468	106	56	[illegible].94	NASA
Polycrystal	466	109	55	7.0	INNOTECH
4cm²	523	117	[illegible]	9.41	NASA
Single Crystal	516	122	58	9.1	INNOTECH
1cm²	463	26	60	7.18	NASA
Polycrystal	470	32	53	8.0	INNOTECH
1cm²	521	29.4	64	9.54	NASA
Single Crystal	524	36	53	10.1	INNOTECH

CRYSTAL SIZE: 5 m – 5mm

PHOTOGRAPH OF
n – TYPE POLYCRYSTALLINE WAFER

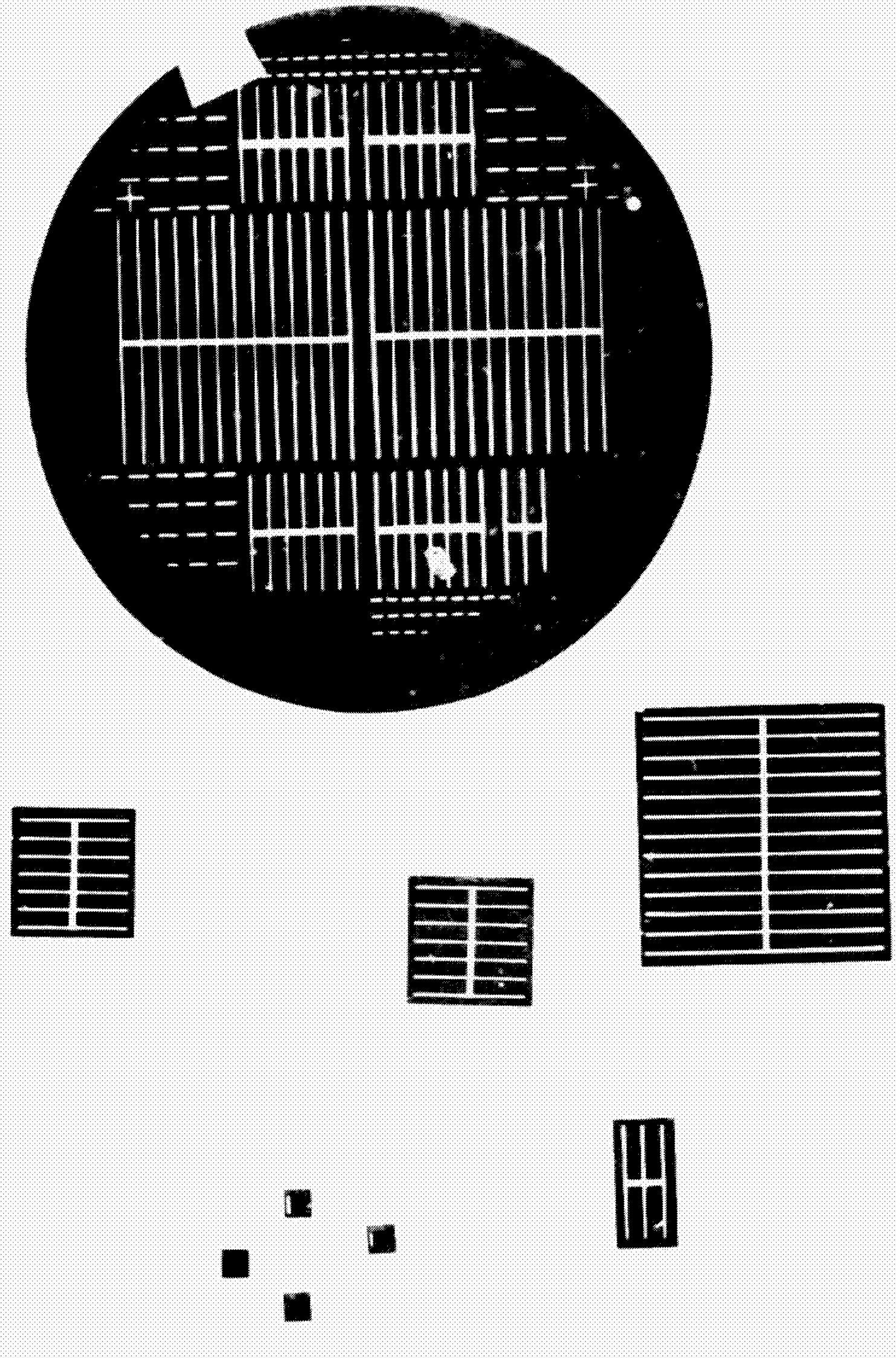

PHOTOGRAPH OF COMPLETED TEST WAFER AND SOLAR CELLS

DEVELOPMENT OF AN ECONOMICAL SILICON SOLAR CELL

GRANT No. GI-43091

18 MONTHS, INITIATED 1JUNE 1974

$114,100

PRINCIPAL INVESTIGATOR:

JOSEPH LINDMAYER

SOLAREX CORPORATION

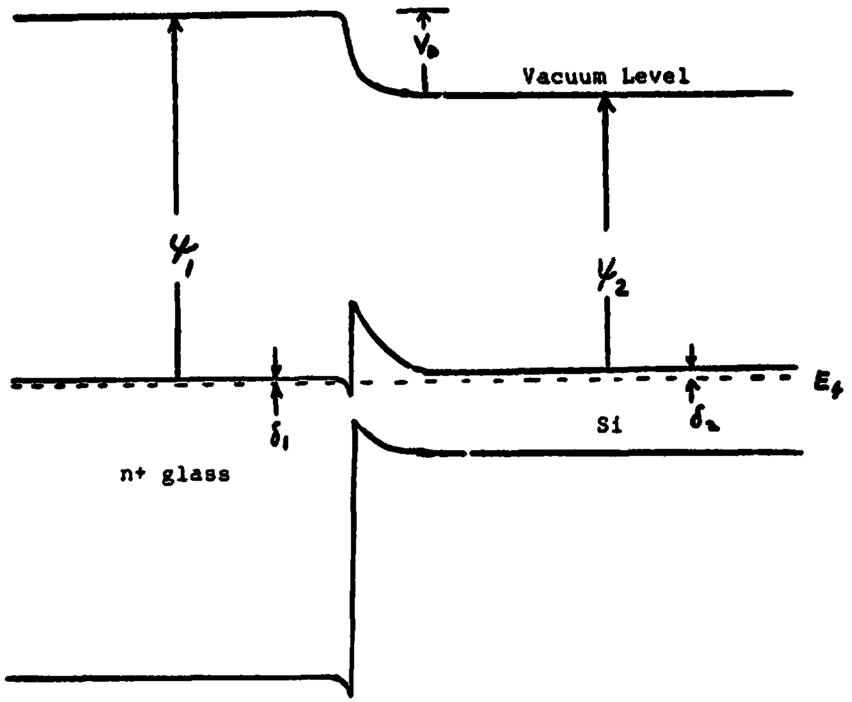

$$V_D = \psi_1 - \psi_2 + -\delta_2 + \delta_1$$

SIMPLIFIED ENERGY BAND DIAGRAM AND BARRIER VOLTAGE EQUATION FOR N+/N HETEROJUNCTION NEGLECTING SURFACE STATES AND SiO_2 BARRIER LAYER

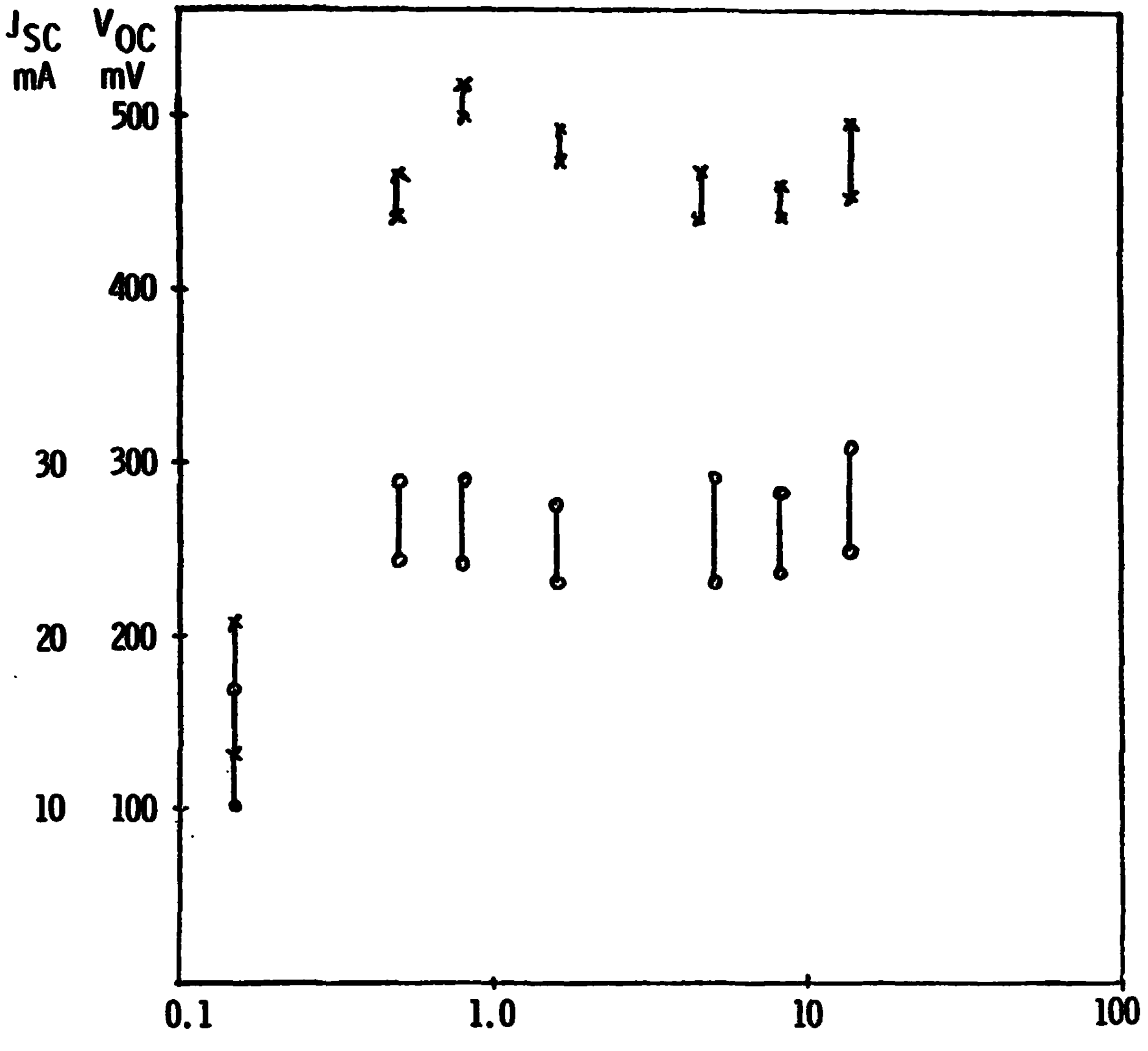

RESISTIVITY OF WAFER vs OPEN-CIRCUIT VOLTAGE AND SHORT-CIRCUIT CURRENT

BEST CELL RESULTS

SPRAY n^+ — SnO_2 / n -Si CELL

@AM 1 100 mW/cm^2

AREA	Voc	Isc	FF	Eff.	Location
	mV	mA	%	%	
4cm^2	4[illegible]	80.5	43	3.49	NASA
Polycrystal	405	83	44	3.7	INNOTECH
4cm^2	514	100.5	48	6.15	NASA
Single Crystal	486	105	46	5.9	INNOTECH
1cm^2	425	19	56	4.49	NASA
Polycrystal	436	23	52	5.2	INNOTECH
1cm^2	468	25.5	54	6.39	NASA
Single Crystal	477	32	45	6.9	INNOTECH

BEST CELL RESULTS

Evap. n^+ — In_2O_3 /p -Si CELL

@AM 1 100 mW/cm²

AREA	Voc	Isc	FF	Eff.	Location
	mV	mA	%	%	
4cm²	337	96	38	3.32	NASA
Polycrystal	332	100	33	2.8	INNOTECH
4cm²	317	95	54	4.09	NASA
Single Crystal	315	100	53	4.4	INNOTECH
1cm²	359	23.1	56	4.61	NASA
Polycrystal	340	2.9	51	5.0	INNOTECH
1cm²	343	24 9	57	4.9	NASA
Single Crystal	322	30	50	5.0	INNOTECH

CRYSTAL SIZE: 5 μm – 5 mm

PHOTOGRAPH OF p-TYPE POLYCRYSTALLINE WAFER

OTHER SILICON SUBSTRATES

- EPI POLYCRYSTALLINE (PROF. CHU-SMU)
  - POOR INNOTECH RUN FOR V_{OC}
  - PHOTOCURRENT - 20mA/cm^2 - ABOUT 2/3 OF SINGLE CRYSTAL IN RUN
- EPI POLYCRYSTALLINE ON SILICON (EPI REACTOR)
  - PHOTOCURRENT - 15 mA/cm^2 - ABOUT 1/2 OF SINGLE CRYSTAL IN RUN
- VACUUM DEPOSITED POLYCRYSTALLINE ON GLASS AND METAL (PROF. FANG - BC)
  - SHORTED THROUGH TO SUBSTRATE
- RIBBON
  - N+ In_2O_3/p Si - GOOD AS SINGLE CRYSTAL - FIRST GROUP
  - N+ In_2O_3/p Si - HIGH LEAKAGE - SECOND GROUP
  - N+ SnO_2/n Si - POOR V_{OC} I_{SC} AND FF

OTHER GLASSES

- V_2O_5
- $.5V_2O_5.\ .5P_2O_5$
- $.85V_2O_5.\ .15P_2O_5$
- CABAL GLASSES
- $2Sb_2O_3.SnO_2$
- TiO_2
- Cd_2SnO_4 (G. HAACKE - AMERICAN CYANAMID)

HETEROFACE CELLS

$N^+In_2O_3/N^+Si/pSi$

- EFFICIENCY 10%
- LOW PRIORITY PROGRAM

SUMMARY OF KEY RESULTS

- 7% EFFICIENCY USING POLYCRYSTALLINE MATERIAL WITH 1 CM^2 AND 4 CM^2 SOLAR CELLS
- 10% EFFICIENCY USING SINGLE CRYSTAL
- BEST RESULTS ON N+/N JUNCTIONS WITH $\mathrm{SnO_2}$ BASED GLASS
- GOOD REPRODUCIBILITY
- SPRAYED GLASS HETEROJUNCTION SHOWS PROMISING INITIAL RESULTS FOR A VACUUM-FREE PROCESS

MAJOR PROBLEMS

TECHNICAL

- UNDERSTANDING EFFECT OF SURFACE STATES AND SiO_2 BARRIER ON V_{OC} AND V_D
- EFFECT OF VARIOUS PROCESSING PARAMETER ON V_{OC} AND V_D
- INCREASE OF V_{OC}
- SUPPLY OF POLYCRYSTALLINE MATERIAL

COST

- FUNDS EXHAUSTED - NEED CONTINUING SUPPORT EFFECTIVE 1 AUGUST

PLANNED ACTIVITY FOR NEXT 12 MONTHS

- DEVELOP BETTER THEORETICAL UNDERSTANDING OF THE GLASS/SI INTERFACE TO ACHIEVE HIGHER V_{OC}

- INCREASE EFFICIENCY
  - HIGHER V_{OC}
  - HIGHER I_{SC}
    - TEXTURE ON SINGLE CRYSTAL
  - HIGHER FILL FACTOR
    - BETTER CONTACT
    - LOWER SHEET RESISTANCE
    - IMPROVE GRID STRUCTURE

- PRODUCE LARGER (> 4 cm^2) POLYCRYSTALLINE AND SINGLE CRYSTAL CELLS

- DEVELOP VACUUM FREE PROCESSING
  - SPRAY GLASS AND OTHERS
  - METALLIZATIONS

- INVESTIGATE OTHER GLASSES

- IMPROVE TEST SETUP - CORRELATE TO ERDA APPROVED TEST LOCATIONS

PLANNED RENEWAL REQUESTS

MAJOR GOAL - 12 MONTHS

- 10% EFFICIENCY ON POLYCRYSTALLINE SILICON
- 14% EFFICIENCY ON SINGLE CRYSTAL SILICON
- HIGH REPRODUCIBILITY
- BETTER JUNCTION UNDERSTANDING
- VACUUM FREE PROCESSING

DATES

1 AUGUST 1975 TO 31 JULY 1975

ESTIMATED COSTS

$449,000 (INNOTECH AND MIT)

N76 12486

DEVELOPMENT OF AN ECONOMICAL SILICON SOLAR CELL

Grant No. GI-43091
18 Months
Initiated 1 June 1974
$114,100

Principal Investigator:
Dr. Joseph Lindmayer
SOLAREX CORPORATION
1335 Piccard Drive
Rockville, Maryland

Presented At:
National Solar Photovoltaic Program Review Meeting
Los Angeles, California
July 22-25, 1975

ABSTRACT

The purpose of this project is to investigate a method of growing electronically viable silicon films on inexpensive foreign substrates, with the objective of creating a technology to radically reduce the overall cost of the silicon employed in photovoltaic solar energy conversion.

The approach employed is to enhance crystalline ordering during film nucleation by confining arriving silicon atoms to a narrow band traveling across a substrate, i.e., the Lateral Growth Technique (LGT). The efforts have employed physical vapor deposition of silicon in a vacuum evaporator on glass and metal substrates with both slit masks and single defining edges, and subsequent chemical vapor deposition (CVD) of thicker films on these thin film structures by pyrolysis of silane at higher temperatures. Efforts will continue on optimizing grain size and film-substrate compatibility for utilization of relatively conventional solar cell processing techniques and temperatures.

The key results to date are: improved ordering with LGT, even using single-edge masking of the silicon flux and reasonable growth rates with the LGT-CVD combination.

OBJECTIVES

ELECTRONICALLY VIABLE SILICON ON DISORDERED SUBSTRATES

- MINIMUM SILICON USAGE
- INEXPENSIVE SUBSTRATE
- CONTINUOUS OPERATION POSSIBILITIES

APPROACH

LATERAL GROWTH TECHNIQUE (LGT) FOR ORDERING

COMBINE LGT & CHEMICAL VAPOR DEPOSITION (CVD) FOR THICKNESS

METAL SUBSTRATE FOR BACK CONTACT

LAST 6 MONTHS ACTIVITY

LGT DEPOSITIONS ON VARIOUS SUBSTRATES & COATINGS

DEPOSITION RATE INVESTIGATIONS

DEPOSITIONS WITH SLITS & SINGLE EDGES

CVD APPARATUS INSTALLATION

COMBINED LGT - CVD DEPOSITIONS

LGT SILICON COST POTENTIAL

PRESENT CZOCHRALSKI : 250 MICRON THICK--$25/SQ.FT. ($270/SQ.M.)

LGT-CVD

CLAD SUBSTRATE---------------------15¢/SQ.FT.
LGT SOURCE, POLY-Si---------------- 5¢/SQ.FT.
TRICHLOROSILANE FOR 50 MICRONS-----50¢/SQ.FT.
TOTAL--------70¢/SQ.FT. ($7.50/SQ.M.)

LGT SILICON TIMETABLE

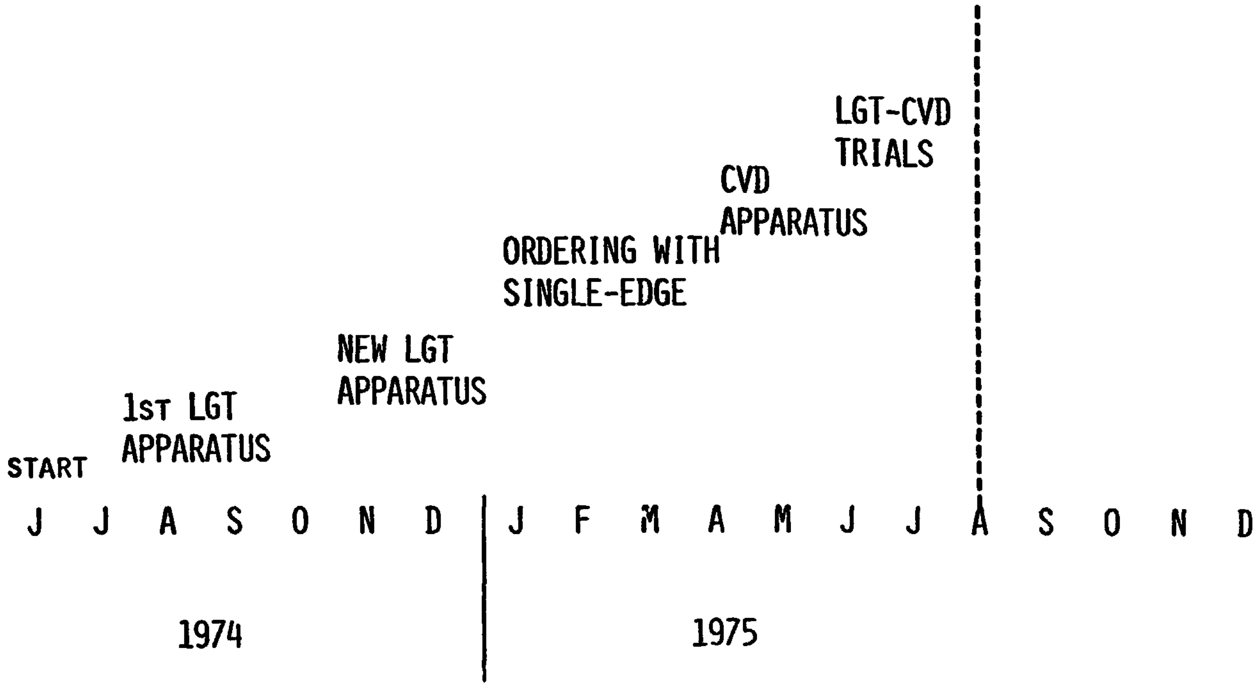

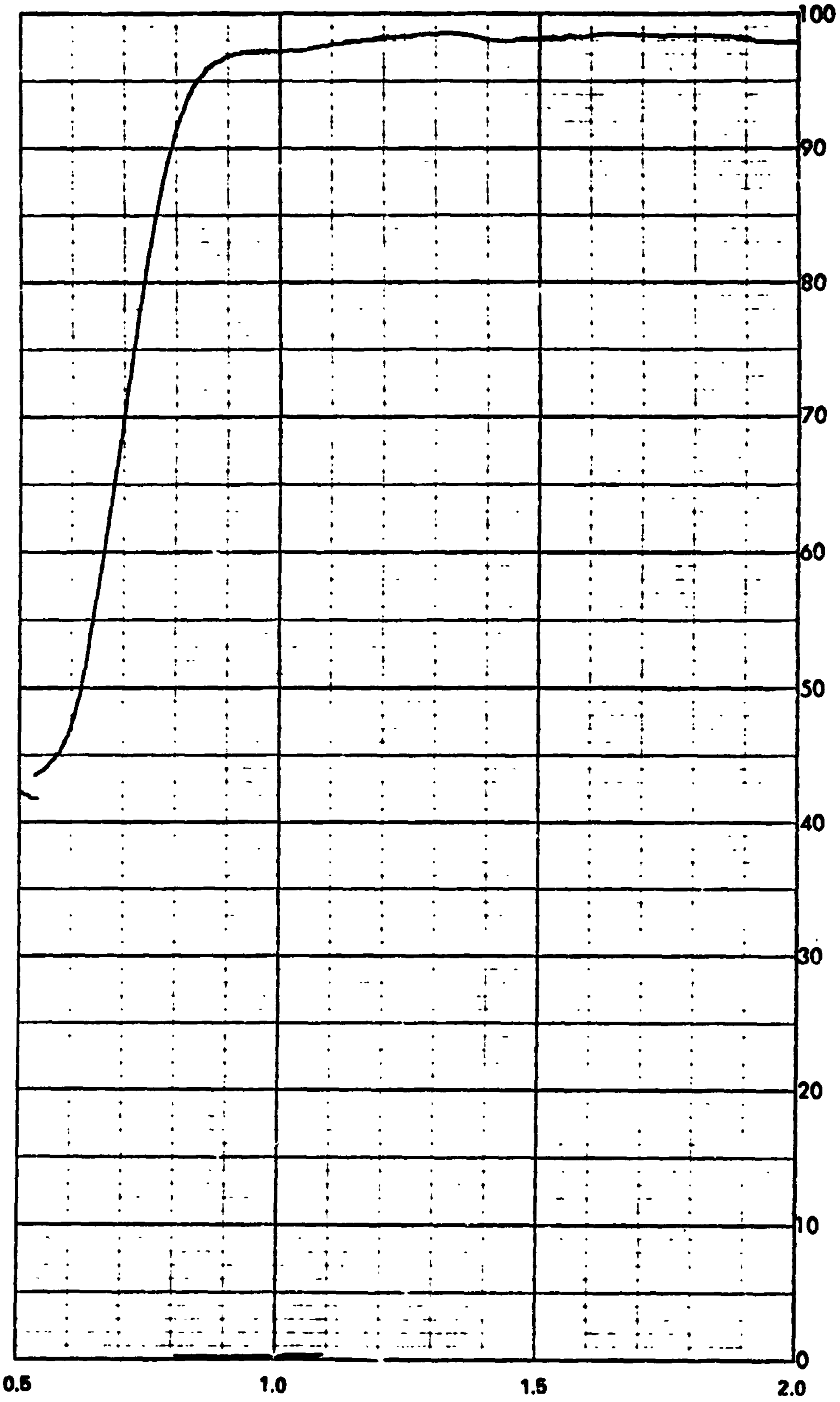

Single edge with slower travel and lowered deposition ra'.e.

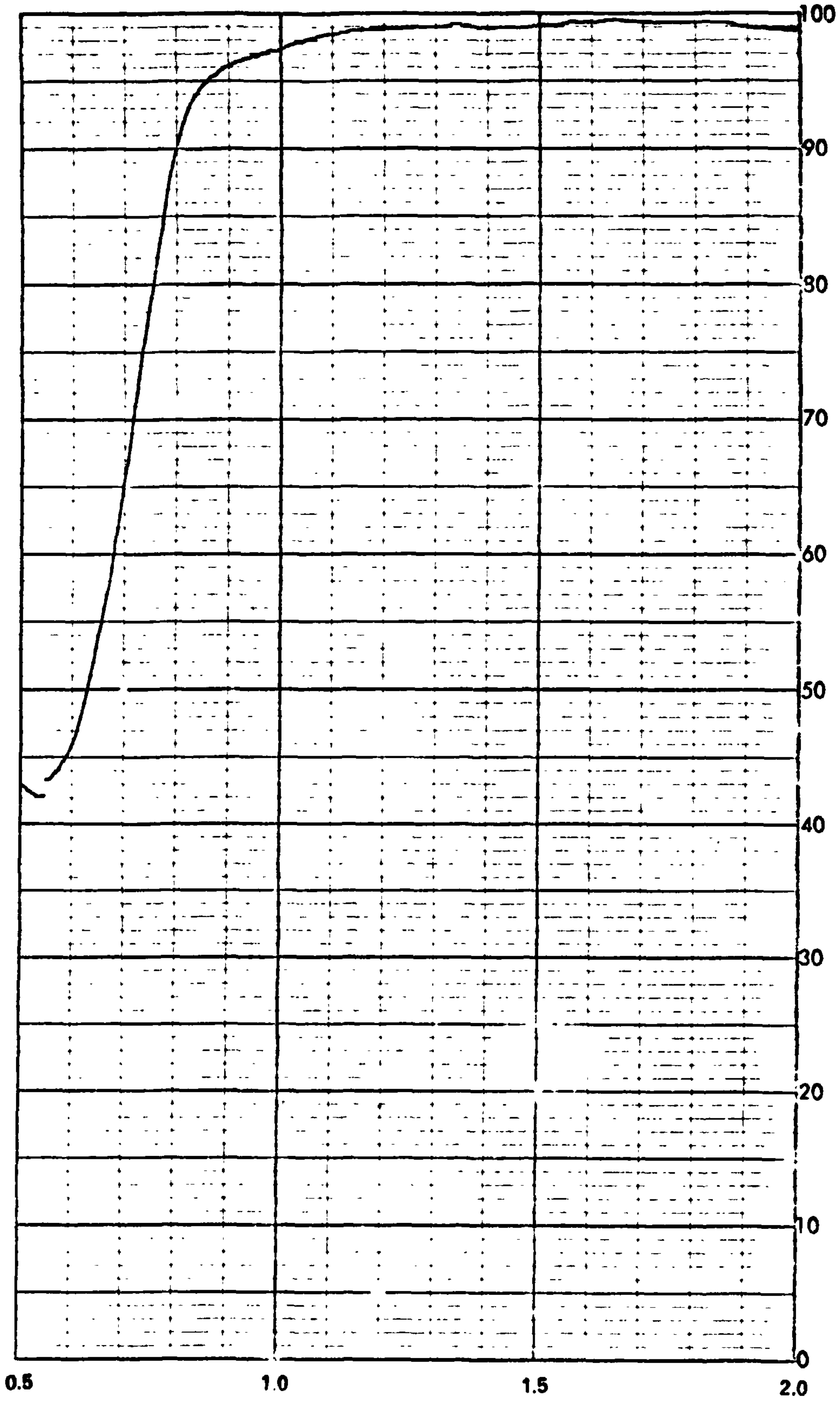

Slit deposition with slower substrate travel.

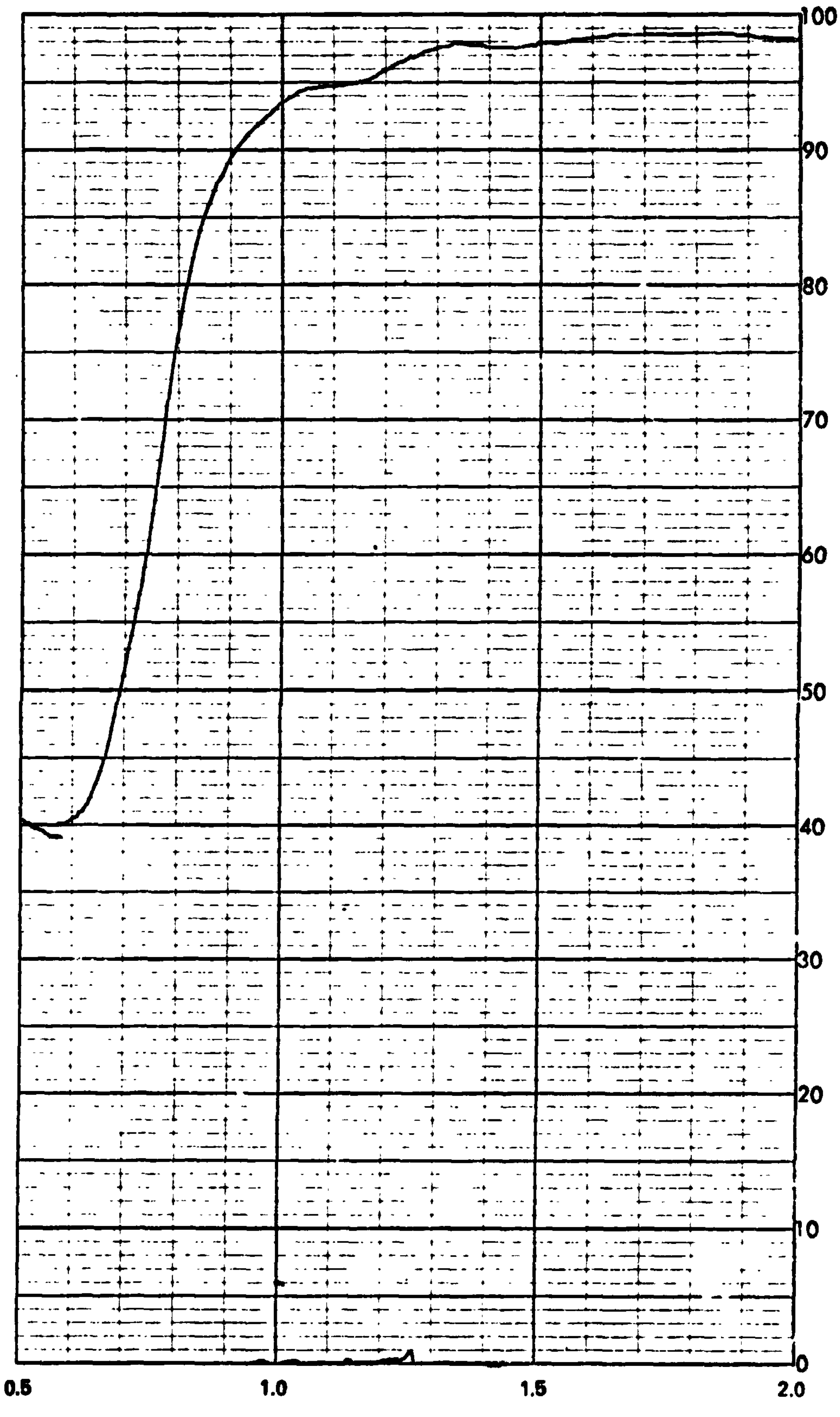

Optical reflection + transmission for LGT silicon film deposited through a slit onto glass.

Slit Deposition

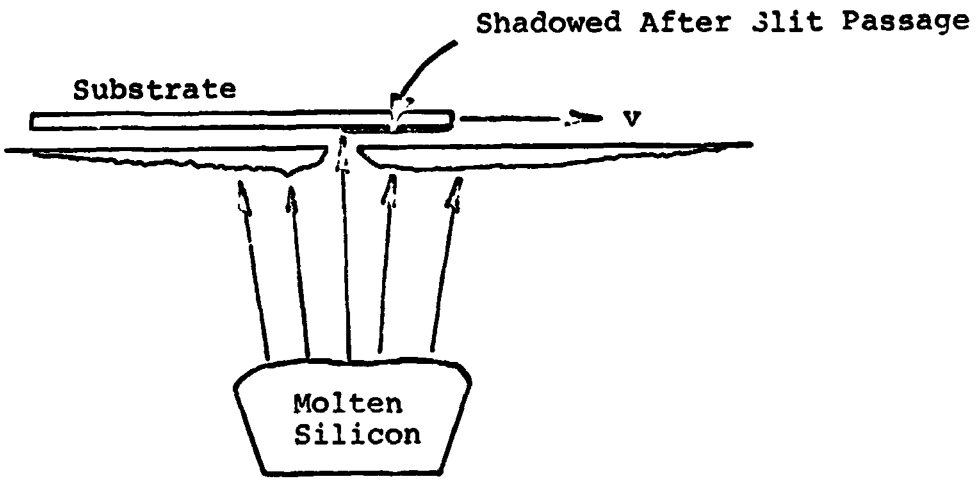

Single-Edge Deposition

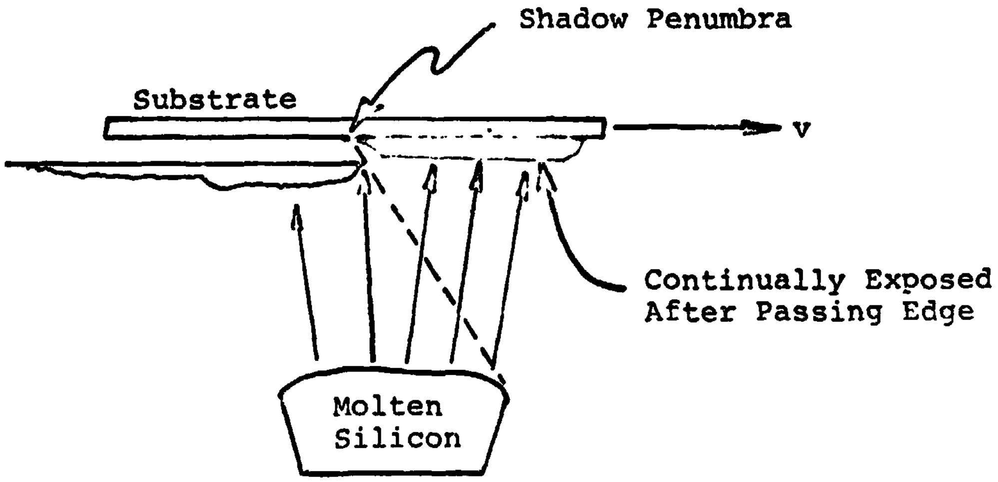

Comparison of Slit and Single-Edge LGT Deposition

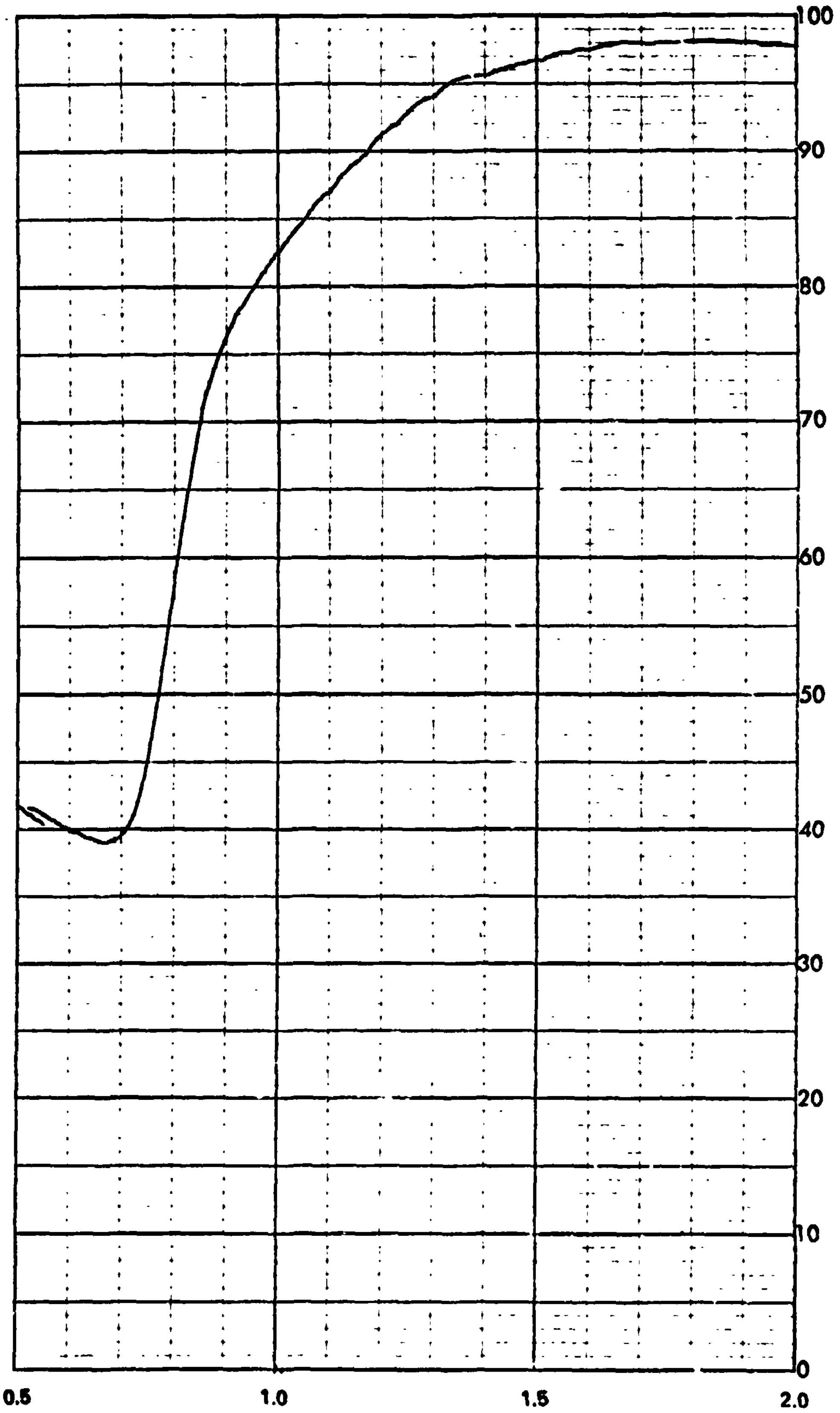

Optical reflection + transmission for fast-deposition with a single-edge mask.

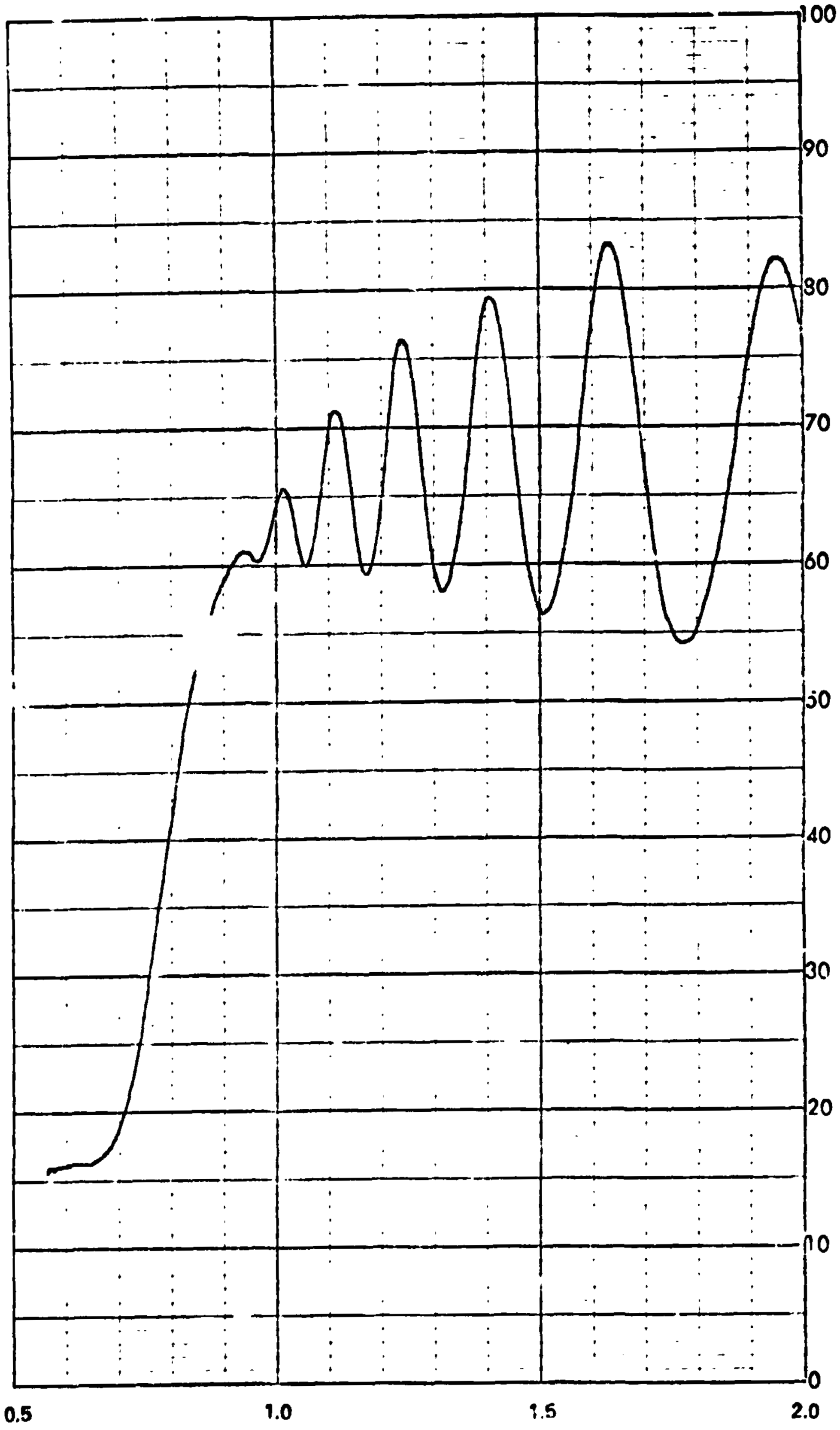

Equal Chromatic Order interference in infra-red transmission of an LGT film.

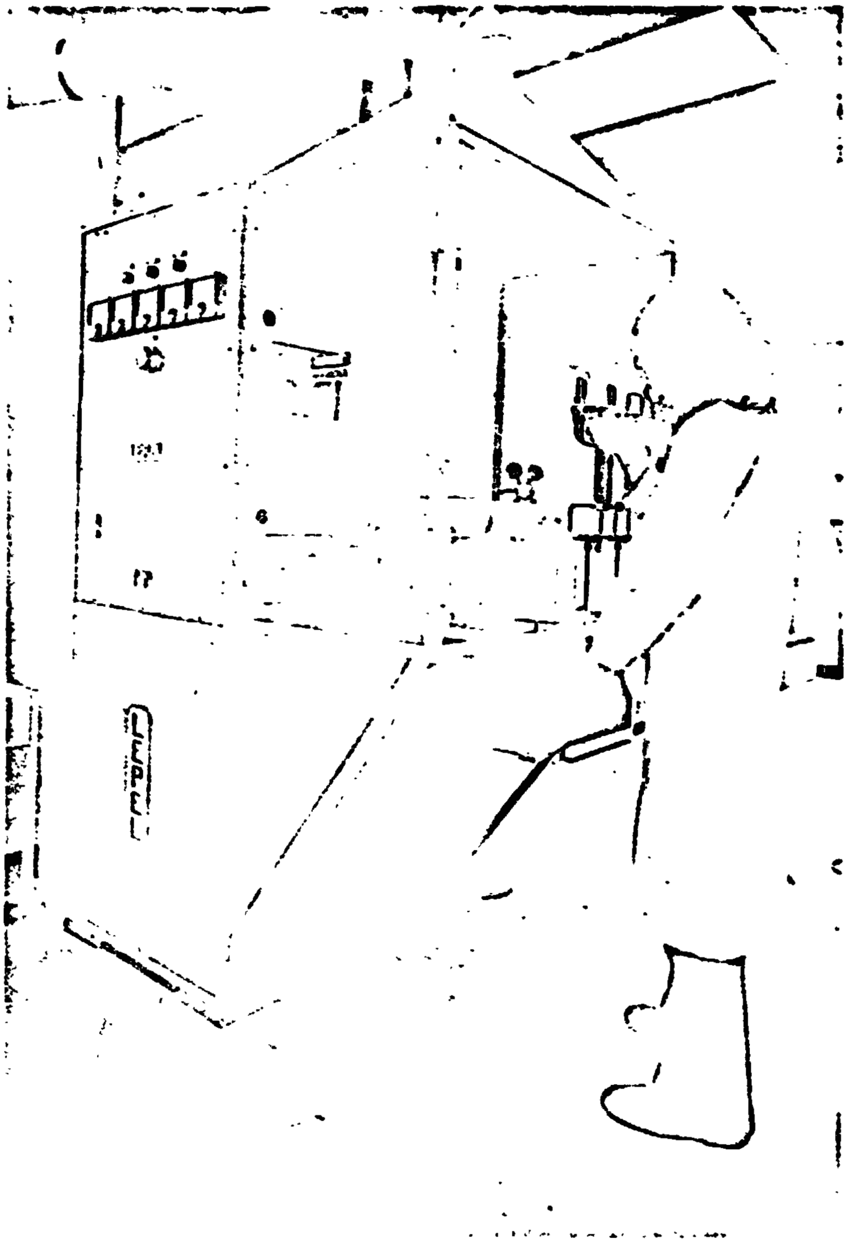

Chemical vapor deposition system for silicon.

c - 5

SUMMARY OF KEY RESULTS

IMPROVED ORDER WITH LGT, EVEN USING SINGLE EDGE

REASONABLE GROWTH RATES

COMBINED LGT - CVD STARTED

PLANNED ACTIVITY FOR NEXT 6 MONTHS

- IMPROVE SUBSTRATE COATINGS
  - NON-REACTIVE OR SLOW REACTION WITH SILICON
  - ADHESIVE TO 1000°C

- COMBINED LGT-CVD DEPOSITIONS
- INCREASE GRAIN SIZE

TITLE

Epitaxial Technology for Low Cost Solar Cells

GRANT

AER 74-15532
(April 1, 1975 - March 31, 1976)
$160,000

CONTRIBUTORS

H. Kressel, R. V. D'Aiello, and P. H. Robinson
RCA Laboratories
Princeton, New Jersey 08540

P. Raccah and F. Pollack
Yeshiva University
New York, New York 10033

PRINCIPAL INVESTIGATORS

H. Kressel
(Program Supervisor)
RCA Laboratories
Princeton, New Jersey 08540

P. Raccah
Yeshiva University
New York, New York 10033

Objective: Study of epitaxial solar cell structures on low cost silicon substrates as a means of improving the cell performance compared to direct diffusion into such substrates, and thus allow a wider use of these low cost materials to obtain useful solar cells. The primary emphasis is presently on the use of EFG ribbon material.

Results: Data obtained during the first three months of this grant are reported. The work has included the following: (1) Comparative X-ray topograph of EFG ribbons (grown by Tyco-Mobil) and epitaxial layers deposited on these materials. (2) Study of diodes and solar cells fabricated by diffusion into the ribbon materials and epitaxially formed on the similar material. (3) Carrier concentration distribution studies of ribbon materials using electroreflectance data.

The major conclusions of the work to date are:

(1) The dislocation density in the epitaxial layers is significantly lower than that of the substrate material. As expected, of course, grain and twin boundaries propagate into the epitaxial layers.

(2) The saturation current density of the diodes epitaxially formed on the substrate is commonly 2-3 orders of magnitude lower than for the diodes formed by direct diffusion. However, large variations in EFG ribbon quality were observed, and it appears that the relative difference between the epitaxial and diffused diodes varies accordingly.

(3) The solar cells made epitaxially (particularly if a graded structure is used) are substantially better than those made by direct diffusion into similar material. The difference is observed both in higher I_{sc} and V_{oc}. (All measurements were made under atmospheric conditions using solar illumination for the most part.)

(4) The devices fabricated so far were intended only as comparative study vehicles rather than as state-of-the-art solar cells. Thus, none of the parameters were fully optimized.

The continuing phase of the program will focus on more detailed characterization, with emphasis on minority carrier lifetime, and local variations in device quality which is correlated with the substrate and epitaxial structure. Different structures and fabrication processes will be evaluated in order to optimize the cell parameters, for as wide a substrate quality range as possible.

TITLE : EPITAXIAL TECHNOLOGY FOR LOW COST SILICON SOLAR CELLS

GRANT #: AER 74-15532

RCA LABORATORIES, PRINCETON, N. J./YESHIVA UNIVERSITY

TOTAL GRANT : $160,000 (ONE-YEAR PROGRAM)

PRINCIPAL
INVESTIGATORS : H. KRESSEL/RCA LABORATORIES (PROGRAM SUPERVISOR)
P. RACCAH/YESHIVA UNIVERSITY

PROGRAM BEGAN ON: APRIL 1, 1975

PROGRAM OBJECTIVE

STUDY OF EPITAXIAL SOLAR CELL STRUCTURES ON LOW COST SILICON SUBSTRATES (EFG RIBBON) AS A MEANS OF IMPROVING THE CELL PERFORMANCE COMPARED TO DIRECT DIFFUSION AND THUS ALLOW A WIDER USE OF THE SUBSTRATES PREPARED TO OBTAIN USEFUL DEVICES.

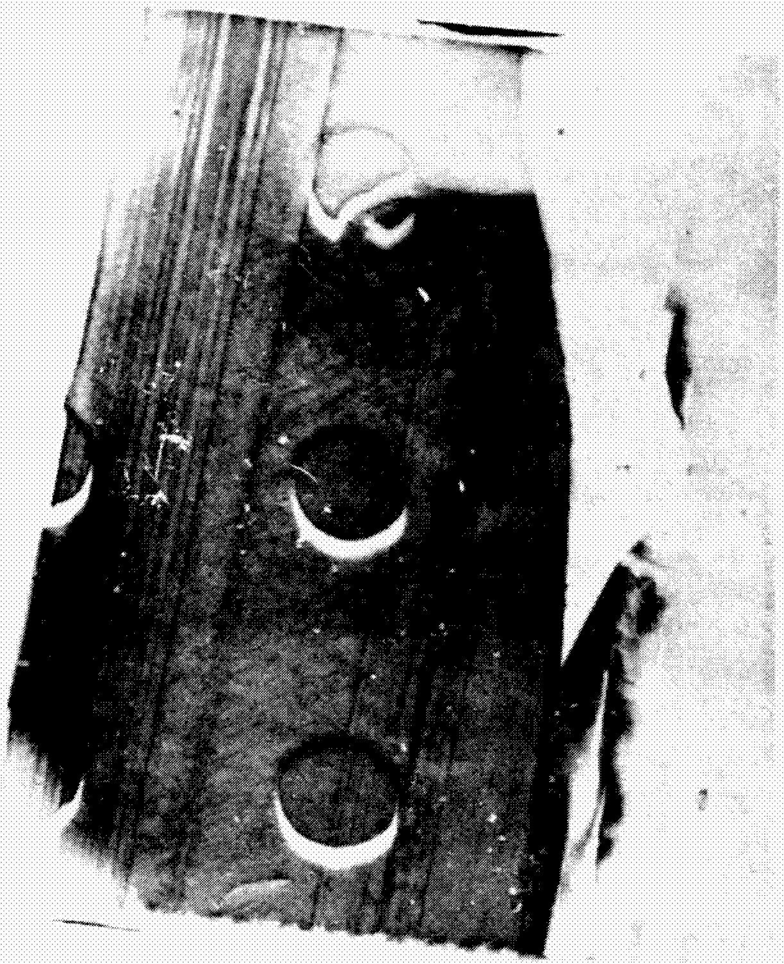

REFLECTION TOPOGRAPH (333)/Cu SHOWING THE REDUCED DEFECT STRUCTURE IN THE EPITAXIAL LAYER (MESAS) COMPARED TO THE ADJOINING EFG SUBSTRATE REGIONS

ORIGINAL PAGE IS
OF POOR QUALITY

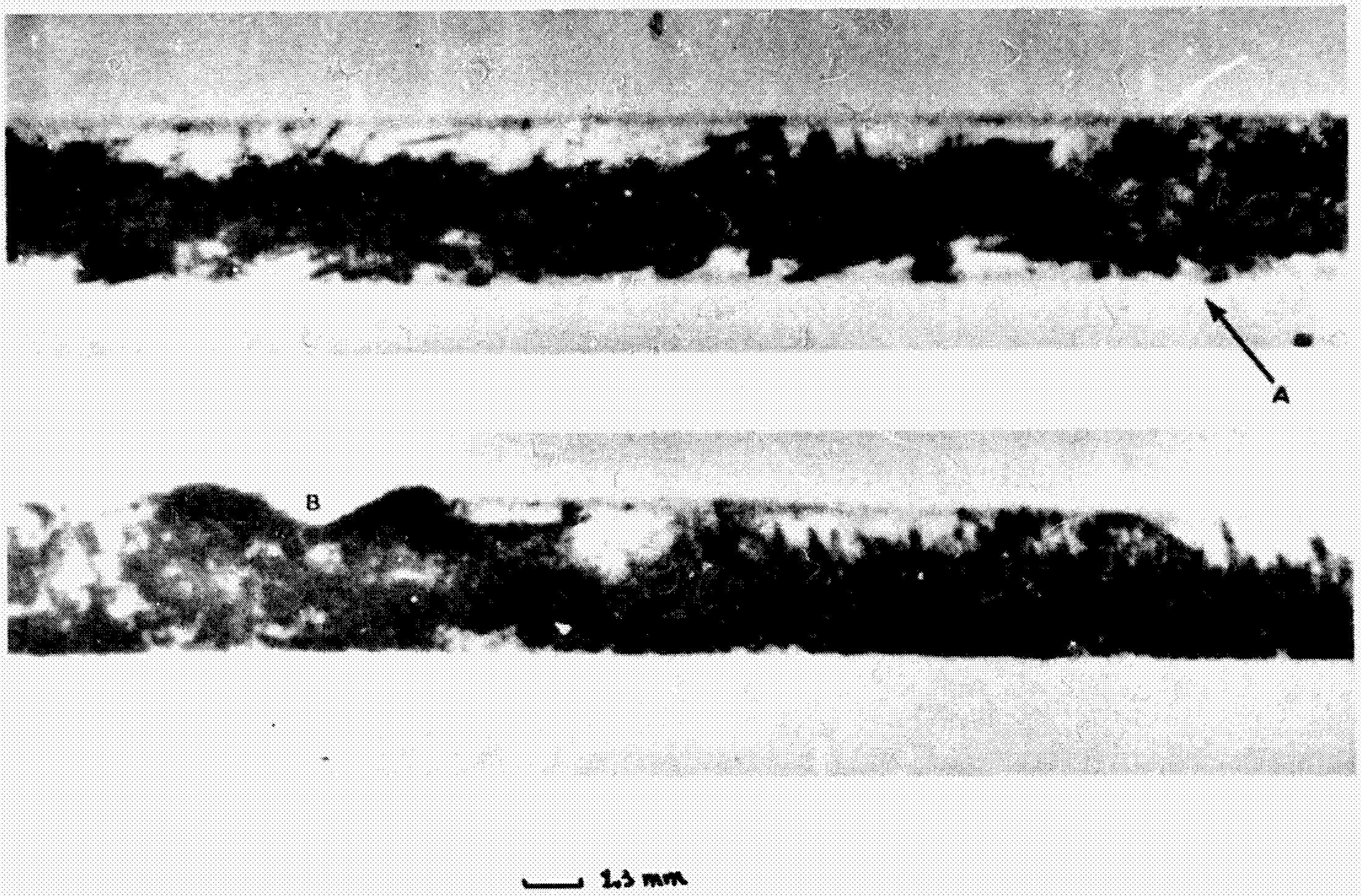

Section topographs showing cross-section defect distribution in silicon/silicon web. The layer is on top and is about 1/3 of the vertical dimension of the image. The high dislocation density in the substrate generally does not propagate into the layer. The twin boundary in the substrate and a growth pit are indicated at A and B, respectively.

ACTIVITY TO DATE

1. DEFECT ANALYSIS OF RIBBONS AND EPITAXIAL LAYERS TO ESTABLISH METALLURGICAL IMPROVEMENT DUE TO EPITAXY (X-RAY TOPOGRAPHY).

2. CELLS AND DIAGNOSTIC P-N JUNCTION STRUCTURES FABRICATED AND CHARACTERIZED.

3. ELECTROREFLECTANCE EQUIPMENT FOR HIGH RESOLUTION MAPPING OF CARRIERS CONCENTRATIONS COMPLETED. PRELIMINARY CORRELATION BETWEEN GROWTH MORPHOLOGY AND CARRIER CONCENTRATION VARIATION.

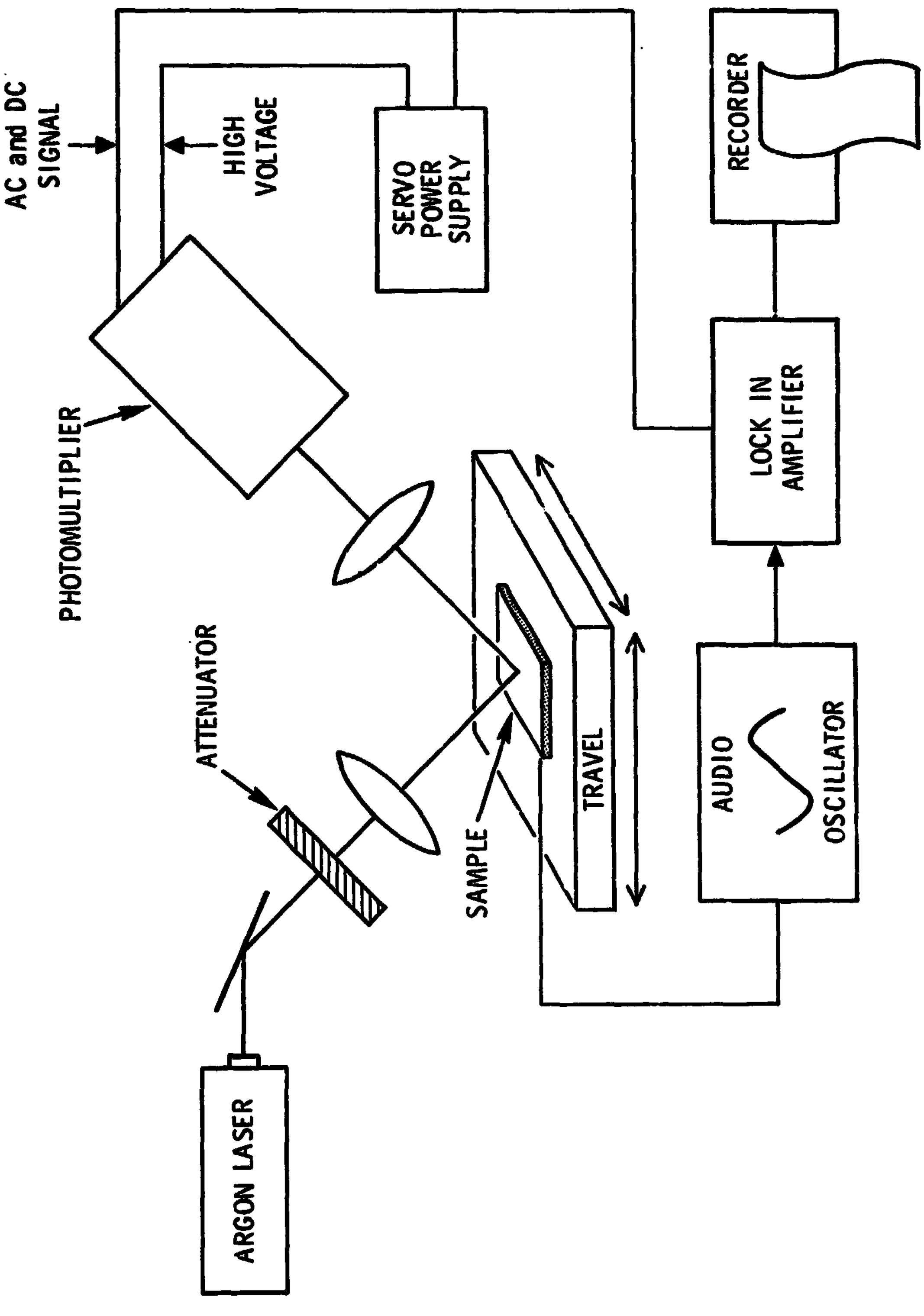
ARGON LASER
ATTENUATOR
SAMPLE
TRAVEL
PHOTOMULTIPLIER
AC and DC SIGNAL
HIGH VOLTAGE
SERVO POWER SUPPLY
AUDIO OSCILLATOR
LOCK IN AMPLIFIER
RECORDER

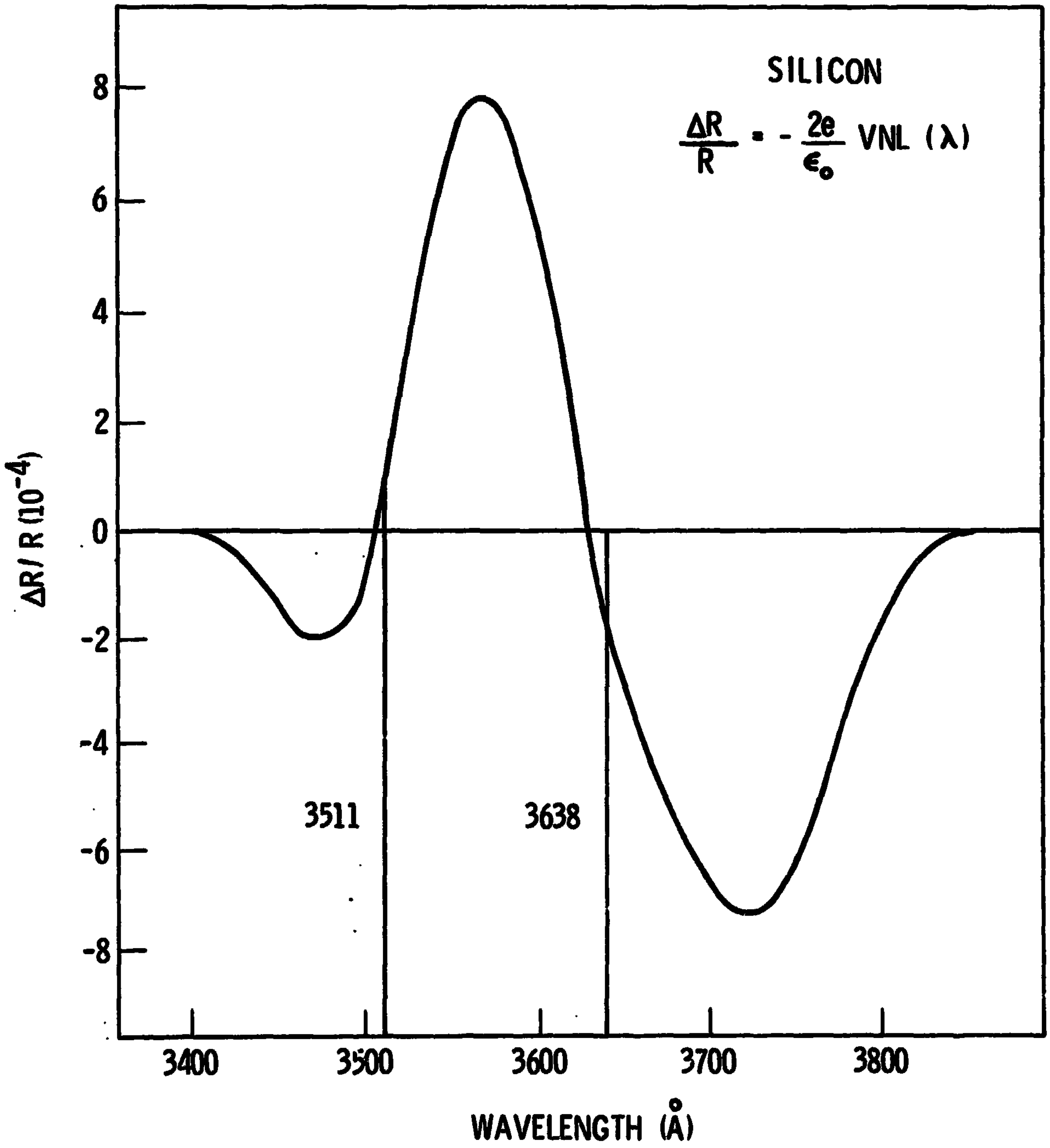
SILICON
$\frac{\Delta R}{R} = -\frac{2e}{\epsilon_0} VNL(\lambda)$
8
6
4
2
0
-2
-4
-6
-8
$\Delta R/R\ (10^{-4})$
3511
3638
3400
3500
3600
3700
3800
WAVELENGTH (Å)

TYR-2

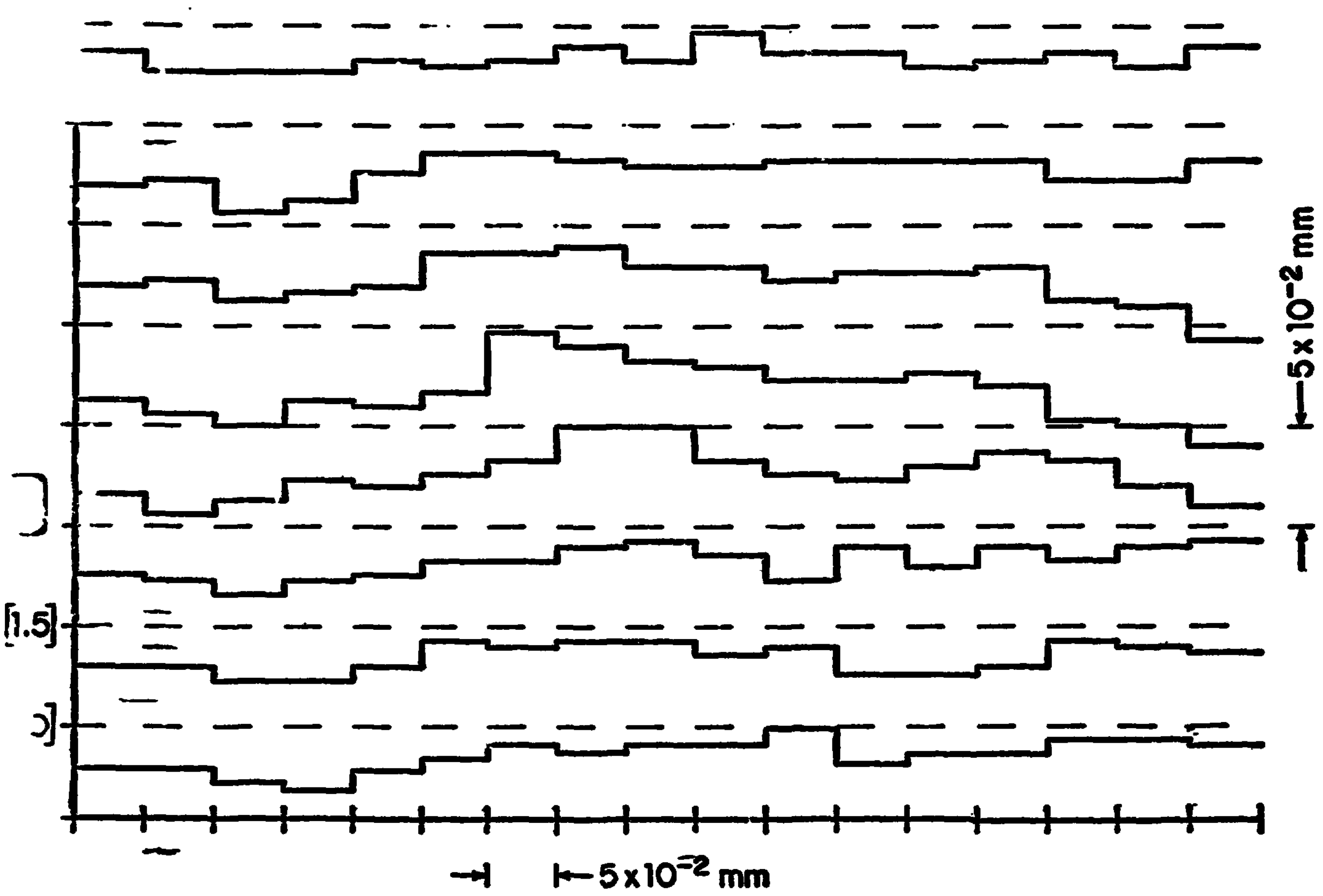

TABLE 1

EPITAXIAL DIODES

#	I_0 (V_a = -2 V), A/cm^3
A1	3.7×10^{-7}
B1	8.6×10^{-8}
C1	9.8×10^{-8}
D1	1.1×10^{-6}
A2	2.2×10^{-7}
B2	2.5×10^{-6}
C2	2.1×10^{-7}
D2	3.5×10^{-7}
A3	1.26×10^{-7}
B3	2.01×10^{-5}
C3	2.15×10^{-5}
D3	5.15×10^{-7}
A4	2.8×10^{-7}
B4	3.4×10^{-7}
C4	5.9×10^{-7}
D4	4.8×10^{-5}

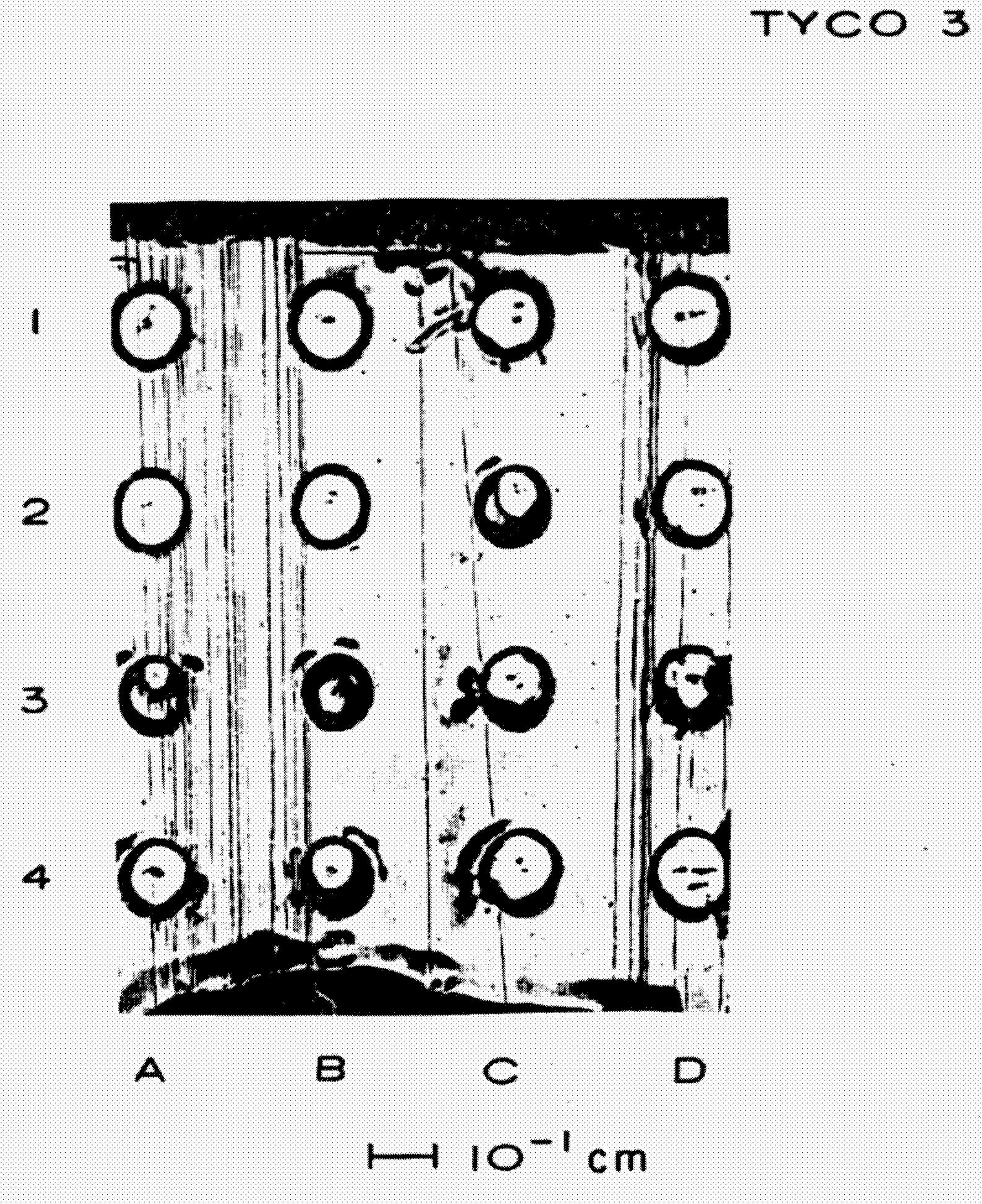

Figure 2 - Microphotograph of mesas etched out from epitaxial material deposited on ribbon substrate. The saturation current density for each of the diodes is given in Table 1.

TABLE 2

DIFFUSED DIODES

#	I_0 (V_a = -2 V), A/cm^2
A1	3.5×10^{-4}
B2	4.5×10^{-5}
B3	3.5×10^{-5}
C1	2.4×10^{-5}
C3	2.7×10^{-5}

STAINED JUNCTION CROSS SECTIONS

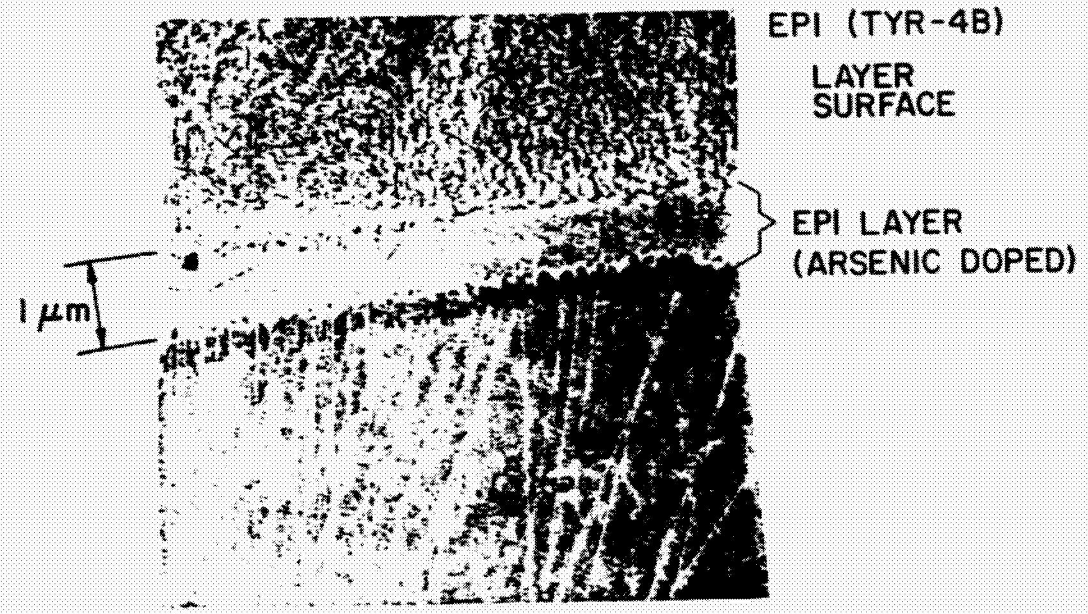

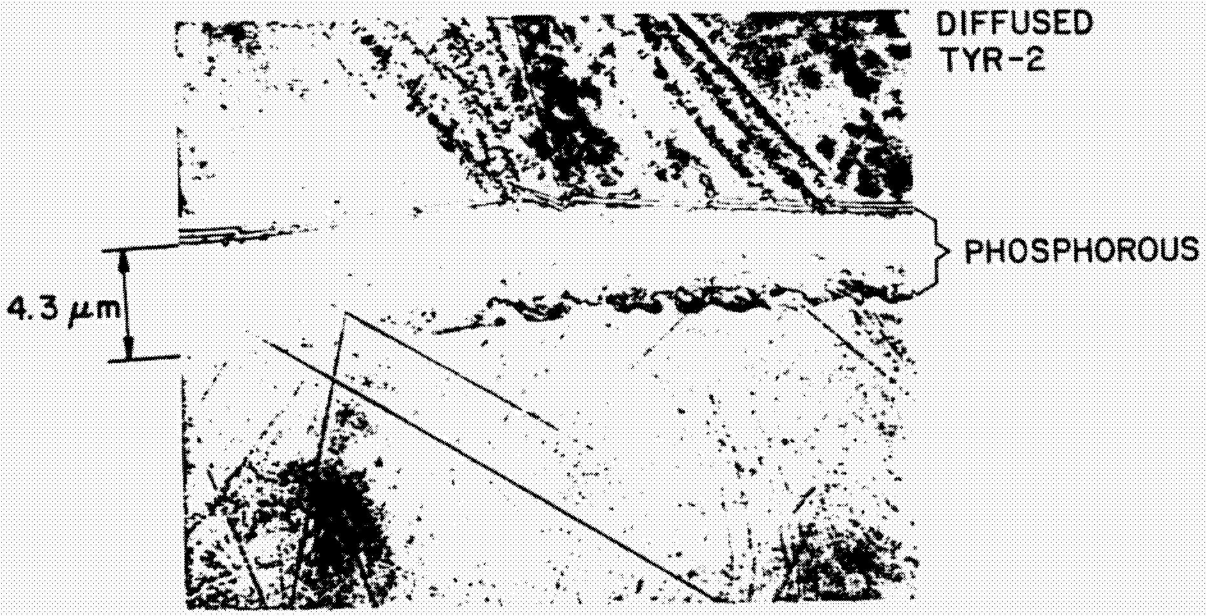

CORRELATION OF PHYSICAL APPEARANCE WITH CELL PERFORMANCE

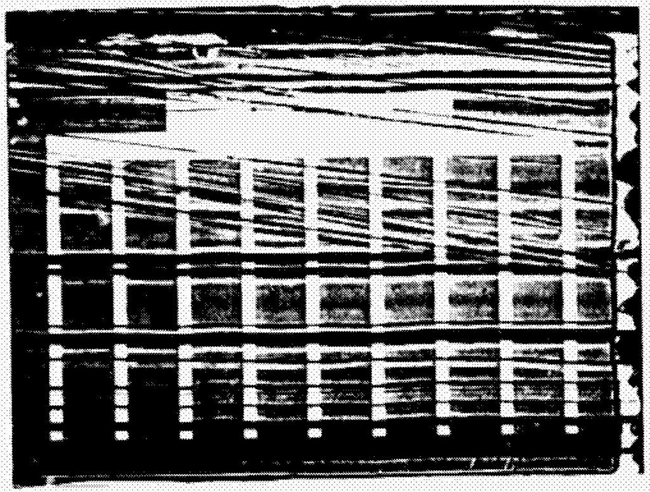

TYR-4A #1

$J_{SC} = 20.1\ mA/cm^2$
$V_{OC} = 539\ mV$

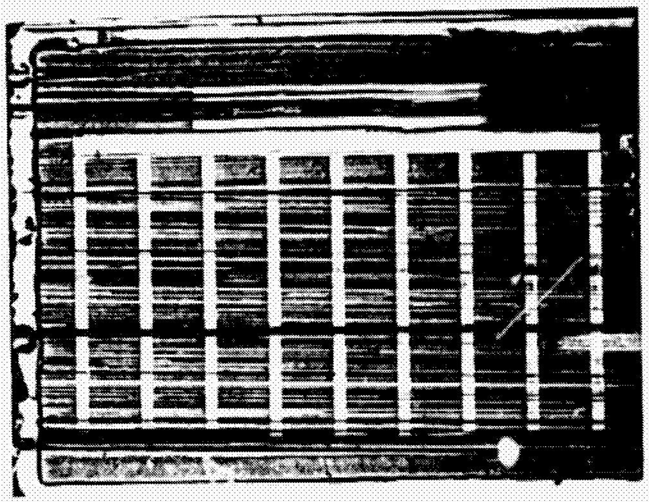

TYR-4A #2

$J_{SC} = 16.8\ mA/cm^2$
$V_{OC} = 477\ mV$

1 cm

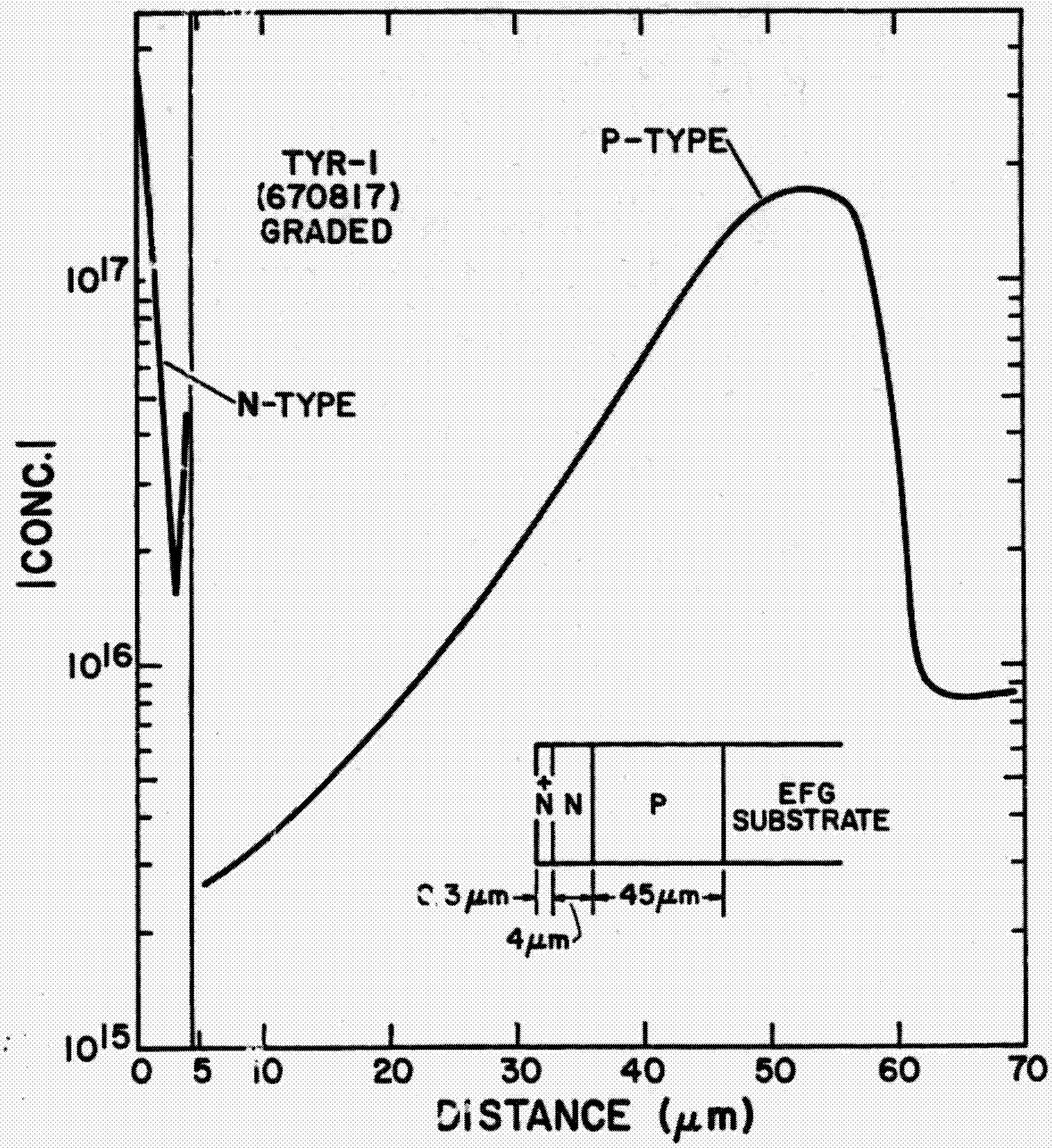
TYR-I
(670817)
GRADED
P-TYPE
N-TYPE
|CONC.|
10^{17}
10^{16}
10^{15}
0
5
10
20
30
40
50
60
70
DISTANCE (μm)
$\overset{+}{N}$
N
P
EFG SUBSTRATE
0.3μm
4μm
45μm

TEST PATTERN

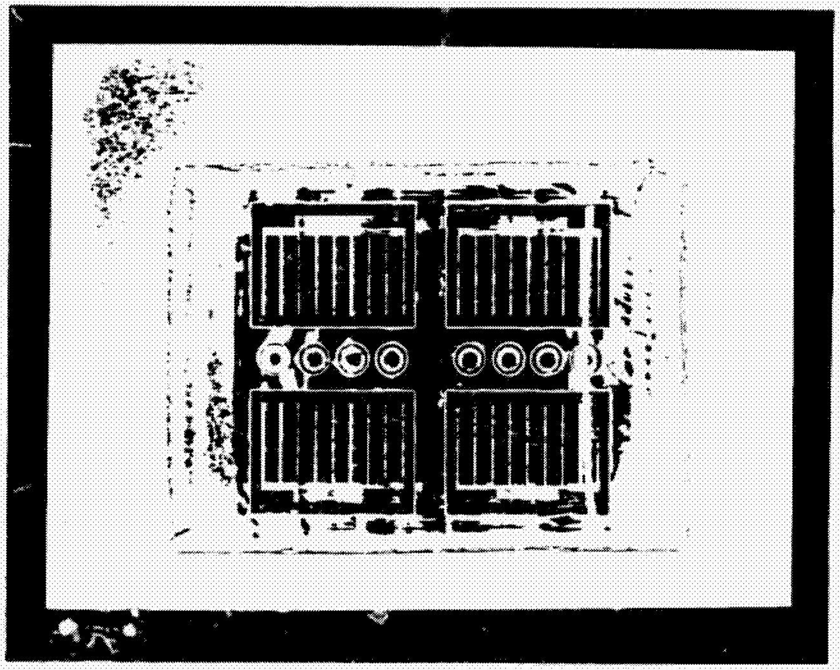

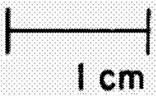

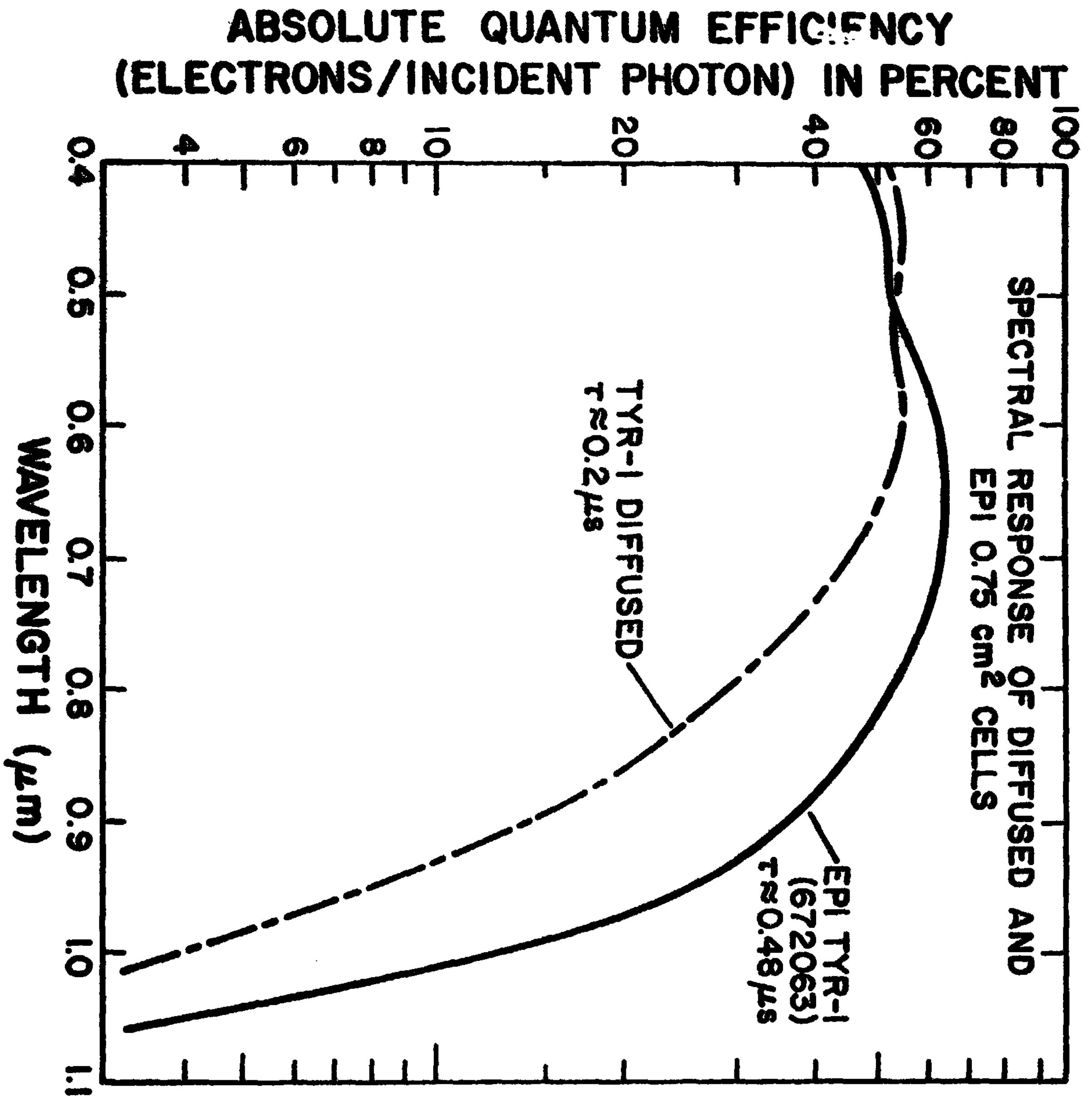
ABSOLUTE QUANTUM EFFICIENCY
(ELECTRONS/INCIDENT PHOTON) IN PERCENT
4
6
8
10
20
40
60
80
100
0.4
0.5
0.6
0.7
0.8
0.9
1.0
1.1
WAVELENGTH (μm)
SPECTRAL RESPONSE OF DIFFUSED AND EPI 0.75 cm² CELLS
TYR-1 DIFFUSED
τ≈0.2μs
EPI TYR-1
(672063)
τ≈0.48μs

COMPARATIVE SOLAR CELL DATA

Device Lot	Process		V_{oc} (mV)	J_{sc} (mA/cm^2)	Max. Power (mW/cm^2)	Fill Factor	Efficiency (%)	Solar Intensity (mW/cm^2)	A.R. Coating
NASA-A[(a)]	Diffused	n/p	545	27.6	10.8	0.72	11.6	93	Ta_2O_5
(TYR-1 (EFC))	Diffused	n/p	504	19.8	6	0.6	6.2	96	SiO_2
	Epi (graded)[(b)]	n/p	523	22.8	7.8	0.65	8.3	94.4	SiO_2
	Epi (uniform)[(c)]	n/p	542	19.2	6.24	0.60	6.6	94.4	SiO_2
(TYR-3 EFC)	Diffused	n/p	78	9	---	---	---	95	SiO_2
	Epi[(b)]	n/p	540	23.3	8.3	0.66	9	92	SiO_2
(TYR-4 EFC)	Epi[(b)]	n/p	539	20.1	4.4	0.41	4.8	91.7	SiO_2
	Epi[(b)]	n/p	477	16.8	---	low	---	91.7	SiO_2

(a) Cell provided by NASA with calibration under atmospheric conditions. It was used as a standard to establish the solar intensity.

(b) Graded impurity profile in p-region.

(c) Uniform impurity profile in p-region.

MAJOR CONCLUSIONS

- DISLOCATION DENSITY IN THE EPITAXIAL LAYER IS LOWER THAN IN THE EFG SUBSTRATE.
- THE SATURATION CURRENT DENSITY OF DIODES EPITAXIALLY FORMED ON THESE SUBSTRATES IS MUCH LOWER THAN OBTAINED BY DIRECT DIFFUSION INTO THE SUBSTRATES.
- THE I_{sc} AND V_{oc} AND EFFICIENCY OF EPITAXIAL SOLAR CELLS ARE GENERALLY HIGHER THAN THOSE MADE BY DIFFUSION INTO THE EFG MATERIAL.
- GOOD QUALITY SOLAR CELLS (∿ 9%) HAVE BEEN MADE EPITAXIALLY IN SOME EFG MATERIAL WHICH DOES NOT YIELD USEFUL DEVICES BY DIRECT DIFFUSION.
- A SENSITIVE ELECTROREFLECTANCE APPARATUS HAS BEEN CONSTRUCTED WHICH ALLOWS THE DIRECT DETERMINATION OF CARRIER CONCENTRATION VARIATIONS. SPATIAL VARIATIONS IN EFG MATERIALS MUCH GREATER THAN THOSE ENCOUNTERED IN CONVENTIONALLY-GROWN BULK Si HAVE BEEN DETECTED.

N76 12488

SHALLOW JUNCTION PHOTOVOLTAIC DEVICE PROGRAM

LAWRENCE LIVERMORE LABORATORY
LIVERMORE, CALIFORNIA

GRANT REQUESTED: ONE YEAR
$245,000

AUTHOR/PRINCIPAL INVESTIGATOR: R. WICHNER

NATIONAL SOLAR PHOTOVOLTAIC REVIEW MEETING
JULY 22-25, 1975
LOS ANGELES, CALIFORNIA

Abstract

SHALLOW JUNCTION SILICON SOLAR CELLS

R. Wichner
Lawrence Livermore Laboratory
Livermore, California

The objective of this program is to develop techniques to produce low cost, high efficiency solar cells, with emphasis on those processes which are applicable to the automated production of both single crystal and defect-laden ribbon or thin film polycrystalline solar cell material. Shallow junction devices are under primary consideration with several types of silicon solar cells having been fabricated, namely, a) epitaxially-grown shallow junction cells, b) Schottky-barrier cells, c) Indium-Tin-Oxide on silicon cells and d) cells produced by a unique process utilizing a corona discharge. Our results with this latter process are described below.

Initial results in producing single crystal silicon solar cells were reported at the Eleventh Photovoltaics Specialist Conference, May, 1975, in Phoenix, Arizona. Cells with efficiencies of over 8% with fill factors of up to 0.76 were reported. These shallow junction cells had enhanced short wavelength response as compared to commercial, deeper junction cells.

Recent work has included the fabrication of polycrystalline silicon cells with AM1 efficiencies of over 3% without an antireflection coating. These cells were 5 mm x 5 mm x 20 microns of $\sim 5\ \Omega$cm silicon grown epitaxially on a 0.01 Ωcm 10 mil thick substrate. Open circuit voltages as high as 0.45 V were obtained.

Preliminary analysis of cells produced by the corona discharge technique indicates a profile of implanted ions which results in a low sheet resistance for the shallow p-layer. Additionally, the presence of heavily-defected regions within a given cell does not seem to grossly

affect the overall performance of the device.

Future activities are geared to optimizing the various process parameters by both experimental and theoretical means, in order to increase the efficiency of cells produced by this new technique.

We have therefore, shown the technical feasibility of the corona discharge technique as a means for producing efficient silicon solar cells and expect that with continued effort, further improvements can be made.

OVERALL PROGRAM OBJECTIVE

DEVELOP TECHNIQUES TO PRODUCE LOW COST, HIGH EFFICIENCY SOLAR CELLS, WITH EMPHASIS ON LOW TEMPERATURE PROCESSES WHICH RESULT IN SHALLOW JUNCTION DEVICES.

ORIGINAL PAGE IS
OF POOR QUALITY

THE CORONA DISCHARGE PROCESS FOR PRODUCING SHALLOW JUNCTION SI SOLAR CELLS

TECHNIQUE:

A CORONA DISCHARGE (UP TO 9 kV) OF BF_3 PRODUCES BORON IONS WHICH ARE IMPLANTED INTO THE SILICON CATHODE TO FORM A SHALLOW P^+ - N JUNCTION.

ATTRIBUTES:

- LOW PROCESSING TEMPERATURES (<500°C) - SUITABLE FOR RIBBON AND THIN FILM POLYCRYSTALLINE SI
- SIMPLE EQUIPMENT AND PROCESSING STEPS
- CELLS WITH HIGH FILL FACTORS
- IMPROVED SHORT WAVELENGTH RESPONSE

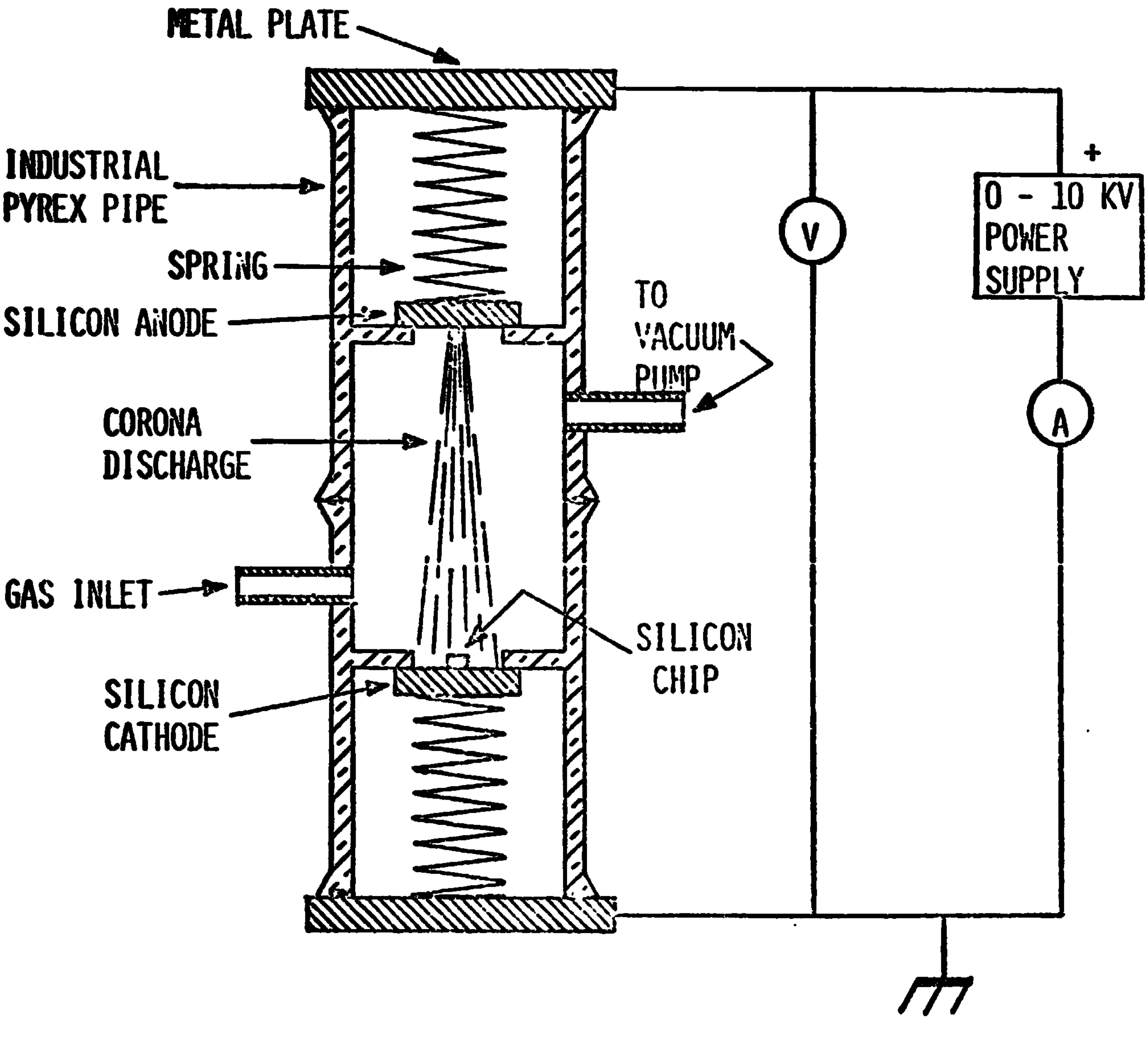

Figure 1. Schematic of Experimental Set-up.

A CORONA-MODE DISCHARGE HAS A UNIQUE FEATURE WHICH CAN BE USED TO ADVANTAGE:

- Potentials of Several Kilovolts can be Sustained
    - Multiply-Ionized Gaseous Species are Generated

      e.g., $BF_3 \rightarrow BF_3^+ \ldots\ldots \rightarrow B^+ \ldots\ldots \rightarrow B^{+5}$
    - The Energy of B^{+5} Falling Through a Potential Drop of 5 kV is equal to 25 keV.

ORIGINAL PAGE IS
OF POOR QUALITY

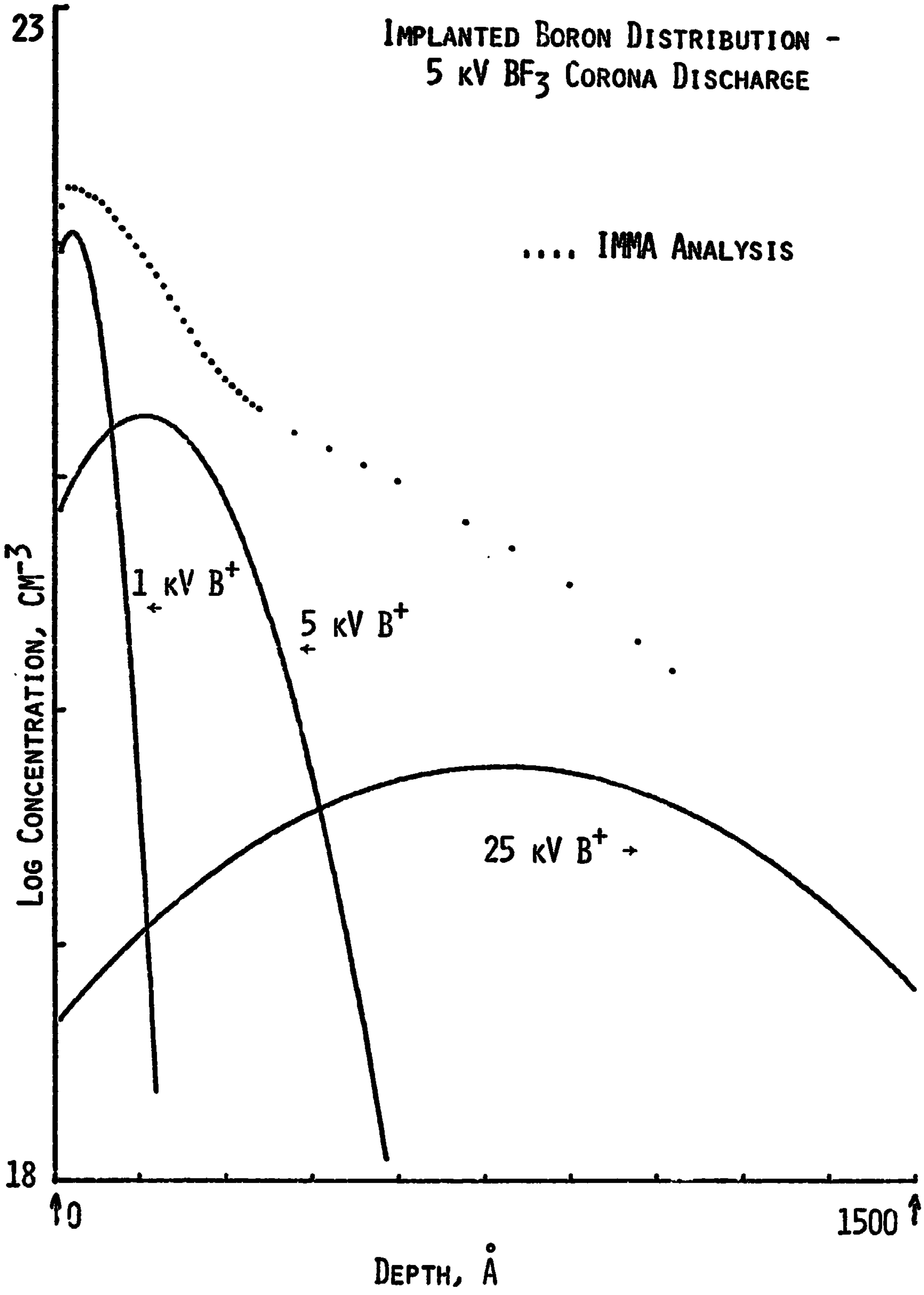
Implanted Boron Distribution -
5 kV BF_3 Corona Discharge
.... IMMA Analysis
1 kV B^+
5 kV B^+
25 kV B^+
23
18
Log Concentration, CM^{-3}
0
1500
Depth, Å

FIGURE 2

FIGURE 3

I-V CHARACTERISTICS
SILICON CORONA CELLS

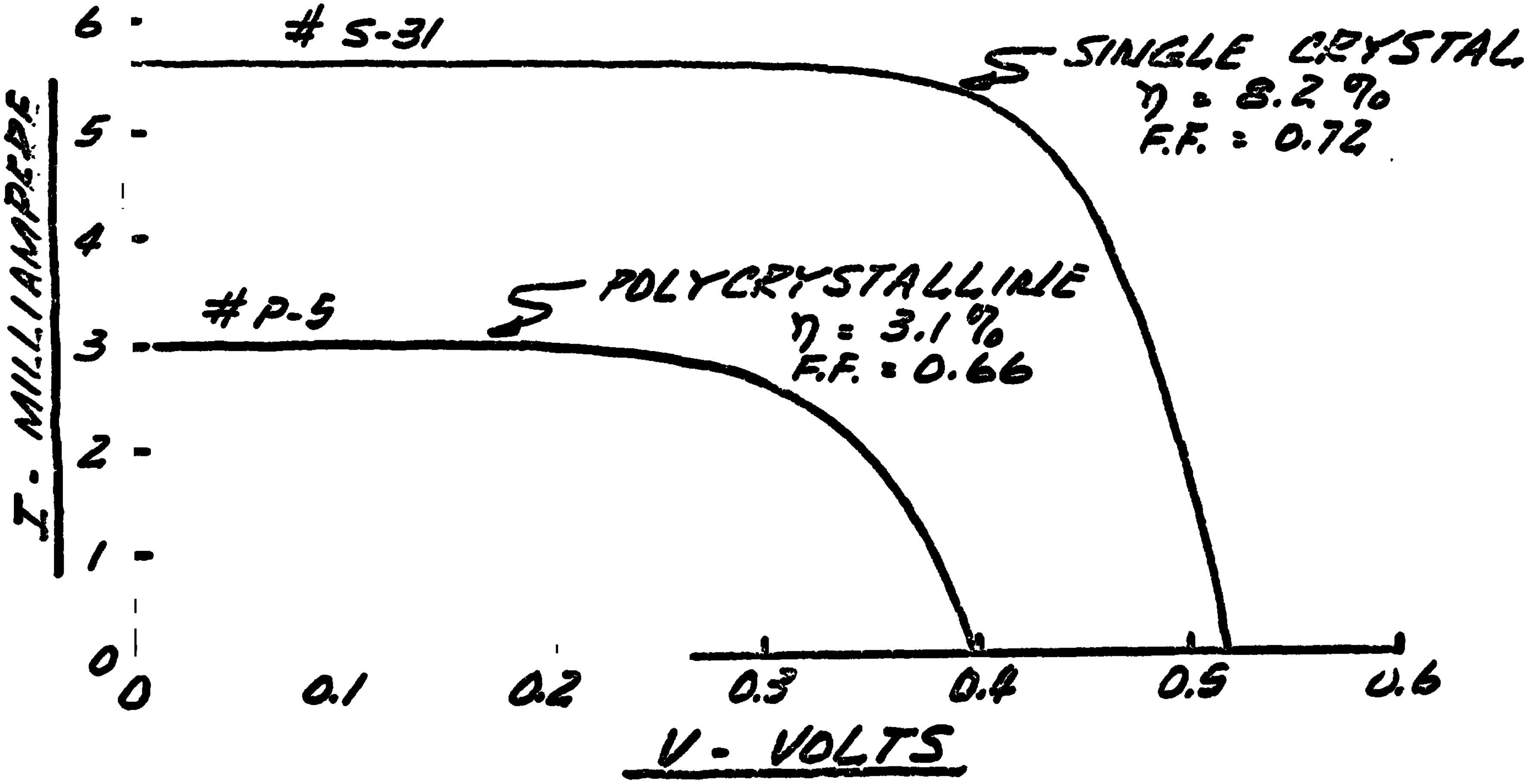

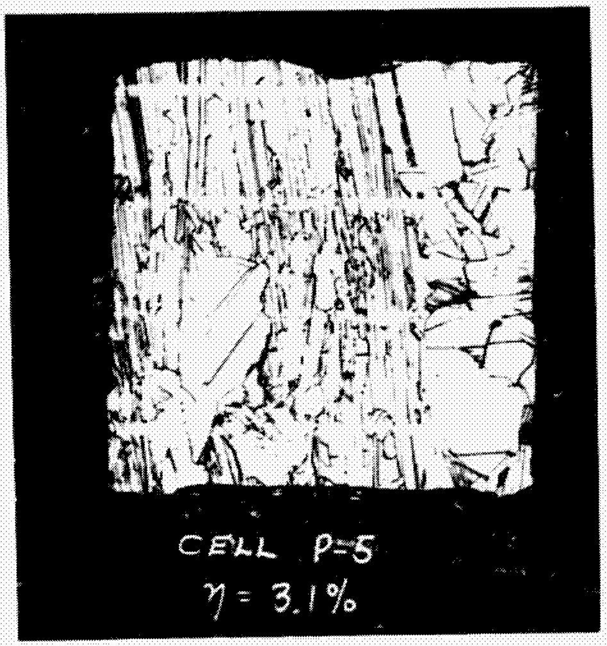

Figure 4. Photograph of Cell P-5. (Dimensions - 5 x 5 mm; Al fingers 0.125 mm wide on 1.25 mm centers.)

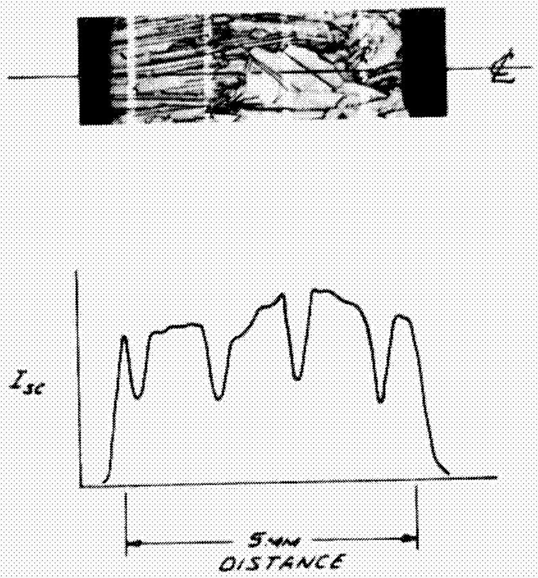

Figure 5. I_{sc} Line Scan of Cell P-5. Light Beam Diameter ~ 0.3 mm.

SUMMARY OF KEY RESULTS

- CONCEPT OF SOLAR CELL FABRICATION BY CORONA DISCHARGE TECHNIQUE HAS BEEN PROVEN
    - SINGLE CRYSTAL CELLS WITH >8% EFFICIENCY (AM1) W/O A-R COATING
    - POLYCRYSTALLINE SILICON CELLS WITH >3% EFFICIENCY (AM1) W/O A-R COATING
- SHALLOW-JUNCTION CELLS ARE NOT GROSSLY AFFECTED BY HIGHLY DEFECTED REGIONS

PLANNED ACTIVITY FOR NEXT 6 MONTHS

- ESTABLISH FABRICATION TECHNOLOGY
- GENERATE THEORETICAL MODEL OF IMPLANTED DOPANT DISTRIBUTION
- DETERMINE EFFECT OF GASEOUS ADDITIVES ON ION POPULATION IN CORONA DISCHARGE
- GENERATE THEORETICAL MODEL FOR SHALLOW JUNCTION CELLS
- SCALE UP CELL DIMENSION
- FABRICATE CELLS WITH INCREASED EFFICIENCY

SESSION VI

COMPOUND SEMICONDUCTOR SOLAR CELLS

N76 12489

ASSESSMENT OF THE INTERNATIONAL WORKSHOP ON CdS SOLAR CELLS

Karl W. Böer
Institute of Energy Conversion
University of Delaware
Newark, Delaware 19711

The National Science Foundation sponsored an International Workshop on CdS/Cu_2S solar cells and other abrupt heterojunctions held at the University of Delaware. Approximately 100 participants, including representatives of NSF, ERDA, NASA and EPRI, discussed during the three day workshop (April 30-May 2) critical questions relating to the performance, stability and economics of these cells with the aim to assess the current state of the art and future potential.

In three parallel sessions, general problems relating to the basic understanding of the cell operation, to material aspects of the cell and to manufacturing methods and cell engineering were discussed.

In a general meeting on the last day of the workshop, a synthesis was attempted in extensive discussions and summarized at a meeting of the Chairmen and Associate Chairmen after the formal adjournment of the workshop. Here it was agreed that the following statement summarized the principal outcome of the meeting. To the extent that there was a definable consensus, these points represent the principal areas of agreement.

Initial Performance and Possible Limits

Peak performances of 7-8.5% conversion efficiency have been demonstrated at room temperature. Peak values of short circuit currents of 25 mamp/cm^2, open circuit voltages of 0.53 volts and fill factors of 75% have been demonstrated. Most investigations show that the highest short circuit currents are obtained with close to stoichiometric Cu_2S.

The highest achievable short circuit current under 100 mwatts/cm^2 natural insolation is about 35 mamps/cm^2 for such cells, allowing 20% optical losses. The theoretical limit for the fill factor is agreed to be about 80%.

Two major approaches to increasing the open circuit voltage were agreed to; namely, recombination at interface states and modifying the band interconnect. A reasonable goal of 0.65 volts was projected and a theoretical upper limit of 0.86 volts was presented.

On the basis of the above individual parameters overall conversion efficiencies in excess of 15% are implied.

Cell Reliability

It was generally agreed that for terrestrial applications, degradation is not an obstacle to utilization of the CdS cell and lifetimes in excess of 20 years are achievable. A major contribution to observed degradation in the past was the result of inadequate protection from atmospheric constitutents. A major degradation mechanism is related to stoichiometry changes in the Cu_2S layer.

Economic Factors

There are at least two production techniques capable of producing economic CdS solar cells. Projected costs/watt were stated to be between 1 and 10 cents/peak watt using the techniques of sensitivity analysis. In order to achieve such projected costs a sufficient production yield of high efficiency cells is necessary. There are indications that such yields are achievable.

General Recommendations

It is recognized by the members of the workshop that the complexity of the heterojunction solar cells warrants a concerted research program with an over-critical mass to systematically approach and solve the key problems to further improvements.

Such improvements shall include an increase of conversion efficiency above 10%, a decrease in thickness of the CdS layer below 10μm, the development of an inexpensive grid and an inexpensive hermetic encapsulation. It must also include the achievement of a production yield in excess of 90% for high efficiency cells within one percentage point deviation. Finally, a life expectancy in excess of 20 years under actual operating conditions is desirable.

The current state of the art shows feasibility of achieving these goals. A great variety of cells have been fabricated using different techniques, electrodes and encapsulations and have demonstrated that cell efficiencies in excess of 5% can be achieved in various ways.

In order to accelerate further progress a systematic research program is recommended:

1. Substrates: A wide variety of substrates is currently used with success including glass, Mo, NiFe, Copper and Kapton with silver pyre. The parameters of influence to cell performance shall be identified and substrates shall be selected which are conducive to high efficient and economic cells.

2. Base Electrodes: Currently predominantly zinc is used but other materials such as Al, Pd-Ag-Ti and conducting glasses are known to produce ohmic contacts to CdS. Other materials and deposition methods shall be identified as ohmic contacts of sufficient conductance and, -for back wall cells - of sufficient optical transparency.

3. CdS Layer: It is know that CdS of different deposition and structure yields good CdS solar cells. Critical parameters shall be identified relating to structure, stoichiometry, doping and surface morphology to obtain high efficiency and stable cells. Alternative methods of deposition and treatments shall be investigated to economically produce such layers.

4. Cu_xS Layer: Evidence is obtained that Chalcocite with $X \geq 1.995$ deposited in a variety of ways yields cells with high collection efficiency. The range of permissible deviation from stoichiometry shall be identified with critical parameters relating to structure and doping to obtain highest collection efficiencies. Means for surface passivation and to stabilize the electrical parameters of the Cu_2S layer shall be investigated as well as alternative means of deposition and post-deposition treatments.

5. Top Electrode: Materials and means of attachment shall be identified to achieve stable ohmic contacts to Cu_2S which could replace the currently used gold.

   Low cost electrodes shall be developed with high collection efficiency (for front wall cells with high optical transparency).

6. Encapsulation: Materials or material combinations shall be identified which can combine antireflection coating with a hermetic sealing and possibly surface passivation. Inexpensive encapsulation techniques shall be developed.

7. Arrays: Critical parameters shall be identified for automatic array fabrication. Means to inexpensively produce and encapsulate such arrays shall be developed.

8. Alternative Heterojunctions: The investigation of alternative material combinations shall be continued and their potential shall be identified in comparison with the CdS/Cu_2 solar cell in respect to maximum possible efficiency, ease of fabrication, degradation mechanism and other relevant parameters influencing reliability and economics.

9. Cell Operation: Efforts shall be continued to improve the understanding of the physics of the cell operation.

10. Diagnostic Tools: Diagnostic tools shall be further developed to identify all essential parameters of the cell and to control reproducible manufacturing of all components of the cell.

11. Life Testing: Meaningful accelerated life tests shall be developed and all newly developed cells shall be promptly submitted to such tests.

12. Documentation and Exchange of Information: All results shall be recorded with attention to ease of access and data retrieval. Close relation of the different parts of the program and swift exchange of information is emphasized.

In addition, systems analyses of the relation between initial cell costs, performance and useable lifetime shall be pursued to give guidance to cell research and development.

This workshop has served a useful function to assess the current state of the art and to provide guidance for future research. It is proposed to hold such workshops periodically.

VERY LOW COST THIN FILM CdS-Cu_2S SOLAR CELL DEVELOPMENT USING CHEMICAL SPRAYING

D. H. Baldwin Company, El Paso, Texas

and

Sandia Laboratories, Albuquerque, New Mexico

Grant Number:	(Not Finalized)
Grant Period:	? (6 Months)
Grant Amount:	Baldwin $110,000 Sandia 30,000

by

George A. Samara

Sandia Laboratories, Albuquerque, New Mexico

Principal Investigators: J. F. Jordan - Baldwin
G. A. Samara - Sandia

presented at

National Solar Photovoltaic Program Review Meeting

July 22-25 (1975) Los Angeles, California

ABSTRACT

Over the past four years the D. H. Baldwin Company has developed a chemical spray process for the production of thin film CdS-Cu_2S solar cells projected to cost less than $60/kW in very large scale production. The average efficiency of these cells has been improved from $< 0.3\%$ in 1971 to about 4.5% at present.

The overall objectives of this program are to further develop the process, to raise the efficiency, and to attain long life stability. In the joint program Sandia Laboratories is to provide the technical support necessary to help achieve these objectives.

The cell consists of a glass substrate onto which is sprayed a thin tin oxide transparent electrode followed by a sprayed film (2-3 μm) of CdS. A very thin film of Cu_xS is then formed by either spraying, dipping, or electrolytic ion exchange. Finally a copper/lead electrode is evaporated on top the Cu_xS layer.

Discussion between Baldwin and Sandia defined several areas for initial investigation by Sandia. These are:

1 - Chemical analysis of the starting chemicals and resulting thin films with emphasis on impurities likely to be electrically active and their effects on cell properties.

2 - Determination of the morphology and crystallography of the various layers.

3 - Determination of the location, depth profile and form of dopants and contaminants known to be in the device and their effects on the morphology and crystallography.

4 - Studies of the electrical and optical properties of the various films and the device.

The results of this work should form the basis for process modification and control and for improving device characteristics and conversion efficiency.

The Sandia effort was recently initiated and the work thus far, on the limited number of available samples, has consisted of a general survey of the potential usefulness of a wide variety of analytical techniques to the understanding of the structure, composition and properties of the films and devices. It is often observed that corroborative results from a combination of techniques are necessary to be able to draw definitive conclusions. Our preliminary findings are summarized in one of the accompanying tables.

It is expected that a more detailed and broader range of studies along with more definitive conclusions will be accomplished by the next Review Meeting.

OVERALL OBJECTIVES

To Further Develop a Process for the Manufacture, on a Large Scale, of Solar Cells Costing Less than 6 Cents per Watt ($60/KW). This Envisages Adapting Chem'cal Spraying Processes to a Float Glass Plant.

Goal 1. Increase Present Efficiency (4.3-4.72%) to 5% Average.

Goal 2. Attain Stability, [illegible] Prove by Life Test, Cells of 5% Effic[illegible]

Goal 3. Obtain Efficiencies Substantially Higher than 5%.

Goal 4. Life Test such Higher Efficiency Cells for Stability.

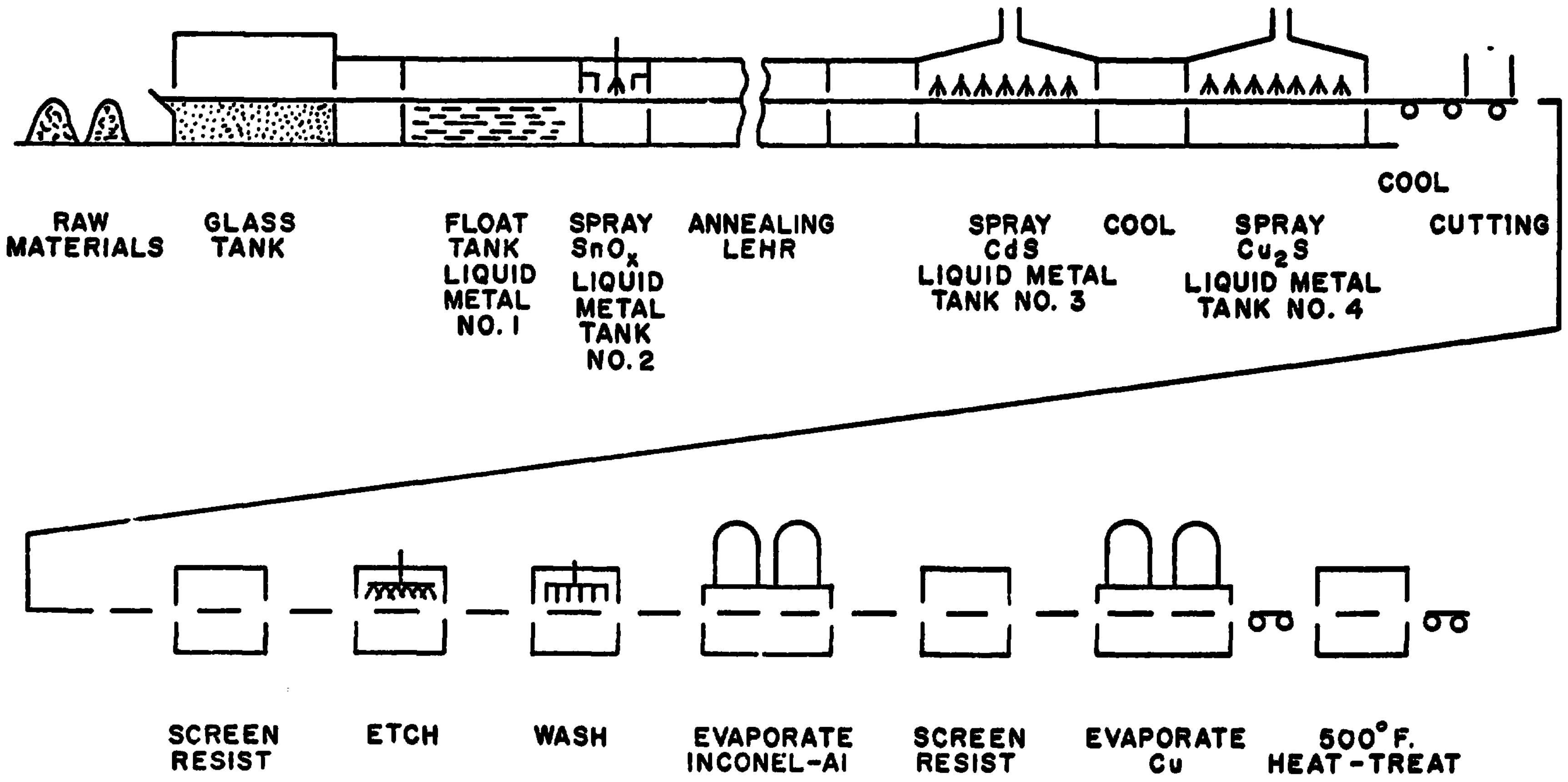

-SCHEMATIC OF A FLOAT-GLASS SOLAR-CELL PLANT

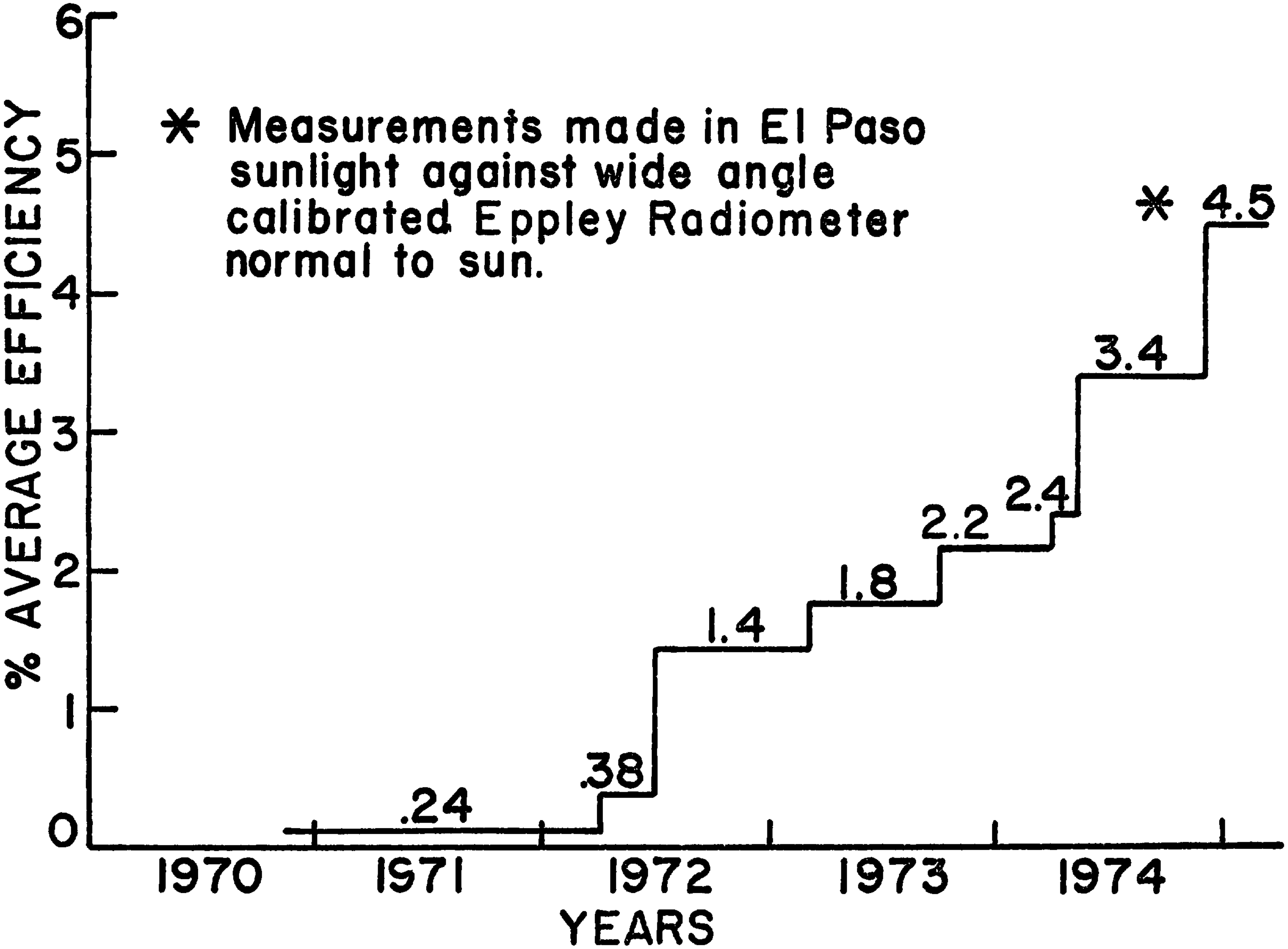

PROGRESS IN IMPROVEMENT OF EFFICIENCY
FOR CHEMICAL SPRAY PROCESS (CELLS)

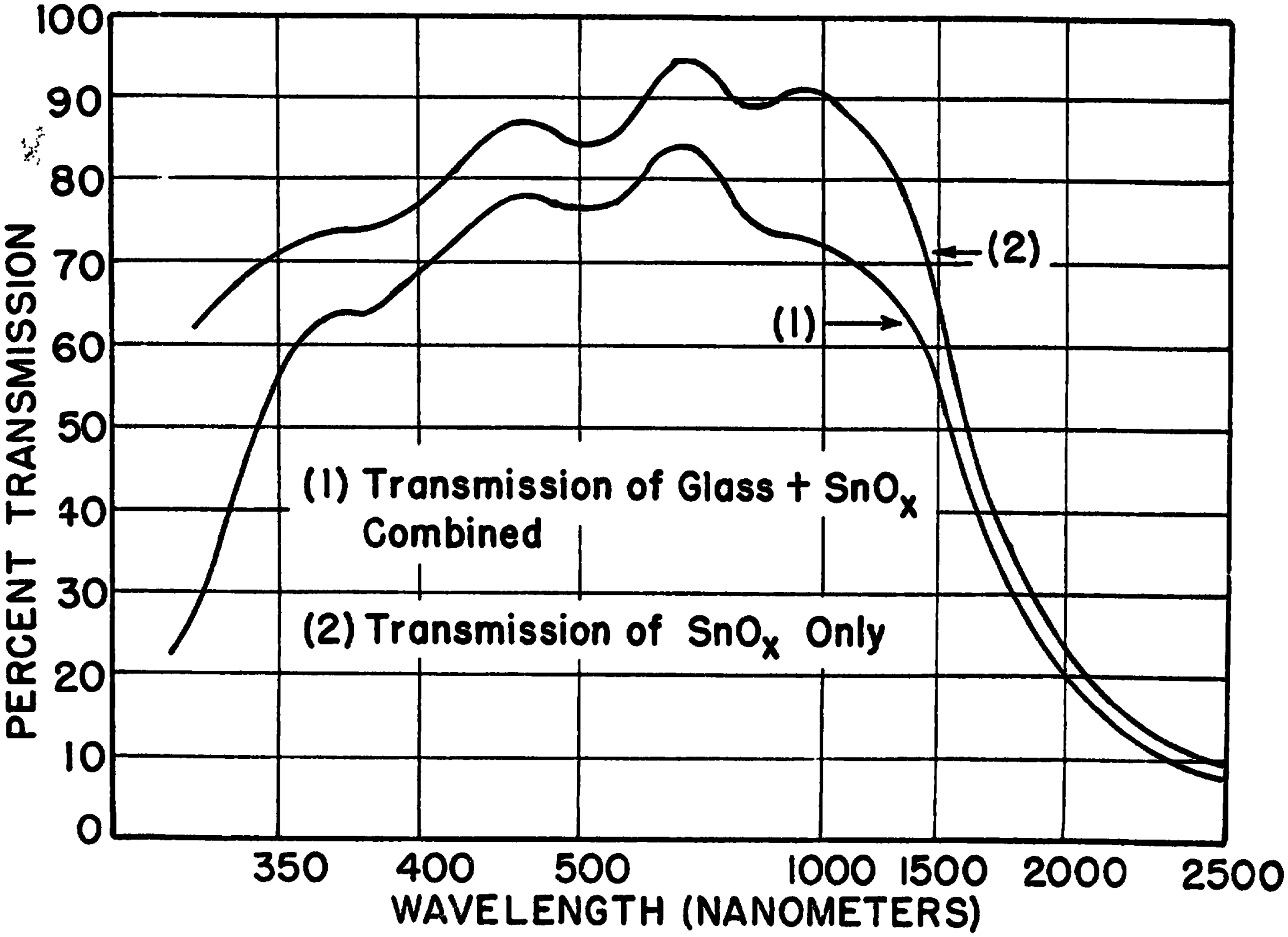
100
90
80
70
60
50
40
30
20
10
0
PERCENT TRANSMISSION
350
400
500
1000
1500
2000
2500
WAVELENGTH (NANOMETERS)
(1) Transmission of Glass + SnO$_x$ Combined
(2) Transmission of SnO$_x$ Only
(1)
(2)

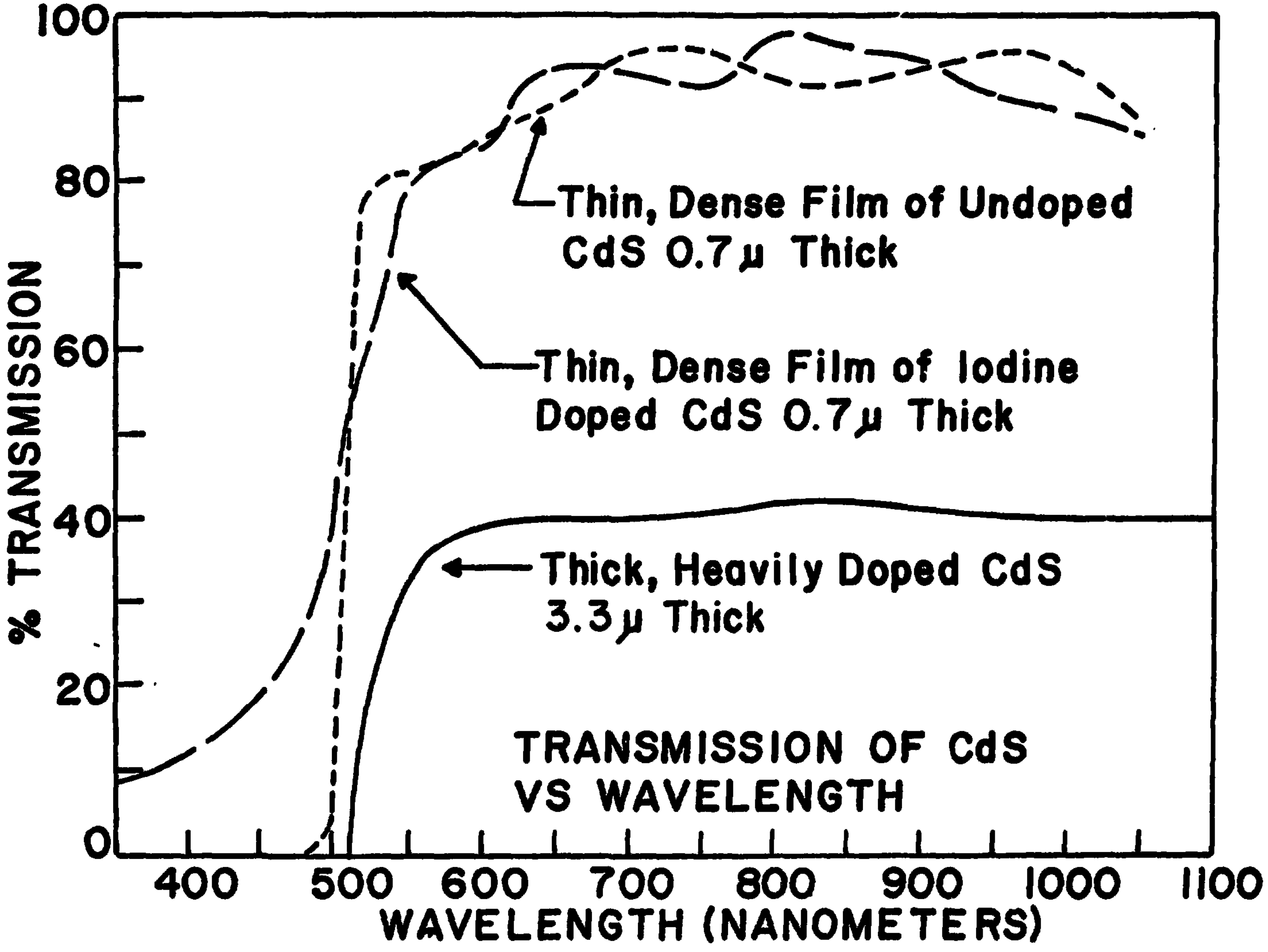
Thin, Dense Film of Undoped CdS 0.7µ Thick
Thin, Dense Film of Iodine Doped CdS 0.7µ Thick
Thick, Heavily Doped CdS 3.3µ Thick
TRANSMISSION OF CdS VS WAVELENGTH
% TRANSMISSION
0
20
40
60
80
100
400
500
600
700
800
900
1000
1100
WAVELENGTH (NANOMETERS)

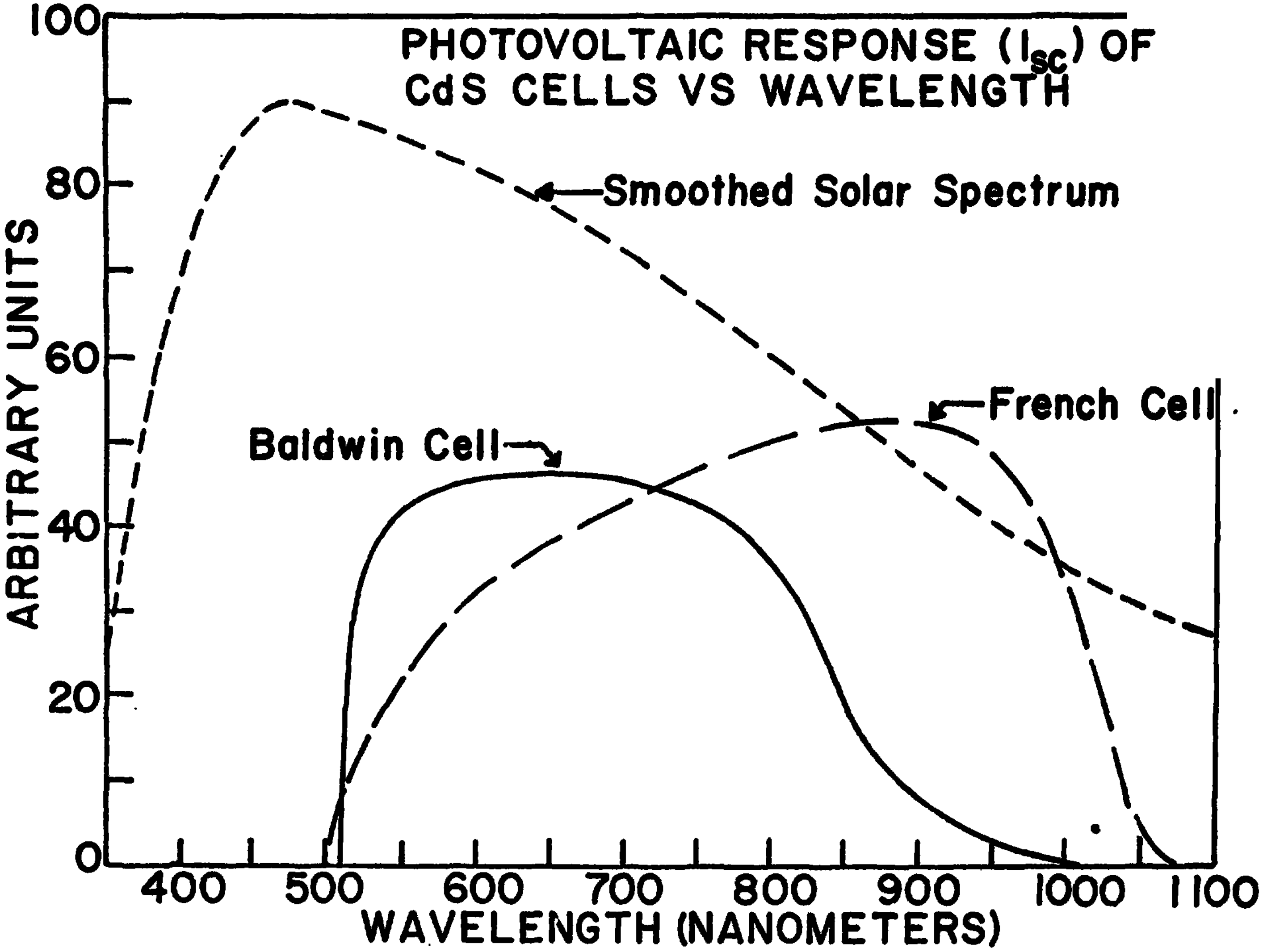
PHOTOVOLTAIC RESPONSE (I_{sc}) OF
CdS CELLS VS WAVELENGTH
Smoothed Solar Spectrum
French Cell
Baldwin Cell
ARBITRARY UNITS
100
80
60
40
20
0
400
500
600
700
800
900
1000
1100
WAVELENGTH (NANOMETERS)

COST SUMMARY: (EXCLUSIVE OF INSTALLATION, SITE PREPARATION, AND POWER HANDLING EQUIPMENT, I.E., CELLS ONLY.)

COSTS AS OF SEPTEMBER 1973.

MATERIALS	DOLLARS PER SQUARE FOOT
GLASS	.1400
OTHER MATERIALS (CHEMICALS AND METALS)	.0509
TOTAL MATERIALS	.1909
ADDITIONAL LABOR COSTS INCIDENT TO CELL MANUFACTURE	.0019
CAPITAL COST-DEPRECIATION AND INTEREST	.0260
PLANT MAINTENANCE COST	.0102
POWER COSTS	.0253
ADDITIONAL G & A (ABOVE THAT INCLUDED IN GLASS COST)	.0068
TOTAL COST	.2611

AT 5% EFFICIENCY, ONE (1) SQUARE FOOT OF GLASS WILL PRODUCE A PEAK POWER OF 4.645 WATTS.

COST PER PEAK WATT	.0562
COST PER PEAK KILOWATT	56.20

JOINT BALDWIN/SANDIA PROGRAM

Sandia Responsibilities:

1. Studies of the Structure and Morphology of Thin Films of CdS, Cu_xS, and SnO_2 Prepared by Baldwin.
2. Chemical Analysis and Dopant Profiles of Above Films
3. Electrical Transport and Optical Properties of Above Films and Cells.
4. Recommendations for Process Modification and Control.

CHARACTERIZATION TECHNIQUES

Technique	Investigator
Electron Diffraction and Reflection Electron Diffraction	F. Gruelich R. Berg
Auge Electron Spectroscopy	P. Holloway
Secondary Ion Mass Spectrometry and Ion Scattering Spectroscopy	G. Nelson
Scanning Electron Microscopy	R. Berg
Rutherford Backscattering	J. Borders
Optical Spectroscopy	H. Stein R. Berg.
Atomic Absorption Spectroscopy	S. Fuller
Emission Spectroscopy	J. Walcott J. Woodworth
Electrical Properties	R. Nasby
High Speed Photography	

PRELIMINARY FINDINGS

1. Impurity Analysis of the Starting Chemicals for the Doped CdS Indicate the Presence of Some Impurities at Levels Potentially Harmful to the Device.
2. After Heating to SnO_x Deposition Temperature the Surface of the Glass (Soda Lime) Becomes Saturated with Na.
3. The Na Causes Fogging of the SnO_x Film and Effectively Limits the Thickness of this Film.
4. The SnO_x Contains Large Amounts of Na. There is Concern that the Na Might Migrate into the CdS Layer.
5. Al is Dispersed in the CdS Layer and Appears to be in the Form of an Oxide Rather than a Sulfide.
6. Morphological Features ("Balls" or Nodules") are Prominant in the CdS Layer, but these Involve no Chemical Inhomogeneities. This Suggests the Great Dominance of the Spray Process Itself in Determining the Film Morphology.
7. The Cu_xS is ~ 400 Å Thick (Average). Surface Coverage of the CdS Layer Appears Incomplete.
8. Both Chalcocite and Djurleite Forms of Cu_xS were Detected. In "One of Better" Cells the Cu_xS Layer was Identified as Chalcocite.

N76 12491

CdS THIN FILM SOLAR CELLS FOR TERRESTRIAL POWER

Grant No. AER74-14918 Westinghouse Research Laboratories

ABSTRACT

The overall objective is the development of very low cost long lived Cu_2S/CdS thin film solar cells for large scale energy conversion. This review covers approximately the second half of the first year's work at Westinghouse.

In this period, the facility for fabricating a modified design terrestrial cell was operated steadily. Cell outputs started out low (at 3.4%), dropped (to 2.0%) when closer controls were placed on the process, increased (to 3.4%) when a revised rinsing process was introduced, and increased further (to 5.0% average) when a revised barrier forming process was put into effect.

Work continued on the development of a low cost grid system. A printed grid, using flake graphite pigment in a polysulfone binder was developed, and gave reasonably compatible grid lines. However, the line width and resistivity were both too high for the required fine mesh grid and further work was postponed.

Excellent evaporated metal grid patterns were obtained using a specially designed aperture mask. Line widths of 1 mil and spacings of 50 and 100 lines per inch were readily obtained. Vacuum evaporated gold and copper grids of 50 lines per inch and 1 micron thickness were adequate electrically for the fine mesh contacting grid. Some difficulty was encountered with such grids dropping cell output to half or less, though usually the outputs could be restored by vacuum annealing. The difficulty is believed to be due to localized shorting of the grid to n-type CdS in crevices in the Cu_2S layer.

Real time roof top sunlight exposure tests of encapsulated

CdS cells show no loss in output after 5 months.

Accelerated life testing of encapsulated cells show no loss of output power after 6 months of 12 hour dark-12 hour AM1 illumination cycles at 40°C, 60°C, 80°C and 100°C temperatures. However, the cells are showing changes in their basic parameters, such as series and shunt resistance and junction capacitance. There are indications that these changes can be correlated with specific degradation modes and hence there is an expectation that the accelerated tests will be of value in predicting cell lifetimes in normal usage.

A- CDS THIN FILM SOLAR CELLS FOR TERRESTRIAL POWER

GRANT NO. AER74-14918

BY

WESTINGHOUSE ELECTRIC CORPORATION
RESEARCH LABORATORIES
PITTSBURGH, PENNSYLVANIA

WITH

THE UNIVERSITY OF PITTSBURGH
PITTSBURGH, PENNSYLVANIA

PERIOD OF GRANT	AUGUST 1, 1974 THRU JULY 31, 1975
AMOUNT OF GRANT	$247,200

PRINCIPAL INVESTIGATOR - F. A. SHIRLAND

B- OVERALL OBJECTIVE OF PROJECT

THE DEVELOPMENT OF VERY LOW COST LONG LIVED
CdS/Cu_2S THIN FILM SOLAR CELLS

THE FIRST PHASE OF A THREE YEAR EFFORT TO CARRY
THE CdS THIN FILM SOLAR CELL TO THE THRESHOLD
OF PRACTICAL APPLICATIONS

C- PLANNED ACTIVITY FOR LAST SIX MONTHS

1- SOLVE PROBLEM OF HIGH R_S AND LOW SCC

2- OPERATE STANDARD PROCESS CELL FABRICATION FACILITY AND ACHIEVE 4% MINIMUM EFFICIENCY LEVEL

3- CONTINUE DEVELOPMENT OF LOW COST GRID SYSTEM

4- STUDY METHODS OF PROTECTING CELLS FROM THE ATMOSPHERE-RECOMMEND APPROACH FOR INTENSIVE DEVELOPMENT

5- OBTAIN FIRST INDICATIONS OF EXPECTED LIFETIMES OF STATE-OF-THE-ART CELLS IN TERRESTRIAL USE

6- START BASIC STUDIES OF CELL STRUCTURE AND OPERATING MECHANISM

7- START STUDIES OF Cu_2S LAYER TO OPTIMIZE STRUCTURE FOR THINNER BASE LAYERS

8- ANALYZE LOSSES IN STATE-OF-THE-ART CELLS TO DEMONSTRATE PRACTICALITY OF HIGHER CELL EFFICIENCIES

D- DESCRIPTION OF PROGRESS MADE

1. Problem of High R_S and Low SCC

High R_S values earlier were apparently due to inadequately formed junctions. They improved greatly when better junctions were were made.

Higher currents (15 to 19 mA/cm^2) were obtained by increased etch to open grain boundaries, and by use of higher CuCl dip temperature

D- DESCRIPTION OF PROGRESS MADE

2- Standard Process Cell Fabrication

A total of 53 standard process cell runs made in 6 month period (3 cells/run)

Initial Process	AVG. EFF. = 3.4%
Tightened Controls	AVG. EFF. = 2.0%
Revised Process - Faster Rinse	AVG. EFF. = 3.4%
Re-Revised Process - New Etch + Dip	AVG. EFF. = 5.0%

Reproducibility - Fair (± 20% at 5.0% level)

Yield - Good 87% in 3rd Qtr.
92% in 4th Qtr.

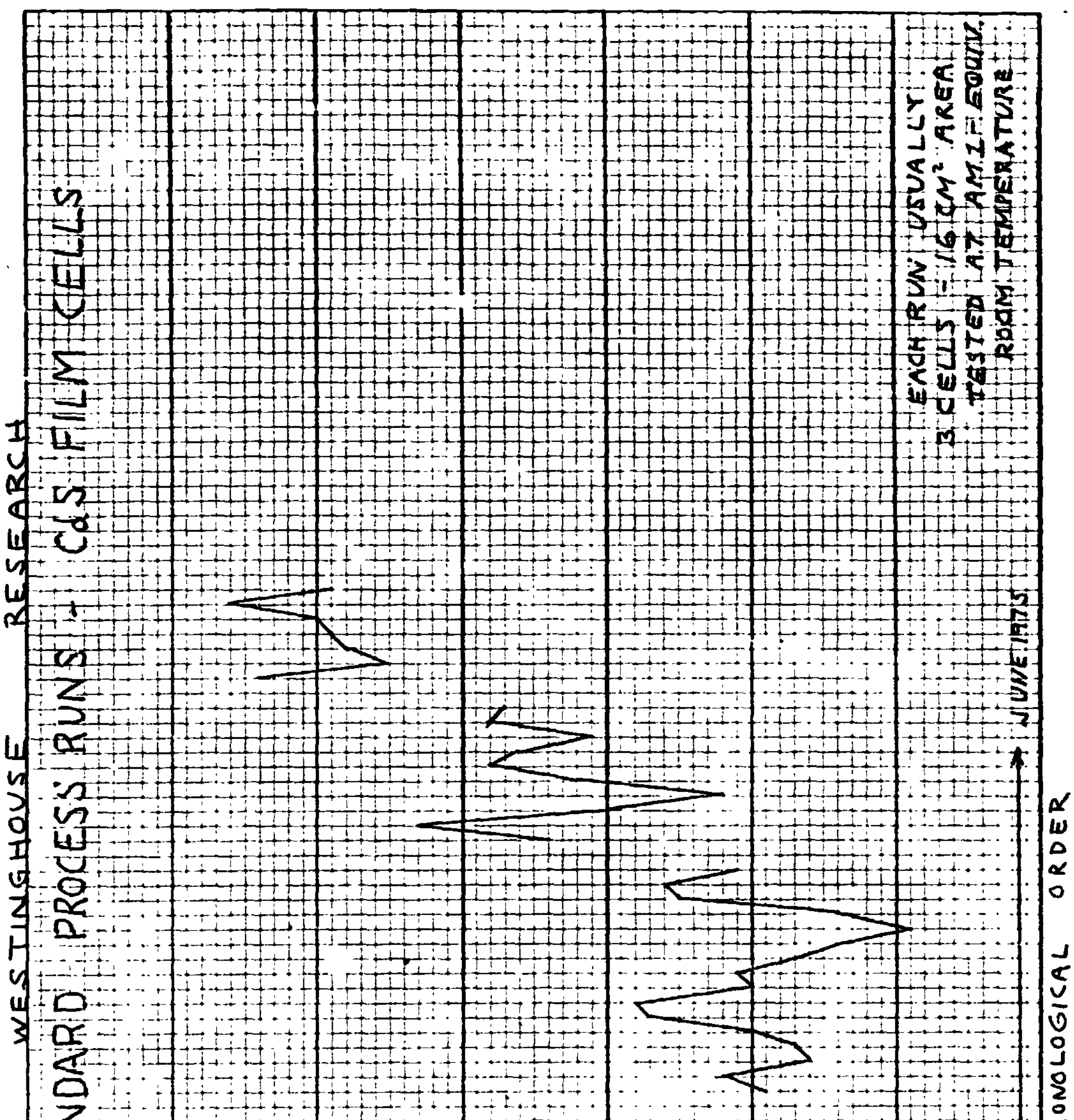
WESTINGHOUSE RESEARCH
STANDARD PROCESS RUNS - CdS FILM CELLS
EACH RUN USUALLY
3 CELLS - 1.6 CM² AREA
TESTED AT AM.1 EQUIV.
ROOM TEMPERATURE
DEC 1974
JUNE 1975
RUNS IN CHRONOLOGICAL ORDER
AVERAGE EFFICIENCY - PER CENT
0
1
2
3
4
5
6

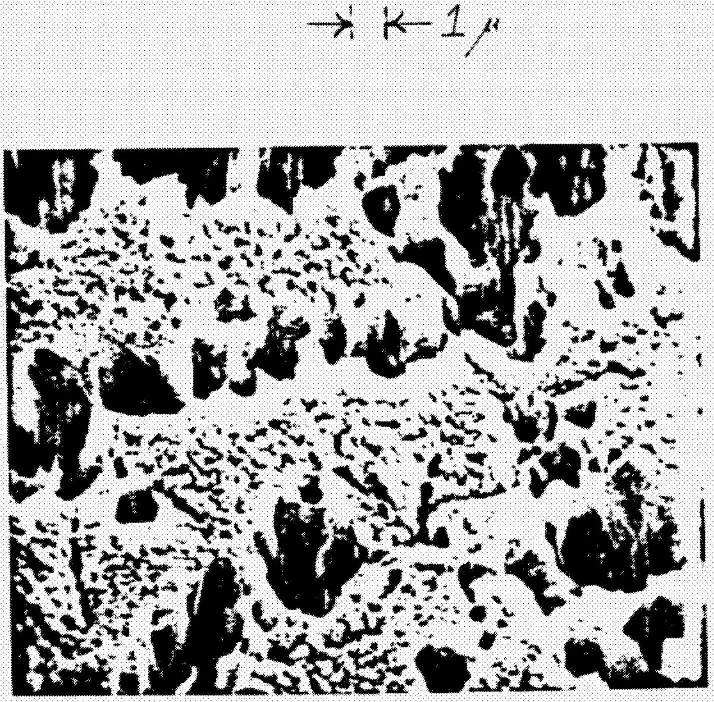

RUN 97-5000X (Old Process)

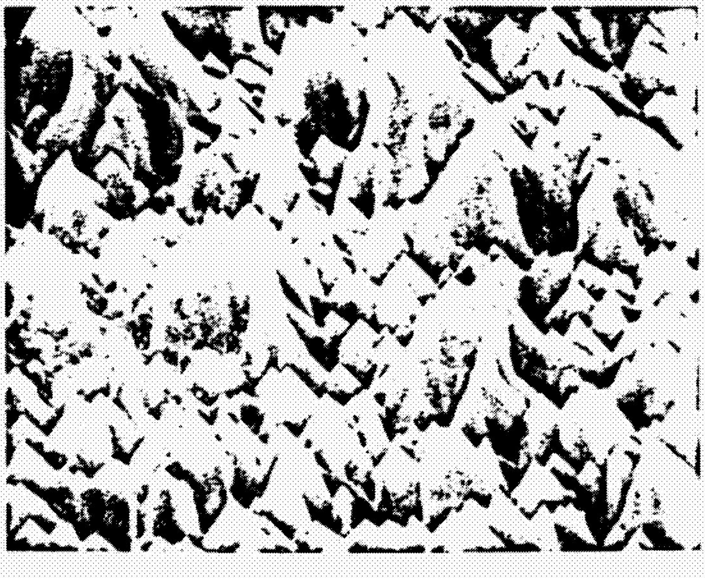

Run 189-5000X (New Process)

SEM PICTURE OF SURFACE OF
Cu_2S/CdS CELL

(5000X)

→||← 1 μ

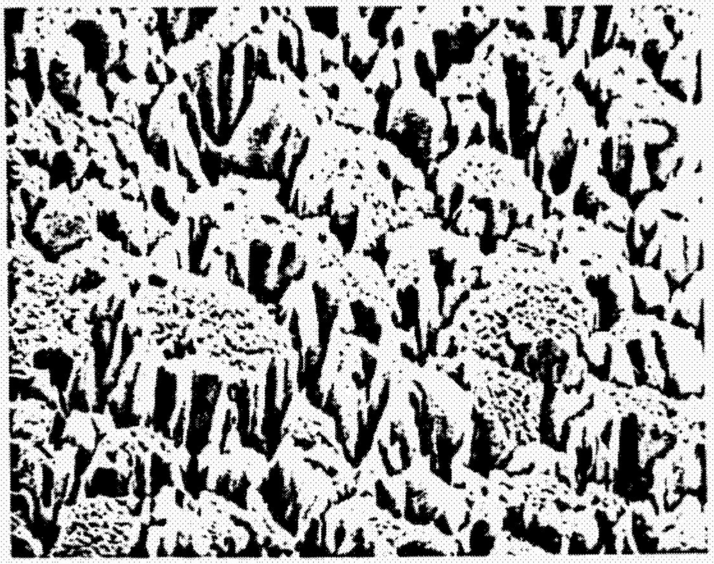

Run 97-2000X (Old Process)

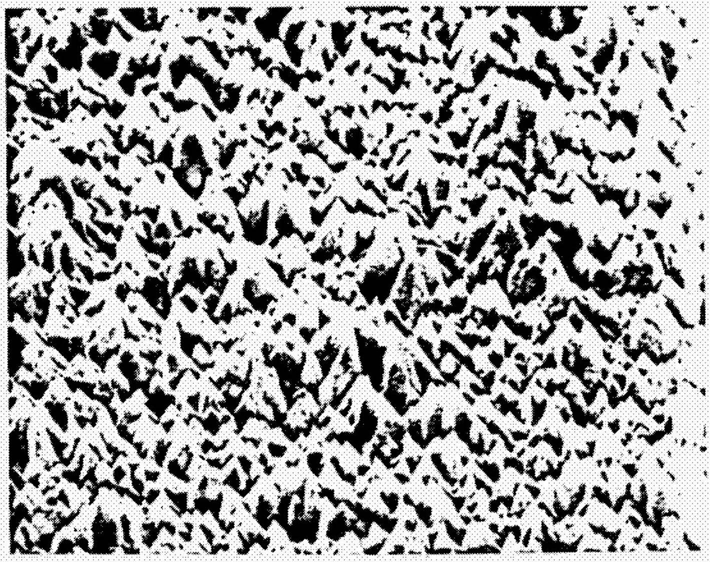

Run 185-2000X (New Process)

SEM PICTURE OF SURFACE OF
Cu_2S/CdS CELL

(2000X)

D- DESCRIPTION OF PROGRESS MADE

3- LOW COST GRID SYSTEM

DUAL GRID SYSTEM SELECTED AS MOST PROMISING
- FINE GRID CONTACT - EVAPORATED OR PRINTED
- COARSE COLLECTOR BUS - METALLIC OVERLAY

PRINTED GRID - FLAKE GRAPHITE PIGMENT, POLYSULFONE BINDER
- RESISTIVITIES WERE TOO HIGH
- RESOLUTIONS WERE TOO LOW

EVAPORATED GRID - MECHANICS OF PROCESS WORKED OUT
- APERTURE MASKS - 1 MIL LINE WIDTHS
  - 50 LPI SPACING UP TO 100
- EXCELLENT PATTERNS OBTAINED - GOOD ADHESION & COND.
- EVAPORATED METALS REDUCE CELL OUTPUT

COARSE COLLECTOR GRID - CONDUCTIVE EPOXY INTERCONNECT - OK
- THERMO-COMPRESSION BONDING - NOT TRIED

D- DESCRIPTION OF PROGRESS MADE

3- LOW COST GRID SYSTEM

PRINTED GRID

PROBLEM:

ORDINARY CONDUCTIVE INKS - MUCH TOO HIGH RESISTANCE

ANALYSIS

PIGMENT SURFACE AREA TOO HIGH TO OBTAIN HIGH LOADING

APPROACHES

A- FLAKE PIGMENT TO REDUCE SURFACE AREA & INCREASE PARTICLE TO PARTICLE CONTACTS

FLAKE GRAPHITE EVALUATED

RESULTS PROMISING - BUT STILL TOO HIGH IN RESISTANCE -- TOO COARSE FOR DESIRED RESOLUTION

FLAKE COPPER MAY HELP

B- CONDUCTIVE BINDER

C- IMPROVED MIXING TO PREVENT COMPLETE WETTING OF PIGMENT

D- DESCRIPTION OF PROGRESS MADE

3- LOW COST GRID SYSTEM

EVAPORATED GRID

PROBLEM:

AFTER GRID IS EVAPORATED, CELL OUTPUT (OCV + EFF.) DROPS.

ANALYSIS:

EVAPORATED METAL PROBABLY SHORTING TO CDS IN GRAIN BOUNDARY CREVICES

APPROACHES:

A- DIFFERENT METALS

VARIOUS METALS HAVE BEEN TRIED. GOLD WORKS BEST, AND COPPER NEXT. MAY TEND TO FORM BLOCKING CONTACT. (AFTER AU OR CU GRID EVAPORATION, OUTPUT OF CELL CAN USUALLY BE RESTORED BY VACUUM ANNEALING.) TRY GRAPHITE.

B- P^+ SEMI-CONDUCTOR UNDER METAL ELECTRODE. (Cu_2S, SI, SE)

Cu_2S REACTIVELY SPUTTERED-GAVE GOOD JUNCTION TO CDS

C- OBLIQUE EVAPORATION TO MINIMIZE PENETRATION IN CREVICES

D- IMPROVE CONTINUITY OF Cu_2S BARRIER LAYER

LONGER CUCL DIP TIME-WEAKER BATH

IMPROVED AGITATION DURING DIPPING

SLOWER ETCH TO REDUCE CREVICING

FORM Cu_2S BARRIER BY SOLID STATE DIFFUSION

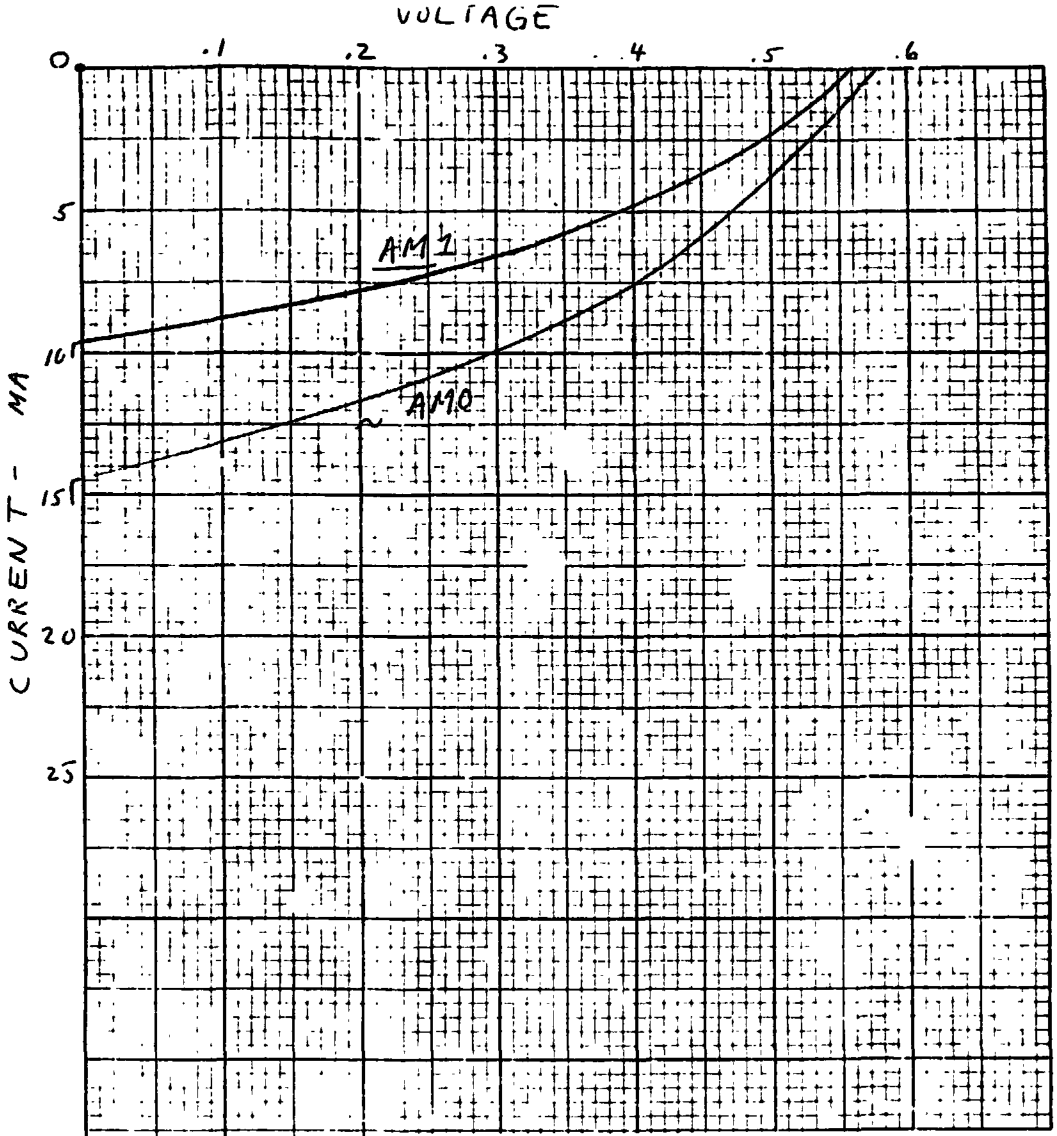

Run: 16ℓ-210 Date: 6/6/75 Area: 4 (cm^2) Oper:

V_{OC}(V)	.558	J_{SC}(mA/cm^2)	2.3
I_{SC}(A)	.0095	P_M(W)	.00200
I_{MP}(A)	.0055	η(%)	0.5 %
V_{MP}(V)	.364	F.F.(%)	37 %
R_{SH}(Ω)	2510	R_S(Ω)	20
ρ_{SH}(Ω/cm^2)	10^4	ρ_S(Ω/cm^2)	80

Comments:

SPUTTERED Cu_2S BARRIER LAYER.

D- DESCRIPTION OF PROGRESS MADE

4- PROTECTING CELLS FROM ATMOSPHERE

R.F. SPUTTERING SYSTEM OBTAINED, SET-UP AND TOOLED

SiO_2, Al_2O_3, AND Si_3N_4 TARGETS OBTAINED

SiO_3, Al_2O_3 AND Si_3N_4 SPUTTERED ONTO GLASS - TO CALIBRATE PROCESS

GOOD ADHERENT, PINHOLE-FREE COATINGS OBTAINED 0.2 TO 1.0μ THICK

READY TO APPLY TO Cu_2S LAYER CELLS

D- DESCRIPTION OF PROGRESS MADE

5- LIFE TESTING

A- ROOF-TOP TEST

5 MONTHS REAL TIME EXPOSURE - NO LOSS OF OUTPUT

B- ACCELERATED LIFE TEST

IN-SITU OUTPUT MEASUREMENTS FOR 6 MONTH ACCELERATED EXPOSURE
- SOME INITIAL DROPS, BUT MOST CELLS HOLDING UP

ACCURATE SIMULATOR TEST BEFORE & AFTER 6 MONTHS ACCELERATED EXPOSURE
- MOST CELLS SHOWING NO LOSS OF OUTPUT
- INTERNAL CELL PARAMETERS SHOWING SOME CHANGES
  - R_S INCREASING - AT ALL TEMPERATURES
  - R_{SH} DECREASING - AT ALL TEMPERATURES
  - C DECREASING - AT 100°C ONLY

SOME CORRELATION BETWEEN IN-SITU AND SIMULATOR DATA, BUT MORE ACCURATE IN-SITU DATA NEEDED FOR BETTER CORRELATION.

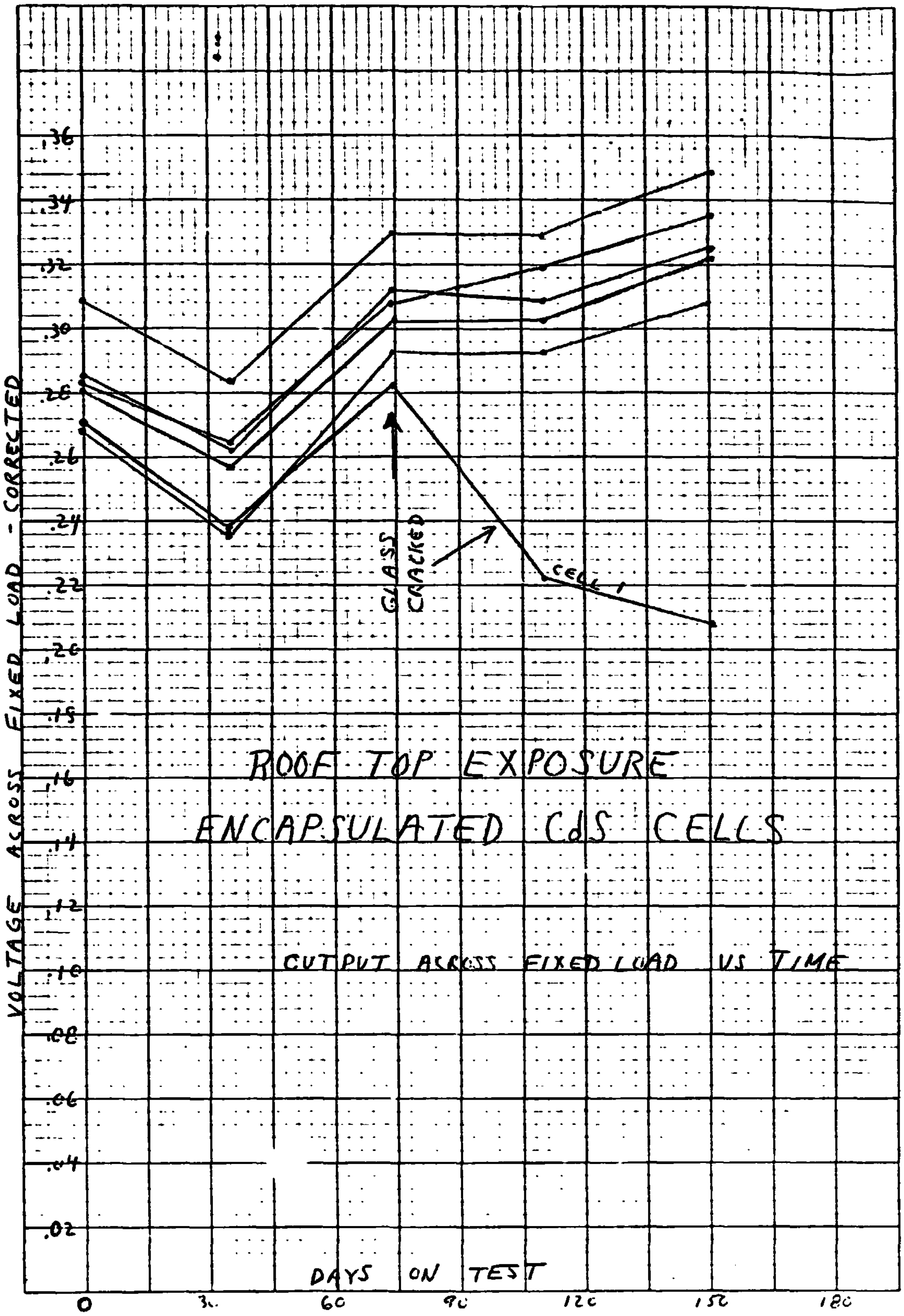ROOF TOP EXPOSURE
ENCAPSULATED CdS CELLS
OUTPUT ACROSS FIXED LOAD VS TIME
VOLTAGE ACROSS FIXED LOAD - CORRECTED
DAYS ON TEST
GLASS CRACKED
CELL 1
.36
.34
.32
.30
.28
.26
.24
.22
.20
.18
.16
.14
.12
.10
.08
.06
.04
.02
0
30
60
90
120
150
180

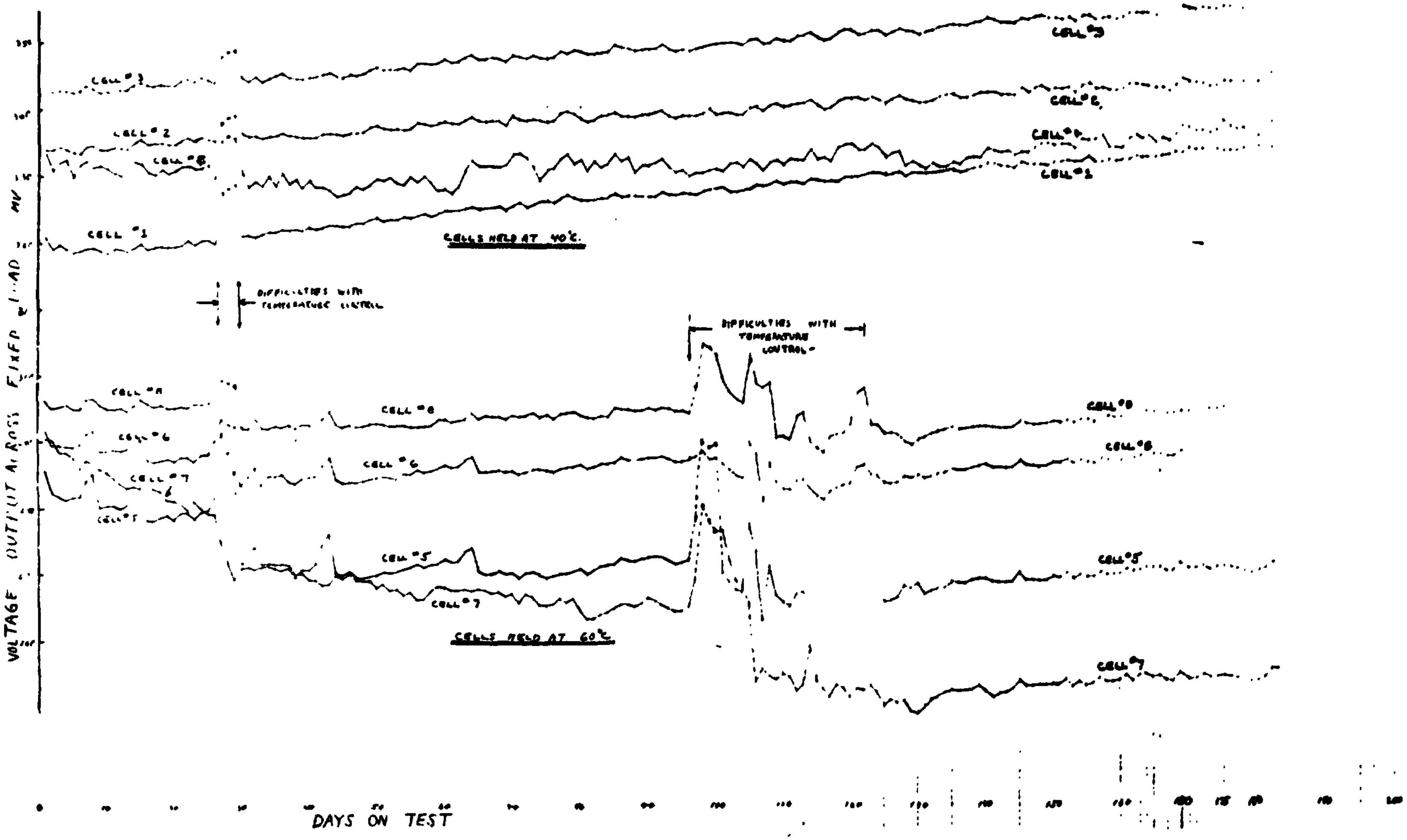
VOLTAGE OUTPUT ACROSS FIXED LOAD MV
CELL #3
CELL #2
CELL #8
CELL #1
CELLS HELD AT 40°C.
DIFFICULTIES WITH TEMPERATURE CONTROL
DIFFICULTIES WITH TEMPERATURE CONTROL
CELL #8
CELL #6
CELL #7
CELL #5
CELLS HELD AT 60°C
DAYS ON TEST

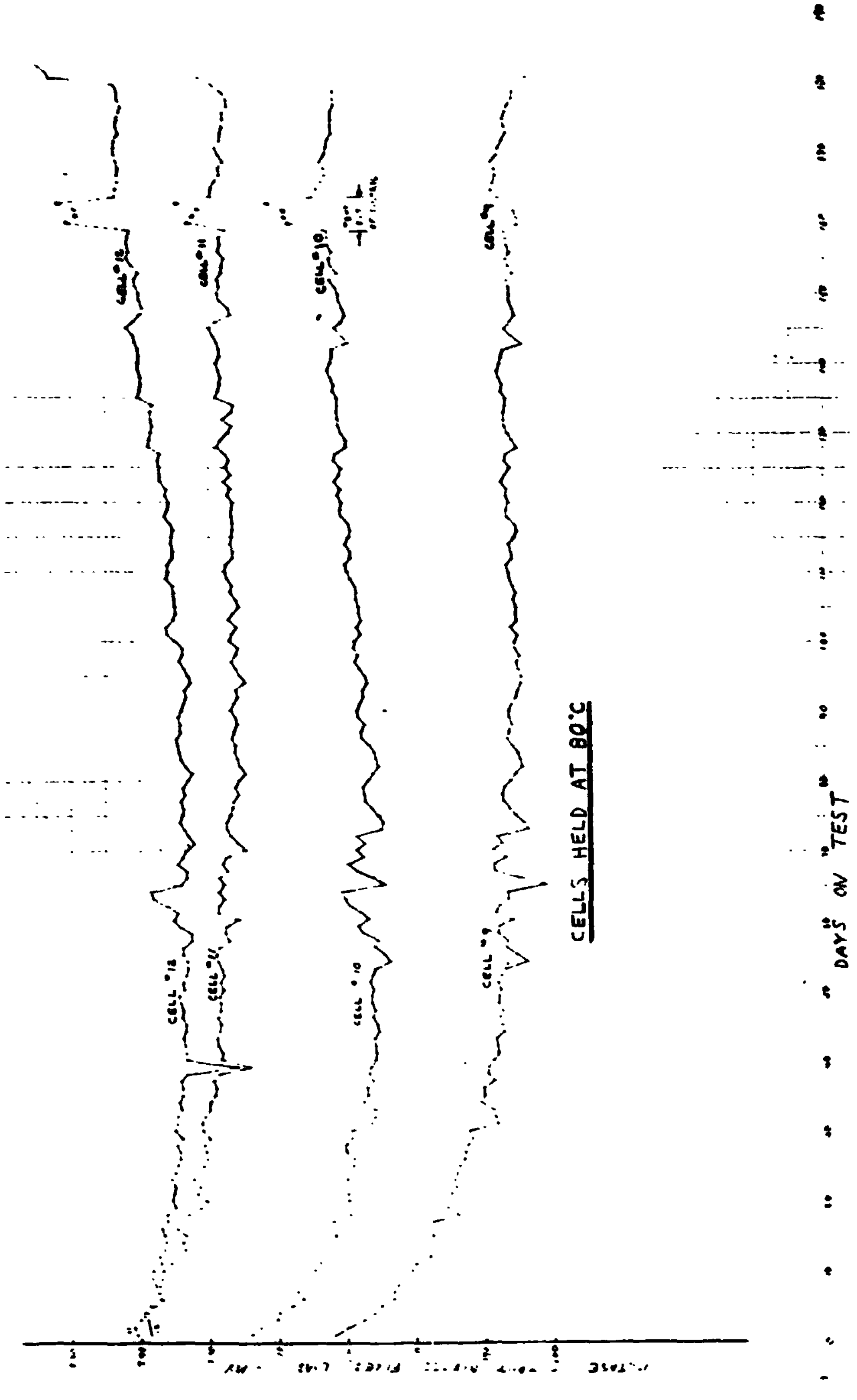
CELLS HELD AT 80°C
DAYS ON TEST
CELL #12
CELL #11
CELL #10
CELL #9

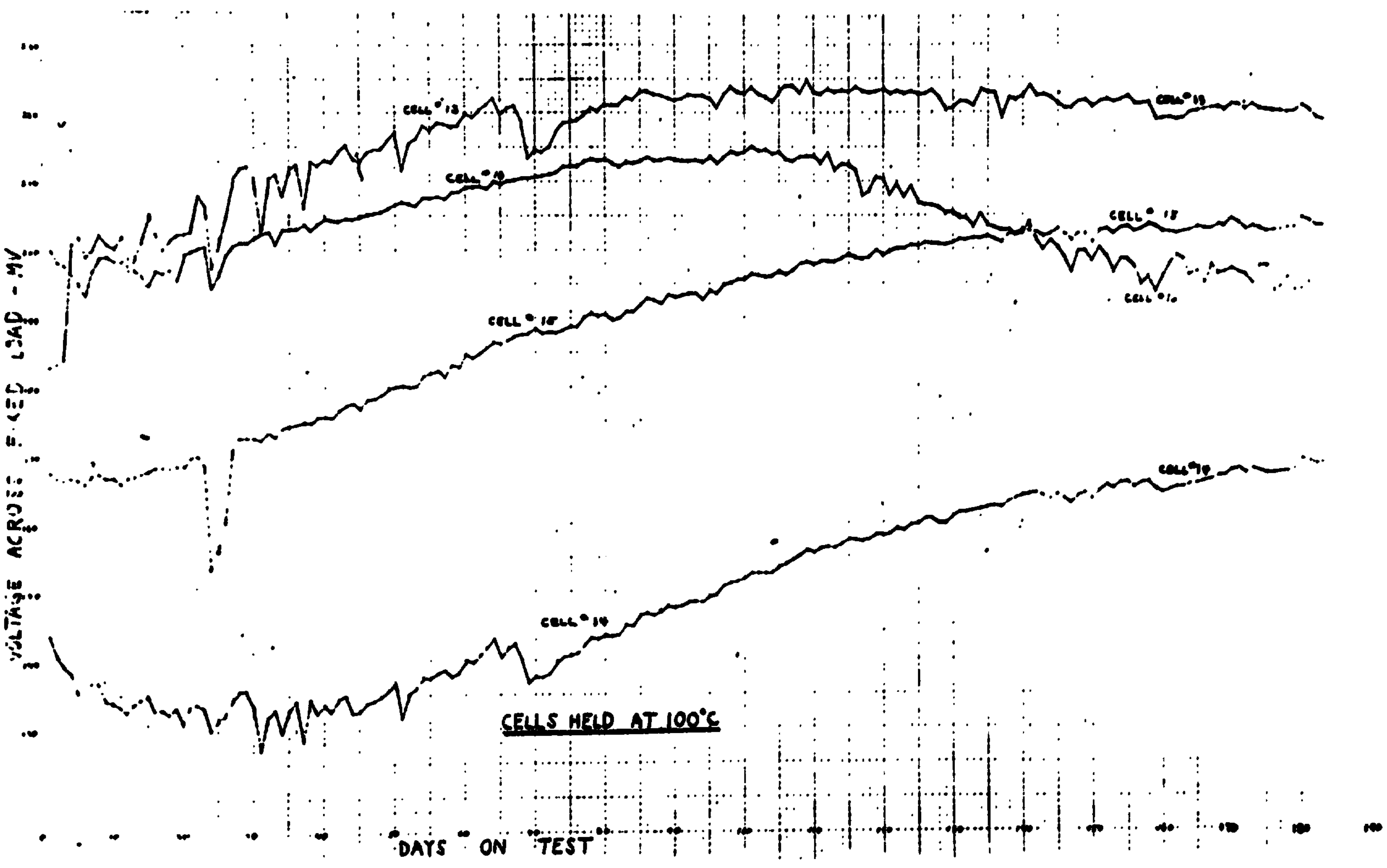
CELLS HELD AT 100°C

CHANGE IN MAX. POWER - AM1 at 25°C
AFTER SIX MONTHS ACCELERATED EXPOSURE
(Tested by NASA, LEWIS)

Temp. of Exposure	Cell No.	CHANGE IN MAX. POWER
40°C	1	-11.4%
	2	- 0.5
	3	0.0
	4	- 6.3
60°C	5	+ 0.9
	6	+ 0.9
	7	- 1.7
	8	+ 3.6
80°C	9	- 2.3
	10	+ 2.3
	11	+ 0.9
	12	+ 3.1
100°C	13	- 9.9
	14	+ 4.7
	15	+ 9.6
	16	-23.4

SUMMARY
CHANGE IN CELL PARAMETERS
AT AM1-25°C
AFTER SIX MONTHS ACCELERATED EXPOSURE

PARAMETER	Average Percent Change at:			
	40°C	60°C	80°C	100°C
OCV	-0.2	+1.4	+1.6	-1.8
SCC	-1.7	+1.1	+3.4	+12.7
M.P.	-4.6	+0.9	+1.0	-4.8
FILL	-2.8	1.6	-3.8	-14.4
R_S	+65	+54	+49	+134
R_{SH}	-51	-36	-51	-60
C	-2.1	-0.4	-1.3	-35.4

E- SUMMARY OF KEY RESULTS

1. CDS CELL FABRICATION FACILITY OPERATIVE
   REACHED 5% AVERAGE AM1 EFFICIENCY FOR STD. PROCESS
   FOR TERRESTRIAL DESIGN CELL. ALL CELLS OVER 4%.

2. METHOD DEVELOPED FOR APPLYING VACUUM EVAPORATED FINE MESH GRID CONTACT - BASICALLY LOW COST METHOD USING APERTURE MASK.

3. PROTECTED CELLS SHOW NO DEGRADATION OF OUTPUT ON REAL TIME TEST AT 6 MONTHS

4- ACCELERATED TEST OF PROTECTED CELLS INDICATE NO PROBABLE DEGRADATION OF OUTPUT UNDER NORMAL CONDITIONS FOR AT LEAST SEVERAL YEARS

5- ACCELERATED TEST AT ELEVATED TEMPERATURES AND HEAVIER DUTY CYCLES IS SHOWING CHANGES IN BASIC CELL PARAMETERS - WHICH SHOULD LEAD TO MORE ACCURATE PROJECTIONS OF CELL LIFETIMES

F- MAJOR PROBLEMS

1. VACUUM EVAPORATED GRIDS APPARENTLY SHORTING CELLS.

2- PRINTED GRIDS TOO HIGH IN RESISTANCE AND TOO COARSE IN RESOLUTION.

G- PLANNED ACTIVITY - NEXT 6 MONTHS

1- UPGRADE STD PROCESS FACILITY FOR
   HIGHER OUTPUT (> 5%), MORE REPRODUCIBLE,
   HIGH YIELDS
   - A- QUALITY & HOMOGENEITY OF CDS FILM
   - B- TOPOLOGY & STRUCTURE OF SUBSTRATE
   - C- DOPING OF Cu_2S LAYER
   - D- OPTIMIZE ETCH & DIP PROCESS

2- CONTINUE DEVELOPMENT OF LOW COST GRID
   - A- EVAPORATED METAL - NON-SHORTING CONTACT
   - B- PRINTED GRID - LOWER RESISTANCE, FINER RESOLUTION
   - C- DEVELOP INTERCONNECTION FOR FINE & COARSE GRIDS

3- DEVELOP ENCAPSULATION - PASSIVATION MEANS
   - A- CONTROL Cu_2S SURFACE STATES - H_2, AR, N_2
   - B- ENCAPSULATION - SiO_2, Al_2O_3, Si_3N_4 EVALUATE
     FOR IMPERMEABILITY, COMPATIBILITY, OPTICAL COUPLING,
     LONG LIFE
   - C- EVALUATE MULTIPLE COATINGS - FOR OPTIMIZATION OF
     CONFLICTING REQUIREMENTS

4- CONTINUE LIFE TESTING
   - A- CORRELATE REAL TIME & ACCELERATED TEST RESULTS
   - B- IDENTIFY MODES OF DEGRADATION
   - C- DETERMINE MAGNITUDES OF EACH & ACTIVATION ENERGY
     WHERE APPLICABLE
   - D- PROJECT LIFETIMES FOR EACH DEGRADATION MODE FOR
     TYPICAL EXPOSURES & DUTY CYCLES

G- PLANNED ACTIVITY - NEXT 6 MONTHS

5- STUDY WAYS TO INCREASE CELL OUTPUT
  A- SCC - INCREASE ABSORPTION, IMPROVE LIFETIME IN Cu_2S
  B- OCV - INCREASE BY SELECTED DOPING
  C- FILL FACTOR - DECREASE R_S - INCREASE R_{SH}
  D- ALTERNATE CELL CONSTRUCTIONS
  E- ANALYSIS OF LOSSES IN CELLS

6- REDUCE EVENTUAL COST POTENTIAL
  A- LOWER COST MATERIALS
  B- THINNER LAYERS - PARTICULARLY CDS
  C- IMPROVE PROCESSING

7- STUDY COMPOSITION & STRUCTURE OF Cu_2S/CdS
  A- HIGH VS LOW OUTPUT CELLS
  B- SEM & DIMA STUDIES OF JUNCTION REGION
  C- BASIC STUDIES AT UNIVERSITY OF PITTSBURGH

N76 12492

DIRECT SOLAR ENERGY CONVERSION
FOR
LARGE SCALE TERRESTRIAL USE

AER 72-03478

Formerly GI-34872

6/1/72 - 6/30/75
$981,000

7/1/75 - 6/30/76
$484,974

Principal Investigators
Karl W. Böer
John D. Meakin

Institute of Energy Conversion
University of Delaware
Newark, Delaware 19711

National Solar Photovoltaic Program Review Meeting

July 22-25, 1973
Los Angeles, California

OBJECTIVES

1) Improve cell performance, stability and life expectancy
2) Improve understanding of cell mechanisms with direct experimental verification
3) Improve gridding and encapsulation to improve life expectancy

PAST ACTIVITIES

As a result of the three year program up to June, 1975, major advances have been made in the reproducible production of CdS cells, the understanding of cell formation and operation mechanisms and the understanding and control of cell degradation mechanisms.

Cells can now be reliably made on copper/zinc, molybdenum, Fe-Ni, zinc and cadmium stannate on quartz. In February, 1975, a run of 60 large (55 cm^2) cells produced a yield of 85% with a mean efficiency of 4.4% and a maximum efficiency of 5.2%. During May, 1975, 20 small (4 cm^2) control cells were produced with a mean efficiency of 5.5% and a maximum efficiency of 6.0%. These efficiencies are under Tungsten-Iodine simulation; the cells are blue sensitive and roof-top testing generally shows a 10% enhancement. The best cell to date shows a 6.8% natural insolation efficiency. Cells are generally made on Cu/Zn substrates with a CdS layer of 20-25 micron thickness.

Procedures and controls have been refined to the extent that transfer to other groups and organizations can be successfully accomplished.

The influence of temperature and illumination intensity on Cell I-V characteristics have been used to identify the effective barrier height, to isolate the effects of blocking contacts and to non-destructively determine the stoichiometry of the surface copper sulfide.

A major improvement in reproducibility and cell performance has been achieved by extensive vacuum heat treatments after cell gridding and lamination. Degradation due to interaction with oxygen and water vapor can be reversed by either hydrogen or vacuum heat treatment.

Roof top testing of cells protected from the atmosphere has shown no detectable degradation after twenty months. Accelerated testing has been conducted at temperatures from 46 to 85°C in various ambients. Lifetimes (degradation to 1/e of initial performance) in excess of twenty years have observed at ≤50°C. It is concluded that suitably hermetically sealed cells will be adequately stable for terrestrial applications.

Quantitative descriptions of the short circuit current have been developed and the importance of reflection from the substrate in front wall cells revealed.

The dominance of interface recombination in controlling the open circuit voltage has been identified.

Structural studies have resulted in a more complete understanding of the cell. Minority carrier diffusion distances have been measured in actual cells. Some changes occurring during degradation have been identified.

During the initial part of the program, studies of toxicity problems and economic assessments established that neither of these considerations presented likely obstacles to large scale utilization of CdS Solar Cells.

CURRENT ACTIVITIES

Various techniques to increase the open circuit voltage are being explored. It had been previously observed that cells made on CdS deposited from a single source gave a consistently higher V_{oc}. Further tests have now shown that this effect may in fact relate to differences in source and substrate temperatures. The resulting differences in CdS structure and crystallinity are being documented. Deposits of mixed CdS and ZnS are being produced and will be initially made into cells using the conventional barriering technique. Precision lattice parameter measurements will be used to monitor composition.

Analysis of I-V characteristics at temperatures between 25 and 110°C is being perfected to provide non-destructive analysis of the Cu_2S. Changes due to vacuum heat treatments and exposure to oxygen are also being monitored by the same technique. In a parallel O.N.R. program, detailed spectral response measurements are being made.

Ultra-high vacuum equipment is being readied to conduct controlled reaction experiments between the copper-sulfide layer and atmospheric components, to be followed by vacuum heat treatments. In situ mass spectroscopy will identify species emitted during these experiments.

Direct observation of the Cu_2S layer and the interface with CdS is under way using transmission electron microscopy. Atmosphere related degradation will also be followed by this technique.

FUTURE PLANS

Primary thrusts during the next 6 months will be directed towards achieving higher open circuit voltages and the fundamental understanding of degradation mechanisms. Techniques to be attempted to achieve the former will include the use of ZnS-CdS mixtures to give a better lattice and electron affinity match to Cu_2S, also the effects of changes in the orientation of the CdS will be explored.

Both theoretical and experimental studies will be made to identify more critically the changes occurring during vacuum heat treatments and exposure to the atmosphere. Support studies of the influence of doping on copper diffusion in CdS, the properties of isolated Cu_2S films and changes in minority carrier diffusion in Cu_2S in various cells are expected to yield valuable results.

KEY RESULTS

- Reliable production technique developed on low cost metallic substrate.
  Large cells (55 cm^2) of mean efficiency ~5%
  Small cells (4 cm^2) of mean efficiency ~6%
  Best cell 6.8%
- Usable cell life in excess of 20 years supported by roof-top and accelerated testing
- Quantitative description of short circuit current. Role of CdS, Cu_2S and the interface region elucidated.
- Dominant role of interface recombination on V_{oc} established. (Conventional model)
- Structure of as-formed cell and effects of degradation substantially established.
- Regeneration accomplished by vacuum and hydrogen heat treatment.

CELL EFFICIENCIES

2/24/75-2/28/75

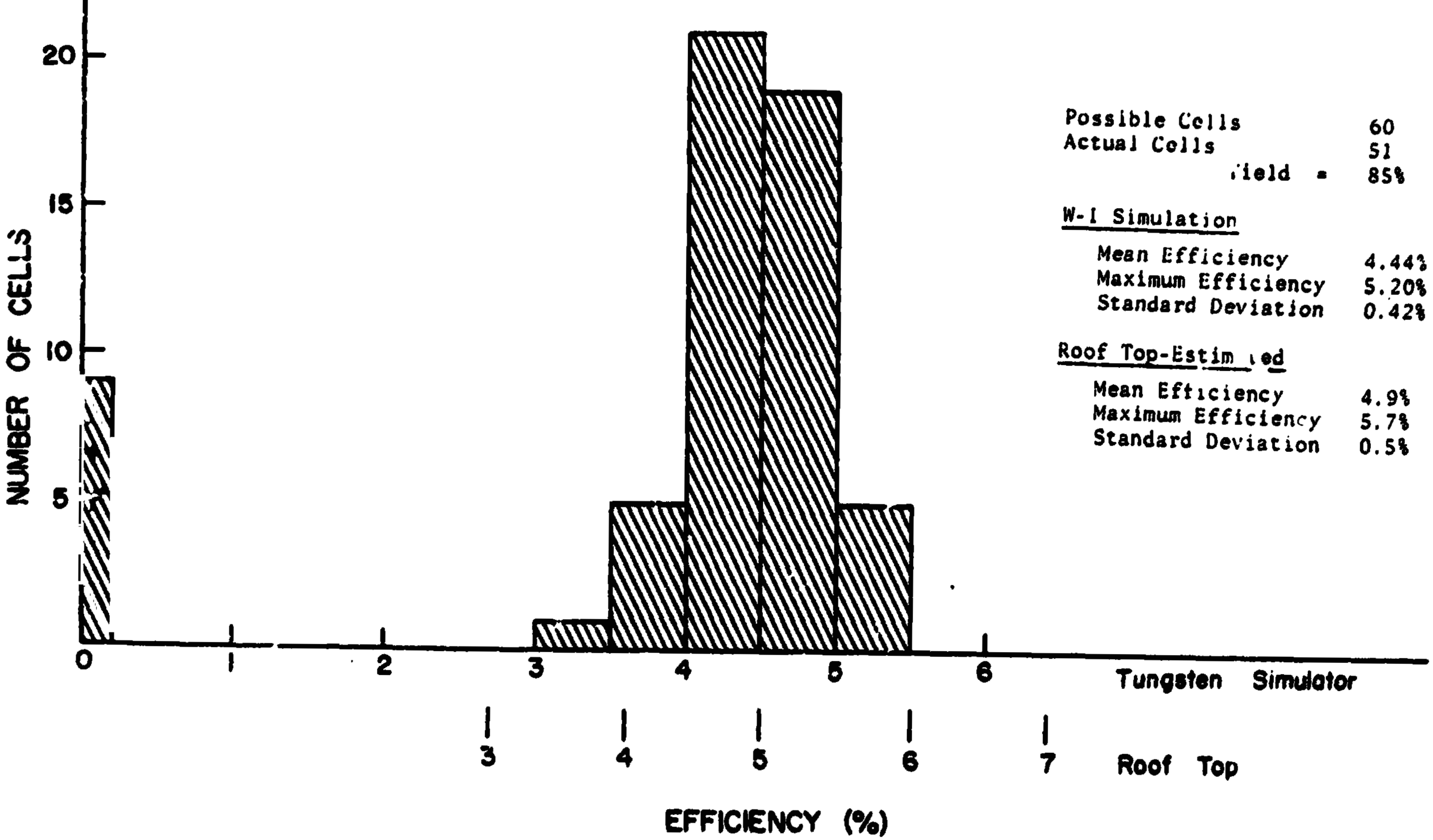

Possible Cells	60
Actual Cells	51
Yield =	85%

W-I Simulation

Mean Efficiency	4.44%
Maximum Efficiency	5.20%
Standard Deviation	0.42%

Roof Top-Estimated

Mean Efficiency	4.9%
Maximum Efficiency	5.7%
Standard Deviation	0.5%

Yield of 4 cm^2 Cells From 5 Copper Substrates
Processed 5/19/75 to 5/29/75.
(Measured on Pilot Line Tungsten - Iodine Simulator)
Average Efficiency = 5.50 % (20 Cells)

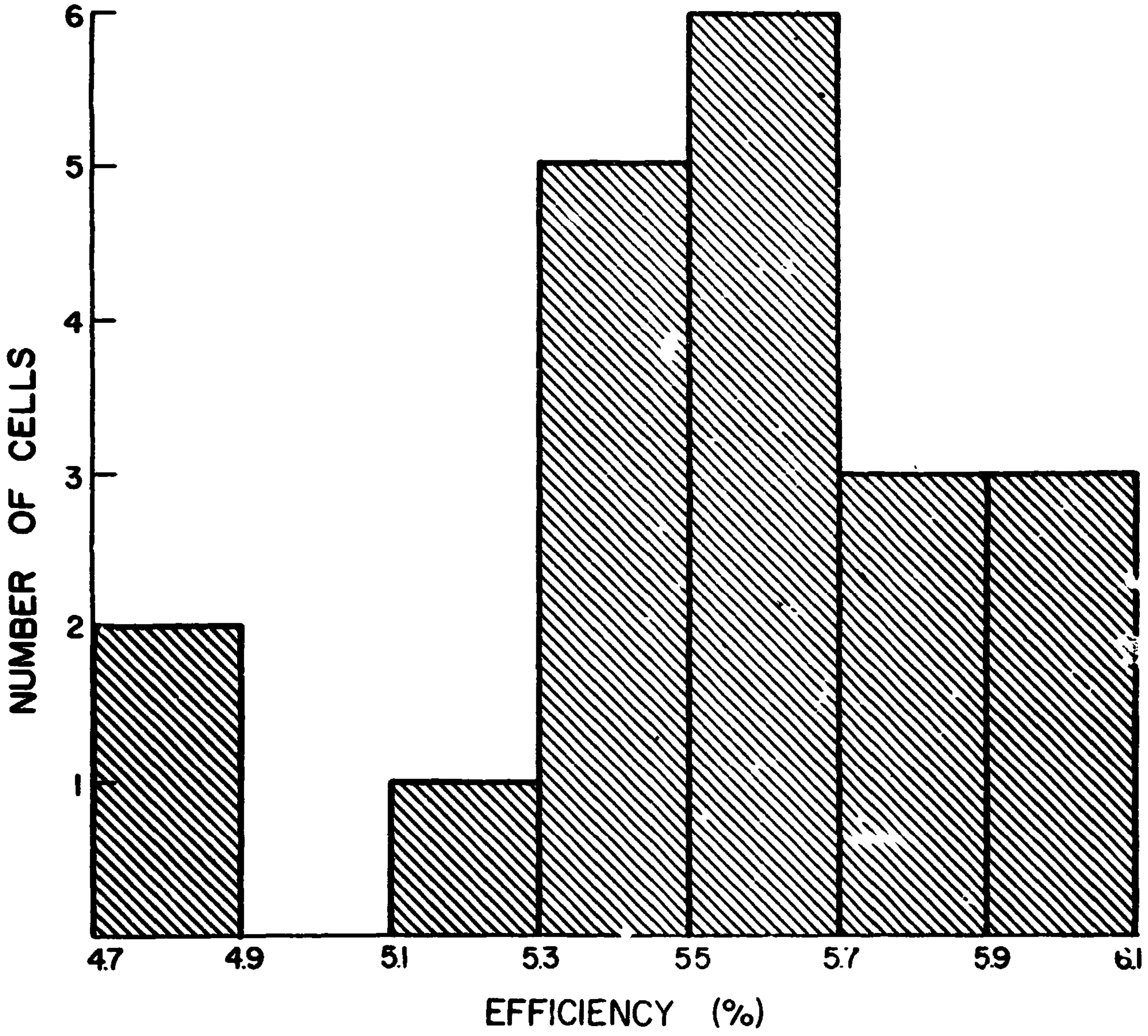

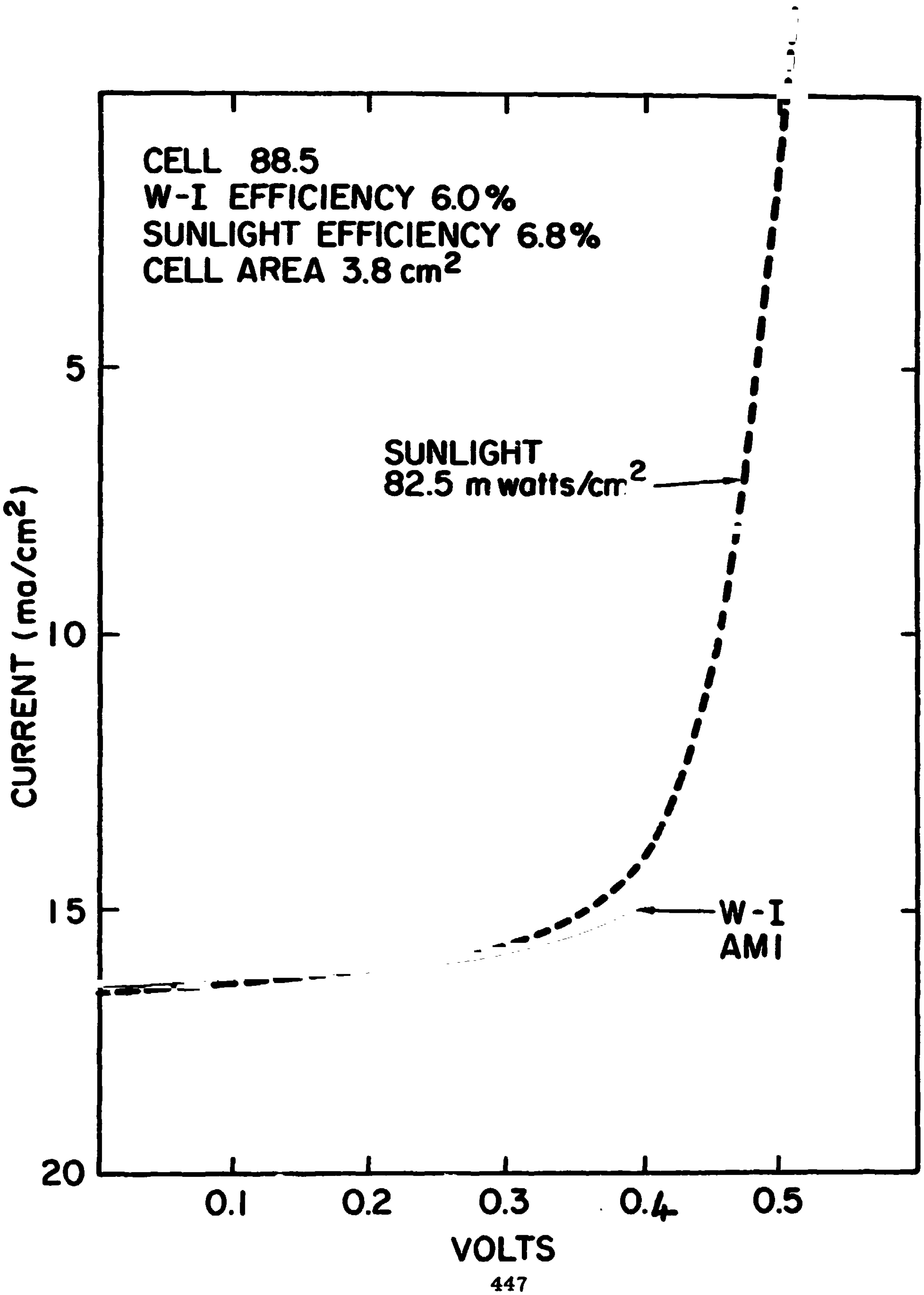
CELL 88.5
W-I EFFICIENCY 6.0%
SUNLIGHT EFFICIENCY 6.8%
CELL AREA 3.8 cm2
SUNLIGHT
82.5 m watts/cm2
W-I
AMI
CURRENT (ma/cm2)
5
10
15
20
0.1
0.2
0.3
0.4
0.5
VOLTS

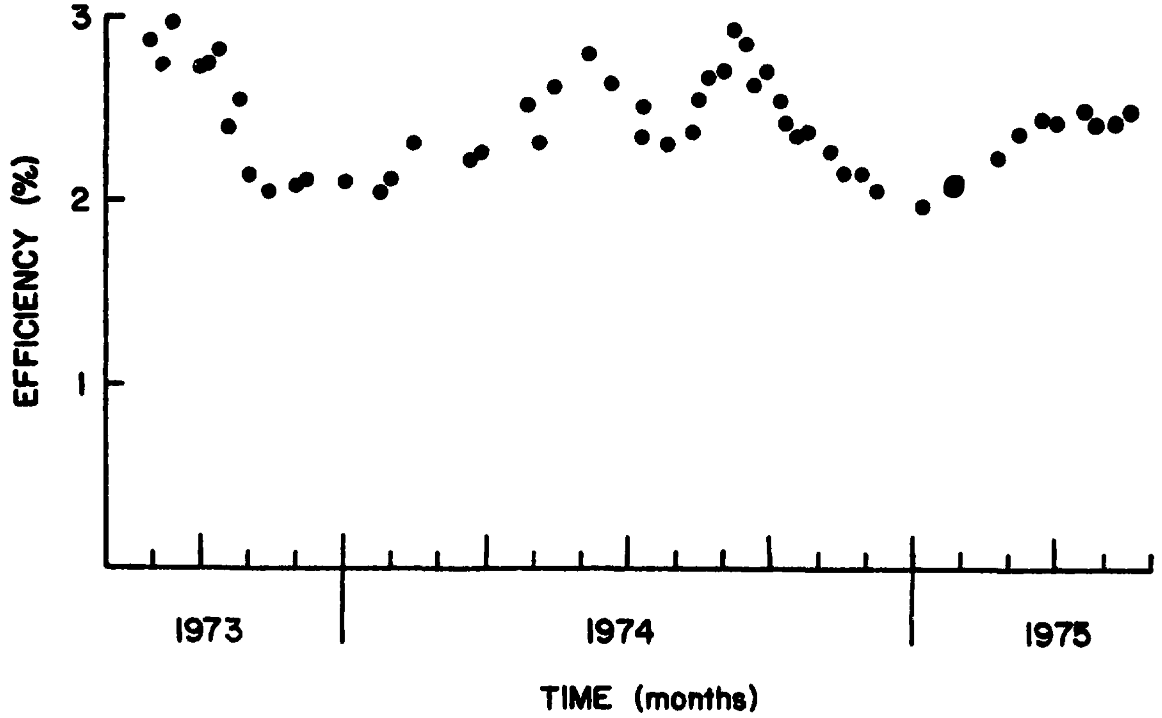

Net ar[illegible] efficiency of 104 cells deployed on Solar One

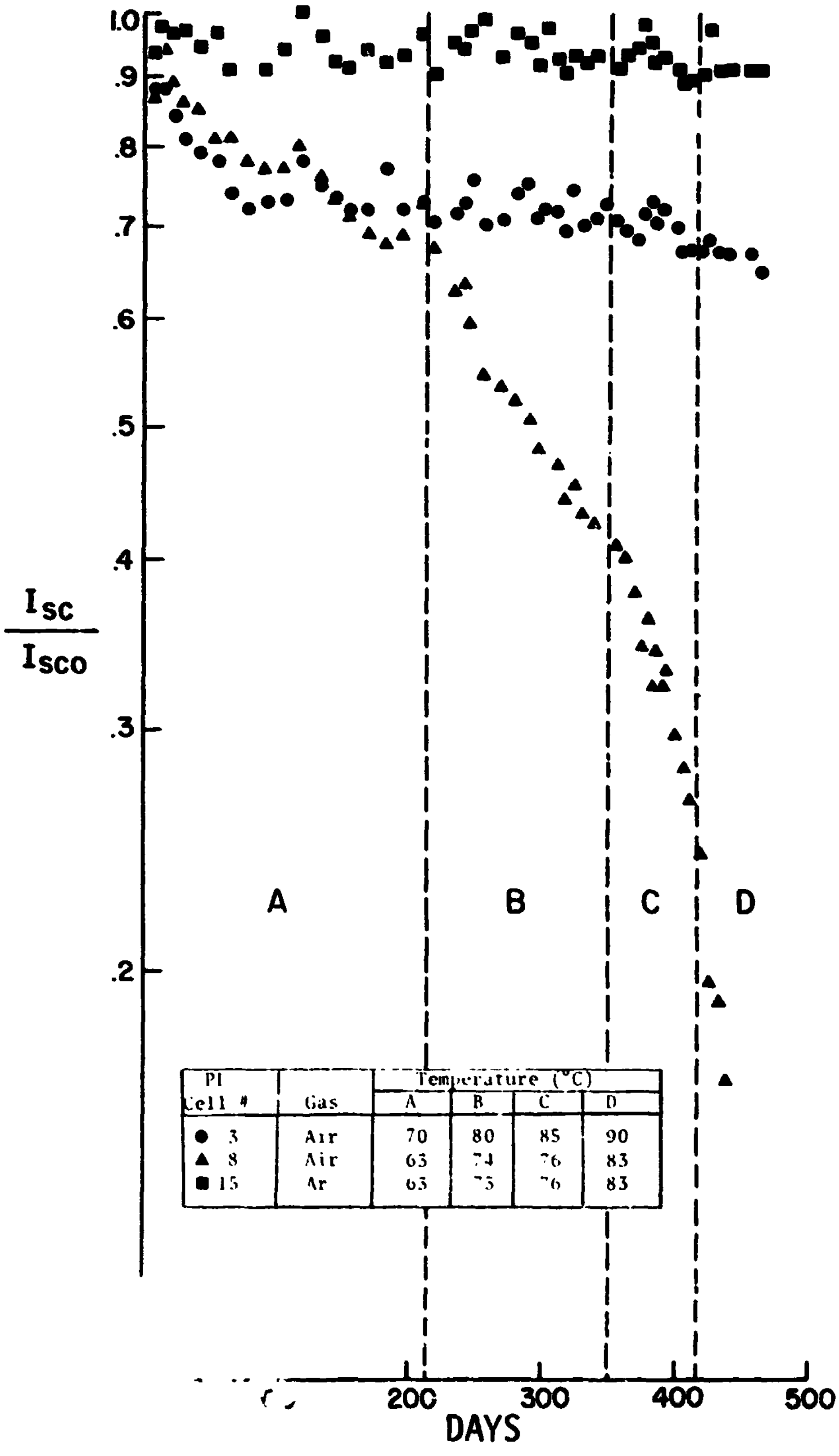1.0
.9
.8
.7
.6
.5
.4
.3
.2
Isc / Isco
A
B
C
D
200
300
400
500
DAYS
PI Cell #
Gas
Temperature (°C)
A
B
C
D
● 3 | Air | 70 | 80 | 85 | 90
▲ 8 | Air | 63 | 74 | 76 | 83
■ 15 | Ar | 63 | 75 | 76 | 83

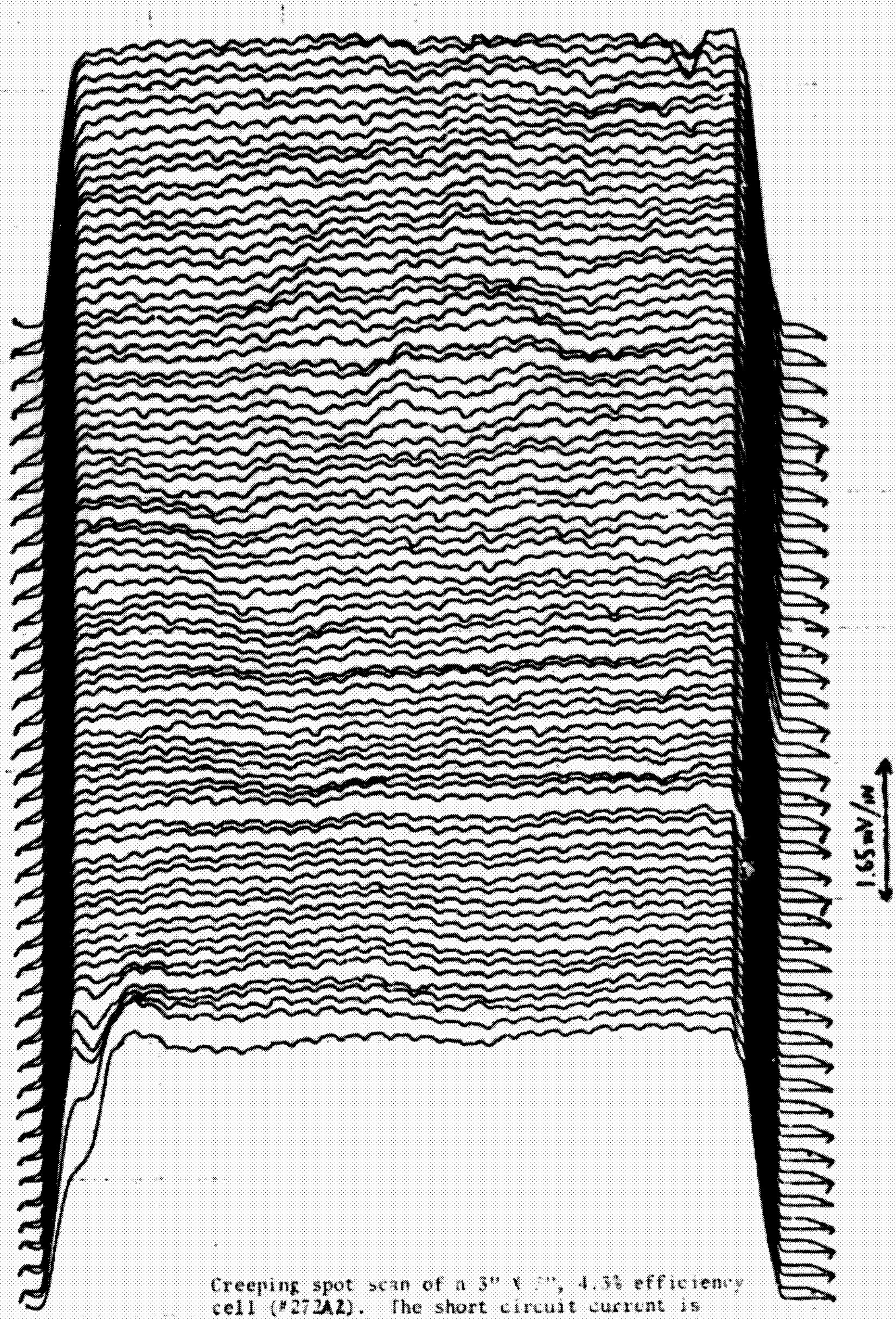

Creeping spot scan of a 3" X 3", 4.3% efficiency cell (#272A2). The short circuit current is plotted as a function of the x-y position of a 4 mm spot.

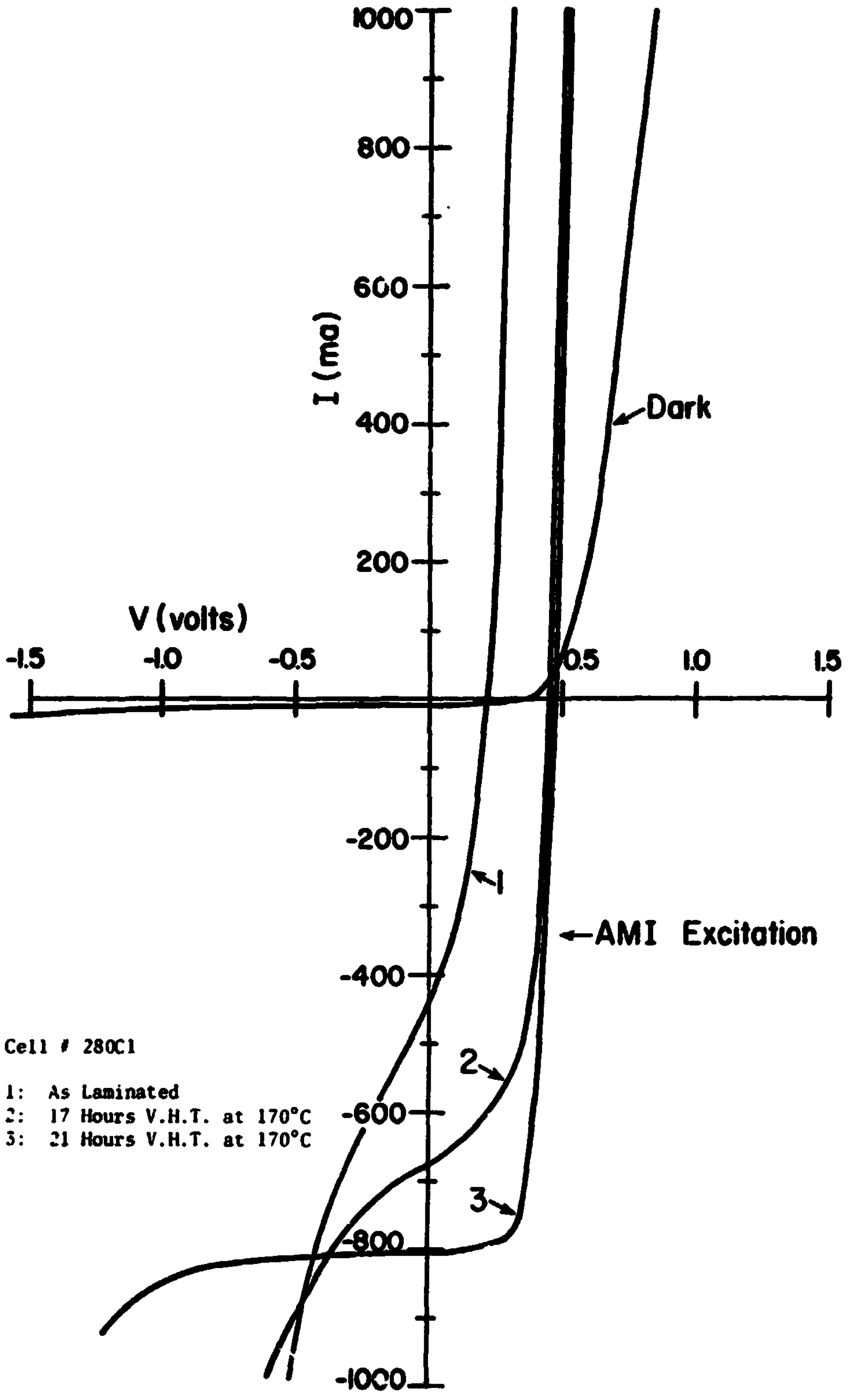1000
800
600
400
200
-200
-400
-600
-800
-1000
I (ma)
V (volts)
-1.5
-1.0
-0.5
0.5
1.0
1.5
Dark
1
2
3
AMI Excitation
Cell # 280C1
1: As Laminated
2: 17 Hours V.H.T. at 170°C
3: 21 Hours V.H.T. at 170°C

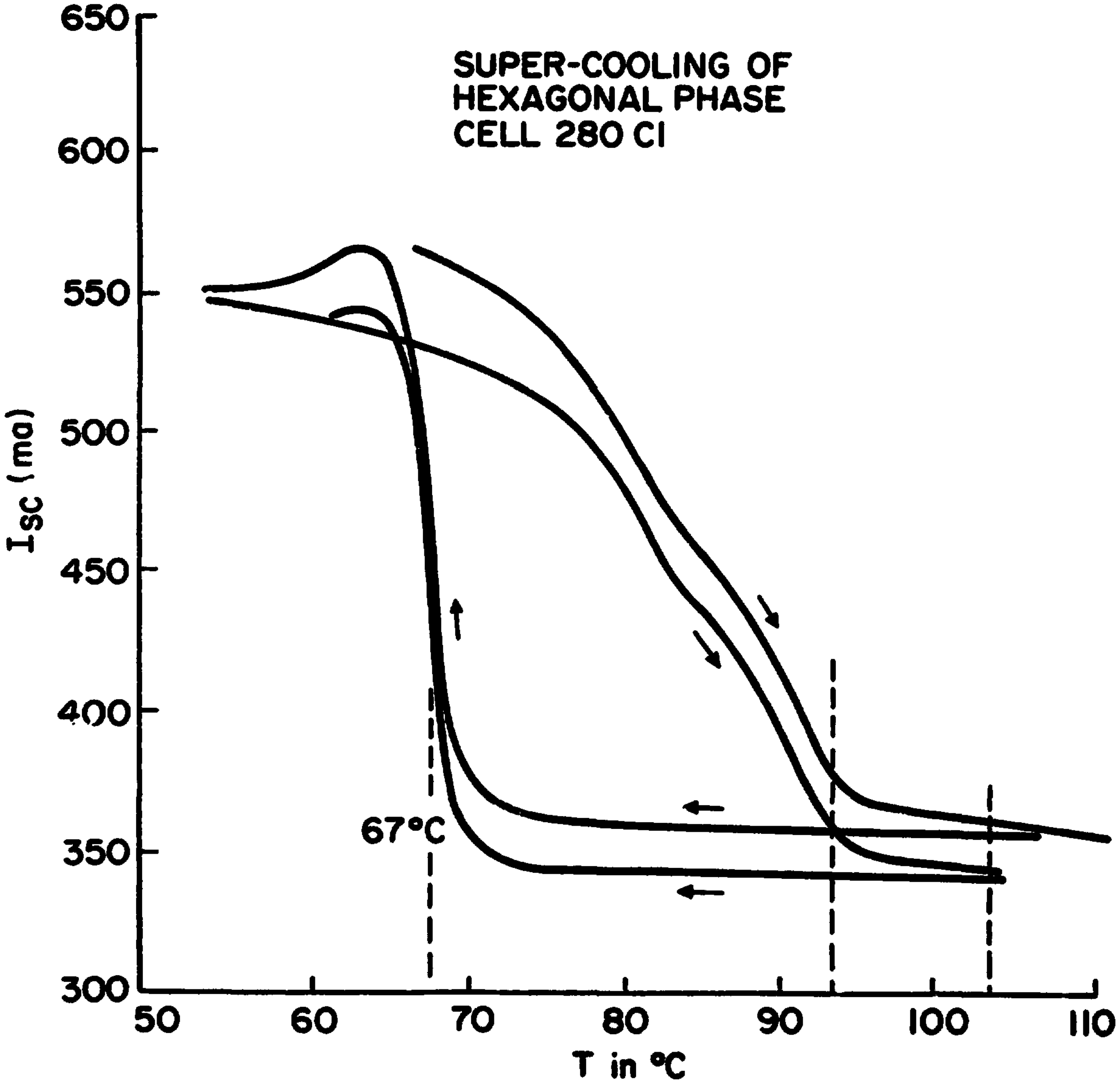
SUPER-COOLING OF
HEXAGONAL PHASE
CELL 280 CI
I_{SC} (ma)
650
600
550
500
450
400
350
300
50
60
70
80
90
100
110
T in °C
67°C

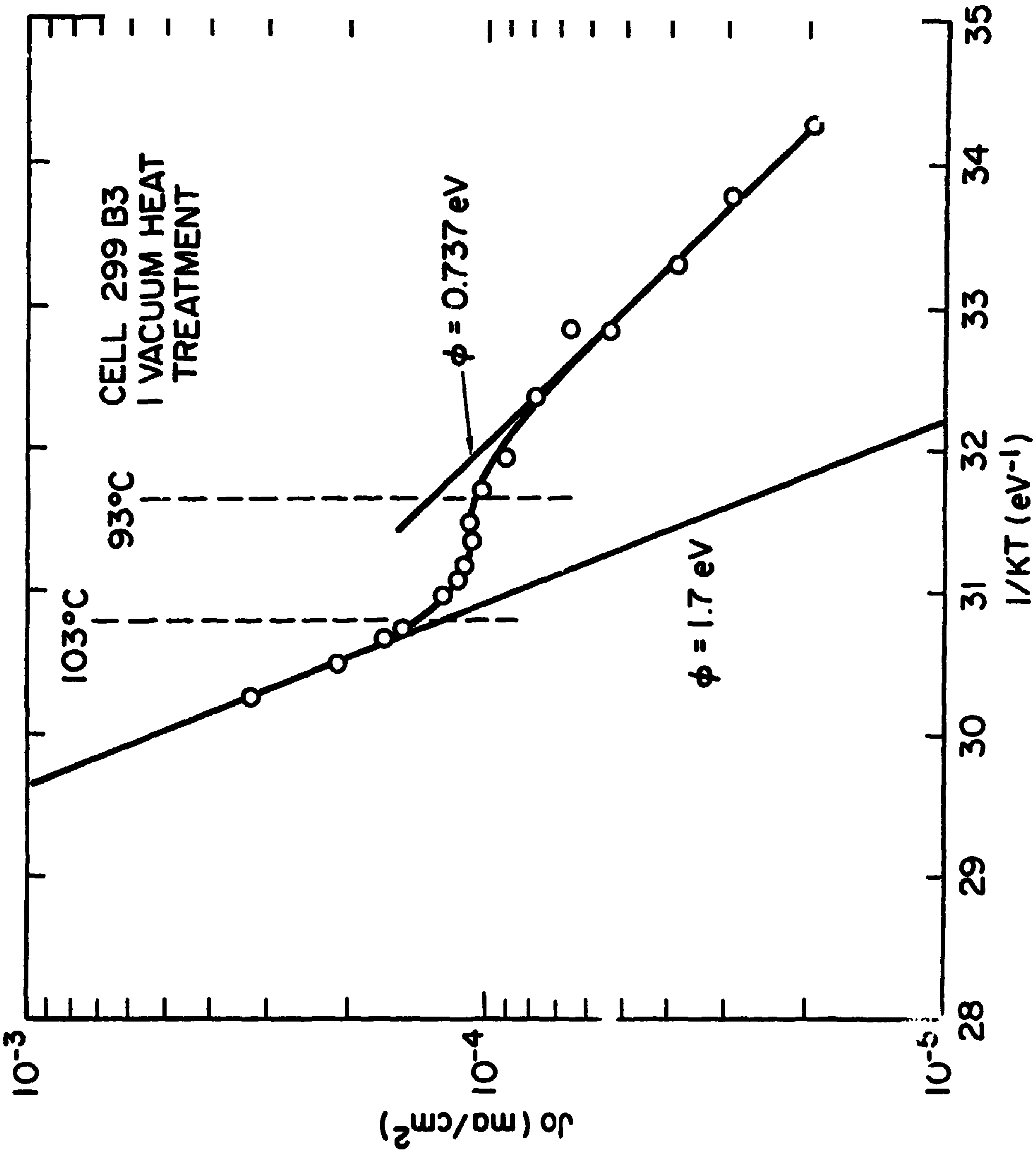
CELL 299 B3
1 VACUUM HEAT
TREATMENT
93°C
103°C
φ = 0.737 eV
φ = 1.7 eV
Jo (ma/cm²)
10^{-3}
10^{-4}
10^{-5}
1/KT (eV⁻¹)
28
29
30
31
32
33
34
35

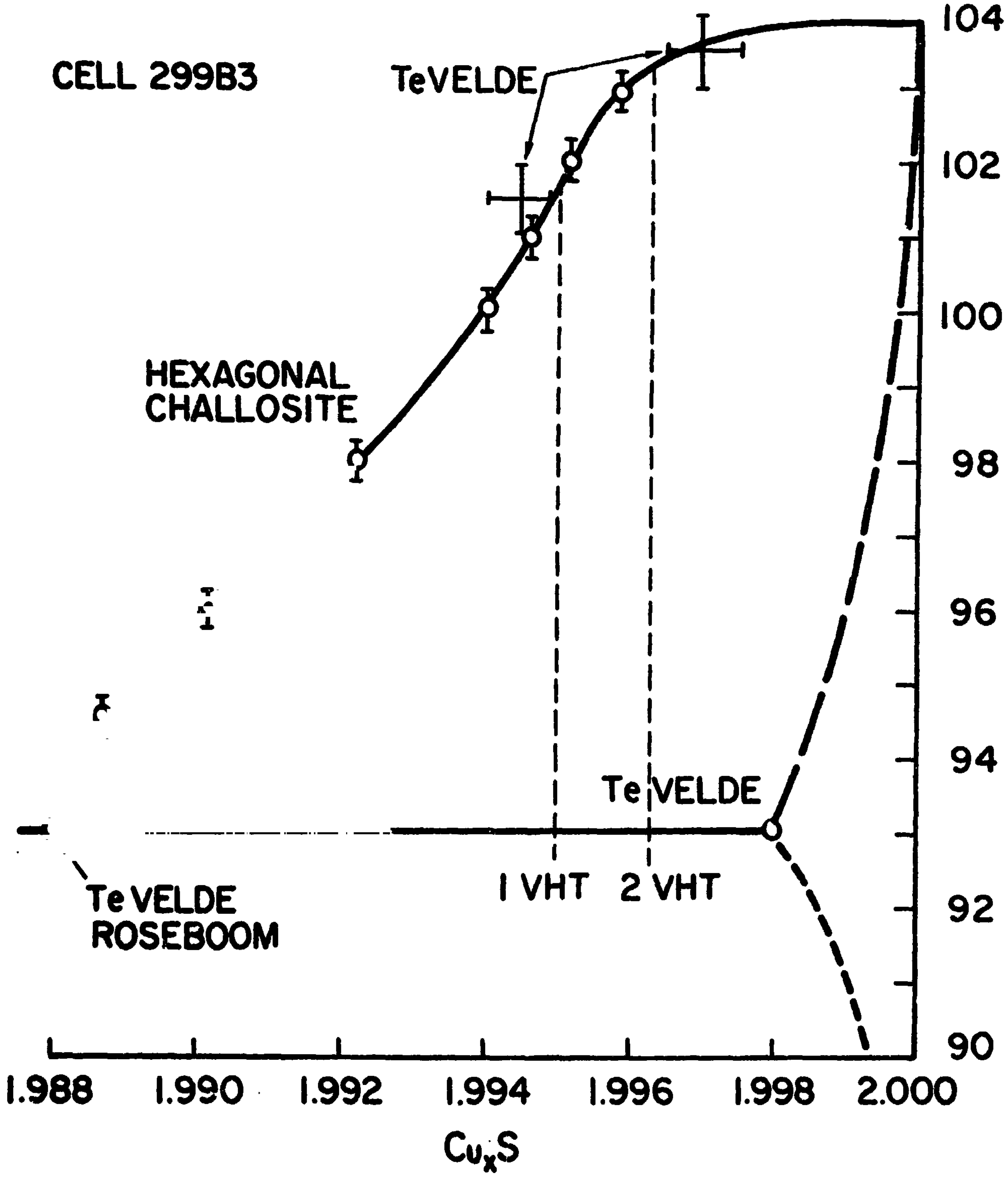

Influence of vacuum heat treatment on the mean composition of Cu-S phase. The hexagonal chalcocite phase boundary is deduced from the temperature variation of j_o.

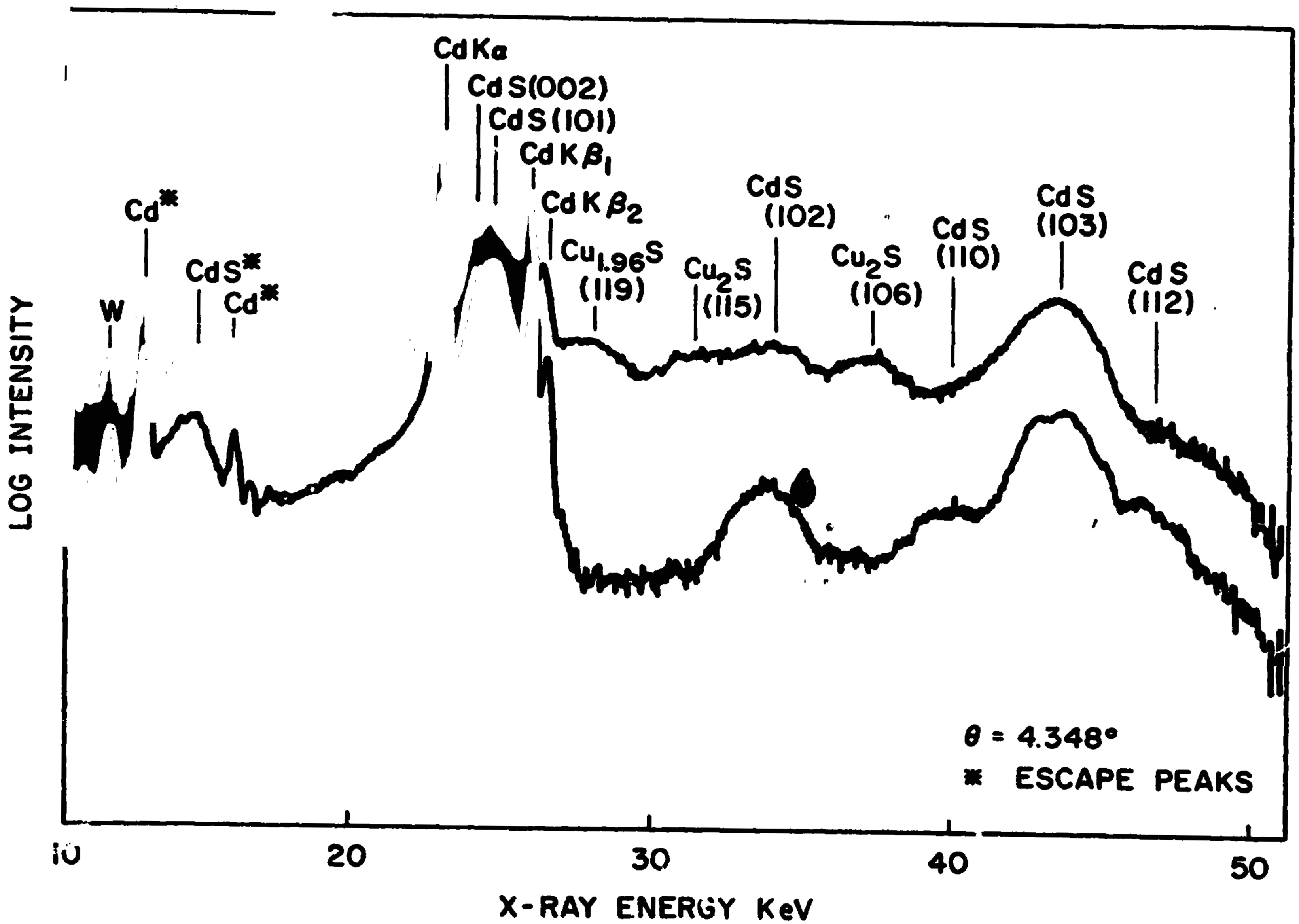

Energy dispersive x-ray scan of a Cu_xS layer. Chalcocite (Cu_2S) and djurleite ($Cu_{1.96}S$) peaks are identified in the top curve. The lower curve resulted after the Cu_xS layer was removed by KCN.

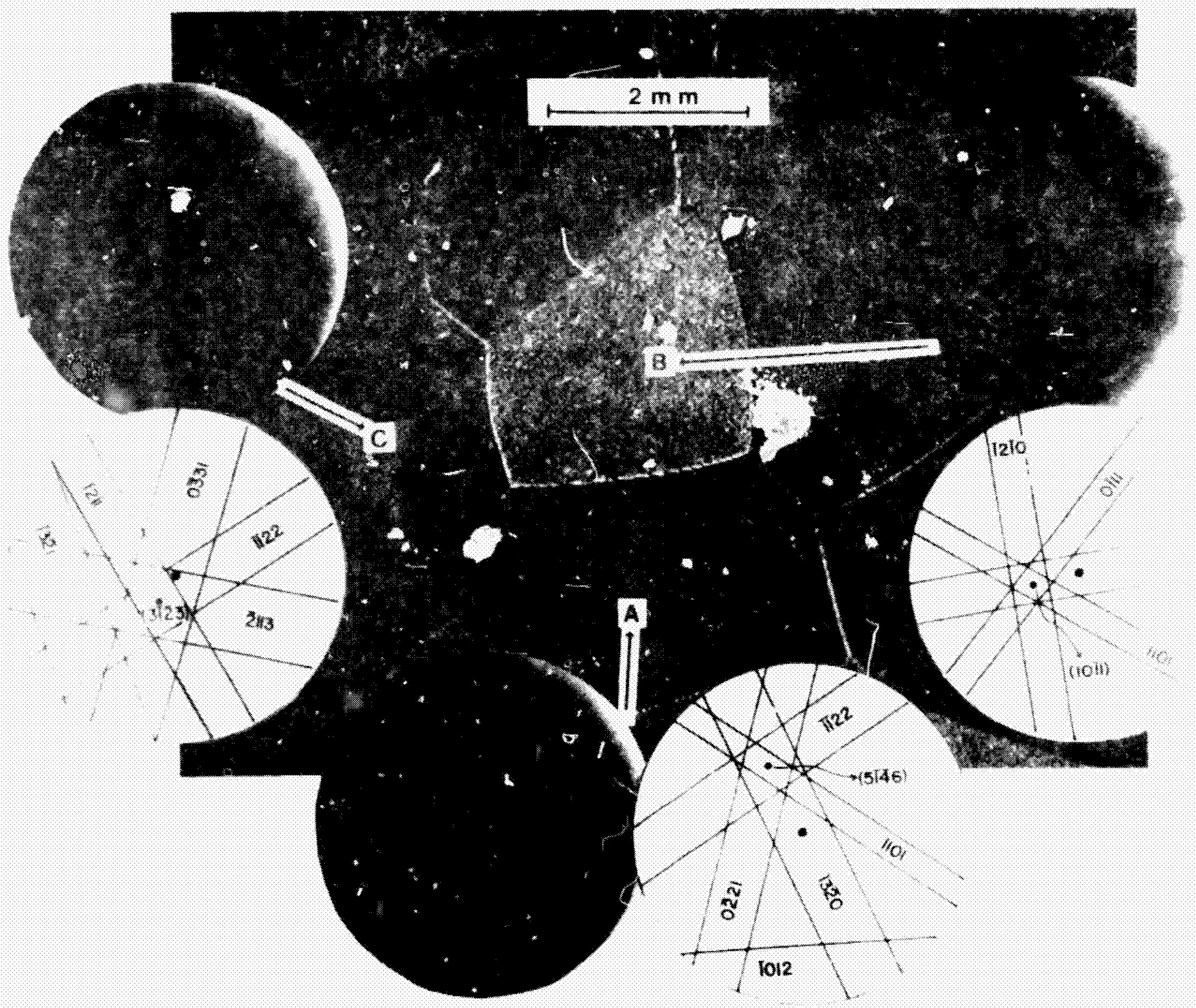

Fig. SEM Micrograph obtained from a vapor-grown CdS film. The insets are channelling patterns from their corresponding grains.

CELL 63-E

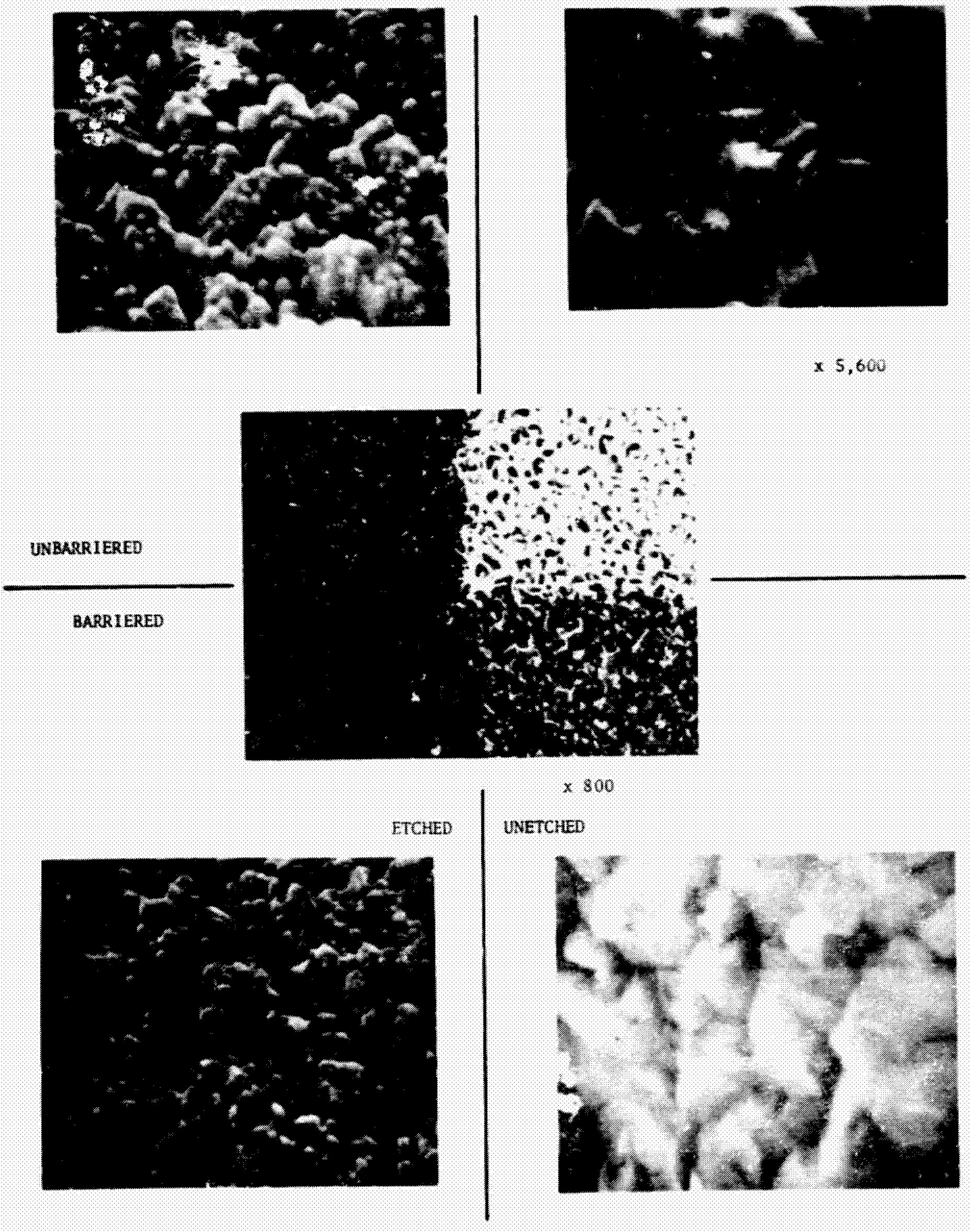

C.6

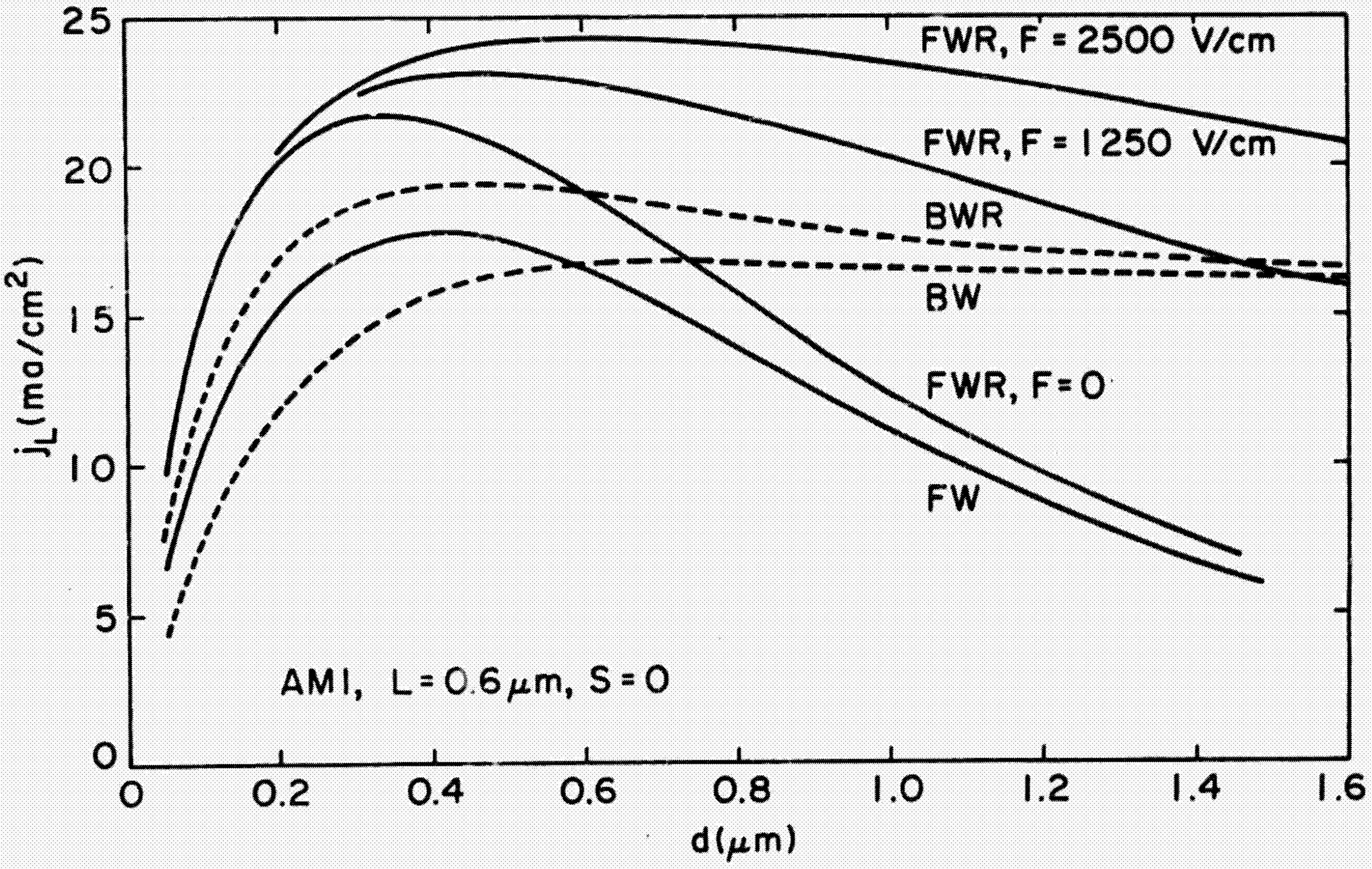

Calculated current densities, including reflection losses for CdS/Cu$_2$S cells.
FW - front wall; BW - back wall; R - with reflection. F - field in CdS.
F=0 unless specified.

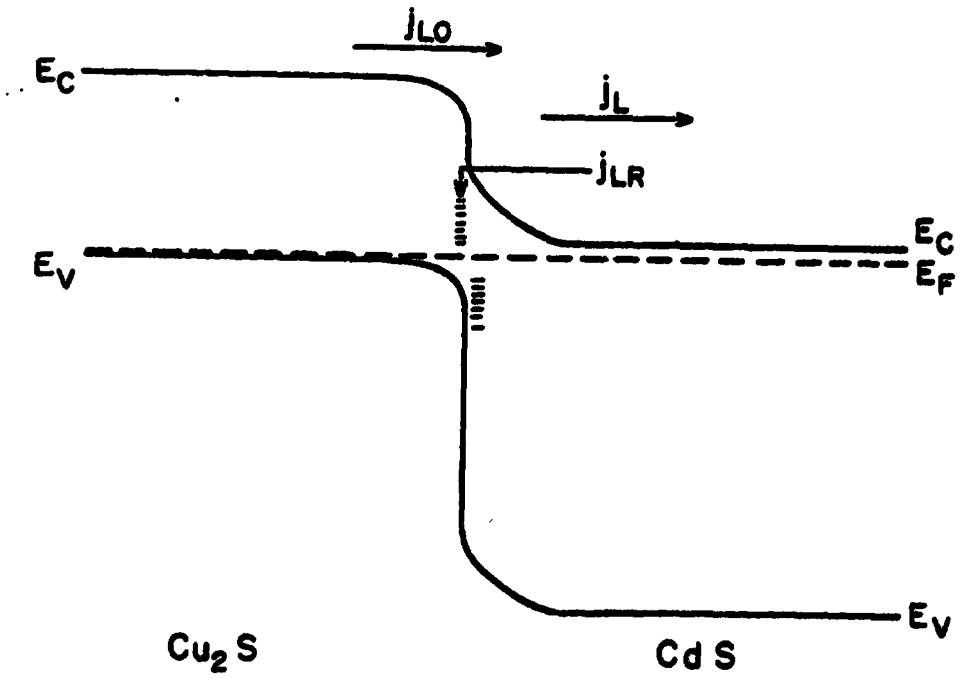

Band diagram for cell showing junction recombination current j_{LR}

INTERFACE DOMINATED CASE

$$j(V) = qS_I\, N_{c2}\, \exp[-(qV_D + \delta)/kT]\, \exp(qV/kT) - j_L(V);\; V \geq 0.3 \text{ volt}$$

$$j_L(V) = j_{LOO}\, [1 - (\frac{d}{R})\, (1-\frac{d}{3R})] \cdot \frac{\mu_2 F_2\, [V,\, \phi\, (\lambda)]}{S_I + \mu_2 F_2 [V,\, \phi\, (\lambda)]}$$

$$V_{oc} = V_D + \delta/q + kT/q\, \ln(j_L(V)/qS_I\, N_{c2})$$

<u>Present Diode Parameters</u>

$S_I \underset{-}{\sim} 10^6$ cm/sec ;

$S_I = v_{th} \cdot \sigma_n \cdot N_I$

Lattice mismatch, $N_I \underset{-}{\sim} 5.10^{13}$ cm^{-2}

$10^{-15} < \sigma_n < 10^{-14}$ cm^2

$v_{th} \underset{-}{\sim} 10^7$ cm/sec

At 25°C

$$V_{oc} = 0.9 - 0.49 + 0.025\, \ln j_L(V)$$

$j_L = 10$ ma/cm^2 $\qquad V_{oc} = 0.468$ V

$j_L = 20$ ma/cm^2 $\qquad V_{oc} = 0.485$ V

<u>Ideal case $S_I = 0$</u>

$$j(V) = qN_{c2}\, L/\tau_n\, \exp(-E_{q1}/kT)\, \exp(qV/kT) - j_L;\; V \geq 0.3 \text{ volt}$$

$$j_L = j_{LOO}\, [1 - (\frac{d}{R})\, (1-\frac{d}{3R})];\; L/\tau_n \underset{-}{\sim} 5.10^4 \text{ cm/sec}$$

Thus $V_{oc} = 1.2 - 0.42 + 0.025\, \ln j_L(V)$

at $j_L = 20$ ma/cm^2 $\quad$ <u>$V_{oc} = 0.86$ volts</u>

N76 12493

REACTIVELY SPUTTERED THIN FILM PHOTOVOLTAIC DEVICES

GRANT APPLICATION

GRANT REQUESTED: ONE YEAR
265 K

AUTHOR/PRINCIPAL INVESTIGATOR: EDMUND J. HSIEH
LAWRENCE LIVERMORE LABORATORY
UNIVERSITY OF CALIFORNIA
LIVERMORE, CALIFORNIA

PRESENTED AT NATIONAL SOLAR PHOTOVOLTAIC PROGRAM
REVIEW MEETING, LOS ANGELES, CALIFORNIA
JULY 22-25, 1975

Abstract

REACTIVELY SPUTTERED THIN FILM PHOTOVOLTAIC DEVICES

Edmund J. Hsieh
Lawrence Livermore Laboratory
University of California
Livermore, California 94550

July 22-25, 1975, Los Angeles, California

The overall objective of our project is to apply thin film sputtering techniques to form low cost thin film photovoltaic devices from materials with direct bandgap absorption characteristics used in existing single crystal solar cells. Also, the sputtering approach will be used to improve the performance characteristics of polycrystalline solar cells. Our immediate objective is to develop a stable, high efficiency thin film CdS-Cu_2S cell by reactive sputtering techniques.

There has been a small internally supported R&D effort at LLL on CdS-Cu_2S solar cells during the last two years. Over the last few months cells have been made by the RF reactive sputtering of Cu in a hydrogen-sulfide and argon atmosphere to form Cu_2S layers on thermally evaporated CdS films. A significant characteristic of this reactive sputtering approach is that there is no dependence on an ion exchange reaction with CdS to form the Cu_2S layer. The major findings so far are:

1. Yield

   We have made over 40 cells by this new process; each exhibited a photovoltaic effect. Even though the evaporation and sputtering parameters of CdS and Cu_2S, respectively, were varied intentionally to examine the latitudes of the new process, no adverse effect on yield has been observed.

2. Efficiency

   The best observed efficiency so far, measured in sunlight, was slightly over 4%. During the short investigation period our aim was primarily to learn more of the new heterojunction-formation process. There was little effort to optimize grid design and other parameters. We observed that open circuit voltage (OCV) can be influenced by sputtering parameters related to formation of the Cu_2S. We measured OCV as high as 0.53 volts in some cells irradiated by 100 mW/cm^2 simulated sunlight. We expect even higher OCV when the process parameters are more thoroughly investigated.

3. Long Term Stability

Within this short period of testing, the new process cells were stable. Since our cells were not encapsulated no long term life test was conducted at this time. In comparison with the wet-dip process for p-n junction formation, the sputtering process minimizes the diffusion of Cu into CdS, and Cd into Cu_2S, and should result in a more stable interface. Also, the solid-state deposition of Cu_2S reduces the chance of formation of shunting paths along the grain boundaries, cracks and pin holes in the CdS substrate and, thus, prevents the start of open circuit degradation.

In the short run, we propose to exploit the additional degrees of freedom made available by the new process to optimize the efficiency of CdS cells. We plan to emphasize Cu_2S identification techniques and specification of the sputtering parameters needed to obtain stoichiometric chalcocite layers. Optimization of evaporated CdS films, including recrystallization and doping, would be a part of the effort. Also, accelerated life tests are planned to verify the cell's long term stability. In the long run, we would like to use reactive sputtering to form both films of the solar cell in a multiple station system, with a closer similarity to a production process. Finally, our sputtering approach would be used in parallel to do some fabrication of other compound semiconductor thin films, such as InP and $CuInSe_2$, for use with CdS.

We have proven in this study the feasibility of a reactively sputtered thin film CdS - Cu_2S solar cell. Identification of the reactively sputtered Cu_2S film was made by x-ray diffractometer and spectro-transmission measurements. Because of its simplicity, economical use of material, and high yield, the reactive sputtering process promises to be a low cost method for producing CdS - Cu_2S solar cells.

REACTIVELY SPUTTERED THIN FILM PHOTOVOLTAIC DEVICES

LAWRENCE LIVERMORE LABORATORY
VERMORE, CALIFORNIA

GRANT REQUESTED: ONE YEAR
265 K

PRINCIPLE INVESTIGATOR: EDMUND J. HSIEH

OBJECTIVE OF PROJECT

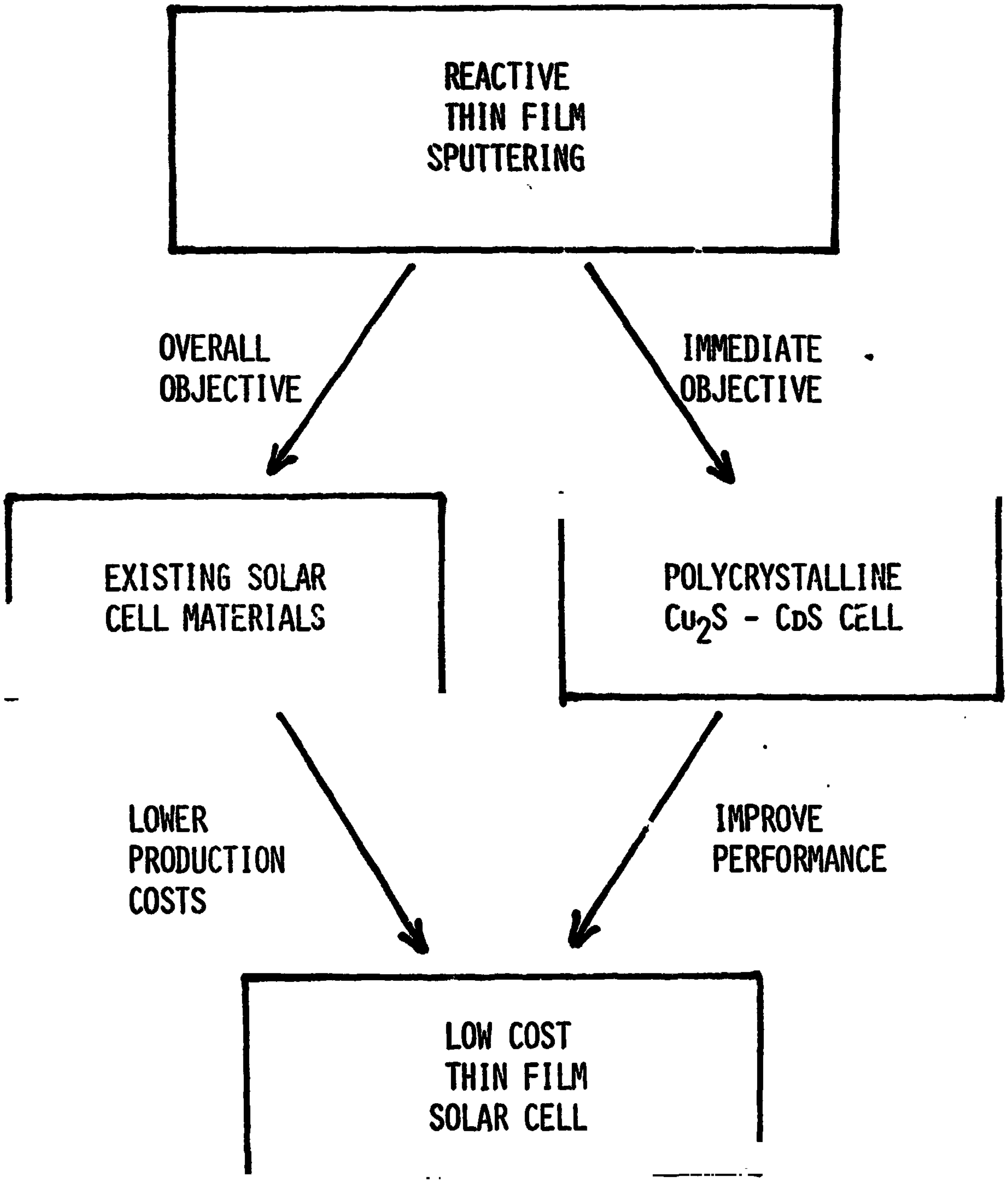

REACTIVE
THIN FILM
SPUTTERING

OVERALL
OBJECTIVE

IMMEDIATE
OBJECTIVE

EXISTING SOLAR
CELL MATERIALS

POLYCRYSTALLINE
Cu_2S - CdS CELL

LOWER
PRODUCTION
COSTS

IMPROVE
PERFORMANCE

LOW COST
THIN FILM
SOLAR CELL

REACTIVE SPUTTERING GIVES COMPOUND FILMS FROM SIMPLE METALS

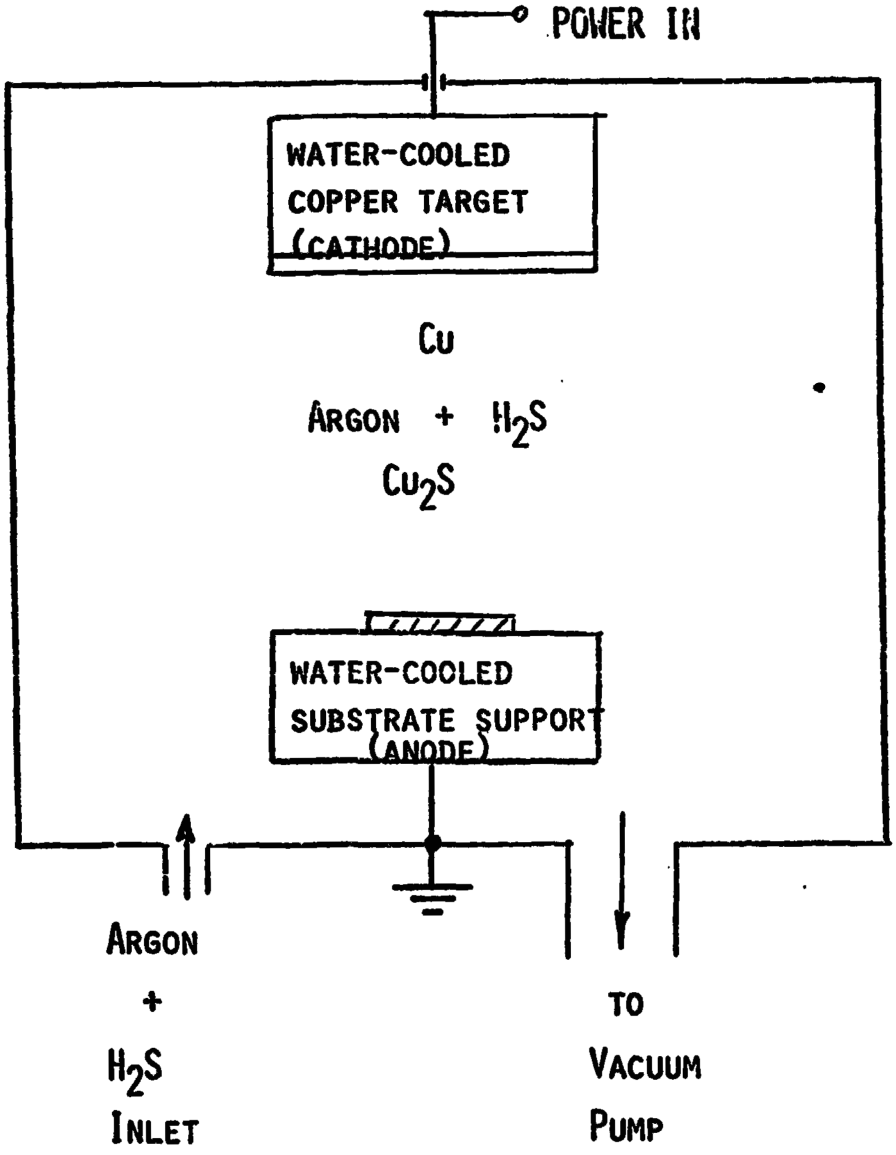

INITIAL SPUTTERED THIN FILM
CdS-Cu_2S CELL CONFIGURATION

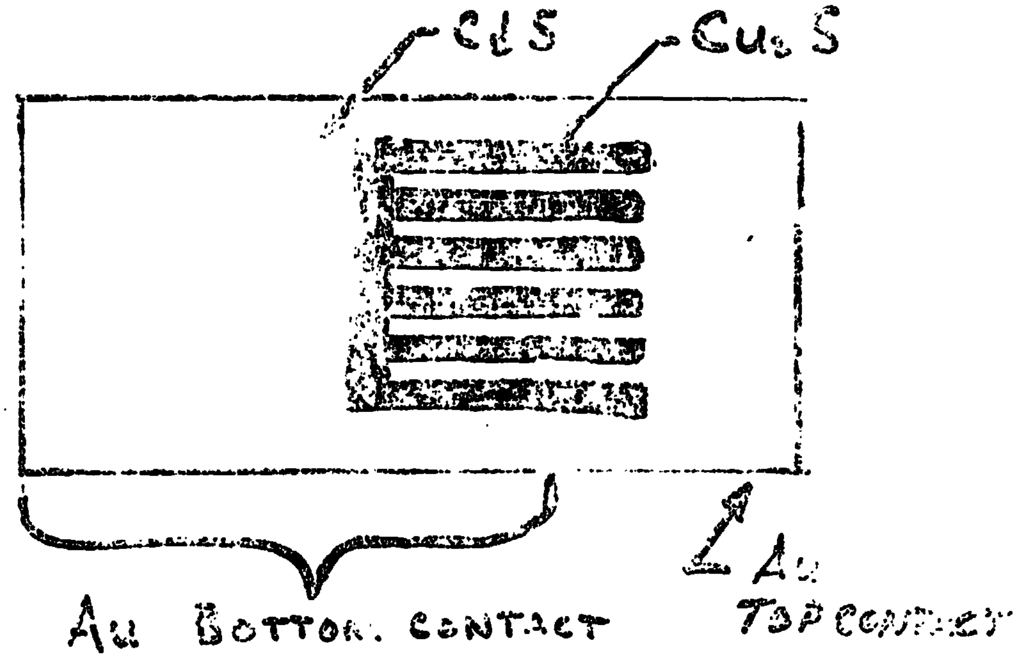

1. Cu_2S THICKNESS ~ 800 Å - 3000 Å
2. CdS THICKNESS ~ 2-5 μ
3. BEST MEASURED EFF IN SUNLIGHT ~ 4%
4. 100% YIELD OVER 40 DEVICES MADE SO FAR

ORIGINAL PAGE IS
OF POOR QUALITY

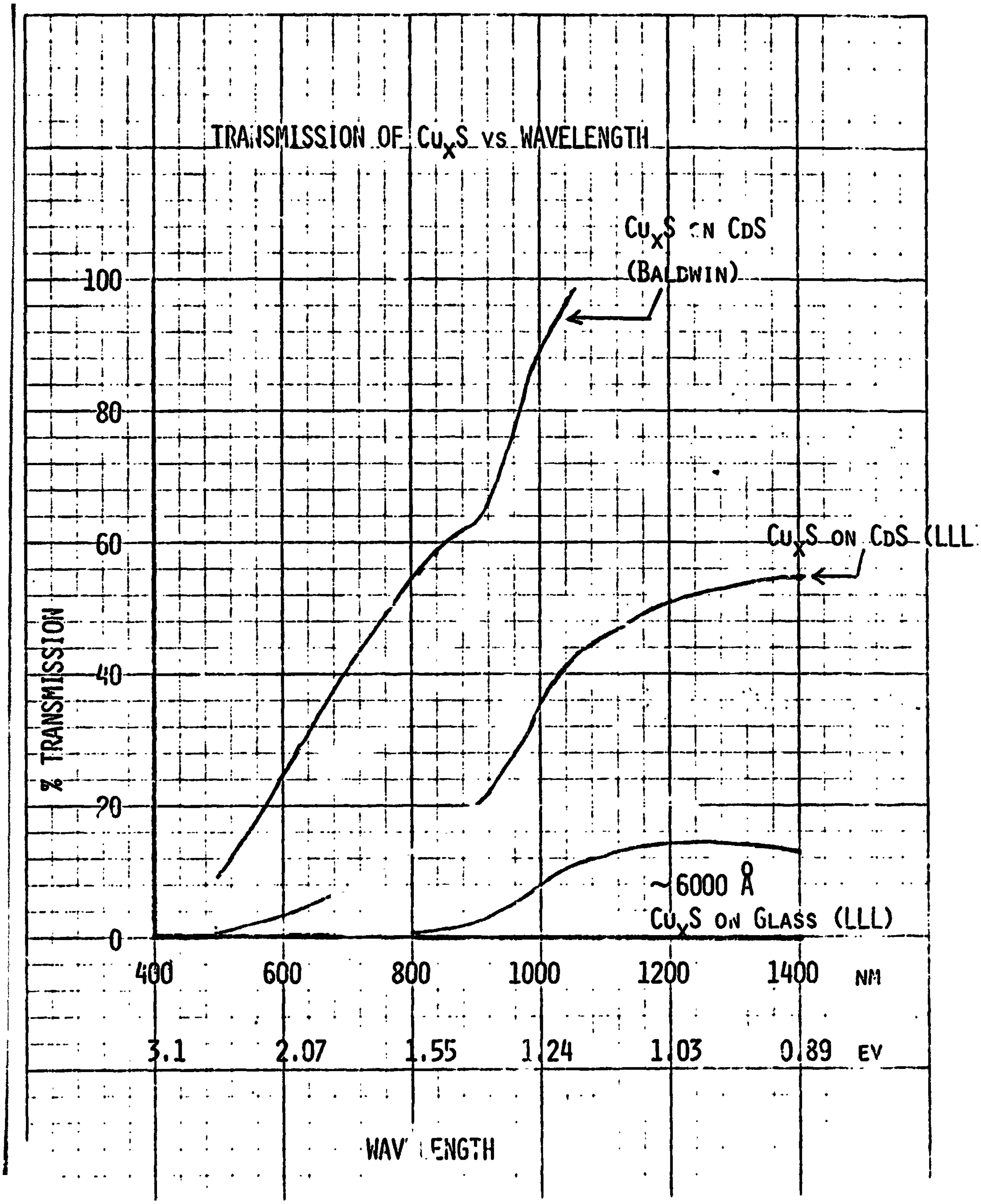
TRANSMISSION OF Cu_xS vs WAVELENGTH
Cu_xS ON CDS
(BALDWIN)
Cu_xS ON CDS (LLL
~6000 Å
Cu_xS ON GLASS (LLL)
% TRANSMISSION
100
80
60
40
20
0
400
600
800
1000
1200
1400
NM
3.1
2.07
1.55
1.24
1.03
0.89
EV
WAVELENGTH

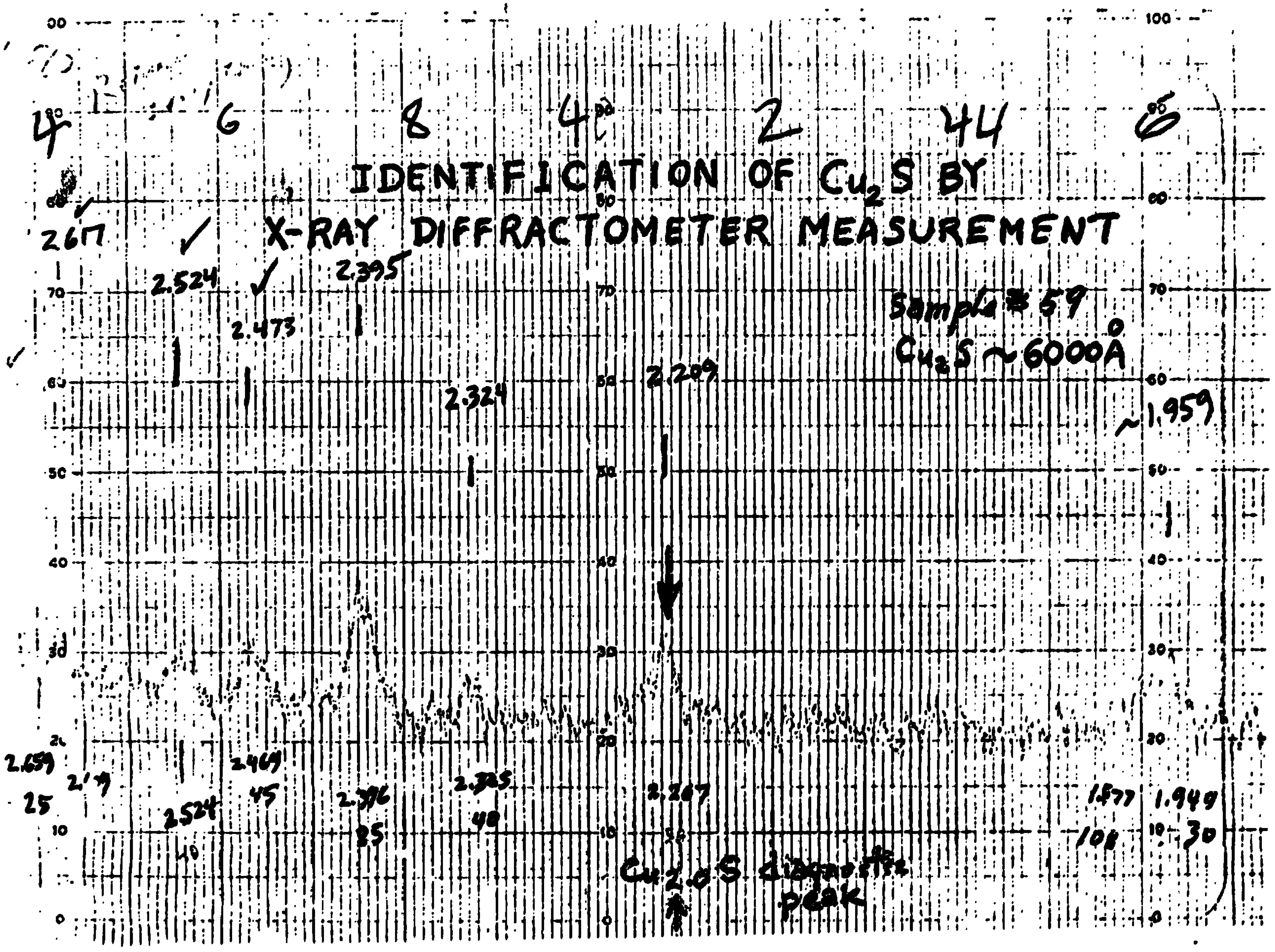

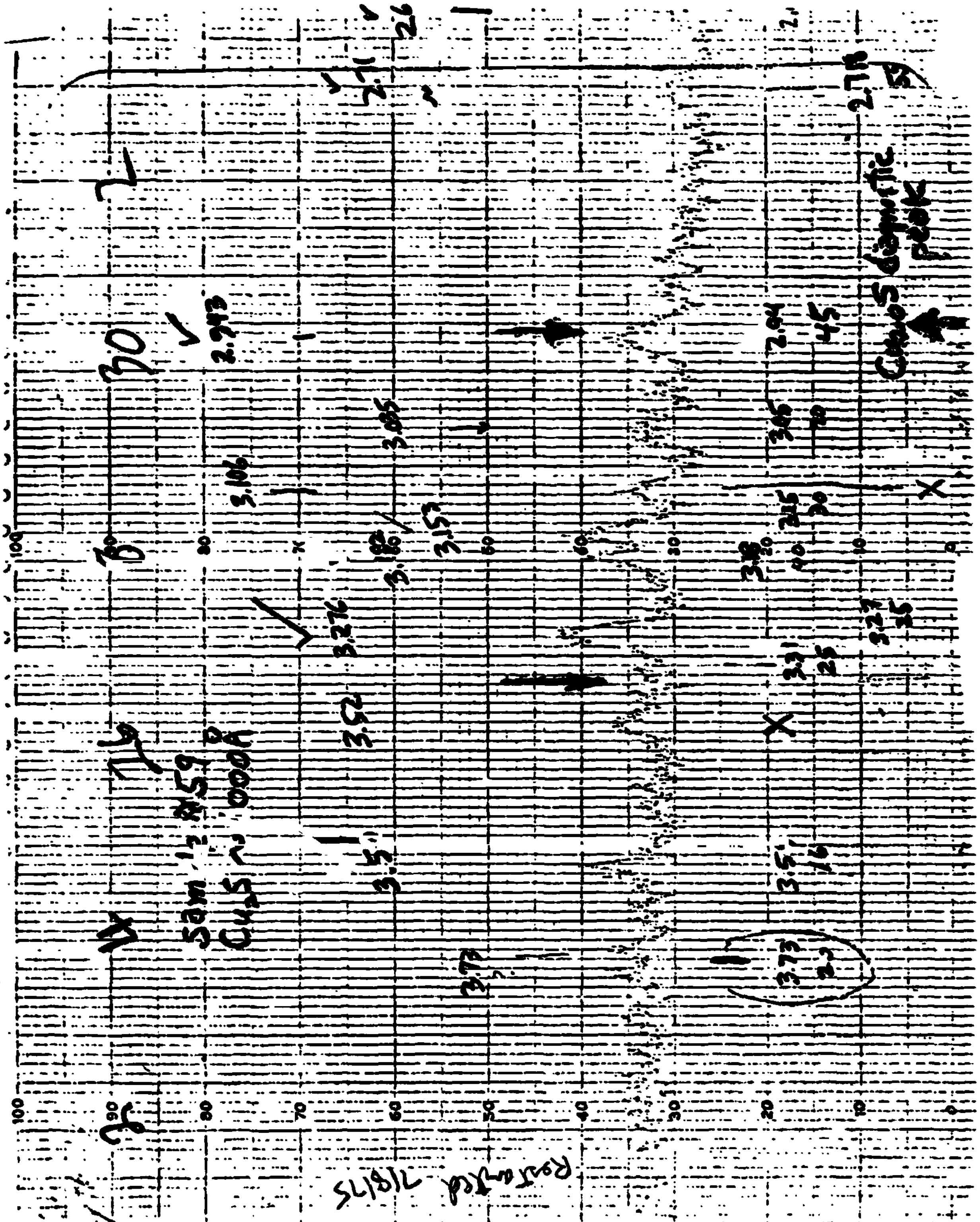

Sam 12 #59 R
CuS ~ 000A
Cu2S diagnostic peak
Rotated 7/8/75
2.71
26
2.718
2.943
3.106
3.085
3.157
3.276
3.22
3.5
3.79
3.06
2.94
45
3.15
30
3.31
25
3.27
35
3.51
16
3.73

I-V CHARACTERISTICS ARE OPTIMIZED BY HEAT TREATMENT IN AIR

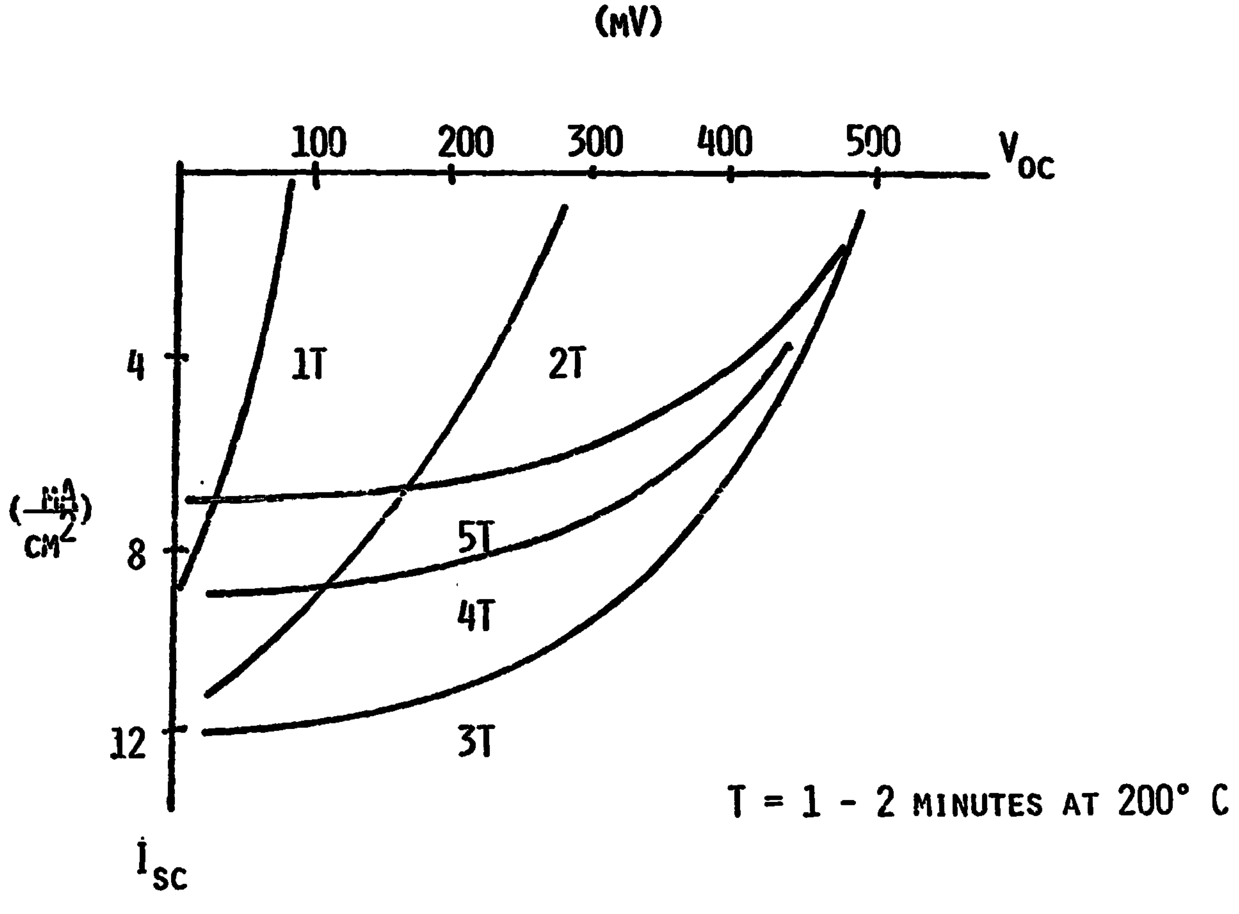

T = 1 - 2 MINUTES AT 200° C

OCV & SCC OPTIMIZATION DEPENDS ON Cu_2S THICKNESS

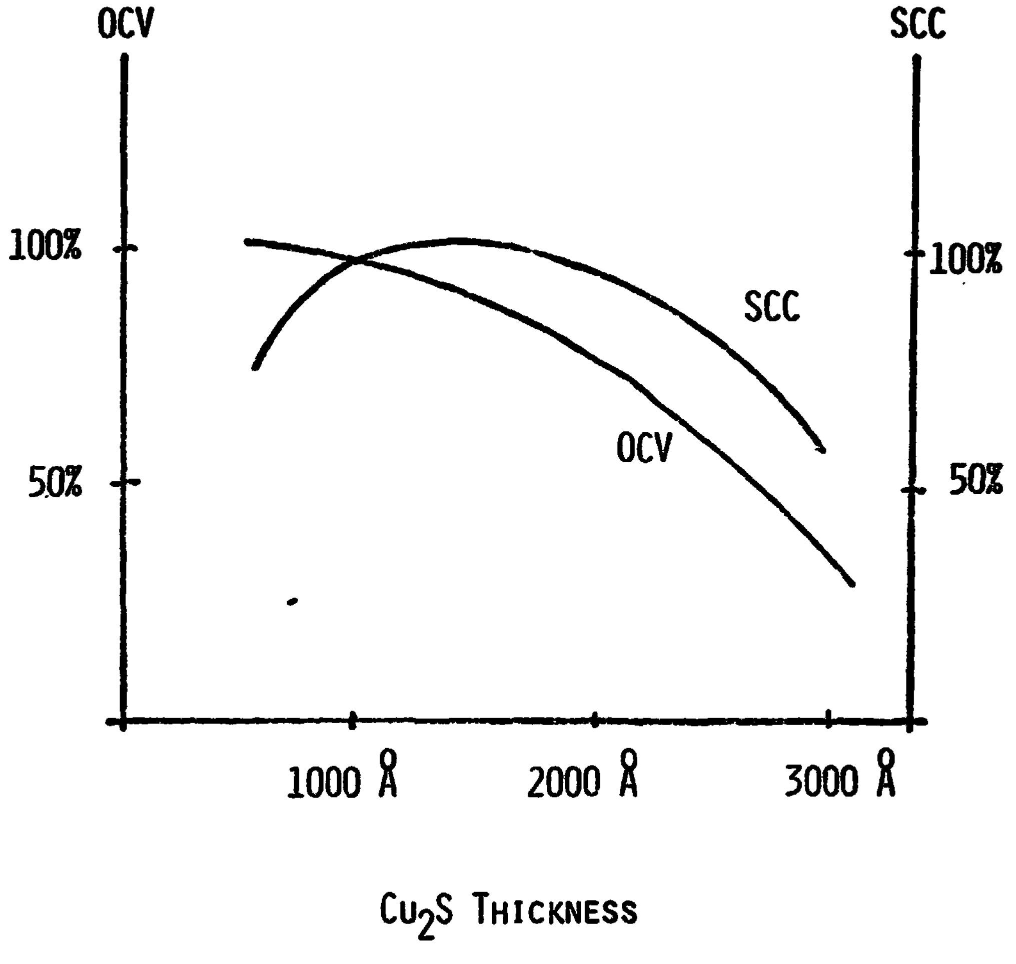

SUMMARY OF KEY RESULTS

1. PROVED FEASIBILITY OF REACTIVELY SPUTTERED CdS-Cu_2S CELL.
   - A. OVER 4% EFFICIENCY MEASURED IN SUNLIGHT
   - B. ALL CELLS MADE SHOWED PHOTOVOLTAIC EFFECT
2. ACQUIRED CAPABILITY TO IDENTIFY THE REACTIVELY SPUTTERED $Cu_{2.0}S$ FILMS.
3. PRELIMINARY CHARACTERIZATION OF THE REACTIVELY SPUTTERED CdS-Cu_2S CELL.
   - A. HEAT TREATMENTS OPTIMIZE CELL PERFORMANCE.
   - B. Cu_2S THICKNESS INFLUENCES OCV & SCC
   - C. THINNER CdS LAYER CAN BE USED.

ACTIVITY FOR NEXT 6 MONTHS

1. ASSEMBLE NEEDED EQUIPMENT AND MATERIAL.

2. IMPROVE CdS CELL EFFICIENCY ABOVE 4% BY
   - A. IMPROVING CELL DESIGN
   - B. IMPROVING STOICHIOMETRY OF SPUTTERED Cu_2S FILM
   - C. DOPING OF CdS (WITH ZnS)

3. START PRODUCING CdS CELLS FOR STABILITY EVALUATION.

4. LITERATURE SEARCH FOR OTHER THIN FILM PHOTOVOLTAIC MATERIALS.

N76 12494

APPLIED RESEARCH ON II-VI COMPOUND MATERIALS FOR HETEROJUNCTION SOLAR CELLS

NSF Grant GI-38445X

July 1, 1974 - June 30, 1975
$ 53,954

Richard H. Bube

Department of Materials Science and Engineering
Stanford University
Stanford, California 94305

Professor Richard H. Bube, Principal Investigator

National Solar Photovoltaic Program Review Meeting
July 22-25, 1975
Los Angeles, California

ABSTRACT

The objective of this grant is the investigation of heterojunction solar cells based on several II-VI compound systems suitable for large-scale terrestrial utilization.

Several II-VI heterojunctions show promise for photovoltaic conversion of solar energy. The three of greatest interest are p-CdTe/n-CdS, p-CdTe/n-ZnSe, and p-ZnTe/n-CdSe. The last of these three is of interest primarily as an opportunity to determine the effects of very small lattice mismatch rather than as an actual solar cell. p-CdTe/n-CdS heterojunction cells have been prepared by close-spaced transport deposition of p-CdTe on single crystal n-CdS, and by two-source vacuum evaporation of n-CdS on single crystal p-CdTe. Both types of cells, in an experimental stage, are quite comparable, exhibiting values of quantum efficiency between 0.5 and 0.9, open-circuit voltages between 0.50 and 0.66 V, fill factors between 0.4 and 0.6, and solar efficiencies up to 4 percent. Cells of p-ZnTe/n-CdSe have also been made by close-spaced vapor transport deposition of n-CdSe on single crystal p-ZnTe.

A detailed program of heterojunction evaluation has been initiated, involving (1) J-V characteristics in the dark vs temperature to determine diode properties in the absence of illumination, (2) J-V characteristics in the light using the solar simulator, (3) V_{oc} vs ln J_{sc} as a function of light intensity at different temperatures to determine magnitudes and temperature dependence of key diode parameters, (4) junction capacitance vs voltage in light and dark, (5) SEM determination of minority carrier diffusion lengths, (6) optical transmission to determine exact variation of absorption constant with photon energy, and (7) spectral response of J_{sc} to determine dependence of quantum efficiency on photon energy.

Measurement of J-V curves in the dark as a function of temperature for evaporated n-CdS on p-CdTe heterojunctions reveals two ranges of behavior: above 250°K, the current is thermally activated, $\eta = 2.4$ and is independent of temperature, and $J_o = 1.9 \times 10^2 \exp(-0.54\ eV/kT)$ A/cm²; below 250°K, tunneling dominates, $\alpha = 21\ V^{-1}$ and is independent of temperature, and $J_o = 5.7 \times 10^{-10}$ A/cm² independent of temperature. J_o and/or η may be light-dependent, as evidenced by the crossover of light and dark J-V curves. Low fill factors may be associated with a bias-dependent quantum efficiency. No transient or quenching effects have been observed in this system at room temperature.

Making ohmic, low-resistance contacts to p-CdTe has been a major problem. Such contacts can be made with Ni to a surface etched with $K_2Cr_2O_7:H_2SO_4:H_2O$, after heat treatment, if the CdTe resistivity is less than 10 ohm-cm. Ohmic, low-resistance contacts have been made with Ni to 133 ohm-cm p-CdTe after implantation of the CdTe with As. Evidence is conclusive from a variety of sources that the contact consists of a thin Schottky barrier with current transport dominated by tunneling.

p-ZnTe/n-CdSe heterojunctions show quantum efficiencies between 0.18 and 0.30, open-circuit voltages between 0.55 and 0.68 V, fill factors between 0.38 and 0.49, and solar efficiencies up to about 1 percent. A bias-dependent quantum efficiency is indicated due to short diffusion length of photoexcited holes in CdSe. V_{oc} vs ln J_{sc} measurements indicate that between 74°C and 221°C α changes from 10.2 to 15.6 V^{-1} (η from 3.25 to 1.49) and $J_o = 1.3 \times 10^{-3} \exp(-0.33\ eV/kT)$, suggesting thermally assisted tunneling as the current transport mode.

Future work includes detailed correlation of diode parameters in p-CdTe/n-CdS and p-ZnTe/n-CdSe with preparation variables, investigation of methods to increase the conductivity of both surface and bulk p-CdTe, determination of the properties of p-ZnTe/n-CdSe junctions made on (111) oriented ZnTe to achieve minimum lattice mismatch condition, and evaluation of p-CdTe/n-ZnSe heterojunctions.

ORIGINAL PAGE IS
OF POOR QUALITY

APPLIED RESEARCH ON II-VI COMPOUND MATERIALS FOR HETEROJUNCTION SOLAR CELLS

NSF Grant GI-38445X

Stanford University

July 1, 1974 - June 30, 1975

$ 53,954

Professor Richard H. Bube
Principal Investigator

PROJECT OBJECTIVES

INVESTIGATION OF HETEROJUNCTION SOLAR CELLS BASED ON SEVERAL II-VI COMPOUND SYSTEMS SUITABLE FOR LARGE-SCALE TERRESTRIAL UTILIZATION.

PLANNED ACTIVITY LAST 6 MONTHS

* PREPARE AND INVESTIGATE ALL FILM p-CdTe/n-CdS CELLS
* OPTIMIZE ELECTRICAL CONTACTS TO p-CdTe
* BRING NEW VACUUM SYSTEM TO FULL OPERATING POTENTIAL
* BEGIN EVALUATION OF OTHER II-VI HETEROJUNCTION SYSTEMS:
  p-ZnTe/n-CdSe, p-CdTe/n-ZnSe, p-ZnTe/n-CdTe

HETEROJUNCTION EVALUATION

- * J-V CHARACTERISTICS IN DARK vs TEMPERATURE
  Diode properties in absence of illumination
- * J-V CHARACTERISTICS IN LIGHT
  Using solar simulator, determine J_{sc}, V_{oc}, fill factor, collection efficiency, solar efficiency
- * V_{oc} vs ln J_{sc} PLOTS AS A FUNCTION OF LIGHT INTENSITY AT DIFFERENT TEMPERATURES
  Diode constant at different temperatures, $J_o(T)$, and effective barrier height for forward currents in light
- * JUNCTION CAPACITANCE vs V IN DARK AND LIGHT
  Width and variation of depletion layer
- * SEM DETERMINATION OF MINORITY CARRIER DIFFUSION LENGTHS
- * OPTICAL TRANSMISSION
  Absorption constant vs photon energy
- * SPECTRAL RESPONSE OF J_{sc}
  Variation of quantum efficiency on photon energy

EVAPORATED n-CdS ON SINGLE CRYSTAL p-CdTe

- * HEAT TREATMENT TO ABOUT 430°C REQUIRED FOR OPTIMUM PERFORMANCE

- * DIODE CHARACTERISTICS IN THE DARK vs TEMPERATURE

$T > 250°K$ $$J = J_o\left[\exp\left(qV/\eta kT\right) - 1\right]$$

$$J_o = J_o^0 \exp\left(-E^*/kT\right)$$

$$\eta = 2.4 \qquad E^* = 0.54\ \mathrm{eV}$$

$T < 250°K$ $$J = J_o\left[\exp(\alpha V) - 1\right]$$

$$J_o = 5.7 \times 10^{-10}\ \mathrm{A/cm^2}$$

$$\alpha = 21\ \mathrm{V}^{-1}$$

- * J_o AND/OR η ARE LIGHT DEPENDENT AS EVIDENCED BY THE CROSSOVER OF LIGHT AND DARK J-V CURVES

- * A BIAS-DEPENDENT COLLECTION EFFICIENCY MAY CONTRIBUTE TO LOW FILL FACTORS

- * NO TRANSIENT OR QUENCHING EFFECTS OBSERVED AT ROOM TEMPERATURE

ELECTRICAL CONTACTS TO p-CdTe

* OHMIC, LOW-RESISTIVITY CONTACT TO SURFACE OF p-CdTe ETCHED WITH $K_2Cr_2O_7:H_2SO_4:H_2O$ FOR RESISTIVITY $\lessdot$ 10 OHM-CM

* OHMIC, LOW-RESISTIVITY CONTACT TO SURFACE OF p-CdTe IMPLANTED WITH As FOR RESISTIVITY OF 133 OHM-CM

* DEVELOPMENT OF A "3-POINT" MEASURING TECHNIQUE THAT ALLOWS CELL EVALUATION EVEN IF CONTACTS NOT IDEAL

* EVALUATION OF OHMIC TO NON-OHMIC TRANSITION BY MEASURING CONTACT PROPERTIES vs TEMPERATURE

* MODEL FOR CONTACT INVOLVING A THIN SCHOTTKY BARRIER WITH CURRENT TRANSPORT DOMINATED BY TUNNELING
  - Chemical effect of etching
  - Auger analysis of contact
  - Low-temperature capacitance
  - Quantitative shape of temperature dependence

OTHER II-VI SYSTEMS: p-ZnTe/n-CdSe

- * 11 HETEROJUNCTIONS MADE BY CLOSE-SPACE VAPOR TRANSPORT OF CdSe ONTO SINGLE CRYSTAL ZnTe
- * OHMIC LOW-RESISTANCE CONTACTS POSSIBLE TO ETCHED p-ZnTe
- * TYPICAL CELL PARAMETERS

V_{oc}	0.55 - 0.68 V	Fill Factor	0.38 - 0.49
Quantum Efficiency	0.18 - 0.30	Solar Efficiency	0.55 - 0.85 percent

- * DIODE CHARACTERISTICS AT 22°C

$\eta_{dark} = 2.38$ $\eta_{light} = 2.41$

$J_o dark = 4.2x10^{-9}\ A/cm^2$ $J_o light = 1.2x10^{-8}\ A/cm^2$

- * TEMPERATURE DEPENDENCE OF DIODE CHARACTERISTICS IN LIGHT

η at 74°C = 3.25 η at 221°C = 1.49

$$J_o = 1.3 \times 10^{-3} \exp(-0.33\ eV/kT)\ A/cm^2$$

SUMMARY OF KEY RESULTS

- CONTACTS TO p-CdTe ARE UNDERSTOOD; OHMIC, LOW-RESISTANCE CONTACTS CAN BE MADE; CELLS CAN BE EVALUATED EVEN IN THE ABSENCE OF IDEAL CONTACTS
- TWO MECHANISMS DETECTED FOR J_o for p-CdTe/n-CdS: HIGH-TEMPERATURE THERMALLY ACTIVATED WITH $E^* = 0.54$ eV, AND LOW-TEMPERATURE TUNNELING
- J_o for p-ZnTe/n-CdSe IS THERMALLY ACTIVATED AT HIGH TEMPERATURES WITH $E^* = 0.33$ eV
- EVIDENCE FOR A BIAS-DEPENDENT COLLECTION EFFICIENCY CONTRIBUTING TO POOR FILL FACTORS
- DEVELOPMENT OF VACUUM EVAPORATOR SYSTEM
- IMPORTANCE OF LIGHT AND PREPARATION VARIABLES ON J_o and η

PLANNED ACTIVITY FOR NEXT 6 MONTHS

* p-CdTe/n-CdS HETEROJUNCTIONS
    - Correlation of E* with preparation variables
    - Determine presence and extent of bias-dependent collection efficiency
    - Transient measurements at low T to determine effect of light on J_o and
    - Optimization of CdS film deposition

* ELECTRICAL CONTACTS TO p-CdTe
    - Evaluations for other metals with different work functions
    - Investigation of methods to make surface high conductivity
    - Contacts to p-CdTe films

* p-ZnTe/n-CdSe HETEROJUNCTIONS
    - Properties of junctions on (111) oriented ZnTe to achieve minimum lattice mismatch (0.35 percent)
    - Full characterization of junction properties

* OTHER SYSTEMS
    - The system of principal interest is p-CdTe/n-ZnSe
        - Larger "window"
        - Larger diffusion voltage
        - Susceptible of extension to p-CdZnTe/n-ZnSSe
    - If results with p-CdTe/n-CdS warrant, then p-CdTe/n-CdZnS

N76 12495

INVESTIGATION OF THIN FILM SOLAR CELLS
BASED ON
Cu_2S AND TERNARY COMPOUNDS SUCH AS $CuInS_2$

BROWN UNIVERSITY

Principal investigator: J.J. Loferski

Talk presented by: J. Shewchun

NSF/RANN GRANT GI-38102X

1 July 1973 to 30 June 1976

∿ $100,000/annum.

Abstract

The work at Brown University is concerned with the production and characterization in film form of Cu_2S and related Cu compounds such as $CuInS_2$ for photovoltaic cells. The low cost process technology being examined,namely the sulfurisation method , is capable of producing films on various substrates. Cathodoluminescence is being used as a diagnostic tool (in conjunction with other aids such as x-rays, scanning electron microscopy, etc.) to identify Cu_xS and $CuInS_2$ compounds. Also, single crystals of $CuInS_2$ are being prepared and it is contemplated that p-n junctions will be made in such crystals.

Cu_2S films have been prepared on silicon, cadmium sulfide, aluminum and silica. X-ray analysis is used to identify the particular phase produced. A film of at least 9000A° of Cu_xS is needed to make a positive identification, although films as thin as 4500A° have been identified. We have been able to employ cathodoluminescence for phase identification below these limits with a minimum detectable limit, at present, of about 1500A° of Cu_2S. Scanning electron microscopy is being employed to determine structural features and homogeneity. The films appear to consist of hexagonal platelets whose size depends on film thickness (1500A° of Cu yields crystallites of ½ μm diameter; 9000A° of Cu yields crystallites of 2 μm diameter). Thinner films show orientation effects which give rise to a characteristic x-ray pattern which we have previously designated UA.

Cathodoluminescence measurements have been further refined. Only Cu_2S of all the phases gives a luminescence response and the response is at

9660A° (77°K) with a half width of about 200A°. This is more characteristic of a direct transition behaviour in contradiction with what is generally assumed about Cu_2S. Cathodoluminescence has also been carried out on heat treated (200°C in air for 5-30 min) and copper treated (60A° Cu, 200°C in air for 10-30 min) films. Short-circuit current increases by factors of about 8 (heat treated)to 17 (copper treated) have been observed. Corresponding to this, cathodoluminescence reveals some interesting behaviour. For heat treated films the Cu_2S peak is retained but there is a strong background due to either Cu impurities or defects. For Cu treated films, the Cu_2S peak disappears. In the case of Cu treated films, x-rays reveal that Cu_2S is still present but other unidentified lines are also present.

Diodes formed on single crystal CdS have reasonable I-V characteristics with $V_{oc} \sim 0.45 - 0.5$ volts. Although method efficiencies have only been about 1% (AM1), no optimization of the process has been carried out.

During the next six months we plan to optimize the process for sulfurization of Cu on single crystal CdS with the objective of cell efficiencies of $\sim$ 5%. We plan to construct all thin film cells consisting of (a) Cu sulfurized on quartz or metal subst tes followed by (b) deposition of a suitable semiconductor - CdS or a more optimum mate. Cathodoluminescence diagnostics will be refined since they appear capable of identifying the phase of Cu_xS responsible for the strong photovoltaic effect. In addition we plan to expand our activity on the growth of $CuInS_2$ crystals and preparation of p-n junctions.

Program Objectives

(1) Preparation and characterization of Cu_xS and $CuInS_2$ films on various substrates for photovoltaic cells using sulfurization of deposited Cu and CuIn films.

(2) Investigate cathodoluminescence as a diagnostic tool for identifying Cu_xS and $CuInS_2$ compounds.

(3) Preparation of single crystals of $CuInS_2$ and p-n junctions

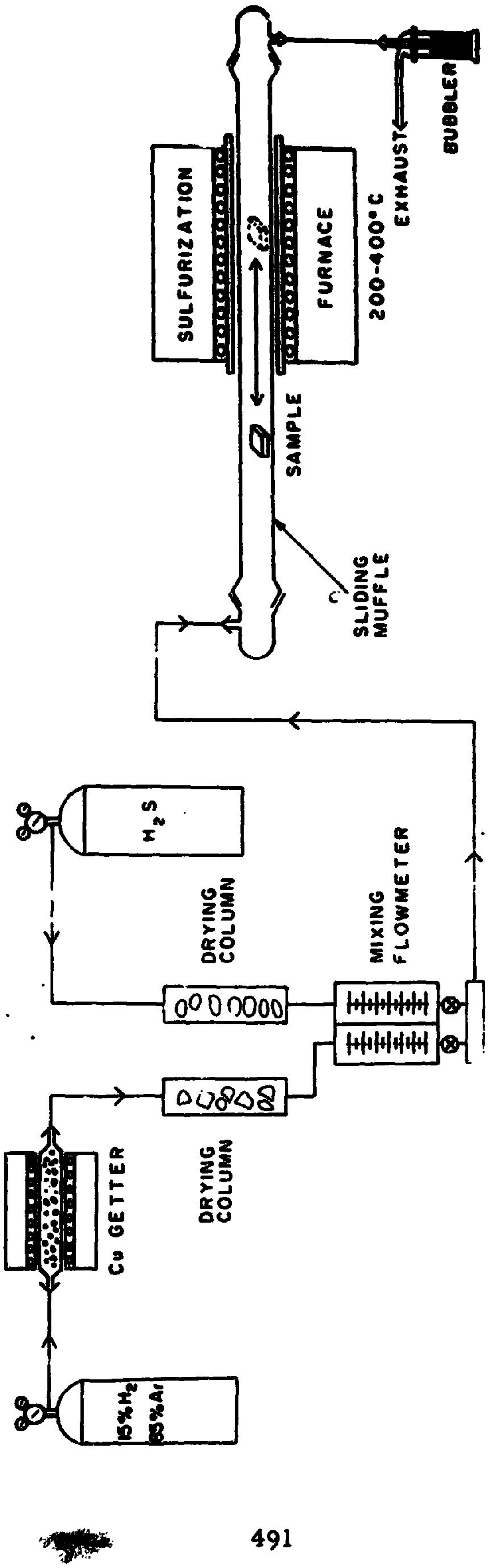
SULFURIZATION
FURNACE
200-400°C
EXHAUST
BUBBLER
SAMPLE
SLIDING MUFFLE
H_2S
DRYING COLUMN
MIXING FLOWMETER
Cu GETTER
DRYING COLUMN
15% H_2
85% Ar

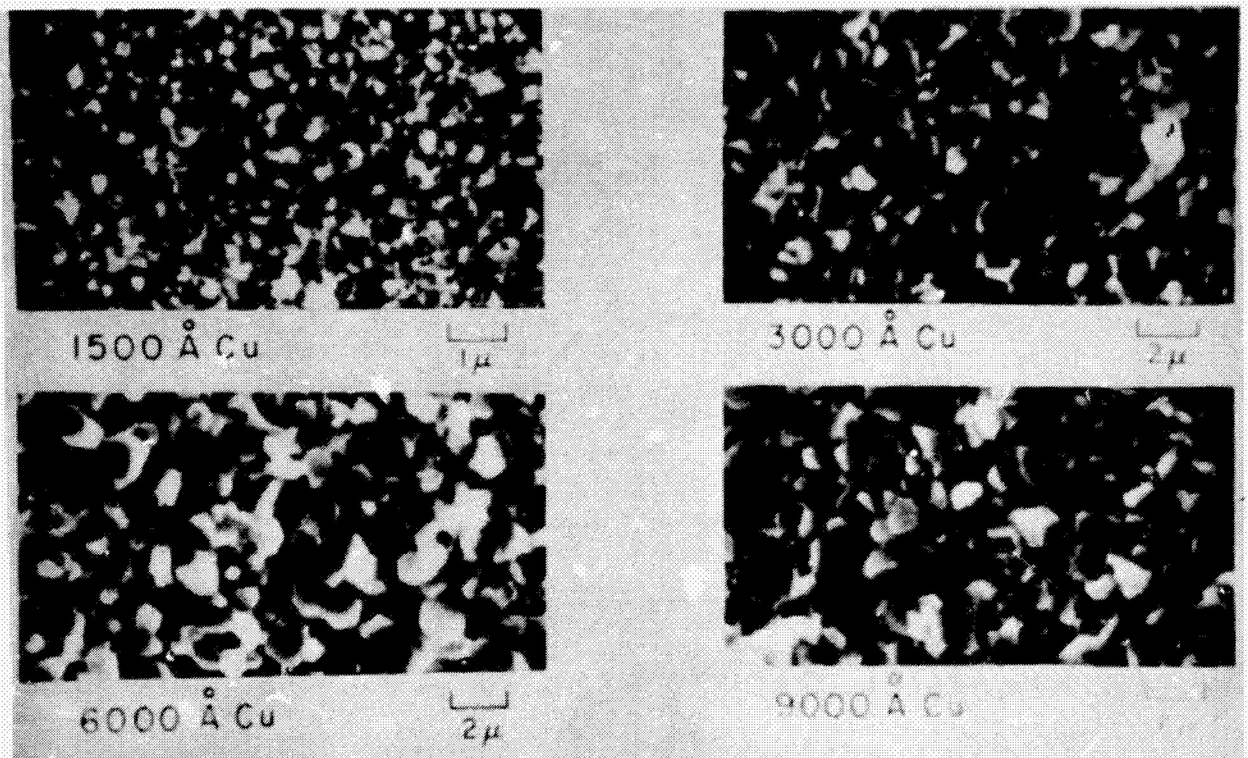

SULFURIZED CuS FILMS ON CdS

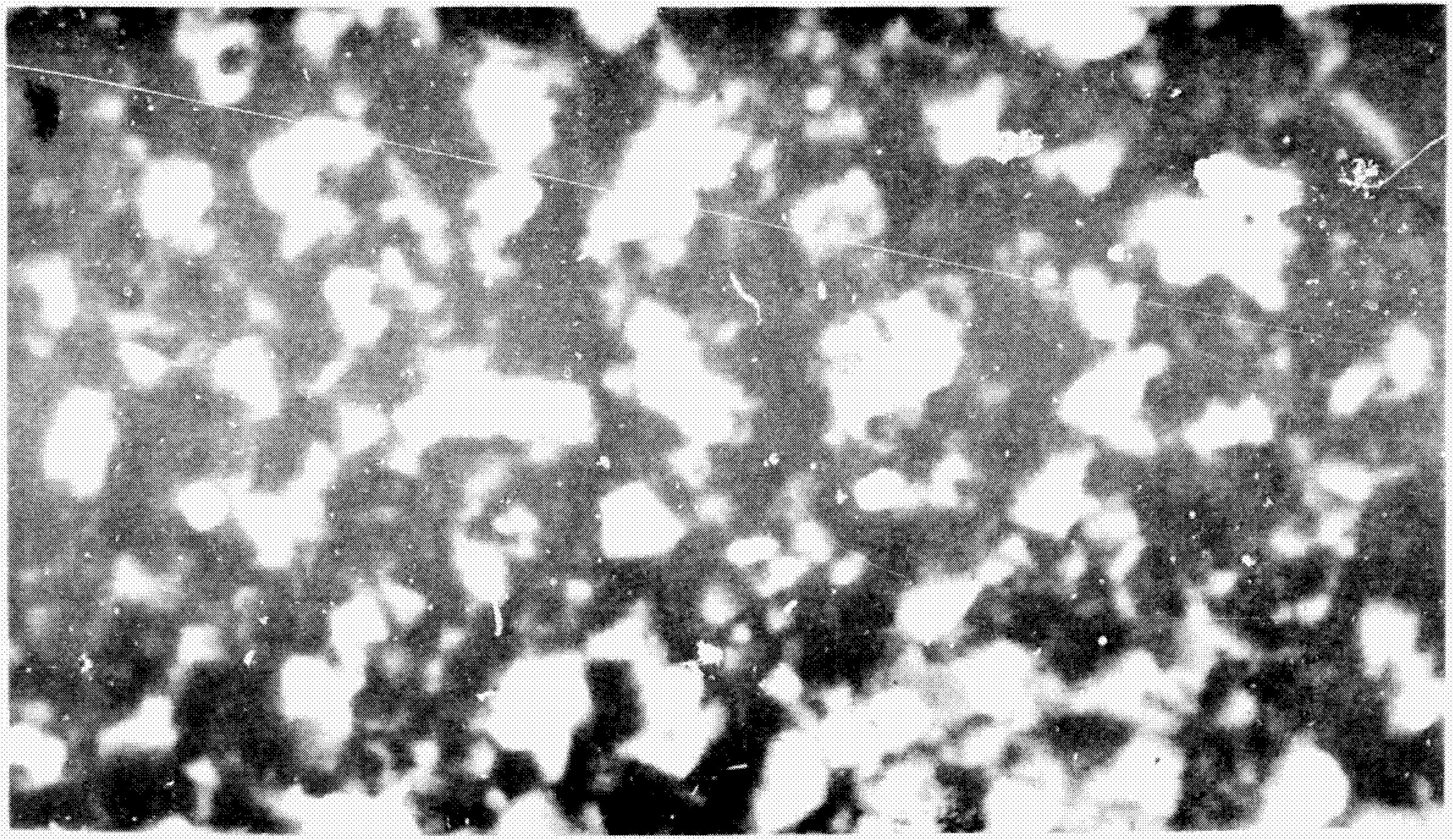

SULFURIZED
4500 Å Cu/1000 Å AL ON SiO_2

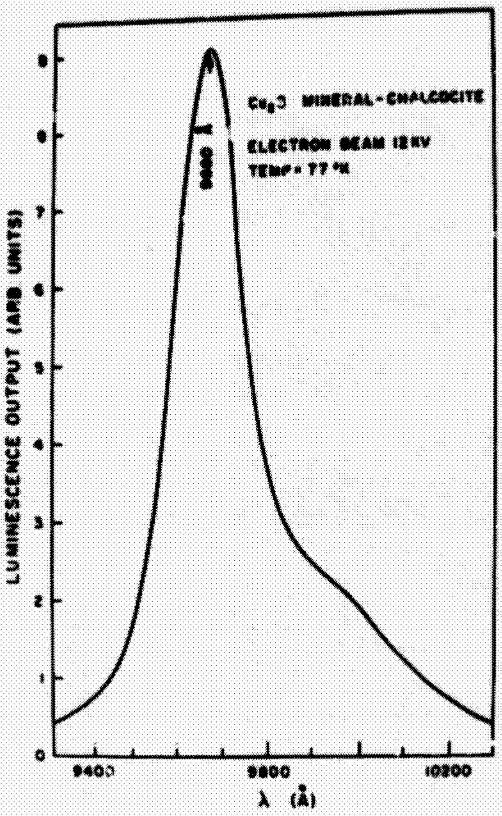
Cu_2S MINERAL-CHALCOCITE
ELECTRON BEAM 12KV
TEMP = 77 °K
9680 Å
LUMINESCENCE OUTPUT (ARB UNITS)
λ (Å)
9400
9800
10200
0
1
2
3
4
5
6
7
8
9

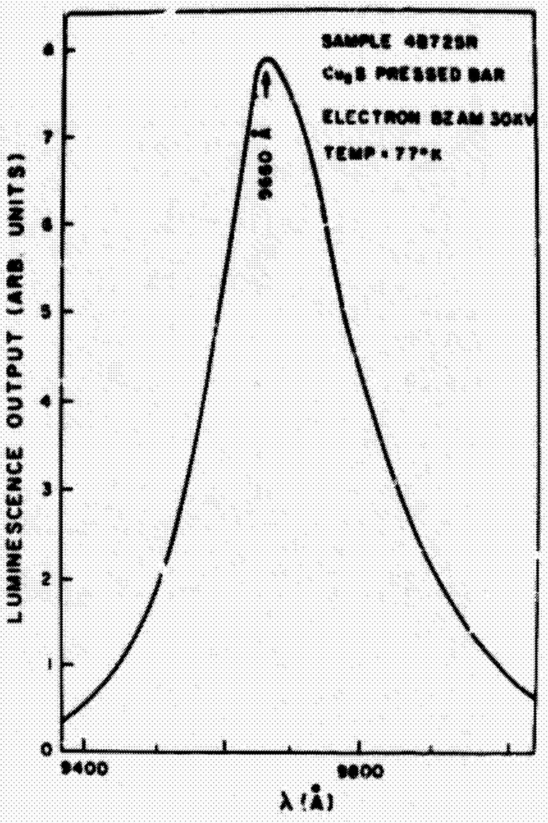
SAMPLE 4872SR
Cu_2S PRESSED BAR
ELECTRON BEAM 30KV
TEMP = 77 °K
9680 Å
LUMINESCENCE OUTPUT (ARB UNITS)
λ (Å)
9400
9800
0
1
2
3
4
5
6
7
8

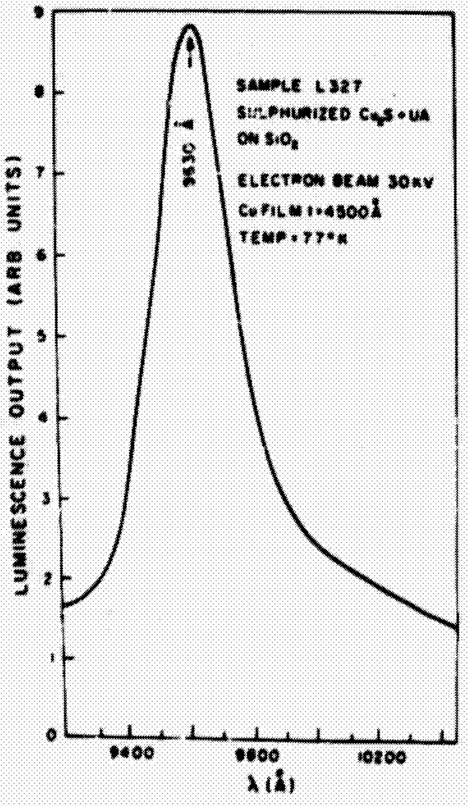
SAMPLE L327
SULPHURIZED Cu_2S + UA
ON SiO_2
ELECTRON BEAM 30KV
Cu FILM t = 4500 Å
TEMP = 77 °K
9630 Å
LUMINESCENCE OUTPUT (ARB UNITS)
λ (Å)
9400
9800
10200
0
1
2
3
4
5
6
7
8
9

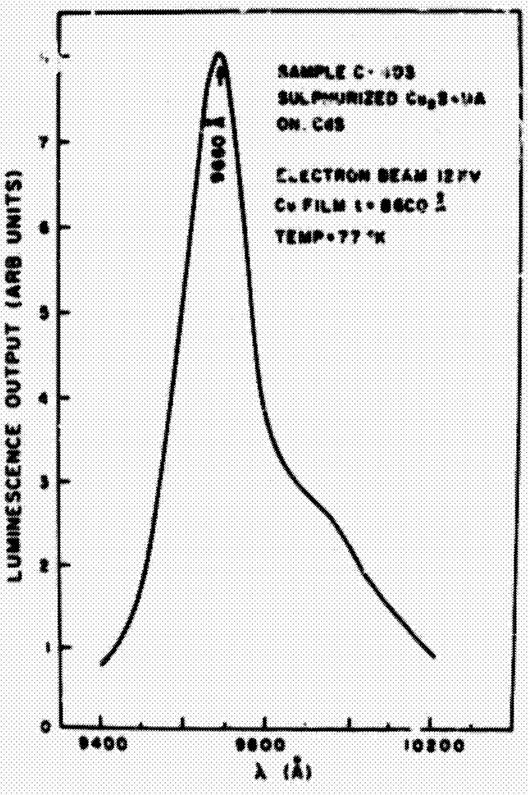
SAMPLE C-403
SULPHURIZED Cu_2S + UA
ON CdS
ELECTRON BEAM 12KV
Cu FILM t = 8600 Å
TEMP = 77 °K
9680 Å
LUMINESCENCE OUTPUT (ARB UNITS)
λ (Å)
9400
9800
10200
0
1
2
3
4
5
6
7

ORIGINAL PAGE IS
OF POOR QUALITY

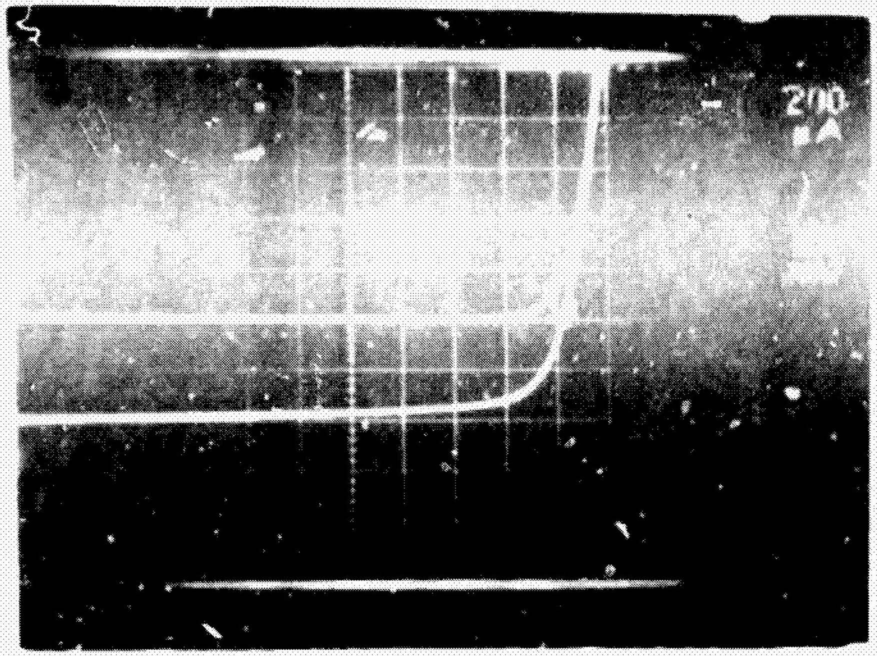

PHOTOVOLTAIC RESPONSE OF DIPPED
Cu_xS-CdS CELL

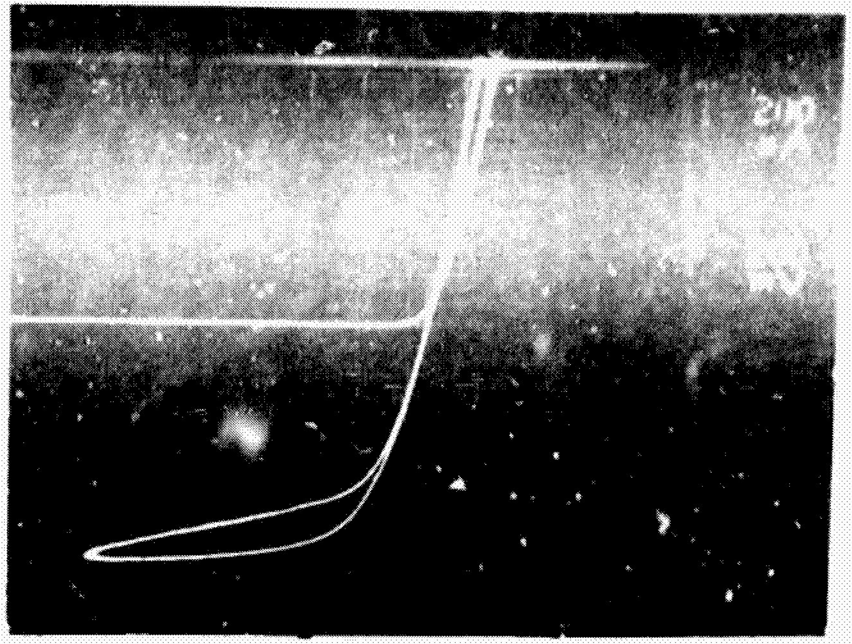

PHOTOVOLTAIC RESPONSE OF SULFURIZED
Cu_xS-CdS CELL

Cell No.	tment (in air)					Copper Treatment (in air)- 60A°				
	temp (°C)	time (min)	I_{sc} (ma) Before	I_{sc} (ma) After	increase factor	temp	time	I_{sc} (ma) Before	I_{sc} (ma) After	increase factor
C 485	200	26	0.14	0.60	4.2					
C 525						200	10	0.019	0.33	17.0
C 430	200	7	0.28	1.9	6.8	200	10	0.09	0.40	4.4
C 525-2	180	7	0.06	0.45	7.5	200	27	0.32	0.60	1.9
C 437	200	9	0.75	2.0	2 7	200	10	0.34	0.50	1.5

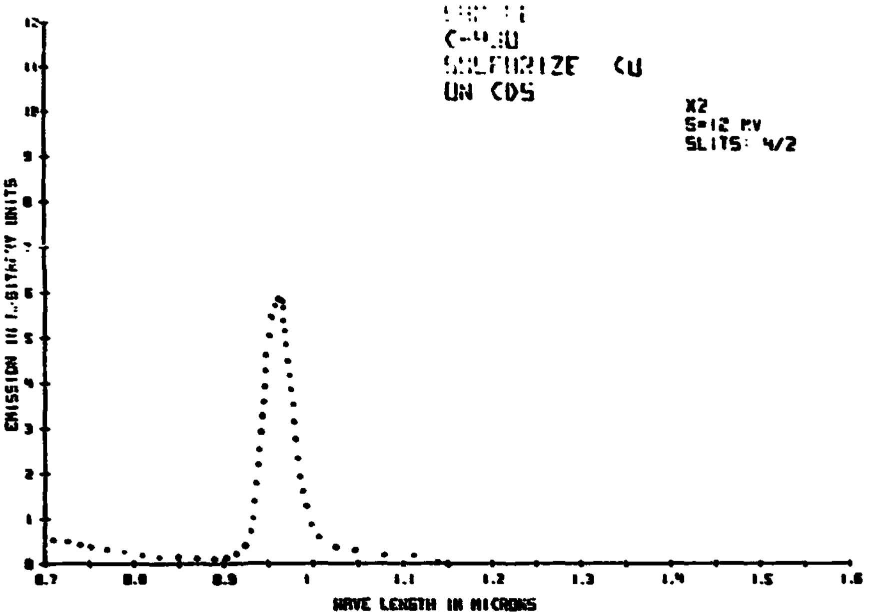
SAMPLE
C-430
SULFURIZE CU
ON CDS
X2
S=12 MV
SLITS: 4/2
EMISSION IN ARBITRARY UNITS
0
1
2
3
4
5
6
7
8
9
10
11
12
0.7
0.8
0.9
1
1.1
1.2
1.3
1.4
1.5
1.6
WAVE LENGTH IN MICRONS

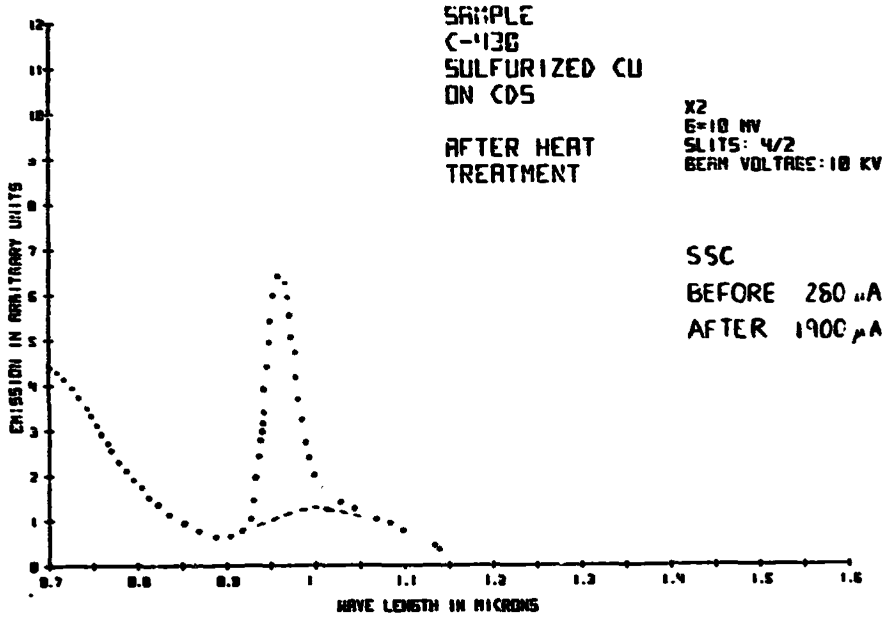
SAMPLE
C-430
SULFURIZED CU
ON CDS
AFTER HEAT
TREATMENT
X2
S=10 MV
SLITS: 4/2
BEAM VOLTAGE: 10 KV
SSC
BEFORE 260 μA
AFTER 1900 μA
EMISSION IN ARBITRARY UNITS
0
1
2
3
4
5
6
7
8
9
10
11
12
0.7
0.8
0.9
1
1.1
1.2
1.3
1.4
1.5
1.6
WAVE LENGTH IN MICRONS

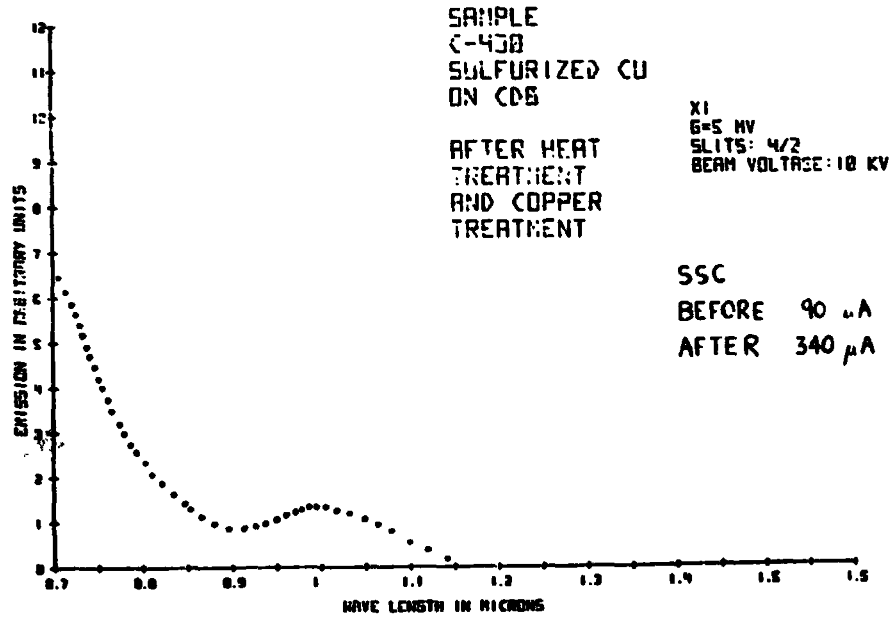
SAMPLE
C-430
SULFURIZED CU
ON CDS
AFTER HEAT
TREATMENT
AND COPPER
TREATMENT
X1
S=5 MV
SLITS: 4/2
BEAM VOLTAGE: 10 KV
SSC
BEFORE 90 μA
AFTER 340 μA
EMISSION IN ARBITRARY UNITS
0
1
2
3
4
5
6
7
8
9
10
11
12
0.7
0.8
0.9
1
1.1
1.2
1.3
1.4
1.5
1.5
WAVE LENGTH IN MICRONS

Summary of results

1) Cu_2S films prepared on Silica, Aluminum, Silicon, CdS - no limitation on substrates.

2) Cathodoluminescence can be used as diagnostic tool to identify Cu_2S and copper impurities.

3) Junctions on CdS and Si exhibit up to 1% η without process optimization.

4) "Heat treatments" and "Cu treatments" can increase SSC by over 1 order of magnitude.

Planned Activity for Next 6 Months

1. Optimize process for sulfurization of Cu on single crystal CdS - objective is cell with ∿ 5% efficiency.
2. All thin film cells
   (a) Cu sulfurized on quartz or metal followed by
   (b) Evaporation of semiconductor - CdS or more optimum mate
3. Growth of $CuInS_2$ crystals and
   Preparation of p-n junctions
4. Refinement of cathodoluminescence diagnostics
5. Co-operation with University of Maine

SESSION VII

OTHER APPROACHES 1

N76 12496

FEASIBILITY INVESTIGATION OF GROWING GALLIUM ARSENIDE SINGLE CRYSTALS IN RIBBON FORM

NSF GRANT GI-43093

July 1, 1974 - December 30, 1975

$164,000 ADL

60,000 MIT

David L. Richardson
Arthur D. Little, Inc.
Cambridge, Mass. 02140

Dr. Joan Berkowitz, Principal Investigator

Presented at the
National Solar Photovoltaic Program Review Meeting
at the
University of California, Los Angeles

July 22 - July 25, 1975

ABSTRACT

An eighteen month program was initiated July 1, 1974 to determine the feasibility of producing GaAs single crystal ribbons suitable for solar cell substrates. Constrained, encapsulated molten zones are passed through rectangular polycrystalline feed material to form single crystal ribbons. The objective of this program is to grow 10 cm x 1 cm x 0.1 cm single crystals by a process that is amenable to continuous growth.

During the past six months, two methods have been used to establish passage of a molten zone through ribbon GaAs feedstock; direct coupling with rf to the GaAs and constrained zone-melting in B_2O_3 sealed graphite boats. Establishment of a narrow molten zone by direct rf coupling to GaAs was shown to be limited by the large skin depth required for heating GaAs as compared to the desired ribbon thickness.

Polycrystalline GaAs ribbons have been grown in graphite boats by passage of a wide zone through B_2O_3-encapsulated feed-stock, confined by a quartz cover plate. Failure to remove the encapsulant above its glass transition temperature, however, resulted in cracking of the ribbons on cooling to room temperature. In order to study the crucial zone melting step in isolation from the encapsulation steps of the continuous process, a horizontal constrained-zone melting apparatus made from graphite was used in which a boron oxide moat serves only as a sealant to suppress arsenic vaporization. Melt zones were passed through 5 and 10 cm long samples of GaAs ribbon feedstock. By controlling the heat flow in the graphite boat and controlling the zoning rate, large grained, single phase polycrystalline samples with directional solidification and good thickness control were achieved. Arsenic vaporization was effectively suppressed at the melting point of GaAs (1240°C) by the B_2O_3 moat and 3 atmospheres of pressure.

A vertical constrained-zone-melting apparatus with a B_2O_3 moat seal, rf heating, and water cooling on the bottom will be used to control the heat flow and temperature patterns required for growth of single crystal ribbons. These conditions will then be adapted to a continuous growth process.

Contribution Personnel: Dr. Joan B. Berkowitz, Principal Investigator
Joseph Wenckus
David L. Richardson
Dr. Peter E. Glaser
Dr. John Haggerty
Wilson Menashi

RIBBON GROWTH OF GALLIUM ARSENIDE

NSF Grant GI–43093

A.D. Little, Inc.

July 1, 1974 – December 30, 1975 (18 Months)

$ 164,000 ADL

$ 60,000 MIT (Crystal Characterization)

Dr. Joan Berkowitz, Principal Investigator

PROJECT OBJECTIVES

- To grow and characterize GaAs substrate ribbon single crystals 10 cm long x 1 cm wide x 0.1 cm thick
- To develop designs for a continuous growth experimental apparatus

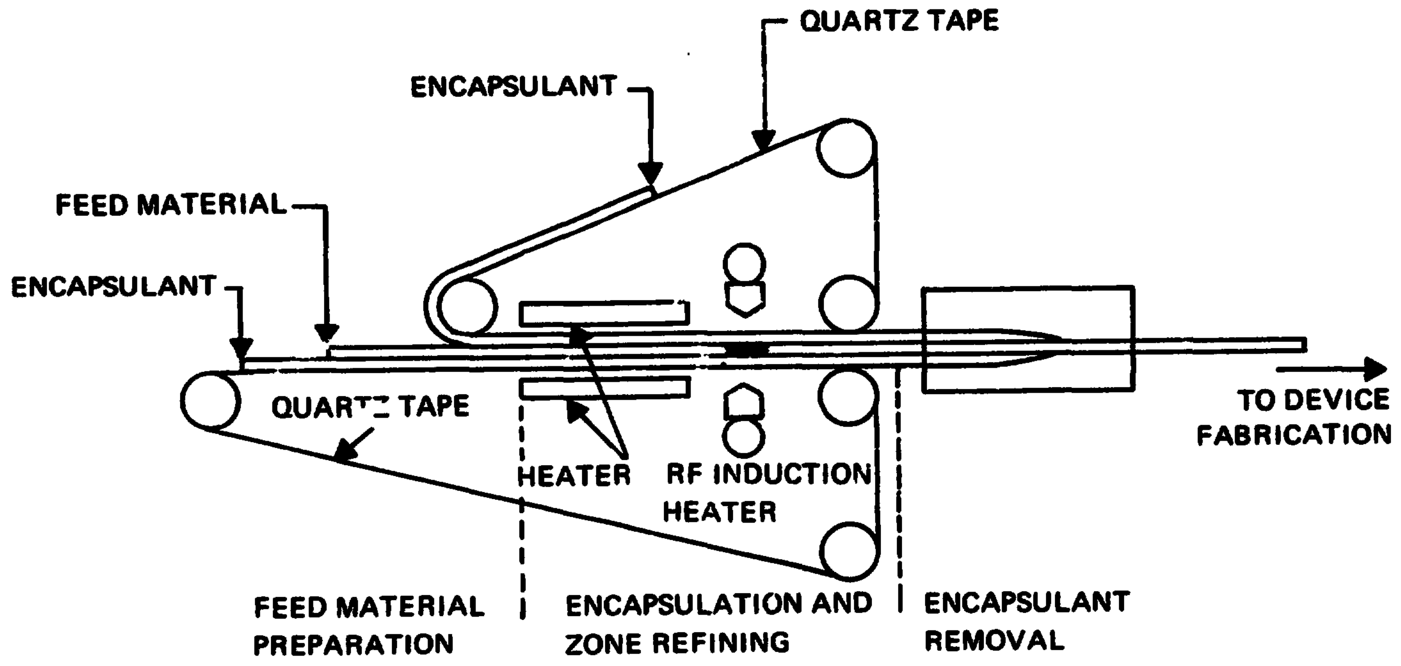
QUARTZ TAPE
ENCAPSULANT
FEED MATERIAL
ENCAPSULANT
QUART'Z TAPE
HEATER
RF INDUCTION HEATER
TO DEVICE FABRICATION
FEED MATERIAL PREPARATION
ENCAPSULATION AND ZONE REFINING
ENCAPSULANT REMOVAL

ACTIVITY DURING THE LAST 6 MONTHS

Tests with Direct Coupling
Horizontal Confined Growth
Characterization of Specimens
Vertical Confined Growth

DIRECT COUPLING

Temperature Limit of 900°C
Skin Depth for RF Heating is Greater Than Crystal Thickness
GaAs Spalled by B_2O_3 in Direct Contact

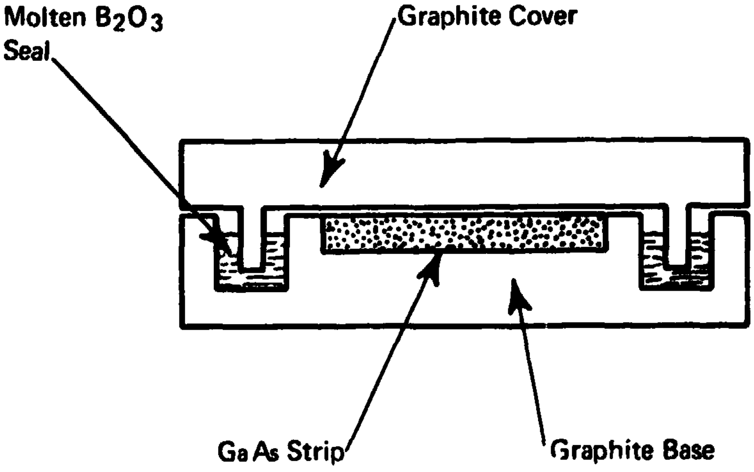

HORIZONTAL CONFINED GROWTH

Constraint of the Molten Zone
B_2O_3 Does Not Contact the GaAs
GaAs Does Not Wet the Graphite

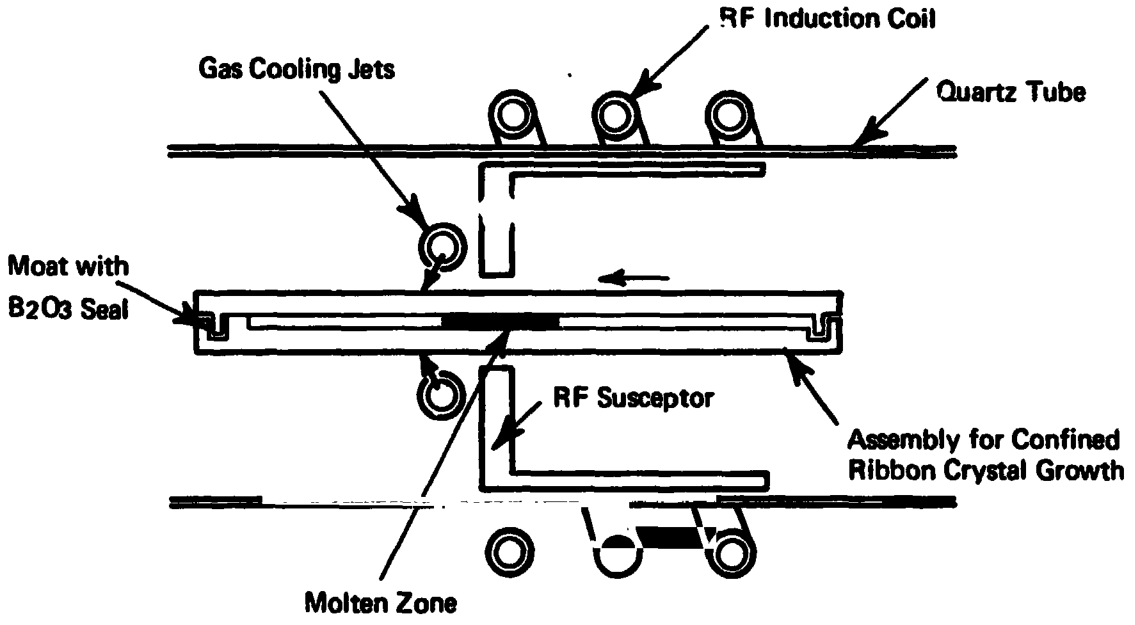

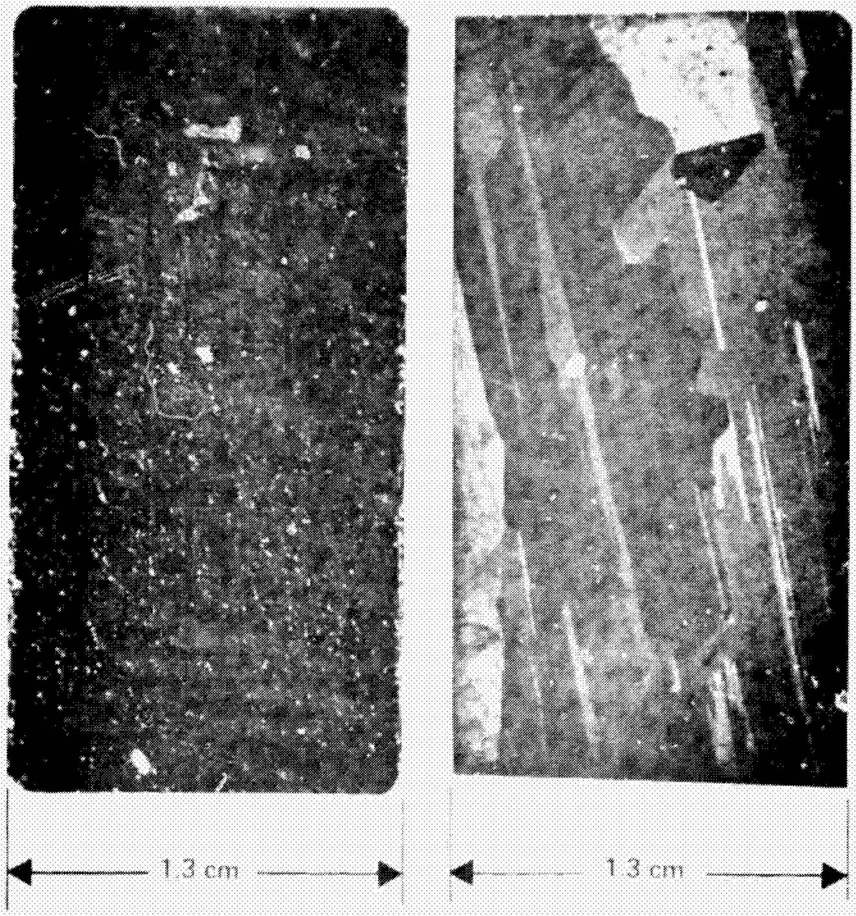
1.3 cm
1.3 cm

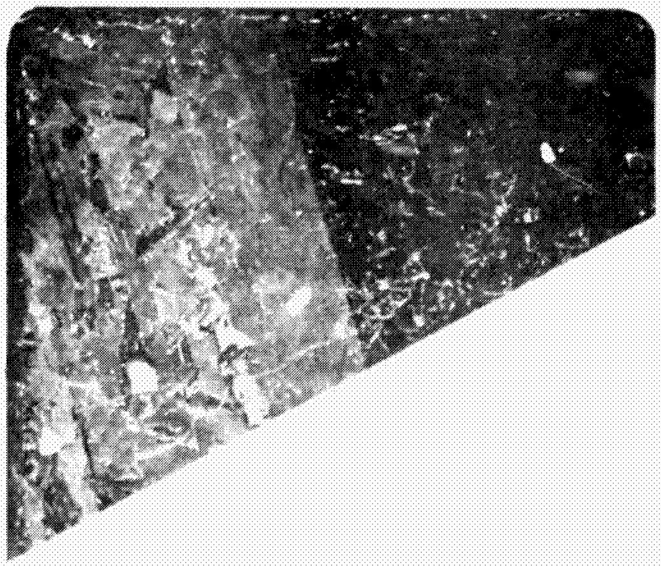

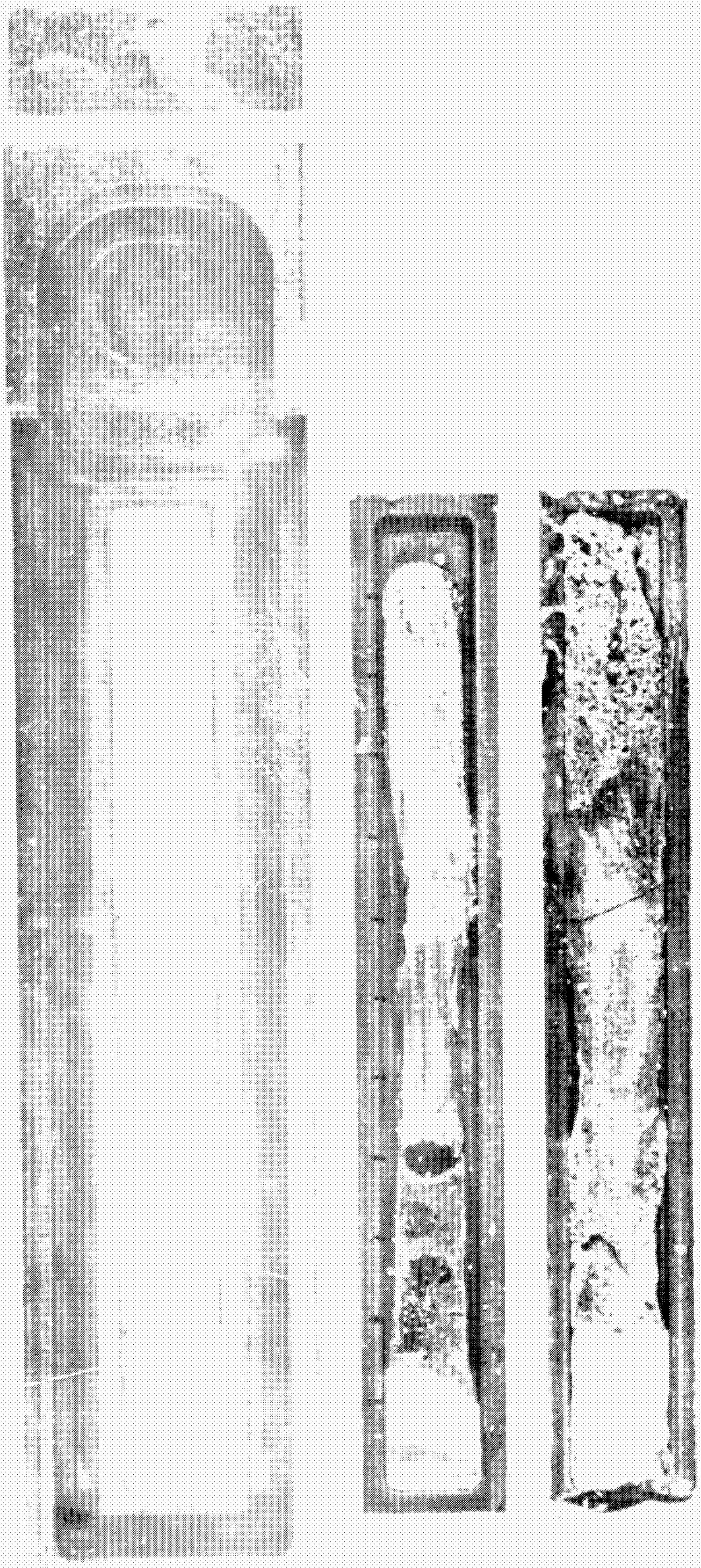

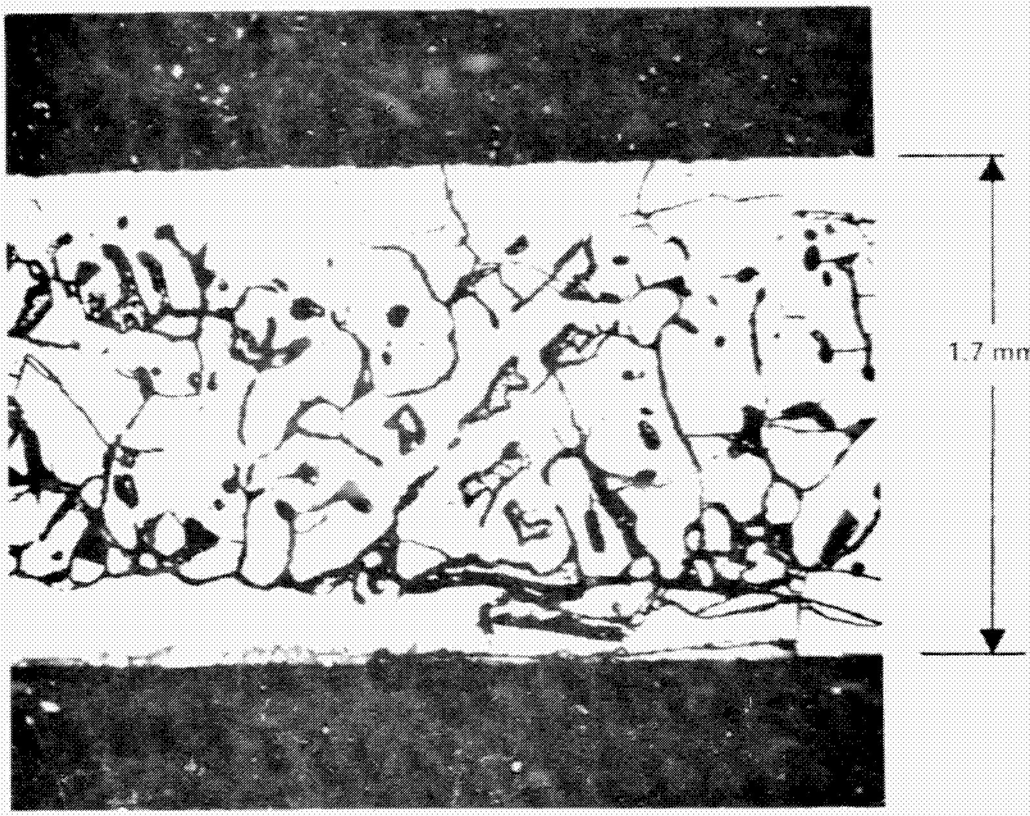
1.7 mm

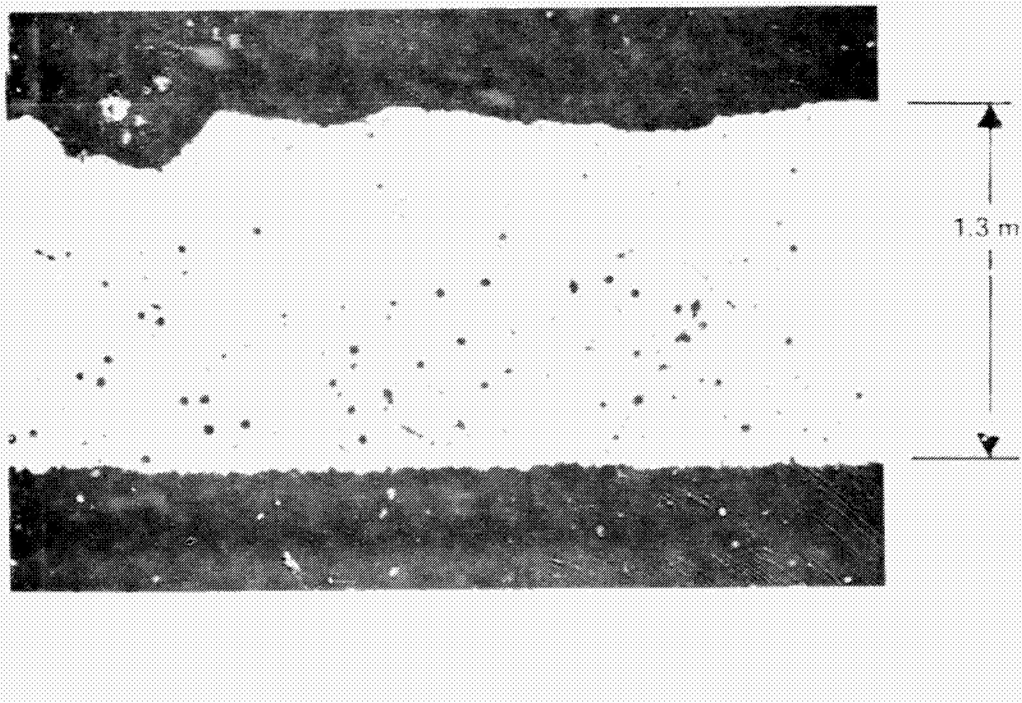
1.3 mm

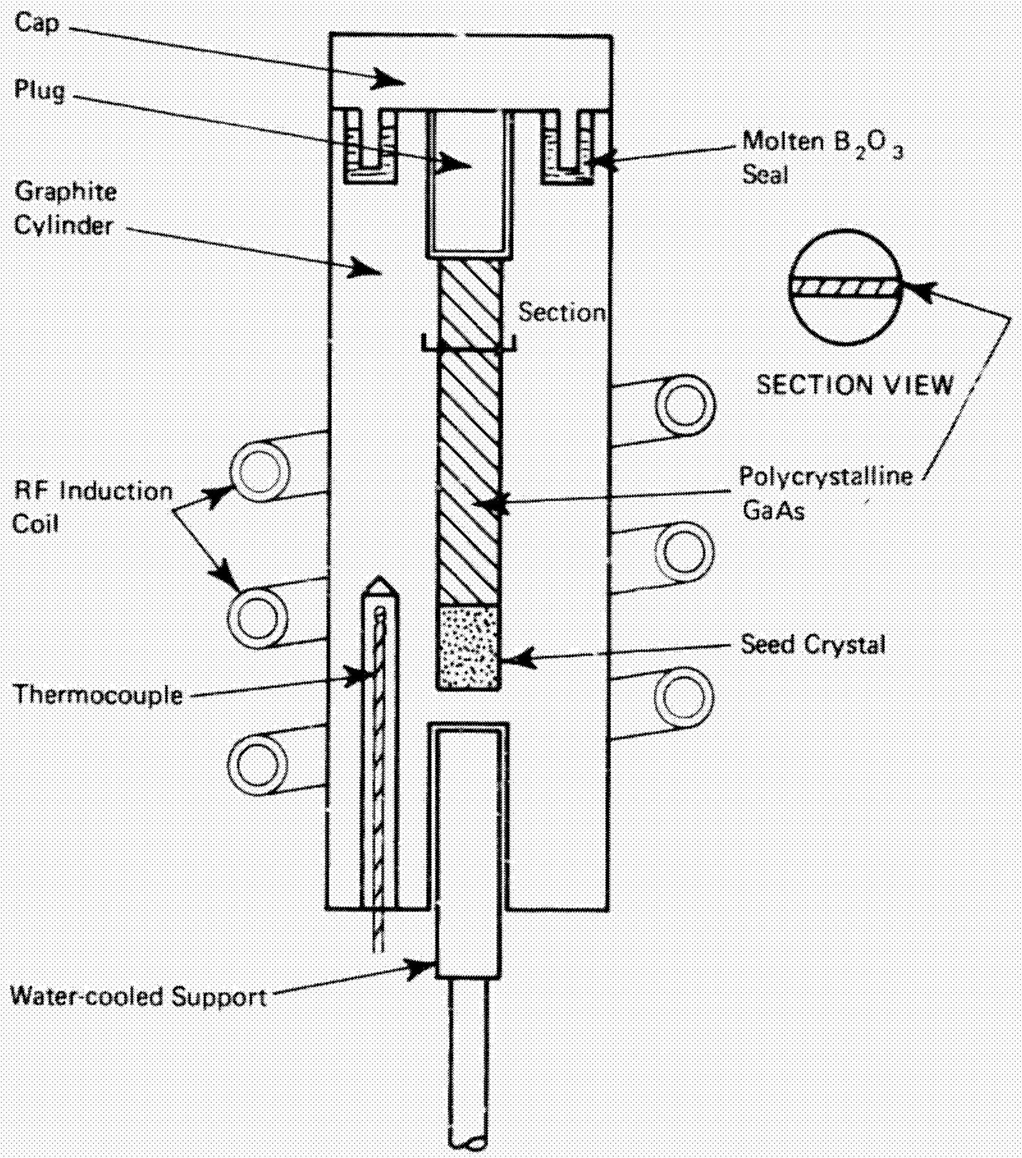

Cap
Plug
Molten B_2O_3 Seal
Graphite Cylinder
Section
SECTION VIEW
RF Induction Coil
Polycrystalline GaAs
Seed Crystal
Thermocouple
Water-cooled Support


Arthur D Little Inc
0 1 2 3 4 5
Centimeter Scale

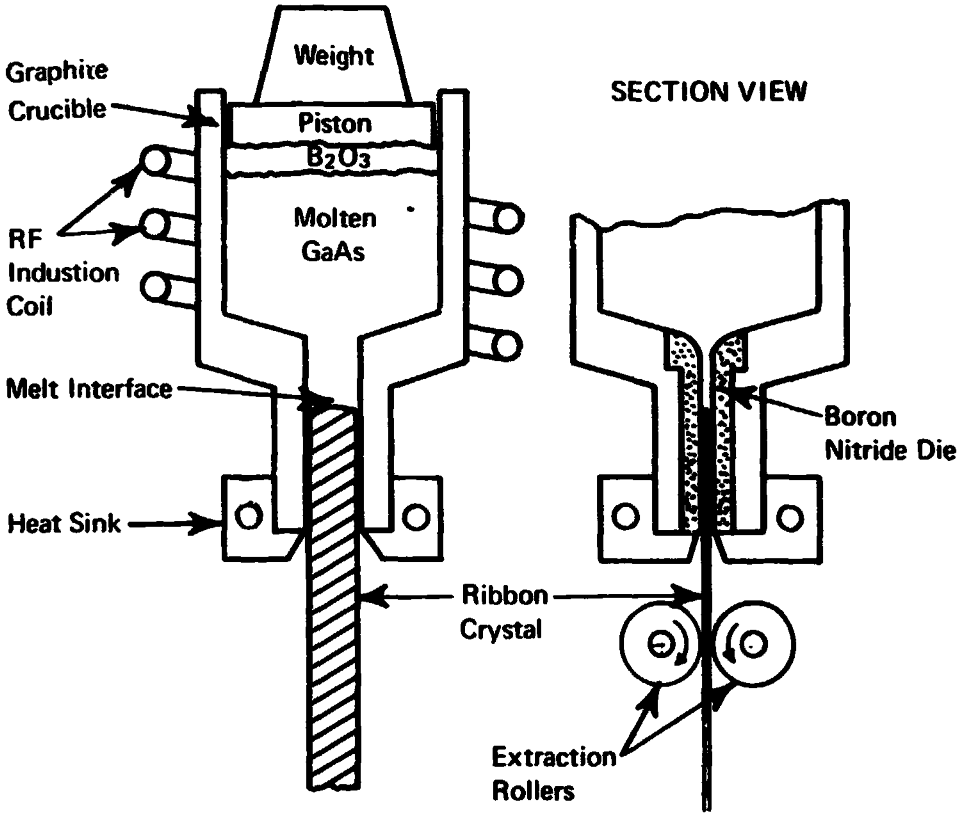
Weight
Graphite Crucible
Piston
B₂O₃
RF Industion Coil
Molten GaAs
SECTION VIEW
Melt Interface
Boron Nitride Die
Heat Sink
Ribbon Crystal
Extraction Rollers

SUMMARY OF KEY RESULTS

- Confined Melt Zone
- Directional Solidification
- Control of Arsenic Vaporization
- Single Phase Polycrystalline Material

PLANNED ACTIVITY FOR THE NEXT 6 MONTHS

- Experiments with Vertical Confined Growth
- Physically Characterize Crystals
- Design Continuous Growth Apparatus

PLANNED RENEWAL REQUESTS – Jan. 1976 – July 1977

- Construction of Experimental Continuous Growth Apparatus
- Optimization of Process with Respect to Energy and Cost
- Solar Cell Development and Characterization

N76 12497

Project Title: EXPLORATORY STUDY ON MICROANALYSIS OF THIN FILMS BY BACKSCATTERING TECHNIQUES

NSF Grant: AER 73-03265
Duration: 24 Months, August 1974 - August 1976
Amount: $130,400.00

Principal Investigators: James W. Mayer
Marc-A. Nicolet

Paper presented on July 24, 1975 at the National Solar Photovoltaic Program Review Meeting, Los Angeles, California, July 22 - 25, 1975.

OVERALL OBJECTIVES

1. To use backscattering spectrometry in the 1-2 MeV range for the determination of the composition and the detection of interdiffusion in thin film structures of interest to photovoltaic conversion.

2. To investigate the solid-phase epitaxial growth (SPEG) of Si layers at low temperatures obtained by interdiffusion processes.

3. To investigate backscattering spectrometry in the sub-MeV range and to assess its possibilities and problems.

Caltech 2

PLANNED ACTIVITY FOR LAST SIX MONTHS

1. Investigate electrical properties of the SPEG layer.

2. Investigate the possibility of SPEG with metal films other than Pd as transport medium.

3. Investigate BS below 1 MeV

EXPLORATORY STUDY ON MICROANALYSIS OF THIN FILMS BY BACKSCATTERING TECHNIQUES

by

James W. Mayer and Marc-A. Nicolet
California Institute of Technology
Pasadena, California 91125

ABSTRACT

I. SPEG

To be potentially useful, SPEG layers must have controllable electrical characteristics, particularly with regards to conductivity type and resistivity value. Efforts were therefore undertaken to establish that such a control is possible.

We added one processing step to the standard sample fabrication procedure by vacuum-depositing a thin layer (nominally 5Å) of Sb before the deposition of the amorphous Si layer, as shown in diagram labelled Caltech 4 (C4). Anneal steps remained unchanged. The resulting SPEG layer was analyzed in four different ways: (a) Auger Electron Spectroscopy (see C5), performed after the uppermost Pd_xSi_y layer was removed, confirmed that Sb was present within the SPEG layer of Si. (b) The I(V) characteristics of the SPEG layer against the Si substrate (<100>, 1-10 Ωcm p-type) was rectifying, and the layer itself afforded good electrical conductivity and easy ohmic contacting with W wires via the Pd_xSi_y layer (see C6). (c) A scanning microprobe picture of a cleaved sampled taken in the electron-beam-induced current mode established the presence of a depletion region more than 1 μ below the surface (see C7 and C8). (d) Hall effect data indicated that the SPEG layer was n-type, had an average free carrier concentration of about 10^{19} cm^{-3} and an average electron mobility $\bar{\mu}_n$ of about 40 cm^2/Vs (see C9). These results apply to a typical sample obtained with initial layers of about 1000Å Pd, 5 Å Sb and 1 μ of amorphous Si annealed in vacuum, first at 280° for 30 min and then under slowly increasing temperatures (≳ 0.2 °C/min) up to 525 °C. The evidence that the layer is n type and well doped is convincing. We plan to determine the properties of the doped SPEG layers more accurately, and to try other methods of introducing the dopant species of various kinds. The main problems are inadequate process control and marginal sensitivity of analytical tools.

SPEG with Pd_2Si as transport layer has two stages (see C10): (a) Initial fast (~10 Å/s at 500°C) transient regime. The growth starts with islands which ultimately join to form a layer (C11). The final thickness is equal to that of the initial Pd_2Si layer (C12). (b) Steady state regime. The growth is much slower (~ 1 Å/s), linear, and independent of the thickness of the transport medium (C13). The rate is thus not diffusion-limited.

SPEG with Ni silicide in lieu of Pd silicide as transport medium has been demonstrated by backscattering spectrometry (C14). As a whole, Ni SPEG is quite similar to that of Pd SPEG (C15). The transient is less distinct, because slower, and in the steady state regime, the boundaries of the transport medium lose their definition as the growth proceeds, which indicates poorer quality of the grown layer. Reactions require temperatures which are typically 90°C above the corresponding temperatures of Pd SPEG.

II. BACKSCATTERING SPECTROMETRY (BS)

To develope BS at energies below 1 MeV, depth calibration must be provided first by absolute measurements of stopping cross sections. Typical past errors of ± 10% are undesirably large. We have compared various methods of data evaluation and their errors with computer programs tested against real ^4He spectra. All methods can attain a few %, but values derived from films of known mass per unit area are generally most reliable. Main sources of errors are caused by detector noise and background signals. Absolute measurements are planned next.

Summaries of main results, major problems, planned activity and renewal proposal are given in C16 to C19.

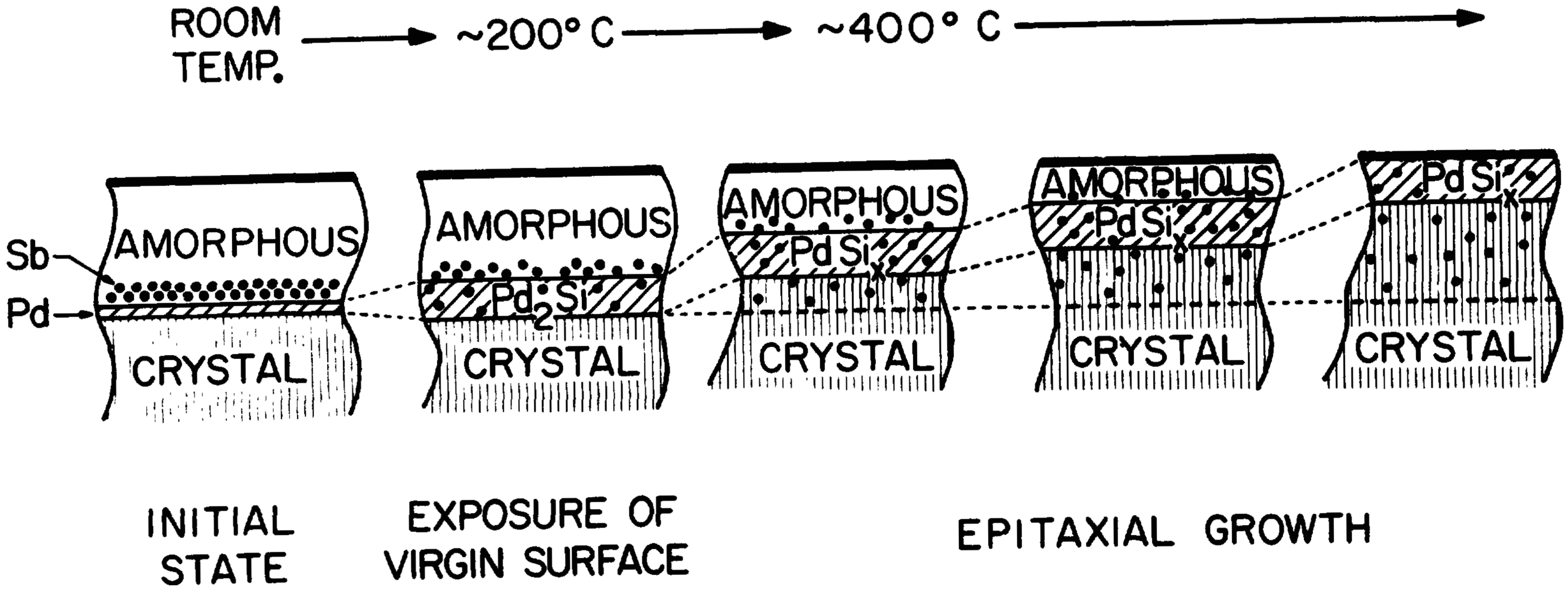
ROOM TEMP.
~200° C
~400° C
Sb
Pd
AMORPHOUS
CRYSTAL
AMORPHOUS
Pd_2Si
CRYSTAL
AMORPHOUS
$PdSi_x$
CRYSTAL
AMORPHOUS
$PdSi_x$
CRYSTAL
$PdSi_x$
CRYSTAL
INITIAL STATE
EXPOSURE OF VIRGIN SURFACE
EPITAXIAL GROWTH

SPEG

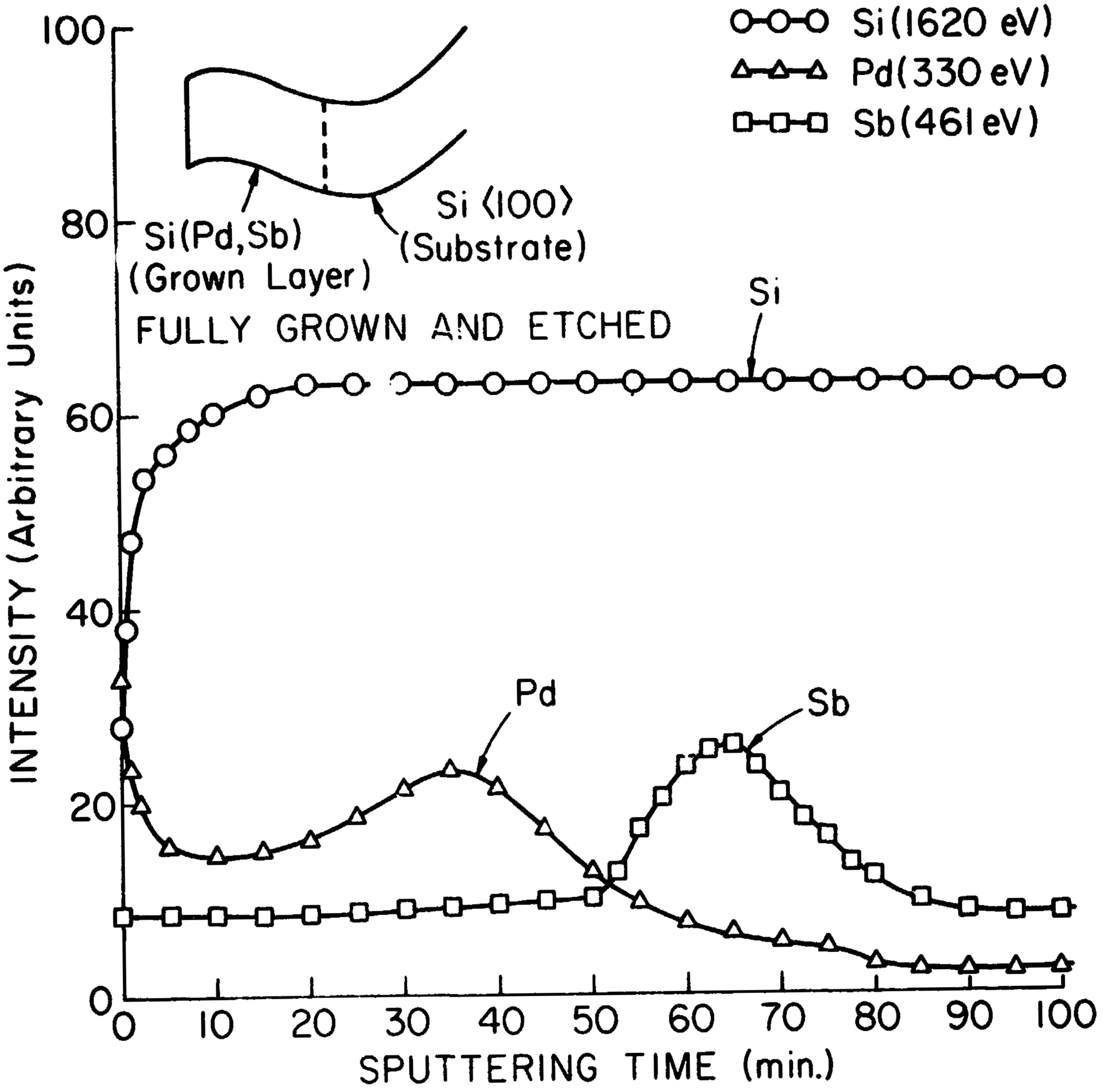
Si(1620 eV)
Pd(330 eV)
Sb(461 eV)
Si(Pd,Sb)
(Grown Layer)
Si ⟨100⟩
(Substrate)
FULLY GROWN AND ETCHED
Si
Pd
Sb
INTENSITY (Arbitrary Units)
0
20
40
60
80
100
0
10
20
30
40
50
60
70
80
90
100
SPUTTERING TIME (min.)

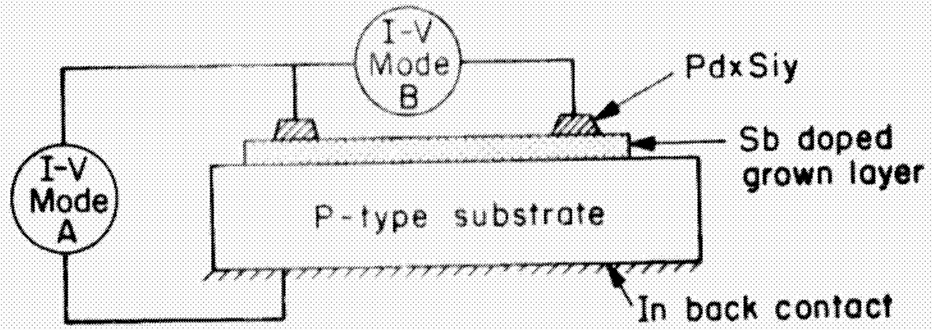
I-V Mode B
PdxSiy
Sb doped grown layer
I-V Mode A
P-type substrate
In back contact

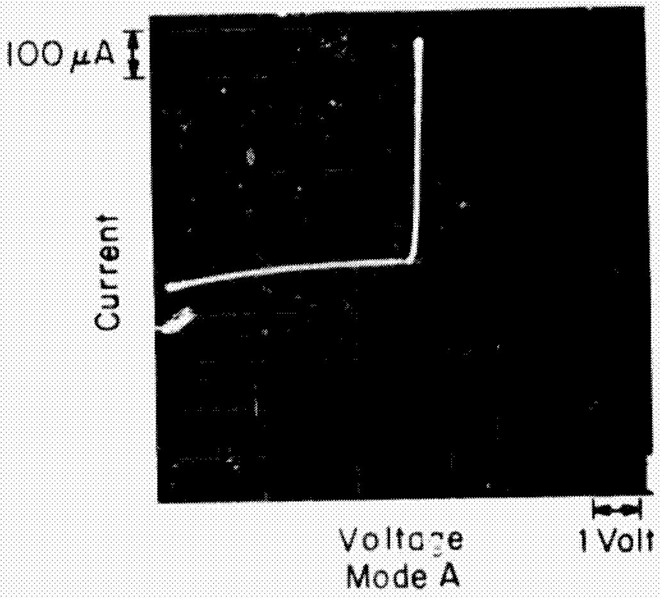
100 μA
Current
Voltage
1 Volt
Mode A

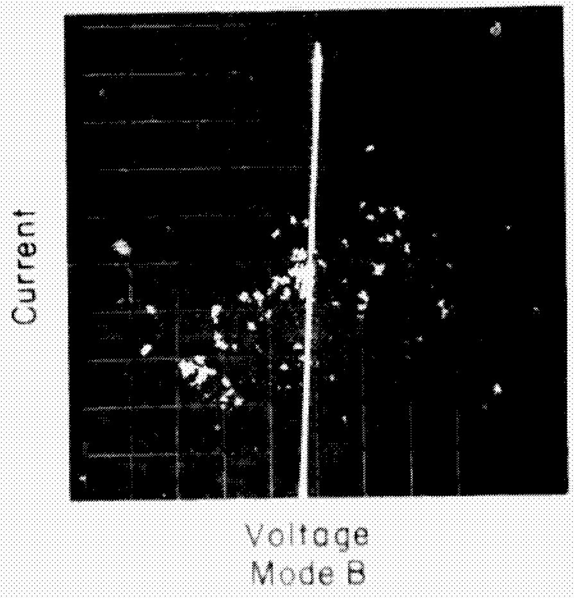
Current
Voltage
Mode B

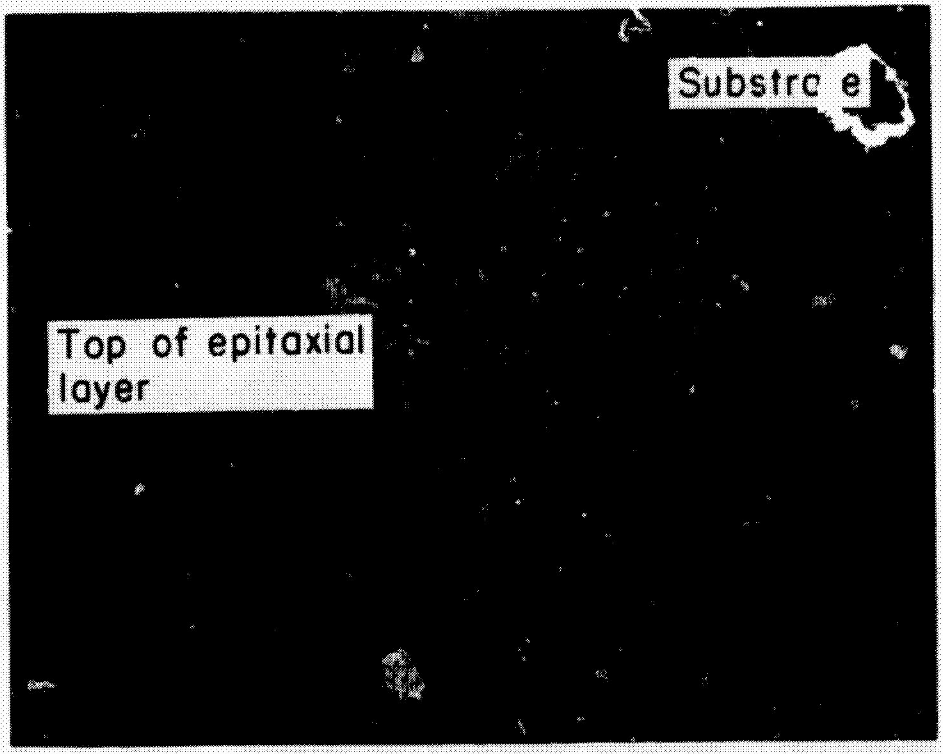

2^{nd} Electron Mode

EBIC Mode

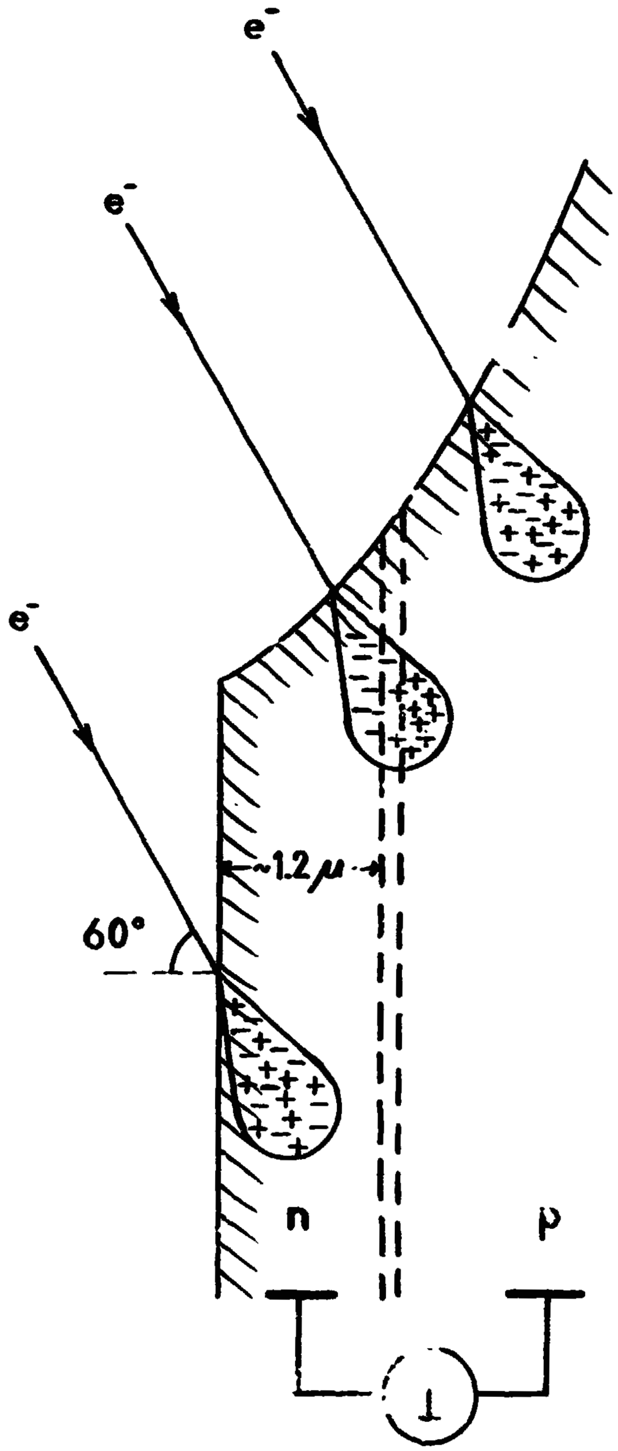

EBIC

HALL EFFECT

Data obtained at room temperature with van der Pauw patterns. Values are averages over the whole thickness (~ 1 μm) of the SPEG layer.

	SPEG Layer	Comparison with bulk single crystal	
Conductivity type	n	n	
Mobility μ_n	~ 40-50	140	cm^2/Vs
Carrier Concentration	10^{19}	10^{19}	cm^{-3}
Resistivity	~ .02	.004	Ωcm

Caltech 9

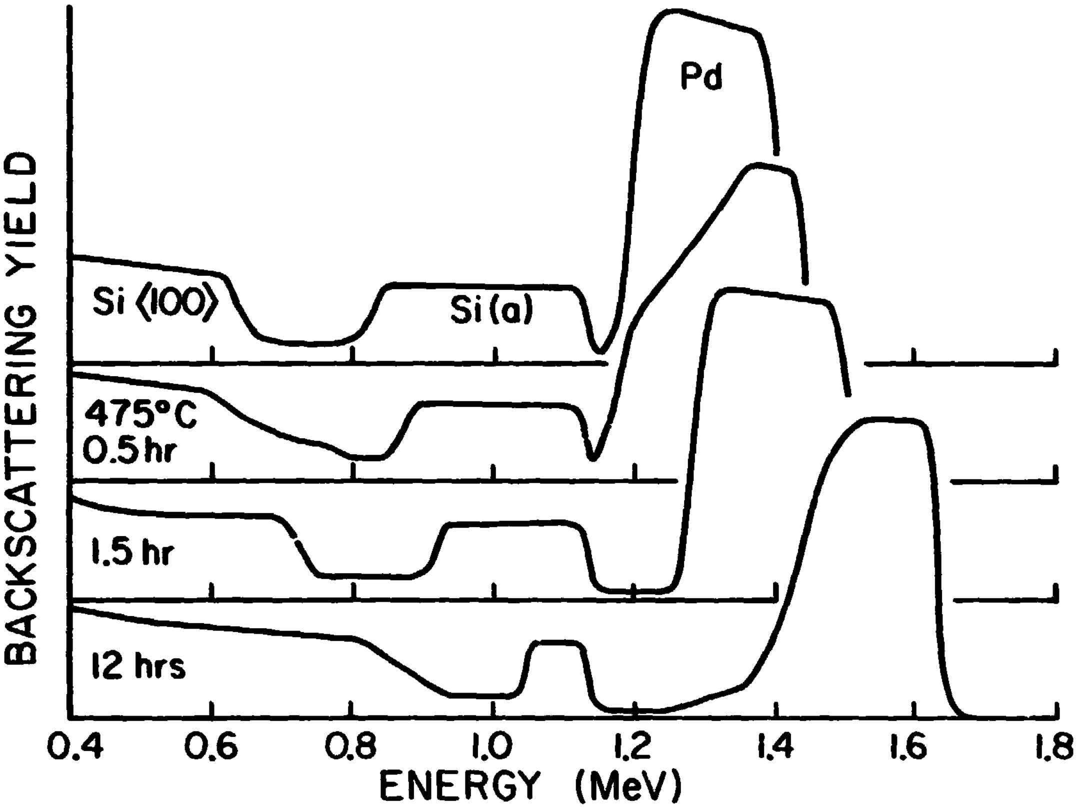
BACKSCATTERING YIELD
Pd
Si ⟨100⟩
Si (a)
475°C
0.5 hr
1.5 hr
12 hrs
0.4
0.6
0.8
1.0
1.2
1.4
1.6
1.8
ENERGY (MeV)

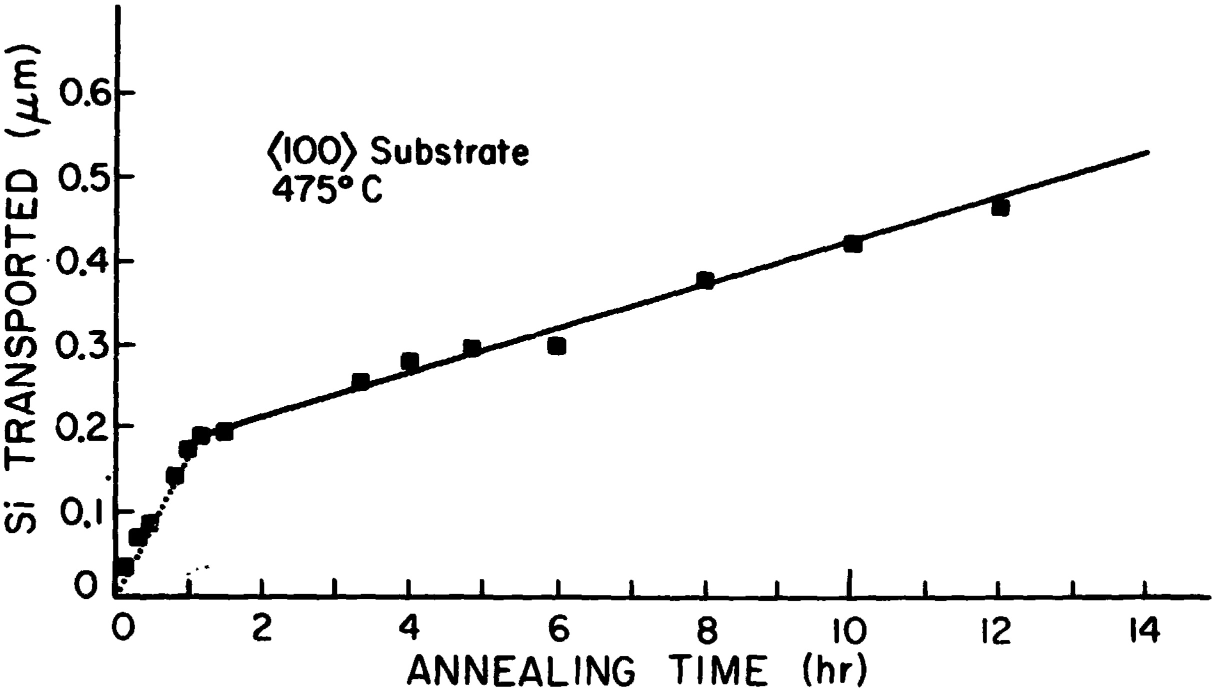
Si TRANSPORTED (μm)
0
0.1
0.2
0.3
0.4
0.5
0.6
⟨100⟩ Substrate
475° C
0
2
4
6
8
10
12
14
ANNEALING TIME (hr)

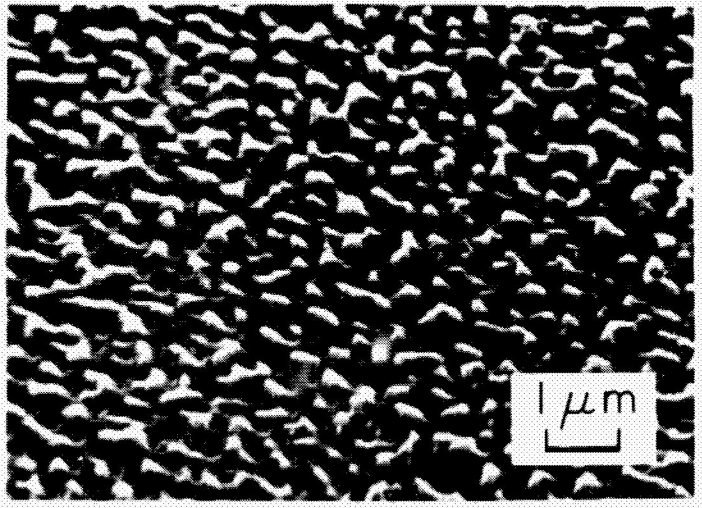

475°C 30min

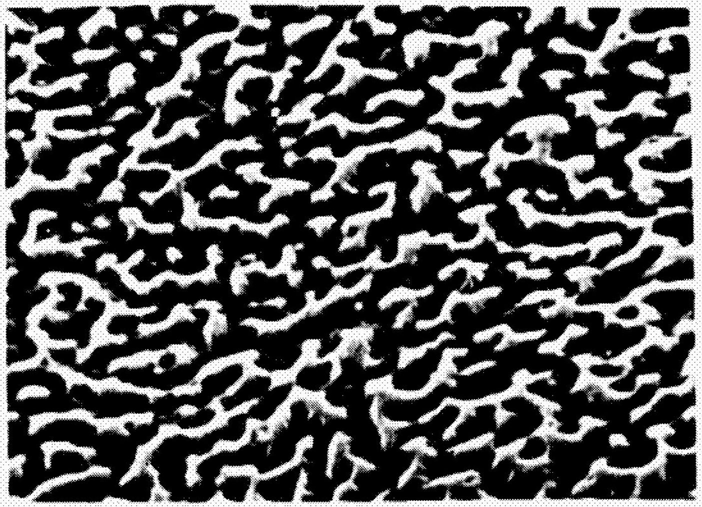

50min

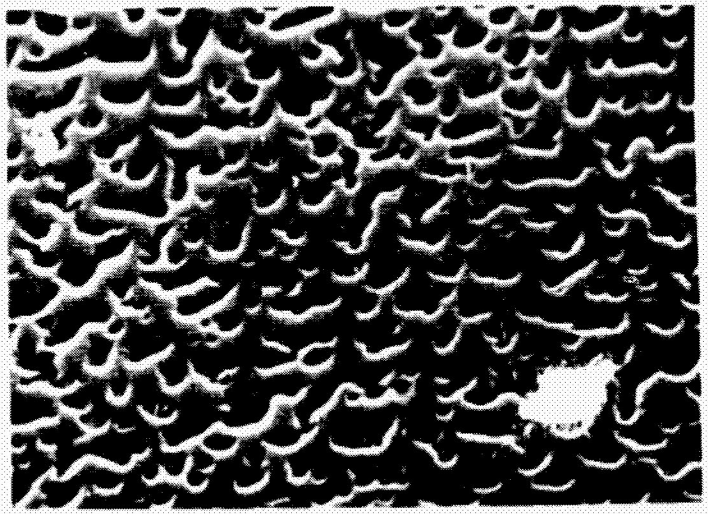

70min

90min

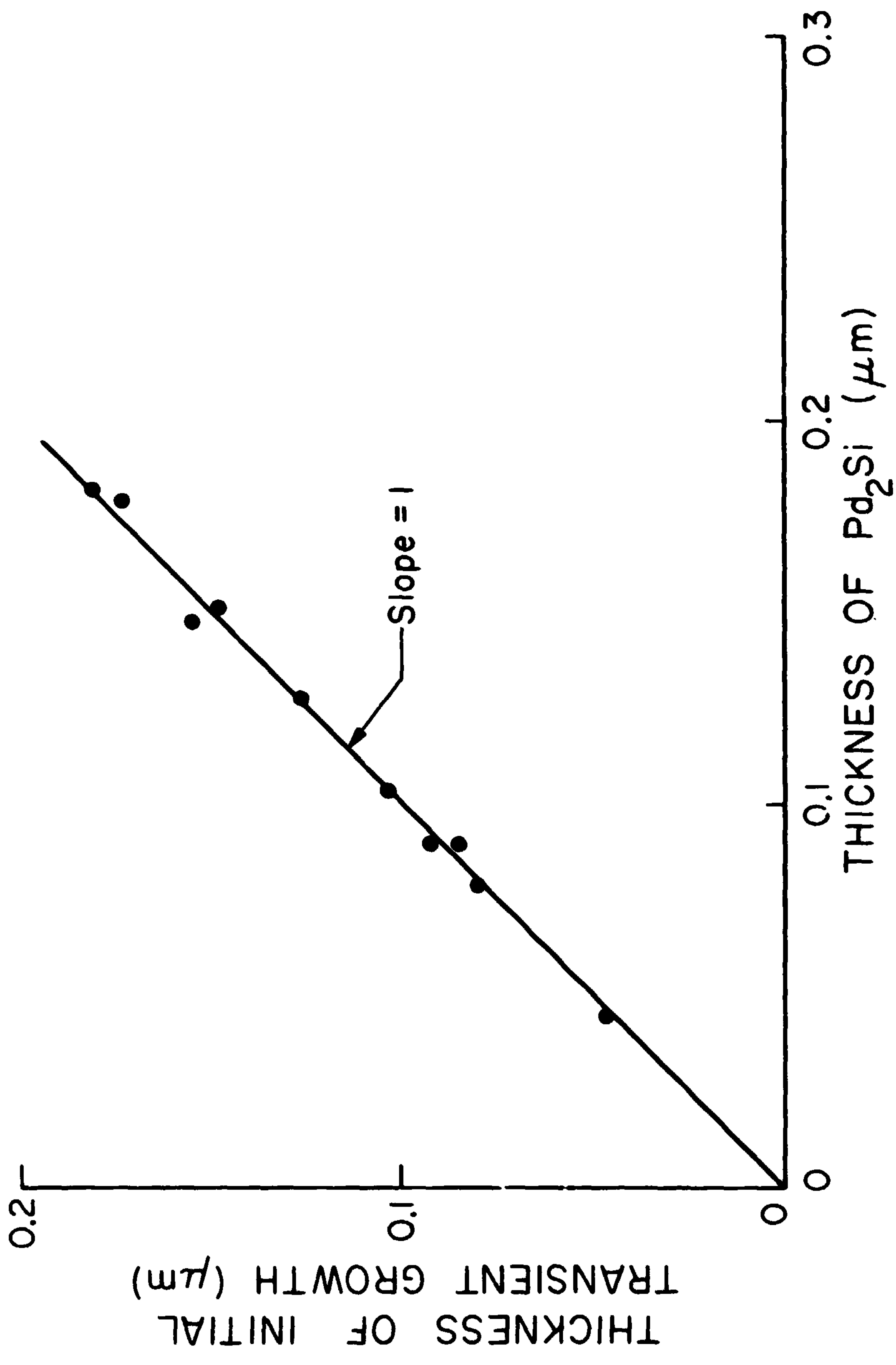
THICKNESS OF INITIAL TRANSIENT GROWTH (μm)
0.2
0.1
0
Slope = 1
0
0.1
0.2
0.3
THICKNESS OF Pd_2Si (μm)

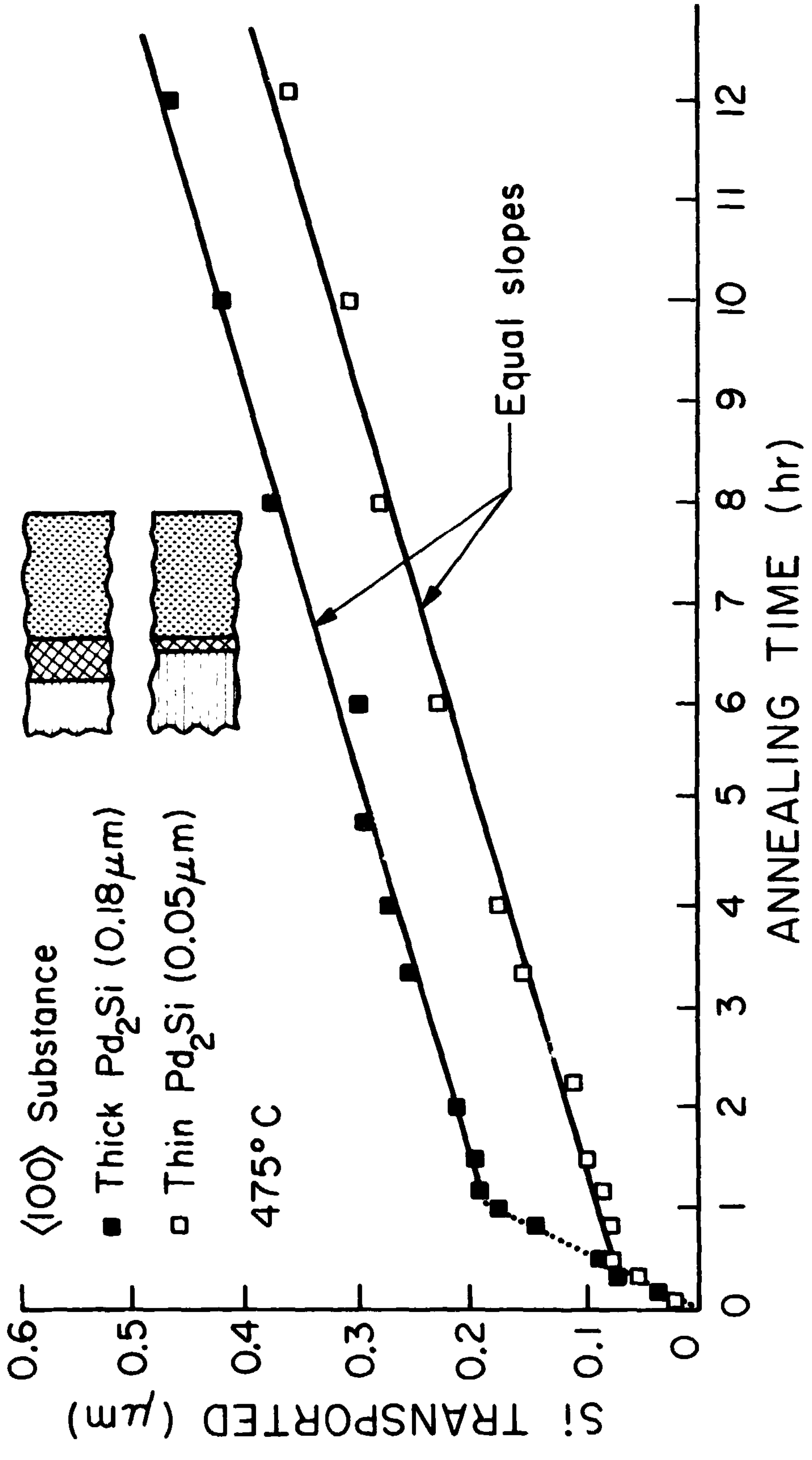
⟨100⟩ Substance
■ Thick Pd_2Si (0.18μm)
□ Thin Pd_2Si (0.05μm)
475° C
Equal slopes
Si TRANSPORTED (μm)
0
0.1
0.2
0.3
0.4
0.5
0.6
ANNEALING TIME (hr)
0
1
2
3
4
5
6
7
8
9
10
11
12

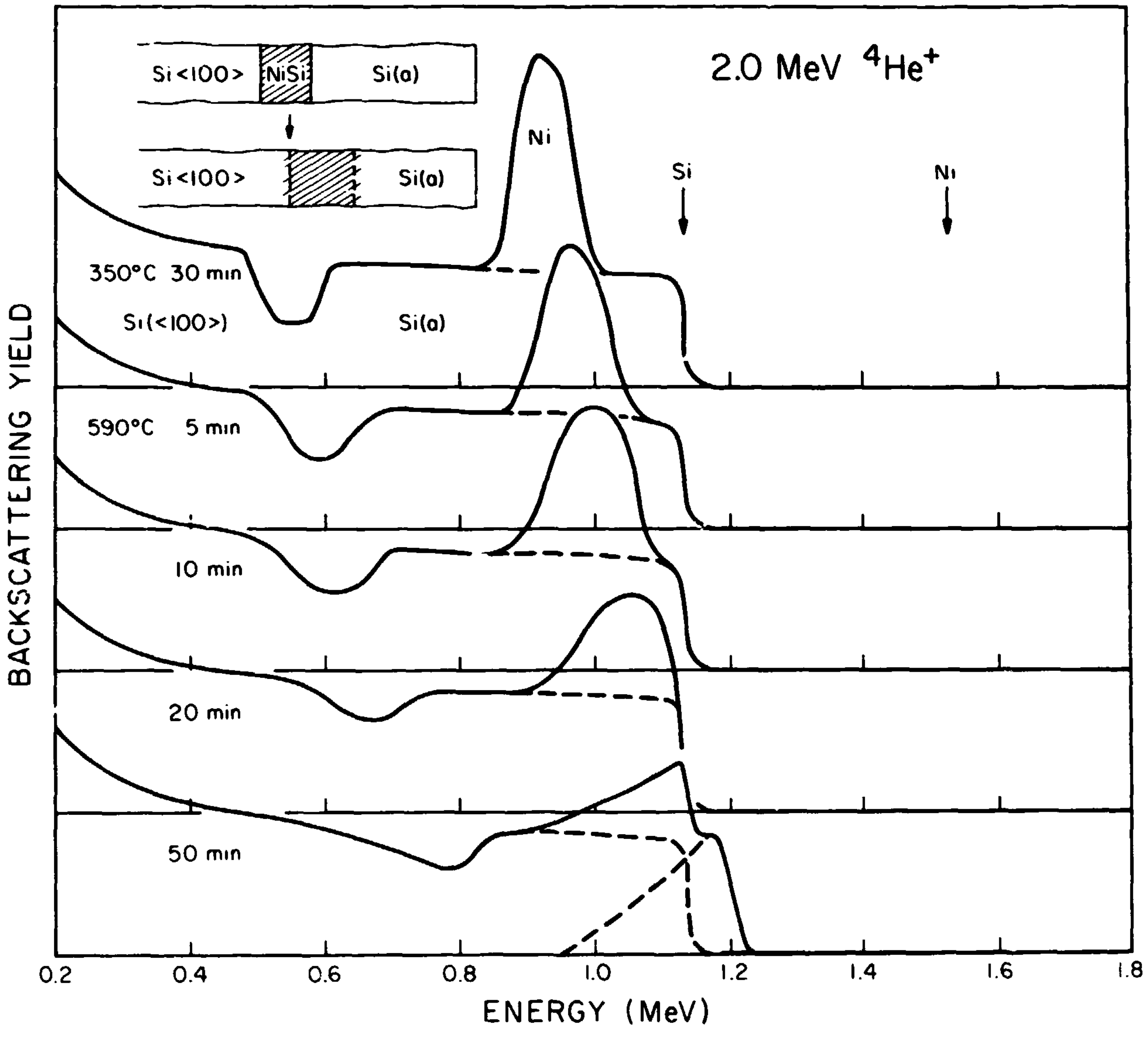
2.0 MeV $^4He^+$
Si<100>
NiSi
Si(a)
Si<100>
Si(a)
Ni
Si
Ni
350°C 30 min
Si(<100>)
Si(a)
590°C 5 min
10 min
20 min
50 min
BACKSCATTERING YIELD
0.2
0.4
0.6
0.8
1.0
1.2
1.4
1.6
1.8
ENERGY (MeV)

COMPARISON OF SPEG WITH Pd AND Ni

	Pd	Ni	
SAMPLE			
Substrate	<100>	<100>	
Metal Film	~1000	~1000	Å
Si(a) Film	~1	~1	μm
FORMATION OF TRANSPORT MEDIUM			
Typical Temperature	280	350	°C
Typical Time	30	30	min
Composition by BS	$\frac{Pd}{Si} = \frac{2}{1}$	$\frac{Ni}{Si} = \frac{1}{1}$	
by X-rays	Pd_2Si	NiSi	
TRANSPORT OF Si			
Typical Temperature	~500	~590	°C
Transient Rate	~10	~2	Å/s
Form	island	no island	(?)
Steady State Rate	~1	~1	Å/s
Structure	epitaxial	epitaxial	(poor)
Apparent Activation Energy	~4	~4	eV

Caltech 15

SUMMARY OF KEY RESULTS

1. Doping of SPEG layers is possible;proof obtained with Sb and established via:
    - I(V) characteristics
    - Hall effect measurements
    - EBIC μ-probe pictures
    - AES
2. SPEG with Pd_2Si has two stages:
    Initial transient regime
    - 10 A°/s rate
    - island growth
    - thickness = that of Pd_2Si layer

    Steady State regime
    - 1 A°/s rate, independent of Pd_xSi_y layer thickness
    - continuous film growth

3. SPEG with NiSi also works; generally similar to SPEG with Pd_2Si:
    - Corresponding process temperatures are typically ~ 90°C higher for Ni
    - Layer quality presently inferior to obtained with Pd_2Si

4. Identified best methods for stopping power measurements below 1 MeV from backscattering spectra.

MAJOR PROBLEMS

SPEG

Control of fabrication processes

- cleanliness of interfaces
- purity of deposited layers
- amount of doping
- annealing ambient

Characterization of final product

- limitations of analytical tools

BS

Limitations in system

- detector noise
- preamplifier noise

Limitations in target

- purity

$$\left.\begin{array}{l}\text{- thickness}\\ \text{- mass/cm}^2\end{array}\right\}\ \text{density}$$

PLANNED ACTIVITY FOR NEXT SIX MONTHS

1. Characterization of doped SPEG layers.

2. Doping of SPEG layers by other dopants or other incorporation methods.

3. Compare SPEG with regrowth of amorphous Si layers on single crystal Si substrates.

4. Obtain stopping cross sections in 0.3 - 1.0 MeV range.

Caltech 18

PLANNED RENEWAL REQUEST

Major Goals

Investigate SPEG

Assess practical potential of SPEG to solar cell, and to semiconductor devices generally

Liberate SPEG from single crystal substrate

Develop sub-MeV backscattering spectrometry

Estimated Dates and Costs

August, 1976 to August, 1978 (24 Months) $150,000.00

Caltech 19

N76 12498

LOW COST AMOS SOLAR CELL DEVELOPMENT

Richard J. Stirn

Jet Propulsion Laboratory, Pasadena, California

ABSTRACT

Recent developments at JPL have demonstrated that high conversion efficiencies are possible with GaAs metal-semiconductor solar cells when a particular heat treatment processing step is used to introduce an interfacial layer between the metal and the semiconductor. The new cell, called AMOS (Antireflection-Coated Metal-Oxide-Semiconductor), has open-circuit voltages of 0.68-0.72 volts and efficiencies of 15% under terrestrial sunlight, as compared to values of 0.45-0.48 volts and 10%, respectively, for similar cells without an interfacial layer. Potentially higher efficiencies are feasible as further improvements are made in optimizing the interfacial layer effect and in increasing the blue response of the cells. These developments clearly indicate the desirability of investigating a thin film version of the AMOS solar cell which could better the economic goal of $0.50 per peak watt with an efficiency greater than 10%.

The thin film AMOS cell proposed is unique in that a thin recrystallized germanium (Ge) layer is used between a low cost metal substrate and the vapor phase epitaxially (VPE)-grown GaAs. It has already been shown that Ge films can be recrystallized to millimeter-sized crystallites by the use of scanning electron beams. Indeed, even lateral growth of single crystal Ge has been demonstrated on tungsten which was dipped and withdrawn from a melt of Ge. In the proposed program, laser beams will be primarily used to investigate recystallization. Later versions of the cell may be able to dispense with the Ge layer, as it may be possible to recrystallize GaAs to sufficient degree using techniques developed for the Ge layer. This possibility will not, however, be explored in the early phases.

The Ge layer, used as a substrate for VPE-grown GaAs, will provide a more ordered, larger-grained GaAs film. The increased order, the use of a semiconductor with high light absorption, and the inherent properties of the

metal-semiconductor contact, should give considerably higher current and voltage outputs than have previously been obtained in polycrystalline thin-film solar cells. The availability and cost of materials are satisfactory for the amounts required and the fabrication steps envisioned for large-scale production are amendable to continuous or quasi-continuous processing.

An ancillary program for optimizing the newly added AMOS processing step, which leads to markedly higher voltage outputs, is proposed. This program will utilize electrical and chemical analysis measurements to better understand the pertinent interface (oxide-semiconductor) properties, so that the appropriate process can be added to the low-cost AMOS cell program when suitable thin films are available.

The electrical MOS-type measurements will be performed at the Pennsylvania State University on a subcontract. This program will supplement an existing theoretical contract with the University (Prof. Stephen Fonash) to investigate the interfacial layer [illegible]. The measurements, along with transient capacitance measurements at JPL, will attempt to determine surface state distribution in the band gap, surface state capture cross sections, surface state type and surface charge, modified to account for the fact that tunneling currents are flowing through the ultra-thin layers. These data will complement studies of the chemistry of the interface region using ESCA (Electron Spectroscopy for Chemical Analysis) facilities at JPL.

The parametric studies for optimum GaAs growth by vapor phase epitaxy on Ge films will be performed by Applied Materials, Inc. The company has been a supplier of exceptionally high quality single crystal GaAs, having minority carrier diffusion lengths for holes of 3-4 microns, even with doping concentrations up to 10^{17} cm^{-3}. The investigation will be focused on the nucleation characteristics of various substrates as to how they are affected by temperature and growth rate. The latter is sensitive to the ratio of the As-and Ga-bearing gases and to the concentrations in each of these gases.

As Ge and GaAs films are developed, the structural characteristics of the films will be examined by optical and scanning electron microscopy, and various x-ray techniques to characterize the grain size and of disorder, preferred orientation and dislocation density. Metal-semiconductor solar cells will be fabricated on GaAs films as they become available with particular interest in the surface preparation required, if any, and the thickness of the semitransparent metal film required for usable sheet resistances.

The standard optical, electrical and photovoltaic measurements will be made on the cells, as well as scanning electron microscopy (in the beam-induced conductivity mode) to observe grain boundary effects on current collection.

The efficiency to be expected may be estimated from the single-crystal cells already constructed. Estimating the current loss at 20% (due to the use of a somewhat thicker semitransparent metal film and a reduced minority carrier diffusion length of about one-half) and a 10% loss in voltage (due to some barrier lowering at the few grain boundaries), a long term goal of 12-14% conversion efficiency for a thin-film AMOS solar cell seems reasonable.

In summary, the research plan involves the interaction of three major groups: (1) the Research Group at JPL, (2) Pennsylvania State University, and (3) Applied Materials, Inc. JPL will select the best substrates for Ge deposition, recrystallize the Ge film by scanning laser or electron beams, characterize the Ge and GaAs films, fabricate and test metal-semiconductor solar cells on the GaAs films, and perform ESCA measurements of the AMOS interface region on single crystal GaAs. Pennsylvania State University will determine the interface electronic properties of the AMOS solar cell and correlate with theoretically determined optimum characteristics. Finally, Applied Materials, Inc., will provide the parametric studies for optimum GaAs growth by vapor phase on Ge films.

LOW COST AMOS SOLAR CELL DEVELOPMENT

GUIDANCE AND CONTROL RESEARCH GROUP

JET PROPULSION LABORATORY

PROPOSED START DATE : SEPTEMBER 1, 1975
$ 225,250

PRINCIPAL INVESTIGATOR : RICHARD J. STIRN

PRESENTED AT : NATIONAL SOLAR
PHOTOVOLTAIC PROGRAM REVIEW
MEETING, UCLA

JULY 22-25, 1975

OBJECTIVE

- DEMONSTRATE THE FEASIBILITY OF A LOW-COST THIN-FILM GALLIUM ARSENIDE SOLAR CELL
    - RECRYSTALLIZE Ge FILMS ON LOW COST SUBSTATES
    - OPTIMIZE GaAs VPE-GROWTH ON Ge FILMS
    - FABRICATE AMOS SOLAR CELLS ON GaAs/Ge FILMS
    - INVESTIGATE INTERFACE PHYSICS AND CHEMISTRY

LIGHT I-V CURVE FOR AMOS CELL

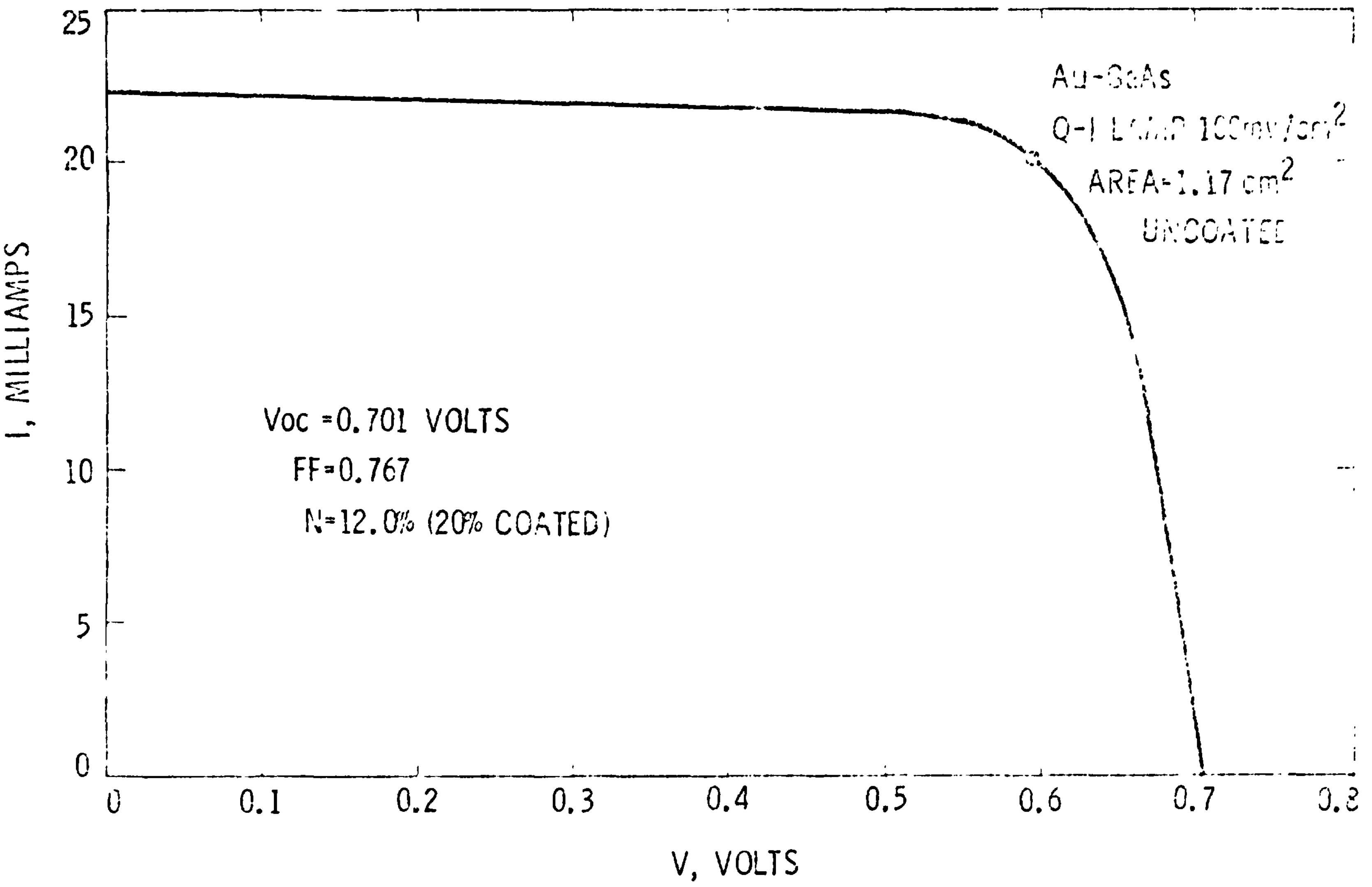

OPEN CIRCUIT VOLTAGE OF [illegible] CELL AT VERY HIGH LIGHT INTENSITY

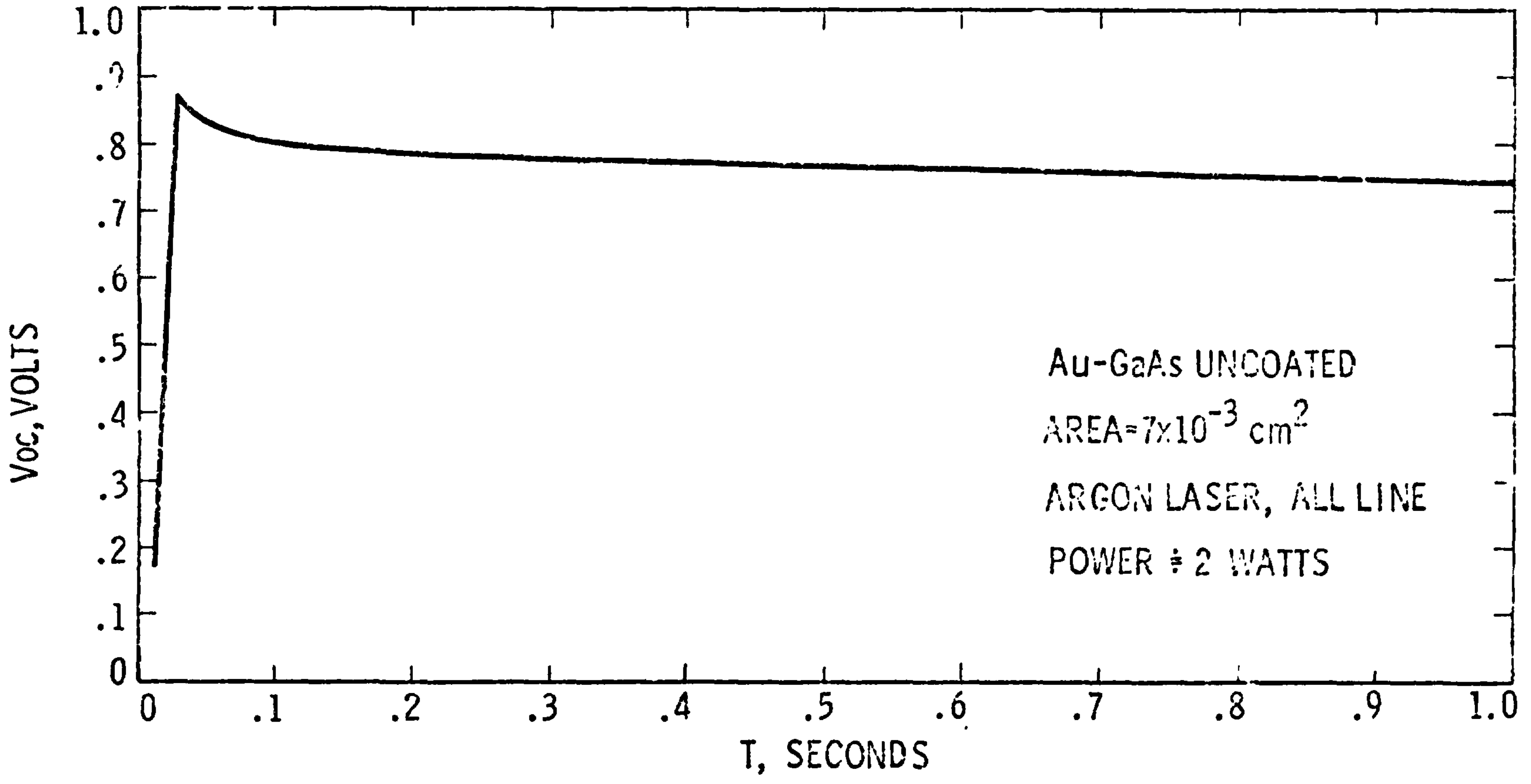

THIN-FILM AMOS SOLAR CELL - FIRST GENERATION (NOT TO SCALE)

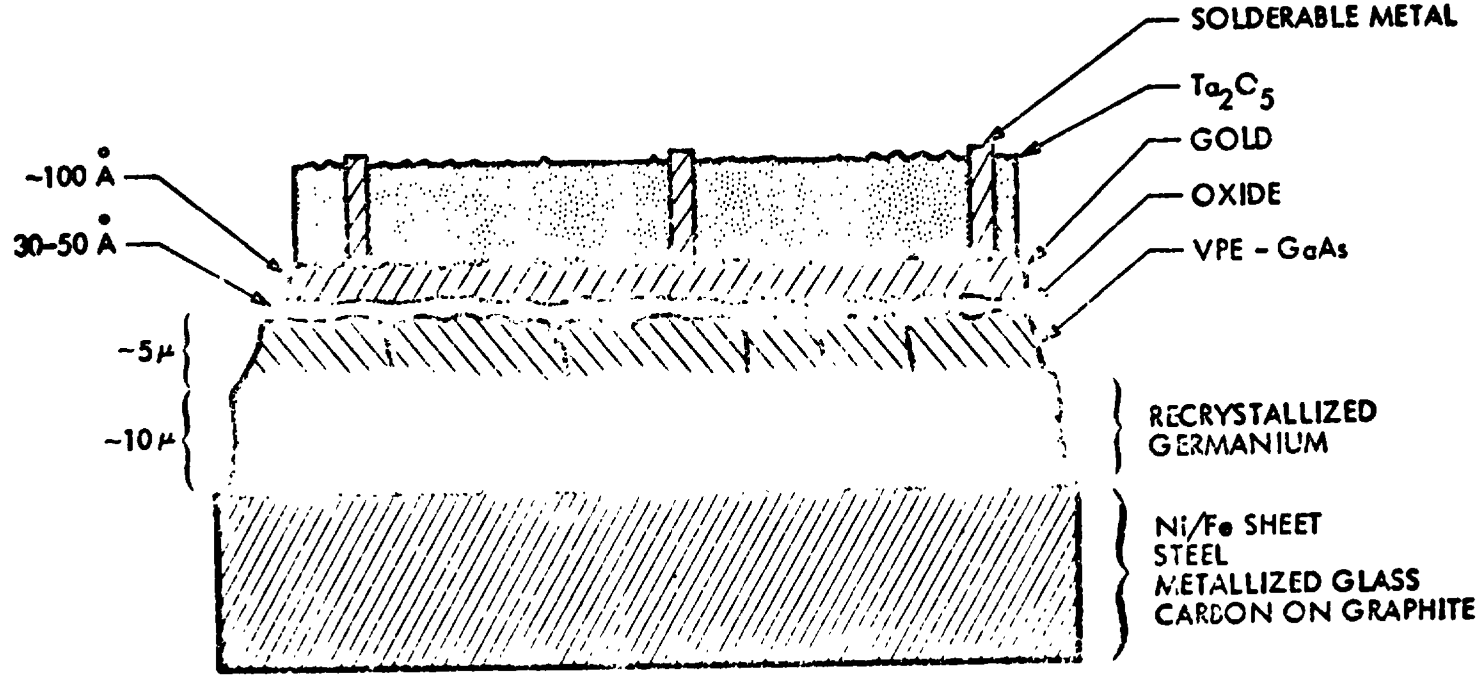

LINEAR COEFFICIENTS OF EXPANSION

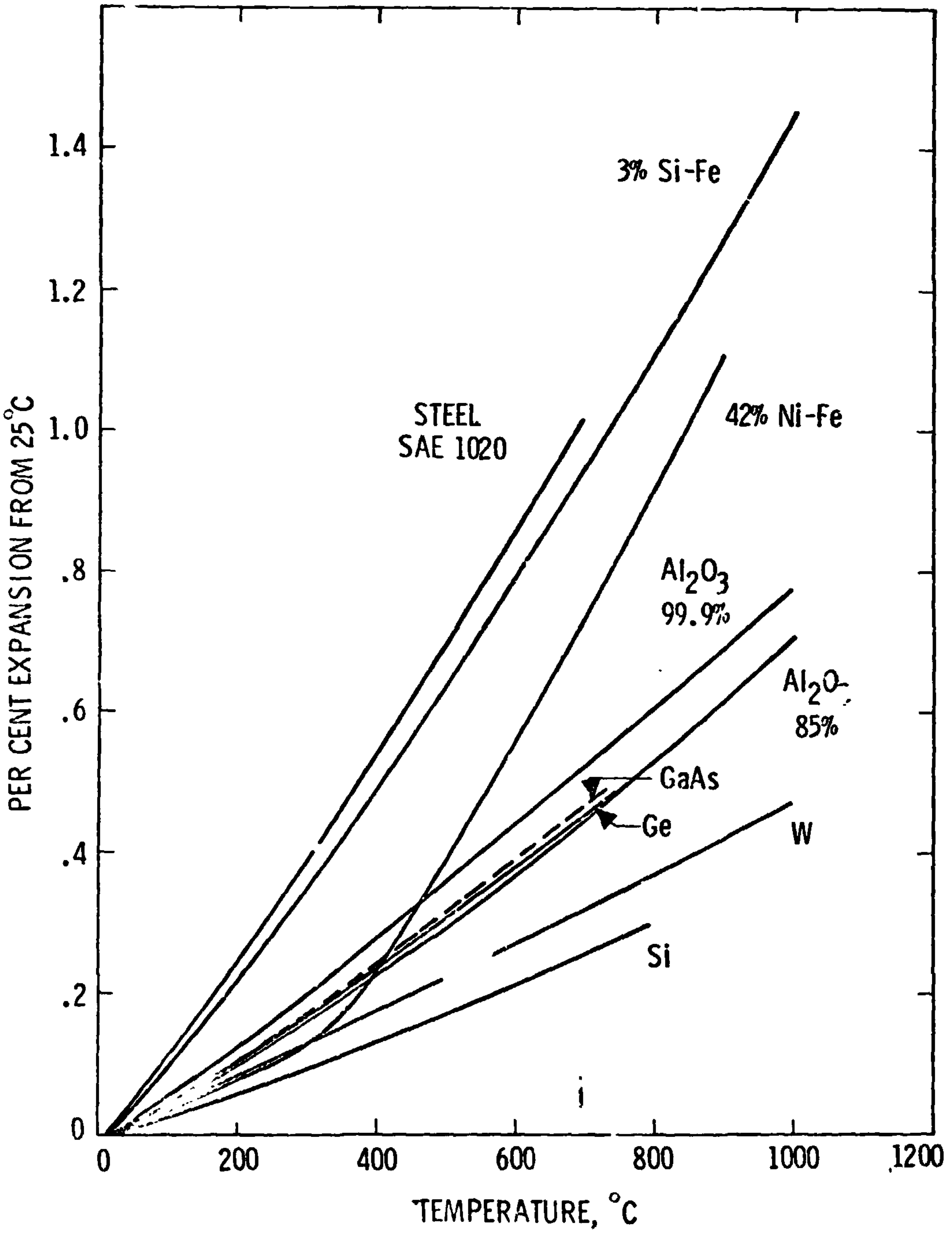

DEPENDENCE OF SHORT-CIRCUIT CURRENT IN A GaAs MS SOLAR CELL ON METAL THICKNESS

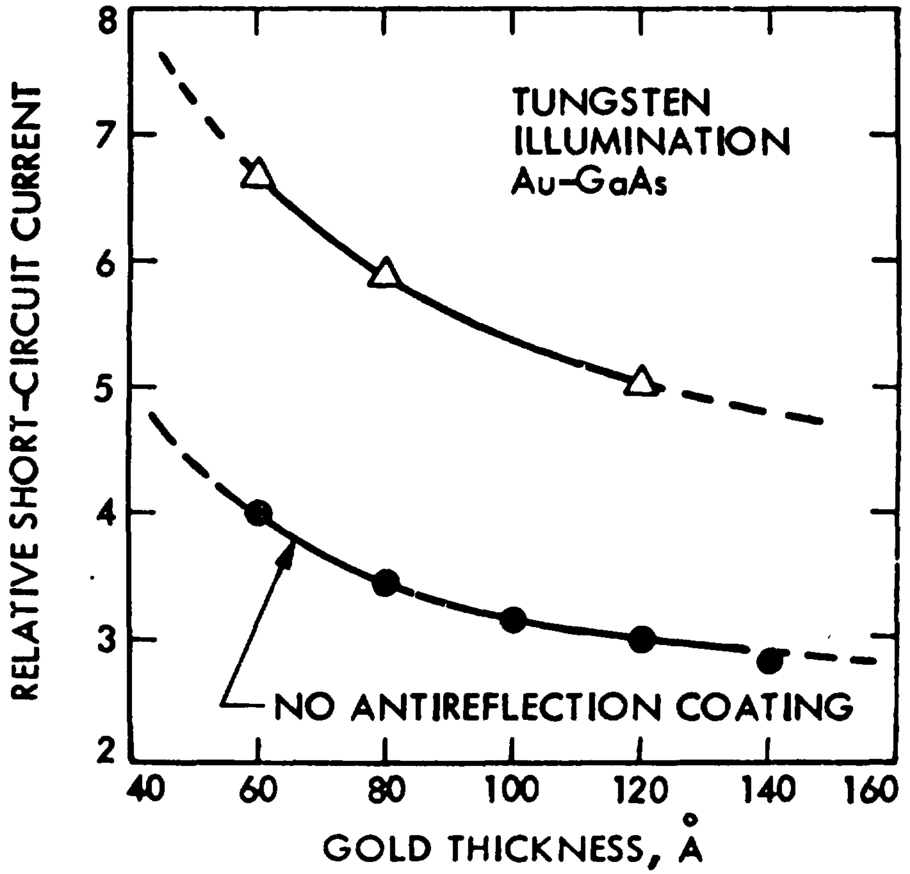

MATERIAL AVAILABILITY
(METRIC TONS)

MATERIAL	ANNUAL REQUIREMENT[a]	PRESENT ANNUAL PRODUCTION[b] (DEMAND LIMITED)	IDENTIFIED WORLD RESOURCES[b]
Ga	92.5	not given	1.3×10^5
As	89.5	5×10^4	1.6×10^7
Ge	168	~100 (1971)	$\sim8\times10^4$
Au	1.9	—	—

[a] ASSUMES 500 MW/YR OR 5×10^6 M^2 @ 10% EFFICIENCY, 80% UTILIZATION, THICKNESS OF GaAs AND Ge LAYERS TO BE 5 UM, 100 Å THICK Au LAYER WITH 10% GRID COVERAGE

[b] U.S. MINERAL RESOURCES, U.S. GEOLOGICAL SURVEY PROF. PAPER 820, 1973

MATERIAL COSTS

MATERIAL	UNIT COST[a]	COST ($1/peak-watt)[b]	
Ga (HIGH PURITY)	60¢/gm	0.111	
As (" ")	15¢/gm	0.027	
Ge (" ")	25¢/gm	0.083	
Au	$175/oz	0.0250	$0.221 (SEMICONDUCTORS)
Fe/Ni (4 mil)	$7.30/m^2	0.0730	
Si-STEEL (12 mil)	2.40/m^2	0.0240	$0.319 TOTAL WITH Fe/Ni SUBSTRATE

---

[a] PRESENT DAY SMALL-LOT PRICES

[b] ASSUMES 10% EFFICIENCY, THICKNESS OF GaAs AND Ge LAYERS TO BE 5UM, 100 Å THICK Au FILM WITH 10% GRID COVERAGE AND 80% UTILIZATION, OF SEMICONDUCTORS AND GOLD.

CONCEPTUAL DIAGRAM OF A POSSIBLE THIN FILM AMOS PRODUCTION LINE

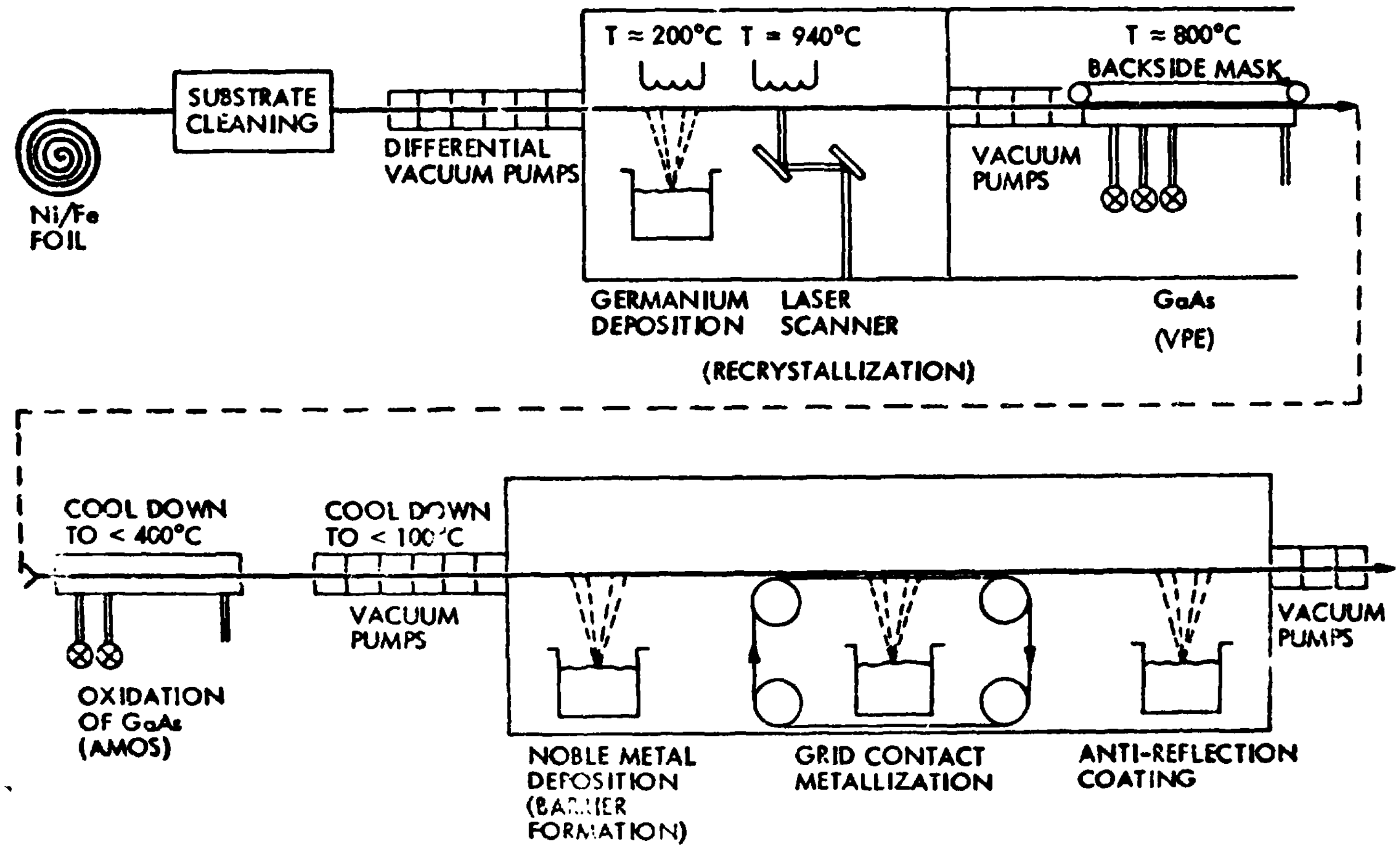

PLANNED ACTIVIES

- SELECT SEVERAL CANDIDATE LOW COST SUBSTRATES
- FABRICATE TWO-DIMENSIONAL LASER SCANNING APPARATAS FOR RECRYSTALLIZATION STUDIES ON GERMANIUM FILMS
- DETERMINE OPTIMUM GaAs GROWTH PARAMETERS ON SINGLE CRYSTAL AND RECRYSTALLIZED GERMANIUM SUBSTRATES
- PERFORM CHEMICAL ANALYSIS OF INTERFACE REGION WITH ESCA SPECTROSCOPY ON SINGLE CRYSTAL AMOS SAMPLES TO INVESTIGATE ALTERNATE PROCESSING STEPS
- LET CONTRACT TO CONDUCT CAPACITANCE-CONDUCTANCE MEASUREMENTS ON SINGLE CRYSTAL AMOS SOLAR CELLS

N76 12499

SILICON SCHOTTKY PHOTOVOLTAIC DIODES FOR SOLAR ENERGY CONVERSION

(GRANT AER73-03197)

RUTGERS, THE STATE UNIVERSITY OF NEW JERSEY
ELECTRICAL ENGINEERING DEPARTMENT
NEW BRUNSWICK, NEW JERSEY 08903

GRANT PERIOD JUNE 1, 1975 - NOV. 30, 1976
GRANT AMOUNT $28,700
PRINCIPAL INVESTIGATOR WAYNE ANDERSON

JULY 1975

C, 7

SILICON SCHOTTKY PHOTOVOLTAIC DIODES FOR SOLAR ENERGY CONVERSION

Wayne A. Anderson
Electrical Engineering Department
Rutgers University
New Brunswick, N.J. 08903

ABSTRACT

Schottky barrier solar cells (SBSC) are fabricated on <100>, 2 Ω-cm, p-type silicon using an Al ohmic contact, 50 Å Cr and then 50 Å Cu Schottky contact, Al current grid, and SiO antireflection coating. Past research was directed towards showing the potential of a SBSC in solar energy conversion. The present project is designed to improve understanding of the SBSC, improve efficiency to 12%, and evaluate potential towards thin film silicon applications.

Figures 4-10 summarize progress in evaluating the various variables in fabrication. At least 40 Å Cr metal is necessary for a good fill factor but Cr alone has too high a sheet resistance. Cu alone gives low open circuit voltage (V_{oc}). About 40 Å Cr and 50-60 Å Cu produce the best combination for high voltage, current (J), and fill factor (F). It has also been shown that removal of the 5-10 Å interfacial oxide layer between silicon and Cr which grows during heat treatment leads to reduced V_{oc}. Both the oxide and Cr are necessary for a high V_{oc}. Modification of the heat treatment cycle changes the oxide thickness leading to modification of V_{oc}. A sputtered Cu layer reduced V_{oc} due to Cu atom penetration into the silicon. <100> silicon gives higher J_{sc} and F than does <111> silicon.

Large area solar cells have lower F than small area ones. This shows the importance of finger design and low sheet resistance. Examination of substrate resistivity effects show 2 Ω-cm silicon to give slightly higher V_{oc} and 0.4 Ω-cm to give slightly higher J_{sc}.

Figures 11 and 12 show results of using "as-sawn" silicon and chemical polishing (only) to produce a smooth surface. Elimination of mechanical polishing could be a cost reducing step in final production procedures. The chemical polished wafers do show greatly improved performance over unpolished ones but more work is necessary to study different polishing sequences. SBSC made from Tyco silicon show a 5% maximum efficiency. More studies of the Tyco silicon are required for complete analysis.

Figure 14 shows results of an activation energy study to explore current conduction mechanisms. These preliminary results indicate that both thermal and tunneling effects exist in the SBSC fabricated at Rutgers. Optical calculations by computer show that 460 Å Nb_2O_5 gives significantly better antireflection (AR) properties than 755 Å SiO. The lesser thickness of Nb_2O_5 should also lead to reduced absorption loss in the AR coating. A solar simulator assembled using a variac, tungsten lamp, and water filter gives photovoltaic data comparable to direct sunlight illumination.

The most significant achievements in this latest research have been increased fill factor (to 0.74) using baking of the vacuum system to remove moisture, improved understanding of the current flow mechanism, and isolation of processing variables which improve efficiency.

OBJECTIVE OF THE PROJECT

The overall objective is to produce a 12% efficient Schottky solar cell using economical silicon and fabrication methods. This is to be accomplished through optimization of current by use of new AR coatings, voltage by interface studies, and fill factor by deposition studies. Further studies include environmental effects, thin epitaxial silicon films, surface effects, and new sources of silicon.

PLANNED ACTIVITY LAST 6 MONTHS

I. Process Variables which Influence Solar Cell Performance

Area

Substrate Resistivity

Substrate Orientation

Heat Treatment

Deposition Procedures

Wafer Polishing

New AR Coatings

II. Miscellaneous

New Computer Programs

Solar Simulator

Current Mechanism Studies

FIGURE 4

PROCESSING STUDY

SAMPLE	PROCESS	V_{OC} (V)	J_{SC} (mA/cm^2)	F	P (mW/cm^2)
134	Cu Schottky metal	0.23	11.8	0.39	0.7
136	25 Å Cr, then Cu	0.46	22.6	0.39	4.0
143	100 Å Cr	0.45	13.3	0.40	2.4

INTERFACE STUDY

	NORMAL	V_{OC} = 0.45-0.53
123 & 124	Re-etch after heating	≈ 0
126 & 127	As above, then re-heat	0.45

FIGURE 5

EFFECT OF ADDITIONAL OXIDE BETWEEN SCHOTTKY METAL AND SILICON

SAMPLE	ADDITIONAL OXIDE	AREA (CM^2)	I_o (MA)	I_{SC} (MA)	V_{OC} (V)
141	18 Å E	0.67	0.055	8	0.23
142	31 Å E	3.0	0.050	1.6	0.20
144	12 Å G	2.7	0.092	0.88	0.17
146	22 Å G	3.3	0.022	0.14	0.14

E - EVAPORATED SRO, THICKNESS MEASURED

G - GROWN IN O_2 @ 620°C, THICKNESS ESTIMATED

FIGURE 6

EFFECT OF HEAT TREATMENT ON PERFORMANCE

Sample	Heat Cycle	I_0 (mA)	J_{SC} (mA/cm^2)	V_{OC} (V)	F	P_0 (mW/cm^2)
147	Standard*	0.012	18.4	0.40	0.62	4.6
148	Inc. N_2	0.003	17.8	0.48	0.37	3.2
149	Soak @ 620°C for 2 min.	0.0015	17.7	0.50	0.25	2.2
150	300-650°C	0.34	27.2	0.51	0.48	6.65

*Standard - Ramp from 25°C to 620°C in air with light N_2 flow.
Cool to 300°C and remove from furnace.

NOTE: Eliminating N_2 or replacing with A_R gives no significant change.

FIGURE 7

EFFECT OF SPUTTERING OF CONDUCTIVE METAL ON SOLAR CELL PERFORMANCE

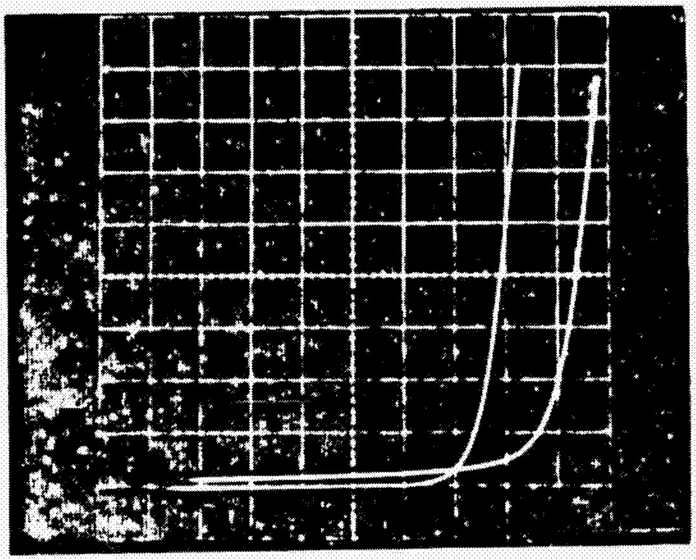

SAMPLE 174

0.1 V/DIV

5 MA/DIV

CURVE ON LEFT-SPUTT. AU

CURVE ON RIGHT-EVAP. AU

FIGURE 8

EFFECT OF SUBSTRATE ORIENTATION ON PERFORMANCE

SAMPLE	ORIENTATION	I_o (mA)	J_{sc} (mA/cm^2)	V_{oc} (V)	F	P_o (mW/cm^2)
171A	100	0,24	20,8	0,43	0,65	5,8
171B	111	0,34	12,1	0,43	0.54	2,8

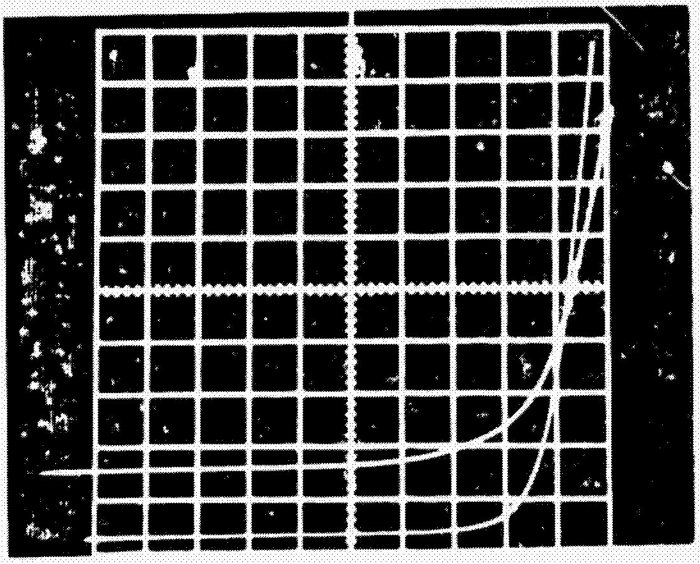

SAMPLE 171

0,1 V/DIV

5 mA/DIV FOR A

10 mA/DIV FOR B

FIGURE 9

EFFECT OF SOLAR CELL AREA ON PERFORMANCE

SAMPLE	V_{oc} (V)	F
167,S	0.43	0.71
167,L	0.41	0.52
153,S	0.47	0.67
153,L	0.47	0.60

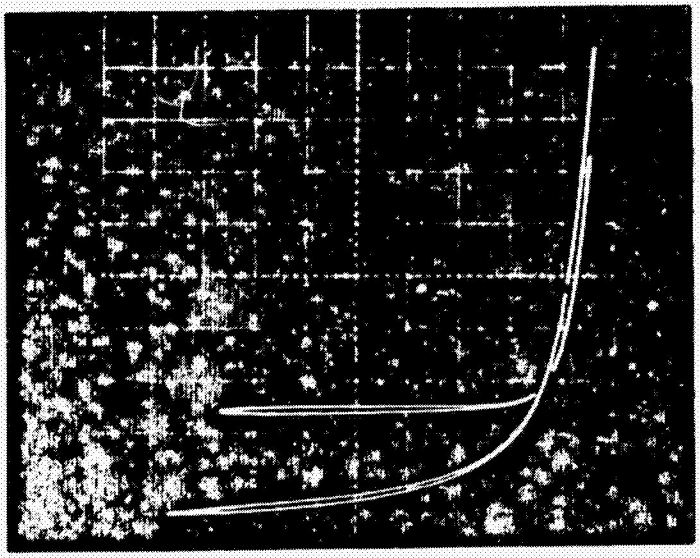

SAMPLE 167

0.1 V/DIV
0.1 MA/DIV SMALL
2 MA/DIV LARGE

FIGURE 10

EFFECT OF SUBSTRATE RESISTIVITY ON PERFORMANCE

SAMPLE	RESISTIVITY (Ω-CM)	I_o (MA)	J_{sc} (MA/CM^2)	V_{oc} (V)	F	P (MW/CM^2)
112	0,4	0,08	5,9	0,40	0,46	1,08
113	2	0,03	5,64	0,42	0,64	1.52
172B	0,4	0,9	19,6	0,41	0,68	5,3
172B	2	0,11	16,9	0,44	0,74	5,2

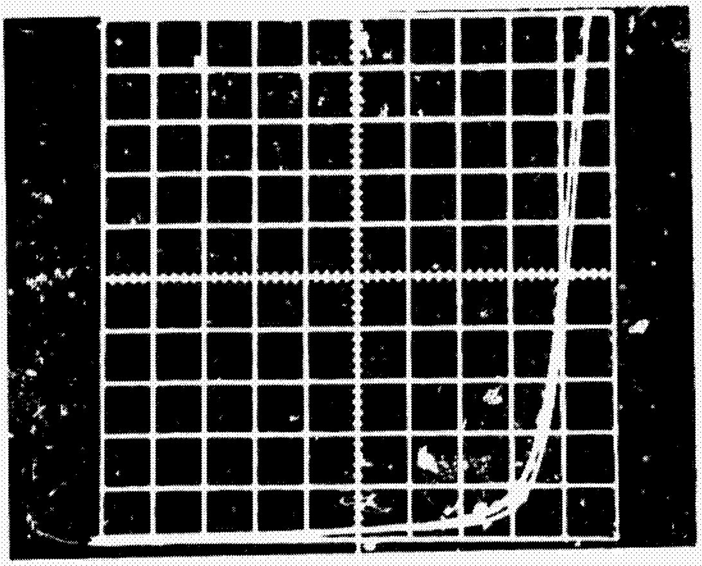

SAMPLE 172

0,1 V/DIV

5 MA/DIV

FIGURE 11

CHEMICAL POLISHING STUDY

STUDY THE FABRICATION OF SCHOTTKY SOLAR CELLS USING "AS-SAWN" SILICON AND CHEMICAL POLISHING

SAMPLE	POLISH	RESULT			
		V_{OC} (V)	J_{SC} (mA/cm^2)	F	P_O (mW/cm^2)
111	"As-sawn"	No photo-response			
117	HF, HNO3	0.31	13.8	.35	1.63
138	HF, HNO3, Acetic	0.27	4.6	.25	.31

FIGURE 12

SCANNING ELECTRON MICROSCOPE STUDY

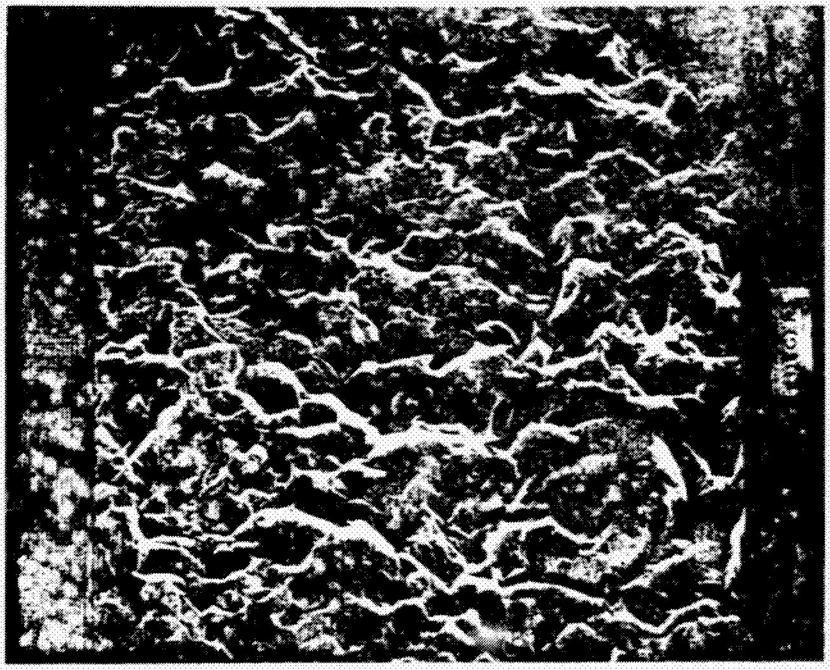

"AS-SAWN"
SILICON
MAG. = 2000

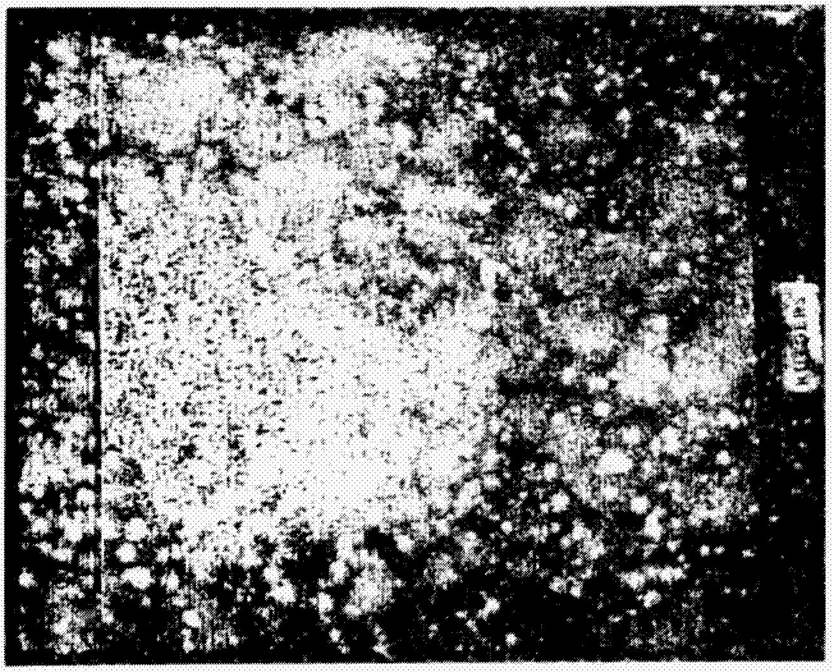

CHEMICAL
POLISHED
SILICON
MAG. = 2000

ORIGINAL PAGE IS
OF POOR QUALITY

FIGURE 13

TYCO 120

AREA = 1.21 CM^2

V_{OC} = 0.43 V

I_{SC} = 25 MA

$V_{OC}\ I_{SC}$ = 8.9 MW/CM^2 } SUNLIGHT

P_O = 4.16 MW/CM^2 } 80-100 MW/CM^2

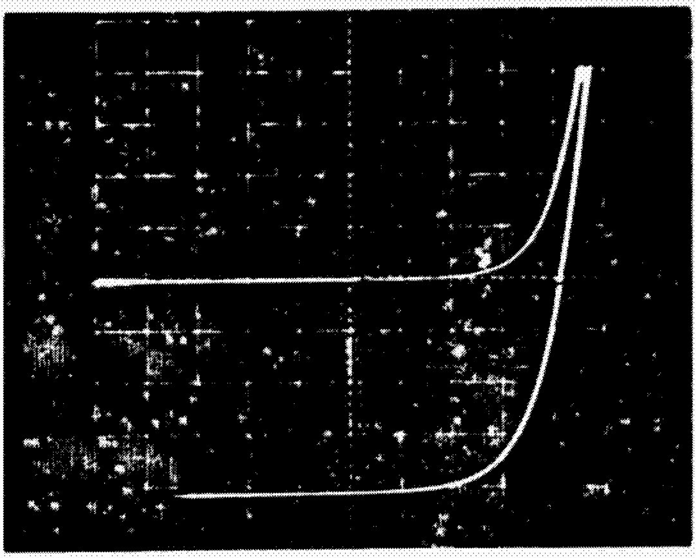

FIGURE 14

ACTIVATION ENERGY

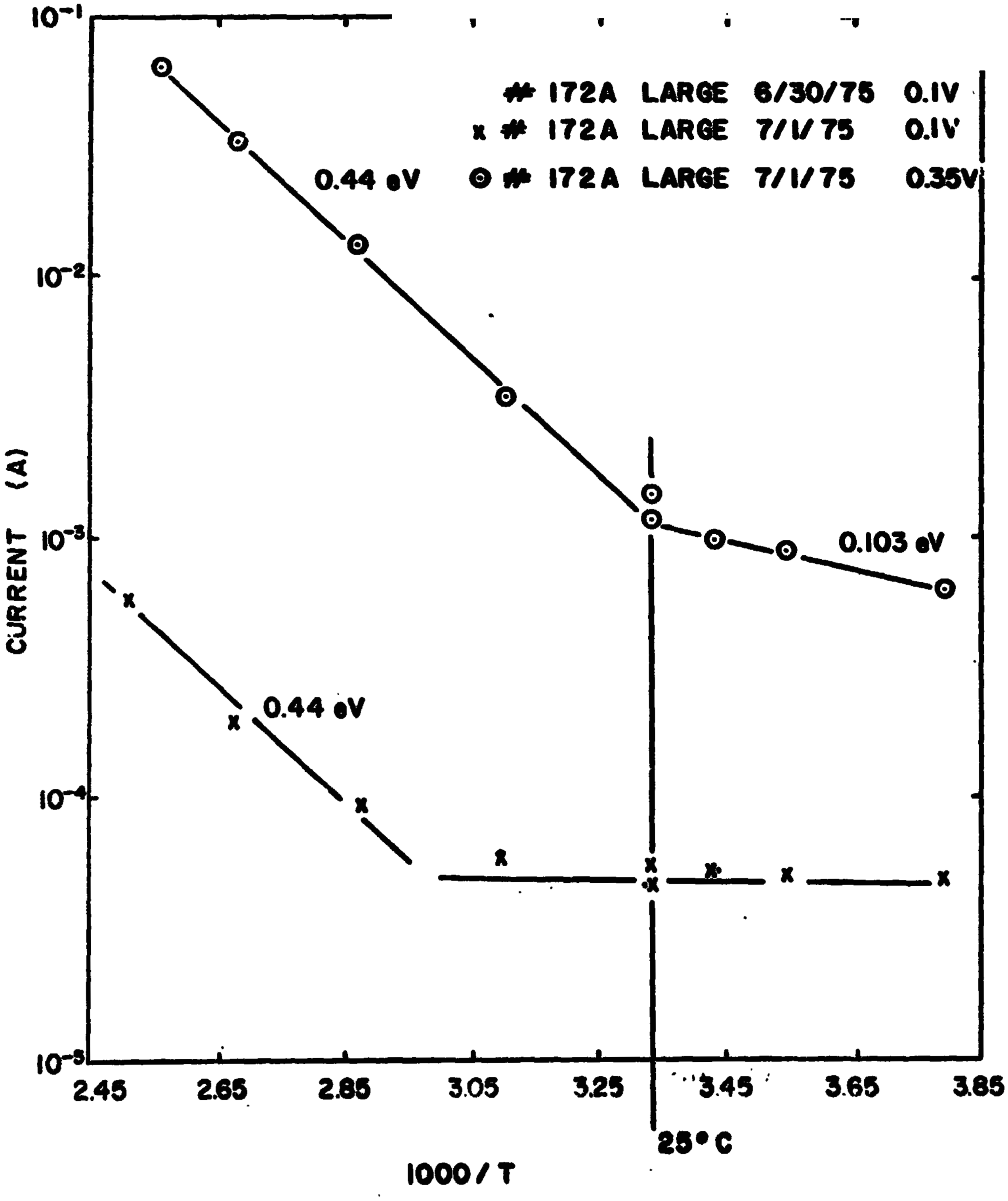

FIGURE 15

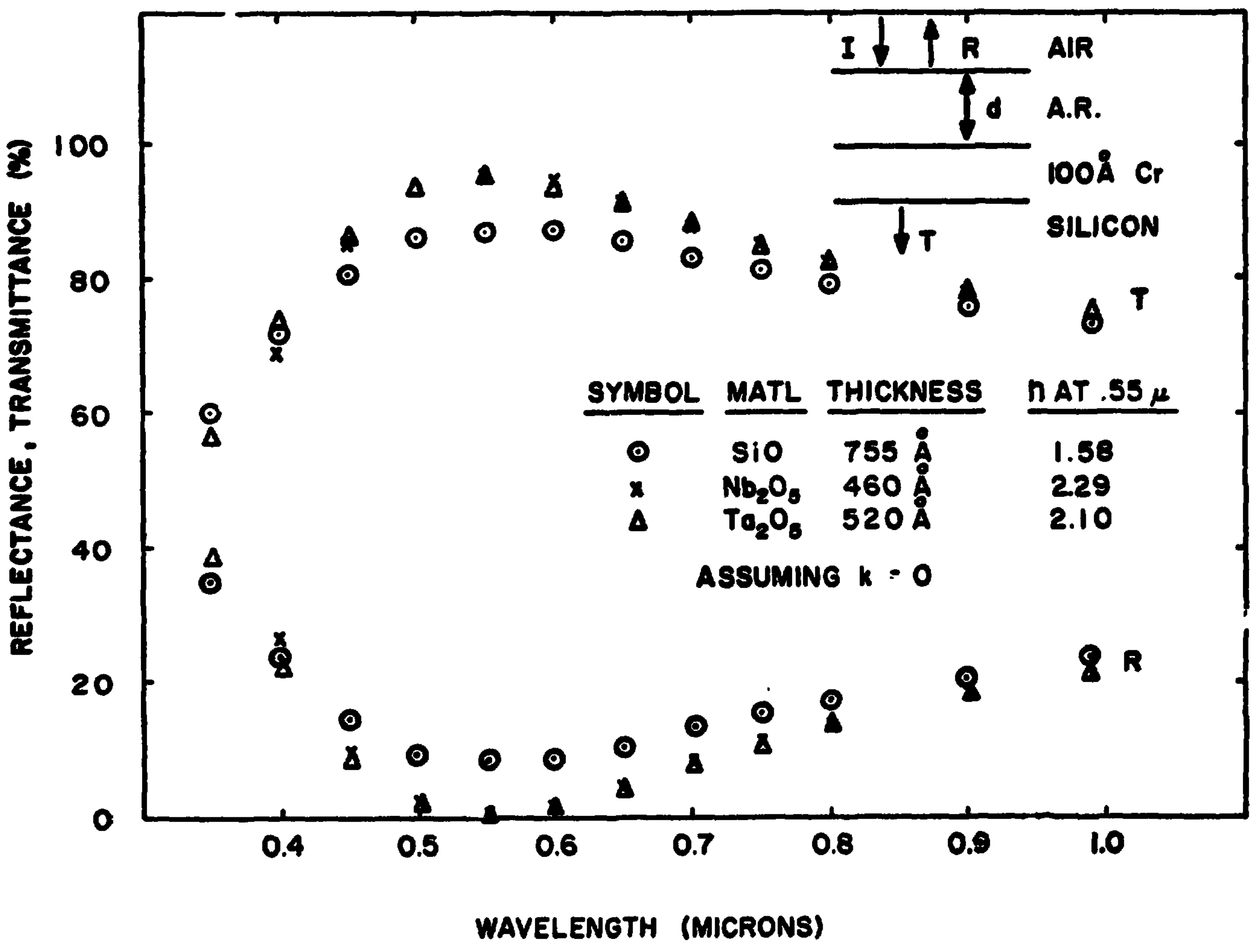
I
R
AIR
d
A.R.
100Å Cr
SILICON
T
T
R
SYMBOL
MATL
THICKNESS
n AT .55 μ
⊙ SiO 755 Å 1.58
x Nb_2O_5 460 Å 2.29
Δ Ta_2O_5 520 Å 2.10
ASSUMING k = 0
REFLECTANCE, TRANSMITTANCE (%)
0
20
40
60
80
100
0.4
0.5
0.6
0.7
0.8
0.9
1.0
WAVELENGTH (MICRONS)

FIGURE 16

MISCELLANEOUS

1. A SOLAR SIMULATOR HAS BEEN ASSEMBLED USING A TUNGSTEN LAMP, VARIAC, AND WATER FILTER. RESULTS COMPARE FAVORABLY WITH DIRECT SUN DATA.
2. 12μ EPITAXIAL LAYER (2Ω-CM) ON A <111>, 0.001 SUBSTRATE GIVES A 50% LOW CURRENT.

SUMMER RESEARCH PARTICIPANTS

B. LALEVIC, ASSOCIATE INVESTIGATOR
A. DELAHOY
S. VERNON
K. NG
P. MATHE
T. POON

FIGURE 17

SUMMARY OF KEY RESULTS

1. CR SCHOTTKY METAL OF 40-50 Å IS BEST.
2. THE OXIDE INTERFACE GIVES HIGH V_{OC}.
3. AN INTERFACE OF 5-12 Å IS PROBABLE.
4. HEAT TREATMENT FROM 300-650°C GIVES HIGH V_{OC}.
5. SPUTTERED SCHOTTKY CONDUCTIVE METAL GIVES LOW V_{OC}.
6. <100> GIVES BETTER J & F THAN <111>.
7. 0.4Ω-CM GIVES HIGHER J.

   2 Ω-CM GIVES HIGHER V_{OC}.
8. TYCO SILICON PRODUCES A PROMISING SCHOTTKY SOLAR CELL.
9. ACTIVATION ENERGY STUDIES MAY LEAD TO ANSWERS ABOUT THE CONDUCTION MECHANISM.
10. Nb_2O_5 AND Ta_2O_5 GIVE PROMISING ANTIREFLECTION IMPROVEMENTS.
11. A SIMPLE SOLAR SIMULATOR GIVES RESULTS COMPARABLE TO SUNLIGHT ILLUMINATION.
12. F = 0.74 HAS BEEN ACHIEVED USING VACUUM SYSTEM BAKING PRIOR TO EVAPORATION.

FIGURE 18

MAJOR PROBLEMS

1. UNDERSTANDING THE CONDUCTION MECHANISMS AND ROLE OF THE INTERFACIAL LAYER.

2. REPRODUCIBILITY OF SHEET RESISTANCE VALUES FROM RUN TO RUN.

3. SIMULTANEOUSLY ACHIEVING HIGH V_{OC}, F, AND I_{SC}.

FIGURE 19

PLANNED ACTIVITY FOR NEXT 6 MONTHS

1. BEGIN STUDIES OF EPITAXIAL LAYERS.
2. EXPAND ELECTRONIC TESTING TO IDENTIFY CURRENT FLOW MECHANISMS.
3. CONDUCT MICROSCOPIC STUDY OF SILICON SURFACE AND INTERFACE.
4. OPTIMIZE THE FABRICATION PROCESS.
5. EXPAND COMPUTER STUDIES.
6. STUDY NEW AR COATINGS.
7. SEND SOLAR CELLS TO NASA LEWIS FOR TESTING.
8. INITIATE ENVIRONMENTAL TESTING AND LIFE STUDIES.
9. CONTINUE FABRICATION OF SCHOTTKY SOLAR CELLS USING NEW SILICON SOURCES (IF AVAILABLE).

FIGURE 20

PLANNED RENEWAL REQUESTS

MAJOR GOALS

1. ACHIEVE 15% EFFICIENCY ON SINGLE CRYSTAL SILICON.
2. ACHIEVE 6% EFFICIENCY ON THIN FILM POLYCRYSTALLINE SILICON.

PERSONNEL

ASSOCIATE INVESTIGATOR IN PHYSICS
ASSOCIATE INVESTIGATOR IN MATERIALS SCIENCE
THREE RESEARCH ASSISTANTS

DATE

JUNE 1, 1976 - MAY 31, 1977

COST

$40,000

EXPLORATION OF UNCONVENTIONAL SOLAR CELLS *

C. F. Grain

Itek Corporation
10 Maguire Road
Lexington, Mass. 02173

Abstract

For the past few months research has been continued on a new concept for the production of low cost photovoltaic cells. The basic concept is that, rather than starting with an inherently high cost process and trying to reduce costs, we have started with a very low cost process for depositing particulate semiconductor layers involving emulsion coating techniques.

It has been shown that the concept is feasible and in fact layers containing ZnO exhibited quantum efficiencies of >50% and power efficiencies up to 3% with exposure to actinic light.

Significant results have recently been obtained with other materials namely Pb_3O_4 and CdS. Pb_3O_4 is a very high resistivity material ($\rho \sim 10^{12}$ ohm-cm), however, we have been able to reduce the resistivity to values of $\sim 10^7$ ohm-cm. This is still approximately two orders of magnitude higher than desired. Nevertheless quantum efficiencies as high as 5% and power efficiencies of the order of 0.1% to an equivalent solar spectrum have been obtained. Figure 1 shows the spectral response characteristics of a typical cell.

Encouraging results have also been obtained with $CdS-Cu_2O$ heterojunction cells. Figure 2 shows the I-V characteristics of a typical cell. The power efficiency is $\sim$ 0.15% while quantum efficiencies are $\sim$ 3%. This represents an improvement in efficiency of about 10^3 in a period of about 4 months. Quantum efficiencies as high as 8% have been obtained, however. power efficiencies were limited by low voltages. The low voltages were the result of leakage at the $CdS-Cu_2O$ junction.

We intend to continue our efforts on both Pb_3O_4 Schottky barrier devices and $CdS-Cu_2O$ heterojunction devices. Problems to be overcome include preparation of "good" non-leaking rectifying contacts, preparation of ohmic contacts and reducing the resistivity of our semiconductor layers.

---

* Supported in part by NSF Grant #AER 74-00928

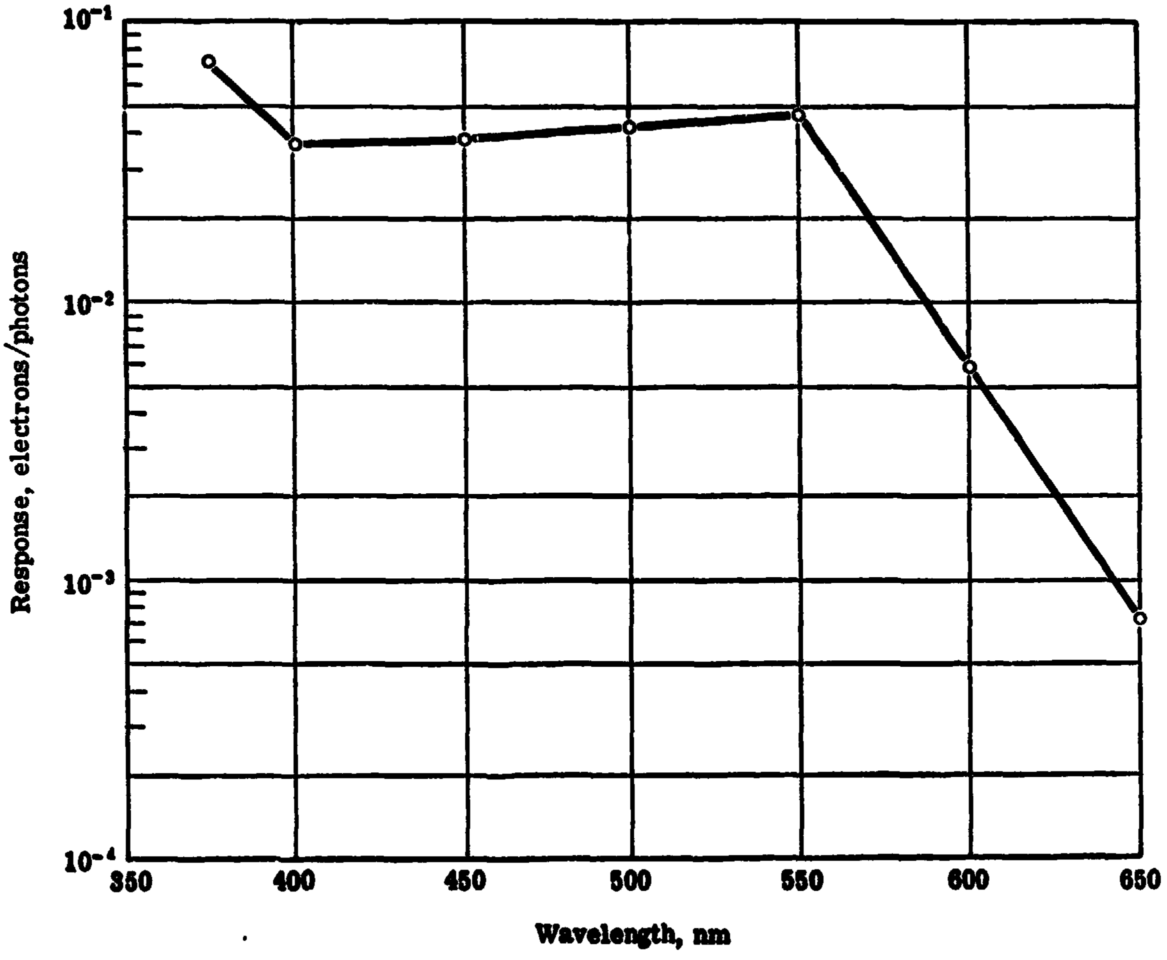

Fig. 1 — Spectral Response, Pb_3O_4

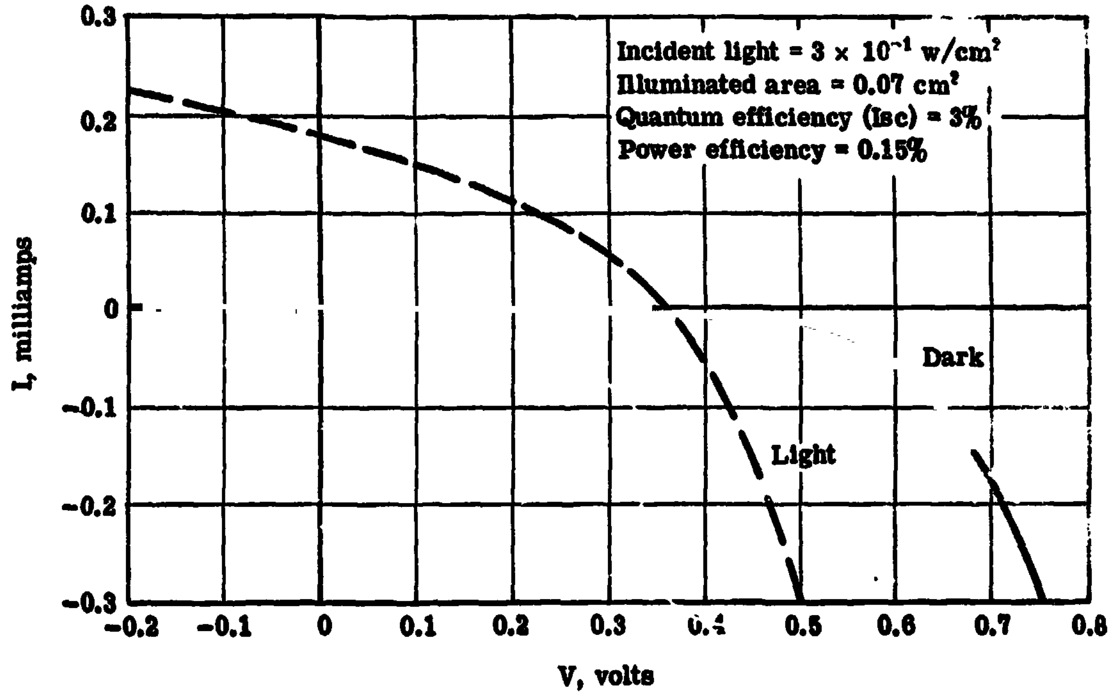

Fig. 2 — I-V curves, CdS-Cu_2O

(a) TITLE: Exploration of Unconventional Solar Cells
(Grant No. AER74-00928)

(b) ORGANIZATION: Itek Corporation, Lexington, Massachusetts
(Central Research Laboratories)

(c) PERIOD: 6 Months (Starting November 15, 1974)

(d) AMOUNT: $57,800

(e) PRINCIPAL INVESTIGATOR: Clark F. Grain

DEFINITION OF OVERALL OBJECTIVE OF PROJECT

Establish the feasibility of producing large area, extremely low-cost solar cells based on particulate semiconductor layers prepared by emulsion coating techniques.

	6 Months	End Goal
Efficiency:	1%	>5%
Cost:	--	~45¢/ft^2(10¢/watt)
Area:	5 cm^2	>3 ft^2

ACTIVITY TO DATE

1. Reduction of resistivity of Pb_3O_4 (via doping)
2. Formation of ohmic contacts to Pb_3O_4
3. Investigation of atmosphere control for further reduction of p
4. Preparation of CdS - Cu_2O heterojunction cells

SUMMARY OF KEY RESULTS

1. Quantum Efficiency of 5% obtained with Pb_3O_4 layers
2. Quantum Efficiencies up to 8% obtained with CdS-Cu_2O
3. Power efficiencies between 01.% - 0.2% with Pb_3O_4 and CdS-Cu_2O
4. Resistivity of Pb_3O_4 reduced from 10^{12} ohm-cm to 10^7 ohm-cm
5. Resistivity of CdS reduced to 10^5 ohm-cm

MAJOR PROBLEMS

1. Further reduction of resistivity of materials (e.g. Pb_3O_4)

2. Establish good Schottky barrier and ohmic contacts to these materials

PLANNED ACTIVITY

1. Experiments to control resistivity and structural phase
    - a) Heat treatments in controlled atmospheres
    - b) Additions of impurity dopants

2. Investigation of contact properties
    - a) Various evaporated or sputtered metals
    - b) Effects of heat treatments
    - c) Other contacts
        - i) Conducting paints
        - ii) Electroless plating

3. Heterojunction devices
    - a) Continue improvement of $CdS-Cu_2O$ cells
    - b) Investigation of other heterojunction pairs (e.g. $ZnO-Cu_2O$)

PLANNED RENEWAL REQUEST

Phase II - Reduction to Practice

12 Months: May 1975 - May 1976

$175,000

Major Goals: Fabricate Solar Cells Using Emulsion Coating Technology and Particulate Materials

Power Efficiency > 3% to Sunlight

Area > 100 cm^2

Life > 1 Month

N76 12500

(a) PROCESS-INDUCED DEFECTS IN TERRESTRIAL SOLAR CELLS

(b)-(e) We are not now a grantee or contractor in either ERDA or NSF sponsored solar photovoltaic research. The results we report have derived from research sponsored by NASA (Grant NSG-3018) beginning June 23, 1974 and still in force at $60,000 per year.

(f)-(g) Authors:

F. A. Lindholm and S. S. Li
(University of Florida, Gainesville)

and

C. T. Sah
(University of Illinois, Urbana)

(h) Principal Investigators of NASA Grant NSG-3018:
F. A. Lindholm and S. S. Li

(i) Part of this paper was presented at the 1975 PSC Conference in May in Phoenix; part has never been presented before.

The expectation of good performance has prompted interest in low-resistivity, shallow-junction solar cells for space applications. Such devices contain, however, regions of high doping and high impurity gradients. Hence the physics underlying their operation is complex; many different mechanisms, traditionally ignored, compete to determine cell behavior.

Thus a major problem in understanding the operation of such cells lies in determining which of these mechanisms are dominant and which may be neglected. A second problem, relating to design, lies in controlling both the dominance and the magnitude of the phenomena via controlling the device structure and the steps used in fabrication.

These problems are the main undertakings of our research sponsored by NASA Grant NSG-3018. Our program includes collateral experimental and theoretical efforts. At present, the experimental effort concentrates on the fabrication of solar cells and related test devices, and on a detailed characterization of the current-voltage properties and of the defects that contribute to them. The experimental tools employed in our study include: current-voltage measurement and transient-capacitance, thermally-stimulated-capacitance and thermally-stimulated-current measurements made on pn junction or Schottky-barrier test vehicles. The theoretical effort anticipates the dominant contributors to the behavior that need experimental study, provides a careful interpretation of the experimental data, and seeks full utilization of the data in calculating its inferences on solar-cell behavior. The theoretical and experimental efforts interplay, each guiding the direction of the other.

Although aimed toward very high-efficiency, low resistivity silicon solar cells for space applications, the results of our studies reached thus far have considerable implications for cells of materials, such as solar-grade silicon, currently being advanced for terrestrial application. A review of our main findings will help clarify these implications.

To examine the issue of dominance among the high-doping mechanisms, we have divided them into two broad categories:

1. Gap shrinkage, as produced, for example, by band tailing, impurity-band widening and impurity misfit; and
2. Altered interband transition rates, arising from Auger-impact or SRH processes or from electronic tunneling via defects.

Which of these mechanisms predominates depends, in general, on the physical make-up of the device, on environmental conditions such as temperature, and on the aspect of cell performance of interest.

To provide a quantitative illustration, we have taken a concrete example: a phosphorous diffused n+p cell, junction depth 0.25 microns, impurity grade constant 10^{23} atoms/cm^4, substrate resistivity 0.1 ohm-cm. Further our attention has centered on the measured open-circuit voltage at 300°K.

To analyze this device, we have extended the traditional analytical theory of silicon solar cells to enable inclusion of the high doping mechanisms. Of these mechanisms, we have concluded that gap shrinkage, taken alone in a one-dimensional model, falls far short of explaining the measured open-circuit voltage. To fit the data, a gap shrinkage of 0.23 eV would be required for impurity concentrations only slightly higher than 10^{18} cm^{-3}, which compares to our upper-bound estimate of 0.07 eV for such concentrations. From a physical standpoint, we predict gap shrinkage to be small because minority carriers can exist in sizable numbers in the dark cell only where the doping is relatively small.

Of all the other mechanisms described until now in this paper, we have proposed the sharp increase in the defect density near the highly-doped surface to be the most likely candidate to explain the data. This result indicates the desirability of additional experiments concerning the properties of the defects near the surface and their relationship to processing, particularly to the processing now used in the solar-cell technology.

To this point in our review, we have considered a one-dimensional model of the cell, the only coordinate of interest having been that measuring the distance from the surface. But the solar cell is a large area device, and inhomogeneities across this area could play a significant role in governing the performance. In particular, we note the existence of a statistical distribution of impurity clusters, thermodynamically stable, occurring in the diffused layer.

Viewing the overall solar cell as a collection of sub-cells roughly in parallel one with another, we propose that those sub-cells with relatively high doping and defect density can severely degrade the performance of the overall device. Hence the area-inhomogeneity mechanism accompanying high doping could play a dominant role and establish a basic limitation on the performance obtainable. We give experimental indications on devices of our fabrication that suggest the importance of area inhomogeneity.

Our work on low-resistivity, high-efficiency cells has suggested the dominant role that defects take in determining performance. For materials being put forward for terrestrial use (EFG, WEB, polysilicon, etc.), the characterization of the defects and their relation to the fabrication processes used will be even more significant. Research similar to ours, conducted presently with NASA, but extended in scope and aimed toward terrestrial solar cells, could thus provide valuable information to the nation's solar photovoltaic program.

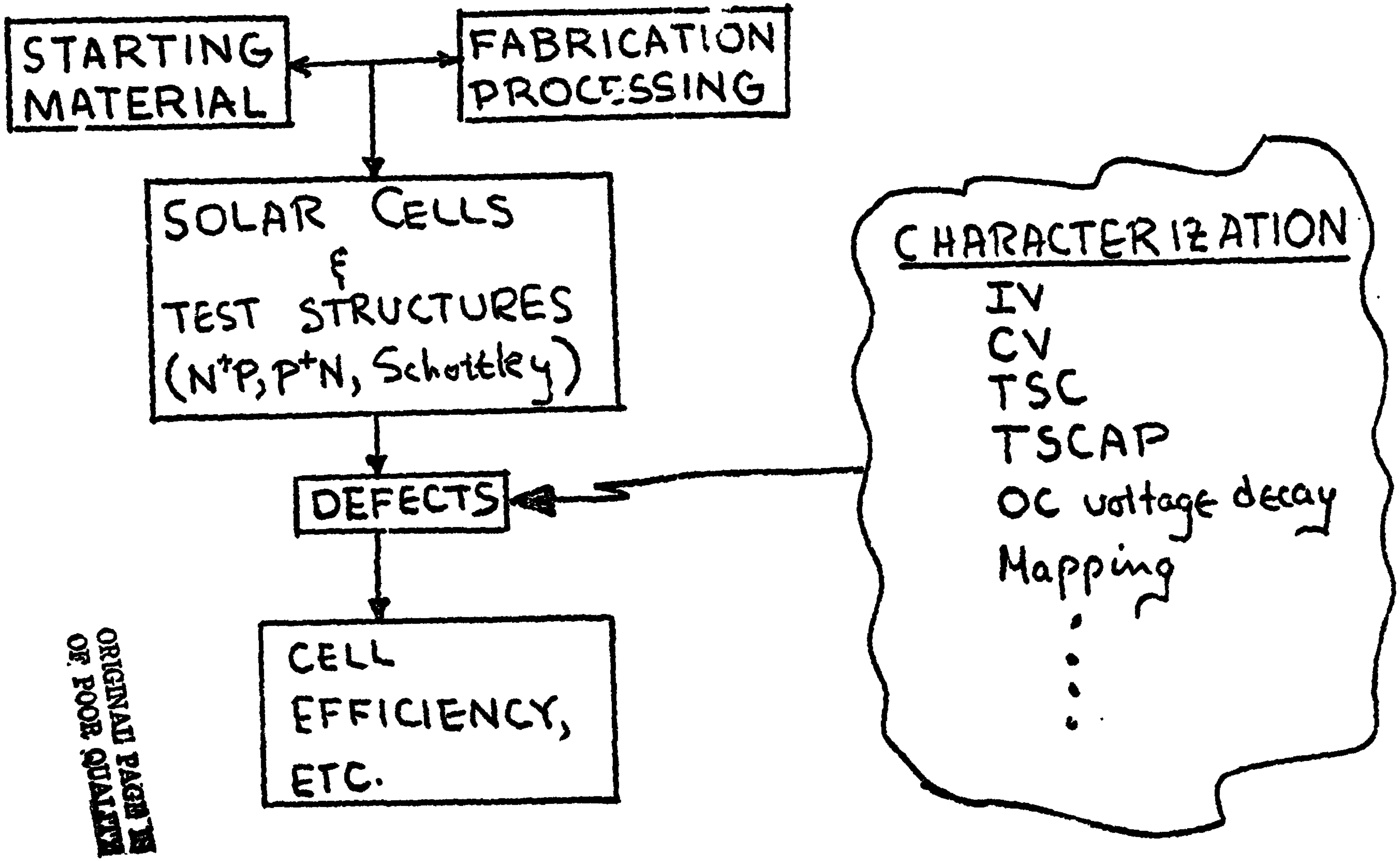
STARTING MATERIAL
FABRICATION PROCESSING
SOLAR CELLS & TEST STRUCTURES (N⁺P, P⁺N, Schottky)
DEFECTS
CELL EFFICIENCY, ETC.
CHARACTERIZATION
IV
CV
TSC
TSCAP
OC voltage decay
Mapping
⋮

HIGH DOPING (1-DIM'L)
[DEGRADING ⇒ LIMITATIONS]

I. GAP SHRINKAGE ΔE_G

$\boxed{Q_E \uparrow}$: $P \propto n_{io}^2 \, \underline{\underline{e^{\Delta E_G / kT}}}$

II. INTERBAND TRANSITIONS

$\boxed{\tau_E \downarrow}$: Auger (high N)

SCR ($T < 300^\circ K$)

tunneling ($T \ll 300^\circ K$)

$\tau = \tau[N_D(x)]$ ($T \simeq 300^\circ K$)

WHICH DOMINATES V_{oc} (IN $0.1 \Omega\text{-}cm$, $300^\circ K$)?

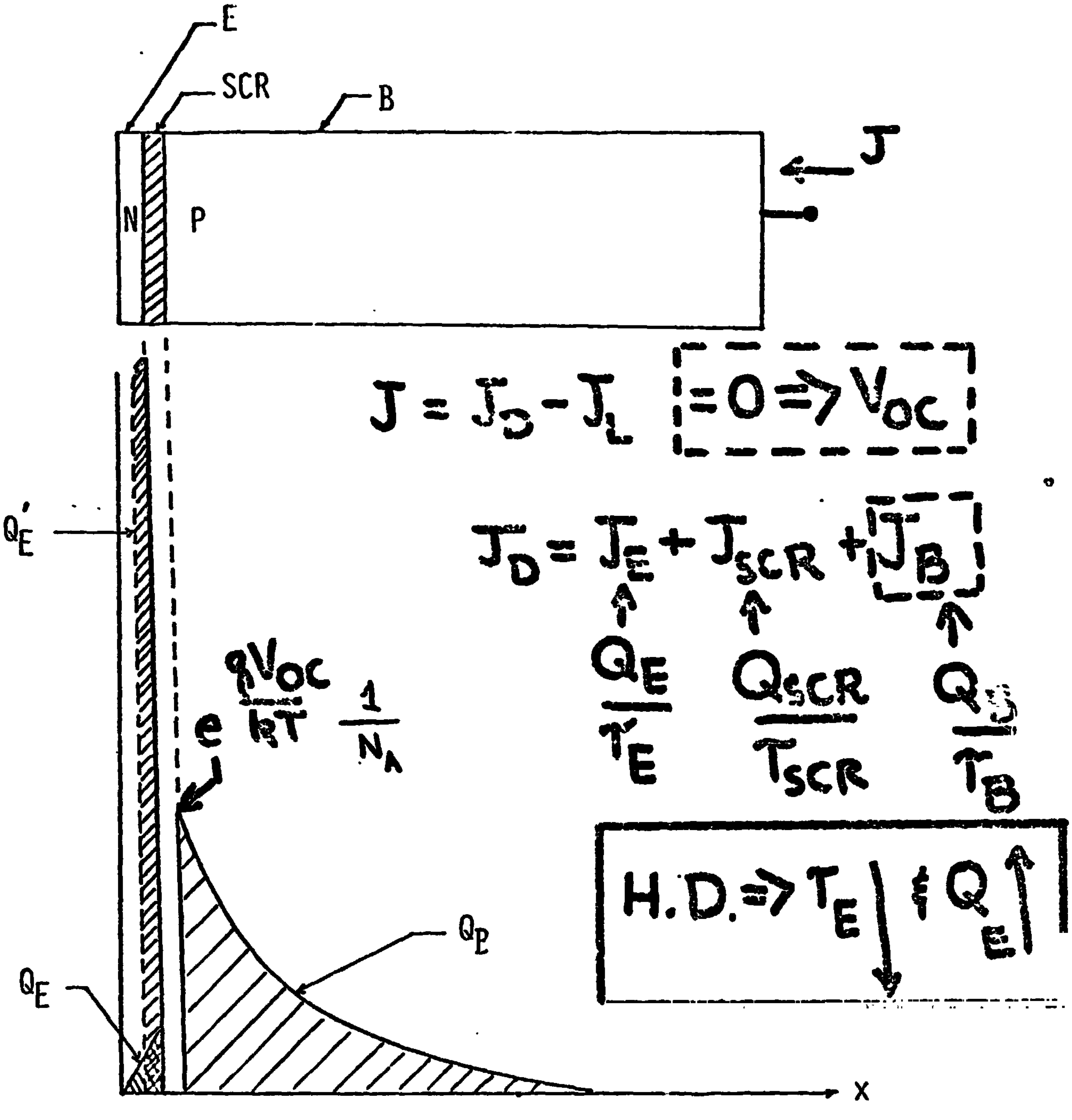
E
SCR
B
N
P
J
$J = J_D - J_L$
$= 0 \Rightarrow V_{OC}$
$J_D = J_E + J_{SCR} + J_B$
$\frac{Q_E}{T_E}$
$\frac{Q_{SCR}}{T_{SCR}}$
$\frac{Q_B}{T_B}$
$e^{\frac{qV_{OC}}{kT}} \frac{1}{N_A}$
Q'_E
Q_E
Q_B
H.D. ⇒ $T_E \downarrow$ & $Q_E \uparrow$
x

GAP SHRINKAGE

BAND TAILS
(RANDOMNESS)

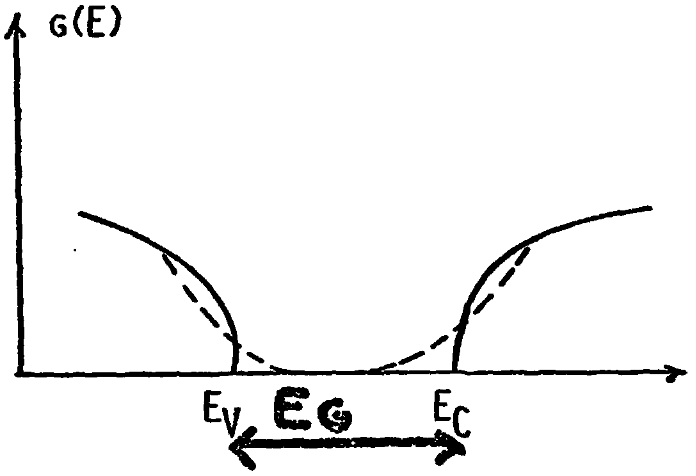

IMPURITY BAND
(OVERLAP)

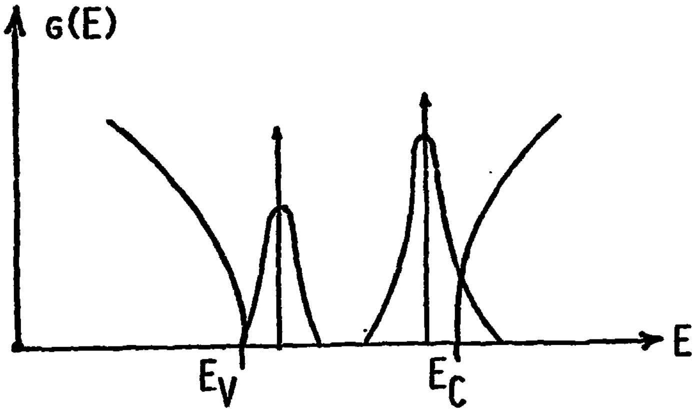

STRAIN
(MISFIT)

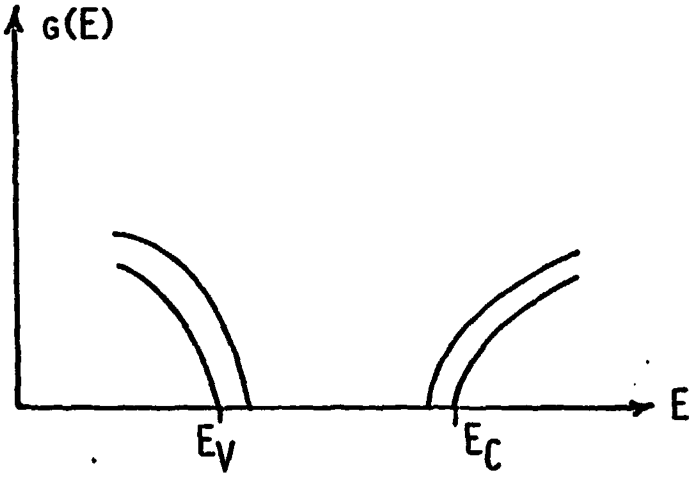

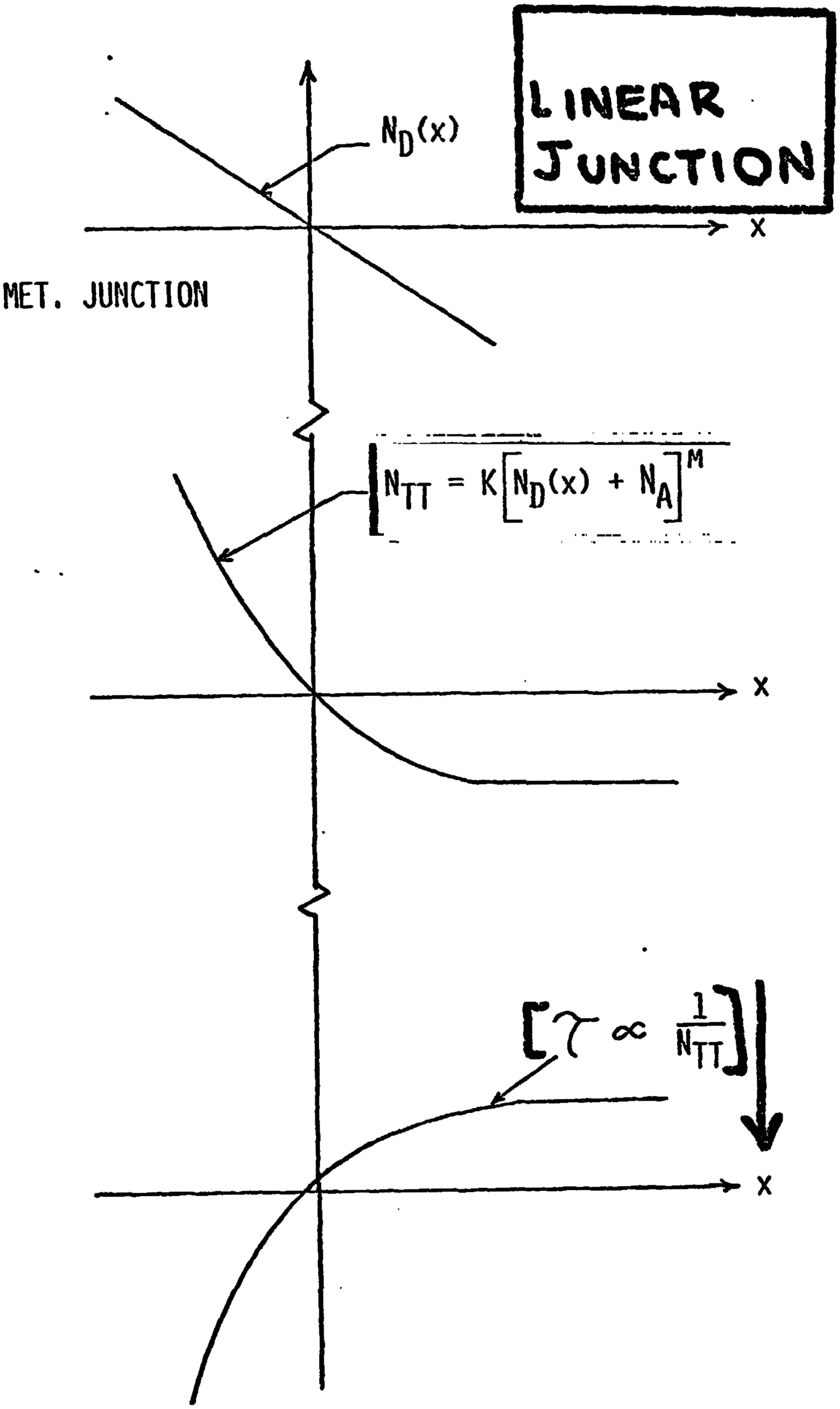
LINEAR JUNCTION
$N_D(x)$
x
MET. JUNCTION
$N_{TT} = K\left[N_D(x) + N_A\right]^M$
x
$\left[\tau \propto \frac{1}{N_{TT}}\right]$
x

HOLES IN EMITTER

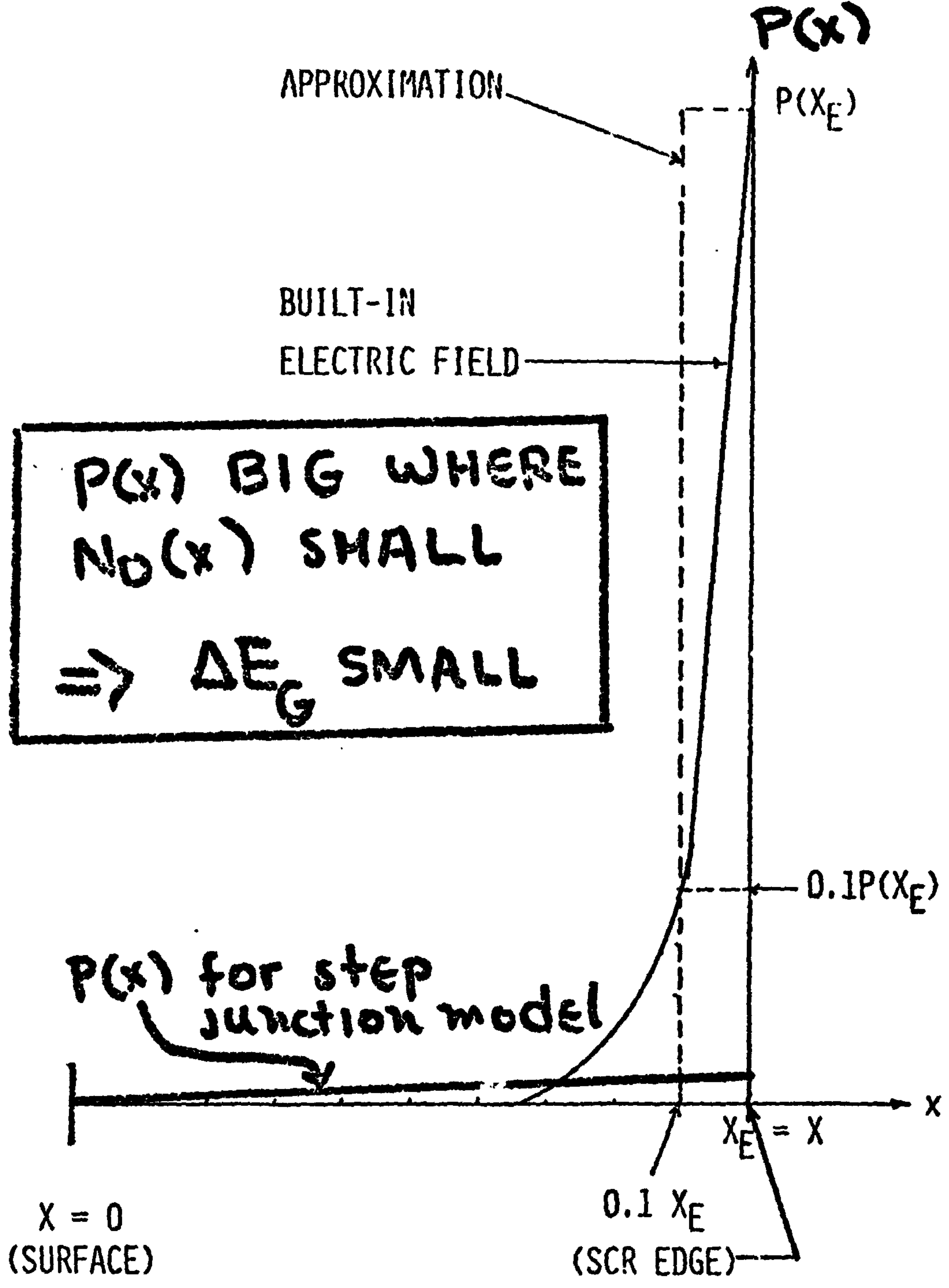

$P(x)$ BIG WHERE $N_D(x)$ SMALL

$\Rightarrow \Delta E_G$ SMALL

WHICH DOMINATES? MATCH TO EXPT.

$0.1\,\Omega\text{-CM}$, 300°K, $n^{+}p$

MEASURED $V_{OC} = 610\,\text{mV}$

$$J_D = J_E + \cancel{J_{SC}} + J_B$$

$$J_E = 14.1\, J_B$$

$$J_E = J_{ET}\,[F \quad G \quad S]$$

field: 0.1

ΔE_G: <15

$\boxed{T(x): 466}$

CONCLUSION : DOMINANT <u>1-DIM'L</u>

H.D. MECHANISM IS

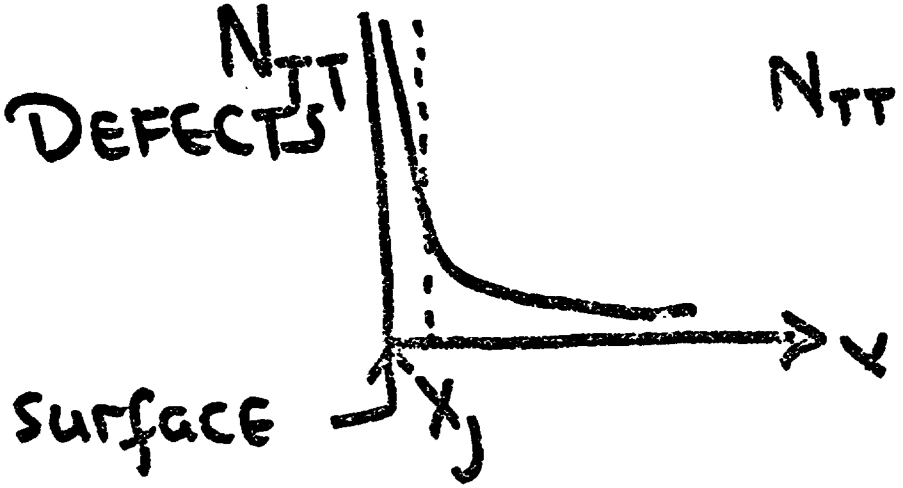

$$N_{TT} = K[N_D(x) + N_A]^m$$

$m \cong 4$ OR $m \simeq 2$

VACANCY COMPLEXES

INCONCLUSIVE

3-DIM'L H.D MODEL:

IMPURITY
CLUSTERS
IN LARGE
AREA DEVICE

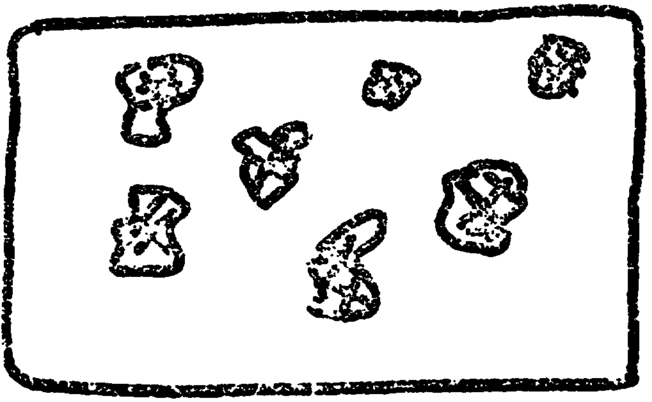

SOME 1-D
MECHANISMS
SENSITIVE:

$e^{\Delta E_G/RT}$,

$\tau \propto N_D^{-m}$

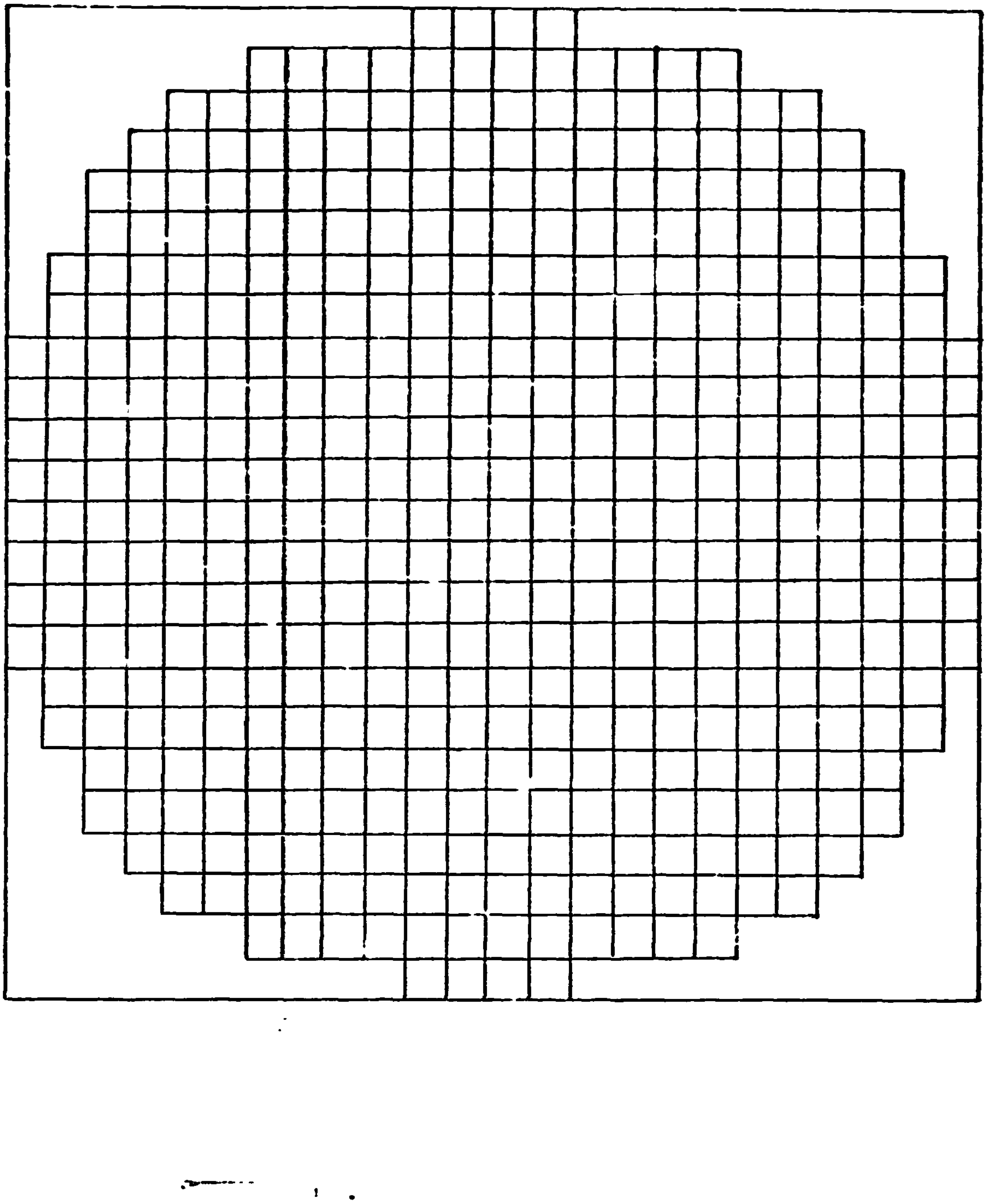

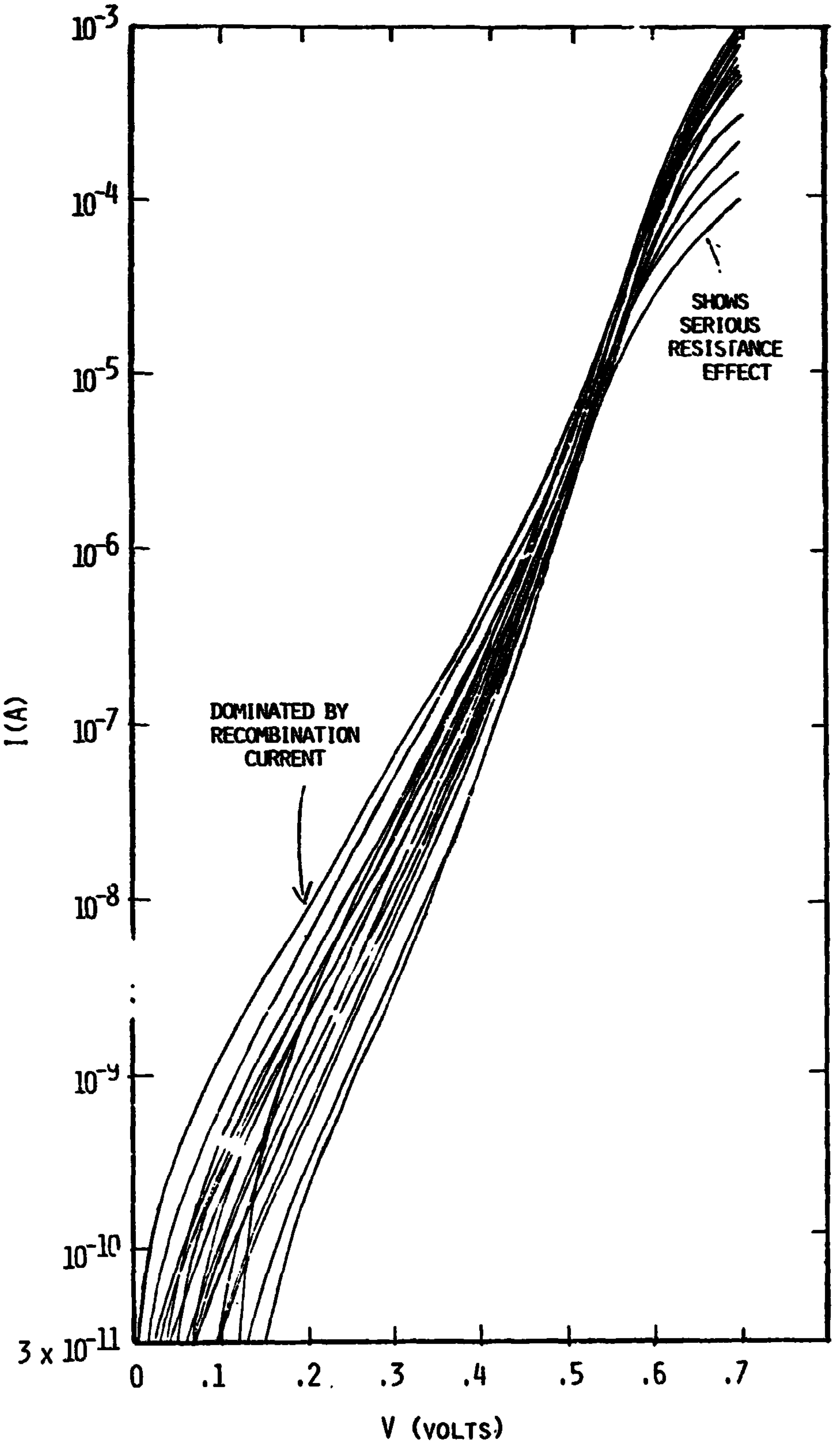

Figure 4.4 Experimental I-V curves for the 0.1 Ω-cm N$^+$P test cells obtained randomly from wafers C-101 and C-102 respectively.

SESSION VIII

OTHER APPROACHES 2

N76 12501

GLASS-SI HETEROJUNCTION SOLAR CELLS

TITLE OF GRANT
GLASS-SI HETEROJUNCTION SOLAR CELLS

GRANT NUMBER
AER74 - 17631

PERIOD OF GRANT
1 AUG. 1974 - 31 JULY 1975

VALUE OF GRANT
$313,900

AUTHOR AND PRINCIPAL INVESTIGATOR

RICHARD L. ANDERSON
DEPARTMENT OF ELECTRICAL AND COMPUTER ENGINEERING
SYRACUSE UNIVERSITY, SYRACUSE, N.Y.

PRESENTATION
NATIONAL SOLAR PHOTOVOLTAIC PROGRAM REVIEW MEETING
25 JULY 1975
U.C.L.A.

ABSTRACT

The purpose of this project is to investigate glass/Si heterojunctions as solar cells of low cost, suitable for terrestrial applications. The Si is the active material, and the glass serves as a window to solar radiation, an antireflection coating of the Si, and a low resistance contact. Fabrication of the cell is simple and inexpensive. Principal specific goals of the project are (i) the fabrication of solar cells by deposition of various window materials on single and polycrystalline Si, (ii) experimental testing and evaluation of the cells, and (iii) the explanation of the characteristics by the development of suitable models.

During the first six months, the concept of the heterojunction solar cell was shown to be valid in the form of an In_2O_3 window on p-type single crystalline Si. Experimental results showed the principal dark current mechanism in the operating range to be recombination through interface states, and the electron affinity of the In_2O_3 was found to be 0.3 eV greater than that of the Si. This difference limits the open circuit voltage and efficiency of such cells to a maximum of 11%, a probable practical efficiency of the order of 7-8%. It was shown that this limitation could be overcome by a shallow diffusion of donors into the surface of the Si. Heteroface cells of this type showed efficiencies of the order of 9% under simulated AM1 irradiation.

During the second six months, investigations of other crystalline window materials have been initiated. Results of measurements on SnO_2/n-Si, single crystal, indicate an electron affinity difference relative to the Si of approximately 0.85 eV. (The size of this difference makes impractical SnO_2/p-Si cells). Electron emission is the principal dark current mechanism. Although their characteristics are not fully understood, they appear to function somewhat like Schottky barrier cells. Under simulated AM1 irradiation, data for the best of these cells are $V_{oc} = 435$ mV, $J_{sc} = 23.7$ mA/cm^2, and $\eta = 6.3\%$.

Experiments with amorphous glasses such as $0.85V_2O_5{:}0.15P_2O_5$ show these materials to be impractical as solar cell windows. The principal limitation is the intrinsically high resistivity, $\rho \gtrsim 10^5$ Ω-cm. The cells tested show high series resistance and severe suppression of photocurrent in the third and fourth quadrants. A layer of amorphous glass between the Si and a low resistivity crystalline glass could, in principle, increase the open circuit voltage without degrading the curve factor or suppressing photocurrent, but the technical problem of depositing a sound layer no thicker than a few nm is non-trivial. Accordingly, such compound heterojunction cells are also judged to be impractical.

Cells of In_2O_3 on grown ribbon and polycrystalline Si of various grades show characteristics differing between runs, between wafers in the same run, and between locations on the same wafer. With few exceptions, open circuit voltages and conversion efficiencies are low, and suppression of photocurrent is evident on many. Since these poor characteristics are also measured on control units made from single crystal wafers, the source of the degradation appears to be in the processing at some stage where an interfacial layer of SiO_2 is grown. Measurements of these cells suggest that grain boundaries do not act as short circuits and that ribbon substrates are comparable to single crystal, but the facts that an oxide layer is evidently present and that all cells tested are 2.3 x 2.3 mm^2, sawed from material with crystallites of size varying from 0.005-20 mm, make such conclusions tenuous at best.

While the oxide layer problem delayed progress toward the project objectives, it provided data to make possible (i) the development of an explanation of the effects of an interfacial insulating layer based on energy bands and (ii) the development of experimental techniques for the identification of such a layer. The model allows qualitative prediction of changes in photocapacitance with voltage and illumination and changes in I-V characteristics with illumination. In particular, it predicts an increase in photocurrent suppression with increased illumination.

Although the stage of oxide growth in the processing is not known, thermodynamic calculations imply that some reduction by the Si of the In_2O_3 and the SnO_2 oxides is unavoidable. Whether or not a stable equilibrium is reached at some particular oxide thickness is directly related to the question of the stability of cells with these constituents under the conditions of terrestrial application. Data from initial experiments indicate rapid growth of SiO_2 interfacial layers on $S\overset{n}{\cancel{i}}O_2$/Si cells when subjected to a temperature of 200°C and less rapid growth when subjected to xenon illumination (without UV filters) at an intensity of 400 mW/cm^2. The same tests of In_2O_3/Si cells yield no conclusive evidence of degradation.

Continued study of the stability question and the inherently connected oxide layer problem is planned for the remaining period. Since photocurrent suppression is a good indicator of the oxide layer, methods for its detection and quantification will be sought. Publication of experimental results and heterojunction solar cell theory is planned.

FIG. 1 AER74-17631

GLASS-SI HETEROJUNCTION SOLAR CELLS
NSF GRANT AER74-17631

DEPARTMENT OF ELECTRICAL AND COMPUTER ENGINEERING
SYRACUSE UNIVERSITY
SYRACUSE, NEW YORK

INNOTECH CORPORATION
NORWALK, CONN.

PERIOD OF GRANT: 1 AUG. 1974 - 31 JULY, 1975

FUNDING: $313,900

PRINCIPAL INVESTIGATOR:

R.L. ANDERSON
SYRACUSE UNIVERSITY

FIG. 2 AER74-17631

OVERALL OBJECTIVES OF PROJECT

THE PURPOSE OF THIS PROJECT IS TO INVESTIGATE GLASS-SILICON HETEROJUNCTIONS AS SOLAR CELLS OF LOW COST, SUITABLE FOR TERRESTRIAL APPLICATIONS. THE PRINCIPAL SPECIFIC GOALS ARE:

A) THE FABRICATION OF GLASS-MONOCRYSTALLINE SI AND GLASS-POLYCRYSTALLINE SI HETEROJUNCTION CELLS.

B) THE EXPERIMENTAL TESTING AND EVALUATION OF THESE CELLS.

C) THE EXPLANATION OF CELL CHARACTERISTICS BY THE DEVELOPMENT OF SUITABLE MODELS.

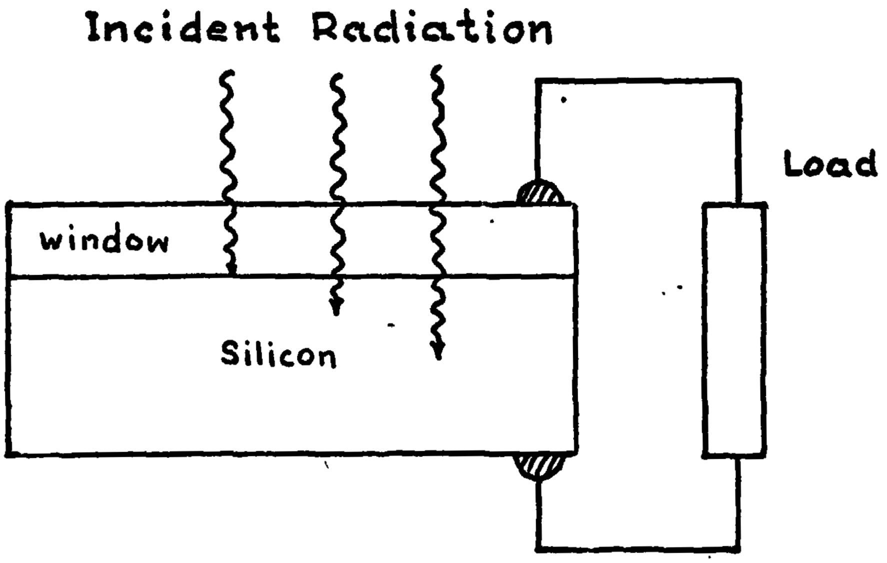

FIG. 3 AER74-17631

ACTIVITY PLANNED FOR 1 JAN - 30 JUNE, 1975

A) INVESTIGATION OF THE FOLLOWING WINDOW MATERIALS ON SINGLE CRYSTAL SUBSTRATES

1) CRYSTALLINE METAL OXIDES: SnO_2, CdO, ZnO . . .
2) AMORPHOUS GLASSES: V_2O_5, TiO_2, V_2O_5:GeO_2 . . .

B) INVESTIGATION OF THE FOLLOWING LOW-COST SUBSTRATES WITH In_2O_3 WINDOWS

1) GROWN RIBBON SI
2) VARIOUS GRADES OF POLYCRYSTALLINE SI

C) DEVELOPMENT OF HIGH EFFICIENCY HETEROFACE SOLAR CELL

D) DEVELOPMENT OF HETEROJUNCTION THEORY

FIG. 4 AER74-17631

OUTLINE OF PROGRESS

I. VALIDATION OF HETEROJUNCTION SOLAR CELL CONCEPT

II. CRYSTALLINE WINDOWS

III. AMORPHOUS WINDOWS

IV. ALTERNATE SUBSTRATES

V. INTERFACE BARRIER LAYER EFFECTS

VI. STABILITY OF CELLS

FIG. 5

In$_2$O$_3$/Si Cells

Reasonably well understood

$\Delta E_C = 0.30$ eV

Dark current mechanism

Recombination via interface states

$$\left.\begin{array}{ll} \text{Max } \eta & \approx 11\% \\ \text{Max } \eta_{\text{PRACTICAL}} & \approx 7\text{-}8\% \\ \text{Max } \eta_{\text{EXP}} & \approx 5\text{-}6\% \end{array}\right\} \text{ for single crystal Si}$$

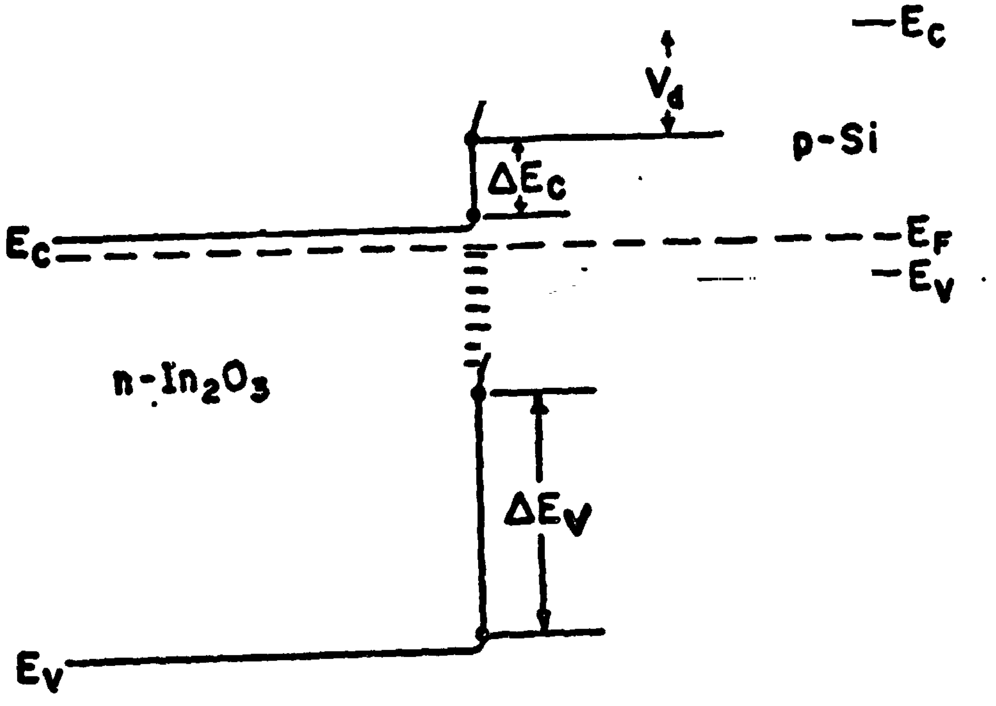

FIG. 6

AER74-17631

HETEROFACE CELLS

1 RUN MADE

EXCESSIVE RESISTANCE BETWEEN In_2O_3 AND SI

($\sim 4 \Omega/cm^2$)

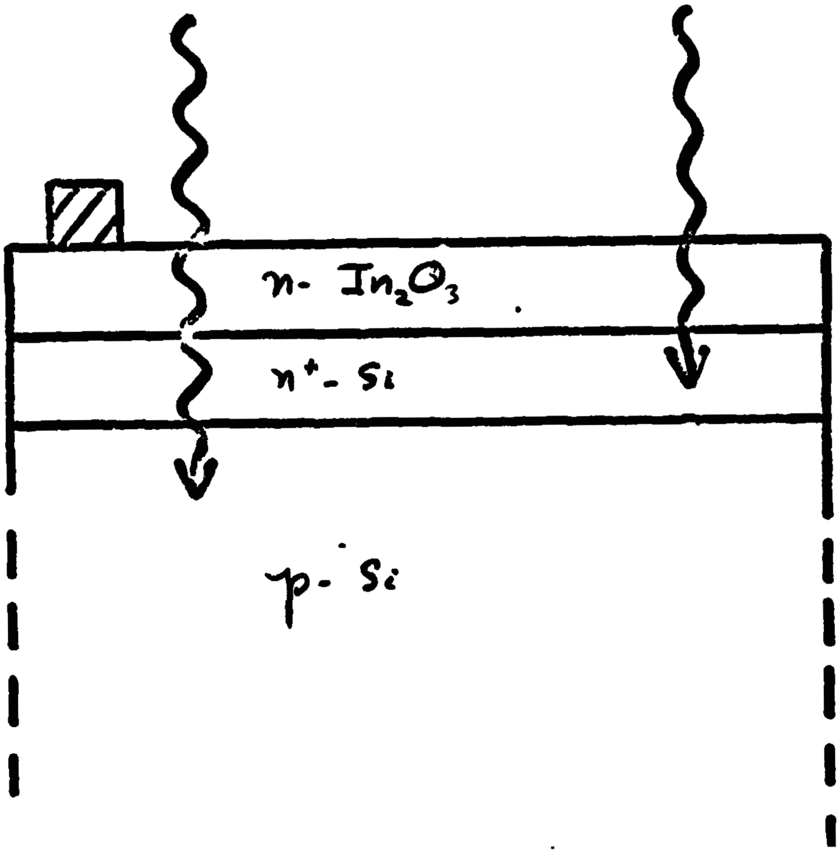

FIG. 7 AER74-17631

SnO$_2$/Si CELLS

SOMEWHAT UNDERSTOOD

$\Delta E_C \overset{?}{\approx} 0.85$ eV

DARK CURRENT MECHANISM: ELECTRON EMISSION

PHOTOCURRENT MECHANISM: RECOMBINATION AT INTERFACE

MAX η NOT DETERMINED

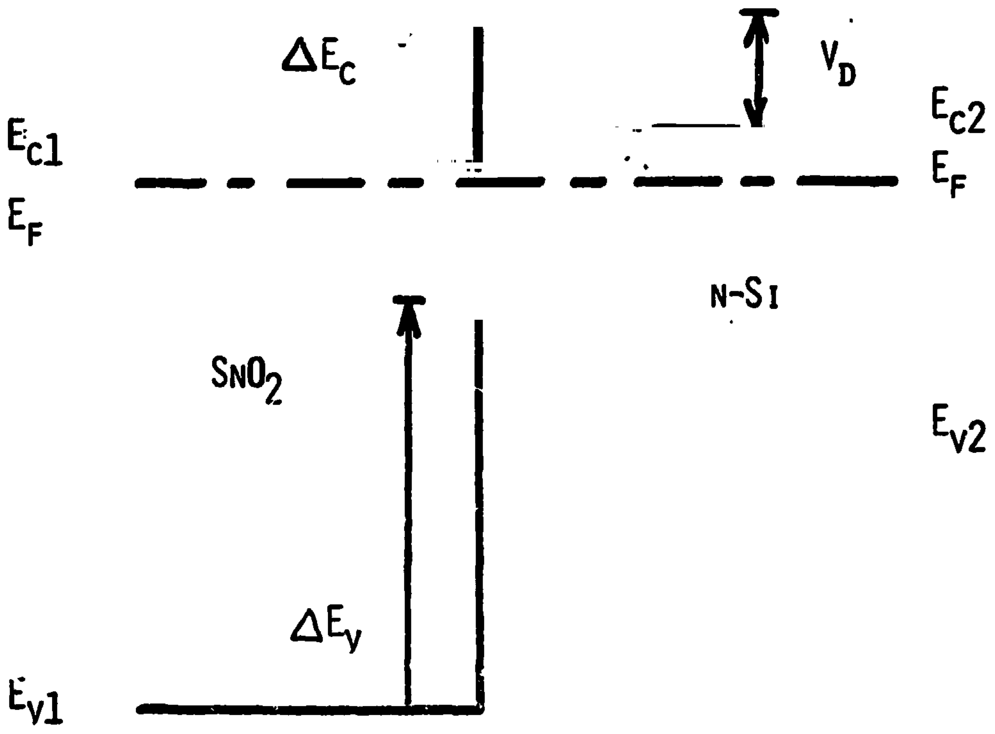

$$T = e^{-\int \sqrt{\frac{2m^*}{\hbar^2}(E_c - E)}\, dx}$$

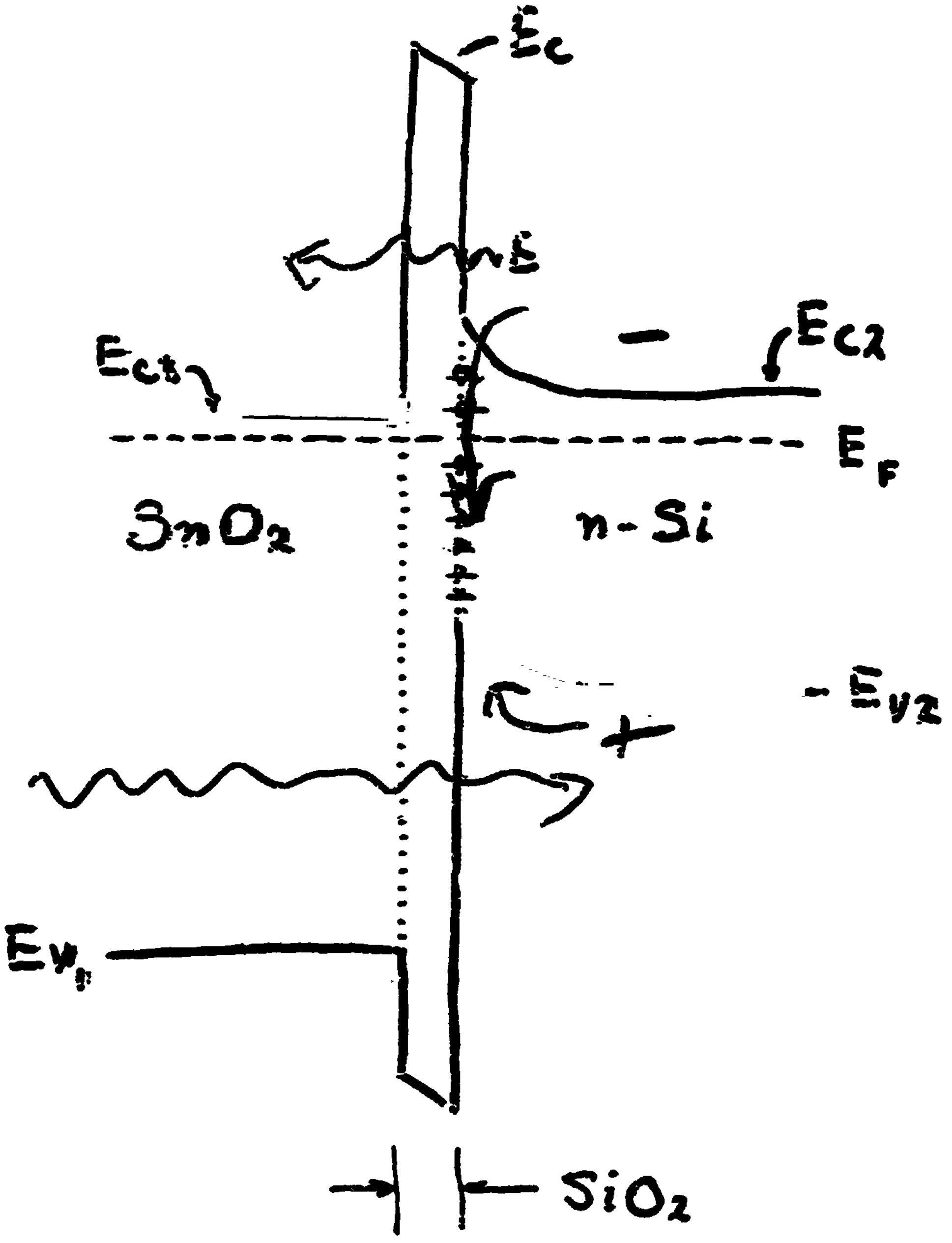

$$SnO_2 + Si \rightarrow Sn + SiO_2$$

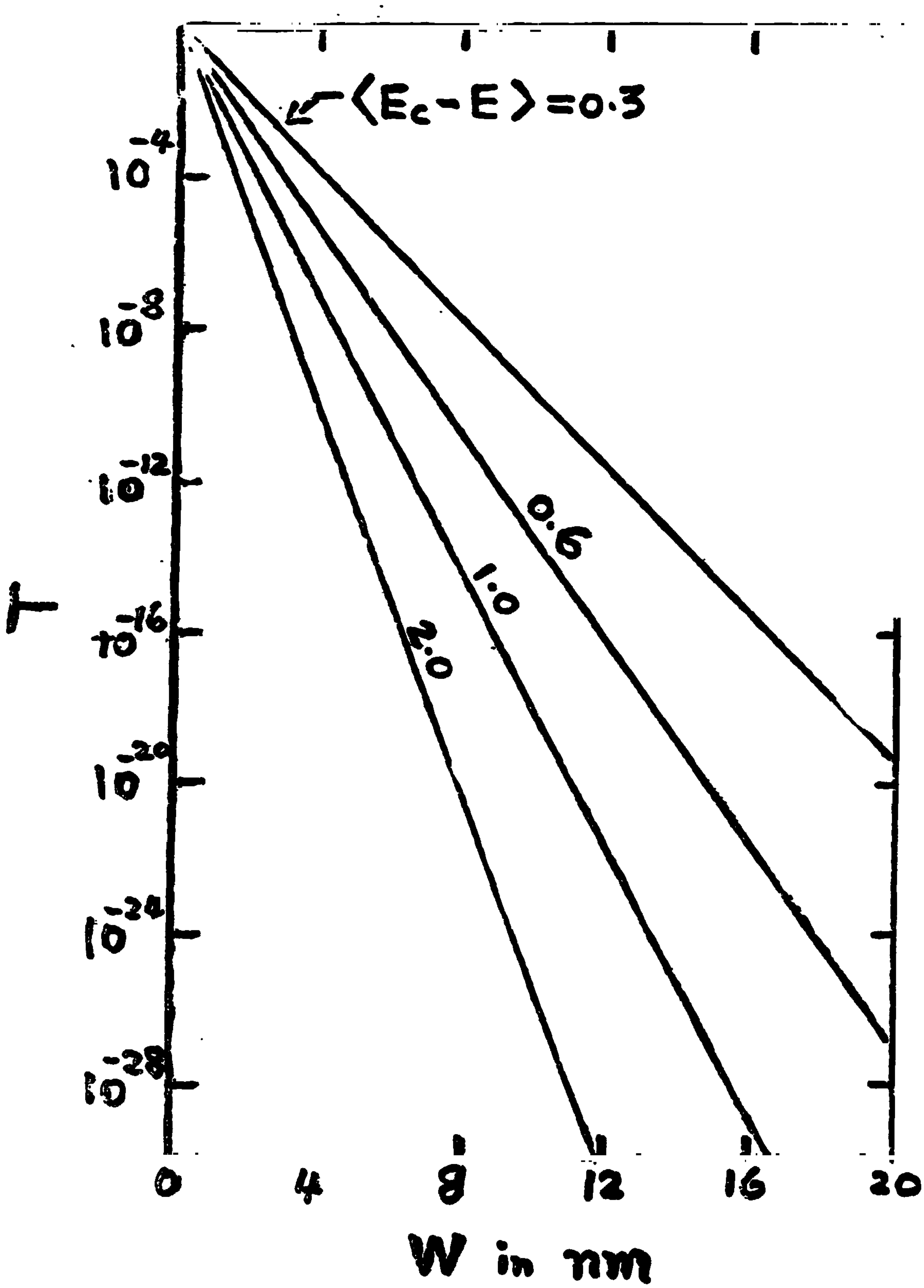
$\langle E_c - E \rangle = 0.3$
0.6
1.0
2.0
10^{-4}
10^{-8}
10^{-12}
10^{-16}
10^{-20}
10^{-24}
10^{-28}
T
0
4
8
12
16
20
W in nm

SnO_2/N-SI

BEST RESULTS

	J_{sc}(MA/CM^2)	V_{oc}(V)	η(%)
SINGLE CRYSTAL 0.23 CM X 0.23 CM	24	0.435	6.3

LATE RESULTS

	J_{sc}	V_{oc}	η
SINGLE CRYSTAL			
2 CM X 2 CM	29	0.523	9.4
1 CM X 1 CM	29	0.521	9.9
POLY (GRAIN SIZE?)			
2 CM X 2 CM	27	0.469	6.9
1 CM X 1 CM	26	0.470	7.2

FIG. 9 AER74-17631

AMORPHOUS GLASS WINDOW

IMPRACTICAL

$\rho_{MIN} > 10^5\ \Omega\text{-CM}$

R_S TOO LARGE

PHOTOCURRENT SUPPRESSION

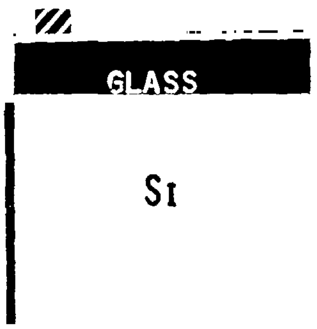

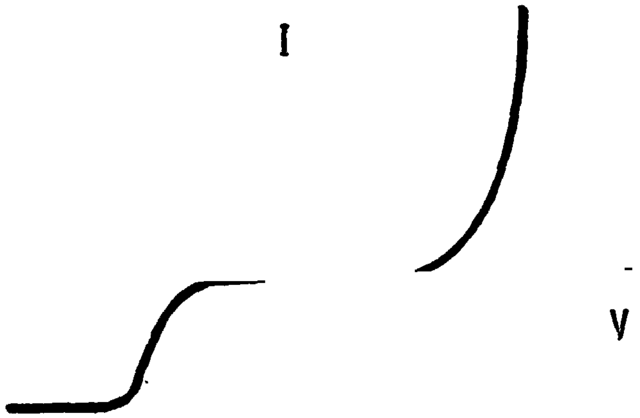

FIG. 10

COMPOUND HETEROJUNCTION

IMPRACTICAL

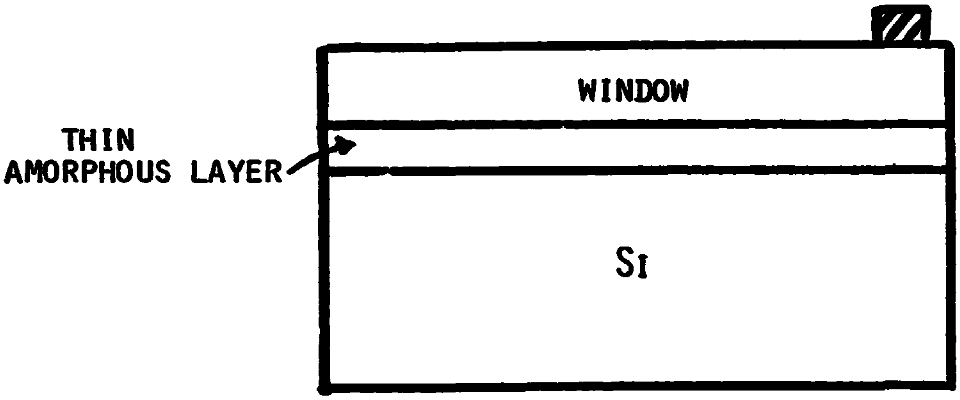

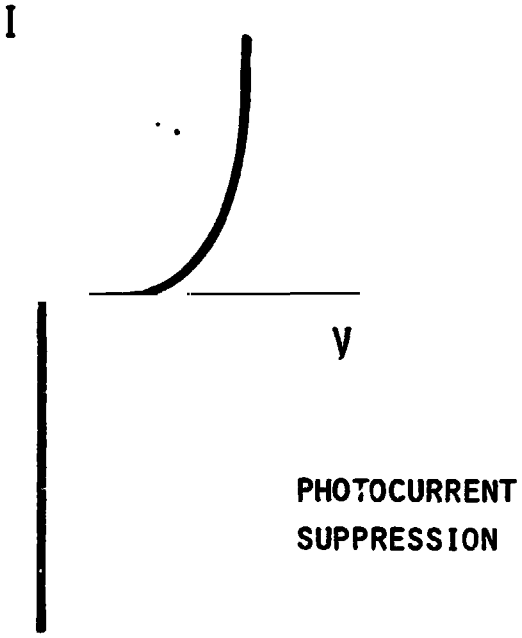

FIG. 11

In_2O_3/P-SI CELLS

SUBSTRATES USED (0.23 CM X 0.23 CM)	BEST η (%)
SINGLE CRYSTAL	4.3
RIBBON	3.4
POLYCRYSTALLINE SI	
LARGE GRAIN	2.9
METAL GRADE	0.5
CVD ON S.C. SUBSTRATE	0.07
CVD EPI ON RECRYSTALIZED MET GRADE (CHU)	1.4
SINGLE CRYSTAL (1 CM X 1 CM)	1.6

MAX V_{OC} 0.323 V

MAX J_{SC} 25 MA/CM^2

LATE RESULTS

	J_{SC} (MA/CM^2)	V_{OC} (V)	η (%)
SINGLE CRYSTAL			
2 CM X 2 CM	24	0.323	4.1
1 CM X 1 CM	25	0.343	4.9
POLY (GRAIN SIZE?)			
2 CM X 2 CM	24	0.357	3.3
1 CM X 1 CM	24	0.359	4.6

FIG. 12 AER74-17631

SiO_2 INTERFACIAL LAYER

COMPETING MECHANISMS

TUNNELING → PHOTOCURRENT

RECOMBINATION → PHOTOCURRENT SUPPRESSION
VIA INTERFACE
STATES

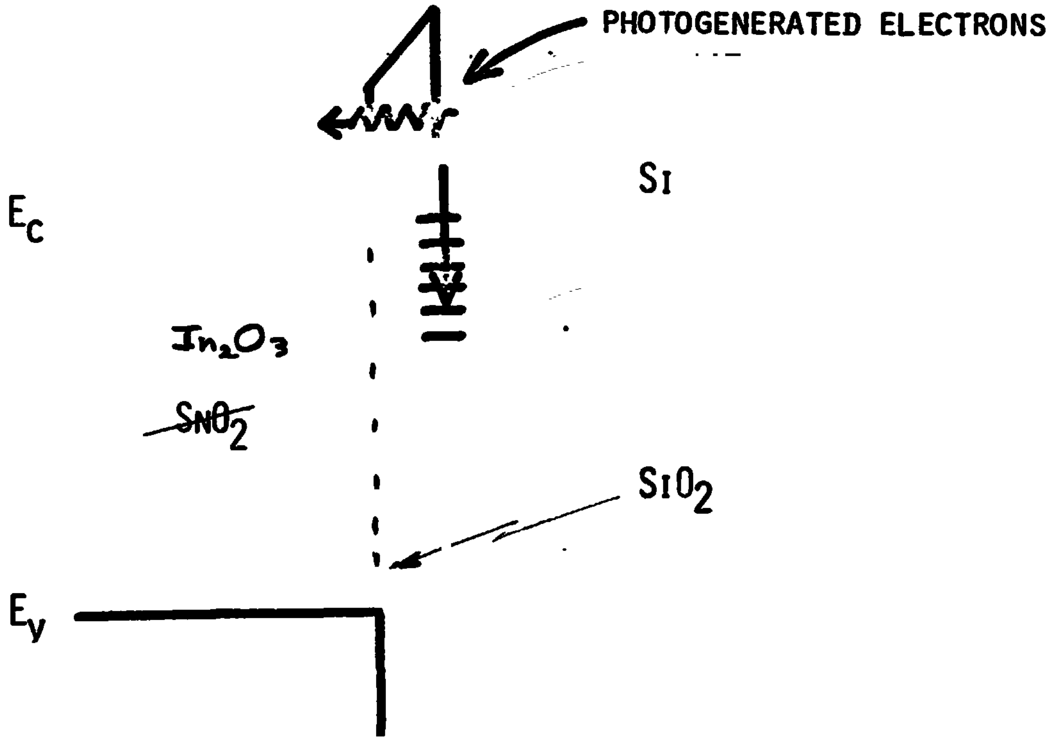

SiO_2 INTERFACIAL LAYER

EFFECTS

A) DECREASE I_0

IF I_{PH} IS INDEPENDENT OF V

$$V_{OC} = \frac{MKT}{Q} \ln\left(\frac{I_{PH}}{I_0} + 1\right)$$

AND V_{OC} IS INCREASED

B) SUPPRESSION OF PHOTOCURRENT FOR THICKNESS 2-3 NM

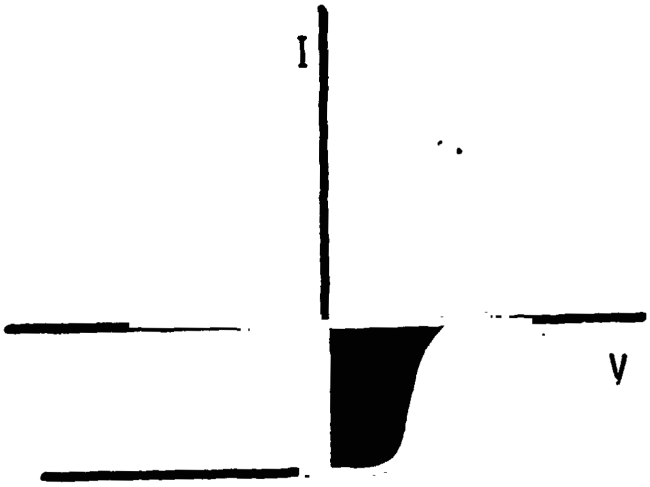

FIG. 14

SiO_2 INTERFACE LAYER

ORIGIN OF SiO_2 LAYER UNKNOWN

PROCESSING?

$SnO_2 + Si \longrightarrow Sn + SiO_2$

$In_2O_3 + \frac{3}{2}\,Si \longrightarrow 2In + \frac{3}{2}\,SiO_2$

AT ROOM TEMP

FIG. 15

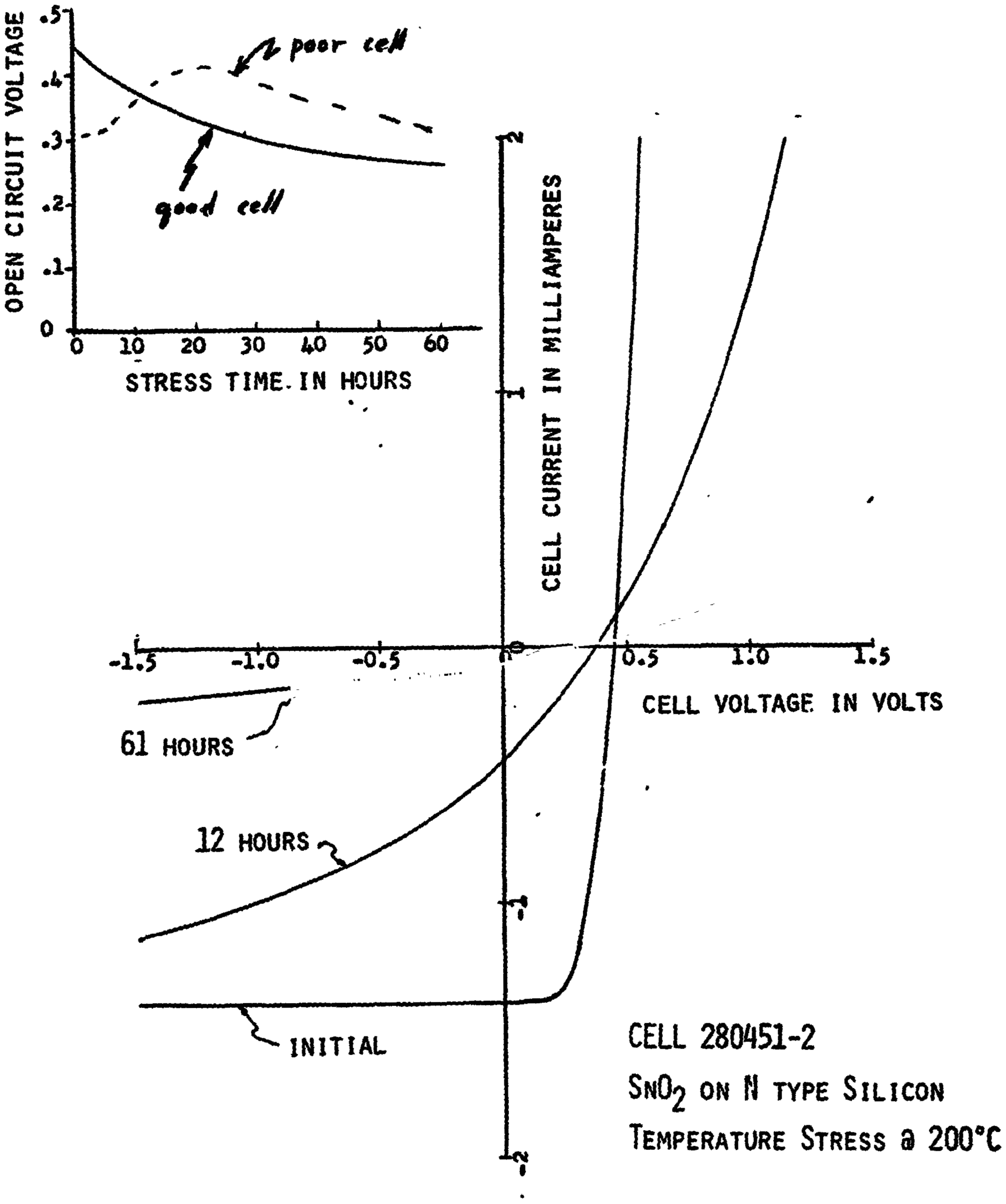
OPEN CIRCUIT VOLTAGE
.5
.4
.3
.2
.1
0
0
10
20
30
40
50
60
STRESS TIME IN HOURS
poor cell
good cell
CELL CURRENT IN MILLIAMPERES
2
1
0
-1
-2
-1.5
-1.0
-0.5
0.5
1.0
1.5
CELL VOLTAGE IN VOLTS
61 HOURS
12 HOURS
INITIAL
CELL 280451-2
SnO2 ON N TYPE SILICON
TEMPERATURE STRESS @ 200°C

FIG. 16 AER74-17631

DEGRADATION OF OPEN CIRCUIT VOLTAGE UNDER 400 mW/cm^2 XENON LAMP ILLUMINATION

CELL 280451-7, SnO_2/n-Si

(At AM 1 V_{oc} goes down 12% in 60 hrs.)

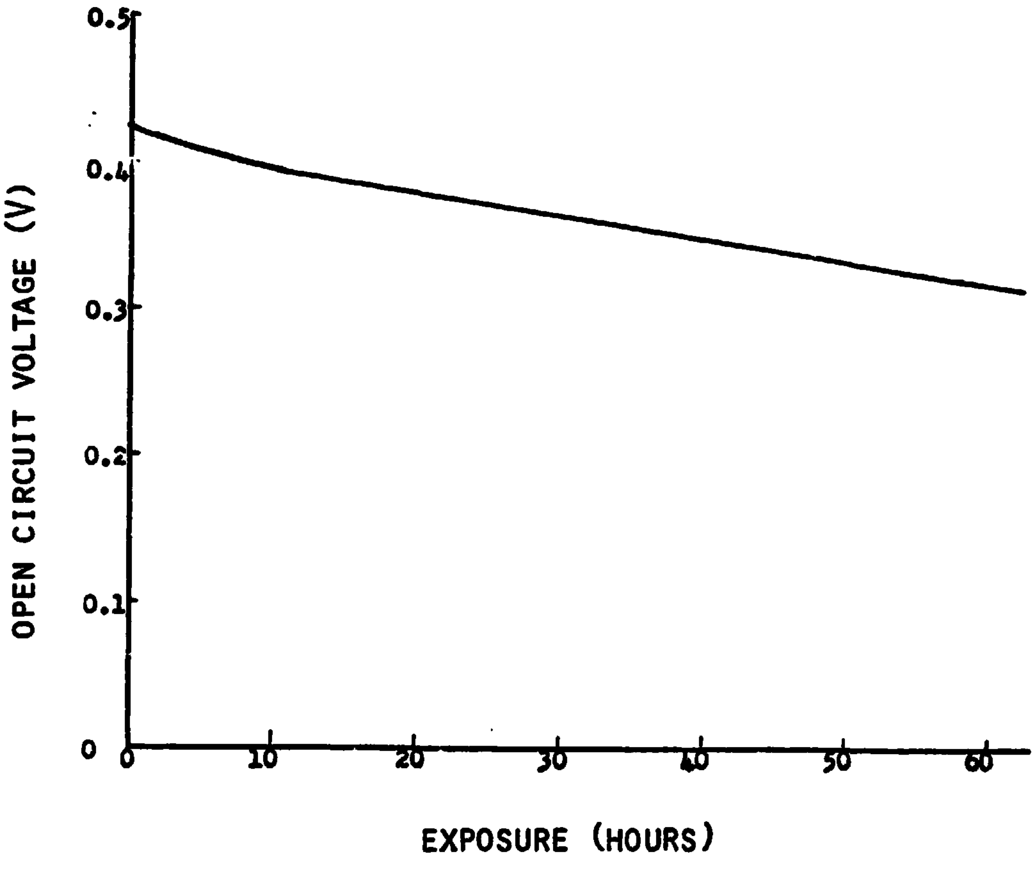

DEVICE S280451 UNIT #3

SnO_2 - Si CELL

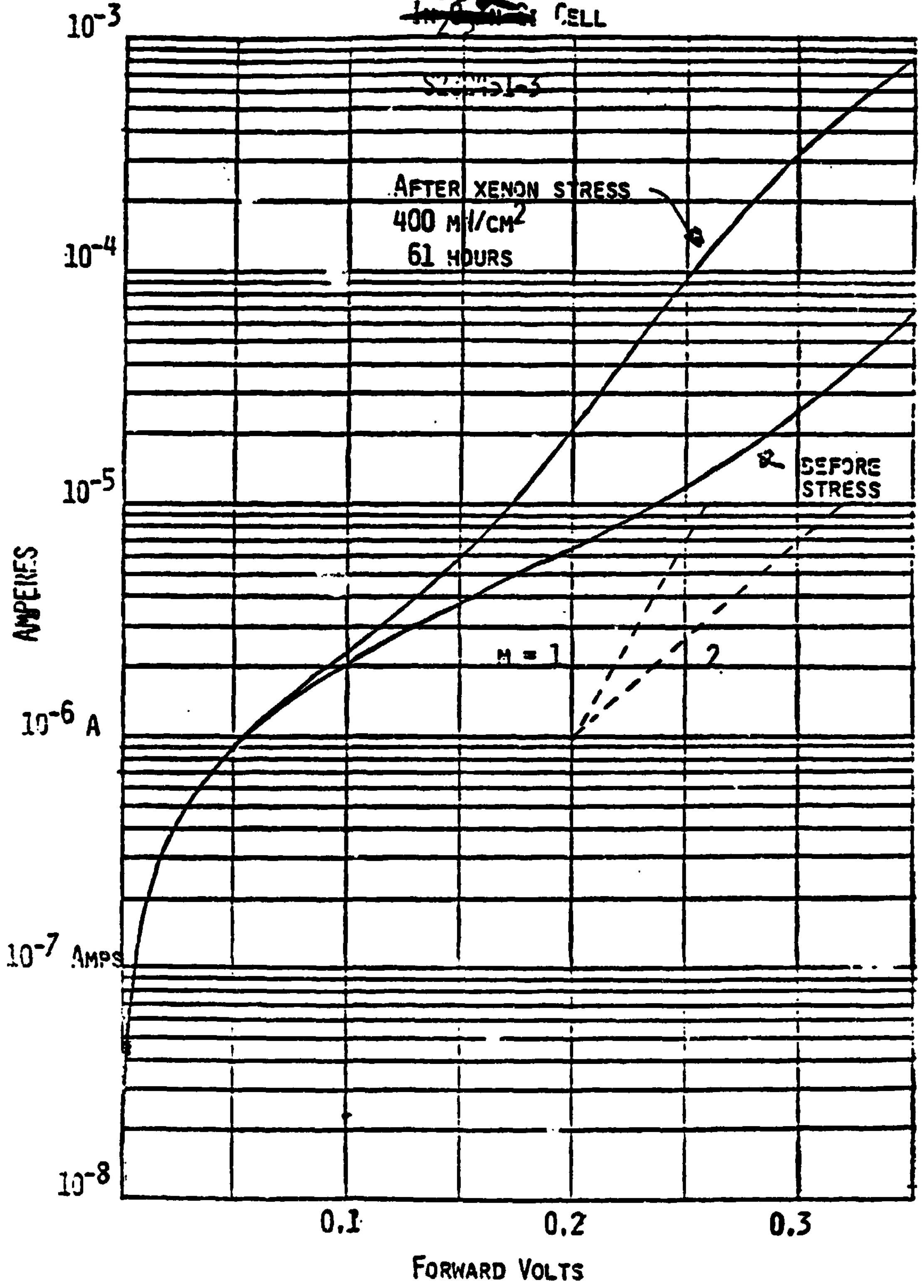

FIG. 17 AER74-17631

SUMMARY OF KEY RESULTS

I. EXPERIMENTAL STUDY AND MODEL OF In_2O_3/Si CELLS ESSENTIALLY COMPLETE. MODEL PREDICTS $\eta_{MAX} \sim 11\text{-}13\%$ AND HIGHER EFFICIENCIES FOR $In_2O_3/N^+\text{-}P\text{-}Si$ CELLS.

II. EXPERIMENTAL STUDY AND MODEL OF $SnO_2/N\text{-}Si$ CELLS NOT COMPLETE, BUT THESE SHOW PROMISE FOR TERRESTRIAL APPLICATION IF STABLE. EFFICIENCY REALIZED 6.3%.

III. AMORPHOUS WINDOWS OR LAYERS SUPPRESS PHOTOCURRENT. NOT PRACTICAL FOR SOLAR CELLS.

IV. INTERFACIAL SiO_2 LAYER SUPPRESSES PHOTOCURRENT AND INCREASES SERIES RESISTANCE. SUPPRESSION INCREASES WITH ILLUMINATION.

FIG. 18 AER74-17631

MAJOR PROBLEMS

I. TECHNICAL

  A. LIMITATION OF V_{OC} BY ΔE_C

  B. PHOTOCURRENT SUPPRESSION

  C. HIGH SERIES RESISTANCE

  D. POOR REPRODUCIBILITY

II. SCHEDULE

  A. START-UP TIME TOO SHORT

FIG. 19. AER74-17631

PLANNED ACTIVITY

I. INVESTIGATE STABILITY OF CELLS

II. INVESTIGATE INTERFACE LAYER EFFECTS

III. DEVELOP METHODS FOR DETECTION OF PHOTOCURRENT SUPPRESSION

IV. PUBLISH EXPERIMENTAL RESULTS AND THEORY OF HJSC's

WHAT SHOULD BE DONE?

I. INVESTIGATE THE THERMODYNAMICS OF VARIOUS WINDOW MATERIALS ON Si, GaAs, ...

II. INVESTIGATE THE CHEMICAL KINETICS OF INTERFACE REACTIONS.

III. DEVELOP EXPERIMENTAL TECHNIQUES FOR ANALYSIS OF INTERFACIAL LAYERS.

IV. DEVELOP METHODS FOR DEGRADATION MEASUREMENT.

V. DEVELOP QUANTITATIVE THEORY OF DEGRADATION.

N76 12502

SURFACE SCIENCE APPLIED TO THE DEVELOPMENT OF ECONOMICAL PHOTOVOLTAIC SOLAR CELLS

1) The effect of dopants on chemical vapor deposition - a surface potential model.
2) Surface segregation of impurities.
3) Silicon recrystallization using a thin Al - layer on carbon.
4) Effect of structure and impurities on surface states.

SURFACE STRUCTURE AND ELECTRONIC PROPERTIES OF MATERIALS

AG 742 $ 87,500

Jan. 1, 1975 - July 1, 1975

W. J. Siekhaus

Energy and Environment Division
Lawrence Berkeley Laboratory

G. A. Somorjai

Inorganic Materials Research Division
Lawrence Berkeley Laboratory

AVS - Chicago 1974

ASME - Palo Alto 1974

ACS - Chicago

International Summer Course - Procidia, Sicily 1975

RESEARCH APPLIED TO THE DEVELOPMENT OF THIN FILM POLYCRYSTALLINE SOLAR CELLS

An economically competetive solar cell consists of a substrate on which a 100 μ thick silicon layer is deposited, covered by a transparent conductor containing a metallic grid.
The problems to which research is directed are identified in the cell by the letters a, b, b', c.

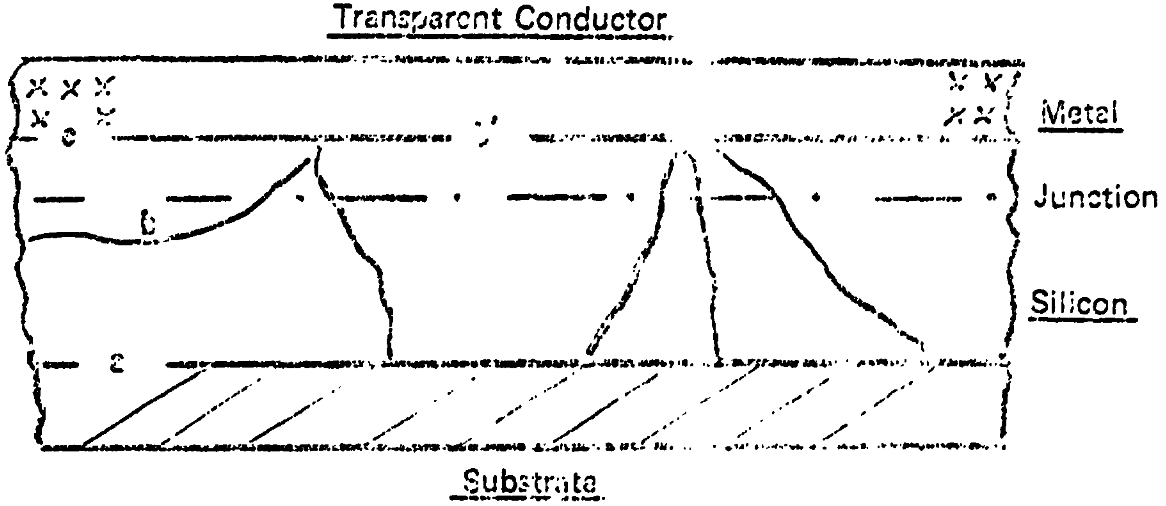

Research Areas:

a) Low temperature catalysis of the decomposition of SiH_4, $SiCl_4$ on a low melting point substrate material (e.g. Al) to form large area silicon sheets.
Research tool: molecular beam deposition.

b) Catalysis of large grain crystallization by use of suitable impurities.
Segregation of impurities onto grain boundaries.
Research tool: low energy electron diffraction, Auger spectroscopy.
a,b,b',c. Dependence of electronic surface states on impurities.
Research tool: photoelectron spectroscopy, energy loss spectroscopy.

PROGRAM OBJECTIVE

ANALYZE INFLUENCE AND BEHAVIOR OF SURFA
AND INTERFACES

DURING CVD FILM DEPOSITION
EFG SHEET FORMATION
CELL LIFE

DETERMINE AND LEARN TO UNDERSTAND, TO CORRECT AND TO USE THE EFFECT OF CHEMICAL COMPOSITION AND PHYSICAL STRUCTURE OF SURFACES AND INTERFACES ON ELECTRONIC STATES.

The objective of this grant is to employ surface science to the problems associated with the development of economical thin film solar cells: to understand and control the mechanism of chemical vapor deposition, to study substrate - film interaction, to analyze impurity segregation onto surfaces and grain boundaries, to determine the effect of selected impurities on grain growth and to investigate the effect of structure and impurities onto surface states.

We have developed a surface potential model to explain dopant effects on chemical vapor deposition. Auger analysis of the interaction between allotropic forms of carbon and silicon films has shown Si-C formation for all forms but glassy carbon. LEED intensity measurements have been used to determine the mean sqare displacement of surface atoms of silicon single crystals, and electron loss spectroscopy has shown the effect of structure and impurities on surface states located within the band gap. A thin film of Al has been used to enhance film crystallinity at low temperature.

At the present time we perform chemical vapor deposition under externally applied electric fields to test the surface potential model of chemical vapor deposition. We use Auger spectroscopy to identify impurities segregating onto surfaces and interfaces, and we are investigating with electron loss spectroscopy the effect of dopants on surface states.

Future experiments are planned to determine dopant spatial distribution on the surface during chemical vapor deposition, the effect of dopants on chemical vapor deposition reaction kinetics using modulated molecular beam analysis, and the effect of impurities on the activation energy for recrystallization. We plan to use UV electron spectroscopy together with improved energy resolution electron loss spectroscopy to determine absolute energy levels of impurity induced surface states.

WORK PLAN

WORK AREA	PROGRAM	RESULTS
Surface states	LEED intensity data on (111) and (7x7(111) Si	Thesis published. Shows correlation between reconstruction and change in bond strength.
	Electron loss spectra on Si(2x1)(111) Si and amorphous Si.	Report. Shows removal of surface state in midgap by oxygen adsorption.
Impurity segregation	Fracture and analyze large and small grain polycrystal line Si to determine grain boundary impurity segregation.	Report. Difficulties. Si does not reproducibly fracture along grain boundaries. Almost always cleaves. Change experimental procedure.

WORK PLAN

WORKAREA	PROGRAM	RESULTS
Effect of Al on Si crystallinity	Thin layer of Al on C before Si deposition	LB L report. Good crystallinity at low temperature without SiC formation.
Effect of surface charge on deposition	Equipment modification and first measurements.	LBL report, theoretical model submitted for publication.
Analytical work for other groups.	"Get" scanning Auger Analyzing system	"Got" it. Measured boron distribution in ion implanted Si.

GRAIN BOUNDARY SEGREGATION OF BORON IN POLYCRYSTALLINE FILMS.

Experimental results reported in J.Electr.Chem.Soc. (first graph - page suggest, that in chemical vapor deposition together with Boron doping the grain boundary will be completely covered with a monolayer of dopant before doping in the grain can be achieved.

To check this hypothesis, polycrystalline films were deposited onto single crystal substrates covered with a thin nitride layer. Deposition was done by CVD using $SiCl_4$ with B_2H_6 doping by Applied Materials Corporation to a thickness of 200 Å. Estimated concentration of B is $6.6 \times 10^{18}/cm^3$.

The next few graphs show, that polycrystalline silicon, under the conditions investigated up to now almost exclusively fractures by cleavage.

Consequently, Scanning Auger Analysis of fractured surfaces allows up to now no consistent analysis of grain boundary segregation.

/ Efforts continue to find suitable conditions, and an alternate approach to find surface segregation is presented in the next section./

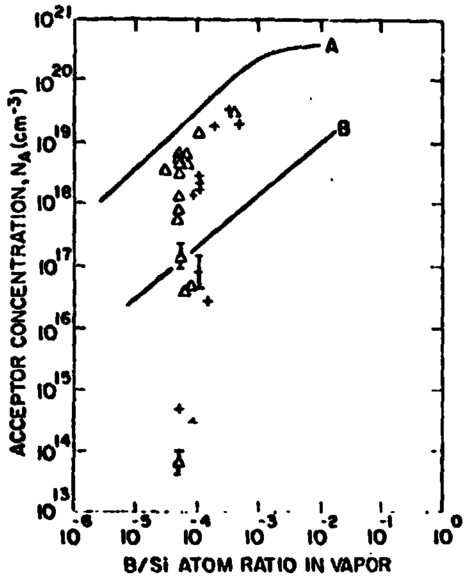

Fig. 2. Acceptor concentration, N_A, vs. B/Si atom ratio in vapor for poly Si samples deposited from SiH_4 at 650°C. △, Thermal SiO_2 substrates; +, fused quartz substrates. Single-crystal doping: -, boron doping of Si from B_2H_6 and $SiCl_4$-H_2 at 1500°K, A (11); B (12).

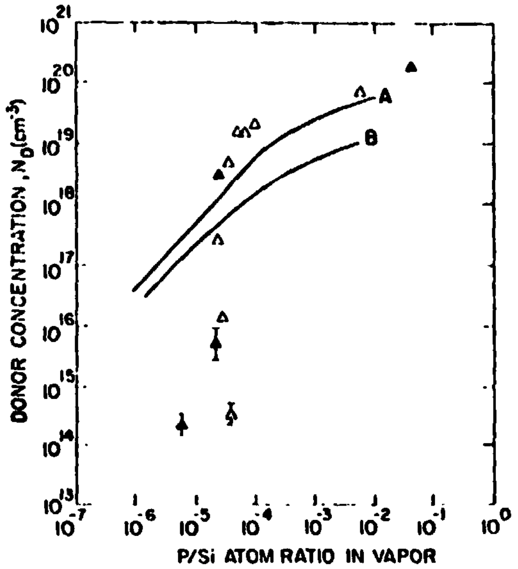

Fig. 3. Donor concentration, N_D, vs. P/Si atom ratio in vapor for poly Si samples deposited on thermal SiO_2 substrates. △ Deposited at 650°C from SiH_4, ▲ deposited at 840°C from $SiBr_4$-H_2. Phosphorous-doped single-crystal silicon, A (14); B (12).

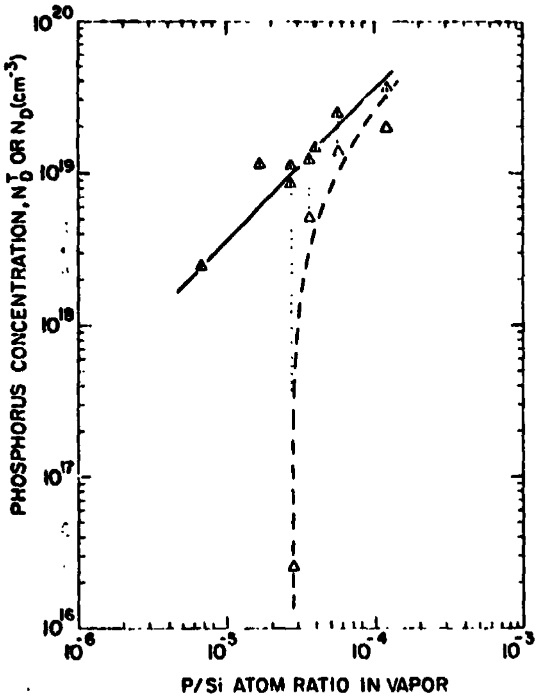

Fig. 4. Total phosphorous concentration, N_D^T, and donor concentration, N_D, vs. P/Si atom ratio in vapor for poly Si deposited from SiH_4 at 650°C. ▲ Total phosphorous concentration, △ donor concentrations, ——+—— see Eq. [1] in text, - - - - calculated from Eq. [4] in text.

M. E. Cowher and T. O. Sedgwick, J. Electrochem. Soc., SSS&T, Nov. 1972

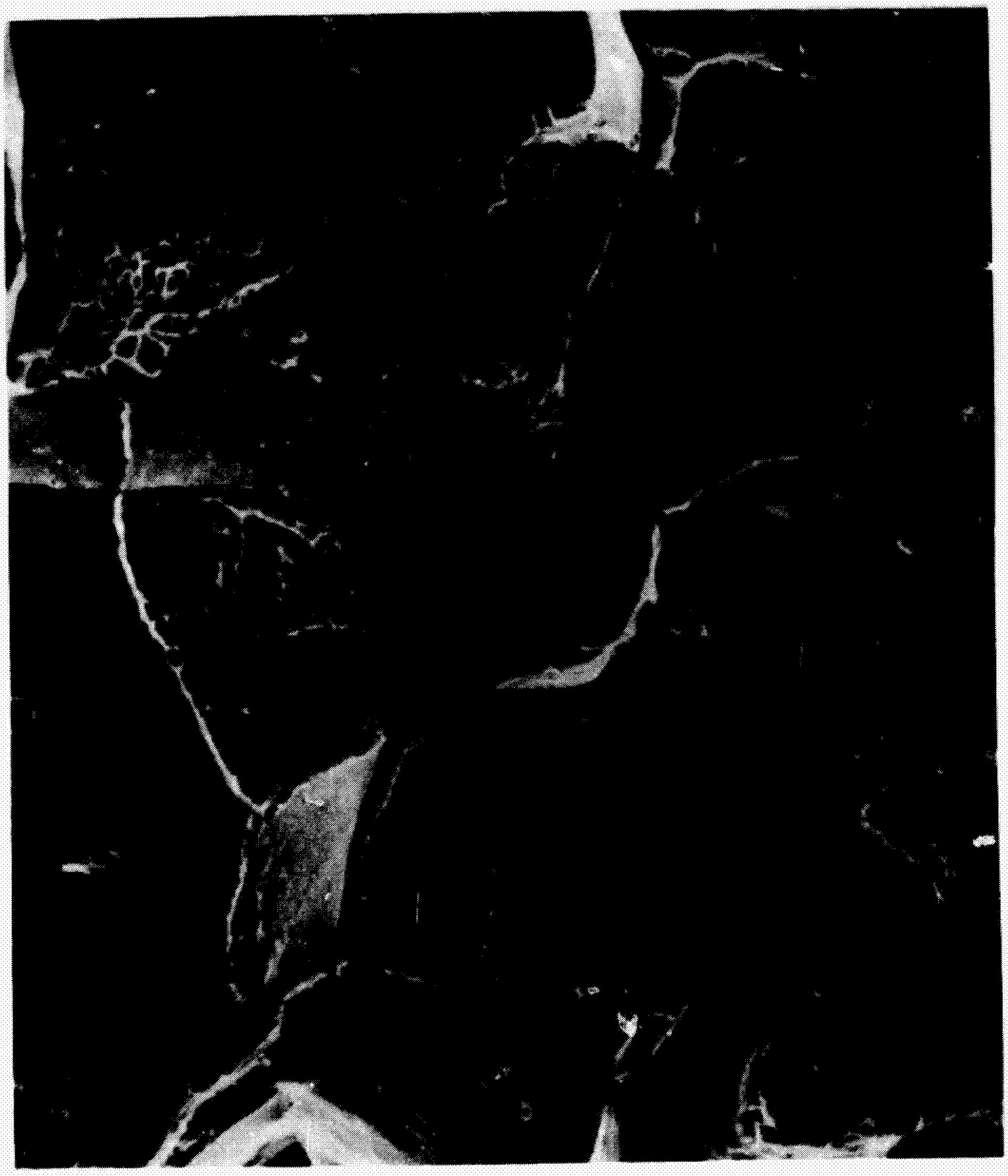

Typical Grain Boundary Fracture of Fe-12 Mn- o.2 Ti, 1000 X

Surface of Pol[illegible] on Siliconnitride (1000X)

FRACTURE VIEW OF POLYCRYST. SILICON CLOSE TO SURFACE, (600)

ORIGINAL PAGE IS
OF POOR QUALITY

FRACTURE VIEW OF POLYCR. SI FILM ON SILICON NITRIDE ([illegible] X)

N76 12503

Dopant Gas Effect on Silicon Chemical Vapor Depositions
A Surface Potential Model

Chin-An Chang[*]

Inorganic Materials Research Division, Lawrence Berkeley Laboratory,
University of California, Berkeley, California 94720

A surface potential model is proposed to consistently explain the known dopant gas effects on silicon chemical vapor deposition. This model predicts that the effects of the same dopant gases on the diamond deposition rate using methane and carbon tetrachloride should be opposite and similar to those of silane, respectively. Available data is in agreement with this prediction.

---

[*] Present address: IBM Thomas J. Watson Research Center,
Yorktown Heights, New York, 10598

Chemical vapor deposition (CVD) has been widely used for thin film depositions. This technique is especially applicable to thin film silicon solar cells. Deposition rate of a few microns per minute can be easily obtained, and p-n junction can be made by mixing silicon chemical vapors (CV), such as silane and silicon tetrachloride, with depant gases, like diborane and phosphine. In general CVD of silicon is carried out at a substrate temperature around 1000 to 1200°C, and single crystal silicon wafer is used for an epitaxial growth of thin films. However, for an economic thin film solar cell, non-crystalline, and oftentimes non-silicon substrates, are required. Furthermore, interaction between the substrate chosen and the silicon thin film deposited should be kept minimal. For example, at a substrate temperature around 1200°C, silicon thin films deposited on graphite show a significant diffusion of silicon and carbon and the formation of silicon carbide[1]. Much less diffusion is noted, however, when the substrate temperature is below 800°C[2]. Similar high temperature interaction between the silicon films deposited and other types of substrate has also been reported[3]. Preferably, one should use the lowest possible substrate temperatures to minimize such interactions and diffusions.

At low substrate temperatures, however, other problems arise. First, silicon film deposited is polycrystalline with small grain sizes[4]. Second, much lower deposition rate than that at high substrate temperature is obtained using the CVD technique[5]. Small grain size means a shortening of lifetime for the charge carriers due to trapping by the grain boundaries[6]; low deposition rate makes CVD a non-economic technique for depositions. To solve the former problem the author has developed a technique to increase the silicon crystallinity at low substrate temperatures[7]. An enhancement of two to four orders of magnitude is obtained for the silicon films deposited on quartz and graphite at 600°C substrate temperature[7,2]. Our next goal is to increase the deposition rate of low temperature CVD. As part of our effort toward this goal we describe in this paper a conceptual model which could lead to a better understanding of the existing information on the variation of CVD deposition rates. This model is shown to consistently explain the known dopant gas effects on the deposition rates of silicon chemical vapors and correctly predicts for those on carbon chemical vapors. The implications and applications of this model to other studies are also discussed.

It has been known that silicon deposition rate using silane, SiH_4, and silicon tetrachloride, $SiCl_4$, is increased by diborane, B_2H_6, and decreased by phosphine, PH_3, and arsine, AsH_3[8]. Existing theories considering active site blocking[8b] and strong bonding between the CV molecules and dopant gas molecules[8c] have not been advanced enough to explain the known effects in a consistent way, nor can they be used to predict the dopant gas effect on other CV molecules. In our approach we make use of the fact that diborane, a p-type dopant gas for silicon, gives an opposite effect on the deposition rate of silicon chemical vapors from those by phosphine and arsine both of which being n-type dopant gases. This implies a possible correlation between the electronic structure of the dopant atoms with the observed effects cited. The mechanism involved in the CVD process is first analyzed, in order to see how this property can be incorporated into the deposition process.

Chemical vapor deposition can be viewed as a two-step process: adsorption of the CV molecule on the substrate surface followed by its thermal decomposition. As an example, deposition of silane follows

$$SiH_4\ (\text{gas}) \rightarrow SiH_4\ (\text{adsorbed}) \xrightarrow{\text{heat}} Si + 2H_2.$$

The thermal decomposition part involves a transfer of thermal energy from the substrate to the CV molecule needed for its decomposition. At a fixed substrate temperature, the maximal amount of thermal energy which can be acquired by the CV molecule is constant. The efficiency of this energy transfer, however, depends on the residence times of the CV molecule on the substrate surface. In other words, for an effective decomposition of the CV molecule to take place on the surface, a sufficient amount of thermal energy necessary for such decomposition should be transferred to the CV molecule before it desorbs from the surface. Therefore, at a fixed substrate temperature, decomposition of the CV molecule will be determined by the adsorption efficiency of this molecule on the substrate surface. This argument is in agreement with the work of Farrow who found that silane adsorption is the rate limiting step for the decomposition of this molecule[8b]. Accordingly, at a given substrate temperature, any factors which enhance the adsorption rate of the CV molecule should also enhance its decomposition and therefore its deposition rate. Our problem is thus simplified to that of the effect of dopant gas on the adsorption of silicon chemical vapor molecules.

From the chemical point of view, silane has the partially ionic $Si^{+}-H^{-}$ bonds[9]. Being tetrahedral, such a molecule possesses no net dipole moment[10]. However, the ionic character mentioned would make silane a molecule with four negatively charged hydrogen atoms surrounding a positively charged silicon atom in the center. Such a molecule would be attracted by a surface with positive surface potential and be repelled from one with negative surface potential. In other words, making the surface potential more positive would [illegible] silane better and enhance its adsorption rate. The same argument applies [illegible] silicon tetrachloride which has $Si^{+}-Cl^{-}$ ionic bonds, similar to those in [illegible]ane.

Next, we study the effect of dopant gas on the surface potential of a substrate. Diborane, arsine and phosphine thermally decompose to release boron, arsenic and phosphorus atoms, respectively. These atoms then adsorb on the surface and become doped into the silicon film deposited. As mentioned earlier, the observed deposition rate dependence of silane and silicon tetrachloride showed possible correlation with the electronic structure of the dopant atoms. Furthermore, during silicon CVD, there is always a silicon surface with freshly adsorbed silicon and dopant atoms[11]. Our problem is therefore similar to the study of the effect of dopant atoms on the [illegible]ce potential of a silicon surface. Supporting this approach is the experimental observation that when the substrate is covered with a monolayer of boron atoms, the deposition rate of silane is the highest among the depositions using the silane-diborane mixtures[8c].

First, we define a reference surface to be a silicon surface with only adsorbed silicon atoms. This is the case when pure silicon chemical vapor is used. A boron adsorbed silicon surface can be seen to be different from the reference one. Boron, being a p-type dopant and electron deficient relative to silicon, should, relative to the reference surface, lower the local electron density on the surface silicon atoms around the adsorption site. This would increase the electron affinity of the silicon surface onto which boron is adsorbed[12]. The effect on the surface potential is seen from the relation defining this property[12].

$$(E_F - E_I)_S = (E_V - E_I) + (\Phi - \phi)$$

Here E_F, E_I, E_V are the energies for the Fermi level, intrinsic level and top of the valence band, respectively, S stands for surface, Φ and ϕ are photoelectric threshold and work function, respectively. Furthermore, $\Phi = X + E_G$, X is the electron affinity, and E_G, the band gap between the bottom of the conduction band and the top of the valence band. An increase in electron affinity, on the surface is seen to make the surface potential more positive than the reference surface defined above[13]. Such a surface would then attract molecules like silane and silicon tetrachloride. This should enhance the adsorption and therefore the deposition rate of these molecules. On the other hand, phosphorus and arsenic, which are n-type dopants and electron-excessive relative to silicon, would make the surface potential more negative than the reference one. Accordingly, the deposition rate of silane and silicon tetrachloride should be lowered when they are mixed with phosphine and arsine. The observed dopant gas effect on the deposition rates of silicon chemical vapors is thus satisfactorily explained. These results are summarized in Table I.

An immediate test of the proposed model is to choose some CV molecule of different bonding character from that of SiH_4 and $SiCl_4$. Different dopant gas effect on the deposition rate of this chosen CV molecule should then be expected. One such molecule is methane, CH_4. Methane is also tetrahedral but has the $C^- - H^+$ type of ionic bonds. The hydrogen atoms are partially positively charged in methane, opposite to that for silane. The dopant gas effect on the deposition rate of methane should then be just the opposite of that for silane. When one goes to another carbon CV molecule, carbon tetrachloride, CCl_4, however, the dopant gas effect should be similar to that for silane. This is because of the $C^+ - Cl^-$ ionic bonding character of this molecule. The predicted dopant gas effect for methane and carbon tetrachloride are also listed [illegible] Table I. For a meaningful test of our model to carbon CVD, data on t[illegible] deposition should be used. Diamond film has the similar st[illegible] film, and differs from the layer structure of a graphite [illegible] The [illegible] literature data on the dopant gas effect on diamond

Table I. Predicted and observed dopant gas effects on the deposition rates of silicon and carbon chemical vapors*

	SiH_4	$SiCl_4$	CH_4	CCl_4
Bonding Characters	$Si^+ - H^-$	$Si^+ - Cl^-$	$C^- - H^+$	$C^+ - Cl^-$
B_2H_6	I	I	D	I
	I^a	I^a	D^b	
PH_3	D	D	I	D
	D^a			
AsH_3	D	D	I	D
	D^a			

*I and D indicate an increase and decrease, respectively, in deposition rate. The first row for each dopant gas is for the predicted effects, the second row for the observed effects.

a. Ref. 9.

b. Ref. 14.

deposition concerns the methane-diborane system[14]. The results clearly show from that observed using only methane. This is just the effect predicted by our model.

Although limited by the existing information for a full test of our model, agreement with the available data is encouraging. It is therefore worthwhile to point out some useful works, both experimental and theoretical, that are necessary for a better understanding of the CVD process. (1) Experiments for the lacking information listed in Table I should be carried out for a complete test of our model. (2) Our model descrives the dopant gas effect through the dopant atom effect on the surface potential. This can therefore be tested by applying a bias voltage to the substrate and observe its effect on the deposition rate of pure CV molecules. Similarly, an electric field can be applied to the surface and tested for its effect on the deposition rate of each CV molecule. (3) Surface properties for silicon and diamond should be studied in the presence of adsorbed boron, arsenic and phosphorus atoms. This includes surface properties such as the surface states and work function. Such study would allow a direct understanding of the adsorbed dopant atom effect on the surface properties and is essential to our final understanding of the problem discussed in this paper. (4) Theoretical calculation on the interactions between an adsorbed dopant atom and another adsorbed CV molecule is also very important. Such interactions could be long ranged and involve coupling with the surface[15]. Calculations of the interactions described in this paper could be very difficult at the moment[16] but certainly are necessary for a better understanding of the adsorption mechanism.

Once the suggested experiments are shown to support our model proposed here, it will then be possible to increase the deposition rate of CVD at low temperatures. By adjusting the surface potential according to the principles described in this paper one should be able to increase the deposition rate beyond the current limit. One can also choose the right combination of CV molecule and dopant gas that allows the maximal increase in deposition rate. Examples from Table I are SiH_4-B_2H_6, CH_4-PH_3, CCl_4-B_2H_6, etc. The remaining limiting factor will then be the amount of thermal energy available at low temperatures. One needs then to find a compromise between the maximal thermal energy needed and the minimal interaction and diffusion allowed between the deposited thin film and the substrate chosen. All these principles should also be applicable to the CVD of other types of thin films, such as those for Si_3N_4, SiC, W, etc.

Finally, since our model is concerned mainly with the effect of one adsorbed species on the adsorption of another molecule, this work should also be useful to surface catalysis studies. In surface catalysis molecular adsorption plays an essential role before decomposition or chemical reaction takes place. By varying the surface potential as described in this paper one should observe changes of the chemical reaction rates between adsorbed molecules. This should allow a better understanding and control of the chemical reactions under study. In addition, varying the magnitude and sign of the surface potential should provide important information on the formation and strength of the chemisorptive bonds between the adsorbed molecule and the surface. Again, more experimental and theoretical work along this line are needed to further advance our idea to surface catalysis.

Acknowledgement

This work was supported by the U. S. Energy Research and Development Administration.

References

1. C.-A. Chang and W. J. Siekhaus, J. Appl. Phys. in press.
2. C.-A. Chang, unpublished results.
3. T. L. Chu, NSF Report, NSF/RANN/SE.GI-38981/PR/73/4, 1974.
4. (a) C.-A. Chang, unpublished results. (b) A. Emmanual and H. M.-Pollock, J. Electrochem. Soc., 120, 1586 (1973).
5. (a) H. C. Theuerer, J. Electrochem. Soc., 108 649 (1961); F. C. Everstegn and G. H. Put, ibid, 120, 106 (1973), L. H. Hall and K. M. Koliwad, ibid, 120 1438 (1973). (b) R. G. Frieser, ibid, 115, 401 (1968). (c) Ref. 4b.
6. T. I. Kamins, J. Appl. Phys., 42, 4357 (1971); Y Maturkura, Japanese J. Appl. Phys. 2, 91 (1963).
7. C-A. Chang, W. J. Siekhaus, T. Kaminska and D. T. Huo, Appl. Phys. Lett., 26, 178 (1975); C.-A. Chang and W. J. Siekhaus, to be published.
8. (a) Ref. 5a. (b) Ria-Choudhury and P. L. Hower, J. Electrochem. Soc. 120, 1761 (1973). (c) R. F. C. Farrow, ibid, 121, 899 (1974).
9. F. A. Cotton and G. Wilkinson, Advanced Inorganic Chemistry, Second Ed., John Wiley and Sons, New York, (1966), p. 466.
10. A. L. McCellan, Tables of Experimental Dipole Moments, W. H. Freeman and Company, San Francisco (1963).

11. This is true for the silicon films deposited on silicon wafers, and also true beyond the first layer of silicon film on non-silicon substrates.

12. F. G. Allen and G. W. Gobeli, Phys. Rev. 127, 150 (1962).

13. W. H. Brattain and J. Bardenn, Bell System Tech. J. 32, 1 (1953); H. C. Montogmery and W. L. Brown, Phys. Rev. 103, 865 (1956).

14. D. J. Poferl, N. C. Gardner and J. C. Angus, J. Appl. Phys., 44, 1428 (1973).

15. T. B. Grimley, Proc. Phys. Soc. 90, 751 (1967).

16. J. R. Schrieffer, private communication.

N76 12504

ENHANCED CRYSTALLINITY OF LOW TEMPERATURE DEPOSITED SILICON FILMS ON GRAPHITE SUBSTRATES

Chin-An Chang* and Wigbert J. Siekhaus

Inorganic Materials Research Division, Lawrence Berkeley Laboratory,
University of California, Berkeley, California 94720

ABSTRACT

The previously developed technique for silicon crystallinity enhancement in silicon films deposited at low temperature is applied to graphite substrates. The measured increase in silicon crystallinity is comparable to that observed earlier using a quartz substrate. The distribution of aluminum in the silicon films is determined using Auger spectroscopic depth profiling. Carbon diffusion from the substrate into the silicon film is shown to be negligible at a substrate temperature of 600°C.

- - -

In a previous paper we have shown a technique to enhance silicon crystallinity at low substrate temperatures for vacuum deposited silicon thin films.[1] An ultrathin Si-Al-Si (100Å-500Å-100Å) sandwich coating was used prior to silicon deposition. The silicon films thus deposited show a lower limit of 5μ for the silicon grain size. Optical microscopic measurement of the etched films further show that silicon grains as large as 200μ are produced.[2]

---

*Present address: IBM, Thomas J. Watson Research Center, Yorktown Heights, NY 10598

In this work the same technique is applied to graphite substrates. Graphite is chosen because of its desirable properties as a substrate material for silicon thin film solar cells. Earlier work in which silicon films were deposited on graphite at high temperature showed significant diffusion of silicon and carbon into each other and the formation of silicon carbide.[3] Later work showed that, at a substrate temperature below 800°C, much less diffusion was observed.[2] Therefore, the Si-Al-Si sandwich coating technique should be applicable to the graphite substrate at 600°C to enhance silicon crystallinity without significant SiC formation. In addition, the difficulty encountered in our earlier study in determining the aluminum distribution is solved in the present work with an extra silicon coating as described later.

Silicon and aluminum were vacuum deposited onto graphite and quartz using conventional electron beam heating. The deposition rate was ca 40Å/min for both Si and Al. Other experimental parameters and Auger depth profiling measurement have been described elsewhere.[1,3] Commercial extruded graphite and fused quartz were used. Graphite substrates cut from a rod were used in both the unpolished and polished form. The latter was polished on Grit 320 SiC paper. Both graphite and quartz substrates were used in each deposition, the latter being used as a reference to be compared with the earlier work.[1] Substrates were outgassed at 800-900°C before deposition in a vacuum of 1×10^{-6} Torr.

An ultrathin Si-Al-Si (100Å-500Å-100Å) sandwich layer was first deposited onto the substrates which were held at room temperature. The substrates were then heated to 600°C and a thick silicon film of ca 2000-3000Å was deposited. Without further annealing the substrates were cooled down to room temperature and another layer of silicon (ca 300Å) was deposited. This last silicon coating is shown to be necessary to prevent the oxidation of aluminum, most of which stays near the surface of the film.[1] It also eliminates the presence of SiO_2 in the aluminum-rich region after exposing the film to air, since SiO_2 formation is restricted to a few monolayers. This technique allows reliable Auger determination of the aluminum distribution in the silicon film.

In this work we present the X-ray diffraction patterns of the silicon films deposited on graphite and quartz. In our earlier work[1] silicon films deposited on quartz showed a highly preferred (111) orientation with the 220/111 peak intensity ratio of ca 10-20%. Transmission electron micrograph of the same films showed spot diffraction pattern which implied a lower limit of 5μ for the silicon grain sizes. Since the same deposition technique is used in both studies,[4] the degree of silicon preferred orientation from the 220/111 intensity ratio is taken as a measure of the crystallinity enhancement over the pure silicon films deposited on quartz at 600°C. The latter showed both a powder-like X-ray diffraction pattern, with 220/111 being ca 60%, and diffused electron diffraction rings.[1]

Figure 1 shows the X-ray diffraction pattern for the silicon films deposited on graphite. Also shown is the X-ray diffraction of a Si film deposited on quartz which is obtained from the same experiment and is used as a reference. The 220/111 intensity ratio is ca 25% and 16% for the silicon films on graphite and quartz, respectively. Unpolished graphite was used in this case. Similar results were obtained using polished graphite substrates. These compare very well with the earlier work. Also seen in Fig. 1 is the (111) peak of aluminum which was not observed in our earlier work. This indicates the necessity of the described final silicon coating for the observation of aluminum. Auger depth profiles for the same films are shown in Fig. 2. Silicon film deposited on quartz shows a higher concentration of aluminum near the surface than in the bulk film. This confirms our earlier observation.[1] For the silicon film on graphite, the aluminum concentration stays nearly the same and is lower than on quartz. Also observed is the diffusion of both aluminum and silicon into the graphite substrate. Quantitative determination of the aluminum distribution in graphite is difficult due to the scattering of data and an uncertainty in the sputtering rate of graphite.

The aluminum distributions described above are consistent with the observation that the aluminum (111) peak is more clearly seen in the silicon film on quartz than in the silicon film on graphite. Carbon diffusion from the graphite substrate into the silicon film is also shown to be negligible from Auger profiling, in agreement with earlier work.[2] In several cases silicon

C.8

deposition was made with a different Si-Al-Si sandwich coating. Using a Si-Al-Si (100Å-500Å-100Å) sandwich coating, the silicon 220/111 intensity ratio was found to be similar to that using the Si-Al-Si (100Å-500Å-100Å) coating.

In summary, our results indicate that, using graphite substrates, an enhancement in silicon crystallinity can be obtained which ic omparable to that using quartz substrates. Carbon diffusion into the silicon film is shown to be negligible at a substrate temperature of 600°C. Silicon diffusion into the graphite substrate is also low compared with that at 1200°C substrate temperature.[3] Furthermore, graphite in the unpolished form gives enhancement in silicon crystallinity similar to that on polished graphite. This may prove to be a further favorable economic factor in using graphite as a substrate material for silicon thin film solar cells.

This work was supported by the U. S. Energy Research and Development Administration.

REFERENCES

1. C.-A. Chang, W. J. Siekhaus, T. Kaminska and D. T. Huo, Appl. Phys. Lett. 26, 178 (1975).
2. C.-A. Chang, unpublished results.
3. C.-A. Chang and W. J. Siekhaus, J. App. Phys, in press.
4. This implies that the same mechanism of silicon crystallization from the Si-Al eutectic melt should be involved in both studies.

FIGURE CAPTIONS

Fig. 1. X-ray diffraction patterns for the silicon films deposited on (a) graphite, and (b) quartz, using the Si-Al-Si sandwich coating technique.

Fig. 2. Auger depth profiles for the silicon films deposited on (a) graphite (a) graphite, and (b) quartz, using the Si-Al-Si sandwich coating technique. Sputtering rate of the silicon films is ca 50Å/min for (a) and ca 30Å/min for (b).

Electron Energy Loss Spectroscopy of the Silicon (111) Surface

The motivation behind this study is mainly two-fold:

(1) In dealing with the usual bulk properties of solids, one always assumes having a crystal with translation symmetry so that one never has to worry about surface effects. However, when we study a specimen using a probe which is sensitive to a few atomic layers, or when we have a specimen which has a large surface-to-volume ratio such as a thin film or micro-particle, surface effects become important. It is therefore interesting to see what the effects are and how they differ from those of the bulk.

(2) In order for silicon solar cells to be economically competitive with conventional energy sources, we are forced to consider using thin silicon films because of high material cost. In using thin films, we are faced with several problems which lower the efficiency considerably, viz. (a) film-substrate diffusion, in which the substrate material can diffuse into the film and hence increases the resistive losses, (b) imperfections and grain boundary scattering and trapping and (c) dominant surface effects because of large surface-to-volume ratio. It turns out that the existence of the surface introduces surface states which can act as electron traps, thereby decreasing the conversion efficiency. Therefore, our aim is to remove all such surface traps. However, we cannot do this without a detailed knowledge of what these surface states are and where they are located in the band structure, because the effectiveness of a surface state as an electron trap depends critically on its location in the band structure. (In fact, the closer the state is to the mid-gap region, the more effective it is as a trap.) Once the location is known, we can then proceed on to introduce some impurities on the surface and study the effects of such impurities on the surface and study the effects of such impurities on the surface states. One such impurity we have studied is oxygen.

Experimental Procedures

The experiment was performed in an ion-pumped stainless steel ultra-high vacuum system, capable of reaching pressures of 2×10^{-9} torr or below. The specimen was a 2500 ohm-cm p-type silicon crystal oriented along the (111) direction, which was polished and degreased prior to introduction into the chamber. The loss spectroscopy was performed by PHI 15-25G Auger electronics at a primary energy of 100 eV with a resolution of approximately 1 eV. At a higher primary energy, we have a fairly good understanding of the energy loss process, but with a poorer resolution. The reverse is true for low primary energies. The present choice is considered to be optimum as far as the loss process, resolution, relative contributions from the bulk and the surface are concerned.

Two surface structures have been studies, viz. the disordered surface and the (2x1) surface. The former was obtained by argon ion bombardment whereas the latter was obtained by cleavage at room temperature. The loss spectra were observed as a function of exposure to oxygen, which was introduced to the system by means of a leak valve.

Results & Discussion

The results we obtained bear close resemblance to those of Rowe and Ibach on the silicon (111) — 7x7 surface. In Fig. 1, we show the loss spectra of the silicon (111) — 2x1 surface as a function of oxygen exposure. On the clean surface, bulk and surface plasmons were observed at loss energies of 16.5 eV and 10.6 eV respectively. The 5 eV transition is possibly a bulk transition. Three surface state transitions were observed, viz. S_1 at 2.5 eV, S_2 at 7.4 eV and S_3 at 14.5 eV, which were also found on the Si(111) — 7 x 7 surface, at slightly different energies. The S_o transition at ~0.6 eV as seen in high resolution energy[2] loss spectroscopy is lost in the elastic background; however, according to a recent theoretical calculation on the 2 x 1 surface the S_o and S_1 transitions have similar initial states and are therefore directly correlated. By exposing the surface to oxygen, the S_1 and S_3 transitions practically disappear at a coverage of 0.1 monolayer, while S_2 increases. Combination with UPS data shows that this is probably due to an oxygen transition. At a coverage of 0.5 monolayer, the plasmon peak splits and this is clearly observable at $\theta = 0.65$. The effect was explained by Rowe and Ibach[3] as due to an oxygen transition close to the surface plasmon peak. One also notices a continuous shift of the bulk plasmon peek towards higher energies at increasing oxygen coverage. At the same time, a loss peak at 3.3 eV appears and becomes well established at monolayer coverage. This can also be attributed to an oxygen transition.

The loss spectrum obtained on the clean disordered silicon (111) surface is identical to that obtained by Rowe and Ibach.[3] The variation of the spectrum as a function of oxygen exposure is similar to that on the (2x1) and (7x7) surfaces, except for one important difference, viz. the plasmon splitting is observable at a much lower coverage of ~0.1-0.2 monolayer. According to the dielectric theory, this is probably due to the larger energy for the oxygen transition (11.5 eV instead of 11 eV on the 7x7 surface). This is physically reasonable because both on the (7x7) and (2x1) surfaces, the structures are relaxed to have stronger back-bonds, leaving a positive weaker potential (due to the silicon ion) on the vacuum side of the interface. Therefore, ELS gives us further information on the relative potential strengths under different surface conditons.

Future Studies

From these studies, one observes that on the disordered and the (2x1) surfaces one monolayer of oxygen is very effective in removing surface states and the states it introduces are deep in the valence band. The only drawback is that the Si-O system is not very stable. Stabilization by further oxidation is possible, but will pose difficulties in making electrical contacts to the surface, which are necessary in solar cell fabrications. So, we are now diverting our attention toward the Si-Al system. Aluminum, besides being a conductor and a dopant, has been used successfully to enhance crystal growth of silicon films at 600° C,[4] and is therefore an interesting material to pursue.

At the same time, we are looking into the possibility of using LEED rotation diagrams as a means of locating surface states, both occupied and empty in the band structure, by using a recent theory on the effects of surface states on LEED measurements.[5] This, together with the results from ultraviolet photoemission studies will give us a complete picture of the surface states in silicon, of different surface structures and with different adsorbates.

References

1. M. Schluter, et al., Phys. Rev. Letters 34, 1385 (1975).
2. J. E. Rowe et al., Surf. Sci. 48, 44 (1975).
3. H. Ibach and J. E. Rowe, Phys. Rev. B9, 1951 (1974).
4. C. A. Chang, et al., Appl. Phys. Letts. 26, 178 (1975).
5. N. Garcia, et al., LBL-3764 (March 1975).

Phosphorus Segregation in Single Crystal Silicon

A 1 in. diameter, p-type, 2.5K Ω-cm silicon single crystal wafer was diffused at 1000° C with phosphorus for 14 hrs. The source was an Emulsitone spin-on solution providing a surface concentration of about 10^{20} p/cm^3. After diffusion the wafer was cooled in air, then etched in phosphor-silica etch (1:1:30, HF:HNO_3:H_2O).

The sample was thereafter placed into an ultra-high vacuum system and outgassed by heating to 800° C for 1 hr. After heating, the surface was sputter etched at room temperature until the auger spectrum no longer changed with time (Fig. A). This spectrum shows the presence of SiO_2, Si, C, and O.

The sample temperature was raised to 800° C in less than one minute and held at this temperature for 4 min. Auger scans for phosphorus were taken at intervals during the temperature treatment (Fig. B). The sample was cooled and a final auger trace made (Fig. C).

Figure B shows the phosphorus signal as a function of time and temperature. It indicates 1) that phosphorus segregates to the surface and 2) that the equilibrium concentration of phosphorus on the surface is a function of sample temperature. Figure C shows the increased phosphorus signal but no other changes.

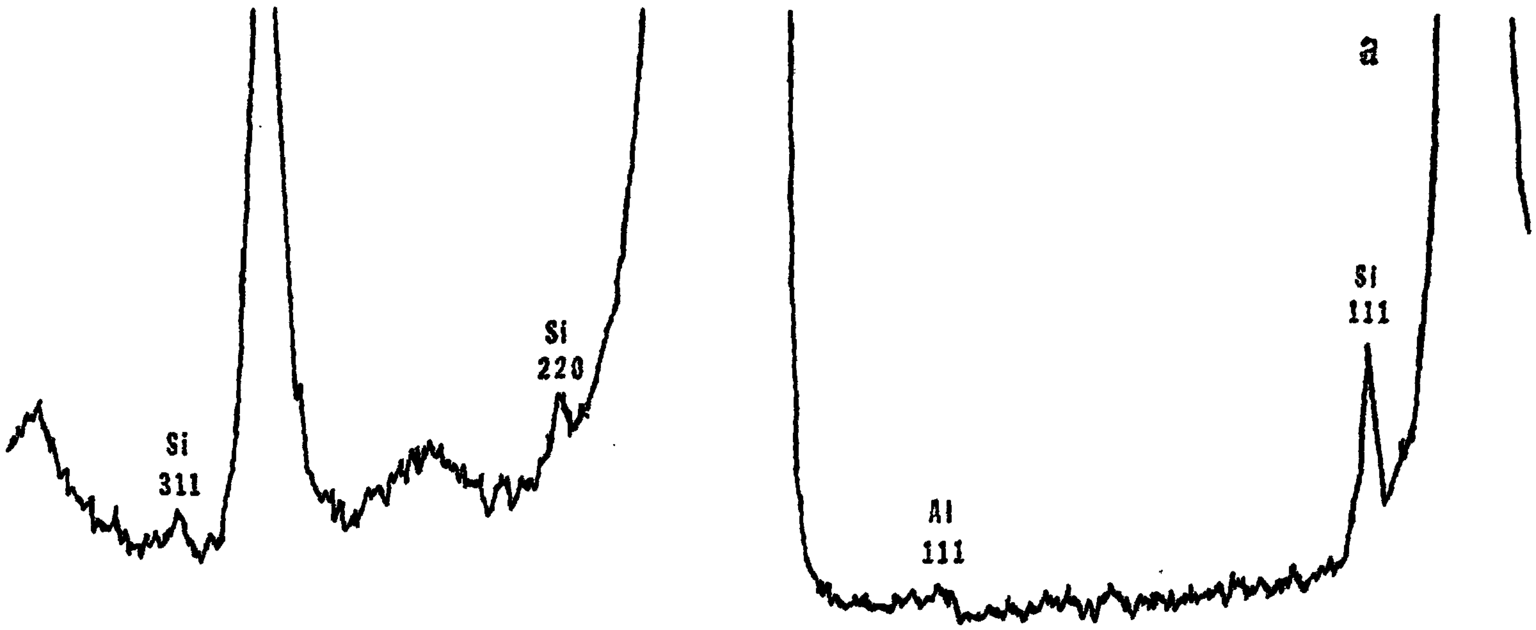

XBL 754-6126

Fig. 1

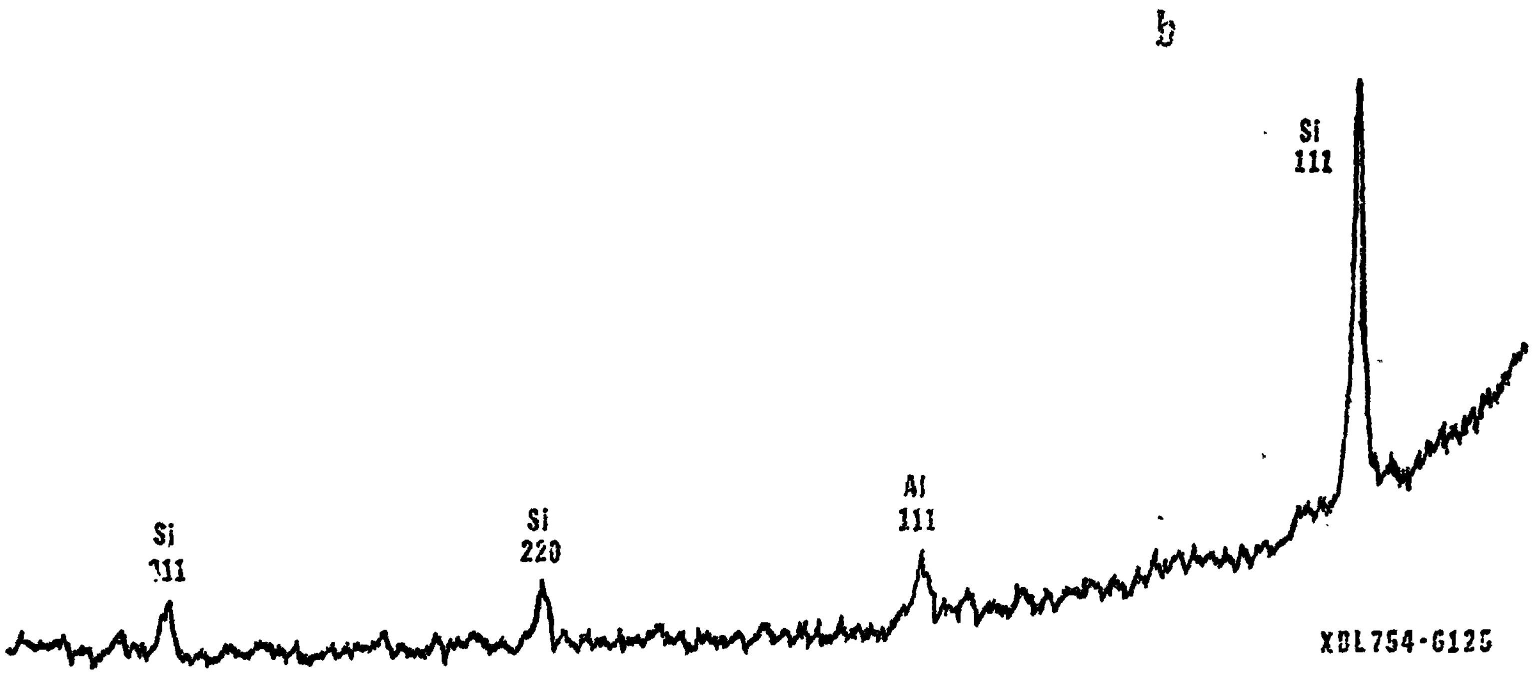

XBL754-G125

Fig. 1 cont.

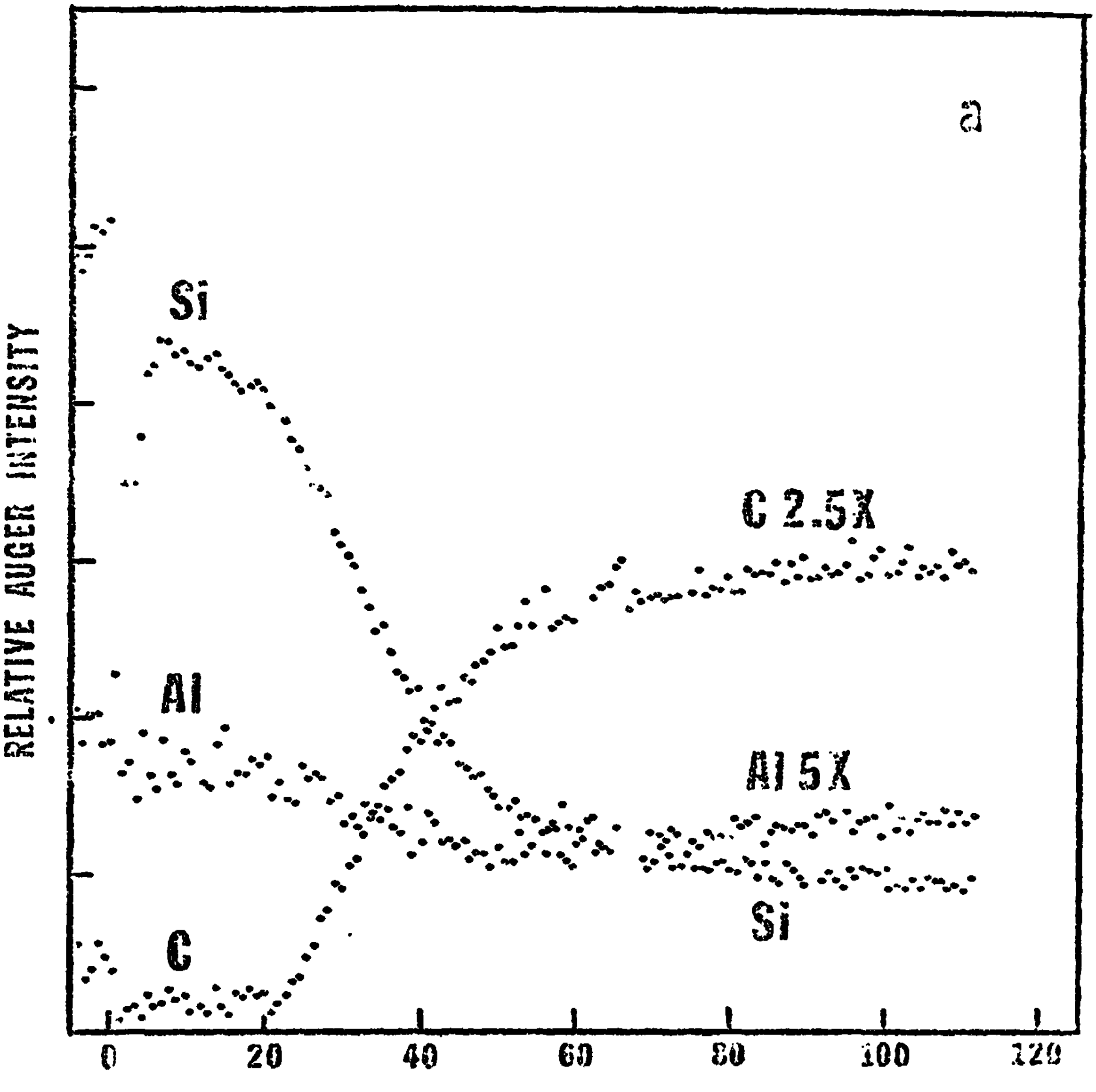
a
Si
Al
C
C 2.5X
Al 5X
Si
RELATIVE AUGER INTENSITY
0
20
40
60
80
100
120
SPUTTERING TIME, MIN
XBL 756-6475

Fig. 2

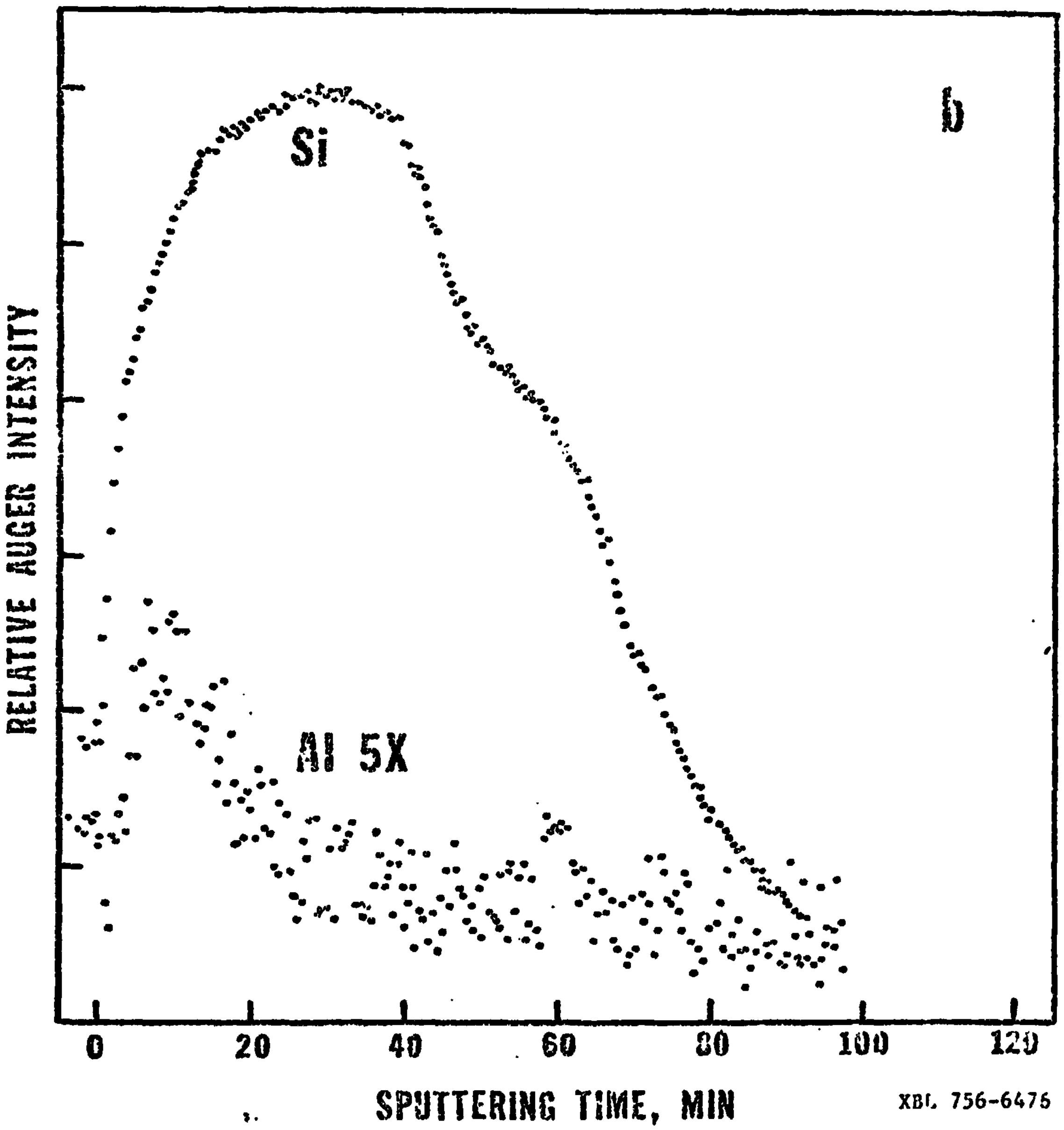
b
Si
Al 5X
RELATIVE AUGER INTENSITY
0
20
40
60
80
100
120
SPUTTERING TIME, MIN
XBL 756-6476

Fig. 2 cont.

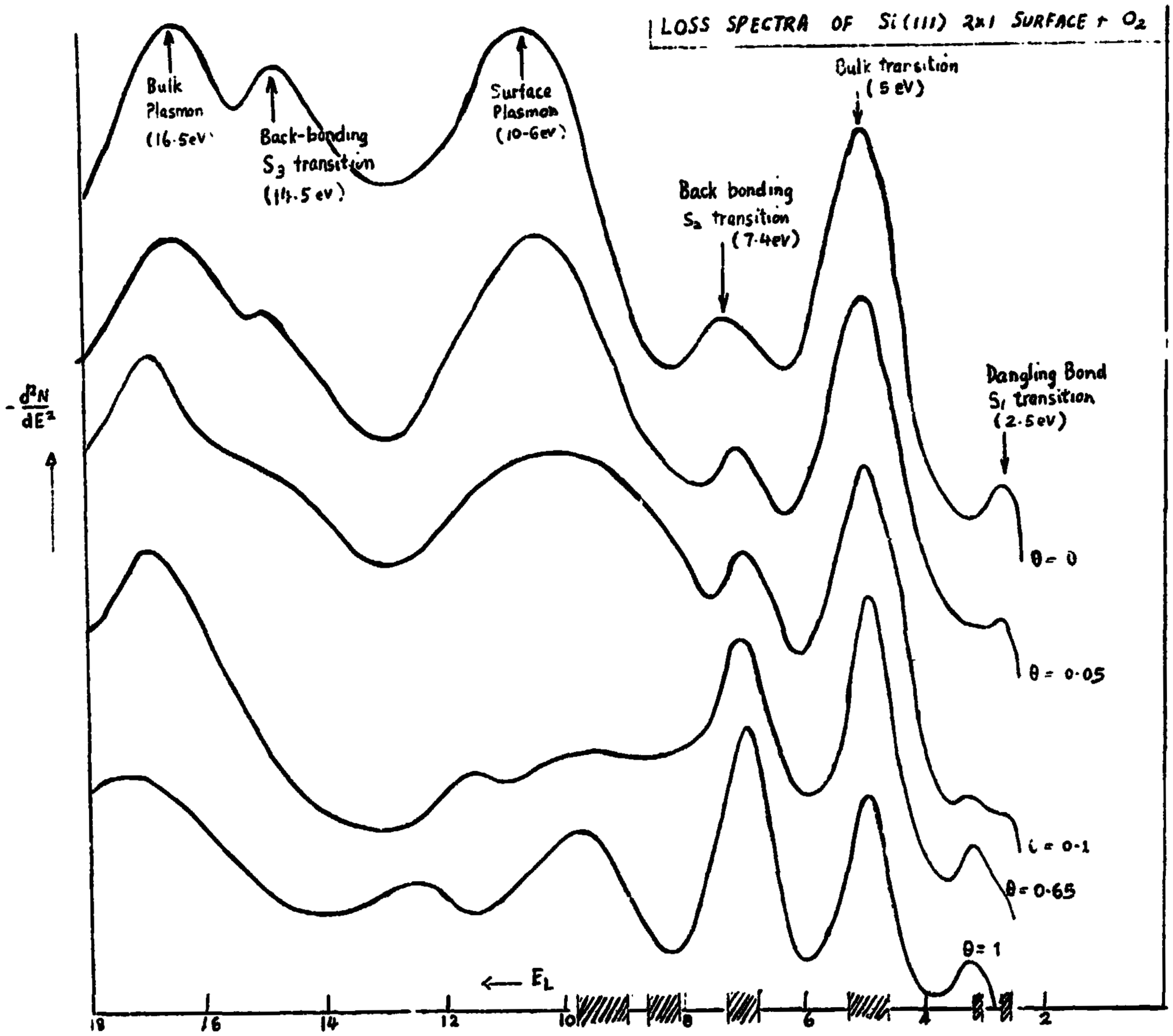
LOSS SPECTRA OF Si(111) 2x1 SURFACE + O2
Bulk Plasmon (16.5eV)
Back-bonding S3 transition (14.5 ev)
Surface Plasmon (10.6ev)
Bulk transition (5 eV)
Back bonding S2 transition (7.4ev)
Dangling Bond S1 transition (2.5eV)
θ = 0
θ = 0.05
θ = 0.1
θ = 0.65
θ = 1
$-\frac{d^2N}{dE^2}$
← E_L
18
16
14
12
10
8
6
4
2

FIG A.

AUGER SPECTRUM OF SPUTTERED SURFACE

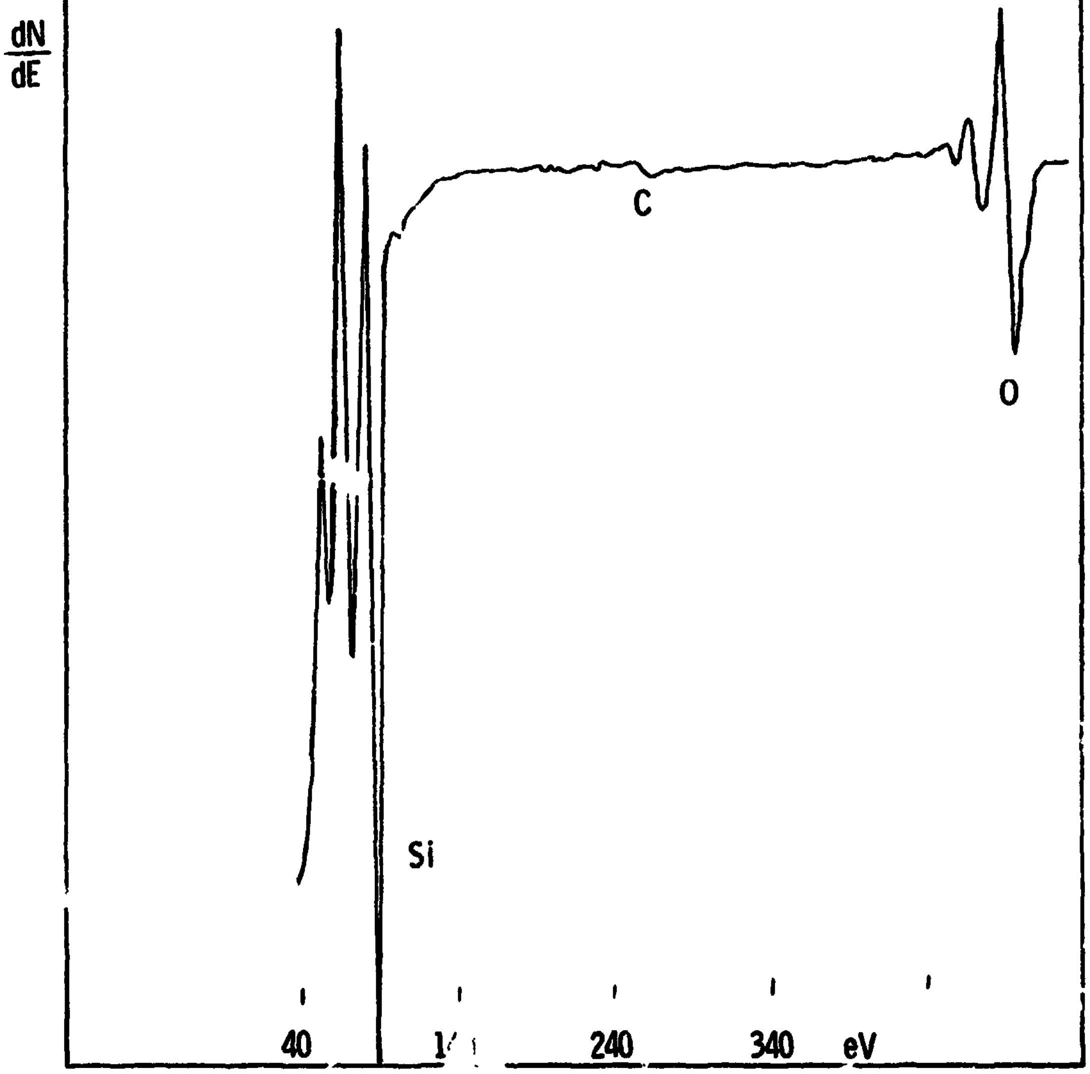

FIG. B

SURFACE SEGREGATION OF PHOSPHORUS

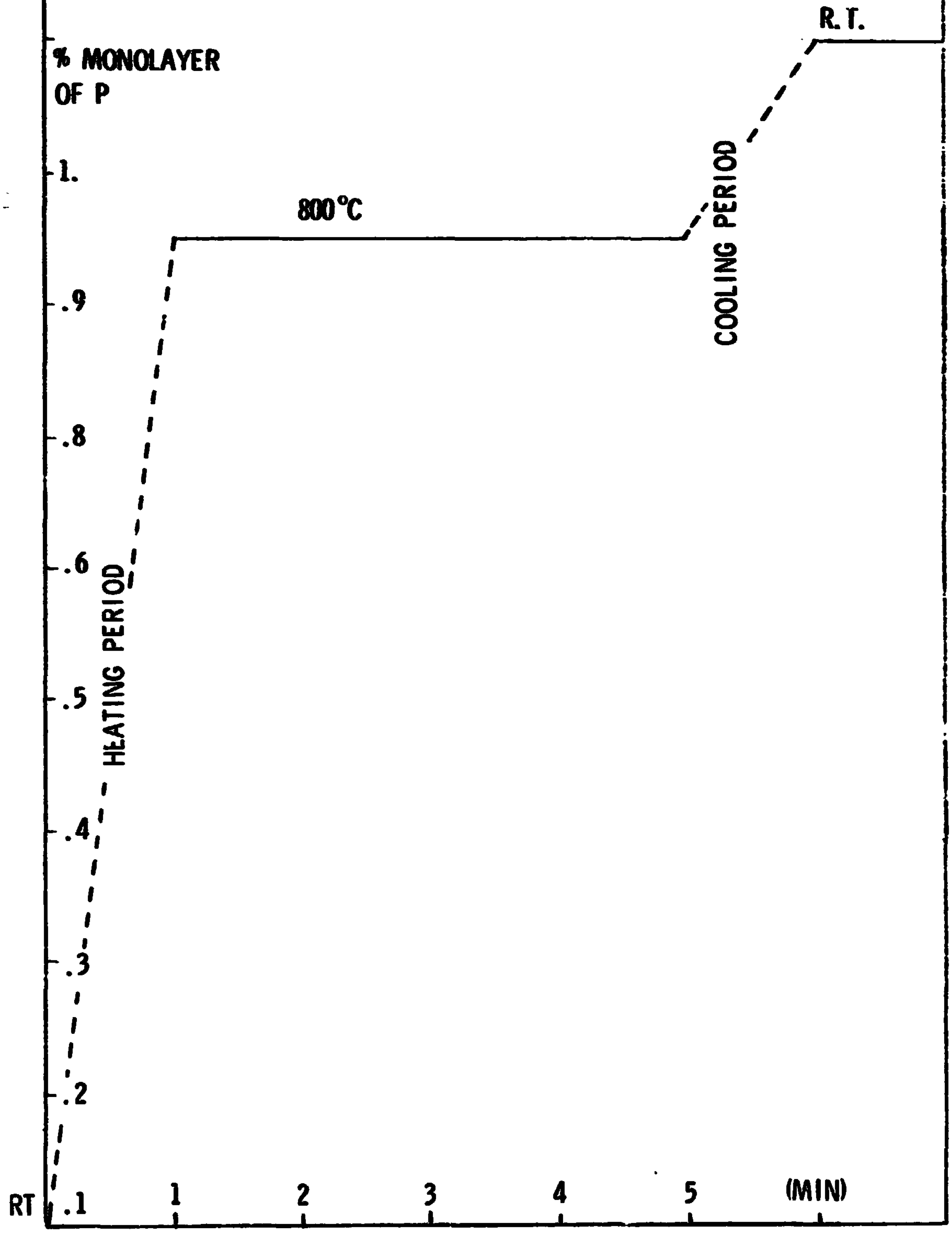

FIG C.

AUGER SPECTRUM OF SILICON AFTER HEATING

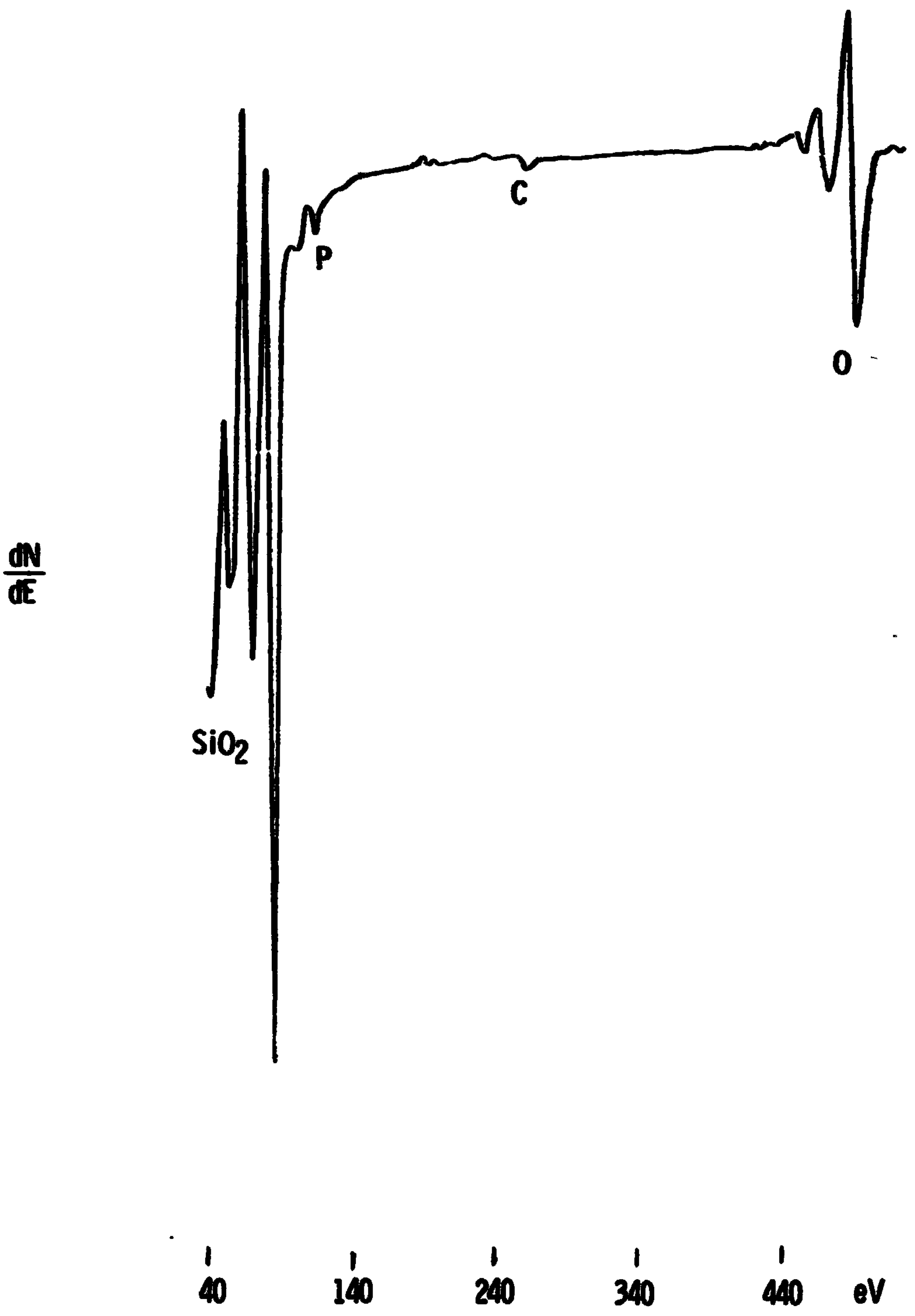

WORK PLAN

WORK AREA	ACTIVITY	GOAL
CATALYSIS OF CRYSTALLIZATION	LEED intensity /vs time at given temperature as f(surface impurity)	Determine activation energy for recrystallization as f(impurity)
	Modify evaporation equipment to allow clean deposition.	
Catalysis of CVD	Deposition rate as f(surface charge)	Low Temperatrue CVD
	Reaction kinetics by modulated molecular beam analysis	Identify critical steps in deposition reaction
	Dopant impurity concentration and distribution at the surface during deposition	Surface charge??
Grain Boundary	Fracture?	What is at grain boundaries?
	Free surface impurity segregation	
Surface States	Install UV system	Surface states as a function of dopant in the energy gap. Absolute energy location.
	Install monoenergetic e- source	
	Analyze single crystal surface plus dopant.	

NLAFSKY'S MA[illegible]E

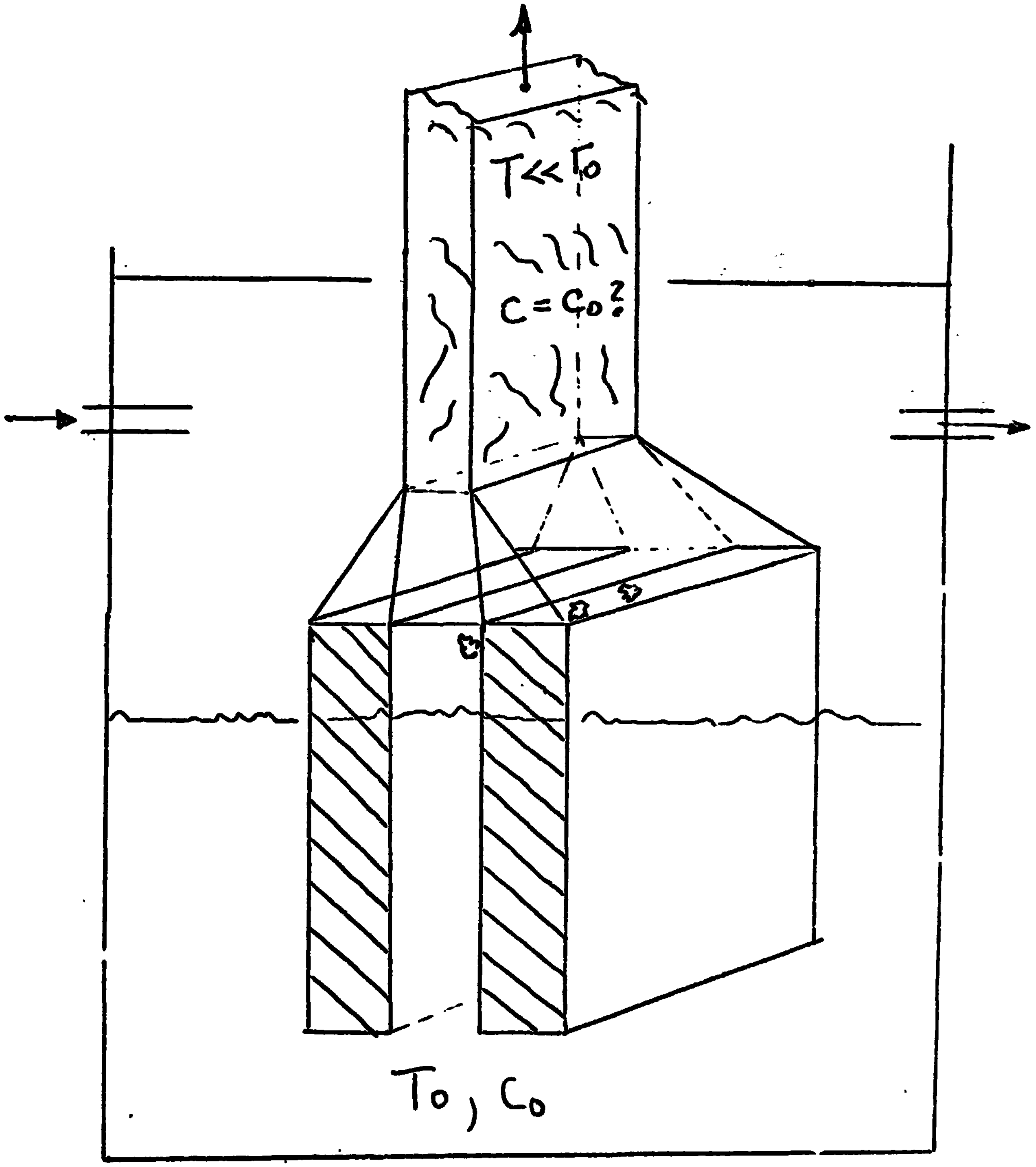

I would like to make a comment on an item listed under program objectives: the influence of surfaces on sheet formation.

EFG - like processes clearly place a very strong emphasis onto an unstable and little understood region: the meniscus, and consequently a majority of present ERDA deadlines teeter and wobble with the rise and fall of the meniscus from the High Meniscus Mode (HMM) to the Low Meniscus Mode (LMM).

The form and the stability of the meniscus depend critically on surface tension, a phenomenon delicately depending on surface composition and chemistry. Surface composition at this point will be fluctuating and unpredictable, since all the impurities dissolved in the melt w[illegible]ant to segregate out at this point, where there are but two places to [illegible] to the surface and to the interfaces (twinning) which the ribbon probably creates for itself to store away the excess impurities which it cannot segregate onto the surface, and which it cannot reject into the remaining liquid through the bottleneck of the capillary.

If my surface science perspective is correct, then

1) the sheet surface is high in impurities (SiC crystals are growing there)

2) the twinning surfaces are high in impurities (Dr. Mlafsky's SEM data indicate this)

3) significant progress will come in size stability and sheet crystallinity if the EFG process is run in an atmosphere capable of removing at the meniscus surface any impurities that might be segregating there. Under these clean surface conditions a stable surface tension would be established. It should be easier to produce a thin (100 Å) film than a thick one, because the very property of the surface, to segregate impurities, has been turned to a constructive advantage.

I certainly would not treat lightly the question raised by Joe Morabito, whether not any starting material of higher impurity might wreck the EFG process entirely, unless one takes the position that things cannot possibly get worse than they are.

I make this point: processes and products of high surface to volume ratio are controlled by surface effects.

RIBBON STARTS

impurities segregate, but return to melt is blocked

in contrast to Czochralsky, ribbon impurity concentration=melt conc.

IMPURITIES SEGREGATE ONTO MENISCUS SURFACE

Surface tension changes, Meniscus changes shape. Surfaces saturates Bulk saturates, reliefs by creating large number of grain and twin boundaries onto which impurities can be deposited. And SiC grains . Repeat.

periodic fluctuations in shape, crystal perfection and impur (Kressel et al.) Boundaries loaded with impurities (Mlafsky's SEM)

C U R E

Zone refining process with impurity removal from surface.

Choose large surface to volume ratio (100) and HMM, and purge with corrosive gas.

Do not try dirty silicon.

Meniscus stable

Purity stable

ERDA stable.

ORIGINAL PAGE IS
OF POOR QUALITY

WORK PLAN

WORK AREA	ACTIVITY	GOAL
SURFACE TENSION	Measure surface tension as f(surface concentration of impurities)	Know thy meniscus
SURFACE SEGREGATION	Measure surface impurity concentration as f(bulk concentration) and f(temperature)	Keep the meniscus clean and produce good ribbons. Investigate EFG - Surface segregation purification process. (EFG _SSPP)
Surface Chemistry	Measure surface concentration at molten Si surface as f(background gas)	

N76 12505

Cadmium Stannate Selective Optical Films
for Solar Energy Applications

NSF Grant AER 73-07957

April 1, 1975 - March 31, 1976

$160,000

Author and Principal Investigator:

G. Haacke

American Cyanamid Company

National Solar Photovoltaic Program Review Meeting

July 22-25, 1975

Los Angeles, California

Abstract

Most of the work discussed in this report has been performed during the last three months of the reporting period after receipt of a renewal grant. At Cyanamid efforts concentrated on reducing the electrical sheet resistance of sputtered cadmium stannate films, installing and testing equipment for spray coating experiments, and sputter deposition of thin cadmium sulfide layers onto cadmium stannate electrodes. In addition, ahead of schedule, single crystal silicon wafers were coated with cadmium stannate. The University of Delaware continued development of the backwall CdS solar cell.

Earlier attempts at sputtering cadmium stannate films with sheet resistances R_s smaller than 1 ohm/square failed because, for thick films, R_s did not decrease proportionally to increasing film thickness. It has now been found that modified post-deposition heat treatment alleviates this problem and 0.7 ohm/square films have been prepared. Visible optical transmission values of these samples reach 80-85%. Approximately 5% of the transmission loss is attributable to a slight haziness which is expected to disappear after refinement of the heat treating procedure.

During the first phase of the spray coating development different spray nozzles were evaluated and a sonic atomizer selected for the current experiments. A substrate heater has been designed and installed which facilitates fast sample heat-up and a wide-range temperature control. Coatings properties achieved during last year's

feasibility study (~100 ohm/square) can now be reproduced at much lower substrate temperatures (400°C vs. 850°C).

In an effort to reduce cadmium requirements and optical absorption of backwall CdS cells thin cadmium sulfide layers (2-5 μ) were sputtered onto Cd_2SnO_4 films. A highly oriented, columnar CdS crystal growth was induced by the Cd_2SnO_4 substrates. However, micropinholes along the grain boundaries caused short circuits and low cell efficiencies. Attempts to eliminate these pinholes were only partially successful. Additional work is planned and will include surface treatment of the Cd_2SnO_4 electrodes before CdS deposition.

At the request of Innotech, Inc. n-type and p-type single crystal Si wafers were coated with Cd_2SnO_4. These experiments proved that low temperature Cd_2SnO_4 deposition (300°C) onto Si is possible. Ohmic contacts formed on n-type Si. The Cd_2SnO_4 sheet resistances were twice as high as expected indicating lower conductivities and/or the presence of a resistive interlayer.

Work at the Institute of Energy Conversion led to backwall efficiencies higher than 5% in $Cd_2SnO_4/CdS/Cu_2S$ cells. This improvement has been achieved by advanced cell lamination techniques and lower series resistances. Heat treatment experiments at 250°C indicate that degradation in cells with Cd_2SnO_4 substrates is less severe than in standard metal substrate cells.

The following activities are planned for the next six months:

1. increase optical transmission of low sheet resistance Cd_2SnO_4 films,
2. reduce sheet resistance of spray coated Cd_2SnO_4 films to 10 ohm/square region,
3. raise backwall efficiency of $Cd_2SnO_4/CdS/Cu_2S$ cells to 6% or higher,
4. investigate deposition of Cd_2SnO_4 onto silicon wafers.

CADMIUM STANNATE
SELECTIVE OPTICAL FILMS FOR SOLAR ENERGY APPLICATIONS

NSF GRANT AER 73-07957

AMERICAN CYANAMID COMPANY
UNIVERSITY OF DELAWARE

GRANT PERIOD: APRIL 1, 1975 – MARCH 31, 1976

AWARD: $ 160,000

PRINCIPAL INVESTIGATOR: G. HAACKE

PROJECT OBJECTIVES

- PREPARE HIGHLY TRANSPARENT, ELECTRICALLY CONDUCTING THIN COATINGS OF CADMIUM STANNATE

- DEVELOP SPRAY TECHNOLOGY FOR FABRICATION OF CADMIUM STANNATE FILMS ON TRANSPARENT SUBSTRATES

- EVALUATE PERFORMANCE OF CADMIUM STANNATE BACKWALL ELECTRODES IN CdS SOLAR CELLS

- DEPOSIT CADMIUM STANNATE FILMS ONTO SILICON SUBSTRATES AND ASSES POTENTIAL FOR FRONT ELECTRODES IN SILICON SOLAR CELLS

PLANNED ACTIVITY TO DATE

- OPTIMIZE SPUTTER CONDITIONS FOR PREPARATION OF LOW SHEET RESISTANCE (1ohm/square) CADMIUM STANNATE FILMS
- INSTALL AND TEST EQUIPMENT FOR SPRAY DEPOSITION OF CADMIUM STANNATE COATINGS
- COAT THIN CADMIUM SULFIDE LAYERS (2-5 microns) ONTO CADMIUM STANNATE ELECTRODES BY SPUTTERING
- INCREASE BACKWALL EFFICIENCY OF $Cd_2SnO_4/CdS/Cu_2S$ SOLAR CELLS

LOW SHEET RESISTANCE FILMS
PROGRESS TO DATE

- MODIFIED POST-DEPOSITION HEAT TREATMENT LOWERS ELECTRICAL SHEET RESISTANCE

- LOWEST SHEET RESISTANCE TO DATE:
  0.[illegible] OHM/SQUARE

OPTICAL TRANSMISSION OF 0.7 OHM/SQUARE CADMIUM STANNATE FILM

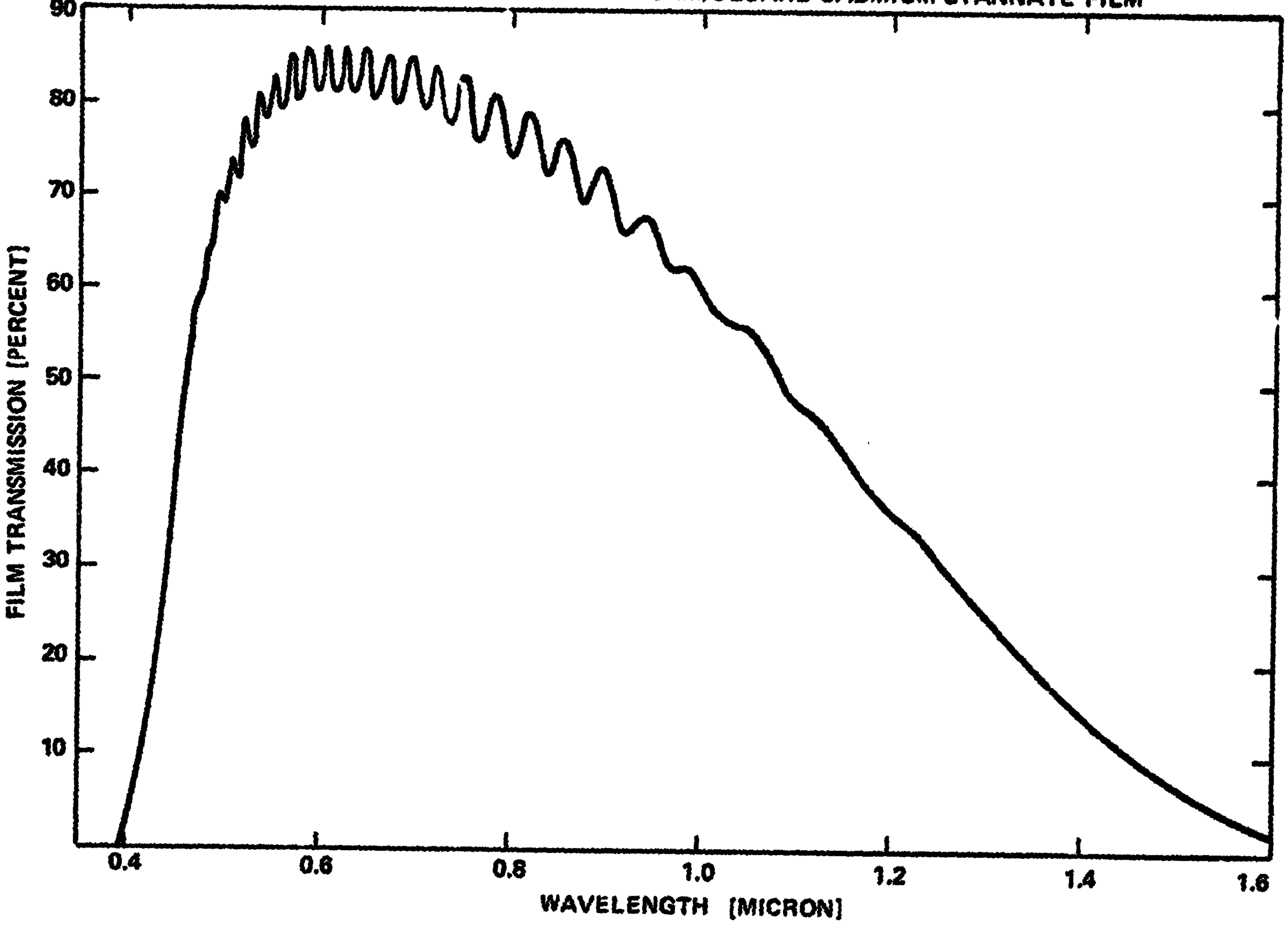

SPRAY COATING DEVELOPMENT

PROGRESS TO DATE

- DIFFERENT SPRAY NOZZLES EVALUATED
- CONTROLLED SUBSTRATE HEATER DEVELOPED AND INSTALLED
- PREVIOUS FILM PROPERTIES REPRODUCED AT LOWER SUBSTRATE TEMPERATURES (400°C *vs* 850°C)

SPUTTERED THIN CdS LAYERS

PROGRESS TO DATE

- HIGHLY ORIENTED CdS LAYERS GROW ON Cd_2SnO_4 SUBSTRATES
- DEPOSITION CONDITIONS ESTABLISHED WHICH MINIMIZE NUMBER OF MICRO-PINHOLES

CROSS SECTIONS OF CdS FILMS SPUTTERED ONTO Cd_2SnO_4 SUBSTRATES

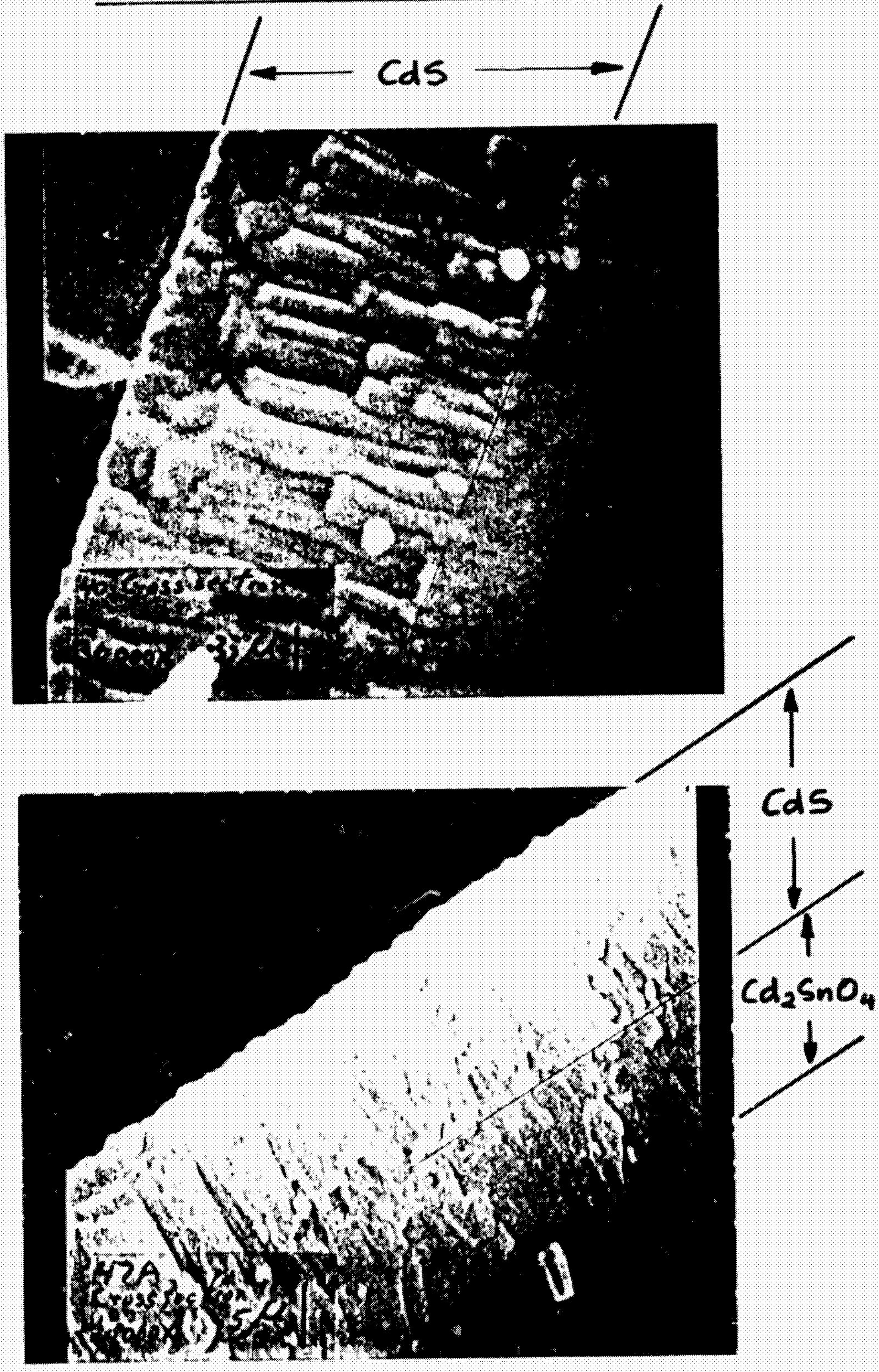

BACKWALL CdS SOLAR CELL DEVELOPMENT

PROGRESS TO DATE

- BACKWALL EFFICIENCIES EXCEED 5%

- HIGH TEMPERATURE (250°C) CELL DEGRADATION APPEARS TO BE LESS SEVERE FOR BACKWALL CELLS

DEGRADATION OF SHORT CIRCUIT CURRENT DENSITY WITH HEAT TREATMENT TIME (AIR - 250°C) FOR METAL AND QUARTZ SUBSTRATE CELLS

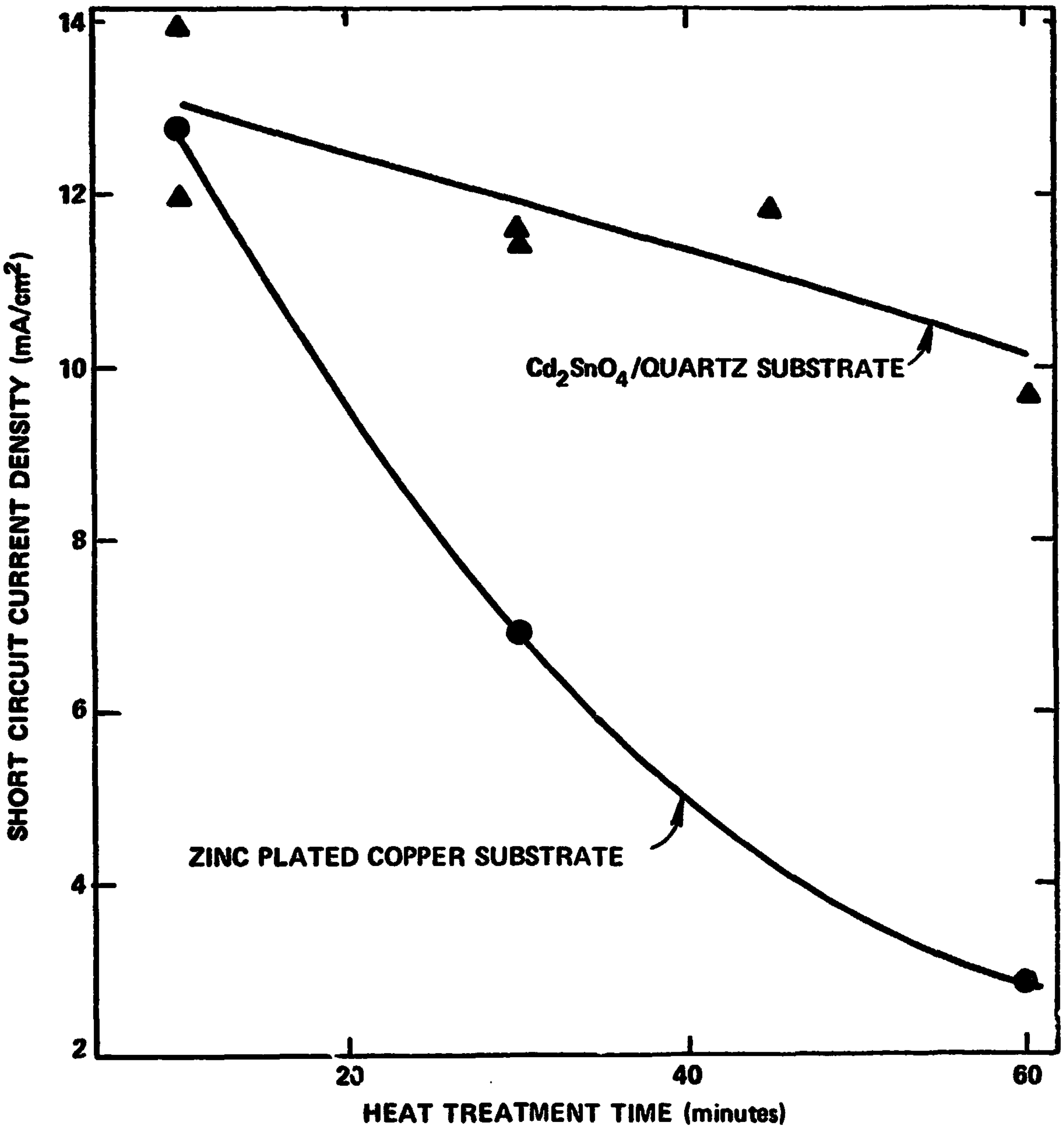

SUMMARY OF KEY RESULTS

- CADMIUM STANNATE ELECTRODES WITH SHEET RESISTANCES BELOW 1 OHM/SQUARE CAN BE PREPARED

- SPRAY COATING TECHNIQUE MODIFIED FOR LOW SUBSTRATE TEMPERATURE DEPOSITION

- BACKWALL EFFICIENCY OF $Cd_2SnO_4/CdS/Cu_2S$ SOLAR CELLS EXCEEDS 5%

- LOW TEMPERATURE COATING OF SILICON WAFERS WITH CADMIUM STANNATE POSSIBLE

MAJOR PROBLEMS

- HIGH ELECTRICAL SHEET RESISTANCE OF SPRAY COATED CADMIUM STANNATE FILMS

- LOW ELECTRICAL CONDUCTIVITY OF CADMIUM STANNATE FILMS ON SILICON SUBSTRATES

PLANNED ACTIVITY FOR NEXT SIX MONTHS

- REDUCE OPTICAL ABSORPTION OF LOW SHEET RESISTANCE CADMIUM STANNATE FILMS
- REDUCE ELECTRICAL SHEET RESISTANCE OF SPRAY COATED CADMIUM STANNATE FILMS
- IMPROVE BACKWALL RESPONSE OF CdS SOLAR CELLS
- INVESTIGATE DEPOSITION OF CADMIUM STANNATE ONTO SILICON WAFERS

ABSTRACT

Title Page

(a) Title of Paper: Thin Film Ternary Compound Solar Cells

(b) Title of Project: Ternary Compound Thin Film Solar Cells

(c) Grant Number: Pending

(d) Period of Grant: 1 September, 1975 - 31 August, 1976.

(e) Value: $34,929 (requested)

(f) Author of Paper: L. L. Kazmerski

(g) Affiliation: Associate Professor
Department of Electrical Engineering
University of Maine at Orono
Orono, Maine 04473

(h) Principal Investigator: L. L. Kazmerski

(i) Paper presented at National Solar Photovoltaic Program Review Meeting
ERDA - NSF
University of California at Los Angeles
July 25, 1975

N76 12506

TERNARY COMPOUND THIN FILM SOLAR CELLS

L. L. Kazmerski
University of Maine at Orono

The investigation of a group of ternary compound semiconductor (I-III-VI_2) thin films for future applications in photovoltaic devices is proposed. The consideration of these materials ($CuInSe_2$, $CuInTe_2$ and especially $CuInS_2$) for long-range device development is emphasized. The major objectives of this research include: (1) The identification and production of device-quality thin films of $CuInS_2$ on suitable substrates; (2) The demonstration of homojunction viability for $CuInS_2$ thin film solar cells; (3) The growth and characterization of $CuInSe_2$ and $CuInTe_2$ for photovoltaic application; and, (4) Possible heterojunction demonstration (e.g. p-type $CuInSe_2$ / n-type CdS thin film solar cell).

Much of the activity to date has been concerned with the growth and properties of $CuInX_2$ films. X-ray (Figs. 4-9) and electron diffraction analyses, Hall mobility and coefficient (Figs. 10, 13), resistivity and carrier concentration variations with substrate and film temperature (Fig. 11), as well as grain size data (Fig. 12) have been determined. Both p- and n-type films of $CuInS_2$ and $CuInSe_2$ have been produced. Single and double source deposition techniques have been utilized. Some data have been recorded for annealed films. (e.g. $CuInS_2$ in H_2S/Ar).

The physical and electrical characterizations of these films are to continue. Photoconductivity data and lifetime measurements are scheduled. A three-source deposition technique is being developed. Films are to be deposited onto several metal substrates, and a thorough investigation of contacts to the ternary films is underway. A tentative schedule (Fig. 15) accompanies this text.

The key results to date include:

1. The deposition of $CuInS_2$, $CuInSe_2$ and $CuInTe_2$ films.
2. Production of n- and p-type $CuInS_2$ and $CuInSe_2$ films on alumina substrates.
3. Development of a double source deposition technique for $CuInS_2$.
4. Report of electrical properties of $CuInS_2$ films.
5. Report of x-ray and electron diffraction studies on ternary compound films.

FIGURE CAPTIONS

Fig. 1. Title Page

Fig. 2. Objectives

Fig. 3. Activity-To-Date

Fig. 4. Chalcopyrite Structure

Fig. 5. Calculated X-Ray Pattern: $CuInS_2$

Fig. 6. Calculated X-Ray Pattern: $CuInSe_2$

Fig. 7. Calculated X-Ray Pattern: $CuInTe_2$

Fig. 8. Tabulated X-Ray Data: $CuInS_2$

Fig. 9. Comparison of Single Phase and Multiple Phase Thin Films of $CuInS_2$ (X-Ray Diffraction Data)

Fig. 10. Mobility Dependence on Inverse Temperature. (a) Single Source Method, $T_{sub} = 280°C$; (b) Single Source Method, $T_{sub} = 160°C$; (c) Single Source Method, $T_{sub} = 400°C$. (d) - (i) Double Source Method. (d) $T_{sub} = 180°C$, $T_{sulphur} = 92°C$; (e) $T_{sub} = 220°C$, $T_{sulphur} = 92°C$; (f) $T_{sub} = 320°C$, $T_{sulphur} = 92°C$; (g) $T_{sub} = 400°C$, $T_{sulphur} = 92°C$; (h) $T_{sub} = 400°C$, $T_{sulphur} = 102°C$; (i) $T_{sub} = 400°C$, $T_{sulphur} = 108°C$. Film Thicknesses are 0.5μ; Substrates are Alumina.

Fig. 11. Resistivity and Carrier Concentration Dependence on Inverse Temperature Curves (d') and (d") Correspond to Curve (d) on Fig. 10. ($T_{sub} = 180°C$). Curves (g') and (g") Correspond to Curve (g) on Fig. 10. ($T_{sub} = 180°C$).

Fig. 12. Grain Size Dependence on Substrate Temperature for Various Substrate Materials.

Fig. 13. Hall Coefficient as a Function of Substrate Temperature for Two Source Method. (a) $T_{sulphur} = 88°C$; (b) $T_{sulphur} = 92°C$; (c) $T_{sulphur} = 102°C$.

Fig. 14. Summary of Film Properties.

Fig. 15. Planned Activity.

TITLE PAGE

(a) TERNARY COMPOUND THIN FILM SOLAR CELLS

(b) University of Maine at Orono

(c) September 1, 1975 - August 31, 1976 (requested)

(d) $34,929. (requested)

(e) Lawrence L. Kazmerski
Associate Professor
Department of Electrical Engineering

Fig. 1.

OBJECTIVES

1. The Identification and Production of Device - Quality Thin Films of $CuInS_2$.
2. Demonstration of Homojunction Viability for $CuInS_2$ Thin Film Solar Cells.
3. Growth and Investigation of Other $CuInX_2$ Materials.
4. Possible Heterojunction Demonstration.

Fig. 2.

ACTIVITY-TO-DATE

1. $\underline{\mathrm{CuInS}}_2$

   (a) Development of Single and Double Source Deposition Techniques.
   (b) X-ray and Electron Diffraction Studies.
   (c) Initial Electrical Characterization of Films (μ, σ, n).
   (d) Production of n and p-type Films.
   (e) Recrystallization.

2. $\underline{\mathrm{CuInSe}}_2$, $\underline{\mathrm{CuInTe}}_2$

   (a) Film Deposition [illegible] rystallization.
   (b) Electrical Char[illegible]tion.
   (c) X-ray, Electron Diffraction Analyses.

Fig. 3.

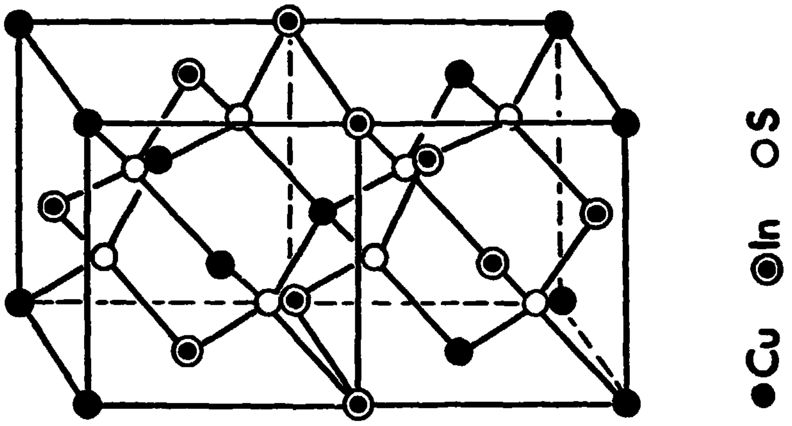

Fig. 4.

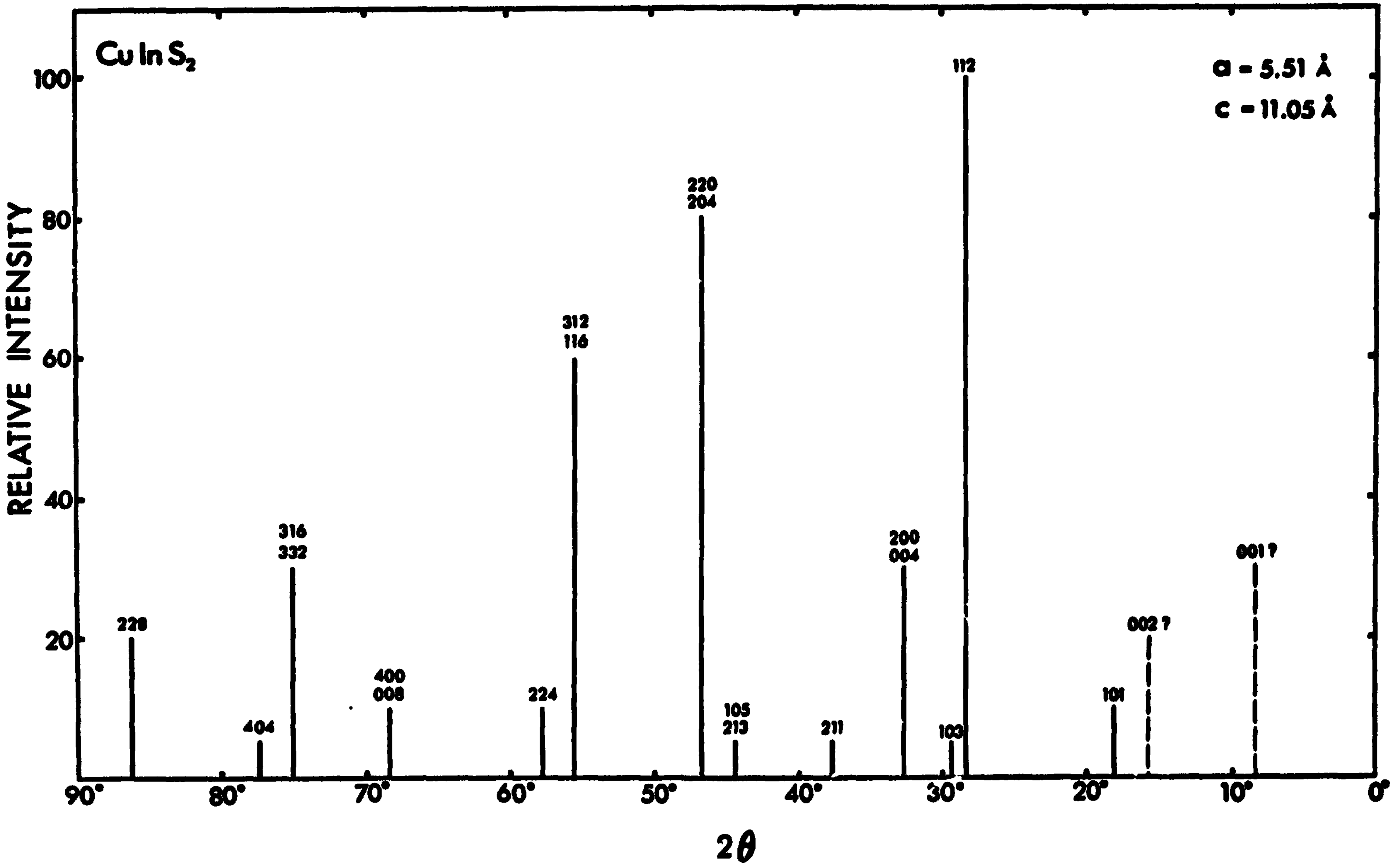
Cu In S_2
a = 5.51 Å
c = 11.05 Å
RELATIVE INTENSITY
100
80
60
40
20
90°
80°
70°
60°
50°
40°
30°
20°
10°
0°
2θ
228
404
316
332
400
008
224
312
116
220
204
105
213
211
200
004
103
112
101
002 ?
001 ?

Fig. 5.

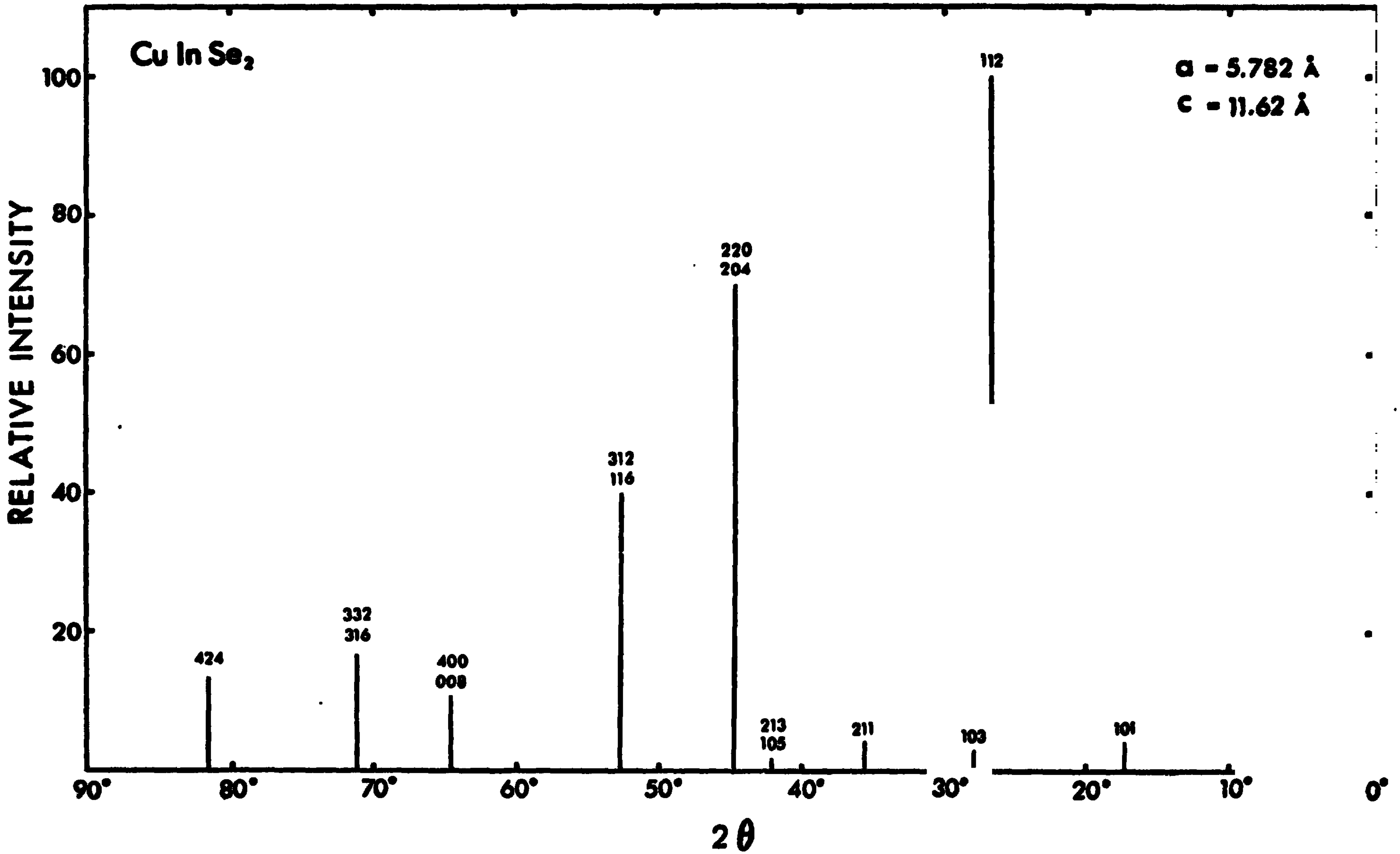
Cu In Se_2
a = 5.782 Å
c = 11.62 Å
RELATIVE INTENSITY
100
80
60
40
20
112
220
204
312
116
424
332
316
400
008
213
105
211
103
101
90°
80°
70°
60°
50°
40°
30°
20°
10°
0°
2 θ

Fig. 6.

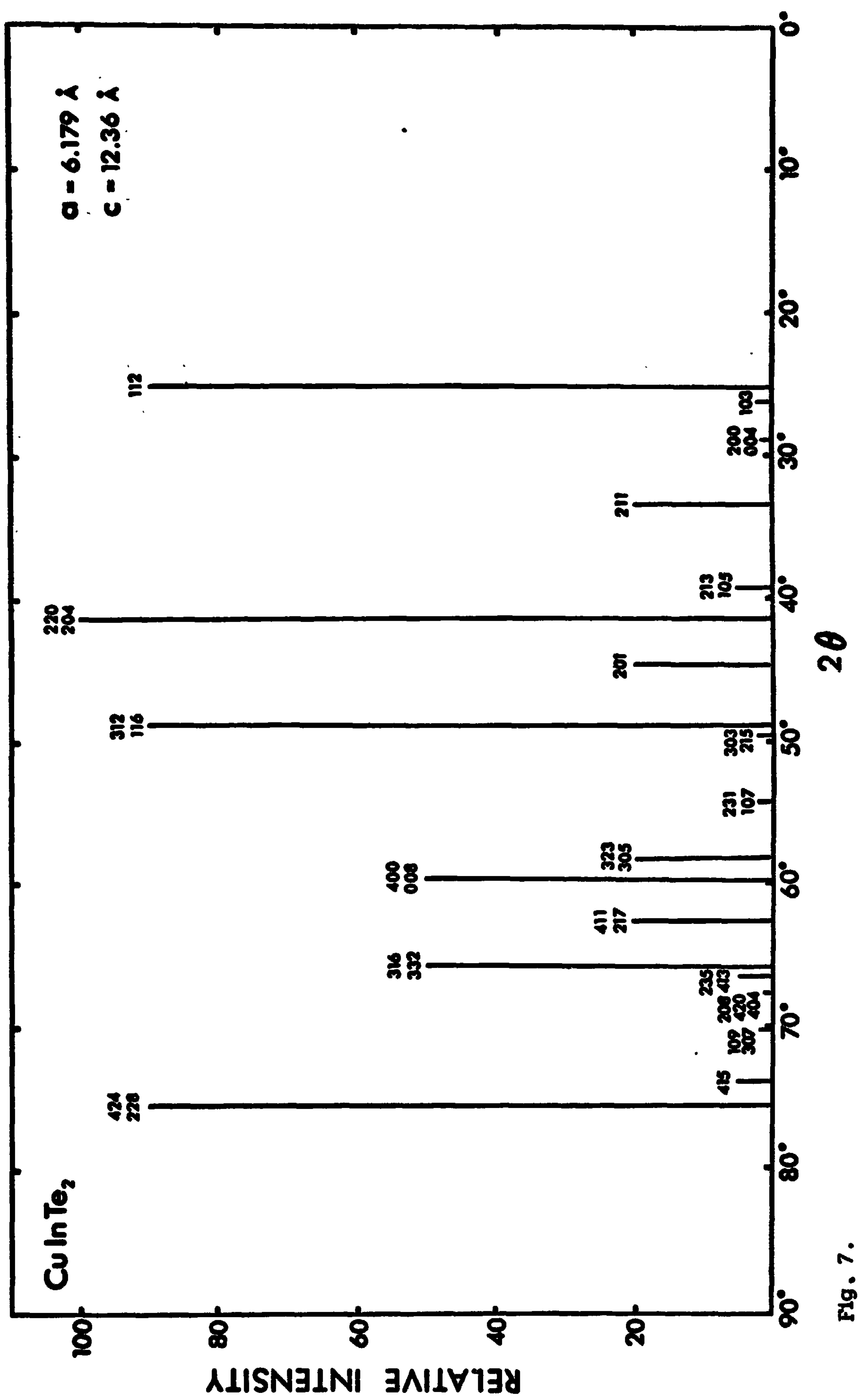
CuInTe₂
a = 6.179 Å
c = 12.36 Å
RELATIVE INTENSITY
100
80
60
40
20
2θ
0°
10°
20°
30°
40°
50°
60°
70°
80°
90°
112
103
200
004
211
213
105
220
204
201
312
116
303
215
231
107
323
305
400
008
411
217
316
332
235
413
208
420
404
109
307
415
424
228

Fig. 7.

TABLE II.

X-ray Diffraction Data (Calculated and Experimental Values)
For $CuInS_2$ Powders and Thin Films.
(Cu Kα and Cr Kα Radiation)

CALCULATED			hkl	Relative Intensity	OBSERVED 2θ		
d	2θ CuKα	2θ CrKα			Powder	Film CuKα	Film CrKα
10.6	8.34°		001?	30	--	--	--
5.56	15.94°		002?	20	--	--	--
4.87	18.20°	27.21°	101	10	18.16°	18.20°	27.2°
3.16	28.24°	42.51°	112	100	28.18°	28.18°	42.4°
3.04	29.38°	44.27°	103	5	29.28°	29.25°	44.2°
2.74	32.68°	49.42°	200,004	30	32.60°	32.60°	49.4°
2.39	37.64°	57.28°	211	5	37.52°	37.50°	57.2°
2.04	44.42°	68.32°	213,105	5	44.36°	44.22°	68.2°
1.94	46.84°	72.38°	220,204	80	46.66°	46.60°	72.3°
1.66	55.36°	87.27°	312,116	60	55.30°	55.28°	87.16°
1.591	57.98°	92.10°	224	10	57.88°	57.86°	92.1°
1.266	65.04	129.6°	316,332	30	64.92°	64.90°	--
1.128	86.24	--	228	20	--	--	--

Fig. 8.

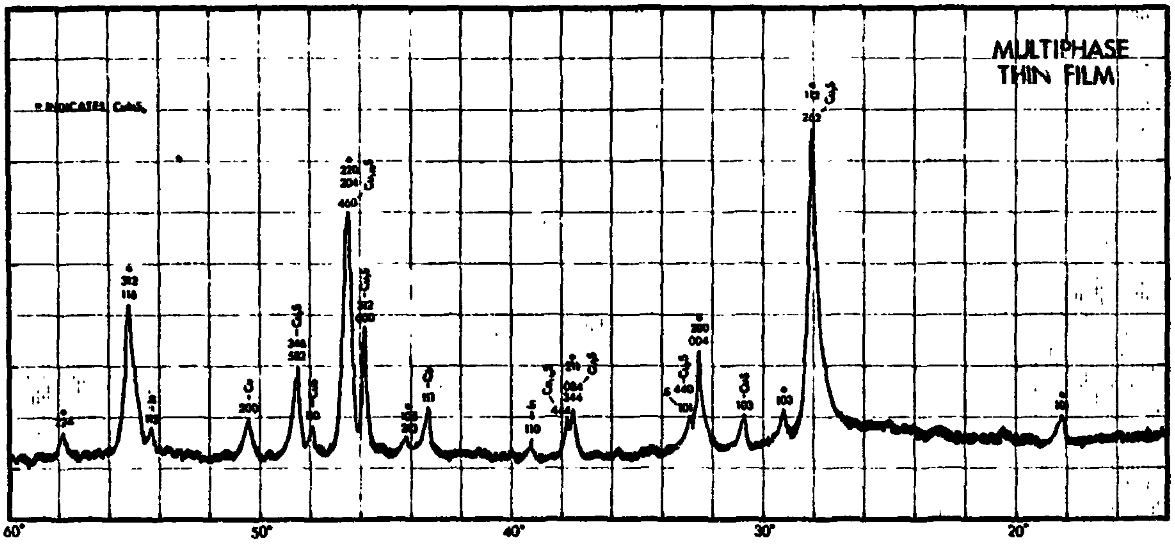
MULTIPHASE THIN FILM
• INDICATES CuInS₂
312
116
200
220
204
460
312
400
211
084
344
200
004
440
101
103
112
60°
50°
40°
30°
20°

Fig. 9.

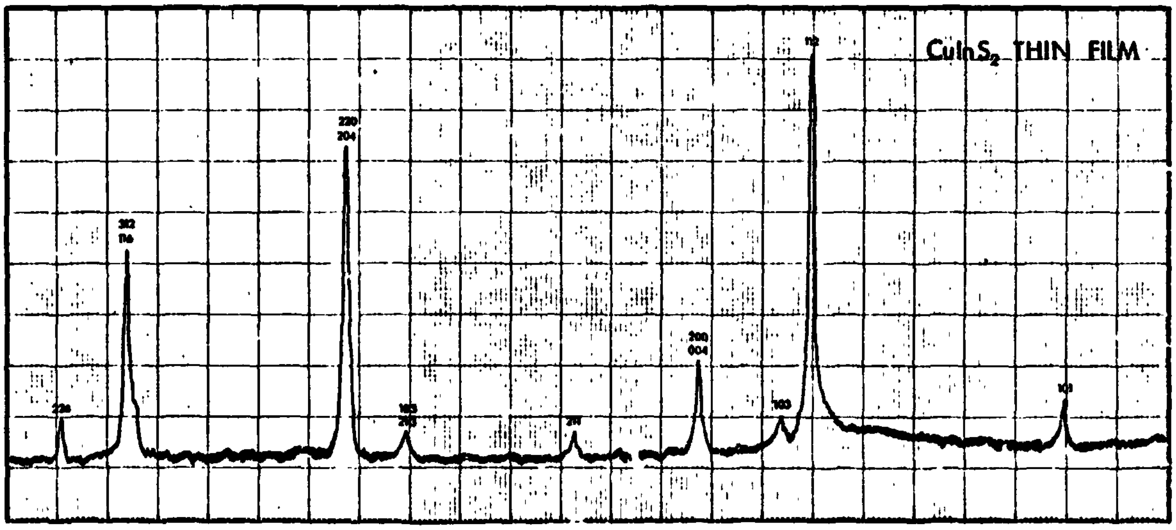
CuInS₂ THIN FILM
312
116
220
204
105
213
211
200
004
103
112
101

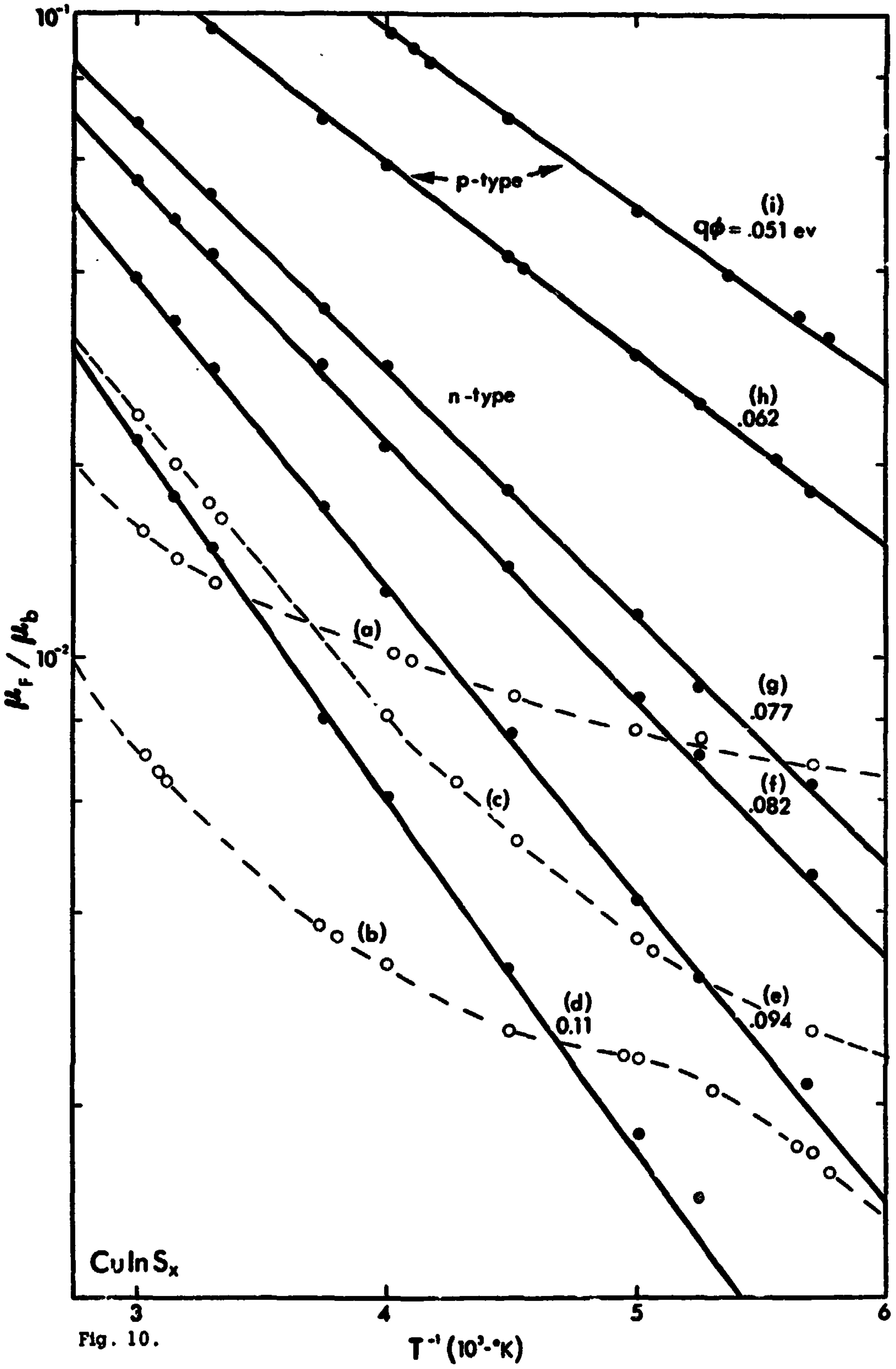
10⁻¹
10⁻²
μF / μb
p-type
n-type
(i)
qφ = .051 ev
(h)
.062
(g)
.077
(f)
.082
(e)
.094
(d)
0.11
(a)
(b)
(c)
CuInSx
3
4
5
6
T⁻¹ (10³-°K)

Fig. 10.

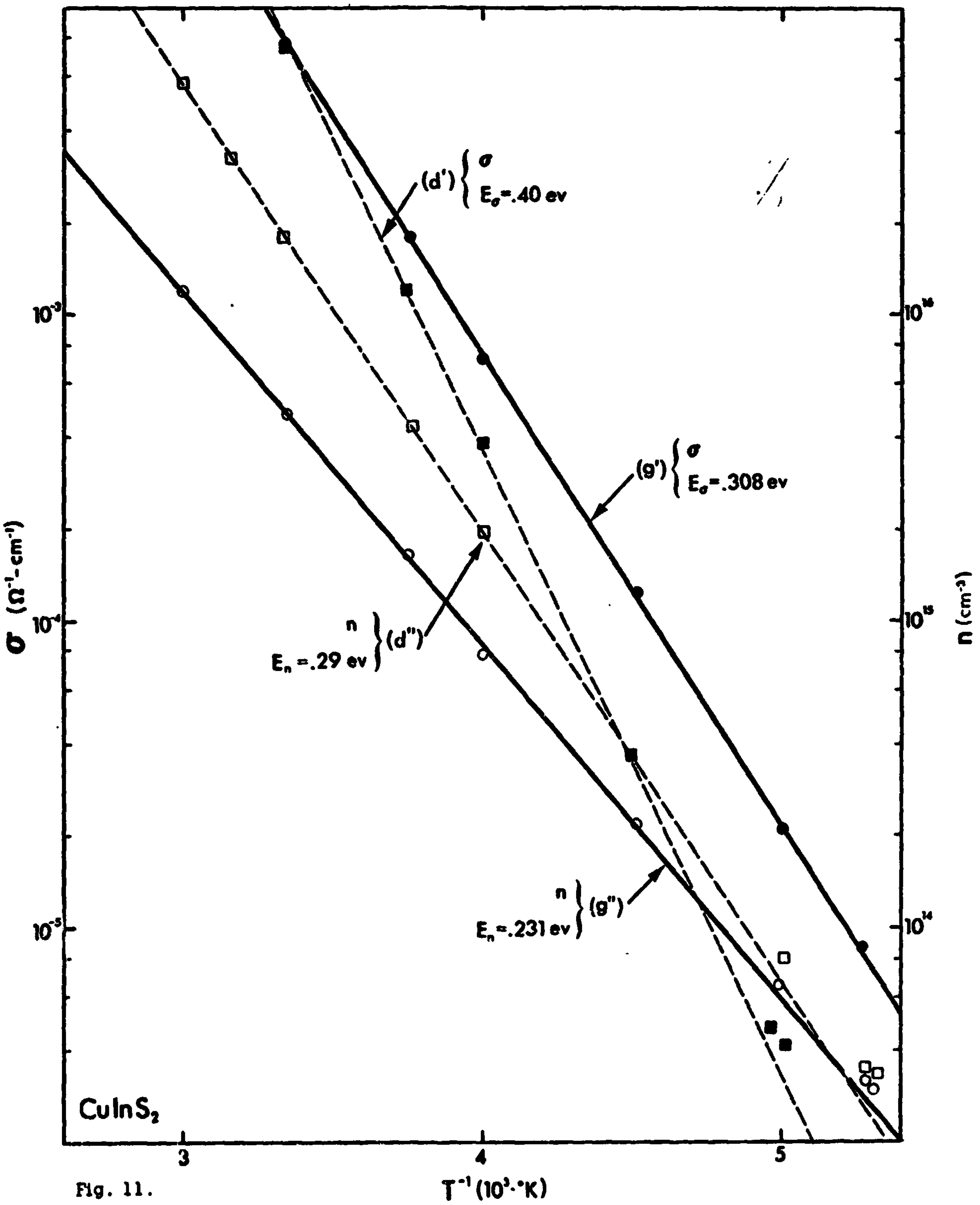

CuInS$_2$
σ (Ω^{-1}-cm^{-1})
n (cm^{-3})
T^{-1} (10^3·°K)
10^{-3}
10^{-4}
10^{-5}
10^{16}
10^{15}
10^{14}
3
4
5
(d') σ E$_\sigma$=.40 ev
(g') σ E$_\sigma$=.308 ev
n E$_n$=.29 ev (d")
n E$_n$=.231 ev (g")

Fig. 11.

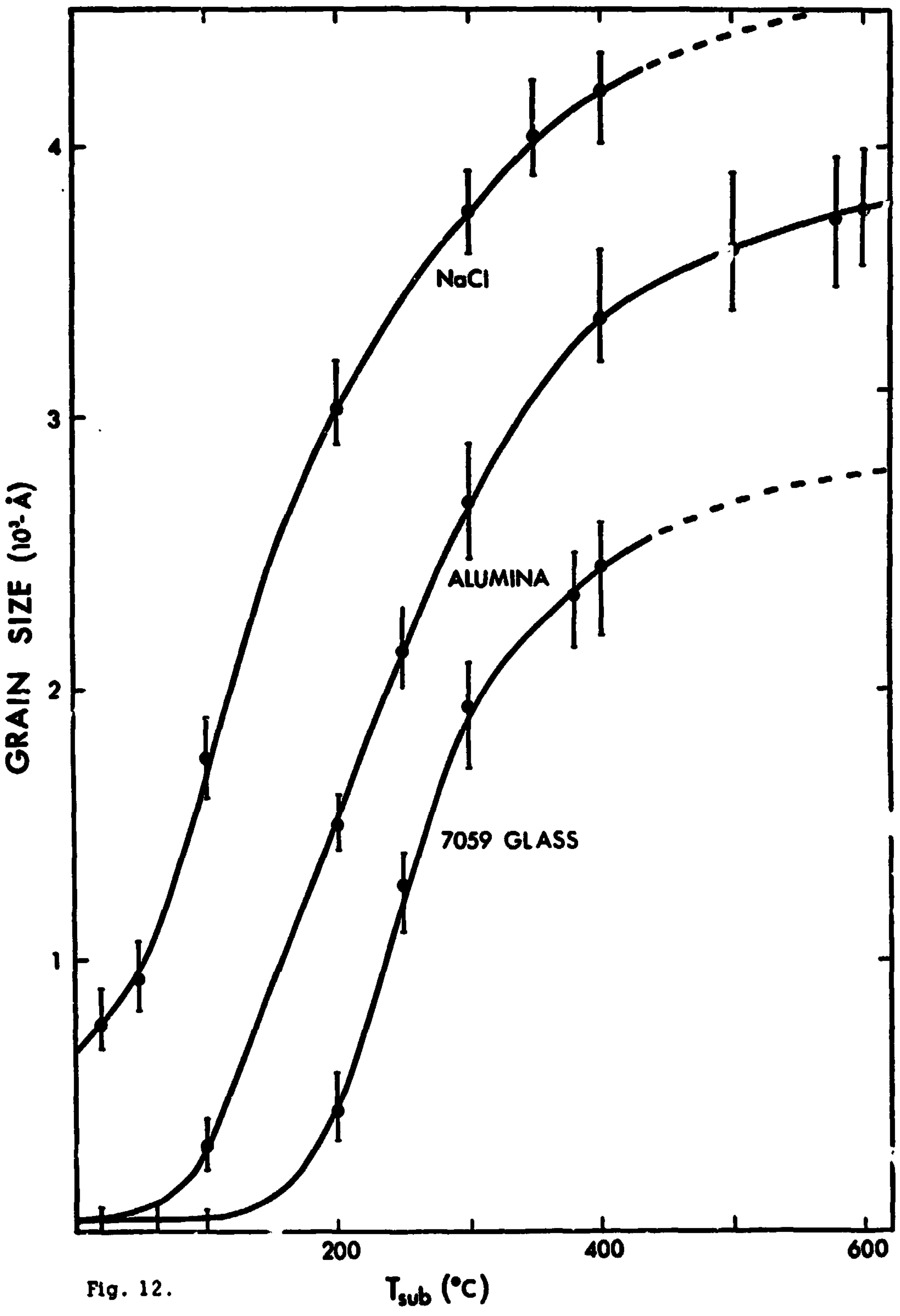
GRAIN SIZE (10^3·Å)
4
3
2
1
200
400
600
T_{sub} (°C)
NaCl
ALUMINA
7059 GLASS

Fig. 12.

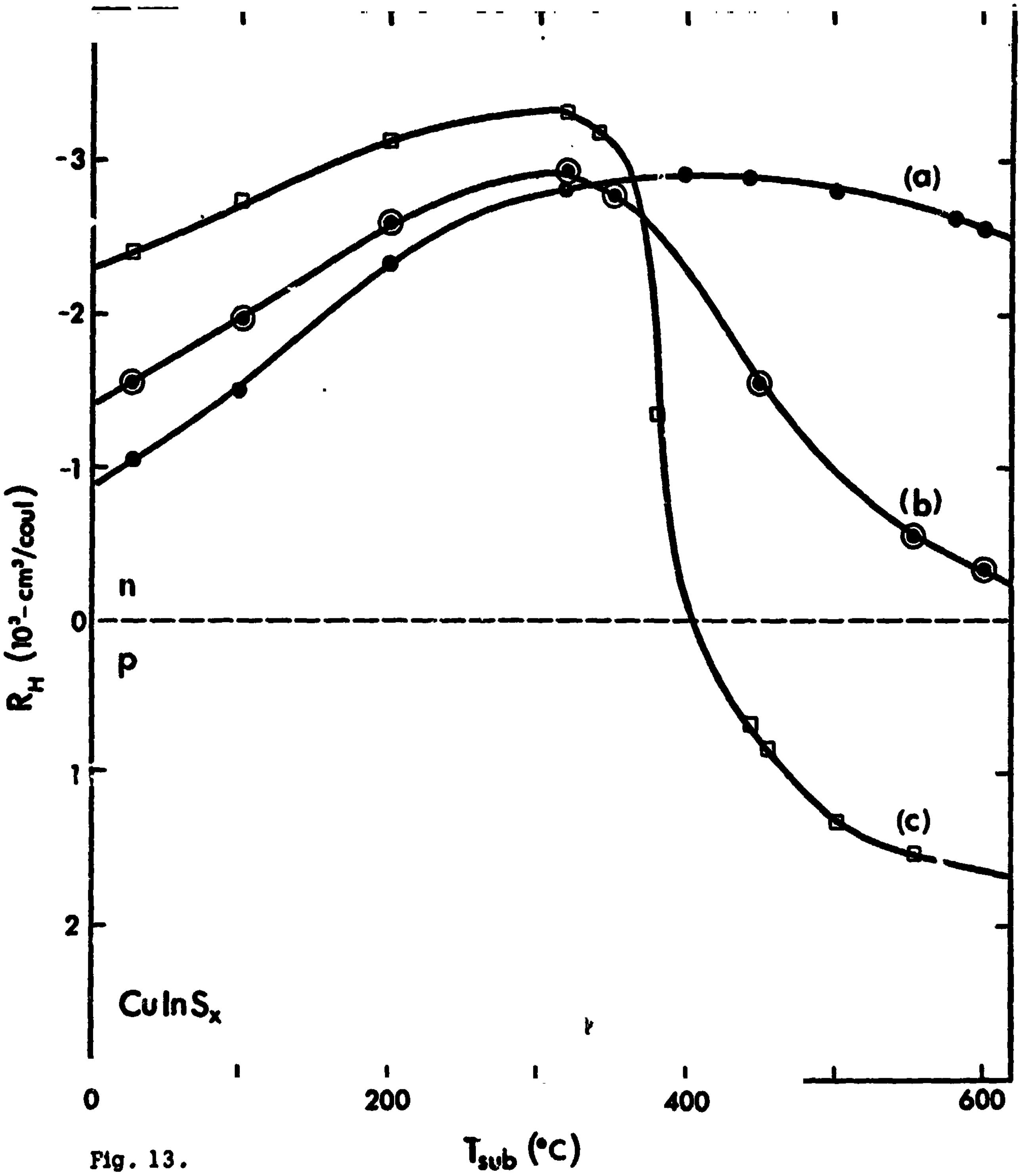

Fig. 13.

Table I. Comparison of properties of the deposited $CuInS_2$ thin films on this study with Single Crystal Values.

		Single Crystals(a), (b)				Films		
		ρ (Ω-cm)	n,p (cm^{-3})	μ ($\frac{cm^2}{v\text{-}sec}$)	E_g (eV)	ρ (Ω-cm)	n,p (cm^{-3})	μ $\frac{cm^2}{(v\text{-}sec)}$
$CuInS_x$	n	1	3×10^{16}	200	1.55	0.1-800	10^{14}-10^{19}	1-10;28(c)
	p	5	1×10^{17}	15		.8-400	10^{13}-10^{16}	~2;3.2(c);8.3(d)

(a) B. Tell, J. Shay and H. Kasper, Phys. Rev. B, 4, 2463 (1971)

(b) B. Tell and H. Kasper, Phys. Rev. B, 4, 4455 (1971).

(c) Recrystallized in H_2S, initially n-type.

(d) Recrystallized in H_2S, initially p-type.

Fig. 14.

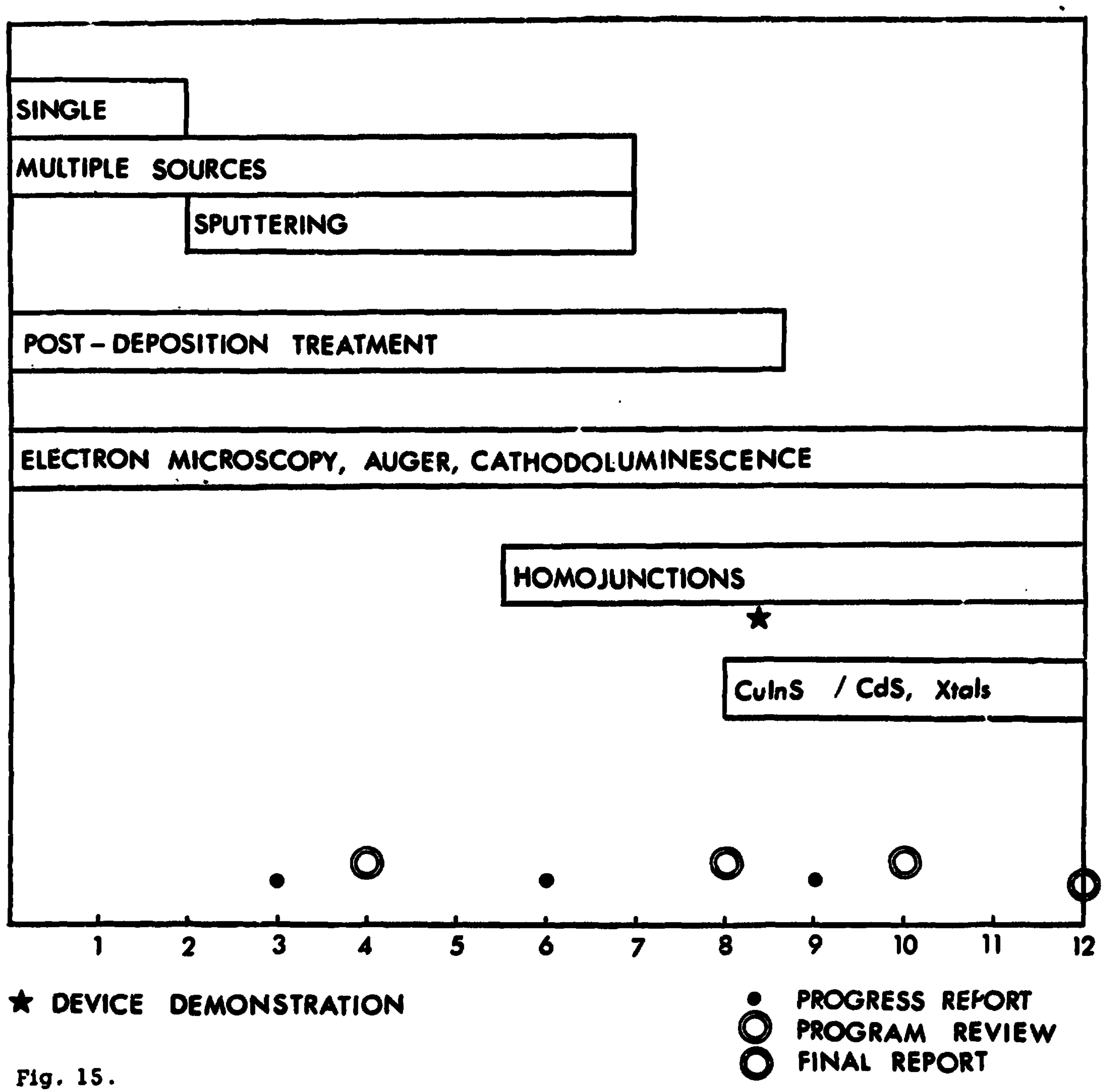
SINGLE
MULTIPLE SOURCES
SPUTTERING
POST-DEPOSITION TREATMENT
ELECTRON MICROSCOPY, AUGER, CATHODOLUMINESCENCE
HOMOJUNCTIONS
CuInS / CdS, Xtals
1
2
3
4
5
6
7
8
9
10
11
12
★ DEVICE DEMONSTRATION
● PROGRESS REPORT
○ PROGRAM REVIEW
○ FINAL REPORT

Fig. 15.

PHOTOCHEMICAL CONVERSION OF SOLAR ENERGY

Grant No. AER 72-035979

Grant Period 6/1/73 - 8/31/75

Grant Amount $304,200

Paper Author
Elliot Berman
Center for Energy Studies
Boston University

Principal Investigator
Norman N. Lichtin
Department of Chemistry
Boston University

National Solar Photovoltaic Program Review Meeting
July 22-25, 1975 Los Angeles, California

ABSTRACT

Objective: Photogalvanic Cell With 5% Efficiency

Past Activity:
An examination of the kinetic and photochemical processes in the iron/thionine system coupled with optimization of cell performance has led to a 600 fold improvement in efficiency. At the same time, progress made in cell design points the way to potential inexpensive systems.

Current Effort/Future Plans:
The emphasis in the program will now be shifted to studying variations in solvent, dye and redox couple to improve cell absorbence, spectrum matching and voltage necessary to a further major improvement in efficiency.

OBJECTIVE

- FIVE PERCENT EFFICIENCY
- STORAGE (?)

PLANNED ACTIVITY

- DIFFUSION LENGTH
  - MULTIPLE LAYER
  - SOLVENT DYE
- SPECTRUM MATCHING
  - MULTIPLE LAYER
- STABILITY

STACKED CELL

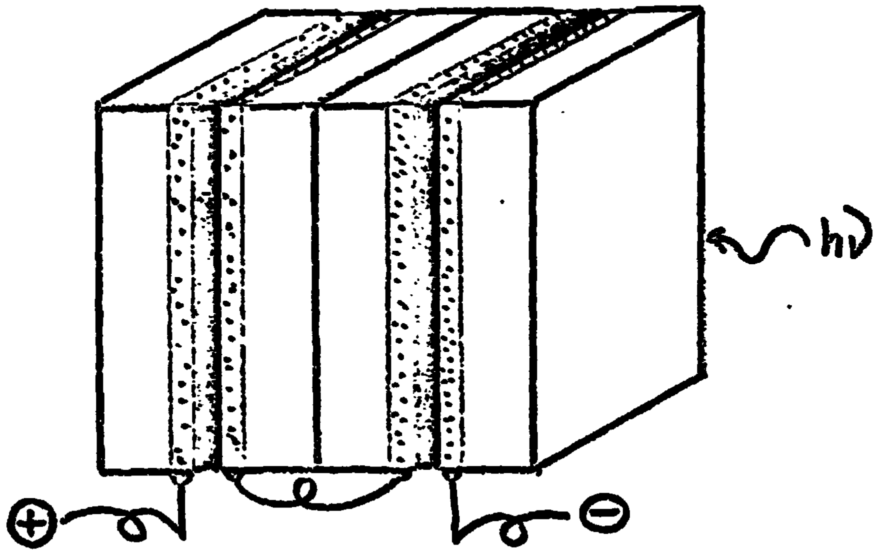

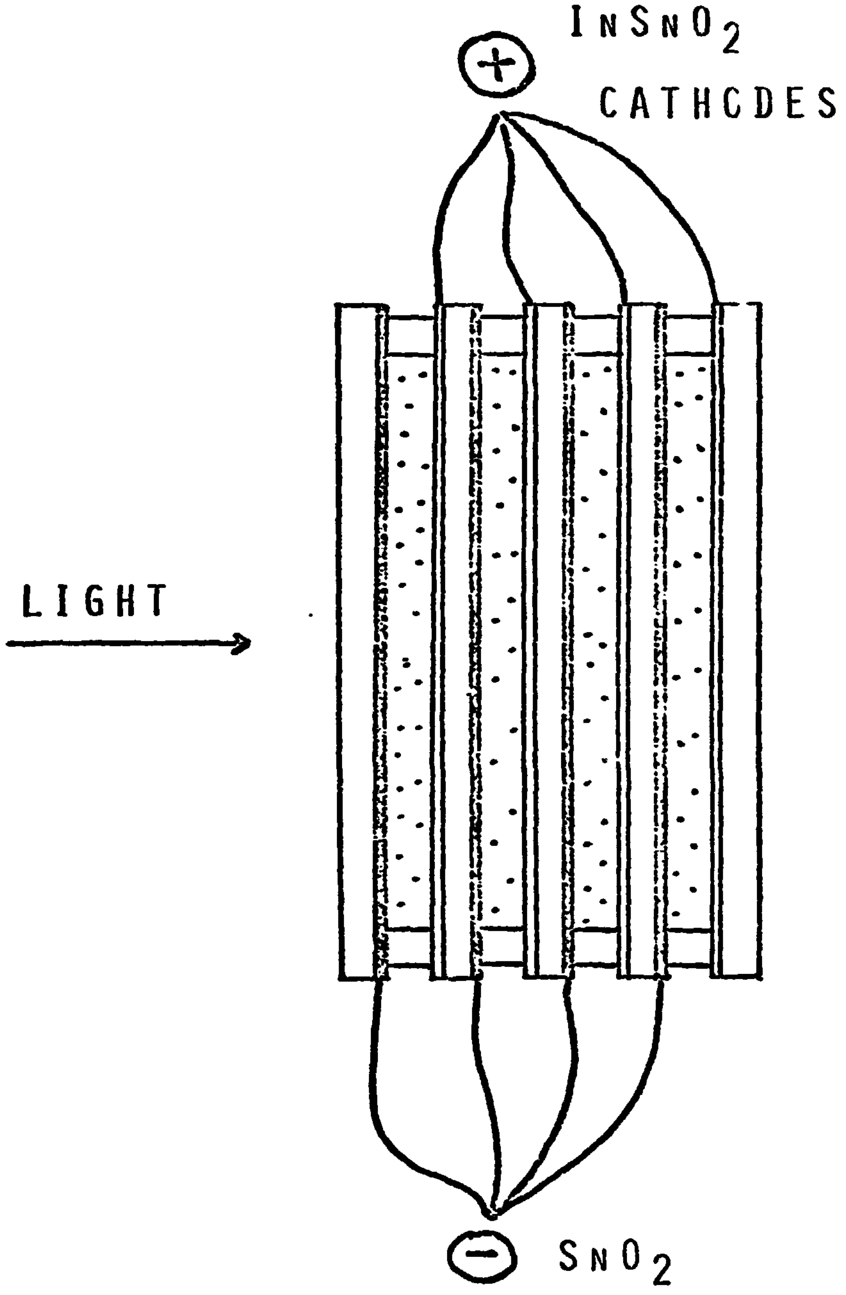

4-ELEMENT STACK CELL

DEVICE PARAMETERS

VOLTAGE EFFICIENCY	∿ 10%
CURRENT EFFICIENCY	∿ 100%
SUNLIGHT EFFICIENCY	
SINGLE LAYER	0.03%
QUADRUPLE LAYER	0.06%
PROGRAM START	0.0001%

FUTURE PLANS

- DYES
- SOLVENT
- ELECTRODE
- REDOX COUPLES

RENEWAL REQUEST

GRANT PERIOD	JULY 24, 1975 - JULY 23, 1976
COST	$181,642

N76 12507

SEMICONDUCTOR-ELECTROLYTE PHOTOVOLTAIC ENERGY CONVERTER

NSF Grant AER 74-13292

From 2/1/75 to 1/31/76

$49,300

Principal Investigators

William W. Anderson, Dept. of Electrical Engineering

Larry B. Anderson, Dept. of Chemistry
The Ohio State University

The goal of this work is the evaluation of the feasibility and practicality of a solar cell consisting of a semiconductor surface in contact with an electrolyte. Preliminary experimental and theoretical work, as well as a literature search, indicates the system merits further study.

Specific semiconductor electrodes and promising electrolytes have been identified for further study. The systems will first be evaluated for efficient energy conversion at typical solar photon irradiances. They will then be evaluated for stability, and finally, for economical and practical solar cell construction.

In Fig. 1 we show the basic components and processes for photovoltaic energy conversion at the surface of an n-type semiconductor in contact with an electrolyte which is oxidizing to conduction band electrons. To date, we have studied characteristics of single crystal CdS, GaAs, CdSe, CdTe and thin film CdS in contact with aqueous and methanol based electrolytes. We have measured open circuit voltages from Mott-Schottky plots and open circuit photovoltage. We have measured short circuit current and quantum efficiency as a function of λ at low photon irradiances and as a function of photon irradiance up to 20 mW/cm^2. Electrode corrosion as a function of current and electrolyte composition has been studied by drift of V_{OC} and I_{SC} with time, by microscopic examination of electrode surfaces and by electrochemical analysis of electrode decomposition products.

The quantum efficiency for short circuit photo current of a CdS crystal and a 20 µm film is shown in Fig. 2 while the electrical and photovoltaic properties are shown in Fig. 3. The highest photon irradiances we have used to date were with the GaAs cell shown in Fig. 4. Significantly higher conversion efficiencies were obtained with a different electrolyte and at low photon irradiances on GaAs as shown in Fig. 5. From an analysis of the short circuit current spectral response shown in Fig. 6, it appears that a significant diffusion contribution to I_{SC} occurs as well as the drift component due to photogeneration of carriers in the space charge region.

As shown in Fig. 1, charge may be transferred from the semiconductor surface to the electrolytic solution in contact with this surface either by simple electron transfer or by deposition on or dissolution from the semiconductor of ionic species. The latter modes are basically undesirable because they inevitably result in changes in the composition and/or dimensions of the electrode. For example, in cadmium sulfide in contact with aqueous solutions, charge appears to be transferred in part by deposition of molecular sulfur and concomitant dissolution of cadmium ion

$$2h^+ + CdS \rightarrow Cd^{2+} + S_{solid} \qquad (1)$$

In methanol solvent, on the other hand, electrolysis of the solvent apparently accounts for a substantial fraction of the current observed.

As a first step in solving the problems of electrode dissolution, we are developing analytical methods suitable for detecting dissolution of CdS, CdSe, CdTe, and GaAs. To do this, it is only necessary to analyze for the level of Cd^{2+} or Ga^{3+} in the photovoltaic cell solution. Anodic stripping analysis is ideally suited for determination of these two metals, and apparatus suitable for this determination is readily available to us. The steps in this procedure are shown in Fig. 7. Analysis of 1 x 10^{-6}, (0.1 ppm) Cd^{2+} is routine by this technique with a precision of 5% A typical replicate analysis is shown in Fig. 8.

Suppression of photo-initiated dissolution of the semiconductor electrode will be attempted. Addition of various redox couples capable of donating electrons to holes at the semiconductor surface will be investigated

$$R + h^+ \rightleftarrows O \qquad (2)$$

When this reaction is more rapid than reaction (1) above, electron transfer will suppress anodic dissolution. This is apparently the case when the electron donor is methanol. However, the oxidation of methanol to formaldahyde is irreversible and causes destruction of the solvent. We are seeking couples R/O which are reversible and may be reduced at the counter electrode, making the solvent-electrolyte system simply an ionic conductor with no permanent change occuring with time.

An attempt to demonstrate comparable photovoltaic energy conversion efficiency in polycrystalline thin film devices will be made. A system for vacuum evaporation of CdS and other II-VI compounds has been set up.

We will obtain a quantitative measure of the electrode dissolution problem for CdS. Cd^{+2} ion concentration in the cell electrolyte will be measured as a function of "exposure", i.e., short circuit current multiplied by time of current flow during illumination at constant intensity. The quantity of interest is in the number of Cd^{+2} ions going into solution for each charge transfer event across the semiconductor-electrolyte interface.

To date, CdS and GaAs have been studied since they were available. Samples of CdTe and CdSe have been obtained which will be evaluated for efficient photovoltaic energy conversion.

It appears that a Becquerel effect solar cell is capable of conversion efficiencies of technological significance. Our measured external conversion efficiency of 30% was for low intensity, almost monochromatic radiation, and so is not directly comparable to commercial state-of-the-art solar cells. However, these are preliminary experiments with the simplest electrolytes on a nonoptimum semiconductor. Use of a semiconductor such as CdTe would optimize the device spectral response to the solar source and comparable efficiencies would then be highly significant. GaAs, which is also well matched to the solar spectrum, gave a 20% conversion efficiency for monochromatic excitation.

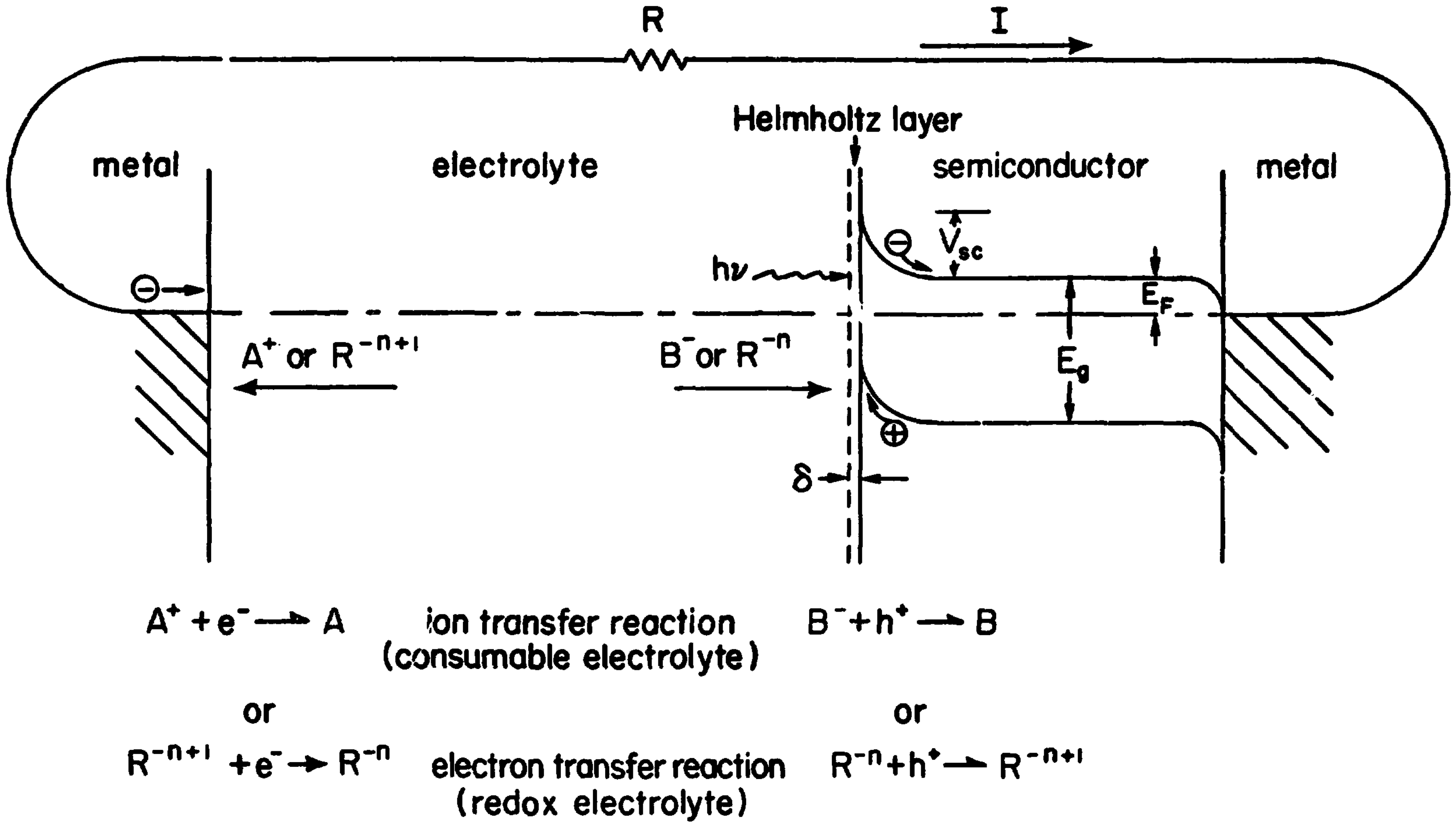

Processes in electrolyte-semiconductor photovoltaic cell.

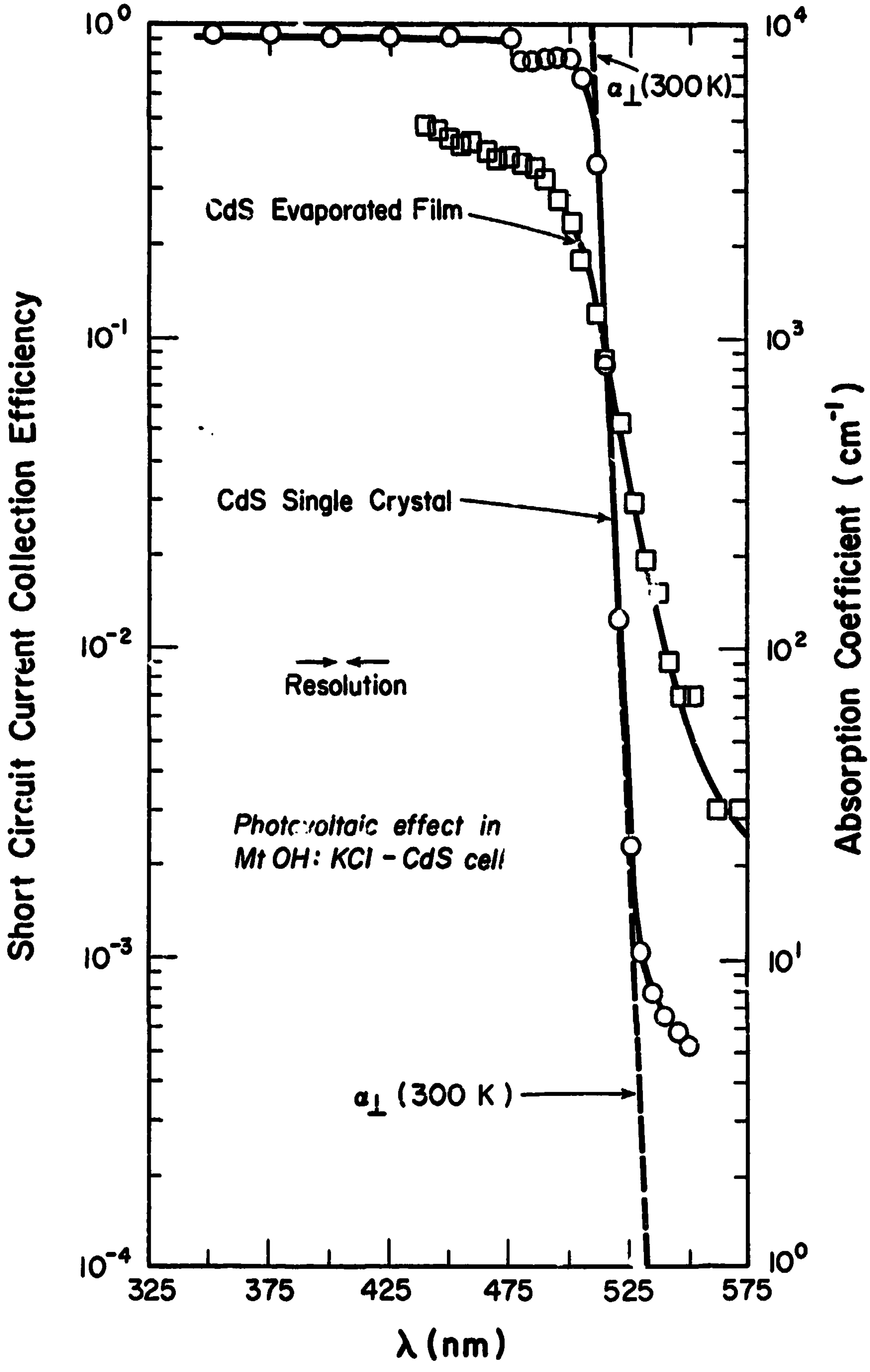
Short Circuit Current Collection Efficiency
Absorption Coefficient (cm^{-1})
10^0
10^{-1}
10^{-2}
10^{-3}
10^{-4}
10^4
10^3
10^2
10^1
10^0
325
375
425
475
525
575
λ (nm)
$\alpha_\perp$(300 K)
CdS Evaporated Film
CdS Single Crystal
Resolution
Photovoltaic effect in
Mt OH: KCl - CdS cell
$\alpha_\perp$ (300 K)

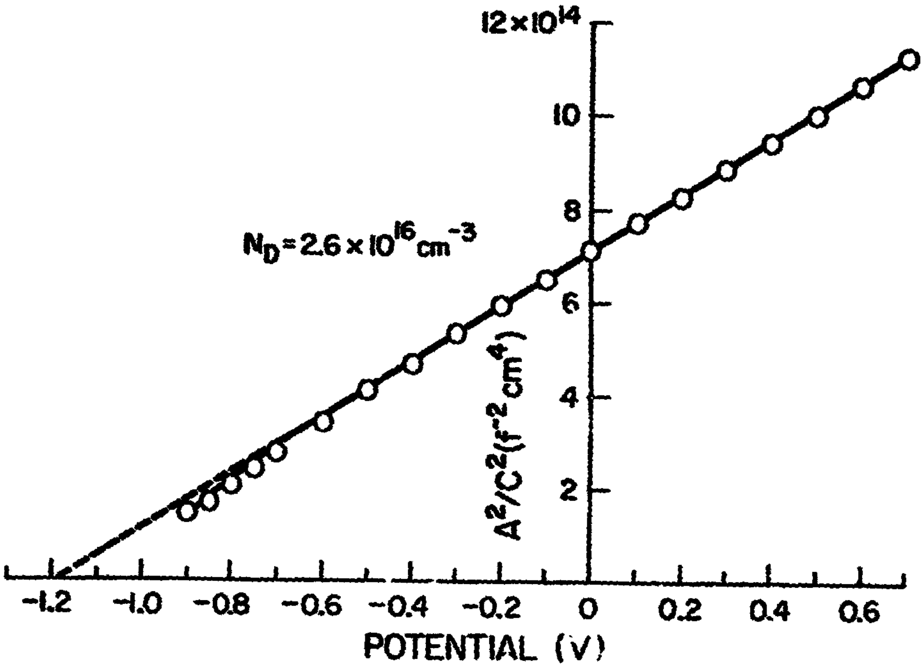

(a) Mott- Schottky plot

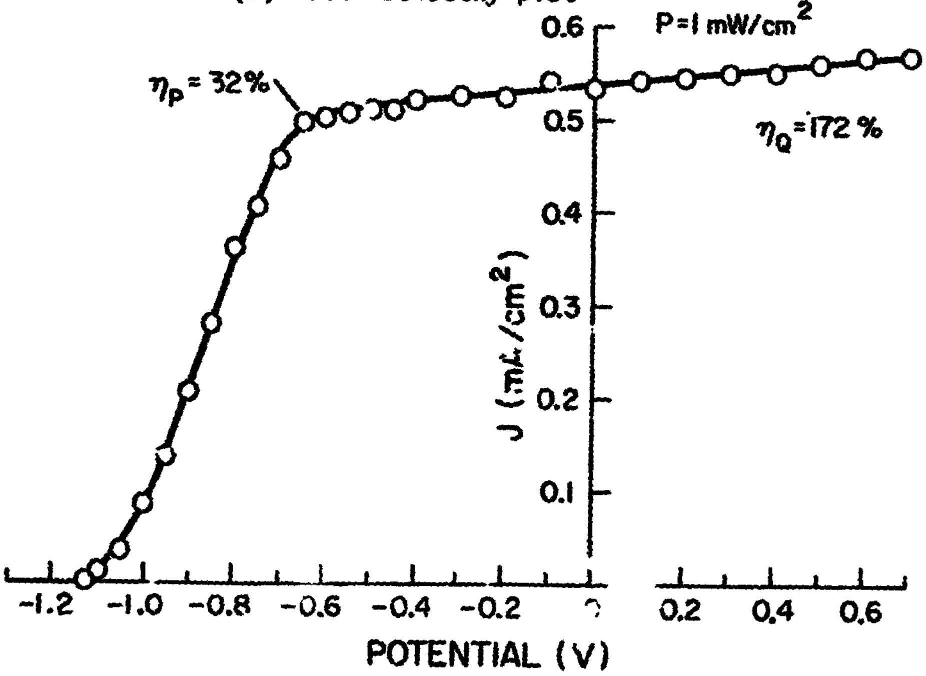

(b) Current - voltage characteristics under 400 nm excitation

Electrical and photovoltaic characteristics of CdS - 0.1M CH_3COOH cell

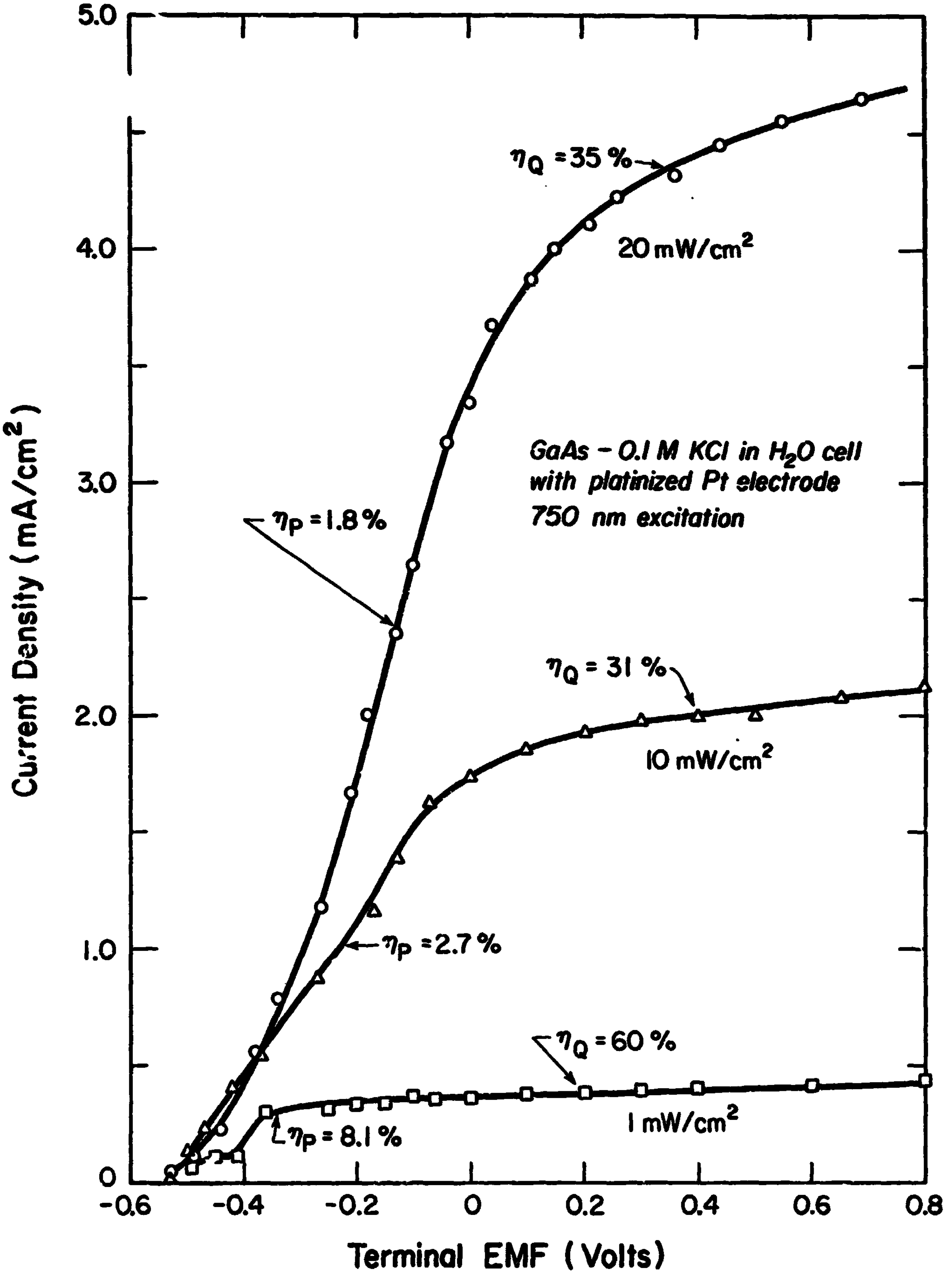
Current Density (mA/cm²)
Terminal EMF (Volts)
5.0
4.0
3.0
2.0
1.0
0
-0.6
-0.4
-0.2
0
0.2
0.4
0.6
0.8
ηQ = 35 %
20 mW/cm²
GaAs – 0.1 M KCl in H₂O cell
with platinized Pt electrode
750 nm excitation
ηP = 1.8 %
ηQ = 31 %
10 mW/cm²
ηP = 2.7 %
ηQ = 60 %
1 mW/cm²
ηP = 8.1 %

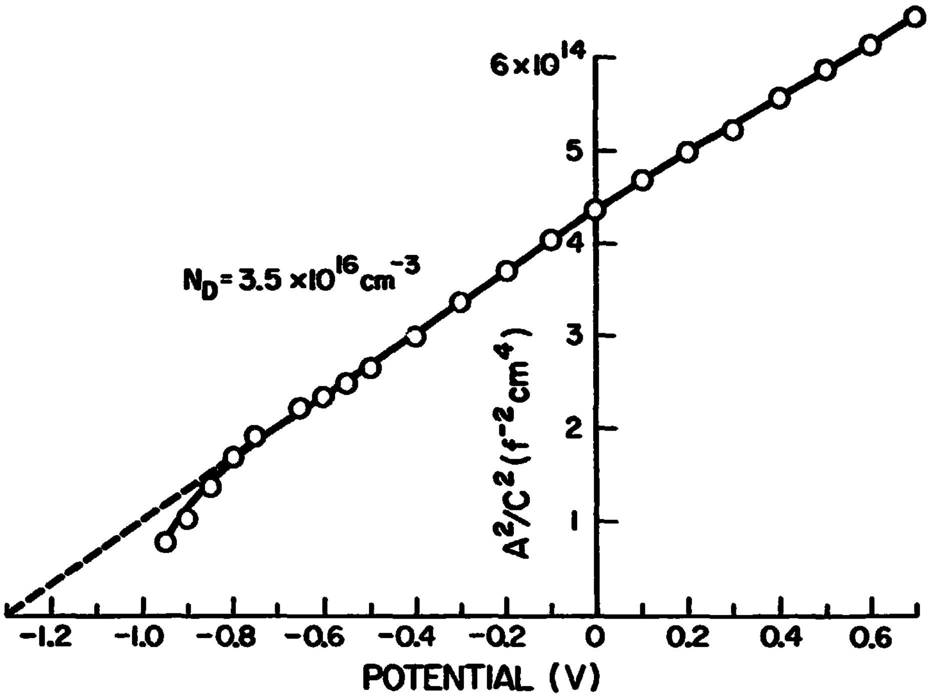

(a) Mott- Schottky plot

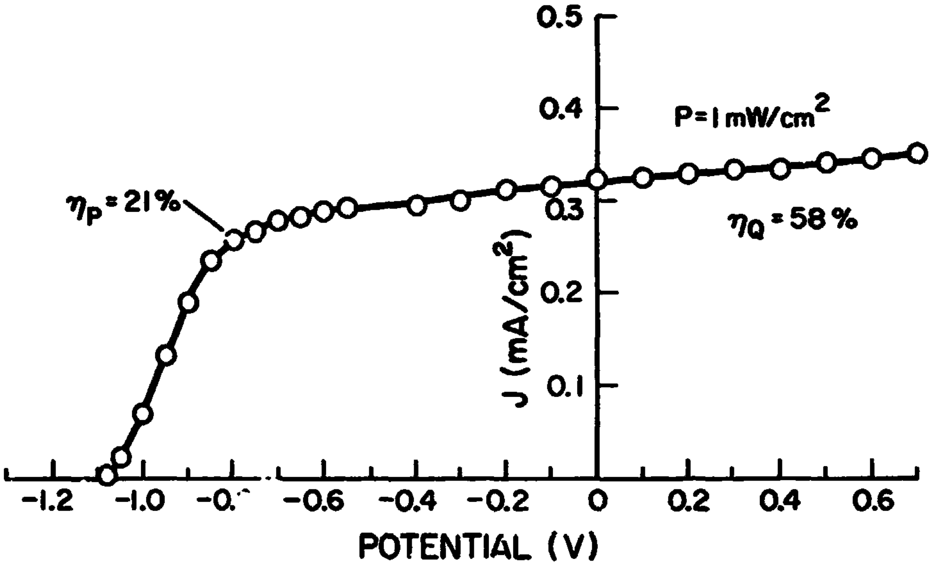

(b) Current - voltage characteristic under 740 nm excitation

Electrical and photovoltaic characteristics of GaAs -. 0.1M HCl cell

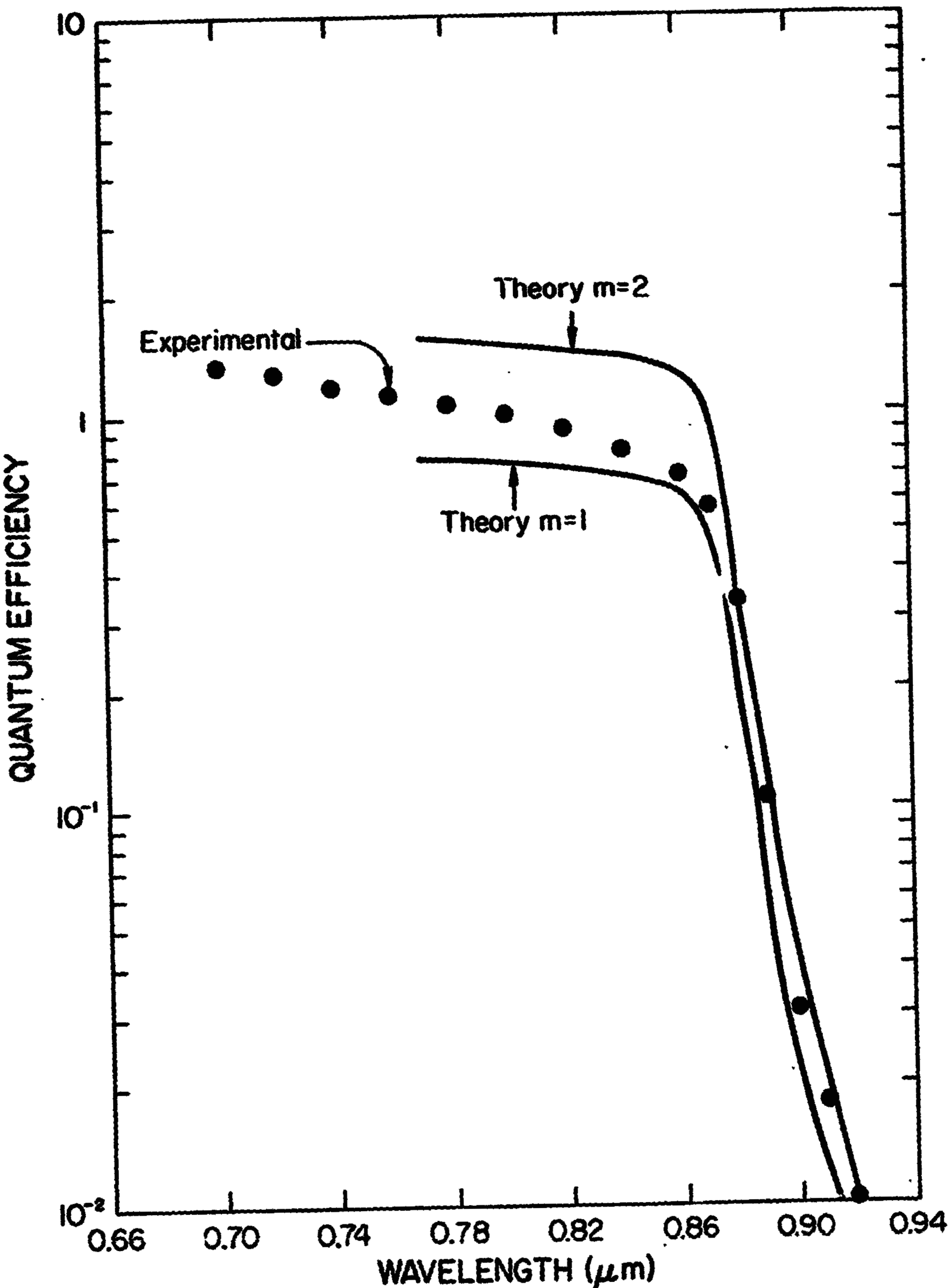

Short circuit quantum efficiency of GaAs-0.1M HCl cell.

Experimental points are shown along with theoretical curves for

L_p = 2μm with and without current doubling.

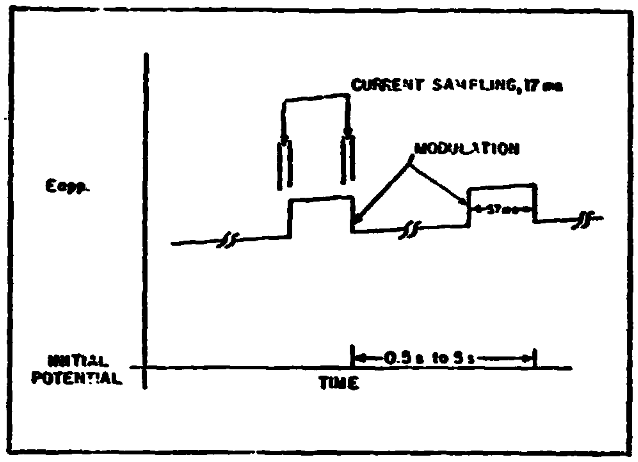

Figure V-9. EXCITATION POTENTIAL WAVEFORM FOR DIFFERENTIAL PULSE POLAROGRAPHY

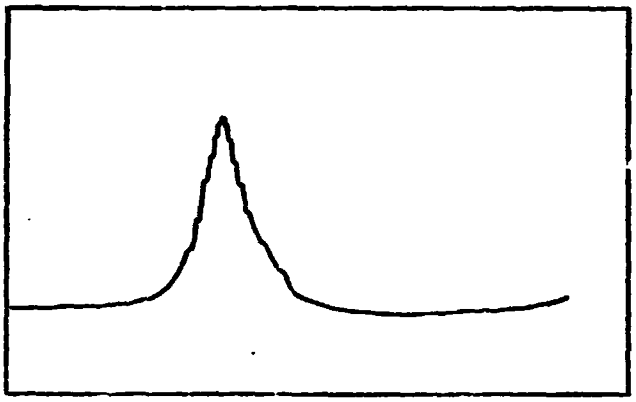

Figure V-10. TYPICAL DIFFERENTIAL PULSE POLAROGRAM

Differential Pulse Stripping
Replicate Analysis of
$1.0 \times 10^{-6}\ \underline{M}\ Cd^{2+}$

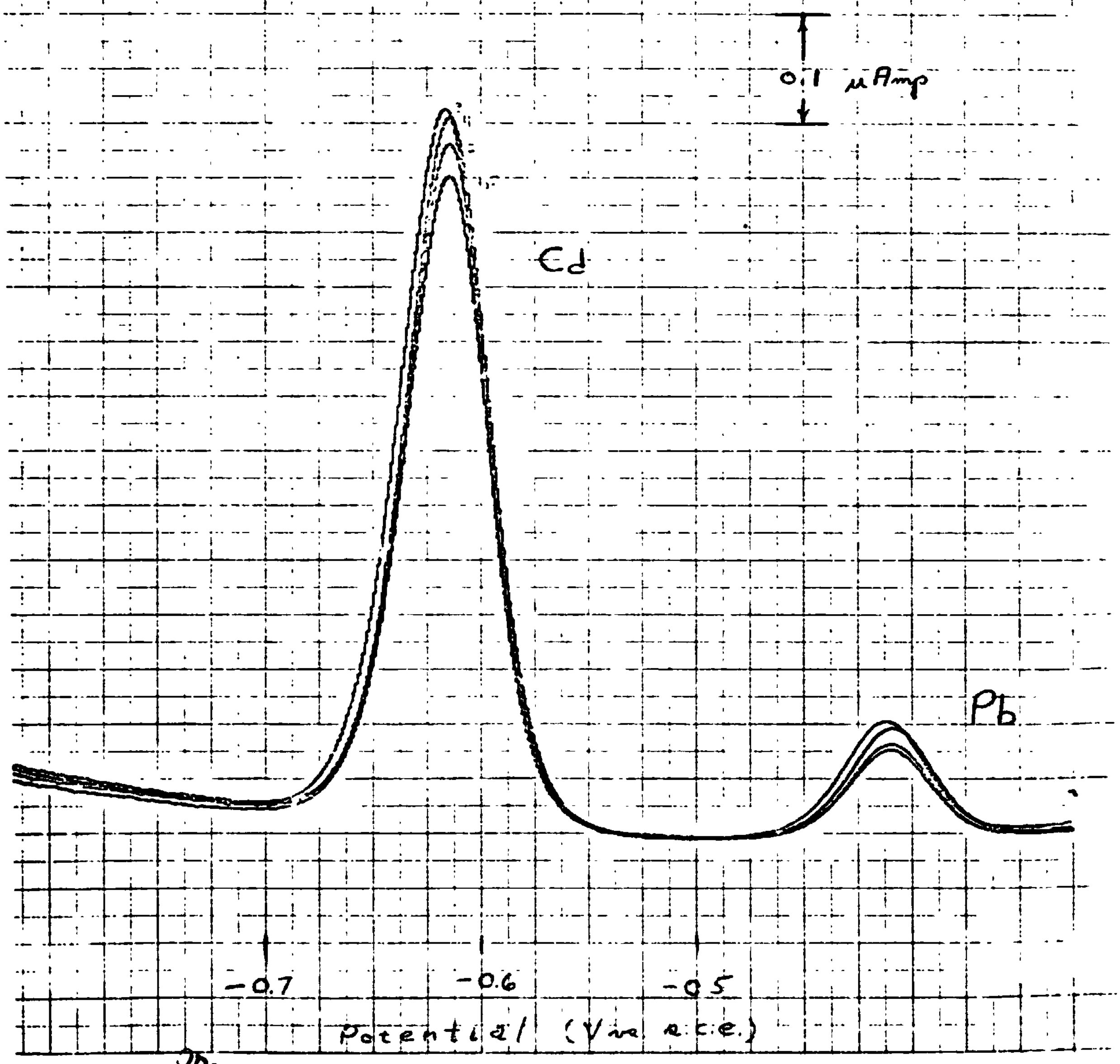

ORGANIC SOLAR CELL EXPLORATORY RESEARCH

GRANT DURATION: 1 YEAR

GRANT AMOUNT: $75,000

DR. STEVEN J. VALENTY

CORPORATE RESEARCH AND DEVELOPMENT

GENERAL ELECTRIC COMPANY
SCHENECTADY, NEW YORK

PRINCIPAL INVESTIGATOR: DR. S. J. VALENTY

July 22-25, 1975

LOS ANGELES, CALIFORNIA

This experimental program is formulated to obtain an understanding of the principles governing the photovoltaic effect in organic materials on the molecular level, and to apply these principles to the design and fabrication of laboratory devices having a photovoltaic organic polymer film as their key element.

The initial part of the program seeks to understand the mechanism of charge generation and separation in extremely thin ($\lesssim$50Å) synthetic organic films, in which one side of the film is a light sensitive electron donor (or acceptor) and the other is an electron acceptor (or donor). The approach may be thought of as a way to study the photovoltaic effect of a single organic junction. By adapting techniques of surface chemistry, it has been possible to form such potential photovoltaic junctions. Further, the use of this methodology provides the capability to vary both the composition of the junction (donor, acceptor, donor-acceptor distance, orientation, concentration) and its environment (aqueous redox electrodes, metal electrodes, semiconducting electrodes and bulk organic electrodes). It is expected that the ability to control these many experimental variables will allow a more detailed description of photovoltaic efficiency in terms of light absorption, charge generation, charge separation and charge collection than heretofore.

Progress to date has been in three areas: (1) materials synthesis, (2) apparatus development, and (3) ultra-thin film fabrication. An initial materials synthesis has provided a variety of surface active dyes, primary electron acceptors and polymers needed as prerequisites to film fabrication. Apparatus development includes the design and construction of devices used: (1) to characterize the surface properties of materials at the air-water interface, (2) to fabricate the asymmetric ultra-thin films, (3) to observe the optical absorption and fluorescence spectra of the films, and (4) to measure the electrical properties of the films. Both symmetrical and asymmetrical ultra-thin films of the synthesized materials have been formed and supported on glass slides for optical study.

The current effort is directed at achieving reproducible formation of a free-standing asymmetric film separating two aqueous redox electrodes.

For the first six months of the grant award, the main objective will be a demonstration of the photovoltaic effect in an asymmetric membrane formed using the surface chemistry methodology developed in this program.

Contributing Personnel: Dr. G. L. Gaines, Jr.
Dr. S. J. Valenty

ORGANIC SOLAR CELL EXPLORATORY RESEARCH

CORPORATE RESEARCH AND DEVELOPMENT
GENERAL ELECTRIC COMPANY

GRANT AMOUNT: $75,000

GRANT DURATION: 1 YEAR

PRINCIPAL INVESTIGATOR: STEVEN J. VALENTY

OVERALL OBJECTIVES OF PROJECT

- EXPERIMENTAL DETERMINATION OF THE MAJOR FACTORS GOVERNING THE PHOTOVOLTAIC EFFECT IN ORGANIC MATERIALS ON THE MOLECULAR LEVEL

- THE DESIGN AND SYNTHESIS OF A NEW CLASS OF ORGANIC PHOTOVOLTAIC POLYMERS AND THEIR FABRICATION INTO LARGE AREA SOLAR CELLS

PHOTOVOLTAIC EFFICIENCY IN ORGANIC MATERIALS

EFF $\propto$ LIGHT ABSORPTION • CHARGE GENERATION • CHARGE MOBILITY • CHARGE COLLECTION

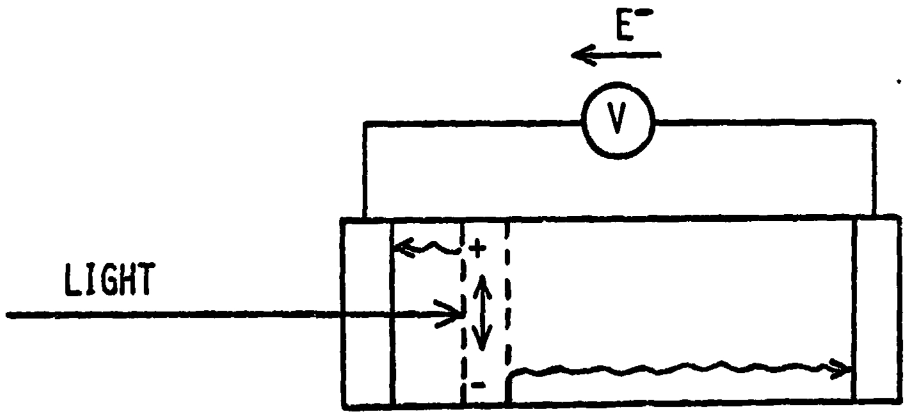

"SINGLE JUNCTION" vs. "CLASSICAL" APPROACH

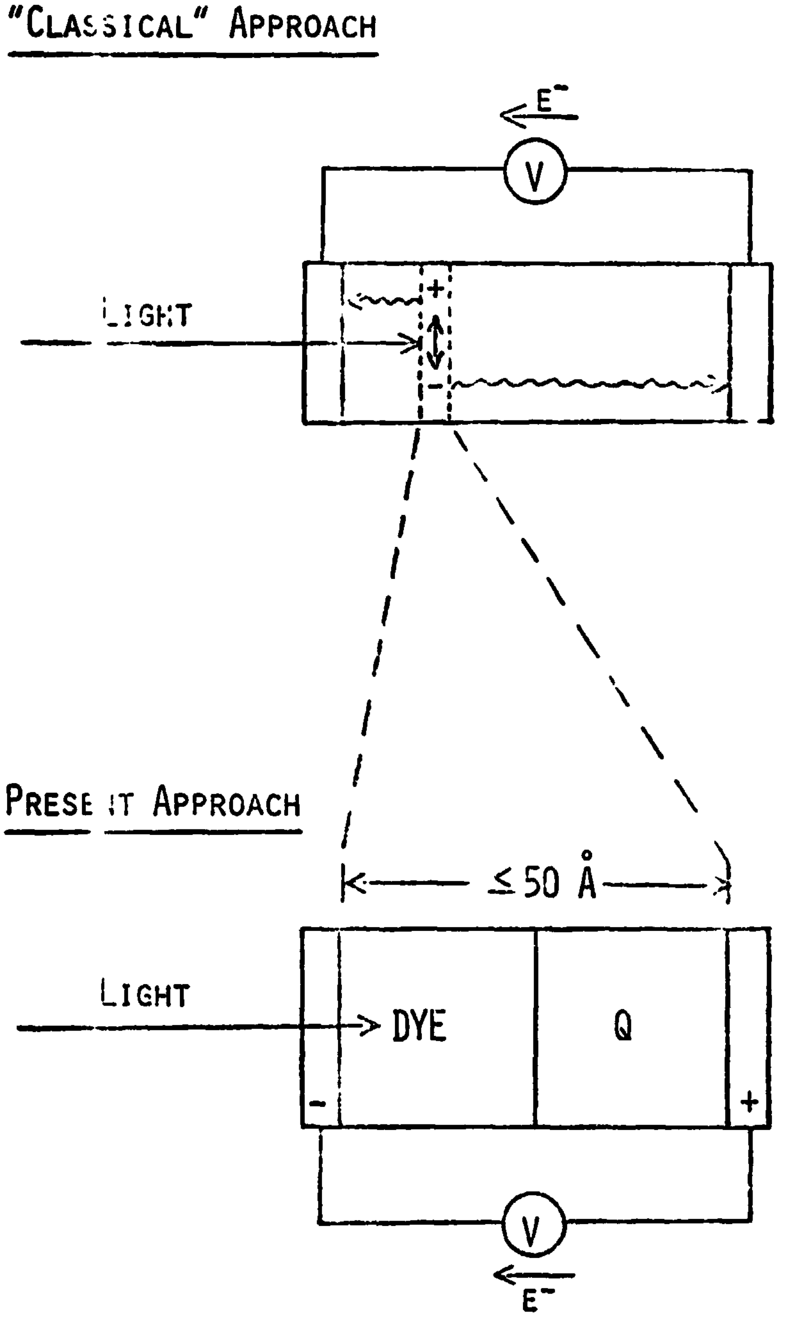

SINGLE ORGANIC JUNCTION EFFICIENCY CONSIDERATIONS

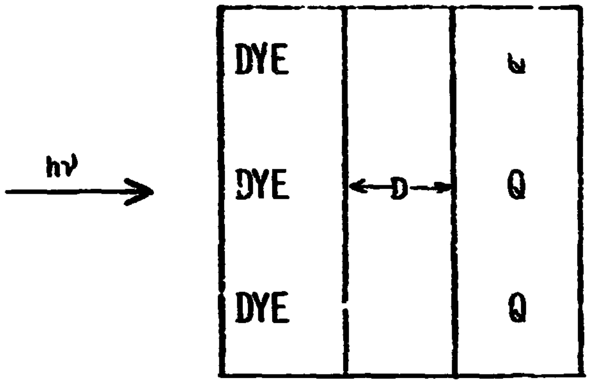

$$\mathrm{DYE} + h\nu \xrightarrow{K_{h\nu}} \mathrm{DYE}^{*}$$

$$\mathrm{DYE}^{*} + \mathrm{G} \underset{K_R}{\overset{K_T}{\rightleftarrows}} \mathrm{DYE}^{+\bullet} + \mathrm{Q}^{-\bullet}$$

$$\mathrm{DYE}^{*} \xrightarrow{K_F,\ K_Q} \mathrm{DYE} + h\nu' \text{ OR } \Delta$$

I	V
LIGHT FLUX	$\Delta G_{\mathrm{DYE}^{*},\mathrm{Q}}$
TUNNELING EFFICIENCY	
$K_T \propto \mathrm{EXP}\left[D \times (V-E)^{1/2}\right]$	
COMPETING PROCESSES	
RECOMBINATION	

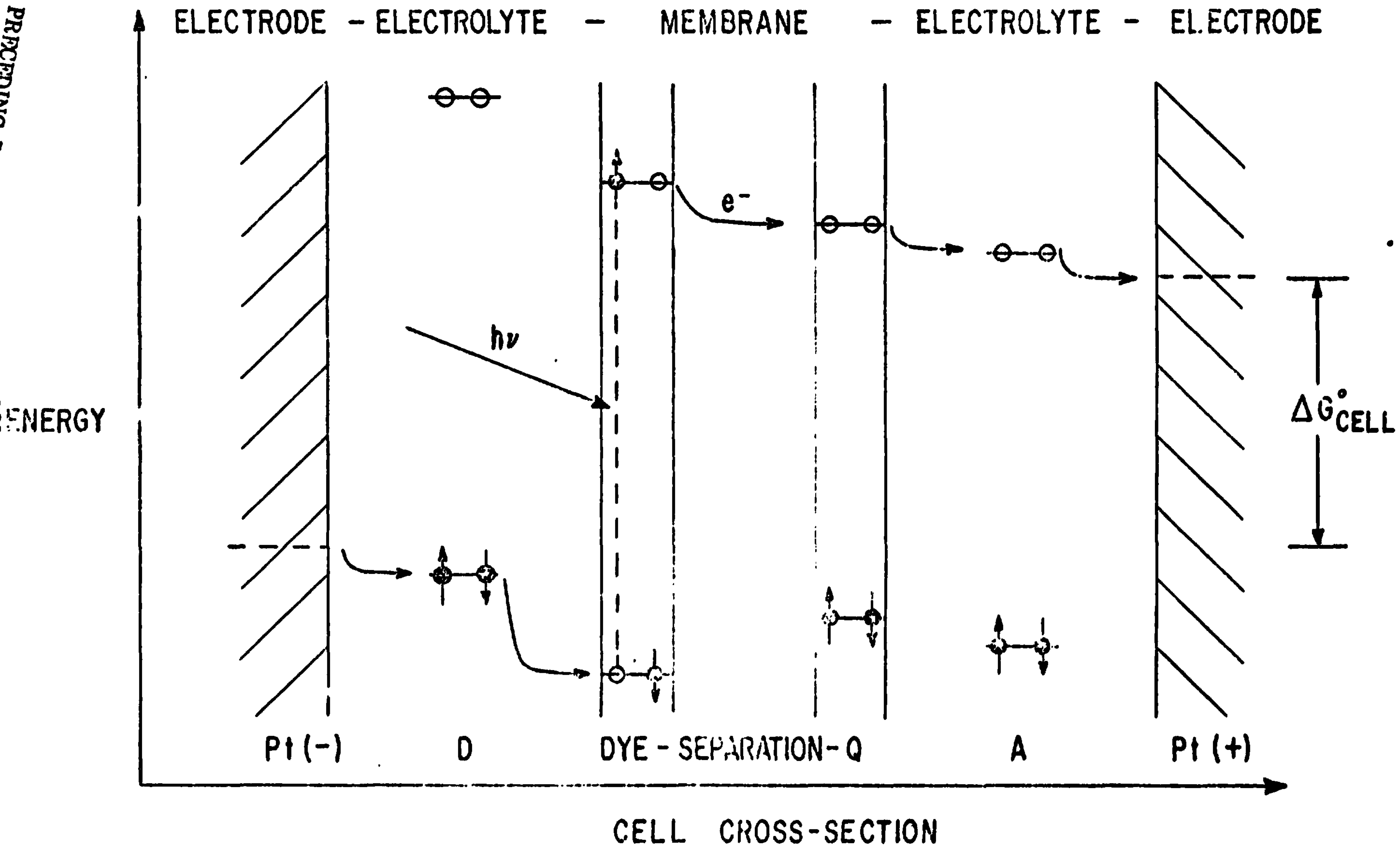

ENERGY LEVELS OF CELL COMPONENTS WHEN ILLUMINATED

PROGRESS TO DATE

- MATERIALS SYNTHESIS
- APPARATUS DEVELOPMENT
- ULTRATHIN FILM FABRICATION

MATERIAL SYNTHESIS

ULTRA-THIN FILM FABRICATION REQUIRES SURFACE ACTIVE MATERIALS

- DYES
  - THIAZINE, AZINE, ACRIDINE
- PRIMARY ELECTRON ACCEPTORS
  - QUINONE, VIOLOGEN
- SURFACE ACTIVE POLYMERS

INSOLUBLE MONOLAYERS AT AIR-H_2O BOUNDARIES

SURFACE ACTIVE DYE:

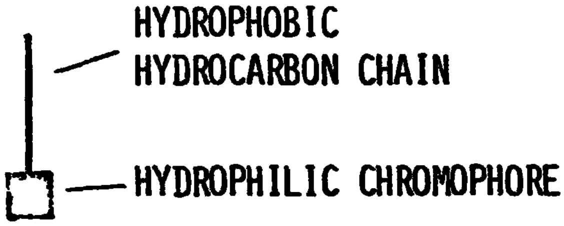

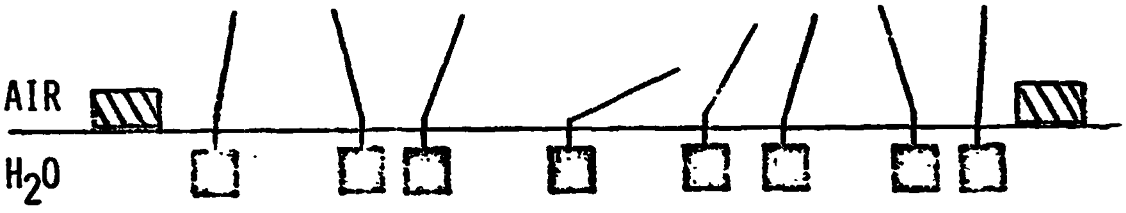

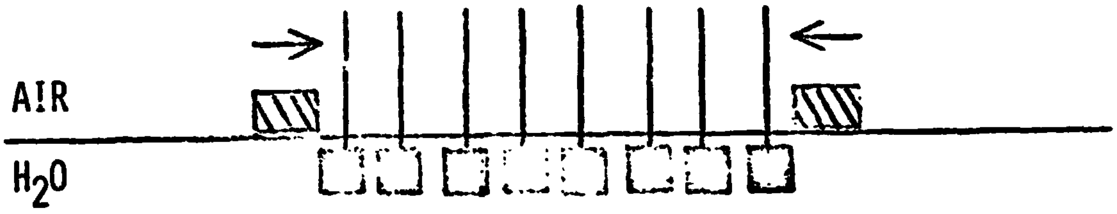

MONOLAYER TROUGHS, FILM BALANCE AND DIPPING MECHANISM

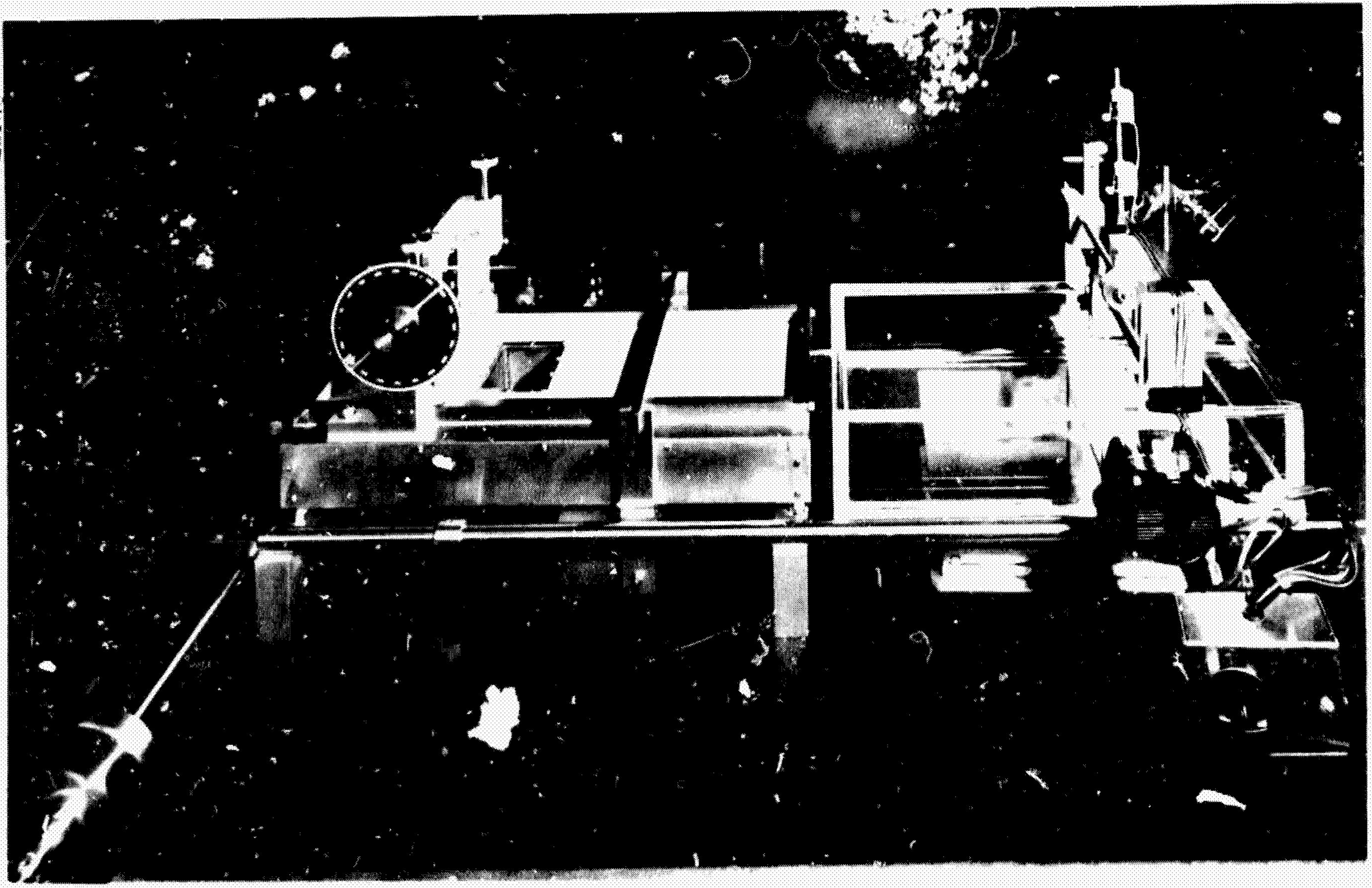

ASYMMETRIC FILM FABRICATION ON SOLID SUPPORTS

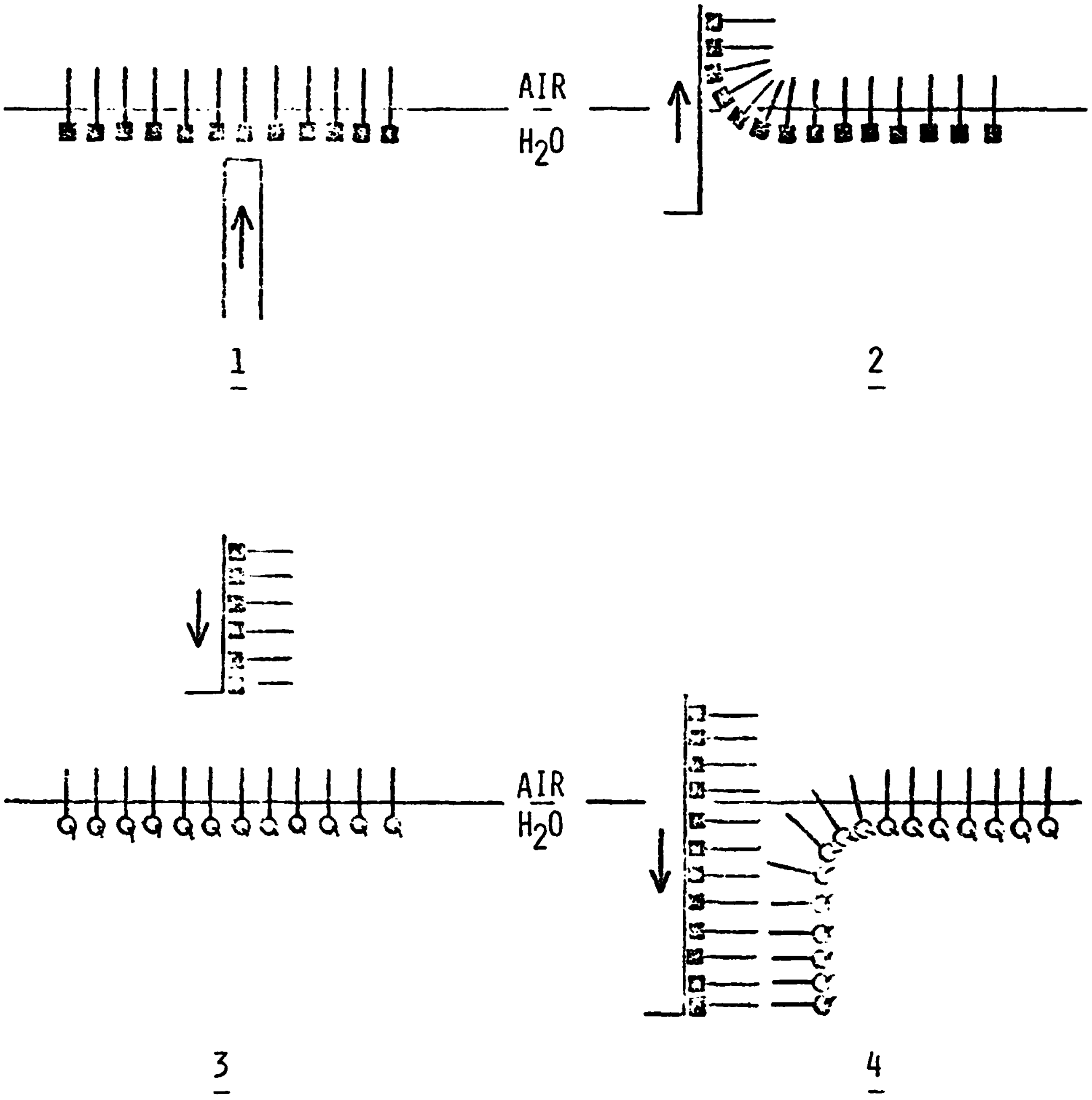

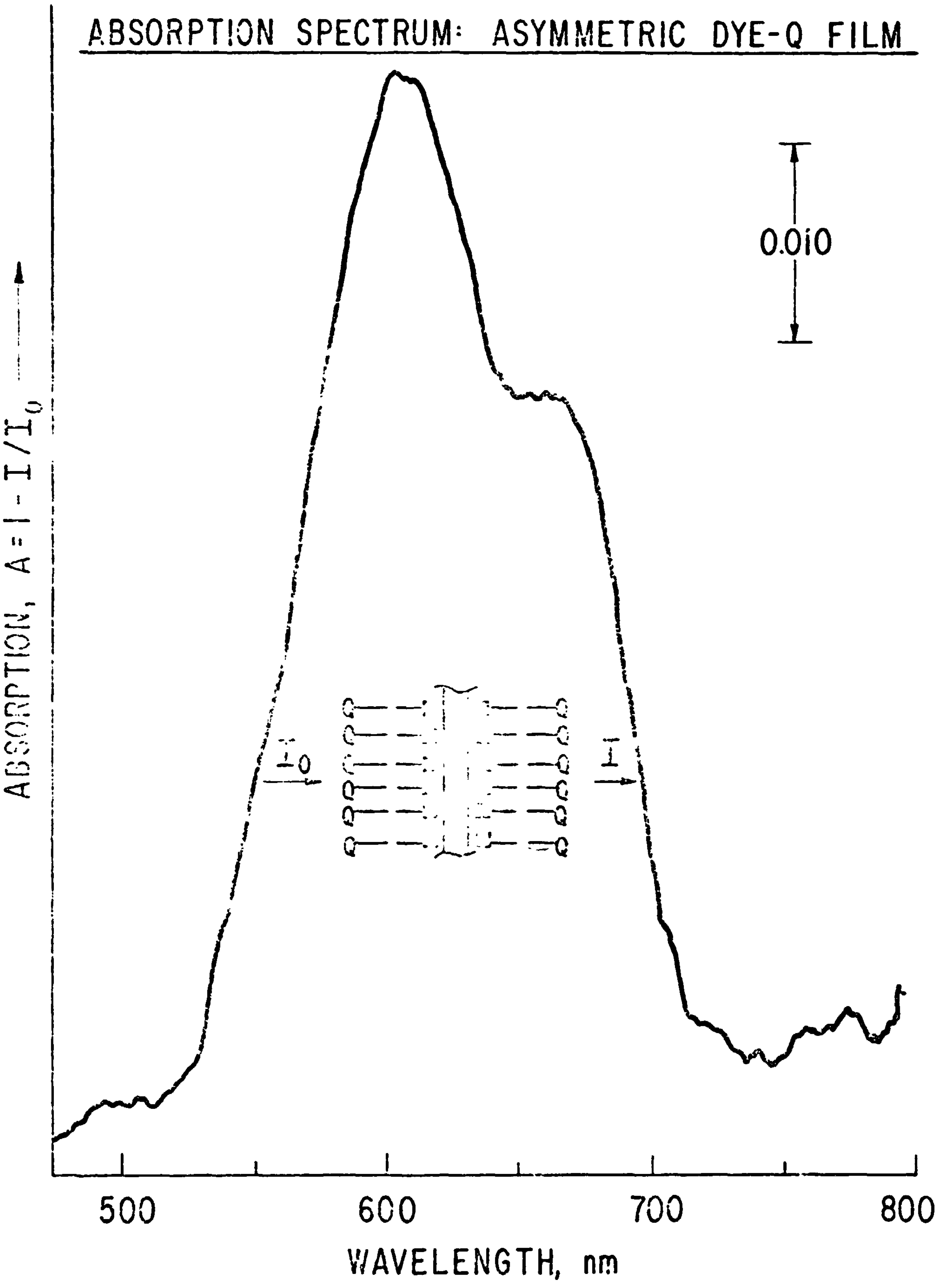
ABSORPTION SPECTRUM: ASYMMETRIC DYE-Q FILM
0.010
ABSORPTION, A = 1 - I/I_0
I_0
I
500
600
700
800
WAVELENGTH, nm

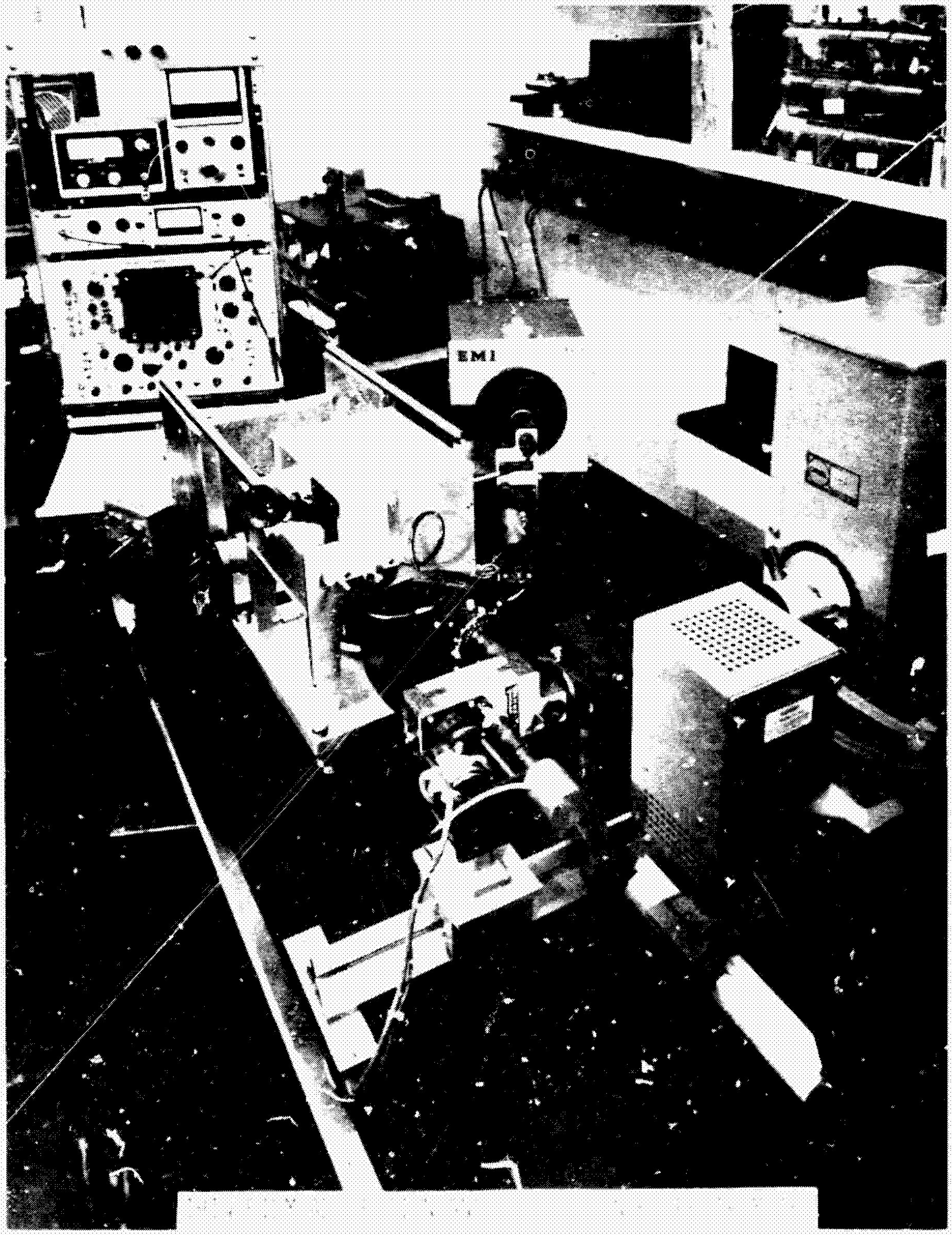
EMI

ASYMMETRIC MEMBRANE FORMATION

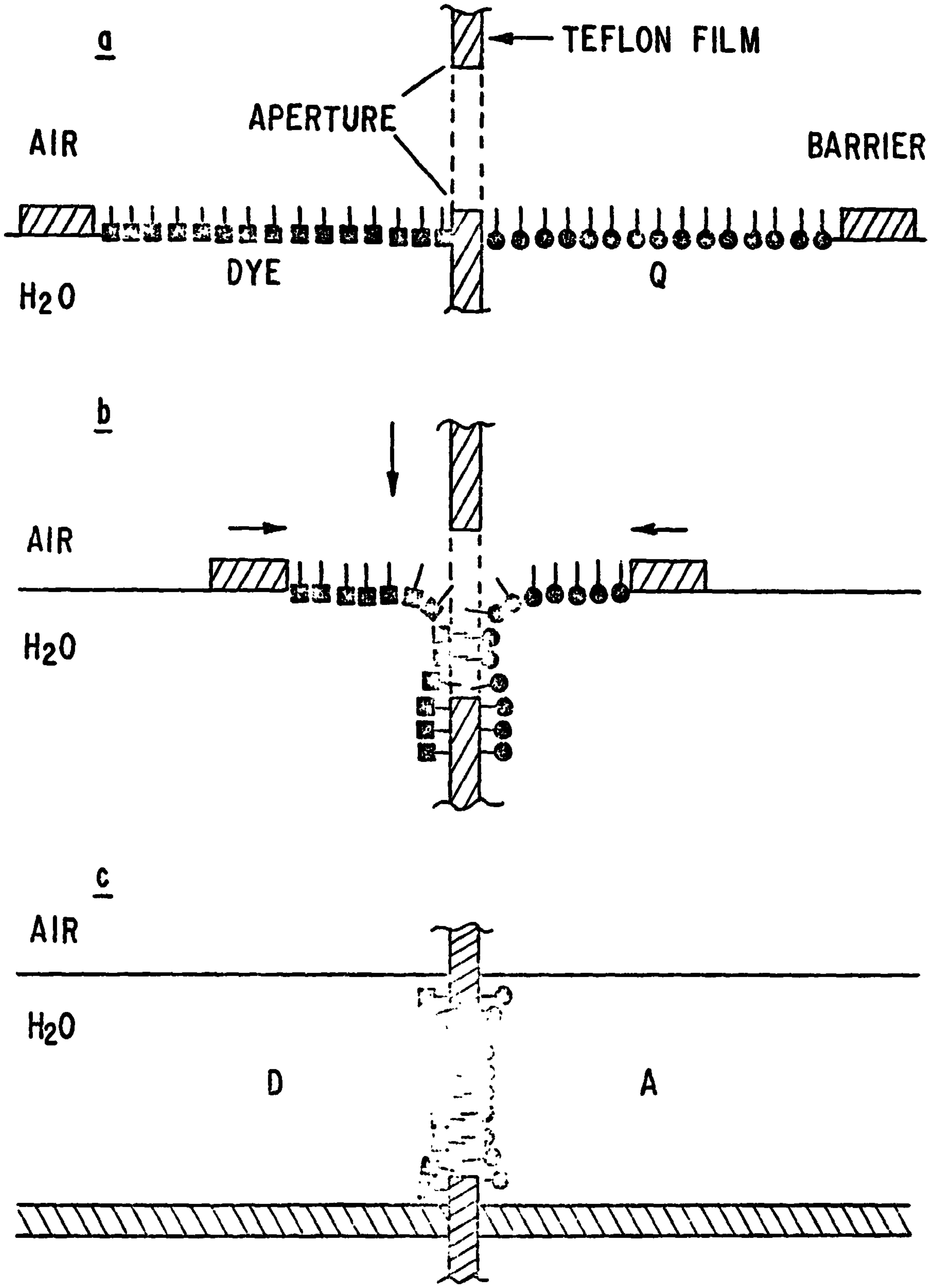

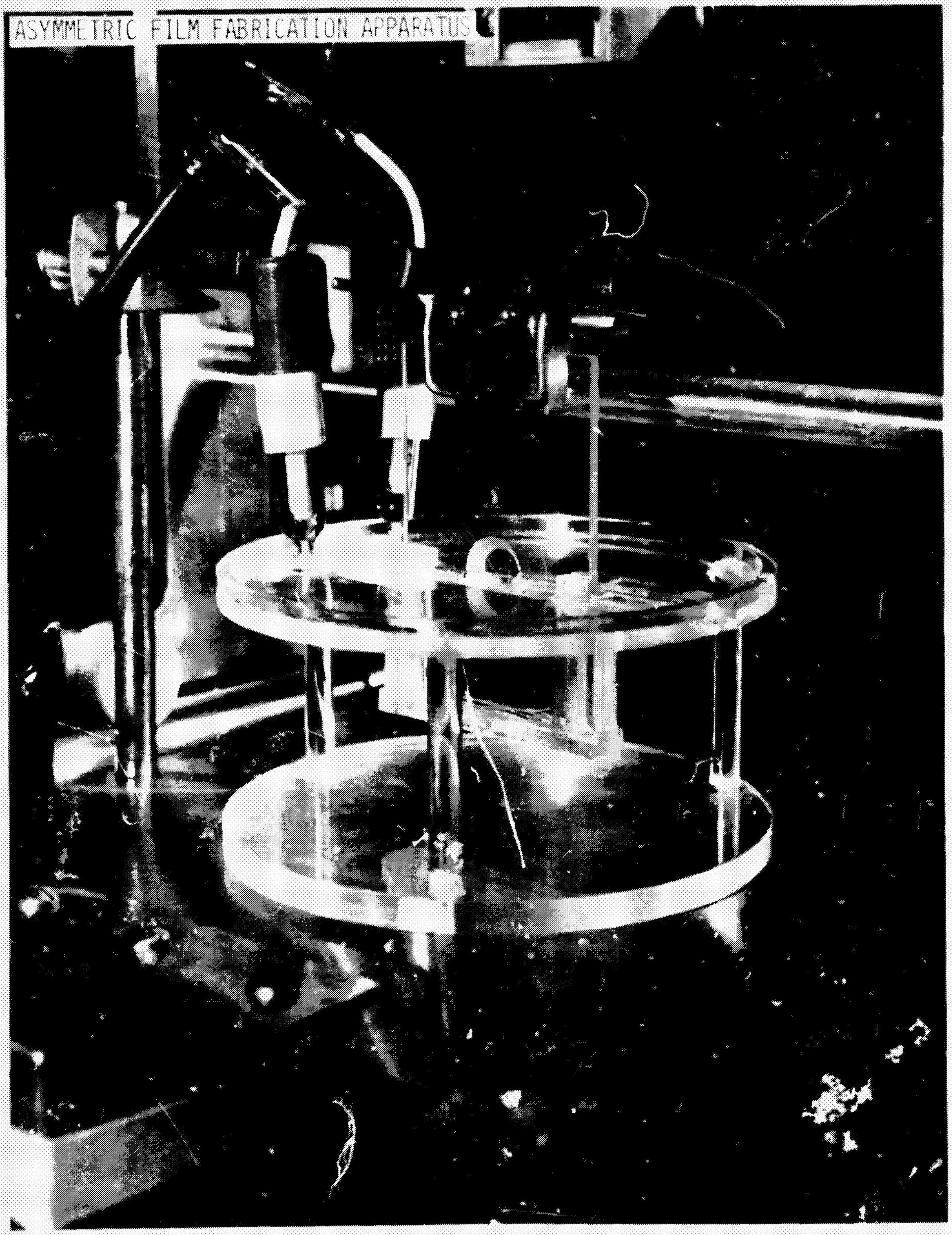
ASYMMETRIC FILM FABRICATION APPARATUS

SUMMARY OF KEY RESULTS

1) APPARATUS DEVELOPMENT -- COMPLETED

   ABSORPTION/FLUORESCENCE SPECTROMETER
   LANGMUIR FILM BALANCES AND MONOLAYER TROUGHS
   ASYMMETRIC FILM TROUGH
   VOLTAGE AND CURRENT CLAMPING CIRCUITRY

2) INITIAL MATERIALS SYNTHESIS -- COMPLETED

   SURFACE ACTIVE DYES, Q AND POLYMERS

3) SUPPORTED ASYMMETRIC FILMS

   SPECTROSCOPIC STUDIES

MAJOR PROBLEMS

- FABRICATION OF FREE-STANDING ASYMMETRIC ULTRATHIN MEMBRANES INTO COMPOSITE FILMS OF ADEQUATE MECHANICAL STRENGTH
- NEED TO DISCOVER EFFICIENT ELECTRON TRANSFER REACTIONS TO UTILIZE ALL THE POTENTIAL ENERGY PRODUCED IN THE ILLUMINATED FILMS

PLANNED ACTIVITY FOR NEXT 6 MONTHS

DEMONSTRATION OF THE PHOTOVOLTAIC EFFECT IN AN ASYMMETRIC MEMBRANE

- MEMBRANE FABRICATION
- PROOF OF MEMBRANE STRUCTURE
- CHOICE D AND A
- WAVELENGTH DEPENDENCE OF OPEN CIRCUIT EMF
- OPEN CIRCUIT EMF AND DYE FLUORESCENCE INTENSITY AS A FUNCTION OF DYE, Q, A, D CONCENTRATION AND pH
- OPEN CIRCUIT EMF AS A FUNCTION OF LIGHT INTENSITY
- I-V CHARACTERISTICS

END